ELSEVIER

World Journal of Gastroenterology®

Supported by NSFC 2005-2006

Volume 11 Number 20
May 28, 2005

National Journal Award 2005

Contents

World Journal of Gastroenterology®
Volume 11 **Number** 20 **May** 28, 2005

Contents

World Journal of Gastroenterology®
Volume 11 **Number** 20 **May** 28, 2005

Contents

Editorial Coordinator for this issue: Umayal Rajarathinam

World Journal of Gastroenterology (*World J Gastroenterol , WJG*), a leading international journal in gastroenterology and hepatology, has an established reputation for publishing first class research on esophageal cancer, gastric cancer, liver cancer, viral hepatitis, colorectal cancer, and *Helicobacter pylori* infection, providing a forum for both clinicians and scientists, and has been indexed and abstracted in Index Medicus, MEDLINE, PubMed, Chemical Abstracts, EMBASE, Abstracts Journals, Nature Clinical Practice Gastroenterology and Hepatology, CAB Abstracts and Global Health. Impact factor of ISI JCR during 2000-2003 is 0.993, 1.445, 2.532 and 3.318 respectively. *WJG* is a weekly journal published jointly by The *WJG* Press and Elsevier Inc. The publication date is on 7th, 14th, 21st, and 28th every month. The *WJG* is supported by The National Natural Science Foundation of China, No. 30224801 and No.30424812, which was founded with a name of *China National Journal of New Gastroenterology* on October 1,1995, and renamed as *WJG* on January 25, 1998.

PUBLISHED JOINTLY BY
The WJG Press and Elsevier Inc

PRINTING GROUP
Printed in Beijing on acid-free paper by Beijing Kexin Printing House

 Print ISSN 1007-9327
CN 14-1219/R.

SPECIAL STATEMENT
All articles published in this journal represent the viewpoints of the authors except where indicated otherwise.

EDITORIAL OFFICE
Editor: *World Journal of Gastroenterology*,
The WJG Press, Apartment 1066 Yishou Garden, 58 North Langxinzhuang Road, PO Box 2345, Beijing 100023, China
Telephone: +86-(0)10-85381901-1023
Fax: +86-10-85381893
E-mail: wjg@wjgnet.com
http://www.wjgnet.com

Public Relationship Manager
Shi-Yu Guo
The WJG Press, Apartment 1066 Yishou Garden, 58 North Langxinzhuang Road, PO Box 2345, Beijing 100023, China
Telephone: +86-(0)10-85381901-1023
Fax: +86-10-8538 1893
E-mail: s.y.guo@wjgnet.com
http://www.wjgnet.com

SUBSCRIPTION INFORMATION
Foreign
Elsevier (Singapore) Pte Ltd, 3 Killiney Road #08-01, Winsland House I, Singapore 239519
Telephone: +65-6349 0200
Fax: +65-6733 1817
E-mail: r.garcia@elsevier.com
http://asia.elsevierhealth.com
Institutional Rates Print-2005 rates: USD1 500.00
Personal Rates Print-2005 rates: USD700.00

Domestic
Local Post Offices Code No. BM 82-261

Author Reprints
The WJG Press, Apartment 1066 Yishou Garden, 58 North Langxinzhuang Road, PO Box 2345, Beijing 100023, China
Telephone: +86-(0)10-85381901-1023
Fax: +86-10-85381893
E-mail: wjg@wjgnet.com
http://www.wjgnet.com

ADVERTISING
Rosalia Da Carcia
Elsevier Science
Journals Marketing & Society Relations Health Science Asia
3 Killiney Road #08-01, Winsland House 1 Singapore 239519
Telephone: +65-6349 0200
Fax +65- 6733 1817
E-mail: r.garcia@elsevier.com
http://asia.elsevierhealth.com

INSTRUCTIONS TO AUTHORS
Full instructions are available online at http://www.wjgnet.com/wjg/help/instructions.jsp If you do not have web access please contact the editorial office.

World Journal of Gastroenterology®

Editorial Board

2004-2006

Published by The WJG Press and Elsevier Inc., PO Box 2345, Beijing 100023, China
Fax: +86-(0)10-85381893 E-mail: wjg@wjgnet.com http://www.wjgnet.com

Bulgaria
Zahariy Alexandrov Krastev, *Sofia*

Canada
Wang-Xue Chen, *Ottawa*
Richard N Fedorak, *Edmonton*
Hugh James Freeman, *Vancouver*
Samuel S Lee, *Calgary*
Philip Martin Sherman, *Toronto*
Alan BR Thomson, *Edmonton*
Eric M Yoshida, *Vancouver*

China
Francis KL Chan, *Hong Kong*
Xiao-Ping Chen, *Wuhan*
Jun Cheng, *Beijing*
Chi-Hin Cho, *Hong Kong*
Zong-Jie Cui, *Beijing*
Da-Jun Deng, *Beijing*
Er-Dan Dong, *Beijing*
Sheung-Tat Fan, *Hong Kong*
Xue-Gong Fan, *Changsha*
Jin Gu, *Beijing*
De-Wu Han, *Taiyuan*
Shao-Heng He, *Shantou*
Fu-Lian Hu, *Beijing*
Wayne HC Hu, *Hong Kong*
Ching Lung Lai, *Hong Kong*
Kam Chuen Lai, *Hong Kong*
Wai-Keung Leung, *Hong Kong*
Zhi-Hua Liu, *Beijing*
Ai- Ping Lu, *Beijing*
Jing-Yun Ma, *Beijing*
Lun-Xiu Qin, *Shanghai*
Yu-Gang Song, *Guangzhou*
Peng Shang, *Xi'an*
Qin Su, *Beijing*
Yuan Wang, *Shanghai*
Benjamin Wong, *Hong Kong*
Wai-Man Wong, *Hong Kong*
Hong Xiao, *Shanghai*
Dong-Liang Yang, *Wuhan*
Xue-Biao Yao, *Hefei*
Yuan Yuan, *Shenyang*
Man-Fung Yuen, *Hong Kong*
Jian-Zhong Zhang, *Beijing*
Zhi-Rong Zhang, *Chengdu*
Xiao-Hang Zhao, *Beijing*
Shu Zheng, *Hangzhou*

Costa Rica
Edgar M Izquierdo, *San José*

Croatia
Marko Duvnjak, *Zagreb*

Denmark
Flemming Burcharth, *Herlev*
Peter Bytzer, *Copenhagen*
Hans Gregersen, *Aalborg*
Jens H Henriksen, *Hvidovre*
Fin Stolze Larsen, *Copenhagen*
Søren Møller, *Hvidovre*

Egypt
Abdel-Rahman El-Zayadi, *Giza*

Finland
Pentti Sipponen, *Espoo*

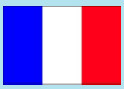

France
Charles Paul Balabaud, *Bordeaux*
Jacques Belghiti, *Clichy*
Pierre Brissot, *Rennes*
Franck Carbonnel, *Besancon*
Bruno Clément, *Rennes*
Jacques Cosnes, *Paris*
Francoise Degos, *Clichy*
Francoise Lunel Fabian, *Angers*
Gérard Feldmann, *Paris*
Jean Fioramonti, *Toulouse*
Rene Lambert, *Lyon*
Didier Lebrec, *Clichy*
Francis Mégraud, *Bordeaux*
Richard Moreau, *Clichy*
Jose Sahel, *Marseille*
Jean-Yves Scoazec, *Lyon*
Jean-Pierre Henri Zarski, *Grenoble*

Germany
HD Allescher, *Garmisch-Partenkirchen*
Rudolf Arnold, *Marburg*
Hubert Blum, *Freiburg*
Peter Born, *Muchen*
Heinz J Buhr, *Berlin*
Haussinger Dieter, *Düsseldorf*
Dietrich CF, *Bad Mergentheim*
Wolfram W Domschke, *Muenster*
Ulrich Robert Fölsch, *Kiel*
Peter R Galle, *Mainz*
Burkhard Göke, *Munich*
Axel M Gressner, *Aachen*
Eckhart Georg Hahn, *Erlangen*
Werner Hohenberger, *Erlangen*
RG Jakobs, *Ludwigshafen*
Joachim Labenz, *Siegen*
Ansgar W Lohse, *Hamburg*
Peter Malfertheiner, *Magdeburg*
Andrea Dinah May, *Wiesbaden*
Stephan Miehlke, *Dresden*
Gustav Paumgartner, *Munich*
Ulrich Ks Peitz, *Magdeburg*
Giuliano Ramadori, *Göttingen*
Tilman Sauerbruch, *Bonn*
Hans Seifert, *Oldenburg*
J Ruediger Siewert, *Munich*
Manfred V Singer, *Mannheim*
Jurgen M Stein, *Frankfurt*
Manfred Stolte, *Bayreuth*
Wolfgang R Stremmel, *Heidelberg*
Hans Ludger Tillmann, *Leipzig*
Siegfried Wagner, *Deggendorf*
Bertram Wiedenmann, *Berlin*

Greece
Arvanitakis C, *Thessaloniki*
Elias A Kouroumalis, *Heraklion*

Hungary
Simon A László, *Szekszárd*
János Papp, *Budapest*

Iceland
Hallgrimur Gudjonsson, *Reykjavik*

India
Sujit Kumar Bhattacharya, *Kolkata*
Chawla YK, *Chandigarh*
Radha Dhiman K, *Chandigarh*
Sri Prakash Misra, *Allahabad*
Kartar Singh, *Lucknow*

Iran
Reza Malekzadeh, *Tehran*

Israel
Abraham Rami Eliakim, *Haifa*
Yaron Niv, *Pardesia*

Italy
Giovanni Addolorato, *Roma*
Alfredo Alberti, *Padova*
Annese V, *San Giovanni Rotondo*
Giovanni Barbara, *Bologna*
Gabrio Bassotti, *Perugia*
Franco Bazzoli, *Bologna*
Adolfo Francesco Attili, *Roma*
Antomio Benedetti, *Ancona*
Giovanni Cammarota, *Roma*
Antonino Cavallari, *Bologna*
Dario Conte, *Milano*
Gino Roberto Corazza, *Pavia*
Guido Costamagua, *Roma*
Antonio Craxi, *Palermo*
Fabio Farinati, *Padua*
Giovanni Gasbarrini, *Roma*
Paolo Gentilini, *Florence*
Edoardo G Giannini, *Genoa*

Paolo Gionchetti, *Bologna*
Roberto De Giorgio, Bologna
Mario Guslandi, *Milano*
Giovanni Maconi, *Milan*
Giulio Marchesini, *Bologna*
Giuseppe Montalto, *Palermo*
Luisi Pagliaro, *Palermo*
Fabrizio R Parente, *Milan*
Perri F, *San Giovanni Rotondo*
Raffaele Pezzilli, *Bologna*
Pilotto A, *San Giovanni Rotondo*
Massimo Pinzani, *Firenze*
Gabriele Bianchi Porro, *Milano*
Piero Portincasa, *Bari*
Giacomo Laffi, *Firenze*
Enrico Roda, *Bologna*
Massimo Rugge, *Padova*
Vincenzo Savarino, *Genova*
Vincenzo Stanghellini, *Bologna*
Calogero Surrenti, *Florence*
Roberto Testa, *Genoa*
Dino Vaira, *Bologna*

Japan

Kyoichi Adachi, *Izumo*
Takashi Aikou, *Kagoshima*
Taiji Akamatsu, *Matsumoto*
Takafumi Ando, *Nagoya*
Akira Andoh, *Otsu*
Taku Aoki, *Tokyo*
Masahiro Arai, *Tokyo*
Tetsuo Arakawa, *Osaka*
Yasuji Arase, *Tokyo*
Masahiro Asaka, *Sapporo*
Hitoshi Asakura, *Tokyo*
Yutaka Atomi, *Tokyo*
Takeshi Azuma, *Fukui*
Nobuyuki Enomoto, *Yamanashi*
Kazuma Fujimoto, *Saga*
Toshio Fujioka, *Oita*
Yoshihide Fujiyama, *Otsu*
Hiroyuki Hanai, *Hamamatsu*
Kazuhiro Hanazaki, *Nagano*
Naohiko Harada, *Fukuoka*
Makoto Hashizume, *Fukuoka,*
Tetsuo Hayakawa, *Nagoya*
Kazuhide Higuchi, *Osaka*
Ichiro Hirata, *Osaka*
Keiji Hirata, *Kitakyushu*
Takafumi Ichida, *Shizuoka*
Kenji Ikeda, *Tokyo*
Kohzoh Imai, *Sapporo*
Fumio Imazeki, *Chiba*
Masayasu Inoue, *Osaka*
Hiromi Ishibashi, *Nagasaki*
Shunji Ishihara, *Izumo*
Toru Ishikawa, *Niigata*
Kei Ito, *Sendai*
Masayoshi Ito, *Tokyo*
Hiroaki Itoh, *Akita*
Hiroshi Kaneko, *Aichi-Gun*
Shuichi Kaneko, *Kanazawa*
Takashi Kanematsu, *Nagasaki*
Junji Kato, *Sapporo*
Mototsugu Kato, *Sapporo*
Shinzo Kato, *Tokyo*
Sunao Kawano, *Osaka*
Yoshikazu Kinoshita, *Izumo*
Masaki Kitajima, *Tokyo*
Tsuneo Kitamura, *Chiba*
Seigo Kitano, *Oita*
Hironori Koga, *Kurume*
Satoshi Kondo, *Sapporo*
Shoji Kubo, *Osaka*
Shigeki Kuriyama, *Kagawa*
Masato Kusunoki, *Mie*
Takashi Maeda, *Fukuoka*
Shin Maeda, *Tokyo*
Osamu Matsui, *Kanazawa*
Yasushi Matsuzaki, *Tsukuba*
Hiroto Miwa, *Hyogo*
Masashi Mizokami, *Nagoya*
Motowo Mizuno, *Hiroshima*
Morito Monden, *Suita*
Hisataka S Moriwaki, *Gifu*
Yoshiharu Motoo, *Kanazawa*
Akihiro Munakata, *Hirosaki*
Kazunari Murakami, *Oita*
Kunihiko Murase, *Tusima*
Masato Nagino, *Nagoya*
Yujl Naito, *Kyoto*
Hisato Nakajima, *Tokyo*
Hiroki Nakamura, *Yamaguchi*
Shotaro Nakamura, *Fukuoka*
Akimasa Nakao, *Nagoya*
Mikio Nishioka, *Niihama*
Susumu Ohmada, *Maebashi*
Masayuki Ohta, *Oita*
Tetsuo Ohta, *Kanazawa*
Susumu Okabe, *Kyoto*
Katsuhisa Omagari, *Nagasaki*
Saburo Onishi, *Nankoku*
Morikazu Onji, *Ehime*
Hiromitsu Saisho, *Chiba*
Hidetsugu Saito, *Tokyo*
Takafumi Saito, *Yamagata*
Isao Sakaida, *Yamaguchi*
Michiie Sakamoto, *Tokyo*
Iwao Sasaki, *Sendai*
Motoko Sasaki, *Kanazawa*
Chifumi Sato, *Tokyo*
Shuichi Seki, *Osaka*
Hiroshi Shimada, *Yokohama*
Mitsuo Shimada, *Tokushima*
Hiroaki Shimizu, *Chiba*
Tooru Shimosegawa, *Sendai*
Tadashi Shimoyama, *Hirosaki*
Ken Shirabe, *Iizuka City*
Yoshio Shirai, *Niigata*
Katsuya Shiraki, *Mie*
Yasushi Shiratori, *Okayama*
Yasuhiko Sugawara, *Tokyo*
Toshiro Sugiyama, *Toyama*
Kazuyuki Suzuki, *Morioka*
Hidekazu Suzuki, *Tokyo*
Tadatoshi Takayama, *Tokyo*
Tadashi Takeda, *Osaka*
Koji Takeuchi, *Kyoto*
Kiichi Tamada, *Tochigi*
Akira Tanaka, *Kyoto*
Eiji Tanaka, *Matsumoto*
Noriaki Tanaka, *Okayama*
Shinji Tanaka, *Hiroshima*
Kyuichi Tanikawa, *Kurume*
Tadashi Terada, *Shizuoka*
Akira Terano, *Shimotsugagun*
Kazunari Tominaga, *Osaka*
Hidenori Toyoda, *Ogaki*
Akihito Tsubota, *Chiba*
Shingo Tsuji, *Osaka*
Takato Ueno, *Kurume*
Shinichi Wada, *Tochigi*
Hiroyuki Watanabe, *Kanazawa*
Sumio Watanabe, *Akita*
Toshio Watanabe, *Osaka*
Yuji Watanabe, *Ehime*
Chun-Yang Wen, *Nagasaki*
Koji Yamaguchi, *Fukuoka*
Takayuki Yamamoto, *Yokkaichi*
Takashi Yao, *Fukuoka*
Hiroshi Yoshida, *Tokyo*
Masashi Yoshida, *Tokyo*
Norimasa Yoshida, *Kyoto*
Kentaro Yoshika, *Toyoake*
Masahide Yoshikawa, *Kashihara*

Lithuania

Sasa Markovic, *Japljeva*

Macedonia

Vladimir Cirko Serafimoski, *Skopje*

Malaysia

Andrew Seng Boon Chua, *Ipoh*
Jayaram Menon, *Sabah*
Khean-Lee Goh, *Kuala Lumpur*

Monaco

Patrick Rampal, *Monaco*

Netherlands

Louis MA Akkermans, *Utrecht*
Karel Van Erpecum, *Utrecht*
Albert K Groen, *Amsterdam*
Dirk Joan Gouma, *Amsterdam*
Jan BMJ Jansen, *Nijmegen*
Evan Anthony Jones, *Abcoude*
Ernst Johan Kuipers, *Rotterdam*
Chris JJ Mulder, *Amsterdam*
Michael Müller, *Wageningen*

Pena AS, *Amsterdam*
Andreas Smout, *Utrecht*
RW Stockbrugger, *Maastricht*
GP Vanberge-Henegouwen, *Utrecht*

New Zealand
Ian David Wallace, *Auckland*

Norway
Trond Berg, *Oslo*
Helge Lyder Waldum, *Trondheim*

Pakistan
Muhammad S Khokhar, *Lahore*

Philippines
Eulenia Rasco Nolasco, *Manila*

Poland
Tomasz Brzozowski, *Cracow*
Andrzej Nowak, *Katowice*

Portugal
Miguel Carneiro De Moura, *Lisbon*

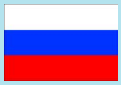

Russia
Vladimir T Ivashkin, *Moscow*
Leonid Lazebnik, *Moscow*
Vasiliy I Reshetnyak, *Moscow*

Singapore
Bow Ho, *Kent Ridge*
Francis Seow-Choen, *Singapore*

Slovakia
Anton Vavrecka, *Bratislava*

South Africa
Michael C Kew, *Parktown*

South Korea
Jin-Hong Kim, *Suwon*
Myung-Hwan Kim, *Seoul*
Yun-Soo Kim, *Seoul*
Yung-Il Min, *Seoul*
Jae-Gahb Park, *Seoul*
Dong Wan Seo, *Seoul*

Spain
Abraldes JG, *Barcelona*
Fernando Azpiroz, *Barcelona*
Ramon Bataller, *Barcelona*
Josep M Bordas, *Barcelona*
Maria Buti, *Barcelon*
Xavier Calvet, *Sabadell*
Antoni Castells, *Barcelona*
Manuel Daz-Rubio, *Madrid*
Juan C Garcia-Pagán, *Barcelona*
Genover JB, *Barcelona*
Javier P Gisbert, *Madrid*
Jaime Guardia, *Barcelona*
Angel Lanas, *Zaragoza*
Ricardo Moreno-Otero, *Madrid*
Julian Panes, *Barcelona*
Miguel Perez-Mateo, *Alicante*
Josep M Pique, *Barcelona*
Jesus Prieto, *Pamplona*
Luis Rodrigo, *Oviedo*

Sri Lanka
Janaka De Silva, *Ragama*

Swaziland
Gerd Kullak-Ublick, *Zurich*

Sweden
Lars Christer Olbe, *Molndal*
Curt Einarsson, *Huddinge*
Lars R Lundell, *Stockholm*
Xiao-Feng Sun, *Linkoping*

Switzerland
Christoph Beglinger, *Basel*
Michael W Fried, *Zurich*
Bruno Stieger, *Zurich*
Arthur Zimmermann, *Berne*

Turkey
Yusuf Bayraktar, *Ankara*
Figen Gurakan, *Ankara*
Cihan Yurdaydin, *Ankara*

United Kingdom
Axon ATR, *Leeds*
Paul Jonathan Ciclitira, *London*
Amar Paul Dhillon, *London*
Stuarts Forbes
Subrata Ghosh, *London*
Brian T Johnston, *Belfast*
David EJ Jones, *Newcastle*
Michael A Kamm, *Harrow*
Hong-Xiang Liu, Cambridge
Giorgina Mieli-Vergani, *London*
Nikolai V Naoumov, *London*
John P Neoptolemos, *Liverpool*
James Neuberger, *Birmingham*
Colm Antoine O'Morain, *Dublin*
Simon D Taylor-Robinson, *London*
Frank Ivor Tovey, *Basingstoke*
Min Zhao, *Foresterhill*

United States
Firas H Ac-Kawas, *Washington*
Gianfranco D Alpini, *Temple*
Paul Angulo, *Rochester*
Jamie S Barkin, *Miami Beach*
Todd Baron, *Rochester*
Kim Elaine Barrett, *San Diego*
Jennifer D Black, *Buffalo*
Xu Cao, *Birmingham*
David L Carr-Locke, *Boston*
Marc F Catalano, *Milwaukee*
Xian-Ming Chen, *Rochester*
James M Church, *Cleveland*
Vincent Coghlan, *Beaverton*
James R Connor, *Hershey*
Pelayo Correa, *New Orleans*
John Cuppoletti, *Cincinnati*
Peter V Danenberg, *Los Angeles*
Kiron Moy Das, *New Brunswick*
Hala El-Zimaity, *Houston*
Ronnie Fass, *Tucson*
Emma E Furth, *Pennsylvania*
John Geibel, *New Haven*
Graham DY, *Houston*
Joel S Greenberger, *Pittsburgh*
Anna S Gukovskaya, *Los Angeles*
Gavin Harewood, *Rochester*
Atif Iqbal, *Omaha*
Hajime Isomoto, *Rochester*
Dennis M Jensen, *Los Angeles*
Leonard R Johnson, *Memphis*
Peter James Kahrilas, *Chicago*
Anthony Nicholas Kalloo, *Baltimore*
Neil Kaplowitz, *Los Angeles*
Emmet B Keeffe, *Palo Alto*
Joseph B Kirsner, *Chicago*
Burton I Korelitz, *New York*
Robert J Korst, *New York*
Richard A Kozarek, *Seattle*
Shiu-Ming Kuo, *Buffalo*
Frederick H Leibach, *Augusta*
Andreas Leodolter, *La Jolla*
Ming Li, *New Orleans*
Lenard M Lichtenberger, *Houston*
Gary R Lichtenstein, *Philadelphia*
Josep M Llovet, *New York*
Martin Lipkin, *New York*

Manuscript reviewers of *World Journal of Gastroenterology*

PO Box 2345, Beijing 100023, China
www.wjgnet.com
wjg@wjgnet.com

ELSEVIER

World J Gastroenterol 2005;11(20):3011-3013
World Journal of Gastroenterology ISSN 1007-9327

• *REVIEW* •

Research progress on *Helicobacter pylori* outer membrane protein

Shi-He Shao, Hua Wang, Shun-Gen Chai, Li-Mei Liu

Shi-He Shao, Shun-Gen Chai, Department of Medical Microbiology and Parasitology, Medical Technology College, Jiangsu University, Zhenjiang 212001, Jiangsu Province, China
Hua Wang, Li-Mei Liu, Graduate Student, Medical College, Northern University, Jilin 132001, Jilin Province, China
Supported by the Research Plan of Jiangsu Provincial Technology Commission, No. BS2004021; Advanced Talent Research Plan of Jiangsu University, No. JDG2004008
Correspondence to: Shi-He Shao, Department of Medical Microbiology and Parasitology, Medical Technology College, Jiangsu University, Zhenjiang 212001, Jiangsu Province, China. ljxwl123@163.com
Telephone: +86-511-2165735
Received: 2004-11-08 Accepted: 2004-12-03

Abstract

Helicobacter pylori (*H pylori*), one of the most common bacterial pathogens on human beings, colonizes the gastric mucosa. In its 95 paralogous gene families, there is a large outer membrane protein (OMP) family. It includes 32 members. These OMP are important for the diagnosis, protective immunity, pathogenicity of *H pylori* and so on. They are significantly associated with high *H pylori* density, the damage of gastric mucosa, high mucosal IL-8 levels and severe neutrophil infiltration. We introduce their research progress on pathogenicity.

Key words: *H pylori*; Outer membrane protein; oipA; Gastric carcinoma

Shao SH, Wang H, Chai SG, Liu LM. Research progress on *Helicobacter pylori* outer membrane protein. *World J Gastroenterol* 2005; 11(20): 3011-3013
http://www.wjgnet.com/1007-9327/11/3011.asp

INTRODUCTION

Helicobacter pylori (*H pylori*) is a noninvasive bacterium. Since Warran and Marshell isolated *H pylori* successfully in 1983, it has been identified as the major causative factor of chronic gastric and peptic ulcer disease and closely related to the occurrence and development of gastric carcinoma, mucosa-associated lymphoid tissue (MALT) lymphoma. In 1994 international cancer institute had determined it being type I carcinogen[1]. Studies regarding the *H pylori* virulence have primarily focused on urease, vacuolating cytotoxin, and cytotoxin-associated antigen. However, in its 95 paralogous gene families there is a large *H pylori* outer membrane protein (Hop) family. It includes 32 members[2,3], such as adhesin protein, proinflammatory protein, and micropore protein. Although some functions of these OMP have still been indefinite, the scholars at home and abroad have paid attention to them on diagnosis, protective immunity, pathogenicity and so on. The documents show that Hop is significantly associated with high *H pylori* colonization, the damage of gastric mucosa, high mucosal IL-8 levels, and neutrophil infiltration. We will review these aspects of OMP.

OMP AND CHRONIC GASTRITIS AND PEPTIC ULCERS

Adhesin protein

We have known that adherence to the epithelium is an important premise that bacteria settle down in the body. Adherence is believed to help protect the bacteria from gastric acidity, as well as from displacement due to peristalsis. HopZ, babA, and babB (blood-group antigen-binding gene), alpAB (adherence-associated lipoprotein) in the OMP are mainly related to adherence.

HopZ (HP9) is a vital adhesin protein. HopZ is primarily located in the bacterial surface, the number of its amino acids largely vary, ranging from 126 to 281. This is primarily because that HopZ gene suffers length-short regulation of different CT dinucleotide repetitive motif of different strains in the translational level. Birgit Peck[4] discovered that the wild-type strain ATCC43504 (HopZ negative) adhered to human gastric epithelial cells whereas a knockout mutant strain showed significantly reduced binding to the cells. Yamaoka[5] concluded: HopZ was significantly related to *H pylori* density and colonization ability in the mouse model.

babA (HP1234) and babB (HP0896) are OMP of having vital relation with adherence. Because their production binds LewisB antigen of human gastric cells, so are called blood-group-antigen-binding gene. Moreover the activity that the product of $babA_2$ (allele of babA) binds LewisB antigen is higher[6]. But because people discovered *H pylori* expresses LewisB antigen, too. Therefore, some scholars doubt whether gastric epithelial cell-LewisB is the receptor of *H pylori*[7]. Ai-Fu Tang in China[8] persistently researched and testified that LewisB antigen expressed by *H pylori* did not affect *H pylori* adherence to LewisB and summit to secretion of host (secretory people have LewisB antigen in humoral fluid). But the author thought that the $babA_2$ gene was not related to peptic ulcer, the same type of LewisB antigen expressed by *H pylori* as their host had the advantage of evading host immune system to survive, then triggered disease. Furthermore, host may trigger disease through producing autoantibody aiming at LewisB antigen. The research by Zambon[9] showed that $babA_2$ and CagA-s1 and m1(allele of Vac) in *H pylori* acted together, which could obviously worsen the degree of inflammation.

AlpAB is also concerned with adhesion of *H pylori*. At present, it is being ascertained that AlpAB are two kinds of channel-forming membrane pore: hopB and hopC, which are organized in an operon[10]. Through designing the mutant strain AlpA or AlpB, Odenbreit testified AlpAB-specific adherence and concluded that the adherence was independent of the composition of the lipopolysaccharide (LPS)[11].

Proinflammatory

oipA (outer inflammatory protein, oipA), encoding OMP gene of relative molecular mass (M_r) of 34 ku, is called HopH (HP0638). The product is called proinflammatory. As early as 1998, Yamaoka[12] discovered that M_r ranging 33 ku to 35 ku OMP were positively correlated with the level of IL-8. However, there was no relationship between other antigens including CagA and production of IL-8. The 33-35 ku antigen was present in 97.5% patients with gastric or duodenal ulcer compared to 70% those with chronic gastritis. In order to ascertain the genic position of the protein, in 2000, Yamoka[13] designed the knockout mutant strain HP0638(M_r34 ku), HP0796(M_r33 ku), HP1501(M_r32 ku), compared with wild-type about inducing to secrete the level of IL-8. The result showed HP0796 and HP1501 had no significant effect on IL-8 product. However, knockout of the HP0638 gene reduced IL-8 product approximately 50%. Cag-negative strains that contained a functional HP0638 gene produced more than three-fold greater IL-8 than Cag-negative nonfunctional HP0638 strains. So the author denoted HP0638 gene as outer inflammatory protein (oipA). The recent data[14] showed that HP0638 frame status was correlated strongly with CagA, vacA iceA genotypes. All of the strains in which HP0638 was in frame were CagA positive and vacAs1, whereas most of the strains in which HP0638 was out of frame were CagA negative (80%) and vacAs2 (70%). So the author thought it suggested that CagA positivity could affect transcription of HP0638. But Yamaoka[15] discovered in his further research that oipA status remained in the final model to discriminate duodenal ulcer from gastritis. Functional oipA was significantly associated with high *H pylori* density, severe neutrophil infiltration and high mucosal IL-8 levels and further research that polyclonal antisera to either a synthetic oipA peptide or a recombinant oipA protein detected oipA expression in *H pylori* and correlated with functional oipA status determined by PCR sequence[16]. Moreover, the recent research showed that the detecting of oipA+HP was 46.6%. But oipA was detected in patients with gastric ulcer and the rate was 100%, which was obviously higher than in patients with gastritis. Thus, it indicated that oipA was significantly more frequent in patients with gastric ulcer[17].

OMP AND GASTRIC CARCINOMAS

Before discovering *H pylori*, people believed that gastric carcinomas evolved from superficial gastritis to chronic atrophic gastritis , then intestinal metaplasia and turned into gland cancer[18]. Hop played an important role in the process. Zambon[9] research testified that coexpressed by the same *H pylori* strain, CagA, s1 and m1Vac worded synergistically, not only were worsening inflammation, but also were at higher risk for intestinal metaplasia. The scholars in Taiwan[19] discovered that a significant association was found between the serum antibodies against lower-molecular-weight proteins of *H pylori*, especially 19.5 ku and 26.5 ku, and malignant outcome of *H pylori* infection. Wei-Hong Yang[20] discovered that antibody titre of 26.5 ku protein in gastritis group was higher than that in ulcer group, in moderate, severe inflammatory gastritis was higher than that in subinflammatory gastritis. These have the advantage of the occurrence and development of tumor. Therefore some scholars believe lower-molecular-weight OMP may act as gastric carcinomas and its hypercrowd screening , it is a kind of marking antigen[21,22].

OMP AND IMMUNITY

Cytokine

When infected by *H pylori*, inflammatory cytokine induced by OMP plays an important role in *H pylori* pathopoiesis. It has been definite that oipA is positively correlated with product of IL-8 as former statement[12]. Petra[23]discovered that HpaA and OMP18(M_r18 000) induced IL-12 and IL-10 to secrete when researching their antigenicity . IL-8 is an main inflammatory promoter and regulatory factor. IL-12 was obviously positively correlated with the degree of T lymphoid infiltration in the mucous membrane and worsen gastric mucous inflammation[24].

Vaccinal research

Most OMP locates the surface of bacterial body, surface exposing, conserving relatively, inducing humoral immunity and so on. Thus, since early, people have begun researching its protective immunogenicity, but can get partial effect on protecting immunity[25,26]. Nowadays, many scholars have researched polyvalent vaccine. Zheng Jiang succeeded in constructing divalent vaccine of HpaA,OMP18 (M_r18 000) and HpaA, OMP26 (26 000), which laid the foundation of constructing *H pylori* protein vaccine[27,28].

CONCLUSIONS AND PERSPECTIVES

There are other OMP which deserve to be further studied. For example, Ping Cao[29]through researching two HopQ alleles discovered that type I HopQ alleles were found significantly more commonly in cag^+/s1-vacA strains from patients with peptic ulcer disease than in cag^-/s2-vacA strains from patients without ulcer disease. But Akihiro[30]through researching OMP29 (M_r29 000) from being isolated ATCC43504 strains discovered that OMP29 could alter its antigenicity through gene modifications mediated by nucleotide transfer. These discovers are looking forward to further probing and studying. At present, genome sequence of *H pylori* OMP have finished, but the function of many OMP has been indefinite: how on earth they induce to disease, the relation with other virulence factor: Cag pathogenicity island and VacA, which antigenicity is more. These are still not clear. However, there are many questions in former research, for example , Yamaoka thought oipA frame status was an unique index that discriminated duodenal from gastritis. But the author didn't examine gene of encoding 35 ku protein. Wei-Hong Yang[20] in China did the correlation research and discovered that in quantitative study ,the antibody titre of 35 ku protein in original duodenal bulb ulcer group was obviously higher than that in chronic superficial gastritis group.

In a word, researching virulence and pathogenicity of *H pylori* is a vital significance. This can discover new strains and further illuminate pathogenic mechanism, on the other hand, can provide basis for vaccinal screening, designing and immunity strategy. This can avail the development of a new particularity diagnosis reagent kit.

REFERENCES

1 NIH Consensus Conference. *Helicobacter pylori* in peptic ulcer disease. NIH Consensus Development Panel on *Helicobacter pylori* in Peptic Ulcer Disease. *JAMA* 1994; **272**: 65-69

2 **Tomb JF**, White O, Kerlavage AR, Clayton RA, Sutton GG, Fleischmann RD, Ketchum KA, Klenk HP, Gill S, Dougherty BA, Nelson K, Quackenbush J, Zhou L, Kirkness EF, Peterson S, Loftus B, Richardson D, Dodson R, Khalak HG, Glodek A, McKenney K, Fitzegerald LM, Lee N, Adams MD, Hickey EK, Berg DE, Gocayne JD, Utterback TR, Peterson JD, Kelley JM, Cotton MD, Weidman JM, Fujii C, Bowman C, Watthey L, Wallin E, Hayes WS, Borodovsky M, Karp PD, Smith HO, Fraser CM, Venter JC. The complete genome sequence of the gastric pathogen *Helicobacter pylori*. *Nature* 1997; **388**: 539-547

3 **Alm RA**, Bina J, Andrews BM, Doig P, Hancock RE, Trust TJ. Comparative genomics of *Helicobacter pylori*: analysis of the outer membrane protein families. *Infect Immun* 2000; **68**: 4155-4168

4 **Peck B**, Ortkamp M, Diehl KD, Hundt E, Knapp B. Conservation, localization and expression of HopZ, a protein involved in adhesion of *Helicobacter pylori*. *Nucleic Acids Res* 1999; **27**: 3325-3333

5 **Yamaoka Y**, Kita M, Kodama T, Imamura S, Ohno T, Sawai N, Ishimaru A, Imanishi J, Graham DY. *Helicobacter pylori* infection in mice: Role of outer membrane proteins in colonization and inflammation. *Gastroenterology* 2002; **123**: 1992-2004

6 **Pride DT**, Meinersmann RJ, Blaser MJ. Allelic Variation within *Helicobacter pylori* babA and babB. *Infect Immun* 2001; **69**: 1160-1171

7 **Clyne M**, Drumm B. Absence of effect of LewisA and LewisB expression on adherence of *Helicobacter pylori* to human gastric cells. *Gastroenterology* 1997; **113**: 72-80

8 **Tang FA**, Zheng PY, Li ZF, Feng CW, Hua JS, Duan CL. No influence of Lewis B expression in *Helicobacter pylori* on bacterial adhesion property. *Zhonghua Xiaohua Zazhi* 2001; **21**: 162-164

9 **Zambon CF**, Navaglia F, Basso D, Rugge M, Plebani M. *Helicobacter pylori* babA2, cagA, and s1 vacA genes work synergistically in causing intestinal metaplasia. *J Clin Pathol* 2003; **56**: 287-291

10 **Odenbreit S**, Till M, Hofreuter D, Faller G, Haas R. Genetic and functional characterization of the alpAB gene locus essential for the adhesion of *Helicobacter pylori* to human gastric tissue. *Mol Microbiol* 1999; **31**: 1537-1548

11 **Odenbreit S**, Faller G, Haas R. Role of the alpAB proteins and lipopolysaccharide in adhesion of Helicobacter pylori to human gastric tissue. *Int J Med Microbiol* 2002; **292**: 247-256

12 **Yamaoka Y**, Kodama T, Graham DY, Kashima K. Search for putative virulence factors of *Helicobacter pylori*: the low-molecular-weight (33-35K) antigen. *Dig Dis Sci* 1998; **43**: 1482-1487

13 **Yamaoka Y**, Kwon DH, Graham DY. A M(r) 34,000 proinflammatory outer membrane protein (oipA) of *Helicobacter pylori*. *Proc Natl Acad Sci USA* 2000; **97**: 7533-7538

14 **Ando T**, Peek RM, Pride D, Levine SM, Takata T, Lee YC, Kusugami K, van der Ende A, Kuipers EJ, Kusters JG, Blaser MJ. Polymorphisms of *Helicobacter pylori* HP0638 reflect geographic origin and correlate with cagA status. *J Clin Microbiol* 2002; **40**: 239-246

15 **Yamaoka Y**, Kikuchi S, el-Zimaity HM, Gutierrez O, Osato MS, Graham DY. Importance of Helicobacter pylori oipA in clinical presentation, gastric inflammation, and mucosal interleukin 8 production. *Gastroenterology* 2002; **123**: 414-424

16 **Kudo T,** Nurgalieva ZZ, Conner ME, Crawford S, Odenbreit S, Haas R, Graham DY, Yamaoka Y. Correlation between *Helicobacter pylori* OipA protein expression and oipA gene switch status. *J Clin Microbiol* 2004; **42**: 2279-2281

17 **Zhang J**, Yu FF, Chen YX, Chen H. Detection of cagA, oipA and iceAl genes of *Helicobacter pylori* and its significance. *Zhongguo Weisheng Jianyan Zazhi* 2004; **14**: 133-134

18 **Guchuan CY**. *Helicobacter pylori* infection and gastric carcinomas. *J Med Introduction* 2003; **24**: 217-218

19 **Shiesh SC**, Sheu BS, Yang HB, Tsao HJ, Lin XZ. Serologic response to lower-molecular-weight proteins of *H pylori* is related to clinical outcome of *H pylori* infection in Taiwan. *Dig Dis Sci* 2000; **45**: 781-788

20 **Yang WH**, Lin SR, Wang LX, Ding SG, Jin Z. The relationship between the pathogenetic factors of *Helicobacter pylori* and gastric diseases. *J Beijing Med University* 2000; **32:** 34-38

21 **Jiang Z**, Huang AL, Wang ZQ, Tao XH, Wang PL, Pu D. Cloning and expression of 18 000u outer membrane proteh gene of *Helicobacter pylori*. *Shijie Huaren Xiaohua Zazhi* 2002; **10**: 266-270

22 **Jiang Z**, Huang AL, Wang PL, Tao XH, Pu D. The cloning and recombinant vector constructing of lower-weight outer membrane protein encoding gene of *Helicobacter pylori*. *Shijie Huaren Xiaohua Zazhi* 2001; **9**: 1316-1318

23 **Voland P**, Hafsi N, Zeitner M, Laforsch S, Wagner H, Prinz C. Antigenic properties of HpaA and Omp18, two outer membrane proteins of *Helicobacter pylori*. *Infect Immun* 2003; **71**: 3837-3843

24 **Bauditz J**, Ortner M, Bierbaum M, Niedobitek G, Lochs H, Schreiber S. Production of IL-12 in gastritis relates to infection with *Helicobacter pylori*. *Clin Exp Immunol* 1999; **117**: 316-323

25 **Chen J**, Chen WH, Zhu SL, Chen W. Immunization against *Helicobacter pylori* infection with *Helicobacter pylori* outer membrane protein vaccine. *Weichangbingxue* 2001; **6**: 75-76

26 **Lin HJ**, Wang JD, Bai Y, Zhang YL, Zhou DY. The *in vivo* and *in vitro* evaluation of the immune protective activity of the recombinant surface proteins of *Helicobacter pylori*. *Zhongguo Weishengtai Zazhi* 2003; **15**: 4-6

27 **Jiang Z**, Huang AL, Tao XH, Wang PL. Construction and characterization of bivalent vaccine candidate expressing HspA and M(r) 18,000 OMP from *Helicobacter pylori*. *World J Gastroenterol* 2003; **9**: 1756-1761

28 **Jiang Z**, Pu D, Huang AL, Tao XH, Wang PL. Construction, expression and antigenic study of bivalent vaccine candidate with 26,000 OMP and heat short protein A of human *Helicobacter pylori*. *Zhonghua Yixue Zazhi* 2003; **83**: 862-867

29 **Cao P**, Cover TL. Two different families of hopQ alleles in *Helicobacter pylori*. *J Clin Microbiol* 2002; **40**: 4504-4511

30 **Sumie A**, Yamashiro T, Nakashima K, Nasu M, Watanabe M, Nishizono A. Comparison of genomic structures and antigenic reactivities of orthologous 29-kilodalton outer membrane proteins of *Helicobacter pylori*. *Infect Immun* 2001; **69**: 6846-6852

Science Editor Guo SY **Language Editor** Elsevier HK

PO Box 2345, Beijing 100023, China
www.wjgnet.com
wjg@wjgnet.com

ELSEVIER

World J Gastroenterol 2005;11(20):3014-3019
World Journal of Gastroenterology ISSN 1007-9327

• *REVIEW* •

Current status of tumor radiogenic therapy

Feng-Ling Min, Hong Zhang, Wen-Jian Li

Feng-Ling Min, Hong Zhang, Wen-Jian Li, Institute of Modern Physics, The Chinese Academy of Sciences, Lanzhou 730000, Gansu Province, China
Feng-Ling Min, Chinese Academy of Sciences, Beijing 100039, China
Supported by the Key Basic Research Project of Science and Technology Ministry of China, 2003CCB00200
Correspondence to: Feng-Ling Min, Institute of Modern Physics, Chinese Academy of Sciences, Lanzhou 730000, Gansu Province, China. fuchenbb@sohu.com
Telephone: +86-931-4969344
Received: 2004-06-16 Accepted: 2004-07-15

Abstract

Although tumor gene therapy falls behind its clinical use, the combination of irradiation and gene therapy is full of promise in cancer therapy based on traditional radiotherapy, chemotherapy and surgery. We have termed it as radiogenic therapy. This review focuses on the following aspects of radiogenic therapy in recent years: improvement of gene transfer efficiency by irradiation, radiotherapy combined with cytokine gene delivery or enhancement of the immunity of tumor cells by transgene, direct stimulation by radiation to produce cytotoxic agents, increase of tumor cell radiosensitivity in gene therapy by controlling the radiosensitivity genes and adjusting the fraction dose and interval of radiation so as to achieve the optimum antitumor effect while reducing the normal tissue damage, radioprotective gene therapy enhancing radiation tumor killing effect while protecting the normal tissue and organs with transgene using transfer vectors.

Key words: Tumor; Radiation; Gene therapy

Min FL, Zhang H, Li WJ. Current status of tumor radiogenic therapy. *World J Gastroenterol* 2005; 11(20): 3014-3019
http://www.wjgnet.com/1007-9327/11/3014.asp

INTRODUCTION

Among the therapies for malignant tumor, the main disease threatening human health, traditional radiotherapy, chemotherapy and surgery still dominate at present. Nevertheless, because the reaction of tumor cells is much severer to chemotherapy than to radiotherapy, the later is so vital to the therapy of tumors. During the past decade, the development in new radiotherapy technologies, such as modern radiotherapy equipment and tumor-shaped stereoadaptability treatment, enables more patients to accept radiotherapy. The therapeutic effect has been improved as well. On the other hand, radiotherapy still faces difficulties, such as recurrence or metastasis after radiation, damage of normal tissues around the tumor. Although the history of tumor gene therapy is not as long as radiotherapy, it has shown some promising results in many *in vitro* experiments. Because therapy of tumors covers many aspects and is quite difficult, gene therapy has not made any breakthrough and falls far behind its clinical application. Molecular biology has provided a theoretical basis for tumor radiotherapy at molecular level, and a breakthrough will be made in increasing the radiation sensitivity and decreasing the damage to normal tissues. Gene therapy technology is also introduced into radiotherapy. How to organically combine gene therapy and radiotherapy has become the new topic in these fields.

RADIATION IMPROVES GENE TRANSFER EFFICIENCY

In 1980s, Perez and Skarsgard[1] successfully used X-ray, ultraviolet radiation and 144 keV/μm of argon ion to increase DNA-mediated gene transfer efficiency, and found that the heavy ion was more noticeable in enhancing transfer efficiency and this enhancement was related to the radiation dose. It was also found that radiation could contribute to the conformity of exogenous DNA and host DNA, as well as to the expression of transferred genes and the expression time was also longer than that with no radiation. Stevens *et al*[2], found that 9 Gy of γ-ray radiation could increase the initial transfection efficiency of DNA mediated by plasmid vectors to 1 400 times. The copies of dissociated plasmid in cells from the γ-ray radiated group were 50% of those from the non-radiated group, but the cell quantity with conformed plasmids was much more than that from non-radiated group, and also the transfection efficiency of linear DNA was higher than that of ring DNA. Zeng *et al*[3], also found that low radiation dose of 3 Gy could increase the Ad5-CMVlacZ-mediated gene transfer efficiency to 40 times. Tang *et al*[4], used adenovirus vectors (AdCMVluc) to infect lung cancer cells of mice radiated by γ-ray, and found that the luc gene encoding products inside a cell increased in a dose-dependent manner, and the efficiency could increase as high as 24 times, which effectively controlled the tumor growth. The mechanism of ion radiation-mediated gene transfer might be as follows. Radiation makes receptors on cell surface damage and perforate, which change both transit of cytomembrane and its electrical level so that the exogenous DNA with negative electricity can go into the cells. The radiation results in DNA damage of cells and activation of their restoration, so the exogenous DNA and host cells DNA can be recombined and conformed[5]. In the later researches,

all the DNA base analogs, H_2O_2, ultraviolet radiation, X-ray, heavy ion had similar effects, indicating that cytotoxin or radiotherapy could make the exogenous DNA go into host cells easily. In addition, similar to the physically electrical perforation-mediated gene transfer, there is no cell specificity for the radiation-mediated gene transfer.

IMMUNE GENE THERAPY AND RADIOTHERAPY OF TUMORS

Human tumor immunity is mostly weak and easy to escape from body's immune system monitoring. Additionally, tumor cells can produce various immuno-suppressive factors so as to suppress the host cellular and humoral immunity. In aid of the molecular biology technology, some immunity-relevant factor genes are transferred to cells and expressed in the body constantly or in tumor cells to stimulate the host immune system or enhance the immunity of tumor cells so that the body immune system can recognize them and take certain killing actions. The combination of immune gene therapy and radiotherapy in tumor treatment can theoretically enhance antitumor immune effect while providing a quick external killing radiotherapy. This kind of therapy can obtain a better result than any single therapy as mentioned above. The facts also proved that clinical use of single cytokines for tumor therapy is not only expensive, but also brings severe toxic and side effects in a large dose, and most clinical applications did not achieve good results[6,7].

Radiotherapy combined with IL-2, INF, TNF cytokines, has obtained preferable antitumor effects. The gene expression of cytokines induced by radiation was first reported by Hallahan *et al*[8], and Sherman *et al*[9]. They found that radiation not only could make DNA damage but also might be related to the tumor killing effect caused by the increase of cytokine secretion. After plasmid pEgr-TNF transfected human tumor cells HL525, Weichselbaum *et al*[10], injected it into squamous cancer cell line SQ-20B of nude mice combined with 20 Gy of radiation. The outcome showed that, in the simple radiotherapy group, the tumor itself shrank by 1.1% on the 36th d and on the 50th d all the other nude mice died except one (1/7); whereas in the combined therapy group, all the other tumors in nude mice were completely vanished on the 20th d, except recurrence in only one (1/7) on the 36th d. It indicates that the combination of TNF and radiotherapy can achieve better therapeutic effects than either one alone. As indicated in some animal experiments[11], radiation combined with Ad-EGR-TNF α vector was carried on human glioma cell line D54, and resulted in complete tumor regression in 71% of xenografts. Its histopathological results showed pronounced vessel thrombosis and tumor necrosis, but no obvious effect was found on the live D54 cells after being treated with TNF α or radiation. Raben *et al*[12], proved that expression of human carcino-embryonic antigen (CEA) could be induced on D54MG human glioma cell line infected with adenovirus vector with CEA gene *in vitro*, and could be recognized by COL-1 antibody of CEA marked by radionuclides. In China, Zhang and Cao[13] and Wei *et al*[14], used adenovirus vectors co-expressing the heterodimer of human IL-12 combined radiation to treat mice with liver cancer. Compared with the methods mentioned above, this combination achieved complete disappearance of 50% cancers. If the mice in combined therapy group were inoculated again with tumor cells, tumor would not form anyway. Moreover, the INF-γ level was notably increased in mice blood serum from the combined group, and induced specific and restricted T cell activity.

On the basis of large experiments *in vitro* and *in vivo*, TNF was also applied to some clinical therapies for solid tumors, such as breast cancer, lung cancer, rectal cancer, pancreatic cancer, melanoma, head and neck tumors. No obvious effect of simplex radiotherapy or chemotherapy was found. During phase I clinical experiment, Hanna *et al*[15], observed seven patients who received Ad-EGR-TNFα injection at doses of 4×10^{9}-$4\times10^{9.5}$ particle units with concurrent radiotherapy. Of the seven patients, two had complete responses, two partial responses, two minor shrinkage and one no change. Meanwhile, the tumors which accepted radiotherapy only at the same dose were not controlled. In the above experiment, complete responses occurred in breast and rectum tumors and the partial responses were observed in pancreatic and lung cancers. There were no obvious toxic and side effects except pain on the injection site and slight chills. No virus was detected in blood or urine from any of the patients. All these have shown the importance, effectiveness and safety of radiogenic therapy.

GENE THERAPY OF TUMORS INDUCED BY RADIATION

The safety and effectiveness of gene therapy of tumors are the key factors in gene therapy, and its control mechanism affects the targets of gene therapy. At present there are two types of control mechanisms, one is called "transcriptional target control", which means to choose tumor-related antigens. For example, some cis-effect elements (such as promoter, enhancer) of AFP and CEA genes are formed into expression boxes with their corresponding target genes, and then are inserted into gene transferring vectors. In this case, the transgene only expresses in tumor cells that produce tumor-related proteins as mentioned above, thereby it can bring a specific killing effect to tumor cells. The other is called "exogenous control of transgene expression", which means to use the cis-effect elements, that can be induced by some factors to express genes, are formed into expression boxes with corresponding target genes and then are inserted into gene transferring vectors. In this case, the transgene will be directly controlled by corresponding inducible factors whether it expresses in the body or not. Among the first genes that were induced by radiation, the early growth gene (EGR)[8] is related to the early growing reaction, c-Jun, β-actin and interleukin-1[16]. These gene encodings can bind to the specific DNA sequences and control other gene expressions. For instance, by means of increasing transcriptional induction of the expression of c-Jun by ionizing, Jun protein could combine DNA at Ap-1 site and activate the downstream gene expression. The vectors constructed by radiation-induced EGR-1 gene and different therapeutic genes have been studied most. EGR-1 encodes a nuclear phosphoprotein containing 533 amino acids. The active oxygen generated

by ionizing can act on the CC (A+T rich) 6GG structural domain of this gene's promoter and promote EGR-1 gene expression[8].

Kawashita *et al*[17], constructed the plasmid vectors, pEGR-TK and pEGR-luc, which meant to insert herpes simplex virus thymidine kinase (HSV-TK) gene or report gene luc into the downstream of early growing gene (EGR-1) promoter. On the next day after the liver cancer cell line was transfected by these two plasmid vectors, 10 Gy of radiation was given and prodrug ganciclovir (GCV) was added as well. As shown in the final results, after transfected by pEGR-luc, the luc gene expression in radiated cells was 15-28 times of that in non-radiated cells. Additionally, the expression level was dependent on the radiation dose. The drug sensitivity of liver cancer cell line transfected by pEGR-TK and radiation to GCV increased by 10^3-10^4 compared with the non-radiated group. The therapeutic effects were good on other cancer cell lines when the vector contained EGR-1 and HSV-TK. Scott *et al*[18], and Marples *et al*[19], designed a type of molecular switch with a recombination system of bacteriophage to establish a radiation-induced gene expression model. EGR-1 enhancer/promoter regulated the expression of Cre recombinase. Through the recombination of loxP site-mediation, the molecule switch was activated and turned on, then was given 1 Gy of X-ray radiation to achieve the goal of completely suppressing the growth of tumor cells. The research on EGR-1 promoted other studies on radiation inducible promoters, such as P21 (WAF1)[20]. Worthington *et al*[20], used WAF1 as a promoter to construct a vector with NO synthetic enzyme gene, and then injected it into the rat tail artery. They found the quantity of nitric oxide synthase increased by four times after a radiation dose of 4 Gy was given.

The study on applying radiotracer combined with the gene therapy, to the tumor targeted diagnosis and therapy has made many progresses. The radiation-inducible gene encodes a type of ligands or transits agents, which can be taken as a target to cytotoxins radiolabeled. The functions are as follows: one is to use the new cytomembrane receptors induced by irradiation for receptor development, the other is to use the transgene products to metabolize the specific substances radiolabeled, and to retain the metabolism of products inside the cells for position display and target study. Tjuvajev *et al*[21], transfected tumor cells by Ad-HSV-TK and then injected a therapeutic dose of FIAU radiolabeled with radionuclide I^{131}, finally the transferring target was improved. Meanwhile, β-ray emitted by ^{131}I-FIAU was incorporated to DNA and the killing effect was enhanced on tumor cells. Auger emitting therapeutics can specifically deliver the ray to receptors bearing tumor cells. Many researches indicated that the ray emitted during radionuclide decay by low-energy Auger electron was highly cytotoxic. In the early experiments, 85 patients with unresectable somatostatin receptor-positive neuroendocrine tumor were given somatostatin analogs with ^{111}In-labeled, 62-69% of the tumors obviously shrank. It was found in research that the dose deposited by γ-ray emission from In^{111} did little damage to the cells, but low-energy Auger electron had a killing effect instead. However, γ-ray emitted by In^{111} could be used for tumor positioning diagnosis[22,23]. The sodium/iodine symporter (NIS) gene concentrates iodine in the thyroid gland, salivary gland, gastric mucosa, *etc*. Radioiodine (^{131}I) has been shown to selectively concentrate on tumor cells transfected with NIS gene and suppressed the growth of tumor cells *in vitro* and *in vivo*. Tissue-specific promoters combined NIS gene such as PAS promoter should be further studied[24,25].

INCREASE OF RADIOSENSITIVITY IN GENE THERAPY

The same type of tumors, even with similar clinical phases, is different in radiosensitivity. In recent years, many genes related to radiosensitivity of tumor cells have been found. The current research focuses on, through controlling radiosensitive genes and adjusting the fraction dose and interval of radiation, how to realize individualization of radiotherapy and how to change tumor cell radiosensitivity, and how to reduce the normal tissue damage so as to achieve the optimum therapeutic effect. P53 and bcl-2 gene play an important role in the tumor generation and development, they have attracted researchers' attention most. Some results of *in vitro* experiments showed that the high expression of bcl-2 protein was related to cell apoptosis induced by radiotherapy and chemotherapy, while to suppress the expression of bcl-2 gene might increase tumor radiosensitivity. Kawabe *et al*[26], compared the ability of adenovirus-mediated wild-type P53 to radiosensitize non-small lung cancer and normal human lung fibroblasts. Ad/CMV/P53 increased the radiosensitivity of two types of non-small lung cancer cell lines and meanwhile the Bax gene expression of lung cancer cells rose, but there was no obvious change of these characteristics in normal lung fibroblast cells. In *in vivo* studies, tumor growth suppression was enhanced by this combination strategy in xenograft tumors in nude mice compared to Ad/CMV/P53 or radiation therapy used alone. Grunbaum *et al*[27], observed tumor cell apoptosis and change of radiosensitivity after P53 mutant and radioresistant soft tissue sarcoma cell line combined treatment with DNA transfection either with mdm2 antisense oligodeoxynucleotides or with a wild-type P53 plasmid and irradiation. At the same radiation dose, the sensitivity of tumor cells with wtP53-plasmid transfection was higher than those without transfection, and clone formation was reduced by two times. Forty-eight and 72 h after radiation, the percentage of apoptotic cells was 25% and 38.9% respectively. Compared with the control group, the apoptotic cell ratio of tumor cells transfected with mdm2 antisense oligodeoxynucleotides was 7.7%. A striking result was obtained with the combined treatment of wtP53 and 12 Gy irradiation, which produced 25% and 38.9% of apoptotic cells 48 and 72 h after transfection, respectively. Besides the regulation of P53 gene, people have also done a lot of work on enhancing the tumor cell radiosensitivity through combining regulation with other genes. Subtraction hybridization identified mda-7 gene as a gene associated with melanoma cell differentiation and growth, which could selectively suppress the growth of various tumor cells without much effect on normal cells. Su *et al*[28], transfected human glioma cell lines by mda-7 adenovirus vector (Ad.mda-7) and found that the expression

of mda-7 could induce growth inhibition and apoptosis in malignant human gliomas with mutants and wild P53, and these effects correlated with an elevation in expression of growth arrest and DNA damage genes. The growth of human glioma cells expressing mutant P53 was inhibited when transfected with AdP53 vector and the sensitivity of the cells increased when transfected with Ad.mda-7 vector. Since the heterogeneity in P53 expression is common in gliomas, it indicates that Ad.mda-7 may, in many cases, be more beneficial to gene-based therapy of malignant gliomas than administration of wild-type P53. Applying Ad-P53 injection to solid tumors, such as breast cancer, lung cancer, rectal cancer, pancreatic cancer, melanoma, head and neck tumors, has been licensed and is in clinic phase III now. Zhang *et al*[29], and Chen *et al*[30], reported that the results of rAd-P53 agent combined with radiotherapy in treatment of head and neck squamous cell carcinomas and nasopharyngeal carcinoma respectively. Randomized controlled study of patients with head and neck squamous cell carcinomas showed that the radio-sensitized enhancement rate was 1.72 times higher at 40 Gy time point and the CR rate of the combined treatment group at the validation point was 1.68 times higher than that of the radiotherapy group. The nasopharyngeal carcinoma was reduced by 95±10% and 80±17% (P<0.001) 8 wk after treatment and the rate of CR of tumor 12 wk after treatment was 75% in the combined treatment group and 15% in the radiotherapy group respectively (P<0.01). Swisher *et al*[31], evaluated the feasibility and mechanisms of apoptosis induction after Ad-P53 (INGN 201) gene transfer and radiation therapy in patients with non-small cell lung cancer in clinic phase II study. They found that 17 of 19 patients completed all planned radiation and Ad-P53 (INGN 201) gene therapy as outpatients with radiation alone. The most common adverse events were grade 1 or 2 fever (79%) and chill (53%). Three months after completion of therapy, pathologic biopsies showed that 12 of 19 patients (63%) had no viable tumor, 3 of 19 patients (16%) had viable tumor, and 4 of 19 patients (21%) were not assessed. Quantitative reverse transcription-PCR analysis of the four P53-related genes (p21 (CDKN1A), FAS, BAK, and MDM2) revealed that BAK gene expression was most closely related to Ad-P53 (INGN 201) gene transfer. In clinical trial no significant toxicity was observed in Ad-P53 patients with mild fever and flu-like symptoms during dose escalation studies. P53 gene can increase the radiosensitivity of tumor cells, and the mechanism has not been fully elucidated. It has been observed that the introduction of P53 induces apoptosis. The clinical trial of head and neck carcinoma treatment by Ad-P53 combined with radiotherapy and chemotherapy is undergoing in 34 centers of the world.

There are many radiosensitive relevant genes. In 1995, ataxia telangiectasia (AT) gene was cloned. The cell lines from AT patients (usually used fibrous cells) showed hypersensitivity to irradiation *in vitro*. The AT cells did not have clear fractionated radiation effect, and high LET ray made much less damage to AT cells than low LET ray. Further research revealed that the activity of DNA topoisomerase suppressor of AT cells was high and highly sensitive to the restricted endonuclease, which influenced its DNA damage repair. Moreover, there was no DNA synthesis suppression in radiated AT cells, so it was characterized with DNA synthetic radioresistance and easy to die from radiation. The high radiosensitivity of AT cells was related to the delayed raise of P53 protein. With the adenovirus vector, Fan *et al*[32], transferred antisense ATM RNA into P53 mutational prostate cancer cells and found that abnormal control of cell-cycle and the radiosensitivity were distinctly increased. Tribius *et al*[33], also proved that, compared with primary glioma cells, the established glioma cells gained adaptive characteristics during cell cultures. The expression of ATM gene products decreased and its radioresistance increased accordingly.

GENE THERAPY AND RADIOPROTECTION

Normal tissue damage around tumors caused by ionizing radiation limits the radiotherapy dose. In order to increase the radiation killing effect on tumor cells, while protecting the normal tissues and organs at the normal tolerant dose, people have been working a lot on physics, chemistry, and biology including the introduction of multileaf collimators, sophisticated immobilization techniques, and intensity modulated radiotherapy *vs* computer-controlled radiotherapy beam modulation, as well as some medicines used to protect the normal organs. However, the medical protection has let people think of tumor cells possibly escaping from radiation killing, so the therapeutic effect would decline[34]. When transgene therapy is used particularly for normal tissues, the radiation dose for tumor cells can be increased while the normal tissue generates tolerance to radiation. The candidate genes involved in radioprotection should have the function to inhibit the apoptotic pathway, repair the damage induced by oxidative stress and radiation, as well as neutralize cytopathic cytokine effects. The transgenic vector should target specific organs and has minimal pathological effects on normal cells. What was studied most was superoxide dismutase (SOD), an important enzyme that widely exists inside the body to clean out the free radicals. The function of this type of enzymes is to protect cells against oxidative stress. SOD can be induced by many environmental factors and chemical substances. Due to the induction to SOD, the ability of body to protect the organs against damage can be strengthened and the body can tolerate these exogenous toxic substances.

Manganese superoxide dismutase (Mn-SOD) gene is an ideal radioprotective gene at present because other genes have some toxic and side effects. The radioresistance mechanism of Mn-SOD gene might be related to the upregulated gene expression after ionizing radiation, probably caused by activating the Mn-SOD gene promoter through the radiation-induced NF-κβ transcriptional activator. Mn-SOD is mainly localized at the mitochondrial matrix of prokaryocytes and eukaryocytes. Because of the importance of mitochondria-mediated irradiation apoptosis, genes associated with stabilization of mitochondrial membranes were first evaluated *in vitro*. Epperly *et al*[35], proved the importance of Mn-SOD positioning in radioprotection of mitochondria. They transferred Cu/Zn-SOD gene and Mn-SOD gene into 32D cl3 cells respectively so as to overexpress the genes. Both groups showed similar antioxidant activity, but Cu/Zn-SOD gene transferring cells

did not have radioprotection effect and this effect was related to the mitochondrial localization signals. Recent data showed that cells which transduced Mn-SOD gene at mitochondria were radiated, the stable mitochondrial membrane could prevent cytochrome C from releasing and going to cytoplasm to activate the cell death pathway[36]. A herpes simplex viral vector containing the full-length human Mn-SOD gene has been successfully expressed on human hematopoietic progenitor cells. Further research will determine whether the hematopoietic progenitor cells transduced Mn-SOD gene has differentiation and self-renewal abilities. Currently the research on human umbilical cord blood transgene would provide experimental information on protecting normal hematopoietic stem cells during total body irradiation in patients receiving chemotherapy who might need marrow transplantation[37,38]. Epperly *et al*[39-41], applied C57BL/6J mouse model to the research on the relationship between radiated TGF, IL-I and TNF-α cell factors and the effect of lung tissue inflammation on MnSOD-PL protection. Before radiation, MnSOD-PL or intra-tracheal administration of adenovirus-mediated Mn-SOD could prevent acute or chronic radiation damage. Administrating 250 μg of MnSOD-PL 24 h before radiation could decrease radiation-inducible electron spin resonant signals. Lung tissue pathology showed that alveolus fibrosis was obviously reduced, compared with the group not given MnSOD-PL and the group given MnSOD-PL at different times after radiation. The mechanism might be as follows. Macrophages and macrophage progenitor cells of bronchoalveolar macrophages from bone marrow are recruited to the vasculature of radiated lung, then by means of the combination of adhesion molecules on its surface and VCAM-1 and VCAM-2 on endothelial cells, they differentiate into macrophages and produce TGF-β1 and TGF-β2 which recruit fibroblast progenitor cells of bone marrow origin to the lungs. Some experiments have proved that TGF-β1 and TGF-β2 produced by bronchoalveolar macrophages could mediate signaling from lung macrophages so as to cause fibroblast progenitor cells moving to the lungs[42]. Other hypotheses include fibroblast progenitor cells in circulation independent on TGF-β1 and TGF-β2, and can directly bind to the upregulated adhesion molecules in the lung tissue. Acute and chronic damages due to esophageal irradiation were similar to the lung damage, but with some differences[43]. Epperly *et al*[44], and Stickle *et al*[45], observed acute apoptosis of esophageal basal squamous stem cells 24 h after irradiation. The apoptotic cells gradually developed into microscopic ulceration and then macroscopic ulceration 10 d later. During the treatment, lots of mice had dehydration, weight loss, high-frequent esophagostenosis or even died. MnSOD-PL administration to mice 24 h prior to single radiation or intermittently during the fractionated radiation every 3-4 d could greatly help to reduce the radiation-induced cell apoptosis, dehydration, weight loss and death, and occurrence of esophagostenosis. At present, the research on esophageal irradiation toxicity is focused on the mechanism of MnSOD-PL radioprotection of esophageal stem cells. The above experimental results showed, compared with the simple radiated control group, giving MnSOD-PL 24 h before radiation could speed-up the recovery of esophageal stem cells.

SUMMARY

The role of genes in human diseases has been gradually identified with the development of human genome planning work. Gene therapy of tumors is becoming one of the important therapies for tumors. In radiogenic therapy, the current problems to be solved are high-efficient gene transferring vectors, efficient targeted genes and the safety of gene therapy.

REFERENCES

1 **Perez CF,** Skarsgard LD. Radiation enhancement of the efficiency of DNA-mediated gene transfer in CHO UV-sensitive mutants. *Radiat Res* 1986; **106**: 401-407
2 **Stevens CW**, Zeng M, Cerniglia GJ. Ionizing radiation greatly improves gene transfer efficiency in mammalian cells. *Hum Gene Ther* 1996; **7**: 1727-1734
3 **Zeng M,** Cerniglia GJ, Eck SL, Stevens CW. High-efficiency stable gene transfer of adenovirus into mammalian cells using ionizing radiation. *Hum Gene Ther* 1997; **8**: 1025-1032
4 **Tang DC,** Jennelle RS, Shi Z, Garver RI, Carbone DP, Loya F, Chang CH, Curiel DT. Overexpression of adenovirus-encoded transgenes from the cytomegalovirus immediate early promoter in irradiated tumor cells. *Hum Gene Ther* 1997; **8**: 2117-2124
5 **Herrlich P,** Bender K, Knebel A, Bohmer FD, Gross S, Blattner C, Rahmsdorf HJ, Gottlicher M. Radiation-induced signal transduction. Mechanisms and consequences. *C R Acad Sci III* 1999; **322**: 121-125
6 **Muc-Wierzgon M,** Baranowski M, Madej K. Tumor necrosis factor in advanced gastrointestinal neoplasms. A clinical trial with a focus on haematological effects. *Haematologia (Budap)* 1996; **27**: 85-92
7 **Niemela M,** Maenpaa H, Salven P, Summanen P, Poussa K, Laatikainen L, Jaaskelainen J, Joensuu H. Interferon alpha-2a therapy in 18 hemangioblastomas. *Clin Cancer Res* 2001; **7**: 510-516
8 **Hallahan DE,** Sukhatme VP, Sherman ML, Virudachalam S, Kufe D, Weichselbaum RR. Protein kinase C mediates x-ray inducibility of nuclear signal transducers EGR1 and JUN. *Proc Natl Acad Sci USA* 1991; **88**: 2156-2160
9 **Sherman ML,** Datta R, Hallahan DE, Weichselbaum RR, Kufe DW. Ionizing radiation regulates expression of the c-jun protooncogene. *Proc Natl Acad Sci USA* 1990; **87**: 5663-5666
10 **Weichselbaum RR,** Hallahan DE, Beckett MA, Mauceri HJ, Lee H, Sukhatme VP, Kufe DW. Gene therapy targeted by radiation preferentially radiosensitizes tumor cells. *Cancer Res* 1994; **54**: 4266-4269
11 **Kianmanesh A,** Hackett NR, Lee JM, Kikuchi T, Korst RJ, Crystal RG. Intratumoral administration of low doses of an adenovirus vector encoding tumor necrosis factor alpha together with naive dendritic cells elicits significant suppression of tumor growth without toxicity. *Hum Gene Ther* 2001; **12**: 2035-2049
12 **Raben D,** Buchsbaum DJ, Khazaeli MB, Rosenfeld ME, Gillespie GY, Grizzle WE, Liu T, Curiel DT. Enhancement of radiolabeled antibody binding and tumor localization through adenoviral transduction of the human carcinoembryonic antigen gene. *Gene Ther* 1996; **3**: 567-580
13 **Zhang W,** Cao X. The construction and application of adenovirus vector coexpressing the heterodimer of human IL-12. *Zhonghua Yixue Zazhi* 1998; **78**: 33-36
14 **Wei DY,** Dai BB, Chen SS. The tumor targeted expression of adenovirus mediated Cdgly TK gene regulated by radiation via Egr-1 promoter. *Zhonghua Yixue Zazhi* 2001; **81**: 994-1003
15 **Hanna NN,** Nemunaitis J, Cunningham CC. A phase II study of human necrosis factor-alpha gene transfer with radiation therapy for advanced solid tumors. *Proc Am Soc Clin Oncol* 2002; **21**: 344
16 **Woloschak GE,** Chang-Liu CM, Jones PS, Jones CA. Modu-

lation of gene expression in Syrian hamster embryo cells following ionizing radiation. *Cancer Res* 1990; **50**: 339-344

17 **Kawashita Y,** Ohtsuru A, Kaneda Y, Nagayama Y, Kawazoe Y, Eguchi S, Kuroda H, Fujioka H, Ito M, Kanematsu T, Yamashita S. Regression of hepatocellular carcinoma *in vitro* and *in vivo* by radiosensitizing suicide gene therapy under the inducible and spatial control of radiation. *Hum Gene Ther* 1999; **10**: 1509-1519

18 **Scott SD,** Marples B, Hendry JH, Lashford LS, Embleton MJ, Hunter RD, Howell A, Margison GP. A radiation-controlled molecular switch for use in gene therapy of cancer. *Gene Ther* 2000; **7**: 1121-1125

19 **Marples B,** Scott SD, Hendry JH, Embleton MJ, Lashford LS, Margison GP. Development of synthetic promoters for radiation mediated gene therapy. *Gene Ther* 2000; **7**: 511-517

20 **Worthington J,** Robson T, Murray M, O'Rourke M, Keilty G, Hirst DG. Modification of vascular tone using iNOS under the control of a radiation-inducible promoter. *Gene Ther* 2000; **7**: 1126-1131

21 **Tjuvajev JG,** Finn R, Watanabe K, Joshi R, Oku T, Kennedy J, Beattie B, Koutcher J, Larson S, Blasberg RG. Noninvasive imaging of herpes virus thymidine kinase gene transfer and expression: a potential method for monitoring clinical gene therapy. *Cancer Res* 1996; **56**: 4087-4095

22 **Tiensuu Janson E,** Eriksson B, Oberg K, Skogseid B, Ohrvall U, Nilsson S, Westlin JE. Treatment with high dose [(111)In-DTPA-D-PHE1]-octreotide in patients with neuroendocrine tumors--evaluation of therapeutic and toxic effects. *Acta Oncol* 1999; **38**: 373-377

23 **McCarthy KE,** Woltering EA, Anthony LB. *In situ* radiotherapy with ^{111}In-pentetreotide. State of the art and perspectives. *Q J Nucl Med* 2000; **44**: 88-95

24 **Boland A,** Ricard M, Opolon P, Bidart JM, Yeh P, Filetti S, Schlumberger M, Perricaudet M. Adenovirus-mediated transfer of the thyroid sodium/iodide symporter gene into tumors for a targeted radiotherapy. *Cancer Res* 2000; **60**: 3484-3492

25 **Cho JY,** Xing S, Liu X, Buckwalter TL, Hwa L, Sferra TJ, Chiu IM, Jhiang SM. Expression and activity of human Na+/I-symporter in human glioma cells by adenovirus-mediated gene delivery. *Gene Ther* 2000; **7**: 740-749

26 **Kawabe S**, Munshi A, Zumstein LA, Wilson DR, Roth JA, Meyn RE. Adenovirus-mediated wild-type p53 gene expression radiosensitizes non-small cell lung cancer cells but not normal lung fibroblasts. *Int J Radiat Biol* 2001; **77**: 185-194

27 **Grunbaum U,** Meye A, Bache M, Bartel F, Wurl P, Schmidt H, Dunst J, Taubert H. Transfection with mdm2-antisense or wtp53 results in radiosensitization and an increased apoptosis of a soft tissue sarcoma cell line. *Anticancer Res* 2001; **21**: 2065-2071

28 **Su ZZ,** Lebedeva IV, Sarkar D, Gopalkrishnan RV, Sauane M, Sigmon C, Yacoub A, Valerie K, Dent P, Fisher PB. Melanoma differentiation associated gene-7, mda-7/IL-24, selectively induces growth suppression, apoptosis and radiosensitization in malignant gliomas in a p53-independent manner. *Oncogene* 2003; **22**: 1164-1180

29 **Zhang SW,** Xiao SW, Liu CQ, Sun Y, Su X, Li DM, Xu G, Cai Y, Zhu GY, Xu B, Lv YY. Treatment of head and neck squamous cell carcinoma by recombinant adenovirus-p53 combined with radiotherapy: a phase II clinical trial of 42 cases. *Zhonghua Yixue Zazhi* 2003; **83**: 2023-2028

30 **Chen CB,** Pan JJ, Xu LY. Recombinant adenovirus p53 agent injection combined with radiotherapy in treatment of nasopharyngeal carcinoma: a phase II clinical trial. *Zhonghua Yixue Zazhi* 2003; **83**: 2033-2035

31 **Swisher SG,** Roth JA, Komaki R, Gu J, Lee JJ, Hicks M, Ro JY, Hong WK, Merritt JA, Ahrar K, Atkinson NE, Correa AM, Dolormente M, Dreiling L, El-Naggar AK, Fossella F, Francisco R, Glisson B, Grammer S, Herbst R, Huaringa A, Kemp B, Khuri FR, Kurie JM, Liao Z, McDonnell TJ, Morice R, Morello F, Munden R, Papadimitrakopoulou V, Pisters KM, Putnam JB, Sarabia AJ, Shelton T, Stevens C, Shin DM, Smythe WR, Vaporciyan AA, Walsh GL, Yin M. Induction of p53-regulated genes and tumor regression in lung cancer patients after intratumoral delivery of adenoviral p53(INGN 201) and radiation therapy. *Clin Cancer Res* 2003; **9**: 93-101

32 **Fan Z,** Chakravarty P, Alfieri A, Pandita TK, Vikram B, Guha C. Adenovirus-mediated antisense ATM gene transfer sensitizes prostate cancer cells to radiation. *Cancer Gene Ther* 2000; **7**: 1307-1314

33 **Tribius S,** Pidel A, Casper D. ATM protein expression correlates with radioresistance in primary glioblastoma cells in culture. *Int J Radiat Oncol Biol Phys* 2001; **50**: 511-523

34 **Andreassen CN,** Grau C, Lindegaard JC. Chemical radioprotection: a critical review of amifostine as a cytoprotector in radiotherapy. *Semin Radiat Oncol* 2003; **13**: 62-72

35 **Epperly MW,** Gretton JE, Sikora CA, Jefferson M, Bernarding M, Nie S, Greenberger JS. Mitochondrial localization of superoxide dismutase is required for decreasing radiation-induced cellular damage. *Radiat Res* 2003; **160**: 568-578

36 **Guo H,** Seixas-Silva JA, Epperly MW, Gretton JE, Shin DM, Bar-Sagi D, Archer H, Greenberger JS. Prevention of radiation-induced oral cavity mucositis by plasmid/liposome delivery of the human manganese superoxide dismutase (SOD_2) transgene. *Radiat Res* 2003; **159**: 361-370

37 **Goff JP,** Shields DS, Boggs SS, Greenberger JS. Effects of recombinant cytokines on colony formation by irradiated human cord blood CD34+hematopoietic progenitor cells. *Radiat Res* 1997; **147**: 61-69

38 **Goff JP,** Shields DS, Wechuck JB, Petersen BE, Zajac VF, Michalopoulos Gk, Greenberger JS. Gene transfer of MnSOD toCD34+Thy1+lin-human cord blood cells using herpes simplex virus vector. *Mol Ther* 2002; **5**: 5407-5411

39 **Epperly M,** Bray J, Kraeger S, Zwacka R, Engelhardt J, Travis E, Greenberger J. Prevention of late effects of irradiation lung damage by manganese superoxide dismutase gene therapy. *Gene Ther* 1998; **5**: 196-208

40 **Epperly MW,** Guo HL, Jefferson M, Nie S, Gretton J, Bernarding M, Bar-Sagi D, Archer H, Greenberger JS. Cell phenotype specific kinetics of expression of intratracheally injected manganese superoxide dismutase –plasmid/liposomes(MnSOD-PL) during lung radioprotective gene therapy. *Gene Ther* 2003; **10**: 163-171

41 **Epperly MW,** Travis EL, Sikora C, Greenberger JS. Manganese [correction of Magnesium] superoxide dismutase (MnSOD) plasmid/liposome pulmonary radioprotective gene therapy: modulation of irradiation-induced mRNA for IL-I, TNF-alpha, and TGF-beta correlates with delay of organizing alveolitis/fibrosis. *Biol Blood Marrow Transplant* 1999; **5**: 204-214

42 **Epperly MW,** Sikora CA, DeFilippi SJ, Gretton JE, Bar-Sagi D, Archer H, Carlos T, Guo H, Greenberger JS. Pulmonary irradiation-induced expression of VCAM-I and ICAM-I is decreased by manganese superoxide dismutase-plasmid/liposome (MnSOD-PL) gene therapy. *Biol Blood Marrow Transplant* 2002; **8**: 175-187

43 **Epperly MW,** Defilippi S, Sikora C, Gretton J, Greenberger JS. Radioprotection of lung and esophagus by overexpression of the human manganese superoxide dismutase transgene. *Mil Med* 2002; **167**: 71-73

44 **Epperly MW,** Kagan VE, Sikora CA, Gretton JE, Defilippi SJ, Bar-Sagi D, Greenberger JS. Manganese superoxide dismutase-plasmid/liposome (MnSOD-PL) administration protects mice from esophagitis associated with fractionated radiation. *Int J Cancer* 2001; **96**: 221-231

45 **Stickle RL,** Epperly MW, Klein E, Bray JA, Greenberger JS. Prevention of irradiation-induced esophagitis by plasmid/liposome delivery of the human manganese superoxide dismutase transgene. *Radiat Oncol Investig* 1999; **7**: 204-217

Science Editor Wang XL and Guo SY **Language Editor** Elsevier HK

PO Box 2345, Beijing 100023, China
www.wjgnet.com
wjg@wjgnet.com

ELSEVIER

World J Gastroenterol 2005;11(20):3020-3026
World Journal of Gastroenterology ISSN 1007-9327

Mismatch repair genes (*hMLH1*, *hPMS1*, *hPMS2*, *GTBP/hMSH6*, *hMSH2*) in the pathogenesis of hepatocellular carcinoma

Abdel-Rahman N. Zekri, Gelane M. Sabry, Abeer A. Bahnassy, Kamal A. Shalaby, Sabrin A. Abdel-Wahabh, Serag Zakaria

Abdel-Rahman N. Zekri, Sabrin A. Abdel-Wahabh, Virology and Immunology Unit, Cancer Biology Department, National Cancer Institute, Cairo University, Egypt
Abeer A. Bahnassy, Pathology Department, National Cancer Institute, Cairo University, Egypt
Serag Zakaria, Tropical Medicine Department, El-Kaser Al-Aini School of Medicine, Cairo University, Egypt
Gelane M. Sabry, Kamal A. Shalaby, Biochemistry Department, Faculty of Science, Ain Shams University, Egypt
Correspondence to: Abdel-Rahman N. Zekri, MSc, PhD, Virology and Immunology Unit, Cancer Biology Department, National Cancer Institute, Cairo University, Kasr El-Aini St., Fom El-Khaig, Cairo 11796, Egypt. ncizakri@starnet.com.eg
Fax: +202-3644-720
Received: 2003-12-10 Accepted: 2004-03-12

Abstract

AIM: DNA mismatch repair (MMR) is an important mechanism for maintaining fidelity of genomic DNA. Abnormalities in one or more MMR genes are implicated in the development of many cancers. We investigated the role of expression of MMR genes (*hMLH1*, *hPMS1*, *hPMS2*, *GTBP/hMSH6*, *hMSH2*) in hepatocellular carcinogenesis.

METHODS: We evaluated the expression level of MMR genes in 33 hepatocellular carcinoma (HCC) cases using the multiplex reverse transcription (RT) PCR assays, as well as in 16 cases of normal adjacent hepatic tissues. β-actin gene was used as an internal control and calibrator for quantification of gene expression.

RESULTS: Out of the 33 studied cases, 25 were HCV positive and 30 (90.9%) showed reduced expression in one or more of the studied MMR genes. Reduced expression was found in *hMSH2* (71.9%), *hMLH1* (53.3%), *GTBP* (51.1%), *hPMS2* (33.3%) and *hPMS1* (6%). A significant correlation was found between reduced expression of *hPMS2* ($P = 0.0069$) and *GTBP* ($P = 0.0034$), *hPMS2* and non-cirrhosis ($P = 0.0197$), *hMLH1* and high grade. On the other hand, 57.1%, 50%, 20%, 18.8%, and 6% of the normal tissues distant to tumors showed reduced expression of *hMSH2*, *hMLH1*, *GTBP*, *hPMS2*, and *hPMS1* respectively. Multivariate analysis revealed a significant correlation between the expression level of *hMSH2* ($P = 0.008$), *hMLH1* ($P = 0.001$) and *GTBP* ($P = 0.032$) and HCC, between *hPMS2*, *GTBP* and HCV-associated HCC ($P<0.001$, 0.002).

CONCLUSION: Reduced expression of MMR genes seems to play an important role in HCV-associated HCC. *hPMS2* is likely involved at an early stage of hepatocarcinogenesis since it was detected in normal adjacent tissues. Reduced expression of *hPMS2* provides a growth advantage and stimulates proliferation which encourages malignant transformation in non-cirrhotic HCV-infected patients via acquisition of more genetic damages.

Key words: Hepatocellular carcinoma; Mismatch repair; Normal distant hepatic tissue

Zekri ARN, Sabry GM, Bahnassy AA, Shalaby KA, Abdel-Wahabh SA, Zakaria S. Mismatch repair genes (*hMLH1*, *hPMS1*, *hPMS2*, *GTBP/hMSH6*, *hMSH2*) in the pathogenesis of hepatocellular carcinoma. *World J Gastroenterol* 2005; 11(20): 3020-3026
http://www.wjgnet.com/1007-9327/11/3020.asp

INTRODUCTION

Hepatocellular carcinoma (HCC) is one of the most common malignant tumors worldwide, with the highest frequencies reported in Asia and Africa. In countries endemic for viral hepatitis, HCC represents 20-40% of human cancers and most of the cases in these areas are late complications of chronic viral hepatitis[1]. The major risk factors for HCC development are now well defined including chronic viral hepatitis, alcohol, aflatoxin and metabolic disorders. These factors induce malignant transformation by increasing cellular turnover as a consequence of chronic liver injury, regeneration and cirrhosis[2]. Although advances in the treatment of HCC have recently been achieved, the prognosis of this disease generally remains very poor[3].

Understanding the molecular basis of HCC is very important, since novel therapeutic approaches, which target these molecules, may lead to improvement in the prevention and treatment strategies of HCC. Therefore, identification of molecular markers related to prognosis is a vital target to improve the clinical outcome and for a more effective therapy[4]. Recently, some of the multisteps involved in hepatocarcinogenesis have been elucidated. Activation of oncogenes, inactivation of tumor suppressor genes, overexpression of certain growth factors and DNA mismatch repair (MMR) defects may contribute to the development of HCC[5].

The DNA MMR system is expressed in all tissues at various levels and plays an important role in the maintenance of genomic integrity as it corrects replicative mismatches of the escaped DNA polymerase proof reading[6]. Biochemical and genetic studies in eukaryotes have defined at least five genes (*MSH2*, *MSH3*, *GTBP*, *MLH1*, and *PMS2*) whose

protein products are required for DNA MMR[7]. Direct evidence for the association of genetic instability and mutant MMR genes is derived from the biochemical studies *in vitro* in which nuclear extracts from human tumor cell lines with mutated MMR genes were unable to efficiently repair heteroduplex DNA fragments[8]. Hence, it was proposed that cells with defective MMR mechanisms had a reduction in the fidelity of DNA and could not correct genetic errors that occurred during cellular replication[9].

Several studies have focused on the impact of defective MMR genes on the pathogenesis of tumors and genes encoding components of the MMR system have been mentioned in relation to several human solid tumors[10-13]. It was shown that defects in MMR genes could lead to a genome-wide instability of the microsatellites[10]. When this occurs in oncogenes or tumor suppressor genes, loss of control over cell growth and proliferation may develop[14]. Moreover, loss of expression of the MMR genes leads to resistance of tumor cells to the damage induced by some chemotherapeutic agents such as 6-thioguanine, some methylating agents, cisplatin and carboplatin[6,15,16]. This acquired resistance could be achieved through several mechanisms including failure to recognize DNA adducts formed by some chemotherapeutic agents or failure to activate signaling pathways that trigger apoptosis[6].

This work was conducted to investigate the possible role of MMR gene defects in the development of HCV-associated HCC through studying the expression levels of *hMSH2*, *GTBP*, *hMLH1*, *hPMS-1* and *hPMS2* genes using the RT-PCR assay.

MATERIALS AND METHODS

Tumor samples

In the present study, 49 samples were analyzed (17 samples of HCC and 32 samples of HCC and their associated normal hepatic tissues obtained from morphologically normal areas distant to the tumor in the same patient). All samples were obtained from patients undergoing hepatectomy at the National Cancer Institute, Cairo University during the period 2000-2002. The mean age of patients was 55.77±11.53 years (range 10-80 years) and the male:female ratio was 1.13:1. Out of the 33 HCC cases, 15 were cirrhotic and 18 showed no evidence of cirrhosis. All clinicopathologic features of the patients are illustrated in Table 1. Fresh tumor and normal distant hepatic tissues (NDHTs) were obtained at the operation theater and immediately divided into two pieces. One was snap frozen in liquid nitrogen and stored at -80 ℃ for subsequent DNA and RNA extraction, the other was fixed in neutral buffered formalin and processed for histopathologic examination to determine tumor type, grade, presence of cirrhosis and percent of neoplastic cells in tumor samples. Only cases composed 75% or more neoplastic cells were included in the study to avoid the neutralizing effect of normal cells. NDHTs were obtained from areas distant to tumors (4-5 cm from the periphery of the tumor) and confirmed to be normal by microscopic examination of hematoxylin and eosin-stained sections. Both normal and neoplastic tissues were examined by two independent pathologists. Unintentional bias was prevented by coding patient tissue samples, so that genomic studies were done without the knowledge of the patient and tumor characteristics. All samples included in this study were HBV-PCR negative.

A written consent was obtained from all studied patients and the Ethical Committee of the NCI approved the protocol according to the ethical guidelines of the 1975 Declaration of Helsinki.

ELISA

Sera collected from 5 mL of coagulated blood were aliquoted and stored at -80 ℃. All sera from patients and controls were tested for HCV antibody and HBsAg by the third generation ELISA using kits from Innogenetics (Belgium) and Equipar (Saronno, Italy). They were also tested for HBs-Ab, anti-HBc total, anti-HbeAg and HBeAg by the third generation ELISA using kits from Innogenetics (Belgium). All tests were done according to the manufacturer's instructions.

DNA extraction

High molecular weight DNA was prepared from 0.5-2.0 g fresh tissue samples according to standard protocols[17].

RNA extraction

RNA from both tumor and normal tissues was extracted using a SV total RNA isolation system (Promega Biotech). The extracted total RNA was assessed for degradation, purity and DNA contamination by a spectrophotometer and electrophoresis in an ethidium bromide-stained 1.0% agarose gel.

Control

Ten samples of normal human DNA and RNA were extracted from PBL and used to optimize the best conditions for the multiplex PCR of β-actin gene *vs* each of the five studied MMR genes. Amplification of β-actin gene (621-bp fragments) was performed to test for the presence of artifacts and to set a base line for each sample that enabled the evaluation of the expression of target genes in the multiplex RT-PCR (i.e., semi-quantitation). The β-actin gene fragments were used to monitor DNA contamination. Since all genes were amplified in the same test tube, designing only one pair of primers should be sufficient for controlling DNA contamination. A water control tube containing all reagents except c-DNA was also conducted in each batch of PCR assays to monitor contamination of genomic DNA in the PCR reagents, negative RT-PCR control was used against each sample.

c-DNA synthesis

Reverse transcription (RT) of the isolated total RNA was done in 25 μL reaction volume containing 1 volume of Superscript II RT enzyme (Gibco-BRL, Gaithersburg, MD, USA), 2.5 μL 10×RT-buffer [250 mmol/L Tris-HCl pH 8.3, 375 mmol/L KCl, 15 mmol/L $MgCl_2$], 0.251 μL of 100 mmol/L dithiothreitol, 1 μL of 25 ng from random primer, 1.5 μL of 10 mmol/L deoxynucleotide triphosphates, 0.5 μL RNAsin (Promega, USA), 5.0 μL of extracted RNA. Samples were then incubated at 50 ℃ for 60 min followed by a 4 ℃ until the PCR amplification reaction.

PCR amplification for the MMR genes

The PCR and quantitation were performed in a 50 μL reaction volume according to Ref.[12] with some modifications. Briefly,

5 μL of the RT reaction mixture (c-DNA), 2.5 units Taq polymerase (Gibco-BRL, Gaithersburg, MD, USA), 1×PCR buffer [500 mmol/L KCl, 200 mmol/L Tris-HCl, 1.5 mmol/L $MgCl_2$, 1 mg/mL bovine serum albumin], 200 μmol/L each of the deoxyribonucleotide triphosphate and 0.25 μmol/L of each primer were mixed. Samples were denatured at 95 ℃ for 5 min and subjected to 35 rounds of thermal cycling (T-gradient, Biometra, Germany). Each cycle consisted of denaturation for 1 min at 95 ℃, annealing for 1 min at different annealing temperatures as shown in Table 2 and extension for 1 min and 30 s at 72 ℃. Samples were then incubated at 72 ℃ for 10 min. All samples were analyzed twice for MMR by RT-PCR on different days with different RT-PCR mixtures to ensure the reproducibility of results.

Quantitation

Fifteen microliters of each PCR product was separated by electrophoresis through a 2.0% ethidium bromide-stained agarose gel and visualized with ultraviolet light. Gels were video-photographed. Then the bands on the photograph were scanned as digital peaks, and the areas of the peaks were calculated in arbitrary units with a digital imaging system (Model IS-1000; Alpha Innotech Co., San Leandro, CA, USA). To evaluate the relative expression levels of target genes in the multiplex RT-PCR, the value of the internal standard (β-actin) in each reaction was used as a normalizing factor and a relative value was calculated for each target genes amplified in the reaction. Reduced expression in any of the studied gene was considered if there was a complete absence or decrease in the intensity of the desired band more than 75% compared to the band of β-actin gene expression which was used as a calibrator. Samples were assayed in batches including both cases and controls. The absence of bands was verified by repeating the multiplex PCR and consistent presence of β-actin gene amplification (Figures 1A-C).

RT-PCR of HCV

The RT and PCR were performed as described in Refs.[18] and[19]. After completion of the reaction, 10 μL of each sample was analyzed by electrophoresis through 1.2% ethidium bromide-stained agarose gel.

Detection of HBV-DNA in tissues

PCR amplification of HBV was done as previously described in Ref.[20], and after the completion of the reaction, 10 μL of each reaction product was analyzed by electrop-horesis through an ethidium bromide-stained 2% agarose gel.

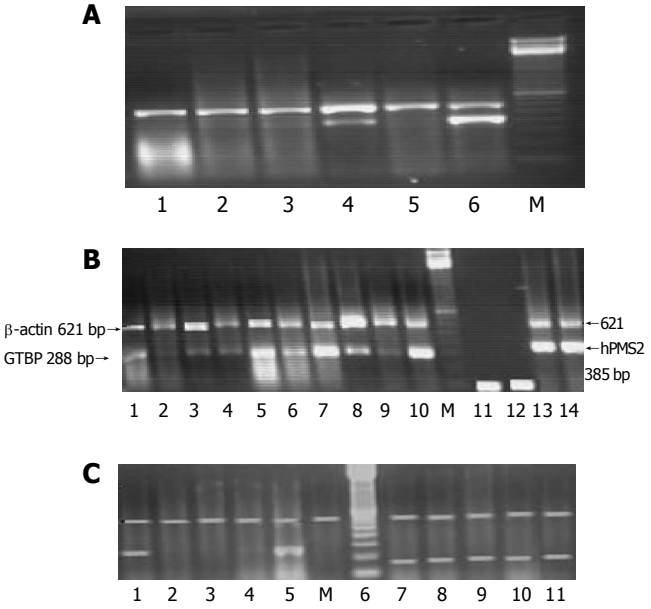

Figure 1 **A**: PCR amplification for MMR genes. **A:** Multiplex RT-PCR of *hMSH2* gene in some HCC cases. M: 100-bp marker; lanes 1-6: *hMSH2* co-amplified with β-actin in HCC cases; lanes 1-3 and 5: *hMSH2* reduction; lane 4: 50 reduced expression of *hMSH2*; lane 6: *hMSH2* co-amplified with β-actin gene in normal PBL as a control. The accepted band of β-actin was at 621 and 492 bp for *hMSH2*. **B:** Multiplex RT-PCR of *GTBP* and *hPMS2* genes in some HCC cases. M: 100-bp marker; lanes 1-10: *GTBP* co-amplified with β-actin in HCC cases; lanes 1 and 6: no reduction; lanes 2, 3, 4, 8 and 9: different expression levels of *GTBP* gene; lane 5: *GTBP* co-amplified with β-actin gene in normal PBL as a control; lane 10: overexpression of *GTBP*; lane 11: *GTBP* co-amplified with β-actin without NA as reagent control; lane 12: *hPMS2* co-amplified with β-actin without NA as reagent control; lanes 13 and 14: overexpression of *hPMS2*. **C:** Multiplex RT-PCR of *hMLH1* and *hPMS1* genes in HCC cases. Lane 1: *hMLH1* co-amplified with β-actin gene in normal PBL as a control; lanes 2, 3 and 6: reduced expression of *hMLH1* gene; lane 5: overexpression of *hMLH1*. M: 100-bp marker; lanes 7-10: *hPMS1* co-amplified with β-actin gene in HCC cases with no changes on the expression level.

Statistical analysis

The results were analyzed using the Graph pad prism computer program (Graph pad software, San Diego, USA). χ^2, *t*-test, and simple correlation tests were used to test for the correlation between the studied parameters. $P \leq 0.05$ was considered statistically significant.

Table 1 Relation between reduced expression of the MMR genes and clinicopathological features of HCC patients

Clincopathological features		No.	*GTBP*	*hPMS1*	*hPMS2*	*hMLH1*	*hMSH2*	HCV-RT-PCR	HBV-PCR
Age (yr)	<50	9	6	0	5	5	7	6	0
	>50	24	11	2	6	11	16	19	0
Gender	M	18	8	2	4	9	13	12	0
	F	15	9	0	7	7	10	13	0
Grade	I and II	24	12	2	8	15	16	17	0
	III	9	5	0	3	1	7	8	0
Cirrhosis	Present	15	7	1	2	8	12	14	0
	Absent	18	9	1	9	8	11	11	0
Total		33	17	2	11	16	23	25	0

Table 2 Oligonucleotide sequences of primers β-actin, MMR genes, HCV, and HBV

Genesequence	Size (bp)	Temperature (℃)
β-actin		
5′-ACA CTG TGC CCA ACG AGG-3′	621	55-59
5′-AGG GGC CGG TCA T AC T-3′		
hMPS-2		
5′-TGC ATG CAG GAT TTG GAA A-3′	385	55
5′-GAA CCC CTC AGA ATC CAC GGA-3′		
GTBP		
5′-CCC TCA GCC ACC AAA GAA GCA-3′	288	56
5′-CTG CCA CCA CTT CCT CAT CCC-3′		
hMLH-1		
5′-GTG CTG GCA ATC AGG GAC CC-3′	215	58
5′-CAC GGT TGA GGC ATT GGG TAG-3′		
hMPS-1		
5′-GCG GCA ACA GTT CGA CTC CTT-3′	174	57
5′-AGC CTT GAT ACC CTC CCC GTT-3′		
hMSH-2		
5′-GTC GGC TTC GTG CGC TTC TTT-3′	429	58
5′-TCT CTG GCC ATC AAC TGC-3′		
HCV		
RB6A		
5′-GTG AGG AAC TAC TGT CTT CAC G-3	266	55
RB6B		
5′-ACT CGC AAG CAC CCT ATC AGG-3′		
HBV		
LBL		
5′-CGG ATC CGT GGA GTT ACT CTG GTT TTT GC-3′	460	55
RBL		
5′-GCA AGC TCT AAC AAC AGT AGT TTC CCG G-3′		

Table 3 Correlation confident analysis of the association between the five MMR gene expressions

MMR	*hMSH2*	*hPMS2*	*GTBP*	*hPMS1*
hMLH1	13/29	6/30	9/30	1/30
	$P = 0.0308^a$	$P = 0.178$	$P = 0.39$	$P = 0.5$
hPMS1	2/32	0/33	1/30	
	$P = 0.407$	$P = 0.391$	$P = 0.95$	
GTBP				
	13/30	8/32		
	$P = 0.149$	$P = 0.0034^a$		
hPMS2	6/32			
	$P = 0.407$			

[a]$P = 0.05$ was considered statistically significant.

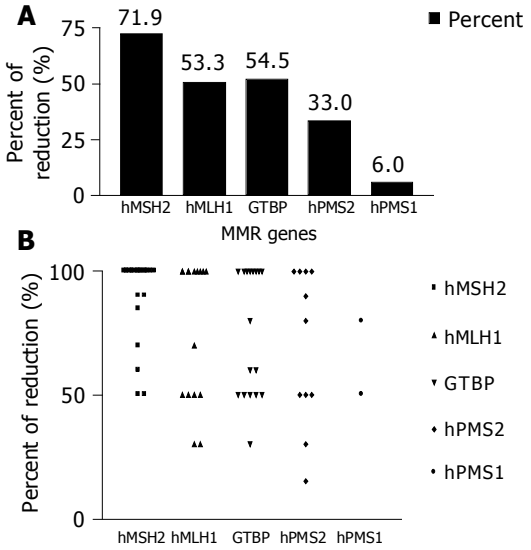

Figure 2 Reduced expression of five studied MMR genes. **A:** Percent of reduction of five studied MMR genes in HCC cases; **B:** percent of reduction of the five MMR genes in each of the studied HCC cases.

RESULTS

Reduction in the expression of one or more of the five studied MMR genes (*hMSH2*, *hMLH1*, *GTBP*/*hMSH6*, *hPMS2* and *hPMS1*) was reported in 30/33 (90.9%) HCC cases, whereas none of the cases showed simultaneous reduction in the five genes. The most commonly affected gene was *hMSH2*, where reduced expression was detected in 23/30 (76.7%) cases, followed by *hMLH1* 16/30 (53.3%) cases, *GTBP* 17/30 (56.7%) cases, *hPMS2* 11/30 (36.7%) cases and *hPMS1* 2/30 (6.7%) cases (Figures 2A and B).

Out of the 30 HCC cases showing reduced expression of one or more genes, 13 (43.3%) had a reduced expression in both *hMSH2* and *hMLH1*, another 13 (43.3%) in both *hMSH2* and *GTBP*, 9 (30%) in both *hMLH1* and *GTBP*, 8 (26.7%) in both *GTBP* and *hPMS2*, 6 (20%) in both *hMSH2* and *hPMS2*, another 6 (20%) in both *hMLH1* and *hPMS2*, 2 (6.6%) in both *hMSH2 and hPMS1*, 1 (3%) in both *hMLH1* and *hPMS1*, and another one (3%) showed a reduction in both *GTBP* and *hPMS1*. None of the cases showed a reduction in both *hPMS2* and *hPMS1*. A significant association was found between reduced expressions of *GTBP* and *hPMS2* ($P = 0.0034$) as well as between *hMSH2* and *hMLH1* ($P = 0.0308$, Table 3).

Relation between MMR gene and cirrhotic HCC

Reduced expression of *hMSH2* was found in 12/15 (75%) patients with cirrhosis compared to 11/18 (61.1%) non-cirrhotic cases as well as in 8/15 (53.3%) compared to 8/18 (44.4%) cases for *hMLH1*, 7/15 (46.7%) compared to 9/18 (50%) cases for *GTBP*, 2/15 (13.3%) compared to 9/18 (50%) cases for *hPMS2* and in 1/15 (6.7%) compared to 1/18 (5.5%) cases for *hPMS1*. No significant relation was found between reduced expression of any of the studied genes and the clinicopathological features of patients except for the relationship between reduced expression of *hPMS2* and non-cirrhotic HCC cases only ($P = 0.0197$, Figure 3A).

Relation between MMR and grade of HCC

Regarding the relationship between the reduced expression of MMR and grade I and II *vs* grade III, strong significant relation was found between reduced expression of *hMLH1* and grade II ($P = 0.0069$, Figure 3B).

Expression level of MMR genes in NDHT

The expression level of *hMSH2* was reduced in 8/16 (50%) NDHT samples compared to 23/30 (71.9%) for their associated HCC samples, 7/16 (43.75%) NDHT compared to 16/30 (53.3%) of HCC cases for *hMLH1*, 3/16 (18.8%) NDHT samples compared to 17/30 (561.7%) of HCC cases for *GTBP*, in 3/16 (18.8%) NDHT samples compared to 11/30 (36.7%) of HCC cases for *hPMS2* and in 1/16

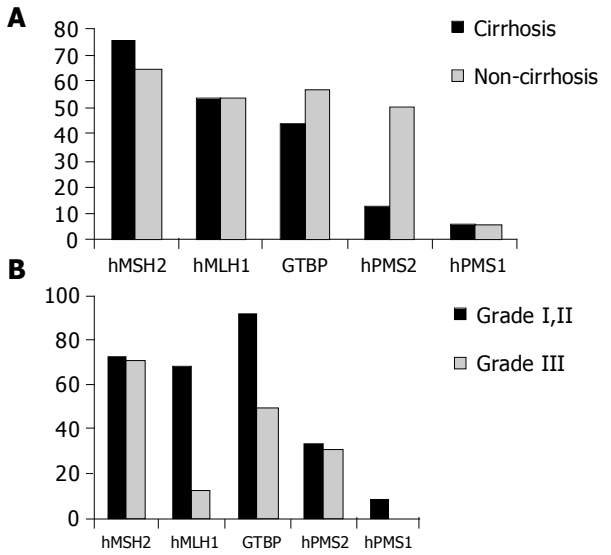

Figure 3 Relation between the five studied MMR genes and cirrhosis (**A**) and grade (**B**) of HCC.

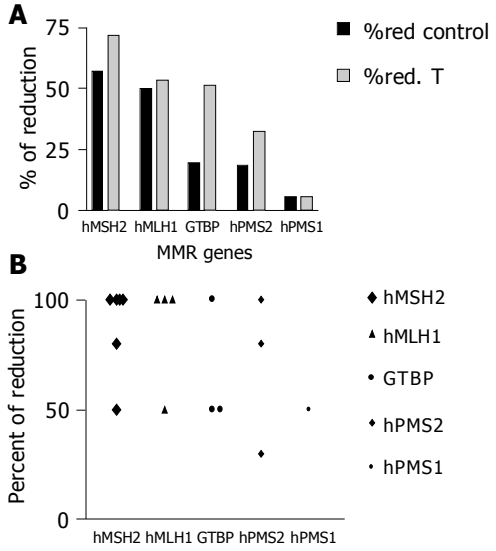

Figure 4 Expression levels of MMR genes in NDHT. Percent of reduction of the five studied MMR genes in HCC cases (**A**) each of the studied normal liver tissues distant to tumor (**B**).

(6.3%) NDHT samples compared to 2/30 (6.6%) of HCC cases for *hPMS1*. A statistically significant difference in the expression levels of *GTBP* was found between cases of HCC and NDHT ($P = 0.04$, Figures 4A and B).

Relation between MMR genes expression and HCV infection

A significant relation was found between reduced expression of *hPMS2*, *GTBP* and the presence of HCV infection in HCC cases ($P<0.001$ and 0.002, respectively).

DISCUSSION

DNA MMR is an important mechanism involved in maintaining the fidelity of genomic DNA. Defective MMR was implicated in a variety of gastrointestinal tumors; however, its role in HCC has been incompletely defined[9]. In this preliminary study, multiplex RT-PCR assay was used to assess the expression levels of five MMR genes in HCV-associated HCCs and their NDHTs.

Reduced expression of *hMSH2*, *hMLH1*, *GTBP* and *hPMS2* but not *hPMS1* was frequently observed in HCC cases. In general, reduced expression of more than one gene was more frequent than in a single gene. The most frequently affected genes in the present study were MSH2 (71.9%), GTBP (56.7%), and MLH1 (53.3%). The reduced expression could be speculative for somatic mutations affecting these genes in particular and might lead to reduced expression. Literature review showed only very few reports with controversial data in this context. In 1999, Yanno *et al*[21], reported the presence of mutations in *hMSH2* gene in HCC patients and demonstrated that these mutations were closely correlated with the overall survival of patients. In a recent study on the gene expression profile of HCC cases using the cDNA array, reduced expression of MSH2 was found to be a frequent event in HCC and was closely associated with tumor metastasis. In contrast, Wang *et al*[22], using immunohistochemical techniques did not find any correlation between the expression level of *hMLH1* or *hMSH2* and the incidence or prognosis of HCC patients. They concluded that defects in *hMSH2*, *hMLH1* did not contribute significantly to hepatocellular carcinogenesis. This controversy in the results of different studies may be attributed to the difference in the detection method of MMR gene defects, the presence of different HCV genotypes of viral infection, epigenetic factors or other factors including race, geographical area, genetic profile and other environmental hazards. It was shown that some mutations could cause premature translation termination that mediates degradation of mutant mRNAs. Moreover, hypermethylation might be another mechanism of gene silencing where hypermethylated genes have reduced mRNA levels. It is also likely that inactivation of transcription factors may reduce the expression of MMR genes with the occurrence of gradual shutdown as a tumor progresses[12].

In addition, several studies demonstrated that the affected MMR genes and the pattern of defects differed according to the type of studied tumors[23]. Whereas in the current study the most frequently affected genes were *MSH2*, *GTBP*, and *MLH1*. Thomas *et al*[24], studied germline mutations of the MMR genes in African Americans with CRC and found an association between germline mutations of *hMLH1* and *hMSH2* and the development of CRC in African Americans. Therefore, it seems possible that defects in MMR genes could be induced by the interplay between several genetic and non-genetic factors and even in the same tumor type we may find different patterns of gene defects.

A novel finding in this work is the frequent involvement of *GTBP* since this gene has not been mentioned before in relation to hepatocellular carcinogenesis. Moreover, in the majority of cases which had a reduced expression of more than one gene, *GTBP* was usually a partner. Therefore, we assume that genetic defects leading to loss of function of *GTBP* might represent an important step in the chain of MMR gene defects involved in hepatocyte transformation especially in the presence of HCV infection. This assumption has been confirmed in the present study by finding a

significant difference between the expression level of *GTBP* in tumor and normal hepatic tissues obtained from the same patients. Additional evidence is provided by the high association reported in the present study between reduced expression of *GTBP* and the presence of HCV in HCC cases.

On the other hand, *hMLH1* was the third most frequently affected gene and commonly associated with reduced expression of *MSH2*. Moreover, reduced expression of *hMLH1* in NHTDT was comparable to that reported in tumor tissues in cases from which paired samples of normal and neoplastic tissues were taken (43.2% *vs* 53.3%). These findings indicate that *hMLH1* is a likely candidate gene in hepatocarcinogenesis and possibly exerts its role in the early steps of hepatocyte transformation. Our data in this regard have confirmed the results of Macdonald *et al*[9], who detected LOH at *hMSH2* and/or *hMLH1* in malignant, premalignant and adjacent normal hepatic tissues. The high association reported in the current study between reduced expression of *hMSH2* and *hMLH1* ($P = 0.03$) suggests the presence of a co-operation between these two genes at a certain stage of hepatocarcinogenesis. Moreover, there was a significant association between reduced expressions of *PMS2* gene and absence of cirrhosis in HCC patients ($P = 0.0197$) since reduced expression of *PMS2* was secondary to *MSH2* in this group of patients. This provides a possible pathogenetic pathway for the development of HCC in non-cirrhotic patients via failure to repair damaged DNA. Subsequently, it could be proposed that defects in *hPMS2* are likely associated with growth advantage and proliferative stimulation which in the absence of effective DNA repair mechanisms may lead to malignant changes in the non-cirrhotic patients. The significant association between reduced expressions of *GTBP* and *hPMS2* in HCC especially in non-cirrhotic cases ($P = 0.003$) could be explained by the presence of a co-operation between these two genes in the development of HCC.

The significant association reported in the present study between the presence of HCV in HCC cases and reduced expression of *hPMS2* and/or *GTBP* ($P<0.001$ and 0.002 respectively) suggests that these genes could be targets for HCV in the genetic cascade controlling HCV-associated hepatocarcinogenesis. Alternatively reduced expression or inactivation of these genes may interfere with (prevent) efficient repair of DNA as a result of HCV infection.

It is now well known that HCV-associated HCC involves alterations in the concerned action of proto-oncogenes, growth factors and tumor suppressor genes. The presence of two nuclear localization signals and a DNA binding motif in the HCV core protein suggests a possible functional role for HCV as a gene regulatory element[25]. Moreover, some studies suggested that this protein could interact with certain cellular proto-oncogenes at the transcriptional level, resulting in the promotion of cell proliferation which in the presence of DNA damage and/or in the absence of efficient DNA repair mechanisms affects normal hepatocyte growth and differentiation. Therefore, the pathogenesis of HCV might contribute at least in part to the upregulation of hepatocyte growth induced by HCV core protein and the loss of DNA repair[26].

To the best of our knowledge, no previous study has revealed the relation between MMR defects and HCV infection in the process of hepatocarcinogenesis. Numerous studies have shown that overexpression of growth factor receptors is associated with altered cellular response to damage and DNA repair. In breast and ovarian cancer cells, overexpression of *c-erbB2* gene products increased sensitivity to drugs through inhibition of DNA repair[27-29] and we previously reported overexpression of *c-erbB2* in HCC and chronic active hepatitis patients in association with HCV genotype-4 which is the predominant genotype in Egyptian patients[25]. It has been clearly indicated that modulation of *c-erbB2* could inhibit DNA repair either directly or indirectly[30]. Finally, the high mutation rate occurring in case of MMR gene defects in the coding or regulatory sequences of other genes could lead to more and more genomic damages with an increased probability for neoplastic transformation[6]. This finding may in part explain the high resistance of HCC to the most known regimen of chemotherapy, since it has been previously reported that a close correlation exists between MMR gene defect and resistance to chemotherapy.

In conclusion, the present study represents a step forward for understanding the genetic events that induce HCC in HCV-infected patients. Reduced expression of *MSH2*, *GTBP*, *MLH1*, and *PMS2* is a frequent event in HCC. Both *GTBP* and *PMS2* are possible candidates for HCC in HCV-infected patients. However, the mechanisms involved in this process have to be clarified. Reduced expression of *hMLH1* occurs in the early stages of hepatocarcinogenesis as evidenced by the finding that there is no significant difference in the expression level of *hMLH1* between tumors and NDHTs, and reduced expression of *hPMS2* most frequently in non-cirrhotic HCC is associated with HCV infection.

REFERENCES

1 **Natoli G**, Ianni A, Costanzo A, De Petrillo G, Ilari I, Chirillo P, Balsano C, Levrero M. Resistance to Fas-mediated apoptosis in human hepatoma cells. *Oncogene* 1995; **11**: 1157-1164
2 **Moradpour D**, Blum HE. Molecular aspects of hepatocellular carcinoma. *Zentralbl Chir* 2000; **125**: 592-596
3 **William H,** Daphne C. Biochemistry and Molecular Biology. Second edition (P. 319- 336). Printed in the USA 2001
4 **John M**, Peter M, Howley A. The Molecular Basis of cancer. Second edition (P: 423 –428). *Printed in the USA* 2001
5 **Blum HE**. Molecular targets for prevention of hepatocellular carcinoma. *Dig Dis* 2002; **20**: 81-90
6 **Fink D**, Nebel S, Norris PS, Aebi S, Kim HK, Haas M, Howell SB. The effect of different chemotherapeutic agents on the enrichment of DNA mismatch repair-deficient tumour cells. *Br J Cancer* 1998; **77**: 703-708
7 **Kolodner R**. Biochemistry and genetics of eukaryotic mismatch repair. *Genes Dev* 1996; **10**: 1433-1442
8 **Risinger JI**, Barrett JC, Watson P, Lynch HT, Boyd J. Molecular genetic evidence of the occurrence of breast cancer as an integral tumor in patients with the hereditary nonpolyposis colorectal carcinoma syndrome. *Cancer* 1996; **77**: 1836-1843
9 **Macdonald GA**, Greenson JK, Saito K, Cherian SP, Appelman HD, Boland CR. Microsatellite instability and loss of heterozygosity at DNA mismatch repair gene loci occurs during hepatic carcinogenesis. *Hepatology* 1998; **28**: 90-97
10 **Benachenhou N**, Guiral S, Gorska-Flipot I, Labuda D, Sinnett D. Frequent loss of heterozygosity at the DNA mismatch-repair loci hMLH1 and hMSH3 in sporadic breast cancer. *Br J Cancer* 1999; **79**: 1012-1017

11 **Han HJ**, Yanagisawa A, Kato Y, Park JG, Nakamura Y. Genetic instability in pancreatic cancer and poorly differentiated type of gastric cancer. *Cancer Res* 1993; **53**: 5087-5089

12 **Wei Q**, Bondy ML, Mao L, Gaun Y, Cheng L, Cunningham J, Fan Y, Bruner JM, Yung WK, Levin VA, Kyritsis AP. Reduced expression of mismatch repair genes measured by multiplex reverse transcription-polymerase chain reaction in human gliomas. *Cancer Res* 1997; **57**: 1673-1677

13 **Zekri AR**, Bahnassi AA, Bove B, Huang Y, Russo IH, Rogatko A, Shaarawy S, Shawki OA, Hamza MR, Omer S, Khaled HM, Russo J. Allelic instability as a predictor of survival in Egyptian breast cancer patients. *Int J Oncol* 1999; **15**: 757-767

14 **Leach FS**, Polyak K, Burrell M, Johnson KA, Hill D, Dunlop MG, Wyllie AH, Peltomaki P, de la Chapelle A, Hamilton SR, Kinzler KW, Vogelstein B. Expression of the human mismatch repair gene hMSH2 in normal and neoplastic tissues. *Cancer Res* 1996; **56**: 235-240

15 **Griffin S**, Branch P, Xu YZ, Karran P. DNA mismatch binding and incision at modified guanine bases by extracts of mammalian cells: implications for tolerance to DNA methylation damage. *Biochemistry* 1994; **33**: 4787-4793

16 **Kat A**, Thilly WG, Fang WH, Longley MJ, Li GM, Modrich P. An alkylation-tolerant, mutator human cell line is deficient in strand-specific mismatch repair. *Proc Natl Acad Sci USA* 1993; **90**: 6424-6428

17 **Sambrook J**, Ritsch E, Maniatis T. Molecular cloning. A laboratory manual (2nd edition) Cold Spring Harbor, NY 1989

18 **Zekri ARN**, Bahnassy AA, Khaled HM, Mansour O, Attia MA. Comparative analysis of different PCR techniques for detection of HCV in hepatocellular carcioma patients. *Cancer J* 1995; **8**: 331-335

19 **Zekri AR**, Sedkey L, el-Din HM, Abdel-Aziz AO, Viazov S. The pattern of transmission transfusion virus infection in Egyptian patients. *Int J Infect Dis* 2002; **6**: 329-331

20 **Boom R**, Sol CJ, Salimans MM, Jansen CL, Wertheim-van Dillen PM, van der Noordaa J. Rapid and simple method for purification of nucleic acids. *J Clin Microbiol* 1990; **28**: 495-503

21 **Yano M**, Asahara T, Dohi K, Mizuno T, Iwamoto KS, Seyama T. Close correlation between a p53 or hMSH2 gene mutation in the tumor and survival of hepatocellular carcinoma patients. *Int J Oncol* 1999; **14**: 447-451

22 **Wang L**, Bani-Hani A, Montoya DP, Roche PC, Thibodeau SN, Burgart LJ, Roberts LR. hMLH1 and hMSH2 expression in human hepatocellular carcinoma. *Int J Oncol* 2001; **19**: 567-570

23 **Heinimann K**, Scott RJ, Chappuis P, Weber W, Muller H, Dobbie Z, Hutter P. N-acetyltransferase 2 influences cancer prevalence in hMLH1/hMSH2 mutation carriers. *Cancer Res* 1999; **59**: 3038-3040

24 **Weber TK,** Chin HM, Rodriguez-Bigas M, Keitz B, Gilligan R, O'Malley L, Urf E, Diba N, Pazik J, Petrelli NJ. Novel hMLH1 and hMSH2 germline mutations in African Americans with colorectal cancer. *JAMA* 1999; **281**: 2316-2320

25 **Arteaga CL**, Winnier AR, Poirier MC, Lopez-Larraza DM, Shawver LK, Hurd SD, Stewart SJ. p185c-erbB-2 signal enhances cisplatin-induced cytotoxicity in human breast carcinoma cells: association between an oncogenic receptor tyrosine kinase and drug-induced DNA repair. *Cancer Res* 1994; **54**: 3758-3765

26 **Ray RB**, Lagging LM, Meyer K, Ray R. Hepatitis C virus core protein cooperates with ras and transforms primary rat embryo fibroblasts to tumorigenic phenotype. *J Virol* 1996; **70**: 4438-4443

27 **Zekri AR**, Bahnassy AA, Shaarawy SM, Mansour OA, Maduar MA, Khaled HM, El-Ahmadi O. Hepatitis C virus genotyping in relation to neu-oncoprotein overexpression and the development of hepatocellular carcinoma. *J Med Microbiol* 2000; **49**: 89-95

28 **Geisler S**, Lonning PE, Aas T, Johnsen H, Fluge O, Haugen DF, Lillehaug JR, Akslen LA, Borresen-Dale AL. Influence of TP53 gene alterations and c-erbB-2 expression on the response to treatment with doxorubicin in locally advanced breast cancer. *Cancer Res* 2001; **61**: 2505-2512

29 **Pietras RJ**, Fendly BM, Chazin VR, Pegram MD, Howell SB, Slamon DJ. Antibody to HER-2/neu receptor blocks DNA repair after cisplatin in human breast and ovarian cancer cells. *Oncogene* 1994; **9**: 1829-1838

30 **Hartwell LH**, Kastan MB. Cell cycle control and cancer. *Science* 1994; **266**: 1821-1828

31 **Soliman AS**, Bondy ML, Guan Y, El-Badawi S, Mokhtar N, Bayomi S, Raouf AA, Ismail S, McPherson RS, Abdel-Hakim TF, Beasley RP, Levin B, Wei Q. Reduced expression of mismatch repair genes in colorectal cancer patients in Egypt. *Int J Oncol* 1998; **12**: 1315-1319

32 **Fink D**, Nebel S, Aebi S, Zheng H, Cenni B, Nehme A, Christen RD, Howell SB. The role of DNA mismatch repair in platinum drug resistance. *Cancer Res* 1996; **56**: 4881-4886

Science Editor Wang XL and Guo SY **Language Editor** Elsevier HK

PO Box 2345, Beijing 100023, China
www.wjgnet.com
wjg@wjgnet.com

ELSEVIER

World J Gastroenterol 2005;11(20):3027-3033
World Journal of Gastroenterology ISSN 1007-9327

Construction and clinical significance of a predictive system for prognosis of hepatocellular carcinoma

Jun Cui, Bao-Wei Dong, Ping Liang, Xiao-Ling Yu, De-Jiang Yu

Jun Cui, Bao-Wei Dong, Ping Liang, Xiao-Ling Yu, De-Jiang Yu, Department of Ultrasound, Chinese PLA General Hospital, Beijing 100853, China
Supported by the Medical and Health Science Foundation of PLA During the 10th five-year plan period, No. 01Z038
Correspondence to: Dr. Jun Cui, Department of Gastroenterology, Yu Huang Ding Hospital, Yantai 264000, Shandong Province, China. cuijun89@hotmail.com
Telephone: +86-535-7062606
Received: 2004-05-07 Accepted: 2004-06-17

Abstract

AIM: The aims of this study were to explore individualized treatment method for hepatocellular carcinoma (HCC) patients whose maximum tumor size was less than 5 cm to improve prognosis and survival quality.

METHODS: Thirty cases of primary HCC patients undergoing tumor resection were retrospectively analyzed (resection group). All the tumors were proved as primary HCC with pathologic examination. The patients were divided into two groups according to follow-up results: group A, with tumor recurrence within 1 year after resection; group B, without tumor recurrence within 1 year. Immunohistochemical stainings were performed using 11 kinds of monoclonal antibodies (AFP, c-erbB2, c-met, c-*myc*, HBsAg, HCV, Ki-67, MMP-2, nm23-H1, P53, and VEGF), and expressing intensities were quantitatively analyzed. Regression equation using factors affecting prognosis of HCC was constructed with binary logistic method. HCC patients undergoing percutaneous microwave coagulation therapy (PMCT) were also retrospectively analyzed (PMCT group). Immunohistochemical stainings of tumor biopsy samples were performed with molecules related to HCC prognosis, staining intensities were quantitatively analyzed, coincidence rate of prediction was calculated.

RESULTS: In resection group, the expressing intensities of c-*myc*, Ki-67, MMP-2 and VEGF in cancer tissue in group A were significantly higher than those in group B ($t = 2.97$, $P = 0.01$; $t = 2.42$, $P = 0.03<0.05$; $t = 2.57$, $P = 0.02<0.05$; $t = 3.43$, $P = 0.004<0.01$, respectively); the expressing intensities of 11 kinds of detected molecules in para-cancer tissue in groups A and B were not significantly different ($P>0.05$). The regression equation predicting prognosis of HCC is as follows: $P(1) = 1/[1+e^{-(3.663-0.412mycc-2.187Ki\text{-}67c-0.397vegfc)}]$. It demonstrates that prognosis of HCC in resection group was related with c-*myc*, Ki-67 and VEGF expressing intensity in cancer tissue. In PMCT group, the expressing intensities of c-*myc*, Ki-67 and VEGF in cancer tissue in group A were significantly higher than those in group B ($t = 4.57$, $P = 0.000<0.01$; $t = 2.08$, $P = 0.04<0.05$; $t = 2.38$, $P = 0.02<0.05$, respectively); the expressing intensities of c-*myc*, Ki-67 and VEGF in para-cancer tissue in groups A and B were not significantly different ($P>0.05$). The coincidence rate of patients undergoing PMCT in group A was 88.00% (22/25), in group B 68.75% (11/16), the total coincidence rate was 80.49% (33/41).

CONCLUSION: The regression equation is accurate and feasible and could be used for predicting prognosis of HCC, it helps to select treatment method (resection or PMCT) for HCC patients to realize individualized treatment to improve prognosis.

Key words: Hepatocellular carcinoma; Prognosis; Prediction

Cui J, Dong BW, Liang P, Yu XL, Yu DJ. Construction and clinical significance of a predictive system for prognosis of hepatocellular carcinoma. *World J Gastroenterol* 2005; 11 (20): 3027-3033
http://www.wjgnet.com/1007-9327/11/3027.asp

INTRODUCTION

Originally resection was the first choice for hepatocellular carcinoma (HCC), however, high recurrence rate after resection was a major problem influencing the therapeutic effect[1]. Percutaneous microwave coagulation therapy (PMCT) plays an important role in the treatment for HCC. Some patients survived for more than 5 years after PMCT. PMCT has the superiority of enhancing immune function both in the tumor and the whole body. An increased systemic immune response directed against the tumor may play an important role in improved survival for HCC patients[2].

Individualized therapy is one new trend in cancer treatment in the 21st century. The purpose of individualized treatment is to improve prognosis, as appropriate therapy method is selected for each patient[3]. There are no sufficient theoretical fundamentals for HCC patients to either select resection or PMCT for therapy. Recurrence and/or metastasis are the main factors affecting prognosis of HCC[4,5]. Patients' clinical conditions before resection and therapeutic measures after operation may be similar, however, their prognosis after resection may differ largely. Some have tumor recurrence within 1 year after resection, while others do not, and the reason leading to this difference is not clear.

The occurrence and prognosis of HCC is related to activation of proto-oncogene, inactivation of tumor suppressor gene, abnormal expression of growth factors and/or their receptors[6-8].

The way to realize individualized treatment is to predict prognosis of HCC patients before treatment, and then according to the prediction suitable treatment methods are selected to best improve prognosis. Therefore, how to predict prognosis of HCC patients becomes the major problem. The aims of this study were: (1) to compare the expressing intensity of 11 kinds of molecules related to HCC in resection group; (2) to construct a regression equation predicting prognosis of HCC patients; (3) to verify the accuracy of the regression equation in PMCT group.

MATERIALS AND METHODS

Patients

Thirty cases of primary HCC patients undergoing resection (resection group) in the Department of Hepatobiliary Surgery in General Hospital of PLA of China (301 Hospital) were retrospectively analyzed. The selecting standards listed were as follows: solitary nodule, maximum size less than 5 cm, no transarterial chemoembolization (TACE) or local thermal therapy performed before resection, no other specific treatments performed after resection. All the tumors were proved as primary HCC with pathologic examination. The patients were divided into two groups according to follow-up results: group A, with tumor recurrence within 1 year after resection; group B, without tumor recurrence within 1 year. The differences of clinical data were not significant ($P>0.05$, Table 1).

Table 1 Clinical data of patients in resection group

Item	Group A ($n=15$)	Group B ($n=15$)
Sex (m/f)	14 /1	14 /1
Age (yr)	54.7±14.3	48.2±8.4
Mean diameter (cm)	3.2±1.0	2.9±1.1
Child–Pugh grade	A	A
Serum AFP (μg/L)	180±200	120±200
ALT (U/L)	58.0±54.1	64.9±56.6
AST (U/L)	49.9±46.8	42.0±37.7
HBsAg positive rate	87% (13/15)	100 (15/15)

Forty-one cases of primary HCC patients undergoing PMCT (PMCT group) in the Department of Ultrasound in General Hospital of PLA of China (301 Hospital) were retrospectively analyzed. The selecting standards were the same as those in resection group. It included 36 males and 5 females. All the nodules were biopsied under ultrasonic guidance and proved as primary HCC with pathologic examination. The patients were divided into two groups according to follow-up results: group A, with tumor recurrence within 1 year after PMCT; group B, without tumor recurrence within 1 year. The differences of clinical data were not significant ($P>0.05$, Table 2).

Table 2 Clinical data of patients in PMCT group

Item	Group A ($n=25$)	Group B ($n=16$)
Sex (m/f)	21/4	15/1
Age (yr)	55.8±13.4	57.2±11.2
Mean diameter (cm)	3.5±1.0	3.0±0.8
Child–Pugh grade	A	A
Serum AFP (μg/L)	160±200	120±160
ALT (U/L)	52.0±42.5	48.1±40.1
AST (U/L)	51.9±38.9	41.2±36.5
HBsAg positive rate	76% (16/21)	95 (20/21)

Immunohistochemical staining

HPIAS-1000 Diagram-Writing Analyzing System was produced by Wuhan Champion Image Technology Corporation Ltd. SP and DAB kit, monoclonal antibodies of AFP, c-erbB2, c-met, c-*myc*, HBsAg, HCV, Ki-67, MMP-2, nm23-H1, P53 and VEGF were all purchased from Beijing Zhongshan Biological Technology Corporation Ltd. Serial sections were made with wax sample of resected tumors, the thickness of the slice was 4 μm. Immunohistochemical staining was performed with SP three-step method using the monoclonal antibodies listed above.

Quantitative analysis of detected molecules

Quantitative analysis of the detected molecules was performed with HPIAS-1000 imaging analysis system. The molecules in cancer and para-cancer tissues were both analyzed. Three fields of view (FOVs) were randomly selected in cancer tissue and para-cancer tissue to quantitatively analyze the expressing intensity. One hundred cells were observed in each FOV, positive-staining cells were calculated, finally the average positive-staining cells in 100 observed cells were determined. The cells were determined as positive-staining cells only if they were stained, without considering their staining intensity. The medium optical density (MOD) of plasm or nucleus in positive-staining cells was calculated, the product of positive-staining cells and MOD was calculated, which was considered as expressing the intensity of positive-staining molecules[9].

Statistical analysis

Data were presented as mean±SD. Paired-sample t test was used to compare the difference, the statistic software SPSS 10.0 was used. Recurrence state after treatment (resection or PMCT) was defined as 0 or 1: that with tumor recurrence within 1 year after treatment was defined as 0 (group A), that without tumor recurrence within 1 year was defined as 1 (group B). Regression equation predicting prognosis of HCC was constructed using binary logistic regression analysis[10]. In this study, $P<0.05$ was considered statistically significant.

RESULTS

Expressing intensity of detected molecules in resection group

The expressing intensities of c-*myc*, Ki-67, MMP-2, and VEGF in cancer tissue in group A were significantly higher than those in group B (Table 3).

Table 3 Expressing intensity of detected molecules in cancer tissue in groups A and B

Molecule	Group A	Group B
AFP	2.72±2.93	1.55±3.00
c-erbB-2	9.44±5.02	6.82±6.10
c-met	2.04±2.68	1.61±3.22
c-*myc*	3.95±2.81[b]	1.34±2.74
HBsAg	0.45±0.96	2.26±5.04
HCV	0.51±1.40	0.96±2.44
Ki-67	1.57±2.20[a]	0.18±0.38
MMP-2	3.70±4.13[a]	0.61±1.70
Nm23-H1	2.18±3.05	1.49±2.20
P53	1.31±3.37	0.39±1.16
VEGF	5.44±4.20[b]	1.04±3.38

[a]$P<0.05$, [b]$P<0.01$ *vs* group B.

The expressing intensities of 11 kinds of detected molecules in para-cancer tissue in groups A and B were not significantly different (Table 4).

Table 4 Expressing intensity of 11 detected molecules in para-cancer tissue in groups A and B

Molecule	Group A	Group B
AFP	0.09±0.35	0.00±0.00
c-erbB-2	0.76±2.50	0.01±0.04
c-met	0.00±0.00	0.00±0.00
c-*myc*	0.00±0.00	0.26±1.00
HbsAg	9.02±5.83	9.11±6.19
HCV	1.32±2.88	0.08±0.20
Ki-67	0.57±2.22	0.01±0.04
MMP-2	0.80±3.10	0.00±0.00
Nm23-H1	0.33±0.81	0.00±0.00
P53	0.00±0.00	0.00±0.00
VEGF	0.04±0.15	0.00±0.00

Micrographs of c-myc, Ki-67, MMP-2 and VEGF

The micrographs of c-*myc*, Ki-67, MMP-2, and VEGF expression are shown in Figures 1-4.

Construction of regression equation

From the tables listed above, it demonstrated that c-*myc*, Ki-67, MMP-2, and VEGF were perhaps key factors determining prognosis difference of patients in groups A and B. Recurrence state (0 or 1) was used as a dependent variable; expressing intensities of c-*myc*, Ki-67, MMP-2, and VEGF in cancer tissue in groups A and B were used as covariates to construct an equation with binary logistic regression analysis.

The regression equation predicting prognosis of HCC is as follow:

$$P(1) = 1/[1+e^{-(3.663-0.412myc\text{-}2.187\text{Ki-}67c\text{-}0.397vegfc)}]$$

The variables in the regression equation are listed in Table 5.

*MYC*C: c-*myc* expressing intensity in cancer tissue; Ki-67c: ki-67 expressing intensity in cancer tissue; VEGFC: vegf expressing intensity in cancer tissue.

Expressing intensity of detected molecules in PMCT group

The expressing intensities of c-*myc*, Ki-67, and VEGF in cancer tissue in group A were significantly higher than those in group B (Table 6).

Table 6 Expressing intensity of detected molecules in cancer tissue in groups A and B

Molecule	Group A	Group B
c-*myc*	8.31±4.71[b]	2.52±2.30
Ki-67	1.53±1.79[a]	0.47±1.19
VEGF	6.23±5.44[a]	2.88±3.57

[a]$P<0.05$, [b]$P<0.01$ *vs* group B.

The expressing intensities of c-*myc*, Ki-67, and VEGF in para-cancer tissue in groups A and B were not significantly different (Table 7).

Table 7 Expressing intensity of detected molecules in para-cancer tissue in groups A and B

Molecule	Group A	Group B
c-*myc*	2.20±3.91	0.95±1.84
Ki-67	$6.40\times10^{-3}\pm3.20\times10^{-2}$	0.00±0.00
VEGF	0.66±1.84	0.54±2.16

Verification of regression equation

The values of expressing intensities of c-*myc*, Ki-67, and

Table 5 Variables in the regression equation

		B	SE	Wald	df	Sig	Exp (B)	95.0% CI for EXP (B)	
								Lower	Upper
Step 1	*MYC*C	–0.357	0.213	2.807	1	0.094	0.700	0.461	1.063
	KI-67C	–2.118	1.251	2.865	1	0.091	0.120	0.010	1.397
	MMP-2C	–0.244	0.306	0.638	1	0.425	0.783	0.430	1.426
	VEGFC	–0.367	0.160	5.269	1	0.022	0.693	0.506	0.948
	Constant	3.680	1.363	7.289	1	0.007	39.640		
Step 2	*MYC*C	–0.412	0.211	3.795	1	0.051	0.663	0.438	1.003
	KI-67C	–2.187	1.271	2.959	1	0.085	0.112	0.009	1.356
	VEGFC	–0.397	0.159	6.222	1	0.013	0.672	0.492	0.918
	Constant	3.663	1.410	6.750	1	0.009	38.991		

Variable(s) entered on step 1: *MYC*C, KI-67C, MMP-2C, VEGFC.

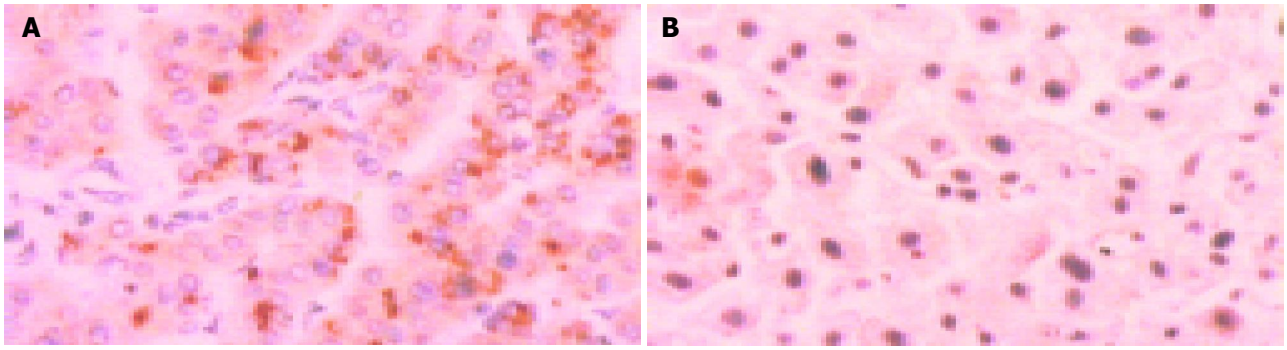

Figure 1 Positive and negative *c-myc* (×400). **A**: Positive *c-myc*; **B**: Negative *c-myc*.

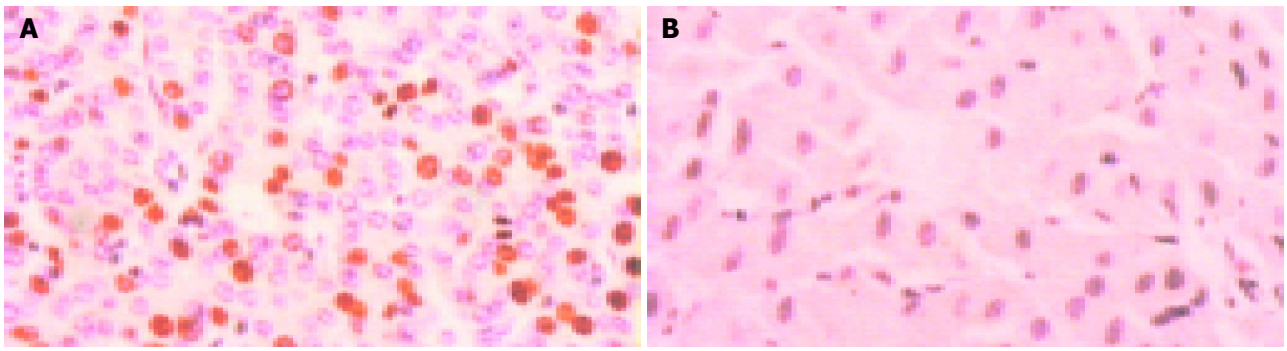

Figure 2 Positive and negative Ki-67 (×400). **A**: Positive Ki-67; **B**: Negative Ki-67.

VEGF in PMCT group were introduced into the regression equation, coincidence rate of prediction was calculated. Coincidence rate in group A was 88.00% (22/25) that in group B was 68.75% (11/16); total coincidence rate was 80.49%.

DISCUSSION

The expressing intensities of AFP, c-erbB2, c-met, c-*myc*, MMP-2, nm23-H1, VEGF in cancer tissue were higher than those in para-cancer tissue in group A. The expressing intensities of c-erbB2 and nm23-H1 in cancer tissue were higher than those in para-cancer tissue in group B. The expressing intensity of HBsAg in para-cancer tissue was higher than that in cancer tissue in groups A and B. The expressing intensities of c-*myc*, Ki-67, MMP-2 and VEGF in cancer tissue in group A were higher than those in group B, the expressing intensities of the 11 kinds of molecules listed in this study in para-cancer tissue in groups A and B were not significantly different.

It was reported in the literature that AFP[11,12], c-erbB-2[13], c-met[14], HBsAg[15], HCV[16], nm23-H1 and P53[17] expressions were related to prognosis of HCC, however, it demonstrated in this study that their expressions were not significantly related to prognosis of HCC in resection group. The reason was probably that the clinical characters of patients in groups A and B were similar. These seven kinds of molecules played minor roles in determining malignancy of HCC in this study. The expressing intensities of c-*myc*, Ki-67, MMP-2, and VEGF in groups A and B in resection group were significantly different. The clinical data in groups A and B were similar, there might be some key molecules closely related to prognosis difference of groups A and B, and these four kinds of molecules were perhaps such key molecules.

Matrix metalloproteinases (MMPs) specially degrade extracellular matrix (ECM) and basement membranes, they are involved in tissue remodeling and angiogenesis of HCC. Ishii *et al*[18], reported that MMP-2 was associated with carcinogenesis and progression of HCC. Kuyvenhoven *et al*, measured serum MMP-2 by ELISA in 91 patients with chronic liver disease, including 25 patients with hepatocellular carcinoma (HCC), and in 60 controls, they demonstrated that MMP-2 was significantly higher in patients with chronic liver disease compared to controls, and increased with Child-Pugh class. There was a significant correlation between MMP-2 and liver function (bilirubin, albumin, and prothrombin time). MMP-2 levels in patients with HCC were significantly higher than those in controls. Serum MMP-2 correlates with the severity of liver disease and may reflect changes in extracellular matrix remodeling[19]. It was demonstrated in this study that the expressing intensity of MMP-2 in cancer tissue was much higher than that in para-cancer tissue in group A, and it was much higher in cancer tissue in group A than that in group B. It seems that MMP-2 was related to prognosis of HCC.

Over-expression of c-*myc* oncogene could promote cellular proliferation and cancerous invasion, it is related to prognosis of HCC. Wang *et al*, evaluated the association of c-*myc* amplification with the prognosis of patients with HCC, they demonstrated that c-*myc* amplifications in single nodular

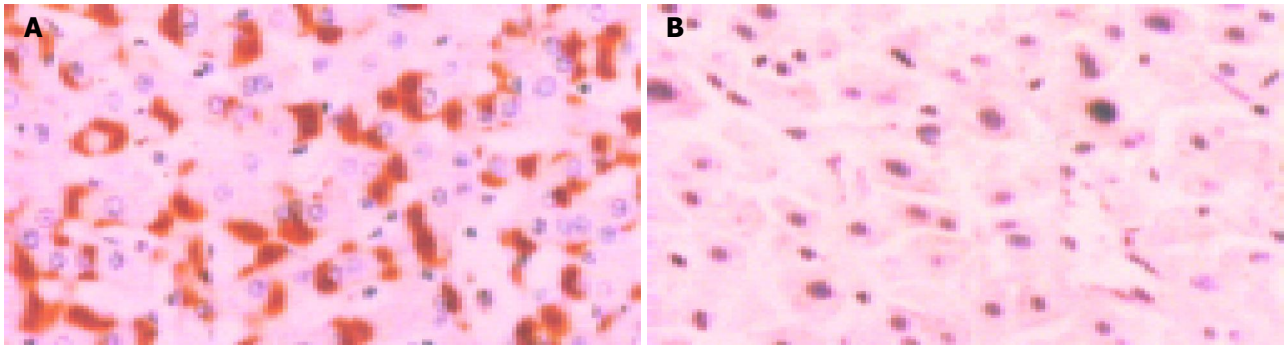

Figure 3 Positive and negative MMP-2 (×400). **A**: Positive MMP-2; **B**: Negative MMP-2.

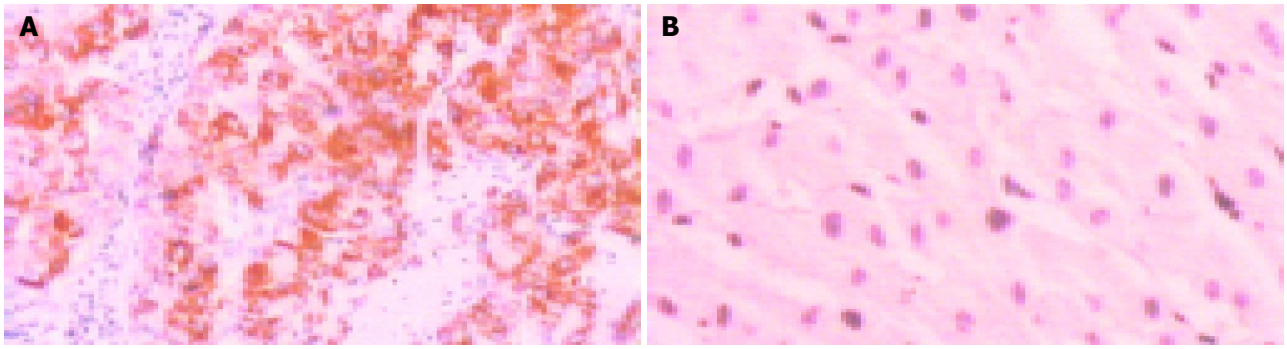

Figure 4 Positive and negative VEGF (×400). **A**: Positive VEGF; **B**: Negative VEGF.

and multiple-nodular HCCs were significantly different (12% *vs* 38%, $P<0.01$). More frequent c-*myc* amplification was detected in metastatic HCC (45%) compared with primary HCC (29%) and in recurrent HCC (60%) compared with primary HCC (38%). The results strongly suggest that amplification of the c-*myc* oncogene was correlated with a poor prognosis[20]. It was demonstrated *in vitro* that the block of c-*myc* expression could suppress the growth of hepatoma cells[21].

Ki-67 proliferation associated antigen was used for determining the cellular proliferation and prognosis of patients with tumor. Ki-67 could label any proliferating cells in cellular cycle except cells in G_0 stage, however, it could not label cells in silent period, so Ki-67 was considered as an objective marker indicating cell proliferation. Ki-67 locates in cell nucleus, it is always in particle shapes in immunohistochemical staining. King *et al*, reported 67 cases of HCC undergoing tumor resection, no other treatment (TAE, TACE) was performed before resection. Immunohistochemical staining showed that Ki-67 labeling index in cancer tissue was much higher than that in normal liver, the survival period of HCC patients with a Ki-67 labeling index >10% was shorter than those with a Ki-67 labeling index ≤10%. Ki-67 expression helped to select treatment method after tumor resection[22]. Ito *et al*[23], reported that HCCs with high expression of Ki-67 had the characters of poor cell differentiation, with portal vein invasion, high chance of stage III and intrahepatic metastasis, short survival period.

Vascular endothelial growth factor (VEGF) is known to promote the development of new blood vessels, which is fundamental to tumor growth and metastasis. Expression of VEGF in HCC tissue was positively correlated with growth and metastasis of HCC, it could be a marker for determining prognosis of HCC[24,25]. Expression of VEGF was strongly correlated with microvessel density (MVD) and tumor size[26,27]. Overproduction of the angiogenic growth factor VEGF by HCC cells may increase vascularity and tumor growth in a paracrine manner[28]. Preoperative serum VEGF was increased in patients with resectable HCC compared with healthy controls. Increased serum VEGF was correlated with HCC recurrence[29]. Multivariate analysis showed that serum VEGF was the most significant predictor of disease-free survival (DFS) and overall survival (OS) in HCC patients after surgical resection. So preoperative serum VEGF is a significant independent predictor of tumor recurrence, DFS, and OS in patients with resectable HCC[30]. The frequency of venous invasion in HCC patients with a high serum VEGF level was significantly greater compared with patients with a low serum VEGF level. It demonstrated that a high preoperative serum VEGF level was a predictor of microscopic venous invasion in HCCs and could be used as a biologic marker of tumor invasiveness and a prognostic factor in HCCs[31,32]. The expression of VEGF mRNA was higher in HCCs with portal vein tumor thrombus (PVTT) than that without PVTT. PVTT was more often seen in HCC patients with positive expression of VEGF mRNA than in patients who had negative expression. VEGF correlated well with the formation of PVTT of HCC[33].

A regression equation predicting prognosis of HCC

using binary logistic regression analysis was constructed, it demonstrated in the equation that c-*myc*, Ki-67, and VEGF expressions were greatly related to prognosis of HCC, however, MMP-2 did not enter the equation, which demonstrated that MMP-2 was not closely related to prognosis of HCC. Taken together, it could be inferred that high expressions of c-*myc*, Ki-67, and VEGF in HCC tissue were related to prognosis of HCC. The regression equation was verified further with patients in PMCT group, it demonstrated that total coincidence rate was 80.49%, it could be used as a kind of prognosis predicting method for HCC patients, and help HCC patients to select individualized treatment method.

Some scholars predicted that the focal point of HCC research in the 21st century would be recurrence and/or metastasis. With currently available techniques (surgical resection or thermal coagulation), it is no problem to have HCC nodules with maximum size less than 5 cm fully resected or coagulated. Post-treatment recurrence is a problem puzzling clinicians. Some recurrence occurs within 1 year after resection. Considering that surgical resection for HCC had the disadvantage of suppressing immunological function at an early stage, PMCT treatment for HCC had the advantage of enhancing local tumor and whole-body immunological functions[2]. The following points should be considered in choosing treatment methods for HCC whose maximum size is less than 5 cm: ultrasound guided biopsy should be performed for suspected HCC patients to confirm its pathological diagnosis; if it is diagnosed as HCC, immunohistochemical staining of c-*myc*, Ki-67, and VEGF and quantitative analysis of the molecules should be performed; the prognosis of the patients could be predicted with the regression equation in this paper. If the predicted value is less than 0.5, then the patient has the tendency of high recurrence even after surgical resection; if the predicted value is more than 0.5, then the patient does not have the tendency of high recurrence after surgical resection. The former, micro-trauma methods such as PMCT or TACE should be chosen for treatment, meanwhile, other auxiliary methods such as biological and traditional Chinese medicine treatment should be adopted, and moreover, close follow-up should be done to detect new lesions. For the latter, surgical resection is suggested.

REFERENCES

1 **Regimbeau JM,** Abdalla EK, Vauthey JN, Lauwers GY, Durand F, Nagorney DM, Ikai I, Yamaoka Y, Belghiti J. Risk factors for early death due to recurrence after liver resection for hepatocellular carcinoma: results of a multicenter study. *J Surg Oncol* 2004; **85**: 36-41

2 **Dong BW,** Zhang J, Liang P, Yu XL, Su L, Yu DJ, Ji XL, Yu G. Sequential pathological and immunologic analysis of percutaneous microwave coagulation therapy of hepatocellular carcinoma. *Int J Hyperthermia* 2003; **19**: 119-133

3 **Levy AE,** Kowdley KV. Unresectable hepatocellular carcinoma: the need for an individualized multidisciplinary approach. *J Clin Gastroenterol* 2001; **33**: 180-182

4 **Harrison LE,** Koneru B, Baramipour P, Fisher A, Barone A, Wilson D, Dela Torre A, Cho KC, Contractor D, Korogodsky M. Locoregional recurrences are frequent after radiofrequency ablation for hepatocellular carcinoma. *J Am Coll Surg* 2003; **197**: 759-764

5 **Chen JY,** Chau GY, Lui WY, Tsay SH, King KL, Wu CW. Clinicopathologic features and factors related to survival of patients with small hepatocellular carcinoma after hepatic resection. *World J Surg* 2003; **27**: 294-298

6 **Daveau M,** Scotte M, Francois A, Coulouarn C, Ros G, Tallet Y, Hiron M, Hellot MF, Salier JP. Hepatocyte growth factor, transforming growth factor alpha, and their receptors as combined markers of prognosis in hepatocellular carcinoma. *Mol Carcinog* 2003; **36**: 130-141

7 **Armengol C,** Boix L, Bachs O, Sole M, Fuster J, Sala M, Llovet JM, Rodes J, Bruix J. p27(Kip1) is an independent predictor of recurrence after surgical resection in patients with small hepatocellular carcinoma. *J Hepatol* 2003; **38**: 591-597

8 **Kobayashi T,** Sugawara Y, Shi YZ, Makuuchi M. Telomerase expression and p53 status in hepatocellular carcinoma. *Am J Gastroenterol* 2002; **97**: 3166-3171

9 **Ling X,** Chen W, Liu S, Wang G. Expression of TGF-beta in region of bone defect repaired by collagen/nano-beta-tricalcium phosphate composite artificial bone. *J Huazhong Univ Sci Technolog Med Sci* 2003; **23**: 302-305

10 **Baech J,** Roer O, Johnsen HE. Individual quality assessment of autografting by probability evaluation: a model estimated by analysis of graft-related end points in 204 patients with malignancies. *Bone Marrow Transplant* 2003; **31**: 453-458

11 **Tan CK,** Law NM, Ng HS, Machin D. Simple clinical prognostic model for hepatocellular carcinoma in developing countries and its validation. *J Clin Oncol* 2003; **21**: 2294-2298

12 **Ueno S,** Tanabe G, Nuruki K, Oketani M, Komorizono Y, Hokotate H, Fukukura Y, Baba Y, Imamura Y, Aikou T. Prognosis of hepatocellular carcinoma associated with Child class B and C cirrhosis in relation to treatment: a multivariate analysis of 411 patients at a single center. *J Hepatobiliary Pancreat Surg* 2002; **9**: 469-477

13 **Ito Y,** Takeda T, Sakon M, Tsujimoto M, Higashiyama S, Noda K, Miyoshi E, Monden M, Matsuura N. Expression and clinical significance of erb-B receptor family in hepatocellular carcinoma. *Br J Cancer* 2001; **84**: 1377-1383

14 **Horiguchi N,** Takayama H, Toyoda M, Otsuka T, Fukusato T, Merlino G, Takagi H, Mori M. Hepatocyte growth factor promotes hepatocarcinogenesis through c-Met autocrine activation and enhanced angiogenesis in transgenic mice treated with diethylnitrosamine. *Oncogene* 2002; **21**: 1791-1799

15 **Chen TH,** Tseng LM, Chau GY, Lui WY, Tsay SH, King KL, Loong CC, Hsia CY, Wu CW. Clinicopathologic and prognostic differences between patients with hepatitis B- and C-related resectable hepatocellular carcinoma. *J Formos Med Assoc* 2001; **100**: 443-448

16 **Mino M,** Lauwers GY. Pathologic spectrum and prognostic significance of underlying liver disease in hepatocellular carcinoma. *Surg Oncol Clin N Am* 2003; **12**: 13-24

17 **Chen GG,** Merchant JL, Lai PB, Ho RL, Hu X, Okada M, Huang SF, Chui AK, Law DJ, Li YG, Lau WY, Li AK. Mutation of p53 in recurrent hepatocellular carcinoma and its association with the expression of ZBP-89. *Am J Pathol* 2003; **162**: 1823-1829

18 **Ishii Y,** Nakasato Y, Kobayashi S, Yamazaki Y, Aoki T. A study on angiogenesis-related matrix metalloproteinase networks in primary hepatocellular carcinoma. *J Exp Clin Cancer Res* 2003; **22**: 461-470

19 **Kuyvenhoven JP,** van Hoek B, Blom E, van Duijn W, Hanemaaijer R, Verheijen JH, Lamers CB, Verspaget HW. Assessment of the clinical significance of serum matrix metalloproteinases MMP-2 and MMP-9 in patients with various chronic liver diseases and hepatocellular carcinoma. *Thromb Haemost* 2003; **89**: 718-725

20 **Wang Y,** Wu MC, Sham JS, Zhang W, Wu WQ, Guan XY. Prognostic significance of c-myc and AIB1 amplification in hepatocellular carcinoma. A broad survey using high-throughput tissue microarray. *Cancer* 2002; **95**: 2346-2352

21 **Cheng J,** Luo J, Zhang X, Hu J, Hui H, Wang C, Stern A. Inhibition of cell proliferation in HCC-9204 hepatoma cells by a c-myc specific ribozyme. *Cancer Gene Ther* 2000; **7**: 407-412

22 **King KL,** Hwang JJ, Chau GY, Tsay SH, Chi CW, Lee TG, Wu

LH, Wu CW, Lui WY. Ki-67 expression as a prognostic marker in patients with hepatocellular carcinoma. *J Gastroenterol Hepatol* 1998; **13**: 273-279

23 **Ito Y,** Matsuura N, Sakon M, Takeda T, Umeshita K, Nagano H, Nakamori S, Dono K, Tsujimoto M, Nakahara M, Nakao K, Monden M. Both cell proliferation and apoptosis significantly predict shortened disease-free survival in hepatocellular carcinoma. *Br J Cancer* 1999; **81**: 747-751

24 **Zhao ZC,** Zheng SS, Wan YL, Jia CK, Xie HY. The molecular mechanism underlying angiogenesis in hepatocellular carcinoma: the imbalance activation of signaling pathways. *Hepatobiliary Pancreat Dis Int* 2003; **2**: 529-536

25 **Dhar DK,** Naora H, Yamanoi A, Ono T, Kohno H, Otani H, Nagasue N. Requisite role of VEGF receptors in angiogenesis of hepatocellular carcinoma: a comparison with angiopoietin/Tie pathway. *Anticancer Res* 2002; **22**: 379-386

26 **Poon RT,** Lau CP, Ho JW, Yu WC, Fan ST, Wong J. Tissue factor expression correlates with tumor angiogenesis and invasiveness in human hepatocellular carcinoma. *Clin Cancer Res* 2003; **9**: 5339-5345

27 **Ng IO,** Poon RT, Lee JM, Fan ST, Ng M, Tso WK. Microvessel density, vascular endothelial growth factor and its receptors Flt-1 and Flk-1/KDR in hepatocellular carcinoma. *Am J Clin Pathol* 2001; **116**: 838-845

28 **Moon WS,** Rhyu KH, Kang MJ, Lee DG, Yu HC, Yeum JH, Koh GY, Tarnawski AS. Overexpression of VEGF and angiopoietin 2: a key to high vascularity of hepatocellular carcinoma? *Mod Pathol* 2003; **16**: 552-557

29 **Zhao J,** Hu J, Cai J, Yang X, Yang Z. Vascular endothelial growth factor expression in serum of patients with hepatocellular carcinoma. *Chin Med J (Engl)* 2003; **116**: 772-776

30 **Chao Y,** Li CP, Chau GY, Chen CP, King KL, Lui WY, Yen SH, Chang FY, Chan WK, Lee SD. Prognostic significance of vascular endothelial growth factor, basic fibroblast growth factor, and angiogenin in patients with resectable hepatocellular carcinoma after surgery. *Ann Surg Oncol* 2003; **10**: 355-362

31 **Poon RT,** Ng IO, Lau C, Zhu LX, Yu WC, Lo CM, Fan ST, Wong J. Serum vascular endothelial growth factor predicts venous invasion in hepatocellular carcinoma: a prospective study. *Ann Surg* 2001; **233**: 227-235

32 **Kwak BK,** Shim HJ, Park ES, Kim SA, Choi D, Lim HK, Park CK, Chung JW, Park JH. Hepatocellular carcinoma: correlation between vascular endothelial growth factor level and degree of enhancement by multiphase contrast-enhanced computed tomography. *Invest Radiol* 2001; **36**: 487-492

33 **Zhou J,** Tang ZY, Fan J, Wu ZQ, Li XM, Liu YK, Liu F, Sun HC, Ye SL. Expression of platelet-derived endothelial cell growth factor and vascular endothelial growth factor in hepatocellular carcinoma and portal vein tumor thrombus. *J Cancer Res Clin Oncol* 2000; **126**: 57-61

Science Editor Zhu LH **Language Editor** Elsevier HK

PO Box 2345, Beijing 100023, China
www.wjgnet.com
wjg@wjgnet.com

ELSEVIER

World J Gastroenterol 2005;11(20):3034-3039
World Journal of Gastroenterology ISSN 1007-9327

Clinicopathological significance of loss of heterozygosity and microsatellite instability in hepatocellular carcinoma in China

Shu-Hui Zhang, Wen-Ming Cong, Zhi-Hong Xian, Meng-Chao Wu

Shu-Hui Zhang, Wen-Ming Cong, Zhi-Hong Xian, Meng-Chao Wu, Department of Pathology, Eastern Hepatobiliary Surgery Hospital, Second Military Medical University, Shanghai 200438, China
Supported by the National Natural Science Foundation of China, No. 30370645 and the Hundred Leading Scientists Program of the Public Health Sector of Shanghai, No. 98BR007
Correspondence to: Wen-Ming Cong, Department of Pathology, Eastern Hepatobiliary Surgery Hospital, Second Military Medical University, Shanghai 200438, China. zhangshuhui100@sohu.com
Telephone: +86-21-25070860 Fax: +86-21-25070854
Received: 2004-06-19 Accepted: 2004-07-22

Abstract

AIM: To determine the features of microsatellite alterations and their association with clinicopathological characteristics of hepatocellular carcinoma (HCC).

METHODS: Loss of heterozygosity (LOH) and microsatellite instability (MSI) of 55 microsatellite loci were detected with PCR-based microsatellite polymorphism analyses in tumors and corresponding noncancerous liver tissues of 56 surgically resected HCCs using the MegaBACE 500 automatic DNA analysis system.

RESULTS: LOH was found in 44 of 56 HCCs (78.6%) at one or several loci. Frequencies of LOH on 1p, 4q, 8p, 16q, and 17p were 69.6% (39/56), 71.4% (40/56), 66.1% (37/56), 66.1% (37/56), and 64.3% (36/56), respectively. MSI was found in 18 of 56 HCCs (32.1%) at one or several loci. Ten of fifty-six (17.9%) HCCs had MSI-H. Serum HBV infection, alpha-fetoprotein concentration, tumor size, cirrhosis, histological grade, tumor capsule, as well as tumor intrahepatic metastasis, might be correlated with LOH on certain chromosome regions.

CONCLUSION: Frequent microsatellite alterations exist in HCC. LOH, which represents a tumor suppressor gene pathway, plays a more important role in hepatocarcinogenesis. MSI, which represents a mismatch repair gene pathway, is a rare event during liver carcinogenesis. Furthermore, LOH on certain chromosome regions may be correlated with clinicopathological characteristics in HCC.

Key words: Microsatellite alterations; Hepatocellular carcinoma

Zhang SH, Cong WM, Xian ZH, Wu MC. Clinicopathological significance of loss of heterozygosity and microsatellite instability in hepatocellular carcinoma in China. *World J Gastroenterol* 2005; 11(20): 3034-3039
http://www.wjgnet.com/1007-9327/11/3034.asp

INTRODUCTION

Hepatocellular carcinoma (HCC) is one of the most frequent human cancers worldwide and has become the second cancer killer in China, since the 1990s[1]. Epidemiological studies in high-risk populations have identified chronic hepatitis B or C virus infections as well as dietary exposure to aflatoxin B1 as major factors in the etiology of this disease[2]. The genesis of human cancers is a multistep process reflecting cumulative genetic alterations that include activation of oncogenes or inactivation of tumor suppressor genes[3,4]. It has been proposed that genetic instability or genomic instability in human cancers can be divided into two types: chromosomal instability or loss of heterozygosity (LOH), which can result from errors in chromosome partitioning, and microsatellite instability (MSI), which is usually equated with DNA polymerase errors. Both LOH and MSI are considered to be phenotypes of genomic instability[5,6]. LOH is frequently observed on chromosomes 1p, 4q, 5q, 8p, 8q, 9p, 10q, 11p, 13q, 14q, 16q, 17p, and 22q in HCC, which suggests that tumor suppressor genes may take part in hepatocarcinogenesis[7-9]. MSI and mutations of mismatch repair gene have been reported in chronic hepatitis, cirrhosis and HCC in recent studies[10-14]. In the present study, we examined the genetic instability in 56 HCCs with 55 high-polymorphic microsatellite markers of chromosomes 1, 4, 8, 16, and 17, and analyzed the association of microsatellite alterations and the clinicopathological characteristics of HCC, in order to further understand the molecular mechanisms of hepatocarcinogenesis.

MATERIALS AND METHODS

Patients and samples

Fifty-six liver cancer specimens from surgically resected tissues were obtained from Eastern Hepatobiliary Surgery Hospital, Second Military Medical University. All patients have not received any prior therapy. All specimens were confirmed with histopathological examination. This study included 43 men and 13 women. The age ranged from 29 to 78 years. Thirty-five of fifty-six patients had serum alpha-fetoprotein (AFP) $\geqslant$20 μg/L. There were 39 cases positive for HBsAg. Twelve cases had small HCCs ($\leqslant$3 cm) and 44 had advanced HCCs (>3 cm). Histopathological diagnosis was made according to the WHO histological classification

of tumors of the liver and intrahepatic bile ducts (2 000). Twenty HCCs were well differentiated, 28 were moderately differentiated and 8 were poorly differentiated. Of the 56 patients, 45 had evidence of intrahepatic metastasis (portal vein invasion and/or intrahepatic dissemination). Forty-seven HCCs were detected accompanying liver cirrhosis.

DNA extraction

Fresh samples were obtained, immediately frozen in liquid nitrogen and stored at -80 ℃ until analysis. A microdissection technique with a cryostat was used to separate tumor cells from corresponding noncancerous liver tissues. Genomic DNA was extracted from carcinoma tissue and corresponding noncancerous liver tissues, using the standard phenol/chloroform method[15]. Concentration of DNA was determined with both spectrophotometric and fluorometric methods.

Microsatellite markers and polymerase chain reaction

Fifty-five microsatellite loci used in this study with chromosomal positions are listed in Table 1. The chromosomal positions and sequences of each microsatellite marker could be referenced to the genome database (http://gdbwww.gdb.org/) and the co-operative human linkage center (http://www.chlc.org/). Each primer pair was fluorescent dye labeled. The PCR mixture contained more than 10 ng of genomic DNA, 200 μmol/L of each dNTP, 1.5 mmol/L $MgCl_2$, 0.5 unit of AmpliTaq Gold DNA polymerase (PE Applied Biosystems, Foster City, CA, USA), 0.5 μmol/L of each primer, and 10× AmpliTaq Gold PCR buffer in a final volume of 10 μL. After denaturation at 94 ℃ for 12 min, DNA amplification was performed for 15 cycles at 94 ℃ for 30 s, at 63 ℃ for 60 s (decreased 0.5 ℃ of each cycle), and at 72 ℃ for 90 s; then for 25 cycles at 94 ℃ for 30 s, at 56 ℃ for 60 s, and at 72 ℃ for 90 s; with a final extension at 72 ℃ for 10 min. PCRs were run in a Biometra thermocycler (Biometra, Germany).

Microsatellite analysis

PCR products were purified by 70% alcohol, twice after amplification. The reaction conditions sometimes yielded an unsatisfactory amplification for certain markers and were modified, and if necessary, these particular markers were run singly. The injection mixture was prepared for each capillary buffer by adding the following to each well of the injection palate: 2 μL purified sample, 0.25 μL ET400-R size standard, and 2.75 μL loading solution (Amersham Pharmacia Biotech). The injection mixture was centrifuged and heat-denatured for 2 min at 94 ℃, then immediately cooled and placed on ice. Samples were electrophoresed on the MegaBACE-500 capillary array electrophoresis sequencer, and the fluorescent signals from different sized alleles were recorded and analyzed using Genetic Profiler version 2.1 software.

Identification of LOH and MSI

The existence of LOH or MSI was determined by comparing the area between cancerous tissues and corresponding noncancerous liver tissues. When two amplified bands per locus were detected in noncancerous liver tissue specimens, the case was defined as informative for analysis (Figure 1A). It was abandoned when only one amplified band per locus was detected in noncancerous liver tissue specimens (Figure 1B). For a given informative marker, LOH was identified when one of two bands was absent between the tumor DNA and normal DNA (Figure 2). MSI was assessed using the five markers recommended by the NCI workshop. MSI high (MSI-H) HCCs were defined as those having two unstable markers of the five markers (D2S123, BAT-26, D5S346, D13S170, and D17S250). MSI was defined as a band shift in one of the two alleles or the presence of novel bands in the two alleles or in the tumor DNA (Figure 3)[16]. Analysis of LOH and MSI was performed at least in duplicate.

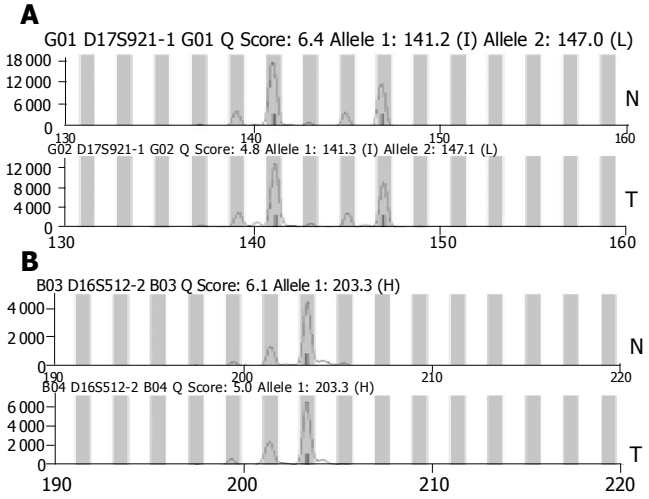

Figure 1 Heterozygosity on loci D17S921 (**A**) and D16S512 (**B**) in a non-informative case. N: non-tumor liver tissue, T: tumor tissue.

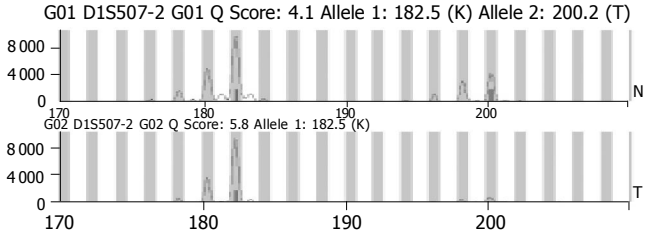

Figure 2 LOH on locus D1S507. N: non-tumor liver tissue, T: tumor tissue.

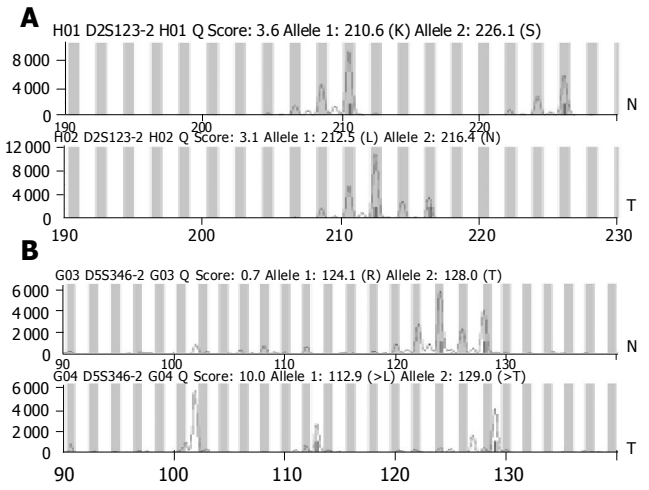

Figure 3 MSI on loci D2S123 (**A**) and D5S346 (**B**). N: non-tumor liver tissue, T: tumor tissue.

Statistical analysis

The differences between the frequency of LOH and clinicopathological features were statistically analyzed using χ^2 test. $P<0.05$ was considered statistically significant.

RESULTS

Frequency of LOH and MSI

LOH was found in 44 of 56 HCCs (78.6%) at one or several loci. The frequency of LOH in HCC at 55 loci is shown in Table 1. Frequencies of LOH on 1p, 4q, 8p, 16q, and 17p were 69.6% (39/56), 71.4% (40/56), 66.1% (37/56), 66.1% (37/56), and 64.3% (36/56), respectively. The loci with the highest frequency of LOH were RIZ (76.7%) on 1p, D4S426 (61%) on 4q, D8S261 (53.5%) on 8p, D16S3091 (59.5%) on 16q and D17S831 (67.6%) on 17p. We performed MSI analysis using the five markers recommended by the NCI workshop. MSI was found in 18

Table 1 Characteristics of microsatellite markers analyzed and patterns of microsatellite alteration in HCC

Locus	Location	Allelic size (bp)	Heterozygosity (%)	Informative cases	LOH *n* (%)	MSI *n* (%)
D1S243	1p36.3	142–170	0.86	35	16 (45.7)	3 (8.57)
D1S468	1p36.3	173–191	0.75	35	13 (37.1)	3 (8.57)
D1S2893	1p36.2	201–223	0.47	44	18 (40.9)	2 (4.55)
D1S2694	1p36.2	241–255	0.65	38	16 (42.1)	1 (2.63)
D1S450	1p36.2	243–267	0.81	38	17 (44.7)	1 (2.63)
D1S434	1p36.2	240–252	0.61	42	15 (35.7)	0
RIZ	1p36.2	–	–	30	23 (76.7)	0
D1S507	1p36.1	183–203	0.78	45	24 (53.3)	2 (4.44)
D1S199	1p36.1	94–116	0.84	39	14 (35.9)	1 (2.56)
D1S234	1p36.1	268–294	0.50	37	14 (37.8)	3 (8.11)
D4S1538	4q22	149–161	0.69	41	17 (41.5)	0
D4S1534	4q22	146–158	0.77	41	22 (53.7)	0
D4S406	4q26	234–258	0.87	42	22 (52.4)	1 (2.38)
D4S1625	4q27-31	182–210	0.74	38	13 (34.2)	1 (2.63)
D4S1652	4q31.1	115–125	0.75	38	16 (42.1)	0
D4S1615	4q34-qter	138–150	0.71	39	19 (48.7)	0
D4S2361	4q	149–164	0.70	42	15 (35.7)	1 (2.38)
D4S1554	4q35	184–208	0.86	37	14 (37.8)	0
D4S426	4q35	177–191	0.78	41	25 (61)	0
D4S2921	4q35	141–163	0.56	44	23 (52.3)	2 (4.55)
D8S264	8p23	121–145	0.83	43	19 (44.2)	1 (2.32)
D8S277	8p23	148–180	0.73	38	18 (47.4)	1 (2.63)
D8S1706	8p23	257–281	0.88	41	20 (48.9)	1 (2.43)
D8S1721	8p23	170–212	0.71	40	21 (52.5)	0
D8S520	8p23	179–199	0.77	40	20 (50.0)	2 (5.00)
D8S549	8p22	166–172	0.61	44	20 (45.5)	2 (4.55)
D8S261	8p22	128–144	0.79	43	23 (53.5)	1 (2.33)
D8S298	8p22	155–167	0.68	44	23 (52.3)	1 (2.27)
D8S1733	8p21	253–257	0.64	38	17 (44.7)	1 (2.63)
D8S1771	8p21	218–240	0.77	40	21 (52.5)	1 (2.50)
D16S408	16q13	–	–	41	17 (41.5)	1 (2.22)
D16S512	16q22.1	201–211	0.77	45	20 (44.4)	6 (13.3)
D16S515	16q22.1	222–244	0.81	36	12 (33.3)	2 (5.56)
D16S507	16q24.1	175–195	0.78	44	20 (45.5)	4 (9.09)
D16S534	16q24.2	296–364	0.87	42	21 (50.0)	5 (11.9)
D16S3091	16q24.2	115–129	0.72	42	22 (59.5)	2 (4.76)
D16S422	16q24.2	188–212	0.79	42	23 (54.8)	2 (4.76)
D16S520	16q24.3	181–197	0.84	44	19 (43.2)	2 (4.55)
D16S413	16q24.2	208–246	0.68	36	16 (44.4)	2 (5.56)
D16S498	16q24.3	131–149	0.84	46	23 (50.0)	1 (2.17)
D17S849	17p13.3	251–261	0.69	39	21 (53.9)	1 (2.56)
D17S926	17p13.3	243–259	0.81	36	21 (58.3)	1 (2.78)
D17S831	17p13.3	224–246	0.81	37	25 (67.6)	3 (8.11)
D17S938	17p13.1-p13.3	164–182	0.76	42	21 (50.0)	0
D17S786	17p13.1	–	–	39	15 (38.5)	1 (2.56)
D17S520	17p13.1	135–157	0.77	40	15 (37.5)	2 (5.00)
D17S799	17p13-p12	–	0.80	42	21 (50.0)	2 (4.76)
D17S921	17p12	186–200	0.70	39	15 (38.5)	0
D17S261	17p11.2	169–185	0.72	41	15 (36.6)	1 (2.44)
TP53	17p11.2	157–171	0.54	7	4 (57.1)	0
D2S123	hMSH-2	197–227		36	3	7 (19.4)
BAT-26		116		37	2	9 (24.3)
D5S346	APC	96–122		41	1	8 (19.5)
D13S170	Rb	220–240		32	4	7 (21.9)
D17S250		151–169		33	3	5 (15.2)

of 56 HCCs (32.1%) at one or several loci. The frequency of MSI was as follows: 10 of 56 (17.9%) HCCs had MSI-H, 8 of 56 (14.3%) had MSI-L. The top two loci were BAT-26 (9/37, 24.3%) and D13S170 (7/32, 21.9%). All seven cases were positive serum HBsAg, of them five were positive for serum HBsAg. There was no significant difference in viral status between the cases with and without MSI. MSI-L was also found in some loci except these five loci.

Relationship between LOH and clinicopathological characteristics

To determine whether LOH was associated with clinicopathological features and to reveal its biological role in HCC development and/or progression, we compared LOH with clinicopathological findings including HBV infection, serum AFP concentration, tumor size, cirrhosis, histological grade, tumor capsule, and tumor intrahepatic metastasis. However, no statistically significant association was found between total LOH and clinicopathological findings. Correlation between clinicopathological features and LOH in HCC is shown in Table 2.

Table 2 Clinicopathologic correlation of LOH in HCC

Parameter	Locus	LOH/informative cases		*P*
HBsAg		Positive	Negative	
	D1S2893	17/31	1/13	0.004
	D1S507	13/21	1/16	0.001
	D4S406	20/26	2/16	0.001
	D8S277	16/22	2/16	0.001
	D8S261	10/27	13/16	0.005
	D8S298	11/29	12/15	0.008
	D8S1733	7/24	10/14	0.011
	D16S512	10/31	10/14	0.014
	D16S515	5/27	7/9	0.001
	D17S831	19/21	6/16	0.001
	D17S938	19/25	2/14	0.001
	D17S926	13/27	8/9	0.032
AFP(μg/L)		<20	⩾20	
	D1S507	3/17	21/29	0.001
	D16S413	9/12	7/24	0.009
Liver cirrhosis		Present	Absent	
	D16S534	20/34	1/9	0.011
	D16S3091	24/33	1/9	0.001
	D16S422	22/34	1/8	0.008
	D17S849	21/31	1/8	0.005
	D17S831	24/39	1/8	0.011
	D17S799	20/35	1/7	0.038
Tumor size		⩽3 cm	>3 cm	
	D8S298	2/9	21/35	0.043
	D8S1771	0/9	21/31	0.001
	D16S498	4/12	19/24	0.007
	D17S926	3/11	18/25	0.012
Histological grade		Well	Moderate and poor	
	D4S426	2/11	23/30	0.002
	D4S1615	2/12	14/26	0.04
	D4S1652	2/11	17/28	0.031
	D16S498	2/18	21/29	0.001
	D17S926	4/13	17/23	0.012
Tumor capsule		Absent or not intact	Intact	
	D8S1721	20/28	1/12	0.001
Intrahepatic metastasis		Not observed	Observed	
	D1S468	8/10	5/25	0.001
	D4S2921	2/21	21/23	0.023
	D8S298	2/10	21/34	0.02
	D8S1771	2/9	19/31	0.039
	D17S926	1/11	20/25	0.001
	D17S786	0/10	15/29	0.004

DISCUSSION

Recently, genomic alterations in HCC have been studied by comparative genomic hybridization, and several chromosome changes have been reported. The gain of 1q, 8q, and 17q and the loss of 4q, 8p, 13q, 16q and 17p were commonly found in HCC. The chromosome regions with gain contained critical oncogenes, whereas those with loss contained tumor suppressor genes[17-19]. Frequent LOH on chromosomes 1p, 4q, 6p, 8p, 13q, 16q, and 17p by whole genome allelotyping suggested that putative tumor suppressor genes on these chromosome regions might play important roles in the development and progression of HCC[7-9].

Frequent deletions and translocations of the short arm of chromosome 1 (1p) have been found in HCCs by cytogenetic analysis, *in situ* hybridization, RFLP and microsatellite analysis, and mapped a commonly affected LOH region to 1p35-36[8,20]. In the present study, LOH was found in 39 of 56 HCCs (69.6%) on at least 1 locus, the top two loci were RIZ (76.7%) at 1p36.2 and D1S199 (53.3%) at 1p36.1. Early studies have demonstrated that high frequency of LOH on chromosome 4q in HCC was mapped to 4q11-q12, 4q12-23, 4q22-24 and 4q35[8,21]. Our data also showed that LOH was found in 71.4% HCCs on at least one locus, the top two loci were D4S426 (61%) at 4q35, and D4S1534 (53.7%) at 4q22. A high frequency of LOH on chromosome 8p has been reported in HCC and other cancers[22,23]. Nagai *et al*[8] reported that 42% of HCCs had LOH on 8p21-23 and argued that a tumor suppressor gene for HCC located in this region. Candidate tumor suppressor genes, such as *PRLTS* gene, *DLC-1* gene, and *EXTR1* gene located on 8p21-22, have been found to be mutated in a variety of tumors, including HCC, ovarian cancers, breast cancer and sporadic colorectal carcinoma[24-27]. Our study showed that LOH was found in 37 of 56 HCCs (66.1%) on at least 1 locus, the top three loci were D8S261 (53.5%) at 8p22, D8S1721 (52.5%) at 8p23 and D8S1771 (52.5%) at 8p21. The highest LOH regions were mapped to 16q12.1, 16q12.2 and 16q22-24[8,21,28]. Our data also showed that 71.4% HCCs harbored LOH on at least 1 locus, the alterations occurring in the top two loci were D16S3091 (59.5%) and D16S422 (54.8%) at 16q24.2. These regions contain many important genes, such as adenine phosphoribosyl transferase (APRT, 16q24.2) and *N*-acetylgalactosamine-6-sulfatase (GALNS, 16q24.2). The deletion of these genes in this region might interfere with cell growth or function[28]. LOH of 17p in 70% has been reported previously[29]. A missense mutation with replacement of arginine by serine at codon 249 has been reported previously in HCCs from Qidong, Shanghai and other geographical areas where aflatoxin and HBV are present[30]. Our data revealed a high level of LOH in D17S831 (67.6%) and D17S926 (58.3%) at 17p13.3. Zhao *et al*[31], also found a novel growth suppressor gene on chromosome 17p13.3 with a high frequency of mutation in human HCC. These results suggest that tumor suppressor genes at 1p36, 4q22, 4q35, 8p22-23, 16q24.2, and 17p13.3 may be involved in hepatocarcinogenesis.

HBV infection has been regarded as an important factor in the development of HCC[32]. However, the molecular mechanism is unclear. Wong *et al*[18], have assessed the

genome-wide chromosomal analysis in 83 tumor samples from Hong Kong, Shanghai, Japan, and USA by comparative genomic hybridization. The most striking feature from the analysis was the high number of aberrations per sample in the HBV-related cases from Shanghai, which was significantly more than that in the other groups. Becker *et al*[33], have shown frequent loss of chromosome 8p in HBV-positive HCC from China. In this study, we found that the incidences of LOH on D1S2893, D1S507, D4S406, D8S277, D17S831, and D17S938 were significantly higher in patients with positive serum HBsAg than in those with negative HBsAg. These data imply that HBV infection might cause genetic changes within chromosomal regions where this is important for the development of some HCCs. Interestingly, LOH on D4S1538, D8S261, D8S298, D8S1733, D16S512, D16S515, and D17S926 occurred more frequently in HBsAg-negative patients than in HBsAg-positive patients. These results suggest that the tumor suppressor genes near these loci might be responsible for HBV-negative HCC.

Aggressive tumor phenotypes such as larger tumor size, poor cellular differentiation, absence of tumor encapsulation and intrahepatic metastasis were associated with LOH at several specific loci[34,35]. LOH was associated with an elevated serum AFP[21]. LOH on D8S298 at 8p22 was closely associated with venous permeation, tumor microsatellite formation, and larger tumor size[22]. LOH on locus D8S1721 at 8p23.1 was seen more frequently in nonencapsulated tumors and LOH on D8S1771 at 8p21.3 was associated with a larger tumor size and poorer cellular differentiation. LOH on D1S214 (lp36.3) and D1S2797 (1p34) was more frequently detected in tumors with intrahepatic metastasis than in those without[9]. In this study, large tumor size (>3 cm) tended to have a higher frequency of LOH on D8S298, D8S1771, D16S498, and D17S926. LOH on D4S426, D4S1615, D4S1652, D16S498, and D17S926 was more frequent in poorly or moderately differentiated HCC than in well-differentiated HCC. LOH frequencies of D8S1721 were significantly higher in patients without intact tumor capsule than in those with intact tumor capsule. LOH on D4S2921, D8S298, D8S1771, D17S926, and D17S786 were more frequently detected in tumors with intrahepatic metastasis than in those without. These results supported that 1p, 4q, 8p, 16q, and 17p deletions at specific loci were associated with tumor progression and aggressive behavior. Association of LOH at specific loci with a more aggressive tumor behavior suggests that loss/inactivation of putative tumor suppressor gene (s) located at these regions may confer a tumor growth advantage and contribute to the progression of HCC. This finding agrees with a previous report using CGH analysis, which suggested that the deletion was associated with tumor metastasis in HCC patients[35].

MSI with associated deficient DNA mismatch repair was first described in hereditary nonpolyposis colorectal cancer and has been implicated in the pathogenesis of a variety of gastrointestinal and other cancers[5]. It is noteworthy that there are some differences in MSI frequency of HCC reported in literatures. The MSI frequencies of HCC were 41-66.6% in Greece, USA and France[11,36]. However, Piao *et al*[37], and Yamamoto *et al*[38], reported the absence of MSI in Korean or Japanese HCCs, and considered that MSI played no role in the development or progression of HCC. Macdonald *et al*[39], found that the frequent LOH of MSI in HCC linked to hMSH2 and/or hMLH1 was only 19. 6%, usually in association with MSI. Besides, another recent study on Chinese HCCs spanning 22 autosomes using 292 highly polymorphic markers showed that MSI was rarely seen[28]. In our study, MSI was found in 18 of 56 HCCs (32.1%) at one or several loci. Ten of fifty-six (17.9%) HCCs had MSI-H. Cases mostly were positive for serum HBsAg. Some studies showed that the incidence of MSI in cirrhotic liver tissues (27%) was almost three times higher than that in noncancerous liver tissues exhibiting findings compatible with chronic hepatitis (10%). In addition, the incidence of MSI in cirrhotic liver tissues did not differ from the incidence in HCCs[40]. The above-mentioned discrepancies may be partly due to the difference in selected cases, the sensitivity of methodology, and the type and number of polymorphic markers used in these studies. The other factors such as different geographic area and different criteria for MSI might contribute to the difference.

In conclusion, frequent microsatellite LOH on chromosomes 1, 4, 8, 16, and 17 existed in HCC. LOH, representing a tumor suppressor gene pathway, plays a more important role in hepatocarcinogenesis. MSI is less frequently found than LOH, suggesting a minor role of DNA mismatch repair deficiency in liver carcinogenesis.

REFERENCES

1 **Tang ZY.** Treatment of hepatocellular carcinoma. *Digestion* 1998; **59**: 556-562
2 **Bosch FX,** Ribes J, Borras J. Epidemiology of primary liver cancer. *Semin Liver Dis* 1999; **19**: 271-285
3 **Thorgeirsson SS,** Grisham JW. Molecular pathogenesis of human hepatocellular carcinoma. *Nat Genet* 2002; **31**: 339-346
4 **Feitelson MA,** Sun B, Satiroglu Tufan NL, Liu J, Pan J, Lian Z. Genetic mechanisms of hepatocarcinogenesis. *Oncogene* 2002; **21**: 2593-2604
5 **Loeb LA,** Loeb KR, Anderson JP. Multiple mutations and cancer. *Proc Natl Acad Sci USA* 2003; **100**: 776-781
6 **Kawai H,** Suda T, Aoyagi Y, Isokawa O, Mita Y, Waguri N, Kuroiwa T, Igarashi M, Tsukada K, Mori S, Shimizu T, Suzuki Y, Abe Y, Takahashi T, Nomoto M, Asakura H. Quantitative evaluation of genomic instability as a possible predictor for development of hepatocellular carcinoma: comparison of loss of heterozygosity and replication error. *Hepatology* 2000; **31**: 1246-1250
7 **Buendia MA.** Genetics of hepatocellular carcinoma. *Semin Cancer Biol* 2000; **10**: 185-200
8 **Nagai H,** Pineau P, Tiollais P, Buendia MA, Dejean A. Comprehensive allelotyping of human hepatocellular carcinoma. *Oncogene* 1997; **14**: 2927-2933
9 **Li SP,** Wang HY, Li JQ, Zhang CQ, Feng QS, Huang P, Yu XJ, Huang LX, Liang QW, Zeng YX. Genome-wide analyses on loss of heterozygosity in hepatocellular carcinoma in Southern China. *J Hepatol* 2001; **34**: 840-849
10 **Dore MP**, Realdi G, Mura D, Onida A, Massarelli G, Dettori G, Graham DY, Sepulveda AR. Genomic instability in chronic viral hepatitis and hepatocellular carcinoma. *Hum Pathol* 2001; **32**: 698-703
11 **Karachristos A,** Liloglou T, Field JK, Deligiorgi E, Kouskouni E, Spandidos DA. Microsatellite instability and p53 mutations in hepatocellular carcinoma. *Mol Cell Biol Res Commun* 1999; **2**: 155-161
12 **Maggioni M,** Coggi G, Cassani B, Bianchi P, Romagnoli S,

Mandelli A, Borzio M, Colombo P, Roncalli M. Molecular changes in hepatocellular dysplastic nodules on microdissected liver biopsies. *Hepatology* 2000; **32**: 942-946

13 **Roncalli M,** Bianchi P, Grimaldi GC, Ricci D, Laghi L, Maggioni M, Opocher E, Borzio M, Coggi G. Fractional allelic loss in non-end-stage cirrhosis: correlations with hepatocellular carcinoma development during follow-up. *Hepatology* 2000; **31**: 846-850

14 **Saeki A,** Tamura S, Ito N, Kiso S, Matsuda Y, Yabuuchi I, Kawata S, Matsuzawa Y. Lack of frameshift mutations at coding mononucleotide repeats in hepatocellular carcinoma in Japanese patients. *Cancer* 2000; **88**: 1025-1029

15 **Sood AK,** Buller RE. Genomic instability in ovarian cancer: a reassessment using an arbitrarily primed polymerase chain reaction. *Oncogene* 1996; **13**: 2499-2504

16 **Berg KD,** Glaser CL, Thompson RE, Hamilton SR, Griffin CA, Eshleman JR. Detection of microsatellite instability by fluorescence multiplex polymerase chain reaction. *J Mol Diagn* 2000; **2**: 20-28

17 **Kusano N,** Shiraishi K, Kubo K, Oga A, Okita K, Sasaki K. Genetic aberrations detected by comparative genomic hybridization in hepatocellular carcinomas: their relationship to clinicopathological features. *Hepatology* 1999; **29**: 1858-1862

18 **Wong N,** Lai P, Lee SW, Fan S, Pang E, Liew CT, Sheng Z, Lau JW, Johnson PJ. Assessment of genetic changes in hepatocellular carcinoma by comparative genomic hybridization analysis: relationship to disease stage, tumor size, and cirrhosis. *Am J Pathol* 1999; **154**: 37-43

19 **Wong N,** Lai P, Pang E, Fung LF, Sheng Z, Wong V, Wang W, Hayashi Y, Perlman E, Yuna S, Lau JW, Johnson PJ. Genomic aberrations in human hepatocellular carcinomas of differing etiologies. *Clin Cancer Res* 2000; **6**: 4000-4009

20 **Leung TH,** Wong N, Lai PB, Chan A, To KF, Liew CT, Lau WY, Johnson PJ. Identification of four distinct regions of allelic imbalances on chromosome 1 by the combined comparative genomic hybridization and microsatellite analysis on hepatocellular carcinoma. *Mod Pathol* 2002; **15**: 1213-1220

21 **Yeh SH,** Chen PJ, Lai MY, Chen DS. Allelic loss on chromosomes 4q and 16q in hepatocellular carcinoma: association with elevated alpha-fetoprotein production. *Gastroenterology* 1996; **110**: 184-192

22 **Chan KL,** Lee JM, Guan XY, Fan ST, Ng IO. High-density allelotyping of chromosome 8p in hepatocellular carcinoma and clinicopathologic correlation. *Cancer* 2002; **94**: 3179-3185

23 **Emi M,** Fujiwara Y, Nakajima T, Tsuchiya E, Tsuda H, Hirohashi S, Maeda Y, Tsuruta K, Miyaki M, Nakamura Y. Frequent loss of heterozygosity for loci on chromosome 8p in hepatocellular carcinoma, colorectal cancer, and lung cancer. *Cancer Res* 1992; **52**: 5368-5372

24 **Fujiwara Y,** Ohata H, Kuroki T, Koyama K, Tsuchiya E, Monden M, Nakamura Y. Isolation of a candidate tumor suppressor gene on chromosome 8p21.3-p22 that is homologous to an extracellular domain of the PDGF receptor beta gene. *Oncogene* 1995;**10**: 891-895

25 **Piao Z,** Kim NG, Kim H, Park C. Deletion mapping on the short arm of chromosome 8 in hepatocellular carcinoma. *Cancer Lett* 1999; **138**: 227-232

26 **Liao C,** Zhao M, Song H, Uchida K, Yokoyama KK, Li T. Identification of the gene for a novel liver-related putative tumor suppressor at a high-frequency loss of heterozygosity region of chromosome 8p23 in human hepatocellular carcinoma. *Hepatology* 2000; **32**: 721-727

27 **Park WS,** Lee JH, Park JY, Jeong SW, Shin MS, Kim HS, Lee SK, Lee SN, Lee SH, Park CG, Yoo NJ, Lee JY. Genetic analysis of the liver putative tumor suppressor (LPTS) gene in hepatocellular carcinomas. *Cancer Lett* 2002; **178**: 199-207

28 **Sheu JC,** Lin YW, Chou HC, Huang GT, Lee HS, Lin YH, Huang SY, Chen CH, Wang JT, Lee PH, Lin JT, Lu FJ, Chen DS. Loss of heterozygosity and microsatellite instability in hepatocellular carcinoma in Taiwan. *Br J Cancer* 1999; **80**: 468-476

29 **Yumoto Y,** Hanafusa T, Hada H, Morita T, Ooguchi S, Shinji N, Mitani T, Hamaya K, Koide N, Tsuji T. Loss of heterozygosity and analysis of mutation of p53 in hepatocellular carcinoma. *J Gastroenterol Hepatol* 1995; **10**: 179-185

30 **Rashid A,** Wang JS, Qian GS, Lu BX, Hamilton SR, Groopman JD. Genetic alterations in hepatocellular carcinomas: association between loss of chromosome 4q and p53 gene mutations. *Br J Cancer* 1999; **80**: 59-66

31 **Zhao X,** Li J, He Y, Lan F, Fu L, Guo J, Zhao R, Ye Y, He M, Chong W, Chen J, Zhang L, Yang N, Xu B, Wu M, Wan D, Gu J. A novel growth suppressor gene on chromosome 17p13.3 with a high frequency of mutation in human hepatocellular carcinoma. *Cancer Res* 2001; **61**: 7383-7387

32 **Rabe C,** Cheng B, Caselmann WH. Molecular mechanisms of hepatitis B virus-associated liver cancer. *Dig Dis* 2001; **19**: 279-287

33 **Becker SA,** Zhou YZ, Slagle BL. Frequent loss of chromosome 8p in hepatitis B virus-positive hepatocellular carcinomas from China. *Cancer Res* 1996; **56**: 5092-5097

34 **Okabe H**, Ikai I, Matsuo K, Satoh S, Momoi H, Kamikawa T, Katsura N, Nishitai R, Takeyama O, Fukumoto M, Yamaoka Y. Comprehensive allelotype study of hepatocellular carcinoma: potential differences in pathways to hepatocellular carcinoma between hepatitis B virus-positive and -negative tumors. *Hepatology* 2000; **31**: 1073-1079

35 **Qin LX,** Tang ZY, Sham JS, Ma ZC, Ye SL, Zhou XD, Wu ZQ, Trent JM, Guan XY. The association of chromosome 8p deletion and tumor metastasis in human hepatocellular carcinoma. *Cancer Res* 1999; **59**: 5662-5665

36 **Salvucci M,** Lemoine A, Saffroy R, Azoulay D, Lepere B, Gaillard S, Bismuth H, Reynes M, Debuire B. Microsatellite instability in European hepatocellular carcinoma. *Oncogene* 1999; **18**: 181-187

37 **Piao Z,** Kim H, Malkhosyan S, Park C. Frequent chromosomal instability but no microsatellite instability in hepatocellular carcinomas. *Int J Oncol* 2000; **17**: 507-512

38 **Yamamoto H,** Itoh F, Fukushima H, Kaneto H, Sasaki S, Ohmura T, Satoh T, Karino Y, Endo T, Toyota J, Imai K. Infrequent widespread microsatellite instability in hepatocellular carcinomas. *Int J Oncol* 2000; **16**: 543-547

39 **Macdonald GA,** Greenson JK, Saito K, Cherian SP, Appelman HD, Boland CR. Microsatellite instability and loss of heterozygosity at DNA mismatch repair gene loci occurs during hepatic carcinogenesis. *Hepatology* 1998; **28**: 90-97

40 **Kondo Y,** Kanai Y, Sakamoto M, Mizokami M, Ueda R, Hirohashi S. Genetic instability and aberrant DNA methylation in chronic hepatitis and cirrhosis-A comprehensive study of loss of heterozygosity and microsatellite instability at 39 loci and DNA hypermethylation on 8 CpG islands in microdissected specimens from patients with hepatocellular carcinoma. *Hepatology* 2000; **32**: 970-979

Science Editor Wang XL and Li WZ **Language Editor** Elsevier HK

PO Box 2345, Beijing 100023, China
www.wjgnet.com
wjg@wjgnet.com

ELSEVIER

World J Gastroenterol 2005;11(20):3040-3045
World Journal of Gastroenterology ISSN 1007-9327

Molecular mechanisms of denbinobin-induced anti-tumorigenesis effect in colon cancer cells

Kuo-Ching Yang, Yih-Huei Uen, Fat-Moon Suk, Yu-Chih Liang, Ying-Jan Wang, Yuan-Soon Ho, I-Hsuan Li, Shyr-Yi Lin

Kuo-Ching Yang, Department of Internal Medicine, Shin Kong Wu Ho-Su Memorial Hospital, Taipei, Taiwan; Department of Internal Medicine, Taipei Medical University, Taipei, Taiwan, China
Yih-Huei Uen, Department of Surgery, Chi-Mei Foundational Medical Center, Yung-Kang City, Tainan, Taiwan, China
Fat-Moon Suk, Department of Internal Medicine, Taipei Medical University Hospital, Taipei, Taiwan, China
Yu-Chih Liang, School of Medical Technology, Taipei Medical University, Taipei, Taiwan, China
Ying-Jan Wang, Department of Environmental and Occupational Health, National Cheng Kung University Medical College, Tainan, Taiwan, China
Yuan-Soon Ho, School of Medical Technology, Taipei Medical University, Taipei, Taiwan, China
I-Hsuan Li, Department of Internal Medicine, School of Medicine, Taipei Medical University, Taipei, Taiwan, China
Shyr-Yi Lin, Department of Internal Medicine, School of Medicine and Department of Internal Medicine, Taipei Medical University Hospital, Taipei Medical University, Taipei, Taiwan, China
Supported by the Shin Kong Wu Ho-Su Memorial Hospital (SKH-TMU-93-16) and the Chi Mei Medical Center (93CM-TMU-09)
Correspondence to: Dr. Shyr-Yi Lin, Taipei Medical University, 250 Wu-Hsing Street, Taipei 110, Taiwan, China. sylin@tmu.edu.tw
Telephone: +886-2-27361661-3210 Fax: +886-2-27393447
Received: 2004-10-26 Accepted: 2004-12-23

Abstract

AIM: To explore both the *in vitro* and *in vivo* effects of denbinobin against colon cancer cells and clarify its underlying signal pathways.

METHODS: We used COLO 205 cancer cell lines and nude mice xenograft model to study the *in vitro* and *in vivo* anti-cancer effects of denbinobin.

RESULTS: Denbinobin at concentration of 10-20 μmol/L dose-dependently suppressed COLO 205 cell proliferation by MTT test. Flow cytometry analysis and DNA fragmentation assay revealed that 10-20 μmol/L denbinobin treatment induced COLO 205 cells apoptosis. Western blot analysis showed that caspases 3, 8, 9 and Bid protein were activated by denbinobin treatment to COLO 205 cells accompanied with cytochrome *c* and apoptosis-inducing factor (AIF) translocation. Pretreatment of MEK 1 inhibitor (U10126), but not p38 inhibitor (SB203580) and JNK inhibitor (SP600125), reversed denbinobin-induced caspase 8, 9 and Bid activation in COLO 205 cells suggesting that extracellular signal-regulated kinase were involved in the denbinobin-induced apoptosis in COLO 205 cells. Significant regression of tumor up to 68% was further demonstrated *in vivo* by treating nude mice bearing COLO 205 tumor xenografts with denbinobin 50 mg/kg intraperitoneally.

CONCLUSION: Our findings suggest that denbinobin could inhibit colon cancer growth both *in vitro* and *in vivo*. Activation of extrinsic and intrinsic apoptotic pathways and AIF were involved in the denbinobin-induced COLO 205 cell apoptosis.

Key words: Denbinobin; Colon cancer; Nude mice; Apoptosis; ERK pathway

Yang KC, Uen YH, Suk FM, Liang YC, Wang YJ, Ho YS, Li IH, Lin SY. Molecular mechanisms of denbinobin-induced anti-tumorigenesis effect in colon cancer cells. *World J Gastroenterol* 2005; 11(20): 3040-3045
http://www.wjgnet.com/1007-9327/11/3040.asp

INTRODUCTION

Colon cancer is one of the most prevalent malignances in the world. It ranked as the second cause of cancer death in the Western societies[1]. In Taiwan, colon cancer is the third most common form of lethal cancer[2]. Although surgical treatment of early stage colon cancer showed promising effect, the prognosis for those advanced staging patients is still not satisfactory, mostly owing to high local recurrent rate and metastasis. Therefore, finding new therapeutic strategies to improve survival rate in colon cancer patients are very important issues.

There are growing evidences that compounds of plant origin have the ability to treat or prevent cancer. For example, the Chinese herbal preparation called PC-SPES, a mixture consisting of extracts from eight herbs, has been used increasingly in prostate cancer[3] and demonstrated activity against androgen independent prostate cancer in a prospective, multicenter, randomized phase II study[4]. Another example was taxol, which was purified from the stem bark of *Taxus brevifolia* and showed anti-tumorigenesis effect on breast and ovarian cancers[5]. Other pure compounds isolated from herb could provide novel therapeutic advantage in the treatment of cancers. For example, solamargine, a pure compound isolated from *Solanum incanum* herb, could be a potential drug for cisplatin-resistant human lung cancer cells[6] and beta-elemene, a wide spectrum anticancer drug derived from the Chinese herb *Curcuma chaeocaulis*, could reverse adriamycin-induced resistance in human breast cancer cell line[7]. Therefore, it is reasonable for us to search

useful anti-cancer drugs from the traditional herbal medicine.

Previous study had demonstrated that denbinobin isolated from *Dendrobium nobile*, *Ephemerantha lonchophylla*, and *E. fimbriata* exerted potential anti-inflammatory, antioxidant, and anti-tumorigenesis effect[8-10]. Denbinobin was found to be cytotoxic against A549 (human lung carcinoma), SK-OV-3 (human ovary adenocarcinoma), and HL-60 (human promyelocytic leukemia) cell lines[9]. However, the anti-cancer effect of denbinobin and its underlying molecular mechanisms remain obscured. The purpose of this study is to explore the *in vitro* and *in vivo* anti-tumorigenesis effects of denbinobin against colon cancer and clarify its underlying molecular mechanisms.

MATERIALS AND METHODS

Cell lines and cell culture

The COLO 205 cell line was isolated from human colon adenocarcinoma (American Type Culture Collection CCL-222). The cells were grown in RPMI 1640 supplemented with 10% fetal calf serum (FCS), penicillin (100 U/mL), streptomycin (100 mg/mL), and 0.3 mg/mL glutamine in a humidified incubator (37 ℃, 50 mL/L CO_2). Denbinobin (Pharmaceutical Industry, Technology and Development Center, Taiwan) was added at the indicated doses in 0.1% dimethylsulfoxide (DMSO). For control specimens, the same volume of DMSO was added in a final concentration of 1 mL/L without denbinobin.

MTT assay

COLO 205 cells were seeded in a 96-well plate at a density of 1×10^4 cells/well and allowed to adhere overnight. After removing the medium, 200 μL of fresh medium per well, containing 10 mmol/L Hepes (pH 7.4) was then added. Then, 50 μL of 3-(4,5-dimethylthiazol-2-yl)-2,5-diphenyl-2H-tetrazolium bromide (MTT) was added to the wells and the plate was incubated for 2-4 h at 37 ℃ in the dark. The medium was removed and 200 μL DMSO and 25 μL Sorensen's glycine buffer was added to the wells. Absorbance was measured using an ELISA plate reader at 570 nm.

Drug treatment, and flow cytometry analysis

At 24 h after plating of cells, cells were washed thrice with phosphate-buffered saline (PBS) and then added with medium containing 10% FCS with various concentrations of denbinobin in a final concentration of 1 mL/L DMSO. The cell cycle stages in the denbinobin and DMSO-treated groups were measured by fluorescence-activated cell sorter (FACS) analysis. Cells were harvested and stained with propidium iodide (50 μg/mL) (Sigma Chemical Co., St. Louis, MO), and DNA content was measured using a FACScan laser flow cytometer analysis system (Becton-Dickinson, San Jose, CA); and 15 000 events were analyzed for each sample.

Analysis of DNA fragmentation

Analysis of DNA fragmentation was performed as previously described[11]. Briefly, the denbinobin and DMSO-treated cells were seeded on 100-mm dishes. The DNA was extracted twice with equal volumes of phenol and once with chloroform-isoamyl alcohol (24∶1 v∶v), then precipitated with 0.1 volume of sodium acetate, pH 4.8, and 2.5 volumes of ethanol at -20 ℃ overnight, and finally centrifuged at 13 000 *g* for 1 h. Genomic DNA was quantitated, and equal amounts of DNA sample in each lane were electrophoresed in a 2% agarose gel. The DNA was visualized by ethidium bromide staining.

Western analysis

Cells were washed with cold PBS, lysed in Golden lysis buffer, and performed Western blotting as described previously[12]. Briefly, cell lysates were prepared, electrotransferred, immunoblotted with anti-bax, bcl-2, cytochrome *c* (Cyto *c*), and apoptosis-inducing factor (AIF) monoclonal antibody or anti-caspases 9, 3 and Bid, total Akt polyclonal antibody (1∶1 000 dilution, Santa Cruz Biotechnology, Santa Cruz, CA); or with anti-caspase 8 and phosphorylated Akt monoclonal antibody (1∶1 000 dilution, Cell Signaling Technology, Beverly, MA); or with anti-glyceraldehyde-3-phosphate dehydrogenase (GAPDH) monoclonal antibody (1∶2 000 dilution, Biogenesis, Kingston, NH), and then with anti-mouse or anti-rabbit or anti-goat IgG antibody conjugated to horseradish peroxidase (1∶5 000 dilution, Santa Cruz Biotechnology) and visualized bands using enhanced chemiluminescence kits (2 min, ECL, Amersham). The expression of GAPDH was used as the control for equal protein loading.

Subcellular fractionation

As previously described[13], COLO 205 cells were harvested in isotonic mitochondrial buffer (210 mmol/L mannitol, 70 mmol/L sucrose, 1 mmol/L EDTA and 10 mmol/L HEPES pH 7.5), supplemented with protease inhibitor cocktail Complete (Boehringer Mannheim), and homogenized for 40 strokes with a Dounce homogenizer. Samples were centrifuged at 500 r/min for 5 min at 4 ℃ to eliminate nuclei and unbroken cells. The resulting supernatant was centrifuged at 10 000 *g* for 30 min at 4 ℃ to separate the heavy membrane pellet, and the resulting supernatant was stored as the cytosolic fraction.

Treatment of COLO 205-derived xenografts in vivo

As previously described[14], COLO 205 cells were grown in RPMI 1640 supplemented with 10% FCS as described above. Cells were harvested through two consecutive trypsinizations, centrifuged at 300 r/min for 5 min, washed twice, and resuspended in sterile PBS. Cells (5×10^6) in 0.2 mL were injected subcutaneously between the scapulae of each nude mouse (purchased from National Science Council Animal Center, Taipei, Taiwan). After transplantation, tumor size was measured using calipers and the tumor volume was estimated according to the formula tumor volume (mm^3) = $L\times W^2/2$, where L is the length and W is the width[15]. Once tumors reached a mean size of 200 mm^3, animals received intraperitoneal injections of either 25 μL DMSO or 50 mg/kg denbinobin thrice per week for 4 wk.

Statistical analysis

Results were expressed as mean±SE for each study. Data were analyzed by Student's *t*-test or linear regression method;

a *P* value of 0.05 or less was considered statistically significant.

RESULTS

Denbinobin suppressed colon cancer cell growth

We first examined the antiproliferative effect of denbinobin on the colon cancer cells. Treatment of the COLO 205 cells with 10 μmol/L denbinobin in a time course study showed significant inhibition of COLO 205 cell growth starting from 12 to 24 h by MTT test (Figure 1A). Dose-dependent study by MTT test further demonstrated that treatment of denbinobin (10-20 μmol/L) to COLO 205 for 24 h suppressed cancer cell growth (Figure 1B).

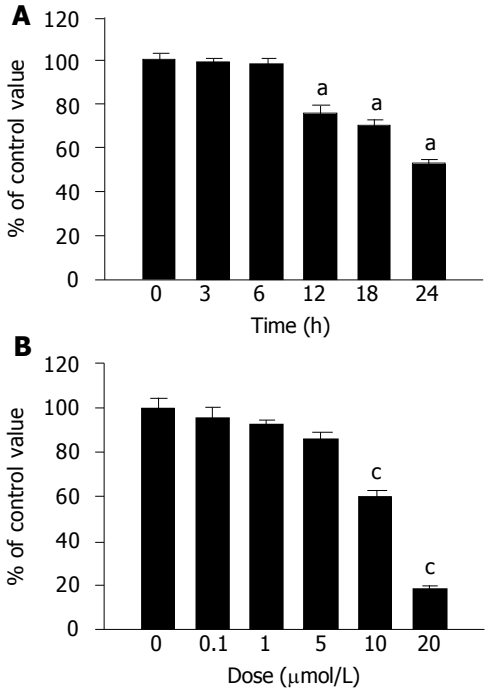

Figure 1 Effect of denbinobin on COLO 205 cell growth. COLO 205 cells were seeded in a 96-well plate until subconfluence and viable cells were determined by MTT assay. **A**: Time course study with 10 μmol/L denbinobin in 0.1% DMSO. Two independent experiments were performed in triplicate. $^{a}P<0.05$ *vs* time 0. **B**: Dose-dependent study after treatment of denbinobin for 24 h. Two independent experiments were performed in triplicate. $^{c}P<0.05$ *vs* DMSO control.

Denbinobin induced apoptosis

To further investigate the cellular mechanism of the denbinobin-induced growth inhibition, FACS analyses of DNA content in both DMSO- and denbinobin-treated COLO 205 cells were conducted. Figure 2A showed that 10-20 μmol/L denbinobin treatment to COLO 205 cells for 24 h induced a significant accumulation of cells at the sub-G_1 phase of the cell cycle, suggesting that the observed growth inhibitory effect of denbinobin was due to induction of cell death. Further study by using DNA fragmentation assay also demonstrated that, at concentrations of 0-5 μmol/L denbinobin, apoptosis was not observed. However, when denbinobin concentration was increased to 10-20 μmol/L, apoptosis was observed in COLO 205 cells (Figure 2B).

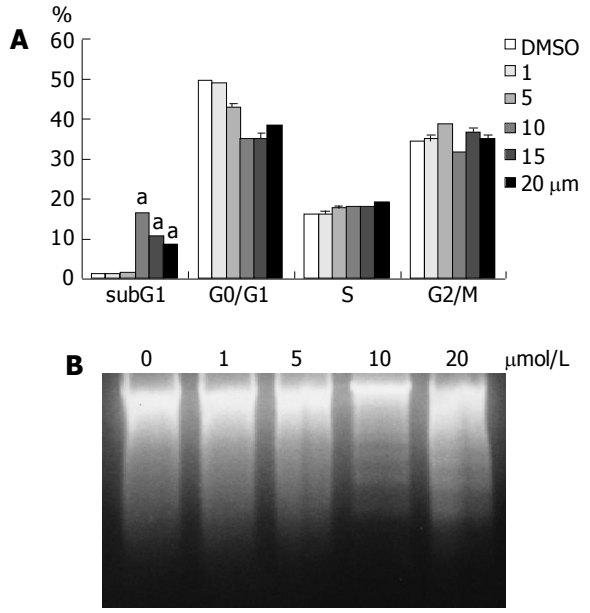

Figure 2 Treatment of COLO 205 cells with denbinobin (10-20 μmol/L) for 24 h induced apoptosis. **A**: FACS analysis of DNA content after 24-h incubation in culture medium supplemented with 10% FCS and 0.1% DMSO or 0-20 μmol/L denbinobin in 0.1% DMSO. Percentages of cells in sub-G_1, G_0/G_1, S, and G_2/M phases of the cell cycle determined using established CellFIT DNA analysis software were shown. Increased sub-G_1 percentage of COLO 205 cells was shown after treatment with 10-20 μmol/L denbinobin. Two independent experiments were performed in triplicate. $^{a}P<0.05$ *vs* DMSO control. **B**: Electrophoresis of genomic DNA from COLO 205 treated with denbinobin. A typical DNA ladder pattern associated with apoptosis was seen at 10-20 μmol/L denbinobin.

Denbinobin activated caspases 3, 8 and 9

Since it has been suggested[16] that the occurrence of apoptosis requires the activation of caspases, we investigated the involvement of caspase activation in the denbinobin-induced apoptosis in COLO 205 cells by Western blot analyses. Treatment of COLO 205 cells with 20 μmol/L denbinobin for 24 h induced caspase 3 activation evidenced by degradation of procaspase 3 bands (Figure 3A). To elucidate the apoptotic pathways involved in the activation of caspase 3, we examined the changes of caspases 8 and 9 protein levels in the denbinobin-treated COLO 205 cells. After treatment of COLO 205 cells with 20 μmol/L denbinobin for 12 h, activations of caspases 8 and Bid were evidenced by the degradation of the proenzymes of caspases 8 and cleavage of Bid proteins. Furthermore, increased expression of activation form of caspase 9 was noted after 18 h of 20 μmol/L denbinobin treatment to COLO 205 cells (Figure 3A).

Denbinobin induced Cyto c and AIF release from mitochondria

It has been demonstrated that activation of caspase 9 occurred during the release of Cyto *c* from mitochondria[17]. To examine whether this occurs in the denbinobin-induced apoptosis in COLO 205 cells, Cyto *c* release was monitored at various times after 10 μmol/L denbinobin treatment. Figure 3B showed that denbinobin treatment resulted in a significant accumulation of Cyto *c* as well as AIF in the cytosol fraction of cell extracts (Figure 3B). This denbinobin-induced elevation of cytosolic Cyto *c* was observed at 12 h and peaked at 24 h after denbinobin treatment. Under the same

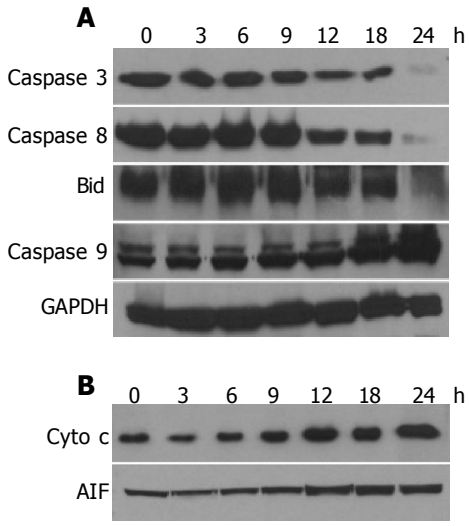

Figure 3 Effect of denbinobin on caspases, Bid protein levels or Cyto *c* and AIF translocation from mitochondria to cytosol. The whole cell proteins (**A**) or cytosolic proteins for Cyto *c*, AIF (**B**) were extracted from the cultured COLO 205 cells, which had been grown in 10% FCS and incubated for the indicated times with 0.1% DMSO or 20 μmol/L denbinobin in 0.1% DMSO. After electrophoresis, proteins were transferred onto Immobilon-P membranes, and then probed with proper dilutions of specific antibodies. Membranes were also probed with anti-GAPDH antibody to correct for difference in protein loading. Denbinobin time-dependently induced the activation of caspases and Bid (**A**), translocation of Cyto *c* and AIF (**B**).

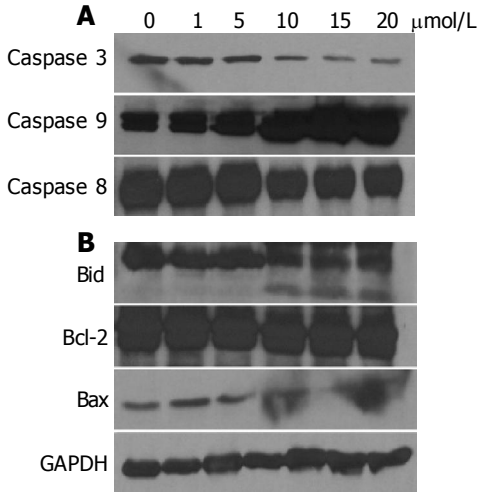

Figure 4 Effect of denbinobin on caspases (**A**) or Bid, bcl-2 and bax protein levels (**B**). The whole cell proteins were extracted from the cultured COLO 205 cells, which had been grown in 10% FCS and incubated for the indicated times with 0.1% DMSO or 20 μmol/L denbinobin in 0.1% DMSO. After electrophoresis, proteins were transferred onto Immobilon-P membranes, and then probed with proper dilutions of specific antibodies. Membranes were also probed with anti-GAPDH antibody to correct for difference in protein loading. Denbinobin dose-dependently induced the activation of caspases (**A**), Bid protein activation and decreased expression of bax (**B**).

conditions, apoptosis was not observed until 12 h after denbinobin treatment (Figure 1A) suggesting that translocation of Cyto *c* and AIF occurred in the denbinobin-treated COLO 205 cells beforehand, and then caspases 9 and 3 activation, and apoptosis followed thereafter.

Denbinobin activated Bid protein

Proteins of the bcl-2 family are also believed to be involved in the control of apoptosis[18]. Activation of Bid by caspase 8 links the extrinsic to the intrinsic apoptotic pathway through mitochondrial damages[19] by releasing Cyto *c* from mitochondria, and thereby initiate apoptosis. Bcl-2 directly or indirectly operates to prevent the release of Cyto *c* from mitochondria. On the other hand, bax can trigger mitochondria to release Cyto *c* from mitochondria, and thereby initiate apoptosis. Accordingly, we examined the changes of bcl-2 protein levels in denbinobin-treated COLO 205 cells. Treatment of COLO 205 cells with 10-20 μmol/L denbinobin caused a dose-dependent activation of caspases 3, 8, and 9 (Figure 4A) as well as Bid activation evidenced by decreased Bid protein and appearance of its cleavage product (Figure 4B). In contrast, bcl-2 protein levels were not changed significantly (Figure 4B). Surprisingly, proapoptotic bax protein showed decreased expression (Figure 4B). These findings suggest that Bid but not bcl-2 or bax participated in the denbinobin-induced COLO 205 cells apoptosis.

Denbinobin-induced apoptosis involved extracellular signal-regulated kinase (ERK) pathway

To further study the signaling pathways involved in the denbinobin-induced COLO 205 cell apoptosis, the following experiments were performed. Since the extracellular signal-regulated kinase (ERK), p38 and JNK pathways have been suggested to be involved in the regulation of apoptotic processes, we applied an MEK 1 inhibitor (U10126), a p38 MAP kinase (p38 MAPK) inhibitor (SB203580) and a JNK inhibitor (SP600125) to examine whether they also participated in the denbinobin-induced COLO 205 cell apoptosis. As illustrated in Figure 5A, pretreatment of COLO 205 cells with 100 nmol/L U10126, but not SB20358 (20 μmol/L) and SP600125 (100 nmol/L), blocked the denbinobin-induced caspases 8, 9 and Bid protein activation in COLO 205 cell, suggesting that the ERK, but not p38 and JNK pathways, was involved in this process.

The serine/threonine kinase Akt is important for anti-apoptotic signaling pathways for normal cells. Accordingly, we tested whether Akt activity was regulated by denbinobin treatment to COLO 205 cells. Time course study in Figure 5B demonstrated that treatment of denbinobin to COLO 205 cells induced activation of Akt evidenced by increased phosphorylated form of Akt peaked from 30 to 60 min after treatment. Pretreatment of PI3K-Akt pathway inhibitor (Wortmannin, 100 nmol/L) failed to affect denbinobin-induced caspases activation (data not shown). These findings suggested that Akt pathway might not be directly involved in the denbinobin-induced apoptosis in COLO 205 cells.

Denbinobin inhibited colon tumor growth in vivo

We further examined the anti-tumor effect of denbinobin *in vivo* by treating athymic mice bearing COLO 205 tumor xenografts. After establishment of palpable tumors (mean tumor volume, 200 mm^3), animals received denbinobin at dosage of 50 mg/kg or DMSO (control) thrice a week. A reduction in tumor volume between denbinobin-treated *vs* the DMSO-treated control group was detected by d 15. This difference became progressively more conspicuous, with the average tumor volume in the denbinobin-treated mice 32% that of the DMSO-treated mice after 4 wk of

treatment (Figure 6A). In mice receiving these treatment regimens, no significant difference of body weight was noted (Figure 6B) and no gross signs of toxicity were observed (visible inspection of general appearance, and microscopic examination of individual organs) (data not shown). Our results indicated that denbinobin might be a potential useful chemotherapeutic agent in treating colon tumor.

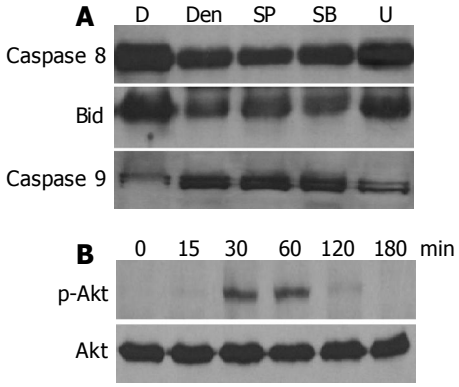

Figure 5 Effect of MAPK and Akt pathways in the denbinobin-induced COLO 205 cells apoptosis. **A**: Cells were pretreated with various kinds of MAPKs inhibitors; U10126 (U, 100 nmol/L), SB203580 (SB, 20 μmol/L), or SP600125 (SP, 100 nmol/L) for 1 h. The whole cell proteins were extracted from the cultured COLO 205 cells, which had been grown in 10% FCS and incubated for the indicated times with 0.1% DMSO or 20 μmol/L denbinobin in 0.1% DMSO for 24 h. After electrophoresis, proteins were transferred onto Immobilon-P membranes, and then probed with proper dilutions of specific antibodies; **B**: Effect of Akt pathway on the denbinobin treatment to COLO 205 cells. Time course study of 20 μmol/L denbinobin-treated COLO 205 cells was used to detect the total Akt proteins and the phorphorylated Akt by Western blot.

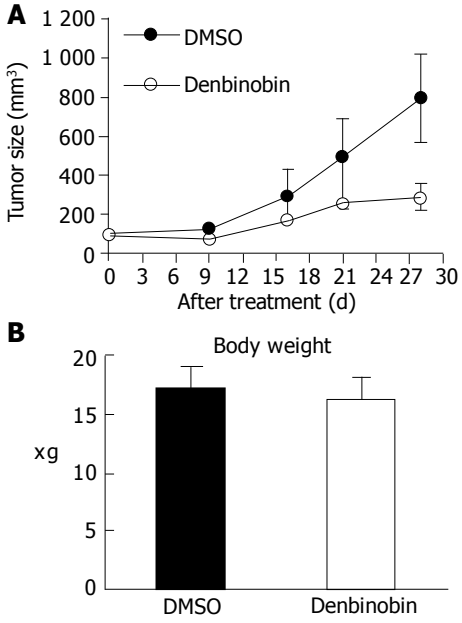

Figure 6 Growth of COLO 205 tumor xenografts in nude mice was suppressed by denbinobin treatment. Athymic nude mice injected with COLO 205 cells into subcutaneous tissue of inter-scapular area. Once tumor volume reached approximately 200 mm^3, the animal received treatment of 50 mg/kg denbinobin or DMSO intraperitoneally thrice per week for 4 wk. (**A**) Average tumor volume (**B**) body weight of DMSO-treated (n = 5, filled circles) *vs* denbinobin-treated (n = 4, open circles) nude mice. Samples were analyzed in each group, and values represent the mean±SE. Comparisons were subjected to linear regression method in (**A**) and showed significant difference between DMSO *vs* denbinobin treatment group.

DISCUSSION

Denbinobin is one of the pure compounds isolated from the stems of *D. moniliforme*, known as Shi-Hu in Chinese medicine, which has been used for a long time to treat respiratory tract infection, fever and heat stroke[10]. Denbinobin has been shown to suppress the lipopolysaccharide-induced TNF-α formation in mouse macrophage cells suggesting that it exerts potent anti-inflammatory effect[10]. Chemical compounds with anti-inflammatory activity has been shown to protect against chemical toxicity and cancer[20,21]. In our *in vitro* study, we demonstrated that denbinobin at concentrations of 10-20 μmol/L inhibited the growth of COLO 205 cells in a dose-dependent manner (Figure 1). These results were not due to inhibition of cell division and indicated that there was an induction of apoptosis by denbinobin in the subcultured cancer cells (Figure 2). *In vivo* studies showed that intraperitoneal administration of denbinobin caused a striking and substantial regression of the COLO 205 tumor in nude mice (Figure 6). To our knowledge, this is the first demonstration that denbinobin inhibits the growth of colon cancer cells both *in vitro* and *in vivo*.

Apoptosis is a cell suicide mechanism that requires specialized cellular machinery. A central component of this machinery is a proteolytic system involving caspases, a highly conserved family of cysteine proteinases with specific substrates[16]. By Western blot analysis, we demonstrated that 10-20 μmol/L denbinobin induces activations of caspases 8 and 9 in COLO 205 cells, evidenced by decreases in the stainable procaspases 8, and increases in the active form of caspase 9 enzyme expression (Figures 3A and 4). Activation of caspases 8 and 9 can cleave and activate downstream caspases such as caspase 3 (Figures 3A and 4), which eventually leads to apoptosis[22].

Bcl-2 family proteins have been suggested to be involved in the regulation of apoptosis by controlling the release of Cyto *c* from mitochondria[18]. Activation of Bid by caspase 8 links the extrinsic to the intrinsic apoptotic pathway through mitochondrial damages[19]. Bcl-2 prevents apoptosis by blocking the release of Cyto *c* from mitochondria[23]. Bax, on the other hand, directly induces Cyto *c* release from mitochondria, and thereby triggers caspase 9 activation[24]. The results of the present study demonstrate that activation of Bid protein by denbinobin treatment in COLO 205 cells seems to be responsible for stimulating the release of Cyto *c* (Figure 3).

One of the major challenges in the cancer treatment is that many tumor cells carry mutations in key apoptotic genes such as p53, Bcl family proteins or those affecting caspase signaling. These defects resulted in failure of traditional chemotherapeutic treatments. Therefore, it is important to search for caspase-independent cell death mechanism in tumor[25]. It has been discovered that, in response to apoptotic stimuli, mitochondria can also release caspase-independent cell death effector such as AIF[26]. AIF is a phylogenetically ancient mitochondrial intermembrane flavoprotein endowed with the unique capacity to induce caspase-independent peripheral chromatin condensation and large-scale DNA fragmentation when added to purified nuclei[27]. In our study, 20 μmol/L denbinobin treatment induced the release of AIF from mitochondria to cytosol. These findings suggest a potential therapeutic advantage of denbinobin in the

treatment of colon cancer.

Mitogen-activated protein (MAP) kinases, including ERK, c-Jun NH2-terminal kinases (JNK) and p38 MAPK are important intermediates of the signal-transduction pathway associated with proliferation or apoptosis[28]. A report has shown that ursodeoxycholic acid could induce colon cancer cell apoptosis through modulation of ERK pathway. Our results demonstrated that MEK 1 inhibitor but not JNK or p38 inhibitors could reverse the denbinobin-induced caspases 8, 9 and Bid activation (Figure 5A) suggesting that ERK pathway was involved in the denbinobin-mediated apoptosis in COLO 205 cells.

Akt promotes cell survival by inhibiting proapoptotic proteins such as Bad, forkhead, and p53, and activating pro-survival proteins such as NF-κB. It is likely that hyperactivity of the PI3K-Akt pathway is a selected mechanism for tumor cells to overcome apoptotic stimuli. In our results, we demonstrated that Akt was not suppressed but transient activated after denbinobin treatment to COLO 205 cells (Figure 5B) and pretreatment of Akt inhibitor has no effect on the denbinobin-induced COLO 205 cell apoptosis. These findings suggest that Akt pathway was not primarily regulated by denbinobin, instead its activation might be a secondary effect.

Our findings introduced our basic observations that denbinobin, a pure compound derived from Chinese herb, could induce apoptosis in colon cancer cells and suppress colon cancer growth in tumor bearing nude mice. The results from the present *in vitro* and *in vivo* studies highlight the molecular mechanisms of denbinobin-induced apoptosis in COLO 205 cells, which might have potential applications in the treatment of human colon cancer.

REFERENCES

1 **Jemal A**, Tiwari RC, Murray T, Ghafoor A, Samuels A, Ward E, Feuer EJ, Thun MJ. Cancer statistics, 2004. *CA Cancer J Clin* 2004; **54**: 8-29

2 **Wei SC**, Su YN, Tsai-Wu JJ, Wu CH, Huang YL, Sheu JC, Wang CY, Wong JM. Genetic analysis of the APC gene in Taiwanese familial adenomatous polyposis. *J Biomed Sci* 2004; **11**: 260-265

3 **Fu Y**, Hsieh TC, Guo J, Kunicki J, Lee MY, Darzynkiewicz Z, Wu JM. Licochalcone-A, a novel flavonoid isolated from licorice root (Glycyrrhiza glabra), causes G2 and late-G1 arrests in androgen-independent PC-3 prostate cancer cells. *Biochem Biophys Res Commun* 2004; **322**: 263-270

4 **Oh WK**, Kantoff PW, Weinberg V, Jones G, Rini BI, Derynck MK, Bok R, Smith MR, Bubley GJ, Rosen RT, DiPaola RS, Small EJ. Prospective, multicenter, randomized phase II trial of the herbal supplement, PC-SPES, and diethylstilbestrol in patients with androgen-independent prostate cancer. *J Clin Oncol* 2004; **22**: 3705-3712

5 **Ozols RF**. Paclitaxel (Taxol)/carboplatin combination chemotherapy in the treatment of advanced ovarian cancer. *Semin Oncol* 2000; **27**: 3-7

6 **Liang CH**, Liu LF, Shiu LY, Huang YS, Chang LC, Kuo KW. Action of solamargine on TNFs and cisplatin-resistant human lung cancer cells. *Biochem Biophys Res Commun* 2004; **322**: 751-758

7 **Hu J**, Jin W, Yang PM. Reversal of resistance to adriamycin in human breast cancer cell line MCF-7/ADM by beta-elemene. *Zhonghua Zhongliu Zazhi* 2004; **26**: 268-270

8 **Chen HY**, Shiao MS, Huang YL, Shen CC, Lin YL, Kuo YH, Chen CC. Antioxidant principles from Ephemerantha lonchophylla. *J Nat Prod* 1999; **62**: 1225-1227

9 **Lee YH**, Park JD, Baek NI, Kim SI, Ahn BZ. *In vitro* and *in vivo* antitumoral phenanthrenes from the aerial parts of Dendrobium nobile. *Planta Med* 1995; **61**: 178-180

10 **Lin TH**, Chang SJ, Chen CC, Wang JP, Tsao LT. Two phenanthraquinones from Dendrobium moniliforme. *J Nat Prod* 2001; **64**: 1084-1086

11 **Lin SY**, Chang YT, Liu JD, Yu CH, Ho YS, Lee YH, Lee WS. Molecular mechanisms of apoptosis induced by magnolol in colon and liver cancer cells. *Mol Carcinog* 2001; **32**: 73-83

12 **Lin SY**, Liang YC, Ho YS, Tsai SH, Pan S, Lee WS. Involvement of both extracellular signal-regulated kinase and c-jun N-terminal kinase pathways in the 12-O-tetradecanoylphorbol-13-acetate-induced upregulation of p21 (Cip1) in colon cancer cells. *Mol Carcinog* 2002; **35**: 21-28

13 **Arnoult D**, Gaume B, Karbowski M, Sharpe JC, Cecconi F, Youle RJ. Mitochondrial release of AIF and EndoG requires caspase activation downstream of Bax/Bak-mediated permeabilization. *EMBO J* 2003; **22**: 4385-4399

14 **Lin SY**, Liu JD, Chang HC, Yeh SD, Lin CH, Lee WS. Magnolol suppresses proliferation of cultured human colon and liver cancer cells by inhibiting DNA synthesis and activating apoptosis. *J Cell Biochem* 2002; **84**: 532-544

15 **Osborne CK**, Coronado EB, Robinson JP. Human breast cancer in the athymic nude mouse: cytostatic effects of long-term antiestrogen therapy. *Eur J Cancer Clin Oncol* 1987; **23**: 1189-1196

16 **Thornberry NA**, Lazebnik Y. Caspases: enemies within. *Science* 1998; **281**: 1312-1316

17 **Zou H**, Henzel WJ, Liu X, Lutschg A, Wang X. Apaf-1, a human protein homologous to C. elegans CED-4, participates in cytochrome c-dependent activation of caspase-3. *Cell* 1997; **90**: 405-413

18 **Reed JC**. Bcl-2 family proteins. *Oncogene* 1998; **17**: 3225-3236

19 **Li H**, Zhu H, Xu CJ, Yuan J. Cleavage of BID by caspase 8 mediates the mitochondrial damage in the Fas pathway of apoptosis. *Cell* 1998; **94**: 491-501

20 **Ma Q**, Kinneer K. Chemoprotection by phenolic antioxidants. Inhibition of tumor necrosis factor alpha induction in macrophages. *J Biol Chem* 2002; **277**: 2477-2484

21 **Na HK**, Surh YJ. Peroxisome proliferator-activated receptor gamma (PPARgamma) ligands as bifunctional regulators of cell proliferation. *Biochem Pharmacol* 2003; **66**: 1381-1391

22 **Li P**, Nijhawan D, Budihardjo I, Srinivasula SM, Ahmad M, Alnemri ES, Wang X. Cytochrome c and dATP-dependent formation of Apaf-1/caspase-9 complex initiates an apoptotic protease cascade. *Cell* 1997; **91**: 479-489

23 **Yang J**, Liu X, Bhalla K, Kim CN, Ibrado AM, Cai J, Peng TI, Jones DP, Wang X. Prevention of apoptosis by Bcl-2: release of cytochrome c from mitochondria blocked. *Science* 1997; **275**: 1129-1132

24 **Jurgensmeier JM**, Xie Z, Deveraux Q, Ellerby L, Bredesen D, Reed JC. Bax directly induces release of cytochrome c from isolated mitochondria. *Proc Natl Acad Sci USA* 1998; **95**: 4997-5002

25 **Cregan SP**, Dawson VL, Slack RS. Role of AIF in caspase-dependent and caspase-independent cell death. *Oncogene* 2004; **23**: 2785-2796

26 **Lorenzo HK**, Susin SA, Penninger J, Kroemer G. Apoptosis inducing factor (AIF): a phylogenetically old, caspase-independent effector of cell death. *Cell Death Differ* 1999; **6**: 516-524

27 **Cande C**, Cohen I, Daugas E, Ravagnan L, Larochette N, Zamzami N, Kroemer G. Apoptosis-inducing factor (AIF): a novel caspase-independent death effector released from mitochondria. *Biochimie* 2002; **84**: 215-222

28 **Tominaga K**, Higuchi K, Sasaki E, Suto R, Watanabe T, Fujiwara Y, Oshitani N, Matsumoto T, Kim S, Iwao H, Arakawa T. Correlation of MAP kinases with COX-2 induction differs between MKN45 and HT29 cells. *Aliment Pharmacol Ther* 2004; **20** Suppl 1: 143-150

Science Editor Guo SY **Language Editor** Elsevier HK

PO Box 2345, Beijing 100023, China
www.wjgnet.com
wjg@wjgnet.com

ELSEVIER

World J Gastroenterol 2005;11(20):3046-3050
World Journal of Gastroenterology ISSN 1007-9327

Matrix metalloproteinase-2 and tissue inhibitor of metalloproteinase-2 in colorectal carcinoma invasion and metastasis

Bing-Hui Li, Peng Zhao, Shi-Zheng Liu, Yue-Ming Yu, Mei Han, Jin-Kun Wen

Bing-Hui Li, Peng Zhao, Shi-Zheng Liu, Yue-Ming Yu, Mei Han, Jin-Kun Wen, Department of Surgery, the Fourth Hospital of Hebei Medical University, Shijiazhuang 050011, Hebei Province, China
Bing-Hui Li, Department of Surgery, the Fourth Hospital of Hebei Medical University, Shijiazhuang 050011, Hebei Province, China
Supported by the Natural Science Foundation of Hebei Province, No. C2004000642
Correspondence to: Dr. Bing-Hui Li, Department of Surgery, the Fourth Hospital of Hebei Medical University, Shijiazhuang 050011, Hebei Province, China
Telephone: +86-311-6033941-347
Received: 2004-06-29 Accepted: 2004-07-22

Abstract

AIM: To explore the relationship between matrix metalloproteinase-2 (MMP-2) and tissue inhibitor of metalloproteinase-2 (TIMP-2) in the development of colorectal carcinoma and to provide a valuable marker for clinical diagnosis.

METHODS: Twenty-five patients with colorectal carcinoma underwent surgical resection. Samples were taken from tumor sites and normal tissues. MMP-2 activity was determined by gelatin zymography. Western blot and ABC immunohistochemical staining were used to detect the expression levels of MMP-2 and TIMP-2 in normal and colorectal carcinoma tissues. Statistical analyses were performed using the Student's *t* test and one-way ANOVA. $P<0.05$ was considered statistically significant. All the statistical analyses were performed using SPSS 10.0 software.

RESULTS: MMP-2 activity could be detected in both normal and colorectal carcinoma tissues. MMP-2 activity in colorectal carcinoma tissues was much higher than that in normal tissues ($P<0.05$, $t = 3.916, 4.227$). MMP-2 activity was positively related to the colorectal carcinoma invasion depth, lymph node metastasis and Duke's stage. Western blot and ABC immunohistochemical staining demonstrated that the expression level of MMP-2 in colorectal carcinoma tissues was much higher than that in normal tissues ($P<0.05$, $t = 9.429$), but the expression level of TIMP-2 in colorectal carcinoma tissues was much lower than that in normal tissues ($P<0.05$, $t = 7.329$). The MMP-2/TIMP-2 ratio of colorectal carcinoma was much higher than that of normal tissues. With the progression of invasion depth, lymph node metastasis and tumor Duke's stage, the activity and expression level of MMP-2 and TIMP-2 gradually increased, but the MMP-2/TIMP-2 ratio gradually decreased.

CONCLUSION: The balance between MMP-2 and TIMP-2 plays a crucial role in the process of colorectal carcinoma invasion and metastasis.

Key words: Extracellular matrix turnover; Colorectal carcinoma; Metastasis

Li BH, Zhao P, Liu SZ, Yu YM, Han M, Wen JK. Matrix metalloproteinase-2 and tissue inhibitor of metalloproteinase-2 in colorectal carcinoma invasion and metastasis. *World J Gastroenterol* 2005; 11(20): 3046-3050
http://www.wjgnet.com/1007-9327/11/3046.asp

INTRODUCTION

Colorectal carcinoma is one of the most common malignant tumors with a relatively high incidence in China. Despite major advances in the diagnosis and treatment of this disease, its mortality has remained unchanged during the last 20 years. Tumor invasion and metastasis are considered to be the major causes of death in colorectal carcinoma patients. Recent researches in the field of mechanism for tumor invasion and metastasis have demonstrated that the degradation of extracellular matrix (ECM) and basement membrane (BM) is an essential step and the contribution of matrix metallopro-teinases (MMPs) is very important during this process[1-4]. MMPs are a family of zinc-dependent endopeptidases that are collectively capable of degrading most components of the BM and ECM[5]. Several studies have proved that there are high expression level and activity of MMPs in many kinds of tumors, such as carcinoma of esophagus, lung, stomach, *etc*. Tissue inhibitors of metalloproteinases (TIMPs), as the main endogenous inhibitors of the metalloproteinases, can reversibly inhibit MMPs in a 1:1 stoichiometric fashion and influence the process of tumor invasion and metastasis[6]. At present, there have been many reports about the overex-pression of matrix metalloproteinase-2 (MMP-2) in colorectal carcinoma tissues. However, few reports concerning the detailed pathophysiological significance of MMP-2 and the relationship between MMP-2 and tissue inhibitor of metalloproteinase-2 (TIMP-2) are available. Therefore, the aim of the present study was to investigate the expression characteristics of MMP-2 and TIMP-2 in colorectal carcinoma tissues and to explore the relationship between MMP-2 and TIMP-2 and the correlation with colorectal carcinoma progression, trying to provide a valuable marker for its clinical prognosis.

MATERIALS AND METHODS

Clinical specimens

Twenty-five patients with colorectal carcinoma were recruited at the Fourth Hospital of Hebei Medical University from March 2002 to July 2002. Paired colorectal tumor and normal mucosal tissue samples (taken at a site 10 cm or more from the primary tumor) were collected immediately after surgical resection. Of the 25 cases, 9 had colon carcinoma, 16 had rectal carcinoma. All colorectal tumors were confirmed by their pathological examination. All the specimens were divided into two parts. One part was stored at -70 ℃, the other part was fixed quickly into formalin solution at pH 7.0, embedded in paraffin and cut into sections (4-μm thick).

Gelatin zymography

MMP-2 activity was analyzed by gelatin zymography. Frozen samples were homogenized in lysis buffer containing 100 mmol/L Tris-Cl, pH 7.6, 20 mmol/L NaCl, 1% Triton X-100. The lysates were incubated on ice for 30 min and insoluble materials were removed by centrifugation. Samples containing 100 μg of protein were mixed with 5×sample buffer (4:1) and electrophoresed (120 V) for 2-3 h at 4 ℃. When the tracking dye at the front reached the bottom of the gel, the gel was removed and shaken gently for 30 min in 2.5% Triton X-100 to remove SDS. Then, the gel was incubated in 50 mmol/L Tris-HCl, pH 8.0, 50 mmol/L NaCl, 10 mmol/L $CaCl_2$, 1% Triton X-100 for 9 h at 37 ℃. At last, following staining with 0.5% Coomassie brilliant blue R250 for 1.5-2 h and decolorized for 1 h. The clear band against a blue background representing the activity of MMP-2 was measured by using a gel image system (Image master 1D analysis software).

Western blot analysis

MMP-2 and TIMP-2 protein levels in normal and colorectal carcinoma tissues were determined by Western blot analysis. Tissue homogenates were prepared as described above for gelatin zymography. Five times loading buffer was added to an equal amount (150 μg) of protein extracts, which was subsequently boiled for 5 min. Then proteins were subjected to SDS-PAGE and transferred to the PVDF membrane for immunodetection. The PVDF membranes were blocked in 5% nonfat milk for 3 h at room temperature and then probed with anti-MMP-2 or anti-TIMP-2 antibody for 9 h at 4 ℃. After that, the membranes were washed thrice with TBS-Tween and incubated with secondary antibody for 2 h at room temperature. Immunoreactive proteins were detected using a color development system (NBT/BCIP) by the standard procedure.

ABC immunohistochemical staining

Streptavidin–biotin complex (SABC) method was adopted in formalin-fixed, paraffin-embedded sections. Sections were de-paraffinized and incubated with 1% hydrogen peroxide in methanol for 10 min to block the endogenous peroxidase activity. After being washed with phosphate-buffered saline (PBS), sections were treated with 0.01 mol/L citric acid buffer to recover the antigen activity. After that, the sections were incubated with 5% normal goat serum for 30 min at room temperature and then incubated with primary antibodies to MMP-2 and TIMP-2 at an antibody concentration of 1:200, overnight at 4 ℃. The negative control was used with PBS buffer replacing the polyclone antibody. ABC immunohistochemical kits and DAB substrate solution were used to detect the immune complex. The procedures of blocking, linkage, and labeling of binding reaction were carried out according to manufacturer's instructions. The peroxidase activity was visualized by a DAB kit (Sino-American Biotechnology Co.). The deep yellow particles were defined as positive.

Statistical analysis

All the experiments were repeated thrice. Statistical analyses were performed using the Student's t test and one-way ANOVA. $P<0.05$ was considered statistically significant. All the statistical analyses were performed using SPSS 10.0 software.

RESULTS

MMP-2 activity analysis

As shown in Figure 1, the major band was 72 000 M_r and the minor band was 62 000 M_r on SDS-PAGE. They corresponded to the latent and active forms of MMP-2 respectively. The MMP-2 activity was much higher in colorectal carcinoma tissues than in normal tissues (Figure 1, $P<0.05$, $t = 3.916, 4.227$). Further, the invasive and metastatic capacity of colorectal carcinoma was significantly correlated with the MMP-2 activity. With the progression of tumor Duke's stage, the MMP-2 activity gradually increased (Figure 2, $P<0.05$, $F = 219.296$). As shown in Figure 3, the MMP-2 activity was much higher in the lymph node metastatic group than in the group without lymph node metastasis (Figure 3, $P<0.05$, $t = 6.042, 20.174$). The MMP-2 activity was also higher in colorectal carcinoma tissues with subserosal invasion than in those with muscularis propria invasion (Figure 3, $P<0.05$, $t = 4.341, 3.151$).

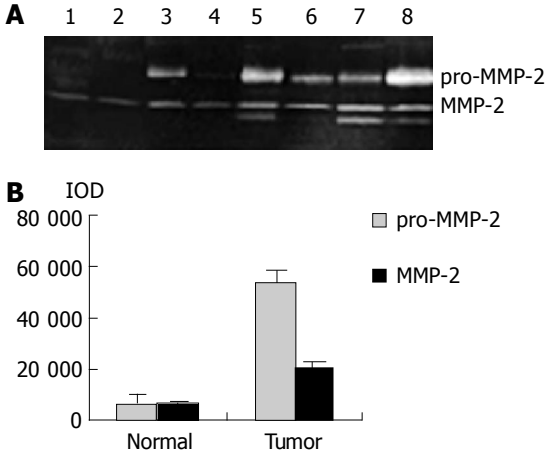

Figure 1 MMP-2 and pro-MMP-2 activity in normal and colorectal carcinoma tissues. **A:** Results of gelatin zymography. Lanes 1-4: normal tissues; lanes 5-8: colorectal carcinoma tissues; **B:** Densitometric intensity of absorbance (IOD) of pro-MMP-2 and MMP-2 activity in normal and colorectal carcinoma tissues.

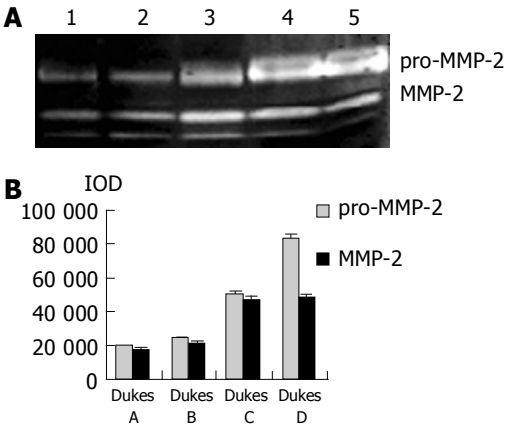

Figure 2 MMP-2 and pro-MMP-2 activity in colorectal carcinoma tissues at different Duke's stage. **A:** Results of gelatin zymography. Lane 1: Duke's A stage, lane 2: Duke's B stage, lane 3: Duke's C stage, lanes 4 and 5: Duke's D stage; **B:** Densitometric intensity of absorbance (IOD) of pro-MMP-2 and MMP-2 activity in colorectal carcinoma tissues at different Duke's stage.

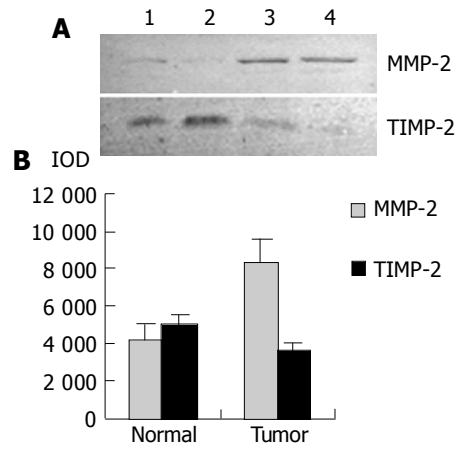

Figure 4 MMP-2 and TIMP-2 expression in normal and colorectal carcinoma tissues. **A:** Western blot analysis for MMP-2 and TIMP-2 expression. Lanes 1 and 2: normal tissues; lanes 3 and 4: colorectal carcinoma tissues; **B:** Densitometric intensity of absorbance (IOD) of MMP-2 and TIMP-2 expression in normal and colorectal carcinoma tissues.

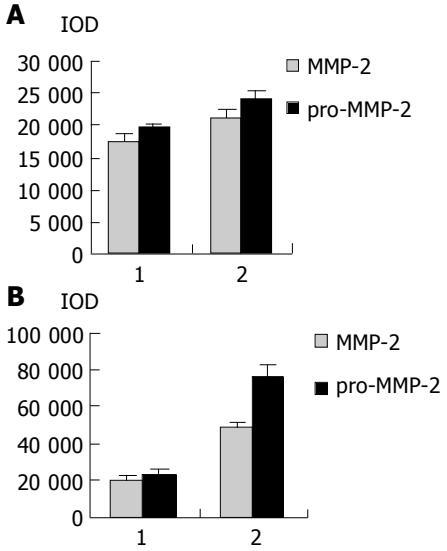

Figure 3 Densitometric intensity of absorbance (IOD) of pro-MMP-2 and MMP-2 activity in colorectal carcinoma tissues. **A:** Different lymph node metastases. 1: lymph node negative; 2: lymph node positive; **B:** Different invasion depths. 1: muscular layer invasion; 2: serous membrane layer or surrounding soft tissue invasion.

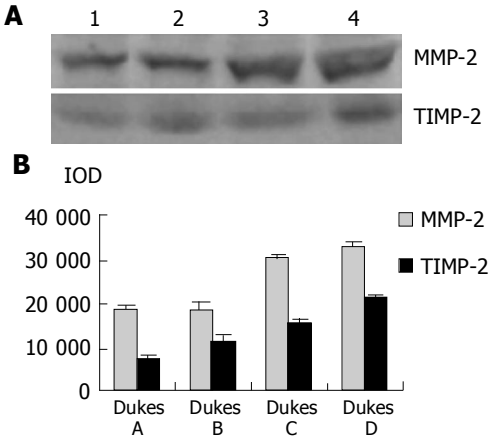

Figure 5 Western blot analysis for MMP-2 and TIMP-2 expression in carcinoma tissues at different Duke's stages. Lane 1: Duke's **A** stage; lane 2: Duke's B stage; lane 3: Duke's C stage; lane 4: Duke's D stage; **B:** Densitometric intensity of absorbance (IOD) of MMP-2 and TIMP-2 expression in colorectal carcinoma tissues at different Duke's stages.

Western blot analysis for MMP-2 and TIMP-2

As shown in Figure 4, Western blot analysis revealed the specific bands of MMP-2 (72 000 M_r) and TIMP-2 (22 000 M_r) in normal and colorectal carcinoma tissues. The MMP-2 expression level was found to be significantly increased whereas significantly decreased in colorectal carcinoma tissues in comparison with normal colorectal tissues ($P<0.05$, $t = 9.429, 7.329$). The MMP-2/TIMP-2 ratio of colorectal carcinoma was much higher than that of normal tissue (Table 1, $P<0.05$, $t = 6.474$). With the progression of tumor Duke's stage, the MMP-2 and TIMP-2 expression levels were gradually increased (Figure 5, $P<0.05$, $F = 74.318, 124.426$). The ratio of MMP-2/TIMP-2 was gradually decreased (Table 1, $P<0.05$, $F = 6.330$). It also could be seen that the MMP-2 and TIMP-2 expression levels in colorectal carcinoma tissues with regional lymph node metastasis were significantly high, while they were very low in those without lymph node metastasis (Figure 6, $P<0.05$, $t = 10.361, 5.609$). The ratio of MMP-2/TIMP-2 in the former was lower than the latter (Table 1, $P>0.05$, $t = 2.252$). The MMP-2 and TIMP-2 expression levels were much higher in colorectal carcinoma tissues with subserosal invasion than in those with muscularis propria invasion (Figure 6, $P<0.05$, $t = 3.042, 4.004$), the MMP-2/TIMP-2 ratio in the former was also lower than that in the later (Table 1, $P>0.05$, $t = 2.476$).

Immunohistochemical staining for MMP-2 and TIMP-2

Figure 7 shows the expression and localization of MMP-2 and TIMP-2 in normal and colorectal carcinoma tissues. Immunohistochemical staining for MMP-2 revealed that normal colorectal tissues were slightly positive while colorectal carcinoma tissues in early stage were strongly positive. In contrast, the positive staining with TIMP-2 in normal colorectal carcinoma tissues was much higher than that in colorectal carcinoma tissues. MMP-2 immunoreactivity was

Table 1 MMP-2/TIMP-2 ratio of normal and colorectal carcinoma tissues (mean±SD)

Variable	MMP-2/TIMP-2	*P*
Tissues		*P*<0.05
Normal	0.5807±0.2061	
Carcinoma	2.4179±0.6534	
Invasion depth		
Muscular layer invasion	2.5781±0.4336	
Serous membrane layer or surrounding soft tissue invasion	2.1308±0.7311	
Lymph node metastasis		
Negative	2.2907±0.5102	
Positive	1.7643±0.2597	
Duke's stage		
A	2.6419±0.5429	
B	1.7081±0.3631	
C	1.9880±0.1551	
D	1.5407±0.1794	

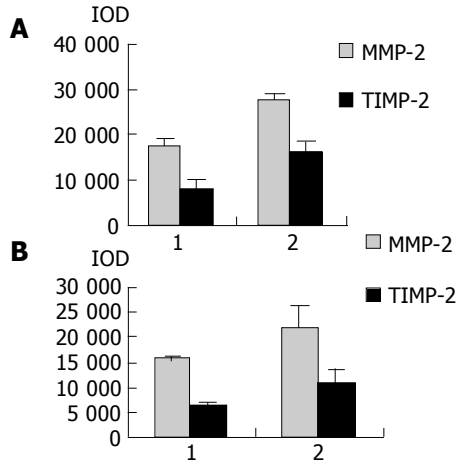

Figure 6 Densitometric intensity of absorbance (IOD) of MMP-2 and TIMP-2 expression in colorectal carcinoma tissues. **A:** different lymph node metastases. 1: lymph node negative; 2: lymph node positive; **B:** Different invasion depths. 1: muscular layer invasion; 2: serous membrane layer or surrounding soft tissue invasion.

observed mainly in the cytoplasm of colorectal carcinoma cells and matrix around tumor cells. It was also observed frequently in stromal cells. However, the positive staining with TIMP-2 was mainly distributed in the matrix around the tumor.

DISCUSSION

Our results in this study demonstrated that MMP-2 activity and expression level were much higher in colorectal carcinoma tissues than in normal tissues. Moreover, there was a significant positive correlation between the MMP-2 activity or expression level and tumor invasion depth, lymphatic metastasis and tumor Duke's stage. These results strongly indicated that MMP-2 expression level was not only associated with the development of colorectal carcinoma, but also played a very important role in the process of colorectal carcinoma invasion and metastasis. Immunohistochemical staining for MMP-2 identified that MMP-2 positive staining mainly occurred in the cytoplasm of colorectal carcinoma cells and matrix around them. It also frequently occurred in stromal cells. This suggests that the major cell source of MMP-2 in colorectal carcinoma is heterogeneous. Western blot analysis also demonstrated that the TIMP-2 (22 000 M_r) expression level in colorectal carcinoma tissues was significantly lower than that in normal colorectal tissues. Furthermore, with the progression of tumor invasion depth, lymph node metastasis and tumor Duke's stage, the TIMP-2 expression level was increased gradually, but did not reach the normal level. Our study also showed that there was an increase in the MMP-2/TIMP-2 ratio in colorectal carcinoma tissues compared to that in normal colorectal tissues. However, with the progression of tumor Duke's stage, the MMP-2/TIMP-2 ratio was gradually decreased. We think that it is related to the increased TIMP-2 expression in the late stage. So we infer that the increased TIMP-2 expression in the late stage of colorectal carcinoma

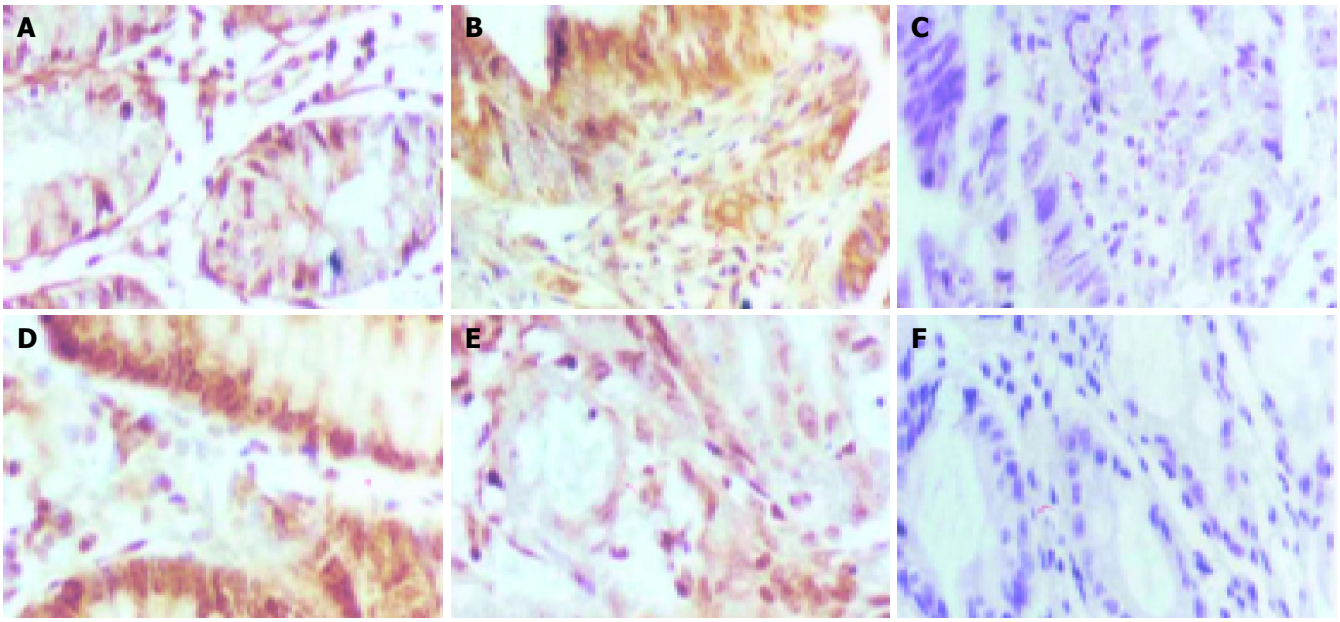

Figure 7 MMP-2 and TIMP-2 expression in normal and colorectal carcinoma tissues (SABC ×40). **A:** MMP-2 expression in normal colorectal tissue, **B:** MMP-2 expression in colorectal carcinoma tissue, **C:** MMP-2 negative control, **D:** TIMP-2 expression in normal colorectal tissue, **E:** TIMP-2 expression in colorectal carcinoma tissue, **F:** TIMP-2 negative control.

is a secondary change towards the increased MMP-2 activity.

Since the dynamic balance between MMP-2 and TIMP-2 is the decisive factor for the maintenance of ECM homeostasis and integrity, the balance disorder between them not only presents the regulation of colorectal carcinoma cells to ECM turnover, but also shows the influence of ECM on the behavior of tumor cells, which is important for colorectal carcinoma invasion and metastasis. During the progression of colorectal carcinoma, TIMP-2 plays a double role. On the one hand it inhibits MMP-2 activity, on the other hand, it is necessary for MMP-2 activation as a major cofactor, which has been reported in several studies[7,8]. In order to expand the growing space, colorectal carcinoma needs to enhance the MMP-2 activation and keep the ECM environment suitable for tumor cells, which must depend on TIMP-2 as a cofactor. In a word, the increase of TIMP-2 expression in the late stage of colorectal carcinoma predicts a worse prognosis.

REFERENCES

1 **Curran S,** Murray GI. Matrix metalloproteinases in tumour invasion and metastasis. *J Pathol* 1999; **189**: 300-308
2 **Chakraborti S,** Mandal M, Das S, Mandal A, Chakraborti T. Regulation of matrix metalloproteinases: an overview. *Mol Cell Biochem* 2003; **253**: 269-285
3 **Yoon SO,** Park SJ, Yun CH, Chung AS. Roles of matrix metalloproteinases in tumor metastasis and angiogenesis. *J Biochem Mol Biol* 2003; **36**: 128-137
4 **Zucker S,** Vacirca J. Role of matrix metalloproteinases(MMPs) in colorectal cancer. *Cancer Metastasis Rev* 2004; **23**: 101-117
5 **Lynch CC,** Matrisian LM. Matrix metalloproteinases in tumor-host cell communication. *Differentiation* 2002; **70**: 561-573
6 **Visse R,** Nagase H. Matrix metalloproteinases and tissue inhibitors of metalloproteinases: structure, function, and biochemistry. *Circ Res* 2003; **92**: 827-839
7 **Egeblad M,** Werb Z. New functions for the matrix metalloproteinases in cancer progression. *Nat Rev Cancer* 2002; **3**: 161-174
8 **Johansson N,** Ahonen M, Kahari VM. Matrix metalloproteinases in tumor invasion. *Cell Mol Life Sci* 2000; **57**: 5-15

Science Editor Wang XL and Guo SY **Language Editor** Elsevier HK

PO Box 2345, Beijing 100023, China
www.wjgnet.com
wjg@wjgnet.com

ELSEVIER

World J Gastroenterol 2005;11(20):3051-3055
World Journal of Gastroenterology ISSN 1007-9327

Antitumor effects and radiosensitization of cytosine deaminase and thymidine kinase fusion suicide gene on colorectal carcinoma cells

De-Hua Wu, Li Liu, Long-Hua Chen

De-Hua Wu, Long-Hua Chen, Department of Radiation Oncology, Nanfang Hospital, Southern Medical University, Guangzhou 510515, Guangdong Province, China
Li Liu, Institute of Cancer Research, Southern Medical University, Guangzhou 510515, Guangdong Province, China
Correspondence to: De-Hua Wu, Department of Radiation Oncology, Nanfang Hospital, Southern Medical University, Guangzhou 510515, Guangdong Province, China. wudh@fimmu.com
Telephone: +86-20-61642135 Fax: +86-20-61642131
Received: 2004-07-23 Accepted: 2004-08-23

Abstract

AIM: To investigate the killing effect and radiosensitization of double suicide gene mediated by adenovirus on colorectal carcinoma cells.

METHODS: Colorectal carcinoma cell line SW480 was transfected with adenovirus expression vector containing cytosine deaminase (CD) and thymidine kinase (TK) fusion gene. The expression of CD-TK fusion gene was detected by reverse transcriptase-polymerase chain reaction. The toxic effect of ganciclovir (GCV) and 5-fluorocytosine (5-FC) on infected cells was determined by MTT assay. The radiosensitization of double suicide gene was evaluated by clonogenic assay.

RESULTS: After prodrugs were used, the survival rate of colorectal carcinoma cells was markedly decreased. When GCV and 5-FC were used in combination, the cytotoxicity and bystander effect were markedly superior to a single prodrug ($\chi^2 = 30.371$, $P<0.01$). Both GCV and 5-FC could sensitize colorectal carcinoma cells to the toxic effect of radiation, and greater radiosensitization was achieved when both prodrug were used in combination.

CONCLUSION: CD-TK double suicide gene can kill and radiosensitize colorectal carcinoma cells.

Key words: CD-TK; Suicide gene; Radiosensitization; Colorectal carcinoma

Wu DH, Liu L, Chen LH. Antitumor effects and radiosensitization of cytosine deaminase and thymidine kinase fusion suicide gene on colorectal carcinoma cells. *World J Gastroenterol* 2005; 11(20): 3051-3055
http://www.wjgnet.com/1007-9327/11/3051.asp

INTRODUCTION

Colorectal carcinoma is one of the most frequent and life-threatening diseases throughout the world, especially in developed and industrialized countries[1]. Despite the improvements in surgery, radiotherapy and chemotherapy, the overall 5-year survival is around 50%[2]. Therefore, interest has been in the development of new treatment modalities due to the significant limitations of currently used local and systemic therapies for colorectal carcinoma. Gene therapy is a promising new treatment which can be used in combination with existing therapies[3]. The most extensively used strategy is suicide gene therapy. The suicide genes are those that have the ability to convert a nontoxic prodrug into a toxin within tumor cells when they are introduced into tumor cells[4]. Two of the best characterized genes are herpes simplex virus thymidine kinase (TK) gene and *Escherichia coli* cytosine deaminase (CD) gene. The enzyme TK efficiently phosphorylates nucleoside analogs such as GCV, and phosphorylated products interact with DNA polymerases, causing an arrest of DNA synthesis and fragmentation and thereby leading to cell death[5,6]. The CD gene is present in many bacteria and fungi but not in mammalian cells. The enzyme CD can convert the relatively non-toxic prodrug 5-FC to 5-flurouracil (5-FU), a metabolite highly toxic to mammalian cells[7,8]. Both TK and CD have been shown not only to kill transfected cells but also to exert toxic effect on neighboring cells, the so called "bystander effect"[9,10]. This is the phenomenon by which small molecules such as active drug metabolites are able to pass between cells so that untransfected cells are subjected to the same effects as those expressing the transgene. It has been shown that experimental tumors can be completely eradicated by cytotoxic gene therapy when only a proportion of the cells have taken up and expressed the relevant gene[11,12].

However, there are contradictions existing about double suicide gene therapy. For example, single suicide gene systems employing TK or CD may be preferable over combinations of the two[13]. In order to develop a protocol for an effective prodrug gene therapy of colorectal carcinomas, we used adenovirus-mediated gene delivery vectors to investigate whether CD-TK fusion gene systems could be combined to produce synergistic antitumor effects and whether CD-TK fusion gene systems could increase radiosensitization on colorectal carcinoma.

MATERIALS AND METHODS

Cell lines and culture conditions

Human colorectal adenocarcinoma SW480 and human

embryonic kidney (HEK) 293 cells obtained from American Type Culture Collection (ATCC) were cultured in Dulbecco's modified Eagle's medium (DMEM) supplemented with 10% heat-inactivated fetal bovine serum. All cells were grown in 50 mL/L CO_2 humidified atmosphere at 37 ℃.

Generation of CD-TK adenoviral vector

Adenoviral backbone vector pAdEasy-1 and shuttle vector pAdTrack-CMV-CD/TK were generous gifts of Cancer Research Institute in Xiangya Medical School of Central South University. Adenoviral vector was generated based on the principle of He *et al*[14]. Briefly, pAdEasy-1 plasmid was transformed into competent BJ5183 bacteria to generate pAdeasy-1 bacteria. pAdtrack-CMV-CD/TK plasmid was linearized with PmeI and transformed into competent pAdeasy-1 bacteria prepared by $CaCl_2$ method to generate recombinant CD-TK adenoviral plasmid. HEK293 cells were transfected by lipofectamine with recombinant adenoviral plasmid which was linearized with PacI. Transfected cells were monitored for green fluorescent protein (GFP) expression and collected 7-10 d after transfection. After three consecutive freeze-thaw cycles, the virus was collected from supernatant. The titer of the virus was determined by plaque assay using HEK293 cells, and expressed as plaque-forming units (PFU). The presence of CD-TK fusion gene in recombinant adenoviral plasmid and viral DNA was identified by PCR with forward primer (5'-GTGAATTCAGGCTAACAGTGTCGAATAACGCT-3') and reverse primer (5'-TCCTTGCGTGTTTCAGTTA-GCCTC-3').

Transfer of HSV-TK gene to colorectal carcinoma cells

SW480 cells were plated one day prior to infection and infected with adenovirus at the desired MOI for 1 h at 37 ℃, followed by the addition of growth media. In order to confirm the successful infection, RT-PCR was performed according to the manufacturer's protocol (Promega Corporation).

In vitro cytotoxicity assays

A total of 1×10^4 infected (SW480/CD-TK) or non-infected cells (SW480) were plated per well into a 96-well tissue culture plate and allowed to adhere overnight. For prodrug treatment, medium was removed and replaced by a fresh medium containing 5-FC or GCV or both of them in different concentrations. Seventy-two hours later, cell survival rate was determined using routine MTT-method and absorbance value (optical density, *A*) was read on a BioRad plate reader at 570 nm wavelength. All experiments were performed at least in triplicate. Survival rate was determined by ratios of absorbance values from test conditions over absorbance values from non-infected cells. Survival rate = (*A* value of the test well/*A* value of the control) ×100%.

Bystander effect assays

SW480 and SW480/CD-TK cells were seeded at a density of 5×10^3 cells/well in 96-well plates with proportion of 1:1. GCV and 5-FC were added at a concentration of 10 and 100 μg/mL, respectively. Then routine MTT assay was performed and assays were tested at least thrice.

Radiosensitivity assays

SW480 and SW480/CD-TK cells were plated in six-well tissue culture plate and allowed to adhere overnight. Then the medium was replaced by a fresh medium containing 100 μg/mL of 5-FC or 10 μg/mL of GCV or both. After 48 h, cells were exposed to a single dose of X-irradiation (0-6 Gy). Clonogenic survival was determined by counting crystal violet-stained clones 14 d after treatment. Cytotoxicity was assessed using cell survival curve.

Statistical analysis

All experiments were repeated at least three times, and SD or standard error (SE) was calculated. χ^2 test was used to analyze the data of *in vitro* cytotoxicity and bystander effect assays. Survival curves were fit using SPSS 10.0 software. Statistical analysis and data fitting of radiosensitivity assays were performed using GraphPad Prism 4.02. A two-sided *t*-test was used to compare the means between sample groups.

RESULTS

Recombinant adenoviruses containing CD-TK gene

HEK293 cells were transfected with the recombinant adenoviral CD-TK plasmid linearized with PacI. After 3 days, 30% of cells expressed green fluorescent protein (GFP) under fluorescence microscope (Figure 1). After three consecutive freeze-thaw cycles, the titer of adenoviruses was 1×10^{12} pfu/mL by plaque assays. We used the recombinant CD-TK adenoviral plasmid and adenoviral DNA as templates to amplify CD-TK fusion gene. The result showed that the CD-TK fusion gene was present (Figure 2).

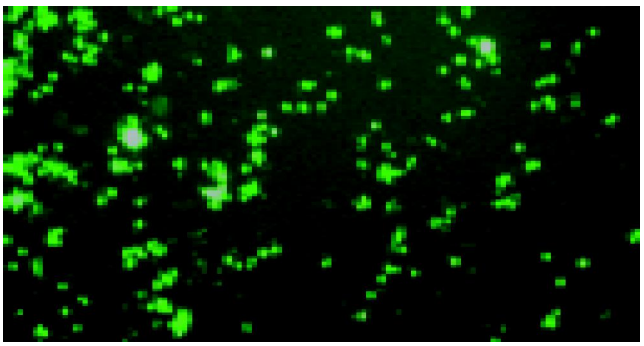

Figure 1 Green fluorescent protein expression of HEK293 cells transfected with recombinant adenoviral CD-TK plasmid under fluorescence microscope (×100).

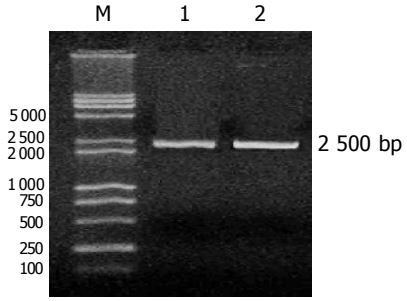

Figure 2 One percent gel electrophoretogram of PCR product (2 500 BP). M: Marker; lane 1: recombinant CD-TK adenoviral plasmid; lane 2: recombinant adenoviral DNA.

Identification of CD-TK fusion gene expression in colorectal carcinoma cells

Total RNA extracted from SW480 and SW480/CD-TK cells was confirmed to have no degradation by agarose gel electrophoresis (Figure 3A). RT-PCR detection of CD-TK gene expression in SW480 and SW480/CD-TK cells is shown in Figure 3B. SW480/CD-TK cells infected with recombinant adenovirus expressed CD-TK gene.

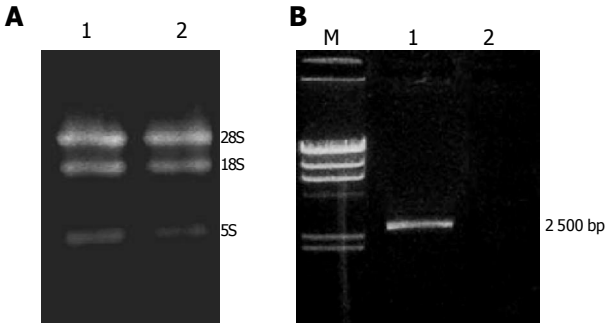

Figure 3 **A:** One percent agarose gel electrophoresis of total RNA from SW480 and SW480/CD-TK cells. Lane 1: SW480/CD-TK cells; lane 2: SW480 cells; **B:** Expression of CD-TK gene in SW480 and SW480/CD-TK cells by RT-PCR. M: λ Hind III marker; lane 1: SW480/CD-TK cells; lane 2: SW480 cells.

Cytotoxicity of double suicide gene treatment

To determine whether double prodrugs could enhance the cytotoxicity of suicide gene *in vitro*, SW480 cells were infected with the recombinant adenovirus containing CD-TK fusion gene and their sensitivity to prodrugs was compared using MTT assays. As shown in Figure 4, both prodrugs yielded killing effects on SW480/CD-TK cells in a concentration-dependent manner. The sensitivity of SW480/CD-TK cells to 5-FC+GCV was greater than that to 5-FC or GCV alone ($\chi^2 = 30.371$; $P<0.01$). To achieve the equal killing effect, lower doses of 5-Fc+GCV should be used. These results demonstrated that double prodrug therapy was superior to a single prodrug. From Figure 5, we found that both GCV and 5-FC had no significant effects on non-infected SW480 cells compared to the control ($\chi^2 = 6.540$; $P>0.05$).

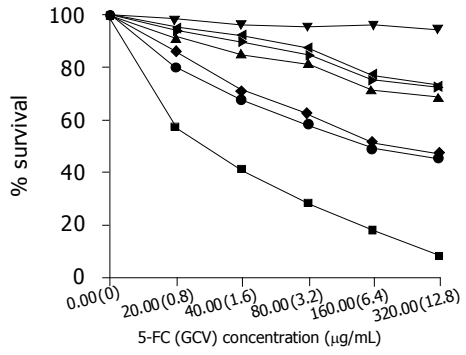

Figure 4 Sensitivity of SW480 and SW480/CD-TK cells to GCV or 5-FC or both of them ■SW480/CD-TK+ GCV+5-FC; ●SW480/CD-TK+ GCV; ◆SW480/CD-TK+5-FC; ▶SW480+ GCV; ◀SW480 +5-FC; ▲SW480+ GCV+5-FC; ▼SW480 (Control).

Bystander effect

SW480/CD-TK cells exhibited a bystander effect when mixed with non-infected SW480 cells. The results showed that the cell inhibitory rate was 75.3±6.8% when both prodrugs were used. The inhibitory rate was 39.3±5.4% and 32.6±6.3%, respectively when 5-FC or GCV was added alone, demonstrating that 5-FC and GCV could be combined to achieve synergistic effect (Figure 5).

Radiosensitization of SW480/CD-TK cells

For radiocytotoxicity studies, SW480/CD-TK cells were treated with fixed concentrations of 5-FC or GCV alone or both for 48 h prior to irradiation. The SER_{SF2} of SW480/CD-TK cells was 1.86 for GCV, 2.96 for 5-FC and 5.05 for both GCV and 5-FC, respectively. Although GCV or 5-FC alone sensitized the tumor cells to radiation, 5-FC and GCV in combination had a more radiosensitizing effect than a single prodrug ($P<0.01$).

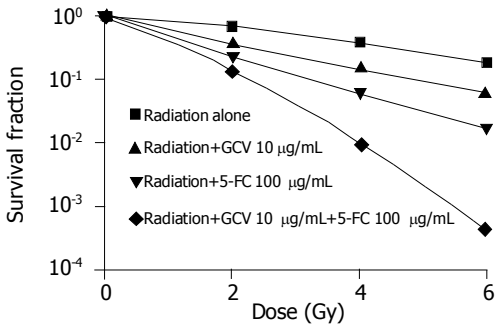

Figure 5 Effects of 5-FC and GCV on radiosensitization of SW480/CD-TK cells.

DISCUSSION

Insertion of genes that activate pro-drugs to produce cytotoxity in tumor cells is considered as a potential therapeutic strategy for cancer treatment. As demonstrated before, double suicide gene therapy is important in controlling tumor growth, reducing cell survival and eradicating tumors such as gliosarcoma[15], mammary adenocarcinoma[16], pancreatic cancer, prostatic[17] and ovarian cancer[18]. We transferred CD-TK fusion gene into human colorectal carcinoma and investigated the *in vitro* efficacy of single and combined prodrugs. The results showed that CD-TK fusion gene had a killing effect on colorectal carcinoma. Although each single prodrug effectively kills tumor cells, prodrugs in combination could have a more powerful killing effect ($P<0.01$). In addition, the advantage of combined prodrugs can also be appreciated by reduction of dose. Taken together, our study demonstrated that strong synergism occurred when tumor cells expressing CD-TK fusion gene were treated with 5-FC and GCV in combination.

Our study also found that SW480/CD-TK cells exhibited a bystander effect when 5-FC and GCV were used alone or in combination. The bystander effect represents the ability of tumor cells expressing a prodrug-activating enzyme to

eradicate neighboring nontransduced tumor cells following prodrug treatment[19,20]. We found that improvement in bystander effect was achieved by double prodrugs. In culture, the bystander effects of these prodrugs probably result from transfer of active metabolites of prodrugs from enzyme-expressing cells to nontransduced tumor cells, either by facilitating diffusion in the case of 5-FC or through gap junctions or apoptotic vesicles in the case of GCV[19,21-23]. The synergy bystander of double prodrugs is important especially in *in vivo* gene therapy, because it can decrease the disadvantage of low gene transfer efficiency and augment the antitumor effect of suicide gene[24].

In humans, treatment of advanced tumors usually requires a more rigorous approach, involving several different modalities. In this regard, we explored the possibility that combining suicide gene therapy with radiation therapy might result in enhanced cytotoxicity, thereby providing a more effective means of eliminating tumor. Our results demonstrated that suicide gene therapy could sensitize tumor cells to radiation therapy. 5-FC and GCV could independently potentiate the killing effects of radiation. Even greater radiosensitivity was observed when both prodrugs were used in comparison with a single prodrug. The advantage of this approach is that it is possible to decrease radiation dose and minimize damage to normal tissues[25]. Suicide gene therapy and radiotherapy produce a synergistic effect and make the combined therapeutic effect even greater[26].

Although current gene therapy techniques are potentially powerful therapeutic tools, practical clinical application of these techniques remains to be studied[27]. One of the rate-limiting factors affecting gene therapy is the development of a safe and reliable vector that can insert the desired gene into the target[28]. Adenoviral vectors can facilitate highly efficient transfection of therapeutic genes into tumor cells. Adenovirus has several characteristics that make it ideal for use in tumor gene therapy. For example, since adenovirus can be efficiently delivered into replicating or nonreplicating cells of epithelial origin, it may be ideal for *in vivo* systemic therapy. The safety of adenoviral gene therapy vectors has been proved in human trials[29]. In conclusion, CD/5-FC and TK/GCV can enhance radiosensitization of colorectal carcinoma.

REFERENCES

1 **Budenholzer B.** Screening for colorectal cancer. *CMAJ* 2001; **164**: 965-966; author reply 967-968
2 **Ohlsson B,** Palsson B. Follow-up after colorectal cancer surgery. *Acta Oncol* 2003; **42**: 816-826
3 **Fibison WJ.** Gene therapy. *Nurs Clin North Am* 2000; **35**: 757-772
4 **Rochlitz CF.** Gene therapy of cancer. *Swiss Med Wkly* 2001; **131**: 4-9
5 **Hlubinova K,** Hlavaty J, Altaner C. Human glioma cells expressing herpes simplex virus thymidine kinase gene treated with acyclovir, ganciclovir and bromovinyldeoxyuridine. Evaluation of their activity *in vitro* and in nude mice. *Neoplasma* 2001; **48**: 398-406
6 **Okabe S,** Arai T, Yamashita H, Sugihara K. Adenovirus-mediated prodrug-enzyme therapy for CEA-producing colorectal cancer cells. *J Cancer Res Clin Oncol* 2003; **129**: 367-373
7 **Koyama F,** Sawada H, Hirao T, Fujii H, Hamada H, Nakano H. Combined suicide gene therapy for human colon cancer cells using adenovirus-mediated transfer of escherichia coli cytosine deaminase gene and Escherichia coli uracil phosphoribosyltransferase gene with 5-fluorocytosine. *Cancer Gene Ther* 2000; **7**: 1015-1022
8 **Ireton GC,** McDermott G, Black ME, Stoddard BL. The structure of Escherichia coli cytosine deaminase. *J Mol Biol* 2002; **315**: 687-697
9 **Pierrefite-Carle V,** Baque P, Gavelli A, Mala M, Chazal M, Gugenheim J, Bourgeon A, Milano G, Staccini P, Rossi B. Cytosine deaminase/5-fluorocytosine-based vaccination against liver tumors: evidence of distant bystander effect. *J Natl Cancer Inst* 1999; **91**: 2014-2019
10 **Cho HS,** Lee HR, Kim MK. Bystander-mediated regression of murine neuroblastoma via retroviral transfer of the HSV-TK gene. *J Korean Med Sci* 2004; **19**: 107-112
11 **Uckert W,** Kammertons T, Haack K, Qin Z, Gebert J, Schendel DJ, Blankenstein T. Double suicide gene (cytosine deaminase and herpes simplex virus thymidine kinase) but not single gene transfer allows reliable elimination of tumor cells *in vivo*. *Hum Gene Ther* 1998; **9**: 855-865
12 **Rogulski KR,** Zhang K, Kolozsvary A, Kim JH, Freytag SO. Pronounced antitumor effects and tumor radiosensitization of double suicide gene therapy. *Clin Cancer Res* 1997; **3**: 2081-2088
13 **Moriuchi S,** Wolfe D, Tamura M, Yoshimine T, Miura F, Cohen JB, Glorioso JC. Double suicide gene therapy using a replication defective herpes simplex virus vector reveals reciprocal interference in a malignant glioma model. *Gene Ther* 2002; **9**: 584-591
14 **He TC,** Zhou S, da Costa LT, Yu J, Kinzler KW, Vogelstein B. A simplified system for generating recombinant adenoviruses. *Proc Natl Acad Sci USA* 1998; **95**: 2509-2514
15 **Chang JW,** Lee H, Kim E, Lee Y, Chung SS, Kim JH. Combined antitumor effects of an adenoviral cytosine deaminase/thymidine kinase fusion gene in rat C6 glioma. *Neurosurgery* 2000; **47**: 931-938; discussion 938-939
16 **Uckert W,** Kammertons T, Haack K, Qin Z, Gebert J, Schendel DJ, Blankenstein T. Double suicide gene (cytosine deaminase and herpes simplex virus thymidine kinase) but not single gene transfer allows reliable elimination of tumor cells *in vivo*. *Hum Gene Ther* 1998; **9**: 855-865
17 **Yoshimura I,** Suzuki S, Tadakuma T, Hayakawa M. Suicide gene therapy on LNCaP human prostate cancer cells. *Int J Urol* 2001; **8**: S5-S8
18 **Kieback DG,** Fischer DC, Engehausen DG, Sauerbrei W, Oehler MK, Tong XW, Aguilar-Cordova E. Intraperitoneal adenovirus-mediated suicide gene therapy in combination with either topotecan or paclitaxel in nude mice with human ovarian cancer. *Cancer Gene Ther* 2002; **9**: 478-481
19 **Aghi M,** Kramm CM, Chou TC, Breakefield XO, Chiocca EA. Synergistic anticancer effects of ganciclovir/thymidine kinase and 5-fluorocytosine/cytosine deaminase gene therapies. *J Natl Cancer Inst* 1998; **90**: 370-380
20 **Kuriyama S,** Mitoro A, Yamazaki M, Tsujinoue H, Nakatani T, Akahane T, Toyokawa Y, Kojima H, Okamoto S, Fukui H. Comparison of gene therapy with the herpes simplex virus thymidine kinase gene and the bacterial cytosine deaminase gene for the treatment of hepatocellular carcinoma. *Scand J Gastroenterol* 1999; **34**: 1033-1041
21 **Dong Y,** Wen P, Manome Y, Parr M, Hirshowitz A, Chen L, Hirschowitz EA, Crystal R, Weichselbaum R, Kufe DW, Fine HA. *In vivo* replication-deficient adenovirus vector-mediated transduction of the cytosine deaminase gene sensitizes glioma cells to 5-fluorocytosine. *Hum Gene Ther* 1996; **7**: 713-720
22 **Imaizumi K,** Hasegawa Y, Kawabe T, Emi N, Saito H, Naruse K, Shimokata K. Bystander tumoricidal effect and gap junctional communication in lung cancer cell lines. *Am J Respir Cell Mol Biol* 1998; **18**: 205-212
23 **van Dillen IJ,** Mulder NH, Vaalburg W, de Vries EF, Hospers GA. Influence of the bystander effect on HSV-tk/GCV gene

therapy. A review. *Curr Gene Ther* 2002; **2**: 307-322
24 **Namba H,** Tagawa M, Iwadate Y, Kimura M, Sueyoshi K, Sakiyama S. Bystander effect-mediated therapy of experimental brain tumor by genetically engineered tumor cells. *Hum Gene Ther* 1998; **9**: 5-11
25 **Lee YJ,** Lee H, Borrelli MJ. Gene transfer into human prostate adenocarcinoma cells with an adenoviral vector: Hyperthermia enhances a double suicide gene expression, cytotoxicity and radiotoxicity. *Cancer Gene Ther* 2002; **9**: 267-274
26 **Freytag SO,** Rogulski KR, Paielli DL, Gilbert JD, Kim JH. A novel three-pronged approach to kill cancer cells selectively: concomitant viral, double suicide gene, and radiotherapy. *Hum Gene Ther* 1998; **9**: 1323-1333
27 **Scanlon KJ.** Cancer gene therapy: challenges and opportunities. *Anticancer Res* 2004; **24**: 501-504
28 **Kay MA,** Glorioso JC, Naldini L. Viral vectors for gene therapy: the art of turning infectious agents into vehicles of therapeutics. *Nat Med* 2001; **7**: 33-40
29 **Freytag SO,** Stricker H, Pegg J, Paielli D, Pradhan DG, Peabody J, DePeralta-Venturina M, Xia X, Brown S, Lu M, Kim JH. Phase I study of replication-competent adenovirus-mediated double-suicide gene therapy in combination with conventional-dose three-dimensional conformal radiation therapy for the treatment of newly diagnosed, intermediate- to high-risk prostate cancer. *Cancer Res* 2003; **63**: 7497-7506

Science Editor Wang XL and Guo SY **Language Editor** Elsevier HK

PO Box 2345, Beijing 100023, China
www.wjgnet.com
wjg@wjgnet.com

ELSEVIER

World J Gastroenterol 2005;11(20):3056-3059
World Journal of Gastroenterology ISSN 1007-9327

Viral and host causes of fatty liver in chronic hepatitis B

Emin Altıparmak, Seyfettin Köklü, Mesut Yalınkılıc, Osman Yüksel, Bahattin Cicek, Ertugrul Kayacetin, Tülin Sahin

Emin Altıparmak, Seyfettin Köklü, Mesut Yalınkılıc, Osman Yüksel, Bahattin Cicek, Ertugrul Kayacetin, Tülin Sahin, Department of Gastroenterohepatology, Yüksek Ihtisas Hospital, Sıhhiye, Ankara, Turkey
Correspondence to: Emin Altıparmak, Associated Professor, Yüksek Ihtisas Hastanesi, Gastroenteroloji, Klinigi, Sıhhiye, Ankara, Turkey. ealtiparmak20@hotmail.com
Telephone: +90-312-3103080 Fax: +90-312-3124120
Received: 2003-12-12 Accepted: 2004-01-30

Abstract

AIM: To investigate the viral and host causes of fatty liver in chronic hepatitis B patients and the role of fat deposits in liver damage.

METHODS: A total of 164 patients (113 males and 51 females, average age 35±11.3 years, and range 10-62 years) with previously untreated chronic hepatitis B were included in the study. The patients were divided into two groups depending on the result of liver biopsy: group without steatosis (100 patients with <5% hepatosteatosis) and group with steatosis (64 patients with >5% hepatosteatosis). The groups were compared in terms of gender, body mass index (BMI), liver enzymes (ALT, AST, ALP, GGT), cholesterol, triglyceride, HBeAg, viral load, and histological findings. In the group with steatosis, the patients were subdivided depending on the degree of steatosis into mild group (45 patients with 5-24% steatosis), and severe group (19 patients with >25% steatosis).

RESULTS: In the group of chronic hepatitis B with steatosis, the mean age, BMI, cholesterol, and triglyceride levels were significantly higher than those in the group without steatosis (P<0.05). Steatosis was found in 53 (46.9%) of male patients and 11 (22%) of female patients (P<0.05). No significant difference was found in the positivity of ALT, AST, ALP, GGT, HBeAg, viral load, histological activity index (HAI) and stage between the two groups (P>0.05). In the group with severe steatosis, the BMI was significantly higher than that in the group with mild steatosis (P<0.05). No significant difference was found in the other parameters between the groups (P>0.05).

CONCLUSION: Steatosis in chronic hepatitis B appears to be a result of metabolic factors of the host rather than the effect of viruses. Steatosis is unrelated to the HAI and degree of fibrosis, which are considered as the histological indicators of liver damage.

Key words: Chronic hepatitis B; Steatosis

Altıparmak E, Köklü S, Yalınkılıc M, Yüksel O, Cicek B, Kayacetin E, Sahin T. Viral and host causes of fatty liver in chronic hepatitis B. *World J Gastroenterol* 2005; 11(20): 3056-3059
http://www.wjgnet.com/1007-9327/11/3056.asp

INTRODUCTION

Hepatosteatosis is defined as fat deposition in the liver that exceeds 5% of the total weight of liver, or with more than 5% of hepatocytes containing fat deposits under light microscopic examination[1]. It occurs under several disease states. The most common causes are alcohol, metabolic diseases, drugs, and nutritional disorders.

Chronic hepatitis C and hepatosteatosis have been shown to occur together often. It is thought that the hepatosteatosis of chronic hepatitis C is associated with the effects of viruses. In these patients, fat deposition appears to be an augmenting factor in liver damage[2-5].

In the literature, few data is available on the role of chronic hepatitis B, which forms an important disease group in hepatology, in steatosis. Some hepatitis C viruses are termed steatovirus[6,7]. No important study investigating the relationship between chronic hepatitis B and fatty liver and the effect of steatosis on the course of the disease is available.

In this study, whether the cause of fatty liver in chronic hepatitis B patients who received no previous treatment is due to viral or host factors and the role of fat deposition in liver damage were investigated.

MATERIALS AND METHODS

The study included 164 patients in 1997-2002 with the diagnosis of chronic hepatitis B (positive for HBsAg, elevated transaminase levels for at least 6 mo, and histopathological findings) who received no antiviral treatment. The following patients were excluded from the study. Those receiving antiviral treatment before the study, those on hepatotoxic drug treatment, those consuming alcohol regularly or excessively, those diagnosed of cirrhosis, anti-HCV or anti-Delta positive patients, those diagnosed as having autoimmune or other metabolic liver diseases. The height and weight of all patients were determined and the body mass index (BMI) was calculated. Based on the BMI, the patients were classified as normal (BMI = 18.5-24.9), over weight (BMI = 25-29.9), obese (BMI = 30-34.9), or extremely obese (BMI = 35-39.9). Liver function, blood glucose, cholesterol and triglyceride levels of each patient were also determined. For each patient HBsAg, HBeAg (Abbot Laboratories, North Chicago, IL, USA) were measured and

HBV DNA was determined by PCR (Amplicor, Roche). The viral load was measured by hybridization (Hybrid Capture Assay, Digene, USA) in 122 patients.

Liver biopsy was performed on each patient. Determination of the histological activity index (HAI) and staging of the biopsy materials were done according to the Knodell's classification[8]. HAI was scored as portal inflammation (0-4), lobular degeneration (0-4), and periportal necrosis (0-10). According to the degree of fibrosis, staging was made from 0 to 4 (0: no fibrosis, I: mild, II: moderate, III: severe, IV: cirrhosis). In the classification of steatosis less than 5% was considered normal, 5-25% as mild, greater than 25% as severe fat deposition.

Statistical analysis

Kruskall-Wallis variance analysis, Mann-Whitney *U* tests and the χ^2 tests were performed.

RESULTS

The 164 chronic hepatitis B patients included in the study were subdivided into group with and without steatosis according to the findings of the liver biopsy materials. One hundred patients had no steatosis, while 64 had steatosis. Fifty-one of the patients were females and 113 were males. The mean age was 35±11.3 years (range 10-62 years). Eleven of female patients (22%) and 53 (46.9%) of the male patients were found to have steatosis. The difference was statistically significant (χ^2: 9.67; $P<0.05$).

The average age, BMI, cholesterol and triglyceride level in the group with steatosis were found to be significantly higher than those in the group without steatosis ($P<0.05$). The differences in the average AST, ALT, ALP, GGT and viral load values showed no statistical significance ($P<0.05$).

The group of patients without steatosis according to the degree of fibrosis showed that 30 (30%) patients were of stage 0, 50 (50%) of stage 1, 7 (7%) of stage 2, and 13 (13%) of stage 3. In the patients with steatosis, however, 24 (37.5%), 29 (45.3%), 3 (4.7%), and 8 (12.5%) of the patients were of stages 0, 1, 2, and 3, respectively. The difference between them was not statistically significant (χ^2: 1.19; $P>0.05$). Examination of the group without steatosis according to the HAI revealed 16 (16%) patients to be of HAI 1 [Knodell score (KS) 0-3], 48 (48%) of HAI 2 (KS 4-8), 23 (23%) of HAI 3 (KS 9-12) and 13 (13%) of HAI 4 (KS 13-18). In the group with steatosis, however, the corresponding number was 7 (10.9%), 34 (53.1%), 16 (25%), and 7 (10.9%), respectively. The differences between the groups were not statistically significant (χ^2: 1.12; $P>0.05$).

Of the 164 patients, 106 were found to be HBeAg (-) and 58 HBeAg (+). Steatosis was discovered in 17 (29.3%) of those with HBeAg (+) and in 46 (44.3%) of those with HBeAg (-). The difference between the two groups was not statistically significant (χ^2: 3.55; $P>0.05$). The findings are summarized in Tables 1-3 and in Figure 1.

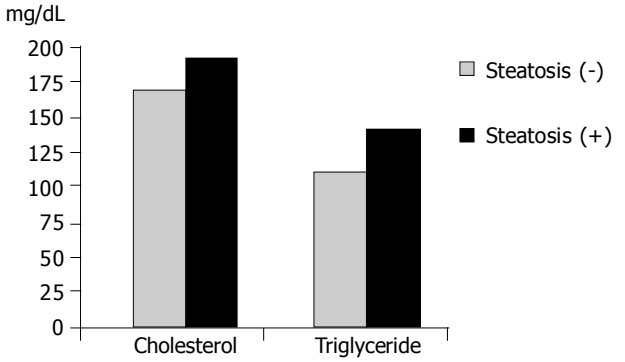

Figure 1 Comparison of cholesterol and triglyceride levels of groups with and without steatosis ($P<0.05$).

The presence of diabetes mellitus or a history of alcohol was considered as a risk factor in the patients. Based on this, 23 patients were found to carry the risk factor, 141 patients did not carry this risk.

Although steatosis was found in 12 (52.2%) patients among those with risk factors, and in 52 (36.9%) of those without the risk factors, the difference between the groups,

Table 1 Comparison of groups according to demographic features

	Steatosis (–) $n = 100$	Steatosis (+) $n = 64$	*P*
Age (yr)	33.23±11.70	37.90±10.09	0.006[a]
BMI	25.25±3.93	27.75±3.70	0.000[a]
Sex (female, %)	40 (78)	11 (22)	0.008[a]
(male, %)	60 (53.1)	53 (46.9)	

[a]$P<0.05$ difference is statistically significant.

Table 2 Comparison of groups according to biochemical features

	Steatosis (–) $n = 100$	Steatosis (+) $n = 64$	*P*
AST	76.50±56.14	70.04±54.61	0.469
ALT	131.62±109.39	113.45±68.19	0.686
GGT	39.67±38.27	44.29±35.33	0.139
ALP	175.08±75.53	173.39±65.68	0.834
Cholesterol	162.20±38.58	184.89±34.54	0.000[a]
Triglyceride	102.50±44.66	133.67±65.96	0.004[a]

[a]$P<0.05$ difference is statistically significant.

Table 3 Comparison of groups according to virological and histopathological features

		Steatosis (-) $n = 100$, %	Steatosis (+) $n = 64$, %	*P*
HBeAg	(–)	58 (58.6)	46 (73)	0.059
	(+)	42 (41.4)	17 (27)	
HBV DNA	(–)			
	(+)	9 (12.2)	12 (25)	0.067
		65 (87.8)	36 (75)	
Viral load	(pg/mL)	1 628.24±2 944.29	781.55±1 292.36	0.063
Stage	0	30 (30)	24 (37.5)	
	1	50 (50)	29 (45.3)	0.754
	2	7 (7)	3 (4.7)	
	3	13 (13)	8 (12.5)	
HAI	0–3	16 (16)	7 (10.9)	
	4–8	48 (48)	34 (53.1)	0.772
	9–12	23 (23)	16 (25)	
	13–17	13 (13)	7 (10.9)	

however, was not statistically significant (χ^2: 1.94; P>0.05).

The 164 patients admitted into the study were subdivided into three groups depending on the biopsy findings: group without steatosis (<5%), group with mild steatosis (5-25%), and group with advanced degree steatosis (>25%). There were 100 patients without steatosis, 45 with mild steatosis, and 19 with advanced degree steatosis. Comparison of the three groups in terms of the mean AST, ALT, ALP, GGT and viral load values showed no statistically significant differences (P>0.05). In terms of the mean age, BMI, cholesterol and triglyceride levels, statistically significant differences were observed between the groups (P<0.05). Comparison of the groups in pairs revealed significantly higher values in BMI and cholesterol levels in the group with mild steatosis than in those without steatosis (P<0.05). In the group with advanced degree steatosis, the BMI, triglyceride and cholesterol levels were found to be significantly higher than those in the group without steatosis (P<0.05). The BMI in the group with advanced degree steatosis was found to be significantly higher than that in the group with mild steatosis (P<0.05, Figure 2).

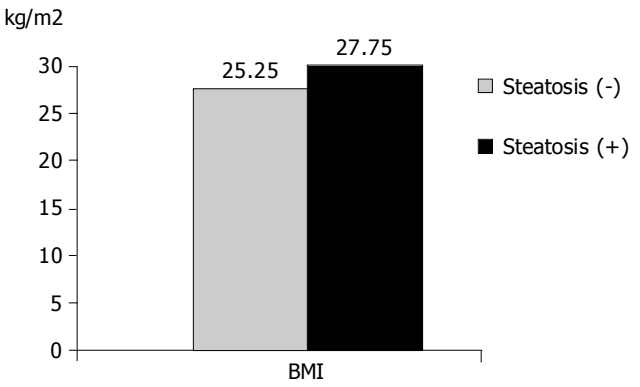

Figure 2 Comparison of BMI of groups with and without steatosis (P<0.05).

DISCUSSION

Viral hepatitis steatosis is thought to be associated with chronic hepatitis C. Steatosis in chronic hepatitis C has been postulated to be associated with the effects of the viruses rather than an immunological response. We, therefore, in our own study, tried to investigate the relationship between chronic hepatitis B virus, another viral agent causing chronic liver diseases, and steatosis. In the end, it was concluded that steatosis in chronic hepatitis B was independent of the viral effect.

In chronic liver diseases other than chronic hepatitis C, no study showing the relationship between steatosis and the disease is available. In these diseases steatosis has been thought to be a different independent pathological entity[9,10]. A study reports that chronic hepatitis B has occurred concurrently with steatosis in 27% of patients[11]. In another study, patients with hepatitis C and B in terms of risk factors were compared, and steatosis was found to occur more frequently in chronic hepatitis C[12]. Unfortunately, the number of chronic hepatitis B patients with steatosis in this study was rather very small.

Some studies, demonstrating the association between steatosis and chronic hepatitis B, described the viruses as "fibroviruses" in some patients and as "steatoviruses" in others[6,7]. One of these studies included patients with relapse of chronic hepatitis B after liver transplantation. This is an interesting study in view of the fact that it was able to compare the histopathological findings of uninfected liver before transplantation and after exposure to the viruses after transplantation[6].

In our study genotyping of the virus could not be conducted due to the combined economic constraints, inadequate laboratory facilities and the fact that this procedure was not yet done routinely. It has been reported that chronic hepatitis C steatosis is associated with some HCV genotypes[2]. There could have been the chance of defining some of the viruses as exhibiting "steatoviruses" based on genotyping.

Steatosis often occurs in some conditions and diseases such as obesity, hyperlipidemia, alcohol consumption and diabetes mellitus. In this study, steatosis was found to be associated with obesity and hyperlipidemia. The BMI was the only factor that was related to the degree of steatosis in a linear fashion. Whereas in some studies this linear relationship between the BMI and degree of steatosis was mentioned[13], other studies showed the opposite[14]. On this issue, the distribution of body fat rather than the quantity should be the determinant[15]. This might explain why steatosis was observed to be associated with the male gender in this study. It has been reported that steatosis is highly associated with the female gender[13,16]. Some recent studies describe equal rates[17]. In our study, the observation that steatosis showed an increase with advancing age is in agreement with what was reported in literature[18].

It was reported that steatosis was a promoting factor for liver damage in HCV infections[2,3]. The effect of steatosis on histopathological damage in chronic hepatitis B is unknown. In our study, no relationship was established between liver damage and steatosis in chronic hepatitis B.

In conclusion, steatosis in chronic hepatitis B seems to be a result of metabolic causes attributable to the host rather than the effect of the viruses.

REFERENCES

1 **Schiff ER,** Sorell MF, Maddrey WC. Disease of the Liver. 6 th ed. Philedelphia: Lippincot- Williams and Wilkins, 1999: 1185-1197

2 **Adinolfi LE,** Gambardella M, Andreana A, Tripodi MF, Utili R, Ruggiero G. Steatosis accelerates the progression of liver damage of chronic hepatitis C patients and correlates with specific HCV genotype and visceral obesity. *Hepatology* 2001; **33**: 1358-1364

3 **Hourigan LF,** Macdonald GA, Purdie D, Whitehall VH, Shorthouse C, Clouston A, Powell EE. Fibrosis in chronic hepatitis C correlates significantly with body mass index and steatosis. *Hepatology* 1999; **29**: 1215-1219

4 **Westin J,** Nordlinder H, Lagging M, Norkrans G, Wejstal R. Steatosis acceleratess fibrosis development over time in hepatitis C virus genotype 3 infected patients. *J Hepatol* 2002; **37**: 837-842

5 **Castera L,** Hezode C, Roudot-Thoraval F, Bastie A, Zafrani ES, Pawlotsky JM, Dhumeaux D. Worsening of steatosis is an independent factor of fibrosis progression in untreated patients with chronic hepatitis C and paired liver biopsies. *Gut* 2003; **52**: 288-292

6 **Phillips MJ,** Cameron R, Flowers MA, Blendis LM, Greig PD, Wanless I, Sherman M, Superina R, Langer B, Levy GA. Post-transplant recurrent hepatitis B viral liver disease. Viral-burden, steatoviral, and fibroviral hepatitis B. *Am J Pathol* 1992; **140**: 1295-1308
7 **Matsumaru K,** Ishii K, Shinohara M, Sumino Y, Aikawa A, Hasegawa A, Nonaka H, Akima M. A renal allograft recipient with viral-burden, steatoviral,and fibroviral hepatitis B who achieved remission with Lamivudine. *J Clin Gastroenterol* 2003; **36**: 187-188
8 **Knodell RG,** Ishak KG, Black WC, Chen TS, Craig R, Kaplowitz N. Formulation and application of a numerical scoring system for assessing histological activity in asymptomatic chronic active hepatitis. *Hepatology* 1981; **11**: 431-435
9 **Samarasinghe D,** Tasman-Jones C. The clinical associations with hepatic steatosis: a retrospective study. *N Z Med J* 1992; **105**: 57-58
10 **Sheth SG,** Gordon FD, Chopra S. Nonalcoholic steatohepatitis. *Ann Intern Med* 1997; **126**: 137-145
11 **Czaja AJ,** Carpenter HA. Sensitivity, specificity, and predictability of biopsy interpretations in chronic hepatitis. *Gastroenterology* 1993; **105**: 1824-1832
12 **Czaja AJ,** Carpenter HA, Santrach PJ, Moore SB. Host-and disease-specific factors affecting steatosis in chronic hepatitis C. *J Hepatol* 1998; **29**: 198-206
13 **Angulo P,** Keach JC, Batts KP, Lindor KD. Independent predictors of liver fibrosis in patients with nonalcoholic steatohepatitis. *Hepatology* 1999; **30**: 1356-1362
14 **Matteoni CA,** Younossi ZM, Gramlich T, Boparai N, Liu YC, McCullough AJ. Nonalcoholic fatty liver disease: a spectrum of clinical and pathological severity. *Gastroenterology* 1999; **116**: 1413-1419
15 **Reid AE.** Nonalcoholic steatohepatitis. *Gastroenterology* 2001; **121**: 710-723
16 **Caldwell SH,** Oelsner DH, Iezzoni JC, Hespenheide EE, Battle EH, Driscoll CJ. Cryptogenic cirrhosis: clinical characterization and risk factors for underlying disease. *Hepatology* 1999; **29**: 664-669
17 **George DK,** Goldwurm S, MacDonald GA, Cowley LL, Walker NI, Ward PJ, Jazwinska EC, Powell LW. Increased hepatic iron concentration in nonalcoholic steatohepatitis is associated with increased fibrosis. *Gastroenterology* 1998; **114**: 311-318
18 **Teli MR,** James OF, Burt AD, Bennett MK, Day CP. The natural history of nonalcoholic fatty liver: a follow-up study. *Hepatology* 1995; **22**: 1714-1719

Science Editor Wang XL and Guo SY **Language Editor** Elsevier HK

PO Box 2345, Beijing 100023, China
www.wjgnet.com
wjg@wjgnet.com

ELSEVIER

World J Gastroenterol 2005;11(20):3060-3064
World Journal of Gastroenterology ISSN 1007-9327

Expression and purification of the complete PreS region of hepatitis B Virus

Qiang Deng, Yu-Ying Kong, You-Hua Xie, Yuan Wang

Qiang Deng, Yu-Ying Kong, You-Hua Xie, Yuan Wang, State Key Laboratory of Molecular Biology, Institute of Biochemistry and Cell Biology, Shanghai Institutes of Life Science, Chinese Academy of Sciences, Shanghai 200031, China
Qiang Deng, You-Hua Xie, Yuan Wang, Sino-France Center for Life Science and Genome Research, Shanghai 200031, China
Supported by the Basic Research Program from Ministry of Science and Technology of China, No. G1999054105, and special funds for Sino-France Center for Life Science and Genome Research from Chinese Academy of Sciences and Pasteur Institute in France
Co-correspondents: Yuan Wang and You-Hua Xie
Correspondence to: Yuan Wang, 320 Yue-Yang Road, Institute of Biochemistry and Cell Biology, Chinese Academy of Sciences, Shanghai 200031, China. wangy@sibs.ac.cn
Telephone: +86-21-54921103 Fax: +86-21-54921011
Received: 2004-05-29 Accepted: 2004-07-11

Abstract

AIM: To express the complete PreS region of HBV in *E.coli* with good solubility and stability, and to establish an effective method for purification of the recombinant PreS protein.

METHODS: The complete PreS region (PreS1 and PreS2) was fused into a series of tags including glutathione S-transferase (GST), dihydrofolate reductase (DHFR), maltose binding protein (MBP), 6× histidine, chitin binding domain (CBD), and thioredoxin, respectively. Expression of recombinant PreS fusion proteins was examined by SDS-PAGE analysis and confirmed by Western blot. Two fusion proteins, thio-PreS, and PreS-CBD, with desirable solubility and stability, were subjected to affinity purification and further characterization.

RESULTS: Recombinant PreS fusion proteins could be synthesized with good yields in *E.coli*. However, most of these proteins except for thio-PreS and PreS-CBD were vulnerable to degradation or insoluble as revealed by SDS-PAGE and Western blot. Thio-PreS could be purified by affinity chromatography with nickel-chelating sepharose as the matrix. However, some impurities were also co-purified. A simple freeze-thaw treatment yielded most of the thio-PreS proteins in solution while the impurities were in the precipitate. Purified thio-PreS protein was capable of inhibiting the binding of HBV virion to a specific monoclonal antibody against an epitope within the PreS1 domain.

CONCLUSION: Increased solubility and stability of the complete PreS region synthesized in *E.coli* can be achieved by fusion with the thioredoxin or the CBD tag. A simple yet highly effective method has been established for the purification of the thio-PreS protein. Purified thio-PreS protein likely assumes a native conformation, which makes it an ideal candidate for studying the structure of the PreS region as well as for screening antivirals.

Key words: Hepatitis B virus; PreS; Expression; Purification

Deng Q, Kong YY, Xie YH, Wang Y. Expression and purification of the complete PreS region of hepatitis B Virus. *World J Gastroenterol* 2005; 11(20): 3060-3064
http://www.wjgnet.com/1007-9327/11/3060.asp

INTRODUCTION

Virally encoded small (HBs), middle (MHBs), and large (LHBs) surface proteins together with cellular phospholipids form the envelope of HBV virion. These proteins are translated from distinct initiation codons, but share a common reading frame and stop codon. The HBs protein contains 226 amino acids and is the major component of the viral envelope. The MHBs protein has 55 extra amino acids (PreS2) located to the N-terminal of HBs and the LHBs protein carries an additional 119 amino acid (or 109 amino acids depending on the viral subtype, PreS1) N-terminal extension with respect to the MHBs protein[1]. All envelope proteins are co-translationally inserted into the endoplasmic reticulum (ER) membrane directed by the topogenic elements in HBs[2,3].

LHBs protein plays pivotal roles in infection and budding processes during the HBV life cycle. The N-terminal PreS region of the LHBs protein can adopt one of two topological conformations depending on whether it undergoes a posttranslational translocation. Thus, LHBs proteins in virions exhibit a mixed population with their PreS region (PreS1 and PreS2) located either inside or outside of viral envelopes[2,3]. Encapsidation of viral nucleocapsids and secretion of mature viral particles require LHBs proteins with cytoplasmic PreS region[4-8]. A stretch of amino acids across the PreS1 and the PreS2 is thought to be involved in the interaction with the cytosolic nucleocapsid before the budding event[7,8]. During the infection process, externally exposed PreS region may mediate the binding of virion to a putative cellular receptor[9,10]. Amino acids 21-47 of the PreS1 domain likely bear the major epitope for cell attachment[9-11].

Given its important functional role in the HBV life cycle and being a potential target for the development of novel antivirals, efforts have been made to express the PreS region

for structural analysis, however, with little success. To date, the PreS region synthesized in *E.coli* is either insoluble or quickly degraded[12-14]. Nunez *et al*[12], produced the PreS region fused with a 6× histidine (6× His) tag that is largely insoluble. Purification of the His-tagged PreS protein under non-denaturing condition failed owing to a severe proteolysis. Structure analysis is difficult due to the fragile nature of the PreS region synthesized in *E.coli* after denature-renaturing cycles. Study with UV-CD spectra indicates that almost half of the proteins display non-ordered conformations[12], which may reflect an inherent instability of the PreS region or the improper folding of the recombinant PreS region. Alternative ways have been adopted to synthesize partial regions of PreS[15,16]. However, it is not clear whether these partial regions retain their original structures.

In this study, we fused the PreS region with different tags respectively and studied the expression of these PreS fusion proteins in *E.coli*, in the hope of stabilizing the PreS region by a structurally linked tag. We observed increased solubility and stability of the PreS fused with the thioredoxin or the CBD tag. We have further established a simple yet highly effective method for purification of thio-PreS. The thio-PreS protein purified with this method is capable of inhibiting the binding of viral particle to a PreS1-specific monoclonal antibody.

MATERIALS AND METHODS

Plasmid construction

Primers (PreS-forward: 5'-ATGGGAGGTTGGTCTTC-CAAAC-3'; PreS-reverse: 5'-GTTCGGTGCAGGGTC-CCCAGTC-3') with adaptors harboring appropriate restriction endonuclease sites were used to amplify the fragment encoding the PreS region from the p3.6II plasmid[17,18] that contains a terminally redundant HBV genome (subtype adr-1). After digestion with appropriate enzymes, the PCR product was inserted into several prokaryotic expression vectors, respectively. Expression vectors used in this study were pET28a+ (Novagen), pQE40 (Qiagen), pMalC2x (NEB), pGEX2T (Pharmacia), pThioHisA (Invitrogen), and pTXB1 (NEB) (Figure 1). Clones containing correct inserts were verified by sequencing (Bioasia, Shanghai).

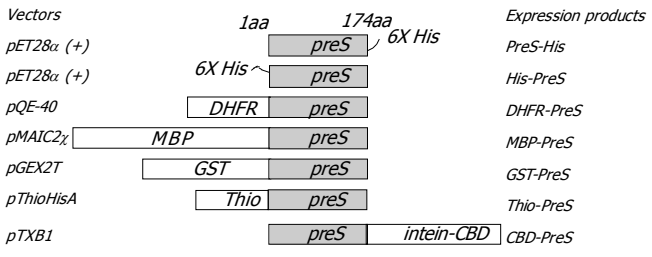

Figure 1 Diagram of various PreS fusion proteins.

Expression of fusion proteins

E.coli Top10 (F') strain was used for the expression of DHFR-PreS and thio-PreS while the BL21 (DE3) strain was used for the expression of other fusion proteins. Expression was induced by IPTG for 4 h at room temperature. Optimized IPTG concentrations were 0.1 mmol/L for DHFR-PreS, 1 mmol/L for thio-PreS, and 0.3 mmol/L for other fusion proteins. Bacteria were harvested and resuspended in PBS with 1 mmol/L EDTA and 100 mmol/L PMSF. Lysates were prepared by sonication on ice and centrifuged before further SDS-PAGE analysis.

Purification of fusion proteins

Purification of PreS-CBD was performed with chitin resin (NEB) according to the manufacturer's instructions. PreS-CBD coupled on the resin was subjected to an inter-mediated self-cleavage, induced by incubation overnight with 50 mmol/L DTT in PBS at 4 ℃. Purification of thio-PreS was performed with ProBond™ nickel-chelating sepharose resin (Invitrogen), taking advantage of a conformational His-Patch motif within the thioredoxin tag. Supernatant of the bacteria lysate was mixed with the resin and rocked gently. The resin was washed thoroughly with PBS, followed by a stringent wash with five column volumes of wash buffer (500 mmol/L NaCl, 5 mmol/L imidazole, 20 mmol/L phosphate, pH 6.0) at a flow rate of 1 mL/min. Recombinant proteins were collected in 2.5 column volumes of elution buffer (500 mmol/L NaCl, 250 mmol/L imidazole, 20 mmol/L phosphate, pH 6.0). Impurities were removed by centrifugation of the thawed sample having undergone an overnight freeze at -70 ℃. Purified proteins were subjected to desalting with Sephadex G25 (Pharmacia). Protein concentration was determined by the Bradford assay.

Virus capture assay

125E11[19,20] is a monoclonal antibody against PreS1. For virus capturing, the antibody was immobilized on a microplate (Nunc) in carbonate buffer. PBS diluted sera of HBV patients (provided by Ruijin Hospital, Shanghai) were added at 10^6 infectious virions per well and incubated for 1 h at room temperature. HBV virions were then detected with HRP conjugated anti-HBs antibody (Sino-America Biotech) and subjected to TMB developed color reaction. The optical density values were measured at 450 nm (A_{450}) with an automatic photometer (Bio-rad). For competitive binding assays, different amount of purified thio-PreS, or thioredoxin as the control, was added to the diluted sera prior to virus capturing.

Western blot

Western blot analyses of PreS fusion proteins were performed according to a standard method[21]. Supernatants of the expression lysates were separated on SDS-PAGE, and transferred to nitrocellulose filters. 125E11 (1∶1 000) was used as the primary antibody for PreS detection. Blots were developed using the ECL method (PerfectBio) with HRP-labeled rabbit anti-mouse Ig (1∶2 000, Dako).

RESULTS

Construction and expression of PreS fusion proteins

A series of prokaryotic expression vectors (Figure 1) were employed to construct PreS expression plasmids. The DNA fragment encoding the PreS region of HBV was amplified

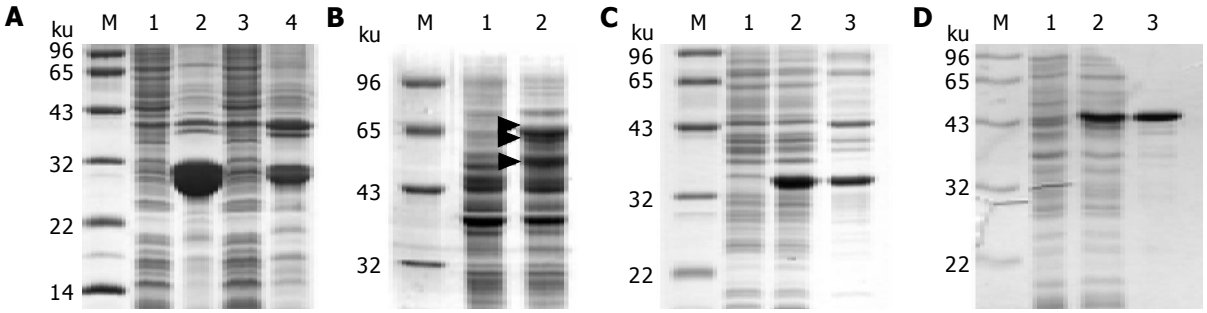

Figure 2 SDS-PAGE of the PreS fusion proteins. **A**: His-tagged PreS. Lanes 1 and 2: His-PreS; lanes 3 and 4: PreS-His; lanes 1 and 3: supernatants of the *E.coli* lysate; lanes 2 and 4: insoluble pellets; **B**: MBP-PreS. Lane 1: bacteria lysate without IPTG induction; lane 2: supernatant of the bacteria lysate after IPTG induction. The 60 kD intact protein and degradation products of MBP-PreS are indicated with triangles; **C**: thio-PreS. Lane 1: bacteria lysate without IPTG induction; lane 2: whole lysate after IPTG induction; lane 3: supernatant of the *E.coli* lysate after IPTG induction; **D**: PreS-CBD. Lane 1: bacteria lysate without IPTG induction; lane 2: PreS-CBD in the supernatant of the bacteria lysate after IPTG induction; lane 3: Purified PreS-CBD coupled to the chitin resin. Molecular weight marker is denoted as M in all figures.

by PCR and inserted into these vectors respectively. 6× His tag was fused to either the N-terminal or the C-terminal of PreS. The CBD tag was joined to the C-terminal of PreS by an intein (Figure 1). Other tags (GST, DHFR, MBP, and thioredoxin) were located at N-terminal respectively.

SDS-PAGE was performed to examine the synthesis of fusion proteins. His-tagged PreS fusion proteins were insoluble, though fairly high yields were achieved (Figure 2A). GST-PreS was found in soluble fraction of the bacteria lysate. However, severe degradation was obvious. Even worse degradation was observed with DHFR-PreS (data not shown). Previous studies by Cho *et al*[14], suggested a more stable recombinant product of MBP fused PreS. In our study, however, moderate proteolysis still occurred. Besides the full-length 60 ku protein, other bands with a smaller molecular weight were observed as indicated on SDS-PAGE, probably represented degraded proteins (Figure 2B). On the contrary, thio-PreS showed an excellent stability in solution (Figure 2C) with a high yield reaching about 0.2-0.5 mg per ml of the bacteria culture. Similarly, PreS-CBD was found predominantly in the supernatant of the bacteria lysate, and importantly, without any obvious degradation by SDS-PAGE analysis (Figure 2D).

Purification of PreS fusion proteins

Given their desirable solubility and stability, PreS-CBD and thio-PreS were subjected to further purification. The chitin matrix was used to purify the PreS-CBD protein. As shown in Figure 2D, PreS-CBD could be successfully separated from the lysate mixture and coupled to the chitin resin. Binding of PreS-CBD to the chitin resin was highly specific, and few contaminants were detected by SDS-PAGE analysis (lane 3, Figure 2D). However, the purification process was handicapped in the elution step. The intact fusion product was difficult to be eluted off the chitin resin, and inter-based cleavage was unsuccessful due to the fragile nature of the free PreS region (data not shown).

Thioredoxin tag as in thio-PreS harbored a His-Patch motif that allowed purification of recombinant proteins on nickel chelating sepharose. The His-Patch motif differed from other linear His-tags in conformation. Thus, recombinant proteins could be purified under a non-denaturing condition. Figure 3A shows the affinity purification of thio-PreS with nickel chelating sepharose. Proteins were eluted with a buffer containing imidazole at different concentrations. An elution buffer containing 250 mmol/L imidazole, 500 mmol/L NaCl and 20 mmol/L sodium phosphate, pH 6.0, gave an optimized elution of thio-PreS. However, some impurities were apparently present even under a highly stringent wash condition. We also tried the resin of thio-bond (Invitrogen) that is specific for the thioredoxin tag rather than the His-Patch motif, but with little success (data not shown).

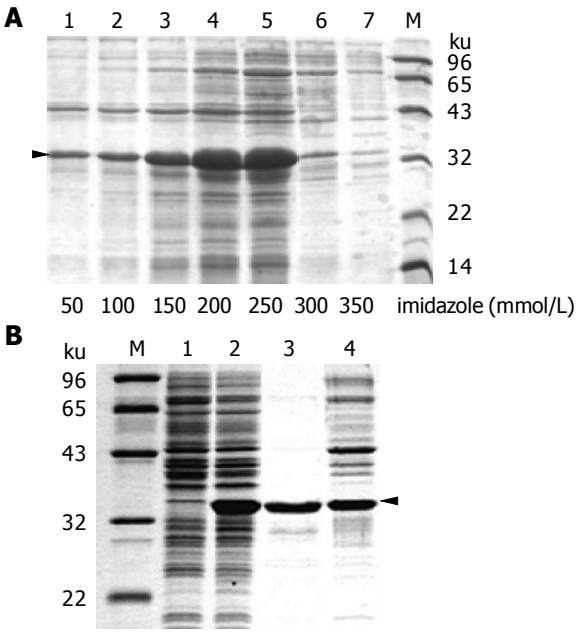

Figure 3 Purification of thio-PreS. **A**: Fractions of thio-PreS eluted with increasing imidazole concentrations listed at the bottom of each lane. The triangle indicates the position of thio-PreS; **B**: Further purification with a freeze-thaw treatment. Lanes 1 and 2: supernatants of the bacteria lysate before or after IPTG induction, respectively; lanes 3 and 4: supernatant and precipitate of the affinity purified thio-PreS sample after a freeze-thaw treatment. Molecular weight maker is denoted as M.

Since thio-PreS showed a great solubility, freezing the affinity purified sample followed by a quick thaw might improve the purity of thio-PreS by eliminating the impurities that were slow in redissolving. As shown in Figure 3B, with

this approach, most impurities were completely fractioned into the precipitate while the majority of thio-PreS remained in the supernatant without any proteolysis. Densitometry scan (Bio-Rad) of the sample on SDS-PAGE suggested a high purity of above 95%. The purified thio-PreS protein was very stable. A procedure of desalting chromatography with Sephadex G25 did little harm to the integrality of this fusion protein even at room temperature (data not shown).

Characterization of the PreS fusion protein

To verify the correctness of synthesized fusion proteins, Western blot was performed with the monoclonal antibody 125E11. As shown in Figure 4, MBP-PreS, PreS-CBD, and thio-PreS with a correct molecular weight could be detected, respectively. Proteolysis of MBP-PreS was also apparent, while only tiny traces of degradation of thio-PreS and PreS-CBD were found. 125E11 could recognize a PreS1 epitope exposed on the surface of the virion. As shown in Figure 5, when immobilized on the solid surface of microplate wells, the antibody could specifically capture viral particles from HBV patient sera. Addition of purified thio-PreS protein to the sera could inhibit the capturing process efficiently and in a dose-dependent manner, suggesting that the PreS region in the thio-PreS protein likely adopts a native conformation that mimics that of the HBV virion.

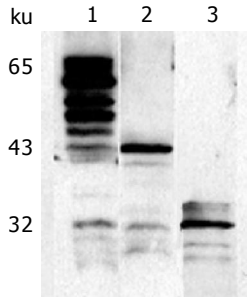

Figure 4 Characterization of the fusion proteins with Western blot.

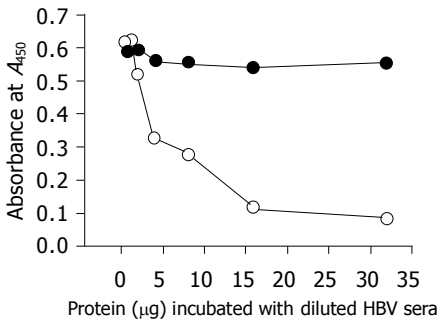

Figure 5 Virus capture assay.

DISCUSSION

The PreS region of LHBs has been implicated in the attachment of HBV virion to the putative receptor on host cells, while its inward conformation is thought to be involved in viral morphogenesis. Other important roles have also been assigned to PreS, including regulation of viral replication and transactivation of a variety of promoter elements[22-24]. Thus, multiple virological functions of the PreS region provide a useful target for anti-HBV drug intervention. Inhibition on viral infection by *E.coli* expressed PreS occurs through a direct interference with the binding of HBV to the putative cell surface receptor[25]. Recombinant PreS product could also be developed as a protein vaccine that elicits B and T cell immune responses on a broader range of MHC haplotypes[26-29]. Nevertheless, detailed structural studies of PreS are complicated by the difficulties in isolating large quantities of LHBs from viral particles and in expressing soluble and stable PreS proteins.

The complete PreS on the surface of HBV virions has been shown as an independent domain with a native structure[2,3,9,10]. Thus, recombinant PreS proteins expressed in the *E.coli* system may accurately reflect the proper structure. However, according to previous works, the PreS region is susceptible to heavy proteolysis during expression and purification. In this paper, attempts have been made to express the PreS fused with various tags in *E.coli*, in the hope of stabilizing the recombinant products by structurally linked tags[30]. Although most PreS fusion proteins expressed in this study are still vulnerable to degradation, or exist as insoluble inclusion bodies, a stable and soluble PreS fusion protein containing the thioredoxin or the CBD tag has been synthesized with a good yield. Thioredoxin is a highly hydrophilic protein tag, designed for achieving increased solubility of fusion proteins expressed in *E.coli*, and usually accumulates at sites on the cytoplasmic inner membrane known as adhesion zones[31]. We proposed that the environment of adhesion zones as well as the great solubility of thioredoxin could contribute to the better folding of the recombinant PreS protein. The impact of intein-CBD (Figure 1) on a better stability of PreS is also obvious. The underlying mechanism is currently unknown. It is possible that the intein-CBD tag forms a structure that may hinder the access of proteases to the proteolytic sites in the PreS region.

Affinity purification based on the His-Patch motif under a non-denaturing condition is not always efficient. In purification of thio-PreS, the contamination of impurities is obvious. Interestingly, after a freeze-thaw treatment, the affinity purified thio-PreS sample is dramatically purified. The majority of thio-PreS remains in the supernatant while the impurities are largely precipitated. This process may take advantage of the differential solubility between thio-PreS and the impurities or act as a salting-out step. The purified thio-PreS might adopt a native structure, since the soluble expression product in a stable fashion usually suggests a proper folding, and His-Patch based affinity purification would imply a correct conformation of the thioredoxin tag. Importantly, thio-PreS can efficiently inhibit the binding of viral particle to the PreS1 specific monoclonal antibody, suggesting exposed eptitopes in the recombinant protein as those on the surface of the native virion. PreS-CBD is also soluble and shows a high stability. Purified PreS-CBD coupled to the chitin resin could be obtained, but the following intein-based cleavage by DTT was unsuccessful which may be due to the fragile nature of the PreS region.

Similarly, thio-PreS was subjected to an enterokinase-cleavage that is engineered in the thio-fusion expression system to separate the desired PreS region from the thioredoxin tag. However, severe proteolysis was observed during this treatment (data not shown), suggesting an important role of the thioredoxin tag in stabilizing the PreS region.

In conclusion, the complete PreS region fused with the thioredoxin or CBD tag has been successfully synthesized. A simple yet efficient method has been established for purification of the thio-PreS protein. The thio-PreS protein is highly stable and soluble. The purified thio-PreS protein may be a valuable candidate for studying the structure of the PreS region as well as for screening antivirals.

ACKNOWLEDGMENTS

125E11 is a kind gift from Professor Zhu-Chuan Zhang. The authors thank Mr. Jie-Hong Jiang, and Mr. Dong-Hua Zhang, Ruijin Hospital, for providing serum samples of HBV patients.

REFERENCES

1 **Neurath AR,** Kent SB. The pre-S region of hepadnavirus envelope proteins. *Adv Virus Res* 1988; **34**: 65-142
2 **Ostapchuk P,** Hearing P, Ganem D. A dramatic shift in the transmembrane topology of a viral envelope glycoprotein accompanies hepatitis B viral morphogenesis. *EMBO J* 1994; **13**: 1048-1057
3 **Prange R,** Streeck RE. Novel transmembrane topology of the hepatitis B virus envelope proteins. *EMBO J* 1995; **14**: 247-256
4 **Poisson F,** Severac A, Hourioux C, Goudeau A, Roingeard P. Both pre-S1 and S domains of hepatitis B virus envelope proteins interact with the core particle. *Virology* 1997; **228**: 115-120
5 **Bruss V,** Vieluf K. Functions of the internal pre-S domain of the large surface protein in hepatitis B virus particle morphogenesis. *J Virol* 1995; **69**: 6652-6657
6 **Bruss V,** Ganem D. The role of envelope proteins in hepatitis B virus assembly. *Proc Natl Acad Sci USA* 1991; **88**: 1059-1063
7 **Bruss V.** A short linear sequence in the pre-S domain of the large hepatitis B virus envelope protein required for virion formation. *J Virol* 1997; **71**: 9350-9357
8 **Ponsel D,** Bruss V. Mapping of amino acid side chains on the surface of hepatitis B virus capsids required for envelopment and virion formation. *J Virol* 2003; **77**: 416-422
9 **De Meyer S,** Gong ZJ, Suwandhi W, van Pelt J, Soumillion A, Yap SH. Organ and species specificity of hepatitis B virus (HBV) infection: a review of literature with a special reference to preferential attachment of HBV to human hepatocytes. *J Viral Hepat* 1997; **4**: 145-153
10 **Cooper A,** Paran N, Shaul Y. The earliest steps in hepatitis B virus infection. *Biochim Biophys Acta* 2003; **1614**: 89-96
11 **Neurath AR,** Kent SB, Strick N, Parker K. Identification and chemical synthesis of a host cell receptor binding site on hepatitis B virus. *Cell* 1986; **46**: 429-436
12 **Nunez E,** Wei X, Delgado C, Rodriguez-Crespo I, Yelamos B, Gomez-Gutierrez J, Peterson DL, Gavilanes F. Cloning, expression, and purification of histidine-tagged preS domains of hepatitis B virus. *Protein Expr Purif* 2001; **21**: 183-191
13 **Delos S,** Villar MT, Hu P, Peterson DL. Cloning, expression, isolation and characterization of the pre-S domains of hepatitis B surface antigen, devoid of the S protein. *Biochem J* 1991; **276**(Pt 2): 411-416
14 **Cho EW,** Park JH, Yoo OJ, Kim KL. Translocation and accumulation of exogeneous hepatitis B virus preS surface proteins in the cell nucleus. *J Cell Sci* 2001; **114**: 1115-1123
15 **Lin Y,** Liu YX, Cislo T, Mason BL, Yu MY. Expression and characterization of the preS1 peptide of hepatitis B surface antigen in Escherichia coli. *J Med Virol* 1991; **33**: 181-187
16 **Maeng CY,** Oh MS, Park IH, Hong HJ. Purification and structural analysis of the hepatitis B virus preS1 expressed from Escherichia coli. *Biochem Biophys Res Commun* 2001; **282**: 787-792
17 **Feng Y,** Kong YY, Wang Y, Qi GR. Inhibition of hepatitis B virus by hammerhead ribozyme targeted to the poly (A) signal sequence in cultured cells. *Biol Chem* 2001; **382**: 655-660
18 **Fu L,** Wu X, Kong YY, Wang Y. Regulation of HBV gene expression by core promoter and its upstream sequence. *Zhongguo Bingduxue* 1997; **13**: 215-223
19 **Yang HL,** Jin Y, Cao HT, Xu X, Li GD, Wang Y, Zhang ZC. Affinity Purification of Hepatitis B Virus Surface Antigen Containing PreS1 Region. *Shengwu Huaxue Yu Wulixuebao (Shanghai)* 1996; **28**: 412-417
20 **Hui J,** Li G, Kong Y, Wang Y. Expression and characterization of chimeric hepatitis B surface antigen particles carrying preS epitopes. *J Biotechnol* 1999; **72**: 49-59
21 **Sambrook J,** Fritsch EF, Maniatis T. Molecular cloning: A laboratory manual.2nd ed. Cold Spring Harbor Laboratory Press, 1989
22 **Lenhoff RJ,** Summers J. Coordinate regulation of replication and virus assembly by the large envelope protein of an avian hepadnavirus. *J Virol* 1994; **68**: 4565-4571
23 **Caselmann WH.** Transactivation of cellular gene expression by hepatitis B viral proteins: a possible molecular mechanism of hepatocarcinogenesis. *J Hepatol* 1995; **22**: 34-37
24 **Natoli G,** Avantaggiati ML, Balsano C, De Marzio E, Collepardo D, Elfassi E, Levrero M. Characterization of the hepatitis B virus preS/S region encoded transcriptional transactivator. *Virology* 1992; **187**: 663-670
25 **Urban S,** Gripon P. Inhibition of duck hepatitis B virus infection by a myristoylated pre-S peptide of the large viral surface protein. *J Virol* 2002; **76**: 1986-1990
26 **Shouval D.** Hepatitis B vaccines. *J Hepatol* 2003; **39** Suppl 1: S70-S76
27 **Pride MW,** Bailey CR, Muchmore E, Thanavala Y. Evaluation of B and T-cell responses in chimpanzees immunized with Hepagene, a hepatitis B vaccine containing pre-S1, pre-S2 gene products. *Vaccine* 1998; **16**: 543-550
28 **Milich DR,** Jones JE, McLachlan A, Bitter G, Moriarty A, Hughes JL. Importance of subtype in the immune response to the pre-S(2) region of the hepatitis B surface antigen. II. Synthetic Pre-S(2) immunogen. *J Immunol* 1990; **144**: 3544-3551
29 **Hui J,** Mancini M, Li G, Wang Y, Tiollais P, Michel ML. Immunization with a plasmid encoding a modified hepatitis B surface antigen carrying the receptor binding site for hepatocytes. *Vaccine* 1999; **17**: 1711-1718
30 **Terpe K.** Overview of tag protein fusions: from molecular and biochemical fundamentals to commercial systems. *Appl Microbiol Biotechnol* 2003; **60**: 523-533
31 **LaVallie ER,** DiBlasio EA, Kovacic S, Grant KL, Schendel PF, McCoy JM. A thioredoxin gene fusion expression system that circumvents inclusion body formation in the *E. coli* cytoplasm. *Biotechnology (N Y)* 1993; **11**: 187-193

Science Editor Wang XL **Language Editor** Elsevier HK

PO Box 2345, Beijing 100023, China
www.wjgnet.com
wjg@wjgnet.com

ELSEVIER

World J Gastroenterol 2005;11(20):3065-3069
World Journal of Gastroenterology ISSN 1007-9327

• *BASIC RESEARCH* •

Ornithine decarboxylase, mitogen-activated protein kinase and matrix metalloproteinase-2 expressions in human colon tumors

Takahiro Nemoto, Shunichiro Kubota, Hideyuki Ishida, Nobuo Murata, Daijo Hashimoto

Takahiro Nemoto, Shunichiro Kubota, Department of Physiological Chemistry and Metabolism, Graduate School of Medicine, The University of Tokyo, 7-3-1 Hongo, Bunkyo-ku, Tokyo 113-0033, Japan
Hideyuki Ishida, Nobuo Murata, Daijo Hashimoto, Department of Surgery, Saitama Medical Center, Saitama Medical School, 1981 Tsujido-machi, Kamoda, Kawagoe City, Saitama 350-8550, Japan
Shunichiro Kubota, Department of Life Sciences, Graduate School of Arts and Sciences, The University of Tokyo, 3-8-1 Komaba, Meguro-ku, Tokyo 153-8902, Japan
Supported by a Grant Under the Ministry of Education, Science, Sports, and Culture, Japan
Correspondence to: Dr. Shunichiro Kubota, Department of Life Sciences, Graduate School of Arts and Sciences, The University of Tokyo, 3-8-1 Komaba, Meguro-ku, Tokyo 153-8902, Japan. kubota@idaten.c.u-tokyo.ac.jp
Telephone: +81-3-5454-6869 Fax: +81-3-5454-6869
Received: 2003-10-08 Accepted: 2004-01-09

Abstract

AIM: To investigate the expressions of ornithine decarboxylase (ODC), MMP-2, and Erk, and their relationship in human colon tumors.

METHODS: ODC activity, MMP-2 expression, and mitogen-activated protein (MAP) kinase activity (Erk phosphorylation) were determined in 58 surgically removed human colon tumors and their adjacent normal tissues, using [1-^{14}C]-ornithine as a substrate, ELISA assay, and Western blotting, respectively.

RESULTS: ODC activity, MMP-2 expression, and Erk phosphorylation were significantly elevated in colon tumors, compared to those in adjacent normal tissues. A significant correlation was observed between ODC activities and MMP-2 levels.

CONCLUSION: This is the first report showing a significant correlation between ODC activities and MMP-2 levels in human colon tumors. As MMP-2 is involved in cancer invasion and metastasis, and colon cancer overexpresses ODC, suppression of ODC expression may be a rational approach to treat colon cancer which overexpresses ODC.

Key words: Ornithine decarboxylase; Human colon tumors; mitogen activated protein

Nemoto T, Kubota S, Ishida H, Murata N, Hashimoto D. Ornithine decarboxylase, mitogen-activated protein kinase and matrix metalloproteinase-2 expressions in human colon tumors. *World J Gastroenterol* 2005; 11(20): 3065-3069
http://www.wjgnet.com/1007-9327/11/3065.asp

INTRODUCTION

Ornithine decarboxylase (ODC) catalyzes the initial step in the biosynthesis of polyamines and ODC activities are associated with malignant status[1]. Overexpression of ODC could lead to cell transformation, tumor invasion, and metastasis[2-4]. A number of studies demonstrated increased expression of ODC in a variety of cancers including colorectal cancer[1].

Invasion and metastasis are a multistep process[5]. Degradation of basement membranes and extracellular matrix is crucial for invasion and metastasis of cancer cells. Basement membranes contain type IV collagen, laminin, heparan sulfate proteoglycan, fibronectin, and other components[5]. Degradation of type IV collagen, a major component of basement membrane, is thought to be a prerequisite for cancer cell invasion[6]. Increased expression or activity of matrix metalloproteinases (MMPs) has been linked to malignancy and tumor cell invasion[7-9]. At least 24 MMPs have been reported so far[7-9]. MMP-2 (72 ku type IV collagenase) which preferentially degrades type IV collagen has been shown to play an important role in invasion and metastasis[5,8]. Several studies have demonstrated increased expression of MMP-2 related to invasion and metastasis of colorectal cancer[10-13].

Mitogen-activated protein (MAP) kinase is a key enzyme of the signal transduction pathways triggered by extracellular signals, including mitogens, growth factors, and cytokines[14-16]. Erk1/2, extracellular signal-regulated kinases that are also termed as p44 and p42 MAP kinases, are ubiquitously expressed. p38 MAP kinase is activated by a variety of cellular stresses, including osmotic shock, inflammatory cytokines, lipopolysaccharides, UV irradiation, and growth factors[17]. Limited information is available concerning MAP kinase expression in human surgically removed colon cancer tissues and its adjacent normal tissues[18]. Hoshino *et al*[18] showed constitutive activation of MAP kinases in 138 human cancer cell lines, and primary tumor tissues including colon cancer. However, it was reported that the activities of Erk1/2, and p38 MAP kinase were downregulated in the majority of human colon cancers[19]. Sakakura *et al*[20] also reported infrequent activation of MAP kinase in human colon cancer. Recently, the p38 MAP kinase signaling pathway was shown to be important for the induction of MMP-1 and MMP-9 by extracellular stimuli[21,22]. Therefore, it is

imperative to analyze the expression levels of MAP kinases (Erk1/2 and p38) in human surgically removed colon cancer tissues and its adjacent normal tissues.

Colon cancer is one of the most common malignancies in the world and is incurable in its advanced stages[23]. Therefore, it is important to understand the mechanism of invasion and metastasis, and to develop better treatments to prevent or cure metastatic colon cancer. As colon cancer has increased expression levels of ODC, MMP-2, and MAP kinase, these three molecules are the candidate targets for treatment of colon cancer. It is important to clarify a correlation among expressions of these three molecules. We previously found that ODC overexpression in fibroblasts led to cellular transformation and invasion with concomitant induction of MMP-2 and Erk1/2[3]. Little information is available concerning the correlation among ODC, MMP-2, and MAP kinase expressions in cancer *in vitro* and *in vivo*. The aim of this study was to investigate the expressions of ODC, MAP kinase, and MMP-2, and further to elucidate the relationship among these expressions in human colon cancer. We discussed the strategies of colon cancer treatment or prevention using α-difluoromethylornithine (DFMO), an irreversible inhibitor of ODC.

MATERIALS AND METHODS

Reagents

Antibodies against phospho-Erk and phospho-p38 MAP kinase were obtained from New England Biolabs (Beverly, MA, USA). MMP-2 ELISA system and DL-[1-^{14}C] ornithine were obtained from Amersham Pharmacia Biotech (Buckinghamshire, UK).

Samples

Paired specimens (tumor and non-cancer tissues adjacent to tumor) were obtained from a total of 58 colon cancer patients who had undergone surgical operation for adenocarcinoma at Saitama Medical University Medical Center. Written informed consent was obtained from all patients before surgical operation. All specimens were immediately stored at -80 ℃ until use.

ODC enzyme assay

ODC activity was determined using [1-^{14}C]-ornithine as a substrate as described previously[3].

MMP-2 ELISA and Western blot analysis

Tissue lysates were prepared by sonicating tissues in lysis buffer (10 mmol/L Tris-HCl buffer, pH 7.5, containing 1 mmol/L EDTA, 0.5 μg/mL aprotinin, 1 μg/mL leupeptin, and 0.2 mmol/L PMSF) and centrifuged at 12 000 *g* for 10 min at 4 ℃. Measurement of protein concentration in supernatant was performed using a Bio-Rad protein assay kit (Hercules, CA, USA). Western blotting was performed as previously described[24]. MMP-2 ELISA was performed according to the manufacturer's protocol. Quantification of the bands was performed using a NIH image.

Statistical analysis

The results were expressed as mean±SD from three independent experiments. The significance was determined by the paired *t*-test or Pearson's test. Statistical analyses were performed using the Statview 4.5 software (Abacus Concepts, Inc., Berkeley, CA, USA).

RESULTS

ODC activity in colon cancer tissues

We examined ODC activities in surgically excised human colon cancer (Figure 1). A remarkable increase in ODC activities was seen in colon cancers. Using the paired *t*-test, a significant increase in ODC activities in colon cancer tissues (6.57±0.94 pmoL CO_2 release/h/mg protein) was shown ($P = 0.0004$ by the paired *t*-test, $n = 58$), compared with those observed in adjacent non-cancer tissues (3.08±0.27 pmoL CO_2 release/h/mg protein). Increased ODC activity over the normal mean±SD level of colon cancer was seen in 17 of 58 (29.3%) cases.

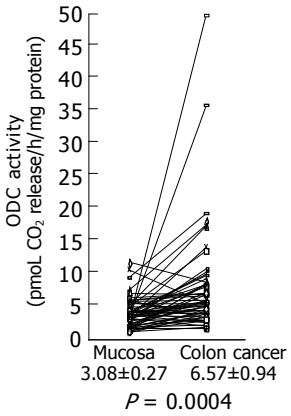

Figure 1 ODC activity in colon cancer tissues and adjacent normal tissues. ODC activities in colon cancer tissues and adjacent normal tissues were assayed as described in Materials and methods, and the data are shown as mean±SD (pmol CO_2 release/h/mg protein).

MMP-2 levels in colon cancer tissues

Next, we investigated MMP-2 expression in colon cancer using a MMP-2 ELISA kit. A significant increase in MMP-2 levels was shown in colon cancer tissues (26.40±5.83 ng/mg protein), compared with adjacent non-cancer tissues (9.02±1.47 ng/mg protein) (Figure 2) ($P = 0.046$ by the paired *t*-test, $n = 58$). Increased MMP-2 expression over the level of the normal mean±SD in colon cancer was observed in 28 of 58 (48.3%) cancers.

Expressions of phosphorylated Erk and p38 MAP kinase in colon cancer tissues

Expression of phosphorylated Erk1/2 and p38 MAP kinase was analyzed by Western blotting using the antibodies against phosphorylated Erk and p38 MAP kinase, respectively. Because of limited amount of tumor tissues, 33 out of 58 samples were used for this experiment. Using the paired *t*-test, a significant increase in phosphorylated Erk1/2 was shown in colon cancer (423.76±71.46 pixel counts) ($P = 0.0002$, $n = 33$), compared with the adjacent tissues (184.15±15.0 pixel counts) (Figure 3). Mean value of phosphorylated p38 MAP kinase had a tendency to

increase in colon cancer (232.00±29.67 pixel counts in colon cancer tissues *vs* 179.54±28.48 pixel counts in adjacent tissues), although *P* value did not reach a significant level (*P* = 0.0627) (Figure 4).

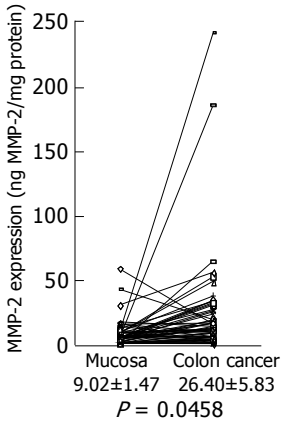

Figure 2 MMP-2 expression levels in colon cancer tissues and adjacent normal tissues. MMP-2 expression levels in colon cancer tissues and adjacent normal tissues were analyzed by MMP-2 ELISA, and the data are shown as mean±SD (ng MMP-2/mg protein).

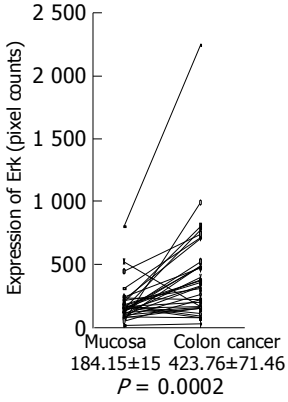

Figure 3 Erk expression in colon cancer tissues and adjacent normal tissues. Expression of phosphorylated Erk1/2 in colon cancer tissues and adjacent normal tissues was analyzed by Western blotting using a specific antibody against phosphorylated Erk1/2, quantitated using a NIH image, and shown as mean±SD (pixel counts).

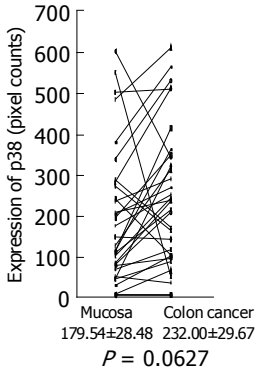

Figure 4 p38 MAP kinase expression in colon cancer tissues and adjacent normal tissues. Expression of phosphorylated p38 MAP kinase in colon cancer tissues and adjacent normal tissues was analyzed by Western blotting using a specific antibody against phosphorylated p38 MAP kinase, quantitated using a NIH image, and are shown as mean±SD (pixel counts).

Correlation between ODC activity, MMP-2 and Erk expressions

A significant correlation was noted between ODC activity and MMP-2 expression in colon cancer tissues and adjacent normal tissues (r^2 = 0.368, P<0.001, n = 58) (Figure 5). Although a correlation between ODC activity and phosphorylated Erk1/2 expression was not found (r^2 = 0.028, P = 0.35) in colon cancers (Figure 6), increased expression of phosphorylated Erk1/2 over the level of the normal mean±SD level was observed in 9 of 33 (27.3%) colon cancers (Figure 3). Increased expression of phosphorylated p38 MAP kinase over the level of the normal mean±SD was observed only in 3 of 33 (9.1%) colon cancers (Figure 4).

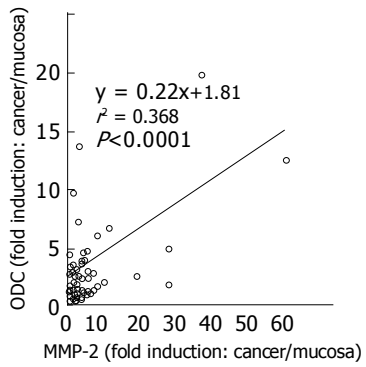

Figure 5 Relationship between ODC activities and MMP-2 expression in colon cancer tissues. Correlation between ODC activities and MMP-2 expression levels in cancer tissues, compared to those in adjacent normal tissues was shown. Statistical significance was analyzed as described in Materials and methods.

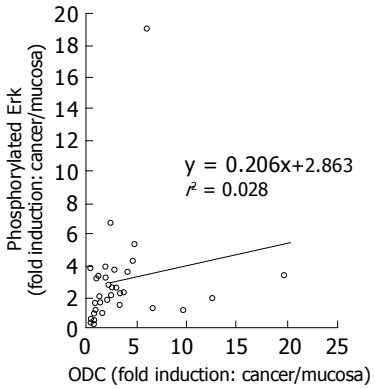

Figure 6 Relationship between ODC activities and Erk expression in colon cancer tissues. Correlation between ODC activities and Erk1/2 expression levels in cancer tissues, compared to those in adjacent normal tissues was shown. Statistical significance was analyzed as described in Materials and methods.

DISCUSSION

In the present study we showed that ODC activities, MMP-2 levels, and Erk1/2 expression had 2.13-, 2.93-, and 2.30-fold increase in colon cancer tissues, respectively, compared to its adjacent normal tissues. Increased ODC activity and MMP-2 levels over the normal mean±SD level in colon cancer were observed in 17 (29.3%) and 28 (48.3%) out of 58 colon cancer patients, respectively. Our results were

essentially consistent with the previous report concerning increased ODC activities[1] and increased expression of MMP-2 in colon cancer[10-13]. The data concerning Erk1/2 expression were consistent with the results of a previous report[18], but not with other reports[19,20]. The reason for the inconsistency is not clear. A new finding in the present study was that there was a relationship between expressions of ODC and MMP-2 in colon cancer. We previously demonstrated that ODC overexpression induced MMP-2 and Erk1/2 expressions in fibroblasts[3]. So, it is reasonably assumed that ODC expression induces MMP-2 expression in human colon cancer. A linkage of ODC and MMP-2 expressions very well explains a basis of invasive phenotype of cancers which overexpress ODC.

Metastasis is a multistep process, which includes local invasion, intravasation and extravasation of cancer cells[5]. Major functional contribution of MMPs is facilitation of degradation of basement membranes between primary tumor and distant metastasis sites. As MMP-2 preferentially degrades type IV collagen, a major component of basement membrane, MMP-2 has been thought to play a major role in invasion process[5,8]. Recent evidence indicates that MMPs including MMP-2 play a much broader role in metastasis both before and after the degradation of basement membrane[25]. For example, MMP-2 contributes to the initiation of tumor growth at both primary and metastasis sites. This may involve regulation of growth environment by regulating access to growth factors from the extracellular matrix surrounding the tumor, either directly or via a proteolytic cascade. The role of MMPs in angiogenesis is considered to be very important, as angiogenesis is required for tumor growth and invasion. Recent studies indicated that MMPs, especially MMP-2, played a pivotal role in angiogenesis[26-28]. In fact, mice deficient in MMP-2 exhibited reduced angiogenesis *in vivo*[29]. As MMP-2 overexpression in colon cancer has been found to be crucial for cancer invasion and metastasis[30], suppression of ODC using DFMO or DFMO in combination with other chemopreventives may be a rational approach to the treatment of colon cancer.

MAP kinase pathways play a major role in converting mitogenic and stress stimuli into nuclear responses. Constitutive activation of the 41-/43-ku MAP kinase (Erk1/2) signaling pathway was shown in human tumors[18]. In the present study we also found increased expression of phosphorylated Erk1/2 in colon cancer. As ODC and Erk1/2 expressions were not correlated in the present study, the data suggested that Erk1/2 expression was not a downstream signal transduction event after ODC expression in human colon cancer. Wang *et al*[19] reported that the activities of Erk1/2, JNK1 and p38 MAP kinase were downregulated in the majority of human colon cancers. The reason for the discrepancy of our result and their result concerning Erk1/2 is not clear. They discussed that protein kinases other than MAP kinases might play a more crucial role in colon carcinogenesis[19]. In the present study we showed that increased expression of phosphorylated p38 MAP kinase over the level of the normal mean±SD was observed only in 3 of 33 (9.1%) colon cancers. This result might be inconsistent with that of their report[19]. p38 MAP kinase was reported to be involved in other MMP (MMP-1 and MMP-9) expression[21,22]. However, our result and Wang's result[19], taken together, suggest that p38 MAP kinase may not be involved in carcinogenesis or invasive phenotype or MMP-2 expression in human colon cancer.

As colon cancer is still incurable at advanced stages, new strategies for prevention and treatment are desired[23]. In the 1980s, DFMO was abandoned due to limited efficacy and significant adverse effects such as nausea, vomiting, abdominal pain, diarrhea, and hearing loss in phase II clinical trials[23,31,32]. In the following decade, DFMO was resuscitated as a chemopreventive agent[33,34]. DFMO (0.2-1.0 g/m^2/d) effectively inhibited ODC activities in target organs such as the colorectum in patients with a personal or family history of colorectal cancer without side effects such as cytotoxicity[35,36]. DFMO is now being tested in phase II/III trials involving patients at risk for colorectal cancer[23]. Recent studies have shown that DFMO had synergistic reductions in intestinal neoplasia when DFMO was administered with cyclooxygenase inhibitors such as piroxicam or aspirin even as the doses of both agents were reduced as much as 50%[37-41]. Thus, DFMO in combination with other chemopreventive agents should be evaluated for the efficacy against colon cancer. As PD 184352 (MEK inhibitor)[42] or BB-94 (MMP inhibitor)[43] has been available for clinical trial, DFMO in combination of PD 184352 or BB-94 may be a rational approach to the treatment of colon cancers overexpressing ODC.

REFERENCES

1 **Cohen SS**. Polyamine metabolism and the promotion of tumor growth. In: Cohen, S.S. (ed.) A guide to the polyamines. *New York; Oxford University Press* 1998: 296-319

2 **Auvinen M**, Paasinen A, Andersson LC, Holtta E. Ornithine decarboxylase activity is critical for cell transformation. *Nature* 1992; **360**: 355-358

3 **Kubota S**, Kiyosawa H, Nomura Y, Yamada T, Seyama Y. Ornithine decarboxylase overexpression in mouse 10T1/2 fibroblasts: cellular transformation and invasion. *J Natl Cancer Inst* 1997; **89**: 567-571

4 **Moshier JA**, Dosescu J, Skunca M, Luk GD. Transformation of NIH/3T3 cells by ornithine decarboxylase overexpression. *Cancer Res* 1993; **53**: 2618-2622

5 **Liotta LA**. Tumor invasion and metastases--role of the extracellular matrix: Rhoads Memorial Award lecture. *Cancer Res* 1986; **46**: 1-7

6 **Chambers AF**, Matrisian LM. Changing views of the role of matrix metalloproteinases in metastasis. *J Natl Cancer Inst* 1997; **89**: 1260-1270

7 **Westermarck J**, Kahari VM. Regulation of matrix metalloproteinase expression in tumor invasion. *FASEB J* 1999; **13**: 781-792

8 **Yu AE**, Murphy AN, Stetler-Stevenson WG. 72 kDa Gelatinase (Gelatinase A): Structure, Activation, Regulation, and Substrate Specificity. In Parks, W.C., and Mecham RP, (ed.) Matrix Metalloproteinases. 1st ed. *San Diego: Academic Press* 1998: 85-113

9 **Nelson AR**, Fingleton B, Rothenberg ML, Matrisian LM. Matrix metalloproteinases: biologic activity and clinical implications. *J Clin Oncol* 2000; **18**: 1135-1149

10 **Levy AT**, Cioce V, Sobel ME, Garbisa S, Grigioni WF, Liotta LA, Stetler-Stevenson WG. Increased expression of the *M*r 72,000 type IV collagenase in human colonic adenocarcinoma. *Cancer Res* 1991; **51**: 439-444

11 **Parsons SL**, Watson SA, Collins HM, Griffin NR, Clarke PA, Steele RJ. Gelatinase (MMP-2 and -9) expression in gastrointestinal malignancy. *Br J Cancer* 1998; **78**: 1495-1502

12 **Liabakk NB**, Talbot I, Smith RA, Wilkinson K, Balkwill F.

Matrix metalloprotease 2 (MMP-2) and matrix metalloprotease 9 (MMP-9) type IV collagenases in colorectal cancer. *Cancer Res* 1996; **56**: 190-196
13 **Papadopoulou S**, Scorilas A, Arnogianaki N, Papapanayiotou B, Tzimogiani A, Agnantis N, Talieri M. Expression of gelatinase-A (MMP-2) in human colon cancer and normal colon mucosa. *Tumour Biol* 2001; **22**: 383-389
14 **Seger R**, Krebs EG. The MAPK signaling cascade. *FASEB J* 1995; **9**: 726-735
15 Hill CS, Treisman R. Transcriptional regulation by extracellular signals: mechanisms and specificity. *Cell* 1995; **80**: 199-211
16 **Mansour SJ**, Matten WT, Hermann AS, Candia JM, Rong S, Fukasawa K, Vande Woude GF, Ahn NG. Transformation of mammalian cells by constitutively active MAP kinase kinase. *Science* 1994; **265**: 966-970
17 **Raingeaud J**, Gupta S, Rogers JS, Dickens M, Han J, Ulevitch RJ, Davis RJ. Pro-inflammatory cytokines and environmental stress cause p38 mitogen-activated protein kinase activation by dual phosphorylation on tyrosine and threonine. *J Biol Chem* 1995; **270**: 7420-7426
18 **Hoshino R**, Chatani Y, Yamori T, Tsuruo T, Oka H, Yoshida O, Shimada Y, Ari-i S, Wada H, Fujimoto J, Kohno M. Constitutive activation of the 41-/43-kDa mitogen-activated protein kinase signaling pathway in human tumors. *Oncogene* 1999; **18**: 813-822
19 **Wang Q**, Ding Q, Dong Z, Ehlers RA, Evers BM. Downregulation of mitogen-activated protein kinases in human colon cancers. *Anticancer Res* 2000; **20**: 75-83
20 **Sakakura C**, Hagiwara A, Shirahama T, Nakanishi M, Yasuoka R, Fujita Y, Inazawa J, Abe T, Kohno M, Yamagishi H. Infrequent activation of mitogen activated protein kinase in human colon cancers. *Hepatogastroenterology* 1999; **46**: 2831-2834
21 **Westermarck J**, Holmstrom T, Ahonen M, Eriksson JE, Kahari VM. Enhancement of fibroblast collagenase-1 (MMP-1) gene expression by tumor promoter okadaic acid is mediated by stress-activated protein kinases Jun N-terminal kinase and p38. *Matrix Biol* 1998; **17**: 547-557
22 **Simon C**, Goepfert H, Boyd D. Inhibition of the p38 mitogen-activated protein kinase by SB 203580 blocks PMA-induced Mr 92,000 type IV collagenase secretion and *in vitro* invasion. *Cancer Res* 1998; **58**: 1135-1139
23 **Umar A**, Viner JL, Hawk ET. The future of colon cancer prevention. *Ann N Y Acad Sci* 2001; **952**: 88-108
24 **Nemoto T**, Kamei S, Seyama Y, Kubota S. p53 independent G (1) arrest induced by DL-alpha-difluoromethylornithine. *Biochem Biophys Res Commun* 2001; **280**: 848-854
25 **Chambers AF**, Matrisian LM. Changing views of the role of matrix metalloproteinases in metastasis. *J Natl Cancer Inst* 1997; **89**: 1260-1270
26 **Hiraoka N**, Allen E, Apel IJ, Gyetko MR, Weiss SJ. Matrix metalloproteinases regulate neovascularization by acting as pericellular fibrinolysins. *Cell* 1998; **95**: 365-377
27 **Stetler-Stevenson WG**. Matrix metalloproteinases in angiogenesis: a moving target for therapeutic intervention. *J Clin Invest* 1999; **103**: 1237-1241
28 **Werb Z**, Vu TH, Rinkenberger JL, Coussens LM. Matrix-degrading proteases and angiogenesis during development and tumor formation. *APMIS* 1999; **107**: 11-18
29 **Itoh T**, Tanioka M, Yoshida H, Yoshioka T, Nishimoto H, Itohara S. Reduced angiogenesis and tumor progression in gelatinase A-deficient mice. *Cancer Res* 1998; **58**: 1048-1051
30 **Stetler-Stevenson WG**, Liotta LA, Kleiner DE. Extracellular matrix 6: role of matrix metalloproteinases in tumor invasion and metastasis. *FASEB J* 1993; **7**: 1434-1441
31 **Ajani JA**, Ota DM, Grossie VB, Abbruzzese JL, Faintuch JS, Patt YZ, Jackson DE, Levin B, Nishioka K. Evaluation of continuous-infusion alpha-difluoromethylornithine therapy for colorectal carcinoma. *Cancer Chemother Pharmacol* 1990; **26**: 223-226
32 **Abeloff MD**, Rosen ST, Luk GD, Baylin SB, Zeltzman M, Sjoerdsma A. Phase II trials of alpha-difluoromethylornithine, an inhibitor of polyamine synthesis, in advanced small cell lung cancer and colon cancer. *Cancer Treat Rep* 1986; **70**: 843-845
33 **Love RR**, Carbone PP, Verma AK, Gilmore D, Carey P, Tutsch KD, Pomplun M, Wilding G. Randomized phase I chemoprevention dose-seeking study of alpha-difluoromethylornithine. *J Natl Cancer Inst* 1993; **85**: 732-737
34 **Meyskens FL**, Emerson SS, Pelot D, Meshkinpour H, Shassetz LR, Einspahr J, Alberts DS, Gerner EW. Dose de-escalation chemoprevention trial of alpha-difluoromethylornithine in patients with colon polyps. *J Natl Cancer Inst* 1994; **86**: 1122-1130
35 **Meyskens FL**, Gerner EW, Emerson S, Pelot D, Durbin T, Doyle K, Lagerberg W. Effect of alpha-difluoromethylornithine on rectal mucosal levels of polyamines in a randomized, double-blinded trial for colon cancer prevention. *J Natl Cancer Inst* 1998; **90**: 1212-1218
36 **Love RR**, Jacoby R, Newton MA, Tutsch KD, Simon K, Pomplun M, Verma AK. A randomized, placebo-controlled trial of low-dose alpha-difluoromethylornithine in individuals at risk for colorectal cancer. *Cancer Epidemiol Biomarkers Prev* 1998; **7**: 989-992
37 **Jacoby RF**, Cole CE, Tutsch K, Newton MA, Kelloff G, Hawk ET, Lubet RA. Chemopreventive efficacy of combined piroxicam and difluoromethylornithine treatment of Apc mutant Min mouse adenomas, and selective toxicity against Apc mutant embryos. *Cancer Res* 2000; **60**: 1864-1870
38 **Nigro ND**, Bull AW, Boyd ME. Inhibition of intestinal carcinogenesis in rats: effect of difluoromethylornithine with piroxicam or fish oil. *J Natl Cancer Inst* 1986; **77**: 1309-1313
39 **Reddy BS**, Nayini J, Tokumo K, Rigotty J, Zang E, Kelloff G. Chemoprevention of colon carcinogenesis by concurrent administration of piroxicam, a nonsteroidal antiinflammatory drug with D,L-alpha-difluoromethylornithine, an ornithine decarboxylase inhibitor, in diet. *Cancer Res* 1990; **50**: 2562-2568
40 **Rao CV**, Tokumo K, Rigotty J, Zang E, Kelloff G, Reddy BS. Chemoprevention of colon carcinogenesis by dietary administration of piroxicam, alpha-difluoromethylornithine, 16 alpha-fluoro-5-androsten-17-one, and ellagic acid individually and in combination. *Cancer Res* 1991; **51**: 4528-4534
41 **Li H**, Schut HA, Conran P, Kramer PM, Lubet RA, Steele VE, Hawk EE, Kelloff GJ, Pereira MA. Prevention by aspirin and its combination with alpha-difluoromethylornithine of azoxymethane-induced tumors, aberrant crypt foci and prostaglandin E2 levels in rat colon. *Carcinogenesis* 1999; **20**: 425-430
42 **Sebolt-Leopold JS**, Dudley DT, Herrera R, Van Becelaere K, Wiland A, Gowan RC, Tecle H, Barrett SD, Bridges A, Przybranowski S, Leopold WR, Saltiel AR. Blockade of the MAP kinase pathway suppresses growth of colon tumors *in vivo*. *Nat Med* 1999; **5**: 810-816
43 **Wojtowicz-Praga S**, Low J, Marshall J, Ness E, Dickson R, Barter J, Sale M, McCann P, Moore J, Cole A, Hawkins MJ. Phase I trial of a novel matrix metalloproteinase inhibitor batimastat (BB-94) in patients with advanced cancer. *Invest New Drugs* 1996; **14**: 193-202

Science Editor Wang XL and Guo SY **Language Editor** Elsevier HK

PO Box 2345, Beijing 100023, China
www.wjgnet.com
wjg@wjgnet.com

ELSEVIER

World J Gastroenterol 2005;11(20):3070-3074
World Journal of Gastroenterology ISSN 1007-9327

• *BASIC RESEARCH* •

MR diffusion-weighted imaging of rabbit liver VX-2 tumor

You-Hong Yuan, En-Hua Xiao, Jun Xiang, Ke-Li Tang, Ke Jin, Shi-Jian Yi, Qiang Yin, Rong-Hua Yan, Zhong He, Quan-Liang Shang, Wei-Zhou Hu, Su-Wen Yuan

You-Hong Yuan, En-Hua Xiao, Jun Xiang, Ke-Li Tang, Ke Jin, Shi-Jian Yi, Qiang Yin, Rong-Hua Yan, Zhong He, Quan-Liang Shang, Wei-Zhou Hu, Su-Wen Yuan, Department of Radiology, the Second Xiangya Hospital, Central South University, Changsha 410011, Hunan Province, China
Supported by the National Natural Science Foundation of China, No. 30070235
Correspondence to: Dr En-Hua Xiao, Department of Radiology, the Second Xiangya Hospital, Central South University, Changsha 410011, Hunan Province, China. xiaogdk@sohu.com
Telephone: +86-731-5550355 Fax: +86-731-4510190
Received: 2004-05-27 Accepted: 2004-06-17

Abstract

AIM: To investigate the implanting method of rabbit liver VX-2 tumor and its MR diffusion-weighted imaging (DWI) characteristics.

METHODS: Thirty-five New Zealand rabbits were included in the study. VX-2 tumor was implanted subcutaneously in 14 rabbits and intrahepatically in 6 for pre-experiments. VX-2 tumor was implanted intrahepatically in 12 rabbits for experiment and three were used as the control group. DWI, T1- and T2-weighted of MRI were performed periodically in 15 rabbits for experiment before and after implantation. The distinction of VX-2 tumors on DWI was assessed by their apparent diffusion coefficient (ADC) values. The statistical significance was calculated by analysis of variance (ANOVA) of the randomized block design using SPSS10.0 software.

RESULTS: The successful rate of subcutaneous implantation of VX-2 tumor was 29% (4/14) while that of intrahepatic implantation of it was 33% (2/6) in the preexperiment. The successful rate of intrahepatic implantation of VX-2 tumor in the experiment was 83% (10/12) and 15 tumors grew in 10 successfully implanted rabbits. The DWI signal of VX-2 tumor was high and became lower when the *b* value increased step by step. The signal of VX-2 tumor on the map of ADC was low. When the *b* value was 100 or 300 s/mm^2, the ADC value of normal group and VX-2 tumor group was respectively 2.57±0.26, 1.73±0.31, 1.87±0.25 and 1.57±0.23 mm^2/s. Their distinction was significant (F = 43.26, P<0.01), the tumor ADC value between *b* values 100 and 300 s/mm^2 was significant (Tukey HSP, P<0.05) and the ADC value between VX-2 tumor and normal liver was also significant (Tukey HSP, P<0.01). VX-2 tumor developed quickly and metastasized early to all body, especially to the lung, liver, lymph nodes of mediastinum, *etc*.

CONCLUSION: The DWI signal of rabbit VX-2 tumor has its characteristics on MR DWI and DWI plays an important role in diagnosing and discovering VX-2 tumor.

Key words: Magnetic resonance imaging; Diffusion-weighted; Liver; VX-2 tumor; Rabbits

Yuan YH, Xiao EH, Xiang J, Tang KL, Jin K, Yi SJ, Yin Q, Yan RH, He Z, Shang QL, Hu WZ, Yuan SW. MR diffusion-weighted imaging of rabbit liver VX-2 tumor. *World J Gastroenterol* 2005; 11(20): 3070-3074
http://www.wjgnet.com/1007-9327/11/3070.asp

INTRODUCTION

The main imaging diagnostic methods of hepatic tumor include computed tomography (CT), magnetic resonance imaging (MRI) and ultrasonography (US)[1-4]. In recent years, however, the application of MRI, especially MR diffusion-weighted imaging (DWI) in the diagnosis of hepatic tumor and evaluation of its progression is much less than that of CT and US[5-8]. With the development of software and scanning technology of MRI, many problems, for example, poor imaging quality, slow scanning speed, have been overcome[8-11] and more studies on it have been reported in recent years[12-15].

Diffusion is caused by the free movement of water molecule[8,10,13-16]. The amount of diffusion is determined by the diffusion coefficient (DC). However, because the measurement of DC *in vivo* may be affected by many factors, such as temperature, perfusion, magnetic susceptibility in the tissue, or other kinds of the motion, the apparent diffusion coefficient (ADC) is used much more in clinic than DC[14,17-19]. DWI was initially used to evaluate early ischemic stages of the brain and its values have been accepted in recent years all over the world. At the same time, several research groups have concluded that DWI has great potential for understanding normal and pathological brain function[20]. But few studies are available on the value of DWI in diagnosing or evaluating the progression of hepatic lesions, especially the VX-2 tumor of rabbits[17,21-23].

Hepatocellular carcinoma (HCC) is one of the most frequent tumors and many studies about its CT, DSA, MRI characteristics have been undertaken in recent years[3-5,6-9,24]. Rabbit VX-2 tumor is the most valuable animal model of HCC in researching its imaging characteristics[25,26], because the blood supply to VX-2 tumor and HCC is similar[23,26,27].

The purpose of our experiment was to investigate the

implanting method of rabbit liver VX-2 tumor and the characteristics of rabbit VX-2 tumor on DWI.

MATERIALS AND METHODS

Animals

Animal studies were carried out under the supervision of a veterinarian according to the guidelines of Ministry of Public Health of China for the use of laboratory animals. All animals were provided by the Laboratory Animal Center of the Second Xiangya Hospital and all protocols were approved by the Animal Use and Care Committee of the Second Xiangya Hospital.

Establishment of VX-2 tumor model[17-20]

The VX-2 tumor strain of rabbit was provided by the Fourth Military Medical University.

Our experiment was divided into two steps: pre-experiment during which subcutaneous and intrahepatic implantation of VX-2 tumor was carried out; experiment during which VX-2 tumor cells were harvested and implanted into the rabbit liver after they grew up under the rabbit derm. Ten of the twenty New Zealand white rabbits in preexperiment were male and 10 were female, their weight ranged from 1.5 kg to 2.0 kg. Six had intrahepatic implantation while 14 had subcutaneous implantation. Eight of the 15 New Zealand white rabbits in the experiment were male and seven were female, their weight ranged from 2.0 to 3.0 kg. Twelve had intrahepatic implantation while the others served as controls.

Procedure of implantation[19-23]

First, we extracted the VX-2 tumor strain from the subcutaneous tumor which was implanted during the preexperiment. After the rabbits were anesthetized, by injecting 3% soluble pentobarbitone into auriborder vein or abdominal cavity at a dose of 1 mL/kg, we incised the skin to expose one cauliflower of the tumor and then excised one cauliflower from it. Then we put the tumor parenchyma into saline containing 40 000 unit gentamycin per 100 mL, and discarded the necrosed tissue and blood clot and then cut it into 1-2 mm^3 microblocks.

Second, we implanted the VX-2 tumor strain into the subcutaneous or liver parenchyma. During the subcutaneous implanting, we pushed the VX-2 tumor strain into the subcutaneous connective tissue through the implanting tube after disinfecting and excising the skin. As the liver parenchyma implanting was concerned, we exposed the lobe of liver after excising the skin and vagina musculi recti abdominis. We put the implanting tube containing the VX-2 tumor strain into the chosen-lobe by rotating and push the VX-2 tumor strain into the liver parenchyma, then put the gelatin sponge into the implanting stoma to prevent bleeding. After the liver stopped bleeding, we sutured the peritoneum, musculi, and skin, respectively. Six of the fifteen New Zealand white rabbits in experiment were implanted in one lobe while six were implanted in two lobes.

After implanting, we injected 200 000-unit penicillin into the muscle daily for 4 d. At the same time, the animal room was kept dry and ventilated.

Magnetic resonance imaging protocol[19]

After animals were anesthetized by injecting 3% soluble pentobarbitone into auriborder vein at a dose of 1 mL/kg or at different doses based on different animal status to make sure that the breathing of animals was slow and stable, T1WI, T2WI, and DWI were performed on a 1.5-Tesla Sigma Twinspeed MR scanner (General Electron Medical Systems, USA) using a small diameter cylindrical brain radiofrequency coil. DWI (axial) and MRI (T1WI and T2WI, axial and coronal) were obtained respectively and periodically 1 d before implanting and 7, 14, 21, or 35 d after implant. The scanning parameters of DWI included spin echo echoplanar imaging (SE-EPI) series, *b*-values 100 and 300 s/mm^2, repetition time (TR) 6 000 ms, echo time (TE) 45 ms, 20 cm×15 cm field of view (FOV), 8NEX, 2 mm thickness layer, 0.5 mm Space, 128×128 matrix, *etc*. The scanning parameters of common MRI included fast reverse fast spin echo (FRFSE) series, T1WI (TR 400/TE 12.3 ms), T2WI (TR3000/TE80 ms), 20 cm×15 cm FOV, 4 NEX, 5 mm thick layer, 0 mm space, 256×192 (T1WI) and 320×256 (T2WI) matrix, *etc*.

Statistical analysis

Based on apparent diffusion coefficient (ADC) value of regions of interest (ROIs), images were evaluated quantitatively, including the difference between normal rabbit liver parenchyma and VX-2 tumor and between different *b*-value groups. ADC values of normal rabbit parenchyma were obtained by the average value of five different ROIs (50 mm^2 each area). We took 80% rabbit VX-2 tumor area as their ROI and measured their ADC values.

The statistical significance was calculated by analysis of variance (ANOVA) of the randomized block using SPSS10.0 software.

RESULTS

Results of rabbit VX-2 tumor implantation

The results of rabbit VX-2 tumor implantation are shown in Table 1.

Table 1 Results of rabbit VX-2 tumor implant

Methods	Number	Success of implant	Postoperative infection	Postoperative death	Cause of death	Rate of success (%)
Pre-experiment						
Intraderm	14	4	0	4	Diarrhea	29 (4/14)
Intrahepatic	6	2	0	2	Diarrhea	33 (2/6)
Experiment						
Intrahepatic	12	10	0	1	Diarrhea	83 (10/12)

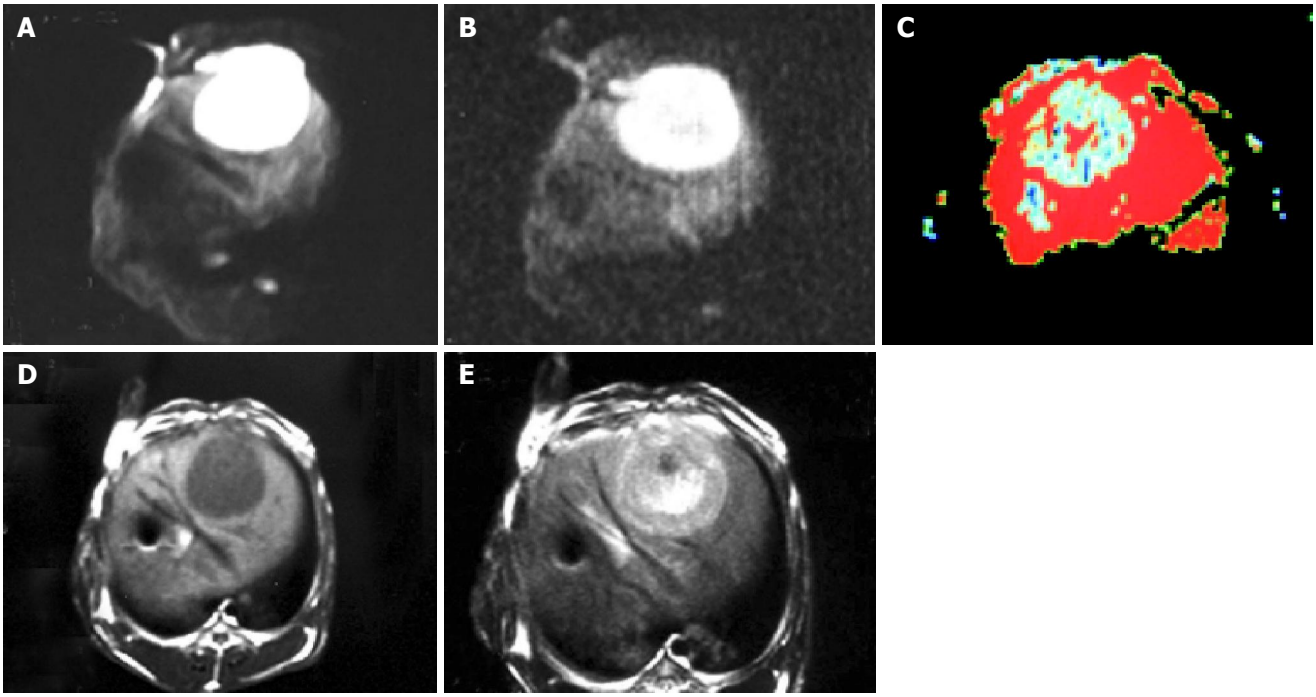

Figure 1 Image manifestations of hepatic VX-2 tumor on DWI. **A**: High signal and distinct, sharp margin of VX-2 tumor on DWI when *b* value is 100; **B**: High signal and distinct margin of VX-2 tumor on DWI when *b* value was 300; **C**: Blue-green VX-2 tumor and red normal liver parenchyma when *b* value was 100; **D**: Low signals and distinct margin of VX-2 tumor on T1WI (note: the no signal area in liver is artifact); **E**: Slightly high signals and distinct margin of VX-2 tumor on T2WI (note: the low signal in the middle of the tumor is gelatin sponge and the no signal area in liver is artifact).

Image manifestations of hepatic VX-2 tumor

Fifteen tumors were detected in 10 rabbit hepatic parenchymas. The diameter of the tumor was 4.73±0.78 on d 7, 11.35±1.73 on d 14, 21.82±3.12 on d 21, and 43.25±4.32 on d 35.

The image quality and tumor signal of DWI were higher when the *b*-value was 100 than those when the *b*-value was 300 (Figures 1A and B). Eight tumors were detected with *b*-value 100 on DWI while 10 tumors were detected with *b*-value 300 on the 7th d after implantation and 15 tumors were detected on DWI with *b*-value 100 or 300 after 14 d. All tumors showed high signals on DWI. The tumor signal on DWI was fairly uniform 14 d after implantation while it was not uniform on the 21th and 35th d and it also showed higher signals in different area tumor sometimes. In addition, one or two low signal areas could be seen in three tumors on the 21th d. T1WI, T2WI or DWI could not be seen on d 35. The margin of 15 tumors not only displayed distinctly but also differed significantly from the structure around. ADC values of all tumors are summarized in Table 2. As shown in Figure 1C, 12 of the 15 cases appeared to have low signals while three were equal or slightly low signals. The number of displayed tumors on T1WI and T2WI was same as that on DWI on the 21th or 35th d. The tumors displayed low signals on T1WI and high signals on T2WI. In addition, the margin of most tumors was distinct but less significant on T1WI or T2WI (Figures 1D and E) between the tumor and the liver parenchyma with different than that on DWI (Figures 1A and B). One of them displayed multi-tumors sizes, the biggest diameter of tumor was about 4 cm×4 cm. They showed different high signals on DWI, and low signals on TIWI and high signals on T2WI. In addition, the size of low signal zones was different in the tumor. The results of autopsy are shown in Figure 2.

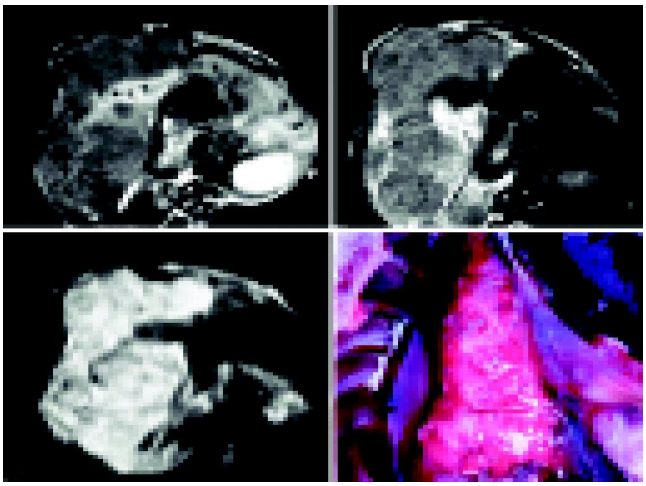

Figure 2 Pleural effusion, abdominal cavity fluid, multi-metastases in the lungs and lymph nodes 21 d after implantation of VX-2 tumor.

Table 2 ADC values of normal rabbit liver and VX-2 tumor (mean±SD)

	ADC values	A[1]	B[1]	C[1]	D[1]	*F*	*P*
A[1]	2.57±0.26		*P*<0.01[2]	*P*<0.01[2]	*P*<0.01[2]		
B[1]	1.73±0.31	*P*<0.01					
C[1]	1.87±0.25	*P*<0.01			*P*<0.05[2]		
D[1]	1.57±0.23	*P*<0.01		*P*<0.05[2]			
ANOVA						43.26	*P*<0.01

[1]A – normal rabbit liver DWI (b = 100 s/mm^2); B – normal rabbit liver DWI (b = 300 s/mm^2); C – VX-2 tumor DWI (b=100 s/mm^2); D – VX-2 tumor DWI b=100 s/mm^2); [2]Difference between different *b*-value groups or between normal liver parenchyma group and VX-2 tumor group.

Table 3 Progression of intrahepatically implanted VX-2 tumor in 12 rabbits

No.	Common conditions[1]						Transferring conditions[2] (MRI and autopsy)								Survival time (d)
	7 d	14 d	21 d	28 d	35 d	40 d	A	B	C	D	E	F	G	H[3]	
1	1	1	2	4			+	+	+	–	–	–	–	–	28
2	1	1	2	3	3	3	–	+	–	–	+	–	–	–	>40
3	1	1	3	3	3	4	+	+	+	–	–	+	+	–	39
4	4						–	–	–	–	–	–	–	–	3
5	1	1	1	1	1	1	–	–	–	–	–	–	–	–	>40
6	2	1	2	3	3	3	+	+	+	–	+	+	–	–	>40
7	1	1	1	3	4		–	+	–	–	–	–	+	–	33
8	3	2	3	3	3	3	+	+	+	–	+	–	–	–	>40
9	1	1	2	3	3	4	+	+	+	–	+	–	+	–	38
10	1	1	2	3	4		–	+	+	–	–	–	+	–	32
11	1	2	3	3	3	3	–	+	–	–	+	–	–	–	>40
12	1	1	3	3	3	4	+	+	+	–	+	–	+	–	39

[1]Common conditions: 1 – well; 2 – common; 3 – bad; 4 – dead. [2]Transferring or metastasizing conditions:– no transferring or metastasizing; + transferring or metastasizing. [3]A – liver; B – lung; C – mediastina; D – brain; E – thoracic or abdominal cavity; F – postperitone; G – diaphragm and heart; H – kidney or pancreas.

Progressing and transferring of rabbit liver VX-2 tumor

MRI and DWI were performed periodically on 12 rabbits in experiment to observe their growing and transferring or metastasizing characteristics (Table 3).

Manifestations of VX-2 tumor dissection and pathology

Intrahepatic VX-2 tumor appeared pale with no envelope and identifiable margin, the extrahepatic surface was uneven (Figure 3). Lung metastases showed many pale nodular foci in size of Mung bean or soybean (Figure 2). After the tumor was removed, the extralayer was thick and tough with rich blood supply. The interior tumor cells were pale. When the tumor grew bigger, irregular cavities could be found in it. Under low power microscope, we could see multilump nests without clear margin. In addition, more parenchyma tissue was found in the tumor than connective tissue in the tumor and there were rich and new blood capillaries between tumor cells. Calcified part in VX-2 tumors could be observed at times. Under high power microscope, VX-2 tumor cells mainly were big and irregular. In addition, the cytoplasm was rich and the nuclei were thickly stained and irregular.

Figure 3 Pale nodular foci of VX-2 tumor 14 d after implanting.

DISCUSSION

VX-2 tumor is induced by the Shope virus and develops after 72 times or more transfer of culture[17,23,24]. Its blood is mainly supplied by the hepatic artery. VX-2 tumor is implanted easily and grows quickly so that the diameter of the tumor can reach 2 cm, 3 or more weeks after implanted and it is able to metastasize to the liver, the lung, mediastinum in the early stage, which is suitable for making animal models. The rate of lung metastasis was 91% (10/11) in our group. In addition, it is advantageous to be manifested by imaging because VX-2 tumor is a solid tumor and rabbit weight is relatively great. Thus, in research of HCC imaging, VX-2 tumor is the widely used animal model[24,25].

The methods of VX-2 tumor implantation mainly include tumor cell injection by hepatic artery catheterization, percutaneous transhepatic injection of tumor cells and direct intrahepatic tumor block implantation[23,24,27]. The successful rate of the last method is the highest, which is usually more than 90%, while that of other two methods is relatively low, which is often lower than 70%[24-26]. In our experiment, we chose tumor block implanting and found the successful rate of intrahepatic implantation was 83% in experiment and 33% in pre-experiment and that of subcutaneous implantation was 29%. For this, on the one hand, we have not gotten the most vigorous tumor cells because of our poor experience and, on the other hand, many rabbits die of diarrhea because of dampness and poorly ventilated animal room as well as rabbits of unsuitable weight and age. In order to increase the successful rate, it is very important to pay attention to these implant technologies. First, we should get the most vigorous tumor cells, the mother of which is no more than 21 d after being implanted and which is observed to be pale or resembling fish flesh and is easy to separate from the tumor. Second, we should choose an appropriate implanting spot, reduce bleeding and prevent abdominal cavity implantation. Finally, clean, ventilated, dry living environment and healthy, strong rabbits are also very important.

Diffusion is caused by the free movement of water molecule, known as "Brown motion". It is able to change the intensity of local magnetic field around hydrogen proton so that its phase position in magnetic field is changed. If we add a powerful polar and quick switching gradient

radiofrequent (RF) pulse, we are able to amplify these phase changes so that we can detect water molecule diffusion motion, known as diffusion-weighted imaging (DWI). The signals on DWI are low when water molecule diffusion motion is high while the signals on DWI are high when water molecule diffusion motion is low. VX-2 tumor is a solid tumor and its body mainly consists of tumor cell nests and other cells so that its water molecule diffusion motion is restricted. The signals of most VX-2 tumor on DWI are high and its margin is usually distinct (Figures 1A and B). When *b* value increases, the signals of VX-2 tumor become lower and lower (Figures 1A and B) but the ability to detect lesions becomes stronger and stronger. All the 15 VX-2 tumors showed high signals in our experiment and the signals of tumors were lower when *b* value was 300 than when it was 100 (Figures 1A and B). The amount of diffusion is determined by the diffusion coefficient (DC). Because DC is affected by many factors, the apparent diffusion coefficient (ADC) is used more clinically rather than DC. In our experiment, the mean ADC value of 15 VX-2 tumors was 1.87±0.25 while that of the normal hepatic parenchyma was 2.57±0.26. When *b* value increased, ADC value became low. The mean ADC value of VX-2 tumor was 1.87±0.25 when *b* value was 100 while it was 1.57±0.23 when *b* value was 300.

In conclusion, the hepatic VX-2 tumor model is a simple and efficient HCC model. DWI has potentially important value in reflecting water molecular motion of tumor, detecting tumor and monitoring tumor progression.

ACKNOWLEDGMENTS

We thank the staff of the Radiology Department and the Laboratory Animal Center of the Second Xiangya Hospital for their help and support, especially Miss Ying-Si He.

REFERENCES

1 **Blomqvist L.** Preoperative staging of colorectal cancer-computed tomography and magnetic resonance imaging. *Scand J Surg* 2003; **92**: 35-43
2 **Vilana R,** Llovet JM, Bianchi L, Sanchez M, Pages M, Sala M, Gilabert R, Nicolau C, Garcia A, Ayuso C, Bruix J, Bru C. Contrast-enhanced power Doppler sonography and helical computed tomography for assessment of vascularity of small hepatocellular carcinomas before and after percutaneous ablation. *J Clin Ultrasound* 2003; **31**: 119-128
3 **Braga L,** Guller U, Semelka RC. Modern hepatic imaging. *Surg Clin North Am* 2004; **84**: 375-400
4 **Vogl TJ,** Schwarz W, Blume S, Pietsch M, Shamsi K, Franz M, Lobeck H, Balzer T, del Tredici K, Neuhaus P, Felix R, Hammerstingl RM. Preoperative evaluation of malignant liver tumors: comparison of unenhanced and SPIO (Resovist)-enhanced MR imaging with biphasic CTAP and intraoperative US. *Eur Radiol* 2003; **13**: 262-272
5 **Taouli B,** Vilgrain V, Dumont E, Daire JL, Fan B, Menu Y. Evaluation of liver diffusion isotropy and characterization of focal hepatic lesions with two single-shot echo-planar MR imaging sequences: prospective study in 66 patients. *Radiology* 2003; **226**: 71-78
6 **Ichikawa T,** Araki T. Fast magnetic resonance imaging of liver. *Eur J Radiol* 1999; **29**: 186-210
7 **Harvey PR.** The modular (twin) gradient coil-high resolution, high contrast, diffusion weighted EPI at 1.0 Tesla. *MAGMA* 1999; **8**: 43-47
8 **Stahlberg F,** Brockstedt S, Thomsen C, Wirestam R. Single-shot diffusion-weighted echo-planar imaging of normal and cirrhotic livers using a phased-array multicoil. *Acta Radiol* 1999; **40**: 339
9 **Ferrucci JT.** Advances in abdominal MR imaging. *Radiographics* 1998; **18**: 1569-1586
10 **Yamashita Y,** Tang Y, Takahashi M. Ultrafast MR imaging of the abdomen: echo planar imaging and diffusion-weighted imaging. *J Magn Reson Imaging* 1998; **8**: 367-374
11 **Chow LC,** Bammer R, Moseley ME, Sommer FG. Single breath-hold diffusion-weighted imaging of the abdomen. *J Magn Reson Imaging* 2003; **18**: 377-382
12 **Colagrande S,** Politi LS, Messerini L, Mascalchi M, Villari N. Solitary necrotic nodule of the liver: imaging and correlation with pathologic features. *Abdom Imaging* 2003; **28**: 41-44
13 **Murtz P,** Flacke S, Traber F, van den Brink JS, Gieseke J, Schild HH. Abdomen: diffusion-weighted MR imaging with pulse-triggered single-shot sequences. *Radiology* 2002; **224**: 258-264
14 **Amano Y,** Kumazaki T, Ishihara M. Single-shot diffusion-weighted echo-planar imaging of normal and cirrhotic livers using a phased-array multicoil. *Acta Radiol* 1998; **39**: 440-442
15 **Kim T,** Murakami T, Takahashi S, Hori M, Tsuda K, Nakamura H. Diffusion-weighted single-shot echoplanar MR imaging for liver disease. *AJR Am J Roentgenol* 1999; **173**: 393-398
16 **Kamel IR,** Bluemke DA, Ramsey D, Abusedera M, Torbenson M, Eng J, Szarf G, Geschwind JF. Role of diffusion-weighted imaging in estimating tumor necrosis after chemoembolization of hepatocellular carcinoma. *AJR Am J Roentgenol* 2003; **181**: 708-710
17 **Ichikawa T,** Haradome H, Hachiya J, Nitatori T, Araki T. Diffusion-weighted MR imaging with single-shot echo-planar imaging in the upper abdomen: preliminary clinical experience in 61 patients. *Abdom Imaging* 1999; **24**: 456-461
18 **Moteki T,** Horikoshi H, Oya N, Aoki J, Endo K. Evaluation of hepatic lesions and hepatic parenchyma using diffusion-weighted reordered turboFLASH magnetic resonance images. *J Magn Reson Imaging* 2002; **15**: 564-572
19 **Chan JH,** Tsui EY, Luk SH, Fung AS, Yuen MK, Szeto ML, Cheung YK, Wong KP. Diffusion-weighted MR imaging of the liver: distinguishing hepatic abscess from cystic or necrotic tumor. *Abdom Imaging* 2001; **26**: 161-165
20 **Lodi R,** Tonon C, Stracciari A, Weiger M, Camaggi V, Iotti S, Donati G, Guarino M, Bolondi L, Barbiroli B. Diffusion MRI shows increased water apparent diffusion coefficient in the brains of cirrhotics. *Neurology* 2004; **62**: 762-766
21 **Ichikawa T,** Haradome H, Hachiya J, Nitatori T, Araki T. Diffusion-weighted MR imaging with a single-shot echoplanar sequence: detection and characterization of focal hepatic lesions. *AJR Am J Roentgenol* 1998; **170**: 397-402
22 **Yuan YH,** Xiao EH. MR diffusion-weighted imaging progressing in liver. *J Practice Radiology* 2003; **19**: 945-948
23 **Geschwind JF,** Artemov D, Abraham S, Omdal D, Huncharek MS, McGee C, Arepally A, Lambert D, Venbrux AC, Lund GB. Chemoembolization of liver tumor in a rabbit model: assessment of tumor cell death with diffusion-weighted MR imaging and histologic analysis. *J Vasc Interv Radiol* 2000; **11**: 1245-1255
24 **Jia HS,** Quan XY, Zeng S, Wen ZB. Dynamic evaluation of rabbit VX2 hepatic carcinoma with CT and MRI. *Diyi Junyi Daxue Xuebao* 2002; **22**: 141-144
25 **Minami Y,** Kudo M, Kawasaki T, Kitano M, Chung H, Maekawa K, Shiozaki H. Transcatheter arterial chemoembolization of hepatocellular carcinoma: usefulness of coded phase-inversion harmonic sonography. *AJR Am J Roentgenol* 2003; **180**: 703-708
26 **Kuszyk BS,** Boitnott JK, Choti MA, Bluemke DA, Sheth S, Magee CA, Horton KM, Eng J, Fishman EK. Local tumor recurrence following hepatic cryoablation: radiologic-histopathologic correlation in a rabbit model. *Radiology* 2000; **217**: 477-486
27 **Merkle EM,** Boll DT, Boaz T, Duerk JL, Chung YC, Jacobs GH, Varnes ME, Lewin JS. MRI-guided radiofrequency thermal ablation of implanted VX2 liver tumors in a rabbit model: demonstration of feasibility at 0.2 T. *Magn Reson Med* 1999; **42**: 141-149

Science Editor Wang XL **Language Editor** Elsevier HK

PO Box 2345, Beijing 100023, China
www.wjgnet.com
wjg@wjgnet.com

ELSEVIER

World J Gastroenterol 2005;11(20):3075-3079
World Journal of Gastroenterology ISSN 1007-9327

• *BASIC RESEARCH* •

Uptake of albumin nanoparticle surface modified with glycyrrhizin by primary cultured rat hepatocytes

Sheng-Jun Mao, Shi-Xiang Hou, Ru He, Liang-Ke Zhang, Da-Peng Wei, Yue-Qi Bi, Hui Jin

Sheng-Jun Mao, Shi-Xiang Hou, Ru He, Liang-Ke Zhang, Da-Peng Wei, Yue-Qi Bi, Hui Jin, West China School of Pharmacy, Sichuan University, Chengdu 610041, Sichuan Province, China
Supported by the National Natural Science Foundation of China, No. 30271613
Correspondence to: Shi-Xiang Hou, West China School of Pharmacy, Sichuan University, Chengdu 610041, Sichuan Province, China. xinba789@yahoo.com.cn
Telephone: +86-28-85501376 Fax: +86-28-85502809
Received: 2004-07-20 Accepted: 2004-08-25

Abstract

AIM: To investigate the uptake difference between bovine serum albumin nanoparticle (BSA-NP) and bovine serum albumin nanoparticles with their surface modified by glycyrrhizin (BSA-NP-GL) and to develop a novel hepatocyte targeting BSA-NP-GL based on active targeting technology mediated by specific binding site of GL on rat cellular membrane.

METHODS: Calcein loaded bovine serum albumin nanoparticles (Cal-BSA-NP) were prepared by desolvation process. Glycyrrhizin was conjugated to the surface reactive amino groups (SRAG) of Cal-BSA-NP by sodium periodate oxidization, which resulted in calcein-loaded bovine serum albumin nanoparticles with their surface modified by glycyrrhizin (Cal-BSA-NP-GL). The morphology of the two types of prepared nanoparticles (NP) was observed by transmission electron microscopy. The diameter of NP was measured with a laser particle size analyzer. The interaction between Cal-BSA-NP-GL and primary cultured hepatocytes was studied through cellular uptake experiments. The uptake amount of Cal-BSA-NP-GL and Cal-BSA-NP by rat hepatocytes was determined by fluorospectrophotometry. Uptake characteristics were investigated through experiments of competitive inhibition of specific binding site of GL.

RESULTS: Both Cal-BSA-NP-GL and Cal-BSA-NP had regular spherical surfaces. The average diameter of Cal-BSA-NP-GL and Cal-BSA-NP was 77 and 79 nm respectively. The uptake amount of the two NP by hepatocytes reached its maximum at 2 h after incubation. The uptake amount of Cal-BSA-NP-GL by rat hepatocytes was 4.43-fold higher than that of Cal-BSA-NP. There was a significant difference in the uptake of Cal-BSA-NP-GL and Cal-BSA-NP by hepatocytes ($P<0.01$). The uptake of Cal-BSA-NP-GL was inhibited when GL was added previously to isolated rat hepatocytes, and the uptake of Cal-BSA-NP was not affected by GL.

CONCLUSION: A binding site of GL is present on the surface of rat hepatocytes, BSA-NP-GL may be internalized via this site by hepatocytes and can be used as a drug carrier for active targeting of delivery drugs to hepatocytes.

Key words: Glycyrrhizin; Surface modified; Bovine serum albumin; Nanoparticles; Hepatocytes

Mao SJ, Hou SX, He R, Zhang LK, Wei DP, Bi YQ, Jin H. Uptake of albumin nanoparticle surface modified with glycyrrhizin by primary cultured rat hepatocytes. *World J Gastroenterol* 2005; 11(20): 3075-3079
http://www.wjgnet.com/1007-9327/11/3075.asp

INTRODUCTION

Liver cells are divided into hepatocytes (hepatic parenchymal cells), Kupffer cells and endothelial cells (hepatic nonparenchymal cells). Parenchymal cells are the main cells of liver. Many fatal diseases occur in hepatocytes, such as chronic hepatitis, cirrhosis, enzyme deficiency and hepatoma. Because of the poor efficiency of current drugs uptaken by hepatocytes, there are few effective therapeutic methods for hepatic diseases. Hence, it is important to target drugs to the hepatocytes.

Application of nanoparticles (NP) in drug delivery systems (DDS) is of particular interest because they provide drug targeting possibilities and sustained release action. However, they have some disadvantages such as rapid uptake by the reticuloendothelial system (RES) within seconds or minutes after injection due to phagocytosis by macrophages in the liver and spleen.

Receptor-mediated drug targeting is a promising approach to selective drug delivery. One particular method exploits the mechanisms of sugar recognition of some specific cells. Among various types of cells in the body, hepatocytes exclusively have high affinity cell-surface receptors that can bind to asialoglycoproteins and subsequently internalize them to the cell interior. Delivery of drugs using liposomes bound to asialoglycoprotein in a specific manner would provide significant therapeutic benefits to hepatic disease. Extensive studies on chemical modification of liposomes with asialoglycoproteins[1-3] or low-molecular weight glycolipid have been carried out to achieve effective targeting to hepatocytes[4-8]. However, it was reported that galactose-bearing liposomes are also taken up by Kupffer cells, and the distribution of these liposomes

in hepatocytes is not very high[9]. Therefore, the discovery of a new ligand instead of using the conventional ones requires investigation.

Glycyrrhizin (GL), a conjugate of one molecule of glycyrrhetinic acid and two molecules of glucuronic acid, is one of the main compounds extracted from the root of *Glycyrrhiza glabra* L (licorice). In 1990s, Negishi *et al*[10], proved that there are specific binding site of glycyrrhizin on the cellular membrane of *in vitro* rat hepatocytes. Based on this research, liposome surface modified with glycyrrhizin was prepared and proved that the uptake amount and *in vivo* distribution of the modified liposomes are considerably higher compared with the conventional liposomes[11,12].

However, liposomes have limitations due to several factors such as leakage of their contents before reaching the target tissue, rapid clearance from the blood stream and their uptake by macrophages of the liver and spleen (RES). Therefore, it is necessary to develop a novel hepatocyte targeting DDS. We have previously prepared albumin NP with their surface modified by glycyrrhizin and studied their pharmaceutical characteristics[13]. In this study, calcein-loaded bovine serum albumin nanoparticles with their surface modified by glycyrrhizin (Cal-BSA-NP-GL) was prepared and the uptake of Cal-BSA-NP-GL by *in vitro* rat hepatocytes was investigated. The interaction between Cal-BSA-NP-GL and isolated rat hepatocytes was determined and the uptake mechanism and influential factors were initially investigated through *in vitro* cell culture experiments.

MATERIALS AND METHODS

Chemicals and reagents

Bovine serum albumin was purchased from Bio Life Science & Technology Co. Ltd (Shanghai, China). Calcein was obtained from SSS Reagent (Shanghai, China). Glycyrrhizin, desoxyribonuclease I and collagenase IV were purchased from Sigma (USA). Carbonate buffer (CBS, pH 9.50, 0.2 mol/L Na_2CO_3 13.0 mL+0.2 mol/L $NaHCO_3$ 37.0 mL), Hank's solution and RPMI-1640 culture medium were provided by the Department of Immunology, School of Preclinical Medicine, Sichuan University. All the other chemicals and reagents used were of analytical grade.

Preparation of Cal-BSA-NP and Cal-BSA-NP-GL

Albumin NP were prepared by a desolvation process as described previously by Weber *et al*[14]. In brief, 100 mg bovine serum albumin was dissolved in 10 mL solvent of calcein (0.1 mg/ mL) by constant stirring at 25 ℃, 20 mL ethanol and 25 μL 2.5% glutaral solution were added gradually into the solvent mixture respectively. After 3-h stirring, ethanol was vacuum distilled and the colloidal solution of calcein-loaded bovine serum albumin nanoparticles (Cal-BSA-NP) was obtained. Glycyrrhizin was dissolved in CBS to make glycyrrhizin solution (0.1 mol/L), 0.1 mol/L $NaIO_4$ solution was added gradually into the glycyrrhizin solution, which resulted in glycyrrhizin oxide solution after stirring for 3 h. Twenty milliliters of glycyrrhizin oxide solution was added into the Cal-BSA-NP solution. After being stirred for 3 h at 25 ℃, Cal-BSA-NP-GL was obtained. The drug amount loaded on NP was determined by fluorospectrophotometry (RF-5000, Shimadzu, Japan), the particle shape was observed under a transmission electron microscope (H-600, Hitachi, Japan) and the particle size was measured with a laser particle size analyzer (Malvern-2000, UK).

Primary culture of rat hepatocytes

Hepatocytes were isolated from normal liver of male Wistar rats weighing approximately 200 g. The livers were purged with Hank's solution and scissored into tissue blocks (1 mm×1 mm). The blocks were treated with 1 mg/mL collagenase IV solution (pH was adjusted to 7.4 using Hepes) at 37 ℃ for 120 min and filtrated via a 200-mesh cell sieve. Hepatocytes were washed thrice by slow centrifugation (500 r/min, 1 min) of the cell suspension to remove cell debris, damaged and nonparenchymal cells. Viability as tested by trypan blue exclusion was over 95%. Isolated hepatocytes were plated onto collagen-coated six-well culture plates at a density of 1×10^6 cells/well, incubated in RPMI-1640 solution in 50 mL/L CO_2 at 37 ℃ for 24 h, and used in the following experiments.

In vitro hepatocyte uptake experiment

Cal-BSA-NP and Cal-BSA-NP-GL solutions were ultracentrifuged (1.5×10^4 *g*) for 20 min, the supernatants were discarded and precipitations were ultrasonically dispersed with 0.5 mL PBS. Then, 0.5 mL Cal-BSA-NP and 0.5 mL Cal-BSA-NP-GL solutions were added to 1 mL preincubated hepatocyte suspension respectively, RPMI-1640 culture solution was added to 2 mL and mixed uniformly. Hepatocytes were incubated with Cal-BSA-NP and Cal-BSA-NP-GL at the indicated concentration in a fresh medium. After incubation for the indicated time, the medium was removed and the cells were washed four times with 12 mL ice-cold PBS, 2 mL distilled water was added into the washed cells and the mixture was stored at -10 ℃ for 2 h. The congelations were defrosted at room temperature to disintegrate the cells. The achieved mixture was centrifuged for 10 min (1×10^4 *g*), and the supernatants were diluted with PBS to 5 mL. The fluorescence strength in the solutions was determined (λ_{ex} = 491.2 nm, λ_{em} = 510.4 nm, slit width = 10 nm). When the concentration of calcein was 0.2-6.4 ng/mL, the standard curve was described as regression equation: $F = -1.51+97.58C$ (ng/mL), $r = 0.9997$. The uptake amount of the two types of NP by hepatocytes was expressed as nanograms of total BSA per 10^6 cells. Each value represented the mean±SD of three experiments. The data were calculated according to the drug amount loaded and the determined strength of fluorescence. For the inhibition experiment, the cells were preincubated with GL solution (GL dissolved in 50 mg/mL $NaHCO_3$) at a concentration of 0-50 mmol/L in medium. The uptake experiments were then carried out as above.

In order to exclude the error caused by calcein absorption of the cell culture plate, parallel processes were followed in all experiments. 0.5 mL Cal-BSA-NP and Cal-BSA-NP-GL solutions were incubated, centrifuged, purged and treated with the above-mentioned method, their strength of fluorescence was determined and deducted while the uptake quantity of hepatocytes was calculated.

RESULTS

Drug amount loaded, morphology and particle size

The drug amount loaded on Cal-BSA-NP and Cal-BSA-NP-GL was 6.02 and 5.93 μg/mg BSA respectively. Transmission electron microscopy (Figure 1) demonstrated that both Cal-BSA-NP (Figure 1A) and Cal-BSA-NP-GL (Figure 1B) had a regular spherical surface. Figure 2 showed that the average diameter of Cal-BSA-NP and Cal-BSA-NP-GL was 77 and 79 nm respectively with a narrow distribution (polyindex 0.42, 0.31).

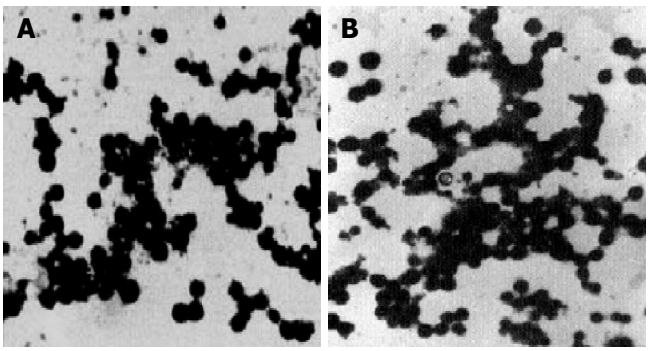

Figure 1 Transmission electron microscopy of Cal-BSA-NP (**A**) and Cal-BSA-NP-GL (**B**) (×15 000).

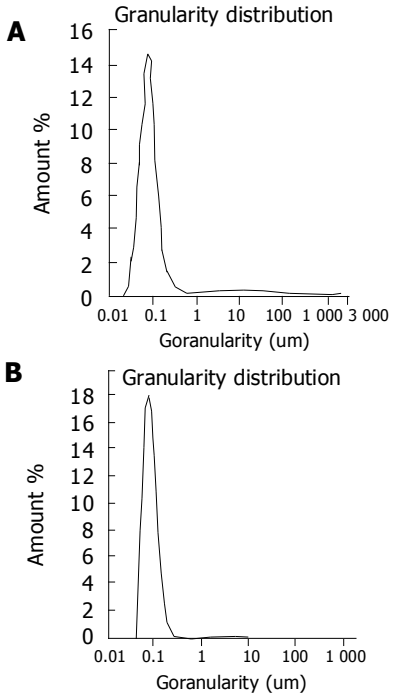

Figure 2 Diameter of Cal-BSA-NP (**A**) and Cal-BSA-NP-GL (**B**).

Dose dependency of uptake of Cal-BSA-NP and Cal-BSA-NP-GL by primary cultured rat hepatocytes

In these experiments, 0.5 mL Cal-BSA-NP and Cal-BSA-NP-GL solutions at the indicated concentration were added respectively to 1 mL previously incubated hepatocyte suspensions, and 0.5 mL RPMI-1640 culture solution was added to each mixture to 2 mL. The amount of BSA added to each culture dish was 6.08, 12.16, 24.25, and 48.58 mg. The mixtures were incubated in 50 mL/L CO_2 at 37 ℃ for 2 h. The dose dependency of the uptake of Cal-BSA-NP and Cal-BSA-NP-GL by primary cultured rat hepatocytes was examined, and the results are shown in Figure 3. Cal-BSA-NP-GL was taken up by rat hepatocytes to a much greater extent than the control Cal-BSA-NP. The uptake of Cal-BSA-NP-GL increased dose-dependently and was saturated at 5 220 ng BSA/dish (10^6 cells) at a dose of 24.25 mg BSA/dish. However, the uptake of Cal-BSA-NP was slightly and linearly increased.

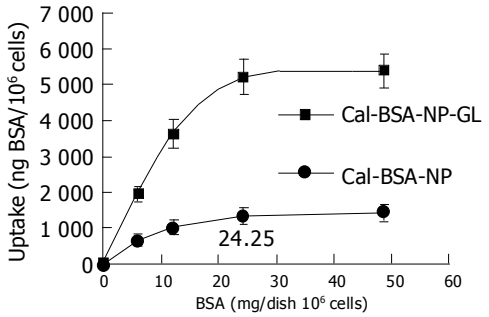

Figure 3 Dose-response curve of uptake of Cal-BSA-NP and Cal-BSA-NP-GL by primary cultured hepatocytes.

Time course of uptake of Cal-BSA-NP and Cal-BSA-NP-GL by primary cultured rat hepatocytes

The time course of the uptake of Cal-BSA-NP and Cal-BSA-NP-GL by hepatocytes is shown in Figure 4. In these experiments, a high affinity of Cal-BSA-NP-GL for hepatocytes was observed. The concentration of calcein in each culture well was 29.1 μg/mL (corresponding BSA in each culture dish was 24.25 mg), at which the uptake of hepatocytes was saturated. The mixtures were incubated in 50 mL/L CO_2 at 37 ℃ for 0, 1, 2, 3, and 4 h respectively, and the incubation was stopped at the indicated time. The incubated mixtures were dealt with following the process in the section "*In vitro* hepatocytes uptake experiment". The time course of the uptake of Cal-BSA-NP-GL was obtained as a biphase curve. The uptake of Cal-BSA-NP-GL and Cal-BSA-NP by hepatocytes reached its maximum after the NP were incubated for 2 h. The uptake amount of Cal-BSA-NP-GL by rat hepatocytes was 4.43-fold higher than that of Cal-BSA-NP. There was a significant difference between Cal-BSA-NP-GL and Cal-BSA-NP ($P<0.01$).

Inhibition experiment of uptake of Cal-BSA-NP-GL by hepatocytes

The high affinity of Cal-BSA-NP-GL for hepatocytes is thought to be due to GL. The presumptive sites on hepatocytes to which Cal-BSA-NP-GL bind are assumed to be specific ones for GL. To demonstrate this theory, we examined whether the uptake of Cal-BSA-NP-GL was inhibited by free GL. Glycyrrhizin was dissolved and diluted to 0.1 mol/L with 50 mg/mL $NaHCO_3$, and 0, 0.2, 0.4, 0.6, and 1.0 mL of glycyrrhizin solution were added to preincubated

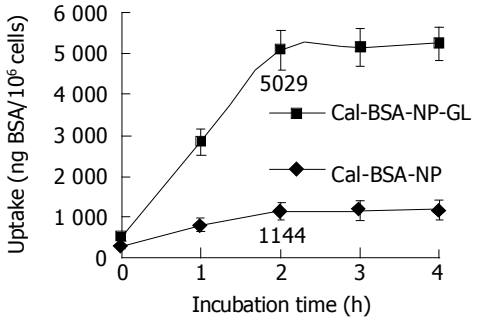

Figure 4 Time course of uptake of Cal-BSA-NP and Cal-BSA-NP-GL by primary cultured rat hepatocytes.

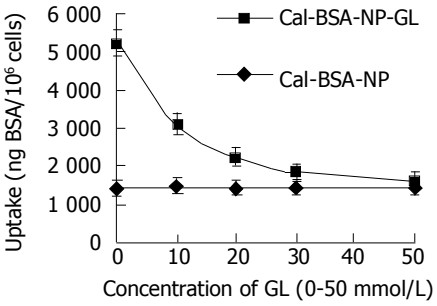

Figure 5 Inhibitory effect of GL on the uptake of Cal-BSA-NP-GL and Cal-BSA-NP by primary cultured rat hepatocytes.

hepatocyte suspensions and the mixtures were incubated in 50 mL/L CO_2 at 37 ℃ for 5 min. Then, 0.5 mL Cal-BSA-NP-GL and Cal-BSA-NP solutions were added to the mixtures respectively, and RPMI-1640 culture solution was added to each mixture to 2 mL (the amount of BSA in each culture dish was 24.25 mg). The culture plate was incubated in 50 mL/L CO_2 at 37 ℃ for 2 h. An identical process was carried out to measure the strength of fluorescence of cell precipitation and the result is shown in Figure 5. The uptake of Cal-BSA-NP-GL was inhibited in response to the concentration of GL in the medium, and the inhibitory ratio was 73% at the concentration of 50 mmol/L of GL.

DISCUSSION

In order to modify the BSA-NP surface with GL, GL was converted into a glycyrrhizin oxide. Aldehyde group of obtained glycyrrhizin oxide was conjugated with surface reactive amino groups of BSA-NP to form Schiff bases, a novel hepatocytes targeting DDS was successfully prepared.

In *in vitro* hepatocyte uptake experiments, the uptake of modified NP depended on the dosage. However, the uptake of Cal-BSA-NP slightly increased linearly. The uptake of drug-loaded NP with their surface modified with glycyrrhizin by hepatocytes could be saturated when the dosage was high enough. Saturation appeared in the dose-response curve of the uptake of Cal-BSA-NP-GL, indicating that the specific binding site of glycyrrhizin is limited on the surface of hepatocytes. The time course of the uptake of NP by hepatocytes accords with the rule of biphase dynamics. During the initial 1 h of incubation, Cal-BSA-NP-GL was rapidly taken up by the cells, and subsequently the uptake of Cal-BSA-NP-GL became slow and increased proportionally to the incubation time. When exogenous glycyrrhizin was added, the uptake of drug-loaded NP with their surface modified with glycyrrhizin, by hepatocytes decreased with increase in the concentration of glycyrrhizin, and the uptake amount approached to traditional NP at last. At the same circumstances, the uptake of traditional NP by hepatocytes increased slowly and linearly. No inhibitory effect was shown on the uptake of Cal-BSA-NP after the addition of GL, suggesting that GL does not diminish the ability of hepatocytes to take up BSA-NP. If the presence of a binding site specific for GL on the surface of hepatocytes is considered, Cal-BSA-NP-GL is likely to bind to this site with the GL moiety. If the specific binding site of glycyrrhizin on the surface of hepatocytes is saturated by exogenous glycyrrhizin, the internalization of Cal-BSA-NP-GL mediated by specific binding site of glycyrrhizin is decreased, with the addition of glycyrrhizin, which is a rational explanation of the excessive uptake of Cal-BSA-NP-GL by hepatocytes compared with Cal-BSA-NP.

It was reported that the uptake of liposomes with their surface modified with glycyrrhizin by hepatocytes increases 10-fold as many as that of traditional liposomes[11]. In our research, the uptake of Cal-BSA-NP-GL by hepatocytes increased 4.43-fold as many as that of Cal-BSA-NP. It might be caused by the following factors. The surface of albumin NP is hydrophilic, its affinity to cell membrane is weaker than liposomes. The structure of bimolecular phospholipid layer of liposomes is similar to that of hepatocyte membrane, the flexible affluxion of phospholipid layer of liposomes makes it easier for GL to combine with the specific binding site of glycyrrhizin on the surface of hepatocyte membrane. The amount of glycyrrhizin on the surface of NP with their surface modified by glycyrrhizin is not enough. The results indicate that the amount of specific binding site of glycyrrhizin on the surface of hepatocyte membrane cannot determine the specific uptake of NP with their surface modified by glycyrrhizin. The ability of GL to combine with the specific binding site of glycyrrhizin and the characteristics of the surface of NP also play an important role in the specific uptake of NP with their surface modified by glycyrrhizin by hepatocytes.

In conclusion, the binding site of GL are present on the surface of rat hepatocytes, BSA-NP-GL may be internalized via this site by hepatocytes and can be used as a promising drug carrier for active targeting of delivery drugs to hepatocytes.

REFERENCES

1 **Tsuchiya S,** Aramaki Y, Hara T, Hosoi K, Okada A. Preparation and disposition of asialofetuin-labelled liposome. *Biopharm Drug Dispos* 1986; **7**: 549-558

2 **Ishihara H,** Hara T, Aramaki Y, Tsuchiya S, Hosoi K. Preparation of asialofetuin-labeled liposomes with encapsulated human interferon-gamma and their uptake by isolated rat hepatocytes. *Pharm Res* 1990; **7**: 542-546

3 **Wu J,** Liu P, Zhu JL, Maddukuri S, Zern MA. Increased liver uptake of liposomes and improved targeting efficacy by label-

ing with asialofetuin in rodents. *Hepatology* 1998; **27**: 772–778
4 **Spanjer HH,** Scherphof GL, Targeting of lactosylceramide-containing liposomes to hepatocytes *in vivo*. *Biochim Biophys Acta* 1983; **734**: 40-47
5 **Ghosh PC,** Bachhawat BK. Targeting of liposomes to hepatocytes. *Targeted Diagn Ther* 1991; **4**: 87-103
6 **Kawakami S,** Yamashita F, Nishikawa M, Takakura Y, Hashida M. Asialoglycoprotein receptor-mediated gene transfer using novel galactosylated cationic liposomes. *Biochem Biophys Res Commun* 1998; **252**: 78-83
7 **Kawakami S,** Fumoto S, Nishikawa M, Yamashita F, Hashida M. *In vivo* gene delivery to the liver using novel galactosylated cationic liposomes. *Pharm Res* 2000; **17**: 306-313
8 **Hirabayashi H,** Nishikawa M, Takakura Y, Hashida M. Development and pharmacokinetics of galactosylated poly L-glutamic acid as a biodegradable carrier for liver-specific drug delivery. *Pharm Res* 1996; **13**: 880-884
9 **Spanjer HH,** Morselt H, Scherphof GL. Lactosylceramide-induced stimulation of liposome uptake by Kupffer cells *in vivo*. *Biochim Biophys Acta* 1984; **774**: 49-55
10 **Negishi M,** Irie A, Nagata N, Ichikawa A. Specific binding of glycyrrhetinic acid to the rat liver membrane. *Biochim Biophys Acta* 1991; **1066**: 77-82
11 **Osaka S,** Tsuji H, Kiwada H. Uptake of liposomes surface-modified with glycyrrhizin by primary cultured rat hepatocytes. *Biol Pharm Bull* 1994; **17**: 940-943
12 **Tsuji H,** Osaka S, Kiwada H. Targeting of liposomes surface-modified with glycyrrhizin to the liver. I. Preparation and biological disposition. *Chem Pharm Bull (Tokyo)* 1991; **39**: 1004-1008
13 **Mao SJ,** Hou SX, Zhang LK, Jin H, Bi YQ, Jiang B. Preparation of bovine serum albumin nanoparticles surface-modified with glycyrrhizin. *Yaoxue Xuebao* 2003; **38**: 787-790
14 **Weber C,** Coester C, Kreuter J, Langer K. Desolvation process and surface characterisation of protein nanoparticles. *Int J Pharm* 2000; **194**: 91-102

Science Editor Wang XL **Language Editor** Elsevier HK

PO Box 2345, Beijing 100023, China
www.wjgnet.com
wjg@wjgnet.com

ELSEVIER

World J Gastroenterol 2005;11(20):3080-3084
World Journal of Gastroenterology ISSN 1007-9327

• *BASIC RESEARCH* •

Inhibition of PMA-induced endothelial cell activation and adhesion by over-expression of domain negative IκBα protein

Jian-Feng Wei, Ke Sun, Shi-Guo Xu, Hai-Yang Xie, Shu-Sen Zheng

Jian-Feng Wei, Shi-Guo Xu, Hai-Yang Xie, Shu-Sen Zheng, Key Lab of Multi-organ Transplantation of Ministry, The First Affiliated Hospital, College of Medicine, Zhejiang University, Hangzhou 310003, Zhejiang Province, China
Ke Sun, Department of Pathology, The First Affiliated Hospital, College of Medicine, Zhejiang University, Hangzhou 310003, Zhejiang Province, China
Supported by the Key Lab of Multi-organ Transplantation of Ministry, College of Medicine, Zhejiang University, Hangzhou, China
Correspondence to: Shu-Sen Zheng, Key Lab of Multi-organ Transplantation of Ministry, The First Affiliated Hospital, College of Medicine, Zhejiang University, Hangzhou 310003, Zhejiang Province, China. zhengss@mail.hz.zj.cn
Telephone: +86-571-87236567 Fax: +86-571-87236570
Received: 2003-06-21 Accepted: 2003-10-12

Abstract

AIM: NF-κB, regulate the expression of cytokine-inducible genes involving immune and inflammatory responses, will be potential therapy approach for allograft from rejection. In this study, we use pCMV-IκBαM vector to inhibit NF-κB activation and investigate the effect of pCMV-IκBαM in inhibition of T cells adhesion to endothelial cells.

METHODS: The NF-κB activity was detected with pNF-κB reporter gene and electrophoretic mobility shift assay. Expression of cell surface molecules was detected by RT-PCR and flow cytometer. The cell-cell adhesion assay was performed to determine the effect of pCMV-IκBαM in inhibition of T cells adhesion to endothelial cells.

RESULTS: We could find that NF-κB activity is inhibited by over-expression of non-degraded IκBα protein. Expression of adhesion molecules like ICAM-1, VCAM-1, and P-selectin as well as cell-cell adhesion were inhibited significantly by transfection of the pCMV-IκBαM vector.

CONCLUSION: Our results indicate that the pCMV-IκBαM, which inhibit the activity of NF-κB through over-expression of non-degraded IκBα protein, can be used for gene therapy in diseases involving NF-κB activation abnormally like organ transplantation via inhibiting cell adhesion.

Key words: Cytokine-inducible genes; Endothelial cells

Wei JF, Sun K, Xu SG, Xie HY, Zheng SS. Inhibition of PMA-induced endothelial cell activation and adhesion by over-expression of domain negative IκBα protein. *World J Gastroenterol* 2005; 11(20): 3080-3084
http://www.wjgnet.com/1007-9327/11/3080.asp

INTRODUCTION

NF-κB, a DNA binding protein complex, is usually present in the cytosol as an inactive complex. IκBα, an associated protein, renders this complex inactive by shielding the nuclear localization signal (NLS). Upon IκB phosphorylation and its subsequent degradation, the NF-κB subunit P65 will translocate to the nucleus, where it binds to specific DNA sequences in the promoter region of several cytokine-inducible genes and up-regulates their transcription[1,2]. Extensive studies have showed that inhibition of NF-κB will be potential therapy approach for allograft from rejection[3-5]. The potent immunosuppressive agents FK506 and cyclosporin A (CsA) are reported to switch off gene transcription by inhibiting a key signaling phosphatase, calcinurin, which is involved in the activation of NF-κB[6,7]. Glucocorticoid, another major immunosuppressive agent, is also believed to work partly via inhibition of NF-κB activation[8]. The detail mechanism about inhibition of NF-κB protecting the graft is not clear till now.

Preview studies have shown that typical procedure of graft rejection is included in three steps: adhesion of alloantigen-activated leukocytes to the vascular endothelial cells, infiltration of alloantigen-activated leukocytes into the graft, activated leukocytes express immune factors which mediate graft tissue destruction[9]. The endothelial cell, as the first barrier faced the alloantigen, is thought to be the most important procedure during allograft rejection[10-13]. We suppose that NF-κB can be an important factor, which participate in the above three steps especially in the adhesion of leukocytes to the vascular endothelial cells.

In the present study, we focus on the transcriptional factor NF-κB in endothelial cells activation and adhesion to T cells. We use the vector encoding domain negative protein mutated at ser-32 and ser-36 IκBα to inhibit activation of NF-κB.

MATERIALS AND METHODS

Materials

ECV304, an endothelial cell line, established from the vein of normal human umbilical cord, were obtained from Cell Bank of Chinese Academy of Science. Human Jurkat cell line was obtained from ATCC (American Type Cell Culture, USA) and cultured for adhesion assay. The following

materials were used in this study: pCMV-IκBα, pCMV-IκBα M, pNF-κB Luc reporter vectors were obtained from Clontech (BD Biosciences, NJ, USA). Luciferase assay system, Gel shift assay system (Promega, WI, USA); MuLV reverase transcriptase, TRIzol, RPMI-1640 medium (Gibco, CA, USA); Geneticin (G418), FuGENE 6 transfection reagent, poly (dI-dC), Protease inhibitors cocktail (Roche, Monnehim, Germany); Protein assay kit (Bio-Rad, CA, USA). Phorbol myristate acetate (PMA) and all other reagents were purchased from Sigma (Sigma Chemical, USA).

Cell culture and transfection for ECV

All of the cells were grown in RPMI 1640 supplemented with 10% fetal bovine serum (FBS), 100 U/mL penicillin and 100 μg/mL streptomycin. Cells were maintained in a standard culture incubator with humidified air containing 50 mL/L CO_2 at 37 ℃.

We performed transfection according to the instruction manual of FuGENE 6 Transfection Reagent with modifications. Briefly, we seeded 1×10^5 cells in 1 mL RPMI 1640 containing 10% FBS medium in 24-well plate and incubated overnight until the ECV cells were 60% confluent. As for stable transfection, added 100 μL serum-free medium (SFM) containing 3 μL FuGENE 6 and 1 μg pCMV-IκBα or pCMV-IκBαM. The plate was incubated for 24 h for expression of reporter gene. Then we added 600 ng/mL G418 in every well and incubated for 7 d. After 7 d incubation, the concentration of G418 was decreased to 300 ng/mL and incubated for more than 3 wk. The over-expression of IκBα protein cells was selected using Western blotting. The cells stably transfected with pCMV-IκBα and pCMV-IκBαM were referenced to ECVWT and ECVMT, separately.

As for transient transfection, 100 μL SFM containing 3 μL FuGENE 6 and 1 μg pNF-κB Luc was added and cells were incubated for 24 h. After treated with PMA for 12 h, the cells were lysed and luciferase activity was measured using luciferase assay system.

Nuclear protein extraction and electrophoretic mobility shift assay

Nuclear extracts were prepared as previously described[14]. Cytoplasmic buffer contained 10 mmol/L HEPES (pH 7.9), 0.1 mmol/L EDTA, 2 mmol/L $MgCl_2$, 10 mmol/L KCl, 0.2% NP-40 and protease inhibitors cocktail solution was prepared to the cell pellet and incubated in ice for 10 min before centrifugation at 13 000 *g* for 1 min. The pelleted nuclei were resuspended in nuclear buffer contained 20 mmol/L HEPES pH 7.9, 1.5 mmol/L $MgCl_2$, 0.2 mmol/L EDTA, 150 mmol/L NaCl and protease inhibitors. The resuspended nuclei were incubated for 30 min on ice with vortexing interruptedly and centrifuged for 20 min at 13 000 *g*.

The concentrations of samples were measured using protein assay kit with BSA protein standard solution as reference. Samples were stored at -70 ℃ until use.

The consensus oligonucleotide of NF-κB was obtained commercially from Santa Cruz and the sequence was shown as the following: NF-κB (5'-AGT TGA GGG GAC TTT CCC AGG C-3'). EMSA were performed according to Holmes's protocol[15]. Briefly, NF-κB consensus oligonucleotide was radiolabeled with [γ-^{32}P]ATP in the presence of T4 polynucleotide kinase. Five micrograms nuclear extract was incubated with labeled probe in 1 μg of poly(dI-dC) for 30 min. Complexes were separated on a 5% polyacrylamide gel in 0.5×TBE and dried using dryer (Bio-Rad, USA) and autoradiographed at -80 ℃.

Reverse transcription polymerase chain reaction

To study cytokine gene expression patterns, we used reverse transcription-polymerase chain reaction (RT-PCR), as previously described. Total RNA was extracted from ECV cells using TRIzol reagent according to the manufacturer's recommendations. For cDNA synthesis, 4 μg total RNA was reverse transcribed with MuLV reverse transcriptase. Primer sequences and reaction conditions: Sequences of the primers used for RT-PCR analysis are described in Table 1. Amplifications were performed under the following conditions: 95 ℃ for 2 min, 94 ℃ for 45 s, 56 ℃ for 45 s, 72 ℃ for 45 s, totally 32 cycles. The final extension step was performed by one cycle at 72 ℃ for 10 min. Twenty-five microliters of reaction system was used including: 2 μL cDNA template, 1 μL sense primer, 1 μL anti-sense primer, 2 μL 25 mmoL $MgCl_2$, 1 μL dNTP and 1.5 u Taq DNA polymerase. Reaction products were run by electrophoresis on a 1.5% agarose gel for 30-40 min at 100 V in 0.5×TBE buffer, and visualized with ethidium bromide staining under UV light. Relative expression level of ICAM-1 and VCAM-1 were defined as optical density ratio (Target gene/GAPDH) analyzed by Kodak digital science scanning system.

Table 1 Sequences of primers for amplifed cDNA of the ICAM-1, VCAM-1, and GAPDH

Genes	Primers	Sequences	Amplifiers
ICAM-1	Sense	5′-CAGTGACCATCTACAGCTTTCCGG-3′	555 bp
	Anti-sense	5′-GCTGCTACCACAGTGATGATGACAA-3′	
VCAM-1	Sense	5′-ACCCTCCCAAGGCACACACAG-3′	533 bp
	Anti-sense	5′-GTAAGTCTATCTCCAGCCTGTC-3′	
GAPDH	Sense	5′-ATGGCACCGTCAAGGCTGAG-3′	225 bp
	Anti-sense	5′-GCAGTGATGGCATGGACTGT-3′	

Analysis of the expression of cell adhesion molecules using flow cytometer

ECVMT and ECVWT cells were treated with PMA (50 nmol/L) for 12 h. Then cells were harvested and washed thrice using cold PBS. Then the cells were incubated with FITC-labeled CD54(ICAM-1), FITC-labeled CD62 (VCAM-1) or PE-labeled CD106(P-selectin) antibodies. The fluorescence densities were determined using flow cytometer (Coulter, USA) and the experiment was repeated thrice.

Adhesion of Jurkat cells to ECV304

We used Jurkat cells for lymphocyte-endothelial cell adhesion assay. The adhesion procedure was performed according to Roy[16]. Briefly, monolayers of cells were seeded at a density of 10^4 cells/well in 96-well plate (Becton Dickinson, NJ, USA). After 24 h of seeding, the cells were treated with PMA (50 nmol/L) for 12 h. Before cell-cell adhesion assay, the ECV monolayers were washed thrice

with PBS. Jurkat T-cells (2×10^5 cells/well) were co-cultured with ECV monolayer for 2 h in a culture incubator. After the co-culture period, the non-adherent Jurkat T-cells were removed by washing each well four times with PBS carefully. Jurkat cell adhesion was determined by visual counting under a phase-contrast microscope. Both Jurkat cells and ECV were counted in five fields of each well at 100× magnification by two individuals, and the average values were taken. The adhesion rate is expressed as the number of attached Jurkat cells per 100 ECV cells.

Statistical analyses

Results are presented as mean±SD of at least three separate experiments. Differences between means of groups were determined by Student's *t*-test. The level of significance was set at $P<0.05$ or $P<0.01$.

RESULTS

Over-expression of domain negative IκBα inhibit NF-κB activation

We stably transfected the ECV304 cells with the pCMV-IκBαM vector, which encoded domain negative IκBα protein mutated at ser-32 and ser-36 and also with the pCMV-IκBα as control. Firstly, we extracted the total protein after being treated with PMA (50 nmol/L) for 45 min. The expression level of IκBα was determined with specific antobody. As shown in Figure 1A, IκBα level was higher in ECVMT cells after treated with PMA compared with ECVWT cells. To determine the NF-κB activity further, the nuclear proteins were extracted after treated with PMA for 45 min. These proteins were applied to EMSA. Figure 1B showed us that pCMV-IκBαM could inhibit the activity of NF-κB significantly.

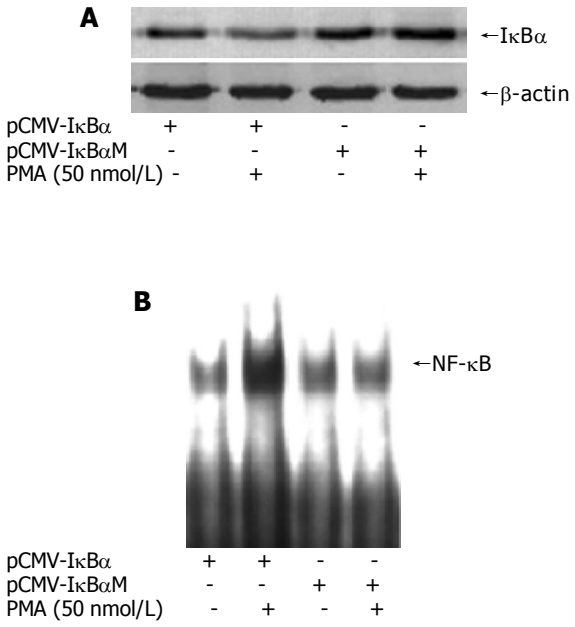

Figure 1 Determining NF-κB activity in ECV304WT and ECV304MT cells. **A**: IκBα level were detected after treated with PMA (50 nmol/L) for 12 h; **B**: EMSA was performed to determine the activity of NF-κB after treated with PMA (50 nmol/L) for 12 h. Band of NF-κB was marked.

Down-regulation adhesion molecules expression under inhibition of NF-κB

Adhesion molecules expression in endothelial cells is dependent, at least in part, on the activation of NF-κB[1]. To determine whether the pCMV-IκBαM can inhibit the expression of adhesion molecules, we performed RT-PCR to determine the mRNA level of adhesion molecules in the total RNA extracted from the cells treated with PMA (50 nmol/L) for 12 h. The results were shown as ratio compared to housekeeping gene GAPDH expression. As shown in Figures 2A and B, we can see that the ICAM-1 and VCAM-1 mRNA levels are inhibited significantly in ECVMT cells compared to ECVWT cells (40.3% *vs* 18.7% for ICAM-1 and 27.3% *vs* 16.7% for VCAM-1). We also compare the protein levels of various adhesion molecules by flow cytometer. The cells were harvested after stimulation with PMA (50 nmol/L) for 12 h. As shown in Figure 2C, the pCMV-IκBαM can inhibit the expression of adhesion molecules including ICAM-1, VCAM-1 and P-selectin. As for ICAM-1, 82.5% cells expressed ICAM-1 in ECVWT cells after being treated with PMA (50 nmol/L) compared 53.2% positive cells in ECVMT cells. Almost the same results were found in VCAM-1 and P-selectin expression between ECVMT cells and ECVWT cells (25.3% *vs* 66.1% for VCAM-1; 65.4% *vs* 35.7% for P-selectin).

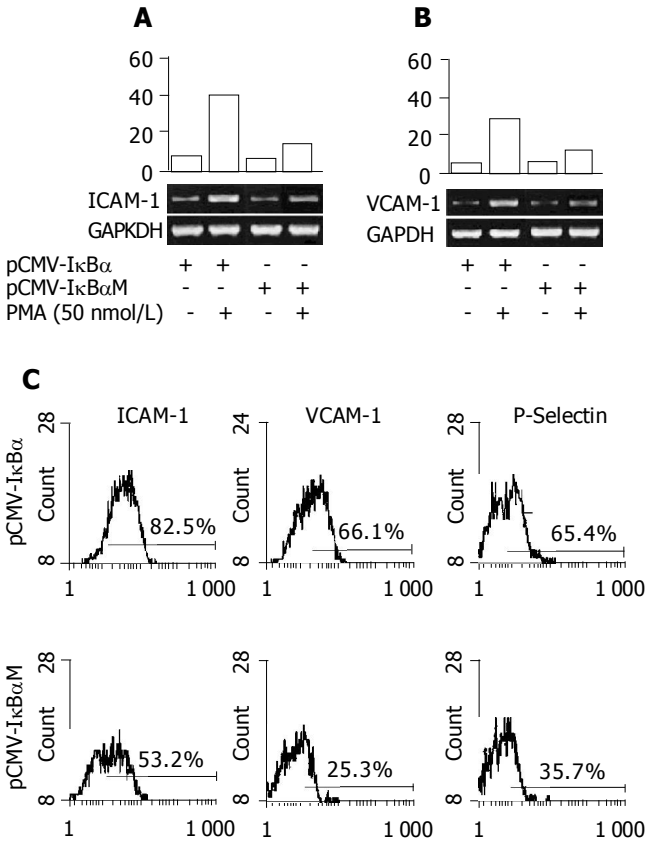

Figure 2 Down-regulation of PMA-induced adhesion molecules expression in ECV cells transfected with pCMV-IκBαM compared with pCMV-IκBα. RT-PCR analysis was performed with primers specific for ICAM-1 (**A**) and VCAM-1 (**B**). **C**: The expression of ICAM-1, VCAM-1 and P-selectin were detected using specific antibodies by flow cytometry. Results are representative of at least three independent experiments.

Inhibit the adhesion of T cells to ECV cells

We then evaluated the effect of pCMV-IκBαM on the adhesion of human T lymphocyte to ECV304 cells as mentioned in Methods section. After the ECV cells were treated with PMA (50 nmol/L) for 24 h, the Jurkat T cells were added and co-incubated for further 2 h. Then we calculated the adherent cells using phase-contrast microscope after non-adherent cells were washed away using cold PBS (Figure 3). We found that the pCMV-IκBαM could inhibit the adhesion of Jurkat T cells to ECV cells from 71.4±5.2% to 42.2±3.7% after being treated with PMA for 12 h (P<0.05).

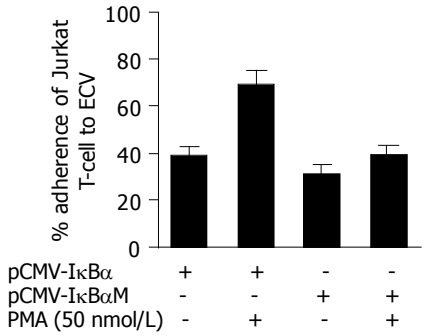

Figure 3 Adhesion of human Jurkat T-cells to PMA-activated endothelial (ECV) cells is inhibited by transfection with pCMV-IκBαM compared with pCMV-IκBα. ECV cells were activated with PMA (50 nmol/L) for 12 h. Cells were washed thrice with PBS and then co-cultured with Jurkat T-cells for 2 h. Then the cells were washed with PBS thrice. Jurkat cell adhesion was determined by visual counting under a phase-contrast microscope. P<0.05 when compared ECVMT with ECVWT.

DISCUSSION

The adhesion of leukocyte to the vascular endothelial cells is a critical step in the immunological response and involves recruitment and infiltration of leukocytes to the site of tissue injury or allograft. The endothelial cell, as the first barrier faced the alloantigen, will be activated upon stimulation like cytokines (e.g., PMA, IL-1, TNF-α,) *in vitro* as well as *in vivo* at sites of allograft. Activated endothelial cells express adhesion molecules to assist adhesion between activated T cells and endothelial cells[18,19]. Among these molecules are P- and E-selectin, intercellular adhesion molecule-1 (ICAM-1), and vascular cell adhesion molecule-1 (VCAM-1), on the endothelial cells, and their respective counter receptors, P-selectin glycoprotein ligand-1 (PSGL-1), leukocyte function-associated antigen-1 (LFA-1) and very late antigen-4 (VLA-4), on the leukocytes[17]. Activated endothelial cells also can secrete chemokines such as IL-6, IL-8 and MCP-1[20,21], which can recruit leukocyte. ICAM-1, which has been studied extensively, binds to its ligand LFA-1 on lymphocytes and promotes lymphocytes binding to the endothelium and facilitates the lymphocytes to invade the graft[22-24]. Blockade of ICAM-1, either with monoclonal antibodies or with antisense oligodeoxynucleotides, has been shown to decrease reperfusion injury and prolong the survival of allograft[25-27].

Activation of endothelial cells requires multiple transcriptional factors. Nuclear factor κB, one of such transcription factors, is held in the cytoplasm by inhibitory IκB proteins (IκBs) and regulates many genes involving immune and inflammatory pathways such as various proinflammatory cytokines, adhesion molecules and apoptosis-associated factors[8,28]. Accumulating evidence clearly demonstrates that blocking the activity of NF-κB might arrest the progression of acute rejection by interrupting the activation of genes of major inflammatory cytokines and adhesion molecules[29]. We use the pCMV-IκBαM vector, which encodes domain negative nondegraded IκBα protein mutated at ser-32 and ser-36 to inhibit the activation of NF-κB. We found that the adhesion molecules including ICAM-1, VACM-1 and P-selectin were down-regulated under inhibition of NF-κB. We also mimic the procedure of cell-cell adhesion *in vitro* between endothelial cells and T cells. The results told us that inhibition of NF-κB could inhibit endothelial cell activation and decrease cell adhesion.

In conclusion, we propose that pCMV-IκBαM vector can be used as novel immunological strategy. Further explorations were needed to verify the effect of pCMV-IκBαM to protect the allograft from rejection *in vivo*.

REFERENCES

1 **Li Q**, Verma IM. NF-kappaB regulation in the immune system. *Nat Rev Immunol* 2002; **2**: 725-734
2 **Makarov SS**. NF-kappaB as a therapeutic target in chronic inflammation: recent advances. *Mol Med Today* 2000; **6**: 441-448
3 **Bonham CA**, Peng L, Liang X, Chen Z, Wang L, Ma L, Hackstein H, Robbins PD, Thomson AW, Fung JJ, Qian S, Lu L. Marked prolongation of cardiac allograft survival by dendritic cells genetically engineered with NF-kappa B oligodeoxyribonucleotide decoys and adenoviral vectors encoding CTLA4-Ig. *J Immunol* 2002; **169**: 3382-3391
4 **Finn PW**, Stone JR, Boothby MR, Perkins DL. Inhibition of NF-kappaB-dependent T cell activation abrogates acute allograft rejection. *J Immunol* 2001; **167**: 5994-6001
5 **Suzuki J**, Morishita R, Amano J, Kaneda Y, Isobe M. Decoy against nuclear factor-kappa B attenuates myocardial cell infiltration and arterial neointimal formation in murine cardiac allografts. *Gene Ther* 2000; **7**: 1847-1852
6 **Kaibori M**, Sakitani K, Oda M, Kamiyama Y, Masu Y, Nishizawa M, Ito S, Okumura T. Immunosuppressant FK506 inhibits inducible nitric oxide synthase gene expression at a step of NF-kappaB activation in rat hepatocytes. *J Hepatol* 1999; **30**: 1138-1145
7 **Frantz B**, Nordby EC, Bren G, Steffan N, Paya CV, Kincaid RL, Tocci MJ, O'Keefe SJ, O'Neill EA. Calcineurin acts in synergy with PMA to inactivate I kappa B/MAD3, an inhibitor of NF-kappa B. *EMBO J* 1994; **13**: 861-870
8 **Baeuerle PA**, Baichwal VR. NF-kappa B as a frequent target for immunosuppressive and anti-inflammatory molecules. *Adv Immunol* 1997; **65**: 111-137
9 **el-Sawy T**, Fahmy NM, Fairchild RL. Chemokines: directing leukocyte infiltration into allografts. *Curr Opin Immunol* 2002; **14**: 562-568
10 **Briscoe DM**, Alexander SI, Lichtman AH. Interactions between T lymphocytes and endothelial cells in allograft rejection. *Curr Opin Immunol* 1998; **10**: 525-531
11 **Denton MD**, Davis SF, Baum MA, Melter M, Reinders ME, Exeni A, Samsonov DV, Fang J, Ganz P, Briscoe DM. The role of the graft endothelium in transplant rejection: evidence that endothelial activation may serve as a clinical marker for the development of chronic rejection. *Pediatr Transplant* 2000; **4**: 252-260
12 **Paul LC**, Baldwin WM, van Es LA. Vascular endothelial al-

loantigens in renal transplantation. *Transplantation* 1985; **40**: 117-123
13 **Rose ML**. Endothelial cells as antigen-presenting cells: role in human transplant rejection. *Cell Mol Life Sci* 1998; **54**: 965-978
14 **Bours V**, Bentires-Alj M, Hellin AC, Viatour P, Robe P, Delhalle S, Benoit V, Merville MP. Nuclear factor-kappa B, cancer, and apoptosis. *Biochem Pharmacol* 2000; **60**: 1085-1089
15 **Holmes-McNary M**, Baldwin AS. Chemopreventive properties of trans-resveratrol are associated with inhibition of activation of the IkappaB kinase. *Cancer Res* 2000; **60**: 3477-3483
16 **Roy S**, Sen CK, Kobuchi H, Packer L. Antioxidant regulation of phorbol ester-induced adhesion of human Jurkat T-cells to endothelial cells. *Free Radic Biol Med* 1998; **25**: 229-241
17 **Dedrick RL**, Bodary S, Garovoy MR. Adhesion molecules as therapeutic targets for autoimmune diseases and transplant rejection. *Expert Opin Biol Ther* 2003; **3**: 85-95
18 **Mozaffarian N**, Casadevall A, Berman JW. Inhibition of human endothelial cell chemokine production by the opportunistic fungal pathogen Cryptococcus neoformans. *J Immunol* 2000; **165**: 1541-1547
19 **Kokura S**, Yoshida N, Yoshikawa T. Anoxia/reoxygenation-induced leukocyte-endothelial cell interactions. *Free Radic Biol Med* 2002; **33**: 427-432
20 **Liu X**, Spolarics Z. Methemoglobin is a potent activator of endothelial cells by stimulating IL-6 and IL-8 production and E-selectin membrane expression. *Am J Physiol Cell Physiol* 2003; **285**: C1036-C1046
21 **Anrather J**, Csizmadia V, Brostjan C, Soares MP, Bach FH, Winkler H. Inhibition of bovine endothelial cell activation *in vitro* by regulated expression of a transdominant inhibitor of NF-kappa B. *J Clin Invest* 1997; **99**: 763-772
22 **Springer TA**. Adhesion receptors of the immune system. *Nature* 1990; **346**: 425-434
23 **Bevilacqua MP**. Endothelial-leukocyte adhesion molecules. *Annu Rev Immunol* 1993; **11**: 767-804
24 **Borthwick NJ**, Akbar AA, Buckley C, Pilling D, Salmon M, Jewell AP, Yong KL. Transendothelial migration confers a survival advantage to activated T lymphocytes: role of LFA-1/ICAM-1 interactions. *Clin Exp Immunol* 2003; **134**: 246-252
25 **Poston RS**, Ennen M, Pollard J, Hoyt EG, Billingham ME, Robbins RC. *Ex vivo* gene therapy prevents chronic graft vascular disease in cardiac allografts. *J Thorac Cardiovasc Surg* 1998; **116**: 386-396
26 **Feeley BT**, Park AK, Alexopoulos S, Hoyt EG, Ennen MP, Poston RS, Robbins RC. Pressure delivery of AS-ICAM-1 ODN with LFA-1 mAb reduces reperfusion injury in cardiac allografts. *Ann Thorac Surg* 1999; **68**: 119-124
27 **Stepkowski SM**. Application of antisense oligodeoxynucleotides for organ transplantation. *Transplant Proc* 1998; **30**: 2142-2145
28 **Baeuerle PA**, Henkel T. Function and activation of NF-kappa B in the immune system. *Annu Rev Immunol* 1994; **12**: 141-179
29 **Vos IH**, Govers R, Grone HJ, Kleij L, Schurink M, De Weger RA, Goldschmeding R, Rabelink TJ. NFkappaB decoy oligodeoxynucleotides reduce monocyte infiltration in renal allografts. *FASEB J* 2000; **14**: 815-822

Science Editor Guo SY **Language Editor** Elsevier HK

PO Box 2345, Beijing 100023, China
www.wjgnet.com
wjg@wjgnet.com

ELSEVIER

World J Gastroenterol 2005;11(20):3085-3090
World Journal of Gastroenterology ISSN 1007-9327

• *CLINICAL RESEARCH* •

Decrease of reactive-oxygen-producing granulocytes and release of IL-10 into the peripheral blood following leukocytapheresis in patients with active ulcerative colitis

Hiroyuki Hanai, Takayuki Iida, Ken Takeuchi, Fumitoshi Watanabe, Yasuhiko Maruyama, Masataka Kikuyama, Tatsuo Tanaka, Kenji Kondo, Kou Tanaka, Kenji Takai

Hiroyuki Hanai, Takayuki Iida, Ken Takeuchi, Tatsuo Tanaka, Kenji Kondo, Department of Endoscopic and Photodynamic Medicine, Hamamatsu University School of Medicine, Hamamatsu, Japan
Fumitoshi Watanabe, Yasuhiko Maruyama, Department of Gastroenterology, Fujieda Municipal General Hospital, Fujieda, Japan
Masataka Kikuyama, Department of Gastroenterology, Hamamatsu Rosai Hospital, Hamamatsu, Japan
Kou Tanaka, Tanaka Clinic, Shizuoka, Japan
Kenji Takai, SRL Inc., Tokyo, Japan
Correspondence to: Dr. Hiroyuki Hanai, MD, Department of Endoscopic and Photodynamic Medicine, Hamamatsu University School of Medicine, 1-20-1 Handayama, Hamamatsu 431-3192, Japan. flw-1013@topaz.plala.or.jp
Telephone: +81-534711013 Fax: +81-534711013
Received: 2004-11-17 Accepted: 2004-12-23

Abstract

AIM: To investigate the clinical efficacy of leukocytapheresis (LCAP) in patients with active ulcerative colitis (UC), and to elucidate the mechanisms by determining the changes in the cytokine levels in the peripheral blood and of the functions of the peripheral blood leukocytes in these patients.

METHODS: The subjects were 19 patients with active UC, with a mean clinical activity index (CAI) of 9.2. The LCAP was conducted using Cellsorba E. In each session of LCAP, 2-3 L of blood at the flow rate of 30-50 mL/min was processed. The treatment was carried out in approximately 1-h sessions, once a week, for 5-10 wk. Blood samples for determination of the cytokine levels were collected from the inflow side of the column (site of dehematization; at the start of LCAP) and outflow side of the column (at the end of LCAP). Blood samples for the determination of reactive-oxygen-producing cells were collected from the peripheral blood before and after LCAP.

RESULTS: LCAP resulted in clinical improvement in all the 19 patients of UC recruited for this study. Remission (CAI: $\leqslant$4) was noted in 15 (79%) of the 19 patients. The blood level of the pro-inflammatory cytokine IL-6 was found to be decreased following treatment by LCAP, and the level of the anti-inflammatory cytokine IL-10 at the outflow side of the LCAP column was found to be significantly elevated as compared to that at the inflow side of the column. The reactive-oxygen-producing granulocytes in the peripheral blood of UC patients was increased as compared to that in healthy persons and the increase was found to be decreased following treatment by LCAP.

CONCLUSION: LCAP exerted a high therapeutic efficacy in patients with active UC. Our findings suggest that LCAP is associated with enhanced production of the inhibitory cytokine IL-10 to indirectly inhibit the functions of the inflammatory leukocytes, and that inflammation is also considerably attenuated by the direct removal of reactive-oxygen-producing neutrophils from the peripheral blood.

Key words: Ulcerative colitis; Reactive-oxygen; Leukocytapheresis; Interleukin-10

Hanai H, Iida T, Takeuchi K, Watanabe F, Maruyama Y, Kikuyama M, Tanaka T, Kondo K, Tanaka K, Takai K. Decrease of reactive-oxygen-producing granulocytes and release of IL-10 into the peripheral blood following leukocytapheresis in patients with active ulcerative colitis. *World J Gastroenterol* 2005; 11(20): 3085-3090
http://www.wjgnet.com/1007-9327/11/3085.asp

INTRODUCTION

Ulcerative colitis (UC), as well as Crohn's disease (CD), is one of the prototype nonspecific inflammatory bowel diseases (IBDs) of unknown cause. Drugs such as salazosulfapyridine[1], 5-aminosalicylic acid[2], corticosteroids[3,4], and immunosuppressants[5] have been used for the treatment of UC; these drugs attenuate the inflammation in the colonic mucosa by their anti-inflammatory and immunosuppressive actions, to cause disease remission. However, some patients with UC are even refractory to the strong anti-inflammatory and immunosuppressive actions of steroids, and surgical treatment often have been considered as the ultimate treatment modality for such patients.

Extracorporeal circulation treatment methods that have been shown to be highly efficacious for the treatment of UC patients refractory to steroids have recently been developed in Japan. One such is the so-called granulocyte and monocyte adsorption apheresis (GMA)[6-8], in which mainly granulocytes and monocytes are removed from the blood, while another is leukocytapheresis (LCAP)[9], in which granulocytes, monocytes, as well as lymphocytes, are

removed from the blood. These treatment modalities have been reported to yield a high therapeutic efficacy in many patients of UC, including those who are refractory to steroids.

The pathogenetic mechanisms underlying the development of the two IBDs, UC, and CD, have not yet been clearly elucidated. However, it has been suggested that inflammation of the intestinal mucosa results from infiltration of the mucosa by inflammatory leukocytes, including neutrophils, monocytes, and lymphocytes. According to several reports, clustering of various leukocytes at the sites of inflammation along the intestinal mucosa and the resultant release of pro-inflammatory cytokines and reactive oxygen species lead to the tissue injury seen in these cases[10-15]. Thus, GMA and LCAP were developed as treatment modalities for UC under the contention that removal of the inflammation-inducing activated leukocytes from the circulation might result in attenuation of the inflammation[6,16,17].

In the present study, the clinical effects of LCAP in cases of active UC were investigated, and the changes in the levels of cytokines and percentage of reactive-oxygen-producing leukocytes (granulocytes, monocytes, and lymphocytes) in the peripheral blood were determined to elucidate the possible mechanisms underlying the clinical efficacy of LCAP in patients of UC.

MATERIALS AND METHODS

Patient background

Nineteen patients with active UC were recruited for this study conducted to determine the efficacy of LCAP. The demographic characteristics of these patients are summarized in Table 1. The patients consisted of 9 males and 10 females, with a mean age of 37.3 years (range, 19-52 years); the mean age of the patients at the time of the first episode was 28.3 years (range, 14-50 years), and the mean duration of the disease was 5.1 years (range, 0.5-19 years).

Table 1 Background factors of the 19 patients selected for LCAP therapy

Demographic characteristics	Measurement
Male/female	9/10
Age (yr)	37.3±16.9 (19–52)
Age at first episode (yr)	28.3±12.7 (14–50)
Duration of UC (yr)	5.1±8.9 (0.5–19)
Number of relapse	3.8±4.2 (2–12)
Classification of severity	
Severe	2
Moderate	11
Mild	6
CAI	9.2 (6–16)
Extent of UC	
Total colitis	12
Left-sided colitis	7

The clinical activity index (CAI) and the endoscopic index (EI) were determined in conformation with the criteria proposed by Rachmilewitz[18]. The mean CAI of the patients at the start of the LCAP treatment was 9.2 (6-16), and the CAI distribution in the patients was as follows: CAI: $\geqslant$12 (severe UC) in 2 patients, CAI: $\geqslant$8, <12 (moderate UC) in 11 patients, and CAI: $\geqslant$5, <8 (mild UC) in 6 patients. Twelve of the nineteen patients had involvement of the entire colon (total colitis), and 7 patients had involvement of the left-sided colitis.

Leukocytapheresis (LCAP)

LCAP was carried out using a column (Cellsorba E) filled with a non-woven fabric made up of polyester fibers. The fabric had a dual structure; an inner layer composed of superfine fibers 0.8-2.8 μm in diameter, and an outer layer composed of fibers 10-40 μm in diameter. The blood is filtrated from the outside into the inside of the non-woven fabric wound into a cylindrical shape in the column, and leukocyte components are removed. The blood, with leukocyte removed, is guided out from the column and heated, and then returned to the corresponding vein of the patient's other arm or leg of the patient. The blood flow rate was set at 30-50 mL/min, and 2-3 L of blood was treated in each session of LCAP. The treatment was carried out in 1-h sessions, once a week, for 10 wk.

Measurement of soluble IL-6 and IL-10

Peripheral blood samples for the measurement of IL-6 and IL-10 were collected before the start of each LCAP session and then 60 min after the LCAP session. Both IL-6 and IL-10 were measured by an ELISA method. The human IL-6 ELISA kit was obtained from R&D Systems (Minneapolis, USA), while the ELISA kit for IL-10 (Human Interleukin-10 Ultrasensitive: hIL-10 US) was obtained from Biosource (CA, USA).

All the assays on the serum samples were performed in an SRL (Special Research Laboratory) in a blinded manner, and the data were processed by an individual who was blinded to both the clinical characteristics of the subjects and the purpose of the study.

Determination of the percentage of reactive-oxygen-producing cells

The percentage of reactive-oxygen-producing cells was determined in conformation with the method established by Bass *et al*[19]. In brief, phosphate-buffered saline (PBS) mixed with 5 μmol/L of 2',7'-dichlorofluorescein diacetate (DCFH-DA) was added to the heparinized vein blood sample, and the sample was heated at 37 ℃ for 15 min under shaking. Then, PBS plus 20 mmol/L of ethylenediamine tetraacetic acid was added to the mixture to prevent agglutination of the neutrophils. The mixture was then centrifuged, washed, and subjected to hemolytic treatment. The reactive-oxygen-producing cells were counted with a flow cytometer using 2',7'-dichlorofluorescein, a product of oxidation with reactive oxygen species, as the indicator.

Statistical analysis

Student's *t*-test or Mann-Whitney's *U*-test was used for statistical analysis.

RESULTS

The therapeutic efficacy of LCAP treatment against active UC was investigated in 19 patients. The results revealed

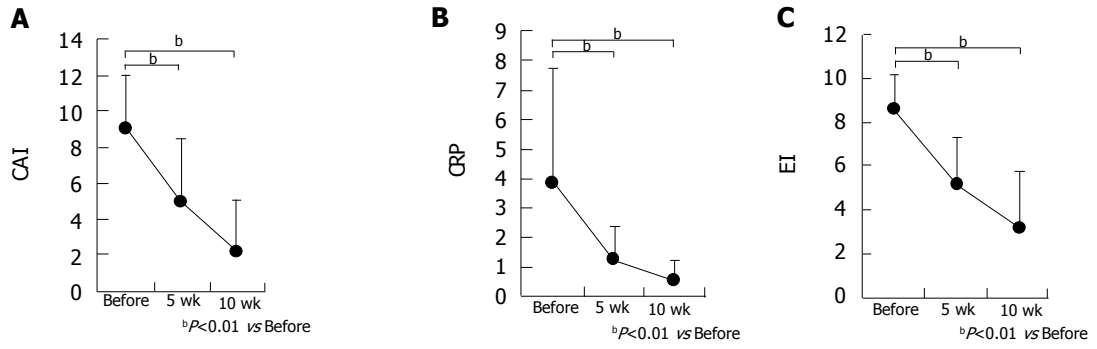

Figure 1 **A**: Average CAI in the 19 patients at wk 5 and 10 following the start of LCAP treatment; **B**: Average CRP level in the 19 patients at wk 5 and 10 following the start of LCAP treatment; **C**: Average EI in 19 patients at wk 5 and 10 following the start of LCAP treatment.

that the CAI, an indicator of the clinical severity of UC, decreased significantly ($P<0.01$) from the mean value of 9.2 before the treatment, to 2.8 following the treatment (Figure 1A). The serum level of C-reactive protein (CRP), a marker of inflammation, decreased significantly ($P<0.01$) from a mean level of 3.9 before treatment to 0.5 after the treatment (Figure 1B). Endoscopic examination revealed a significant decrease ($P<0.01$) of the EI score from a mean of 8.7 before treatment to 3.2 after the treatment (Figure 1C). Evaluation 12 wk after the LCAP treatment revealed that remission (CAI$\leqslant$4) had occurred in 15 (79%) of the 19 patients; in the remaining 4 patients, even though remission had not occurred, the values of each of the above-described markers had nevertheless decreased, showing a beneficial therapeutic effect of the treatment against the disease. Dull headache as a side effect of LCAP treatment was observed in only one patient. Based on the above results, LCAP was confirmed to be a highly safe treatment modality.

The blood levels of IL-6, a pro-inflammatory cytokine, and IL-10, an inhibitory cytokine, were determined during the treatment in randomly selected patients. A decrease of IL-6 level in the peripheral blood during the treatment was observed in six patients (Figure 2A). The IL-10 level, on the other hand, was found to be increased in the blood in the outflow side of the LCAP column as compared to that in the inflow side of the LCAP column (Figure 2B). This elevation of IL-10 production was found to be particularly marked in the early stages of the treatment.

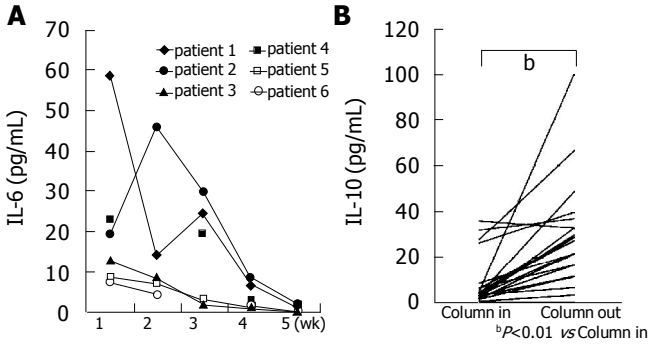

Figure 2 **A**: The serum IL-6 concentrations in six patients at wk 1, 2, 3, 5, and 10 following the start of LCAP treatment; **B**: The serum IL-10 concentrations measured at the Cellsorba inflow (at the start of LCAP) and outflow (at the end of LCAP).

IL-10 has been reported to markedly inhibit the protein and mRNA expression of IL-1, a pro-inflammatory cytokine produced in response to lipopolysaccharide (LPS) stimulation of neutrophils and monocytes[20]. It was revealed that the production of IL-10 was stimulated by LCAP treatment. Based on this observation, the effects of LCAP on the functions of neutrophils and monocytes were investigated, using the percentage of reactive-oxygen-producing cells as an indicator. The percentages of reactive-oxygen-producing cells in the peripheral blood of healthy persons and UC patients prior to LCAP were determined first. The percentage of these cells was found to be significantly increased in the peripheral blood of UC patients as compared in that of healthy persons (7.1±4.9 *vs* 20.1±12.0) (Figure 3A). On the other hand, there were scarcely any reactive-oxygen-producing cells among the lymphocytes and monocytes in the peripheral blood of either healthy persons or UC patients in the absence of stimulation (data not shown). The percentage of reactive-oxygen-producing cells before LCAP treatment (one occasion) was compared with that determined after the treatment (one occasion) in the UC patients. The percentage was found to be significantly decreased after the LCAP treatment (20.8±12.4 *vs* 12.0±9.5) (Figure 3B). Representative results of fluorescein-activated cell-sorter (FACS) analysis before and after LCAP treatment in the UC patients are shown in Figure 4.

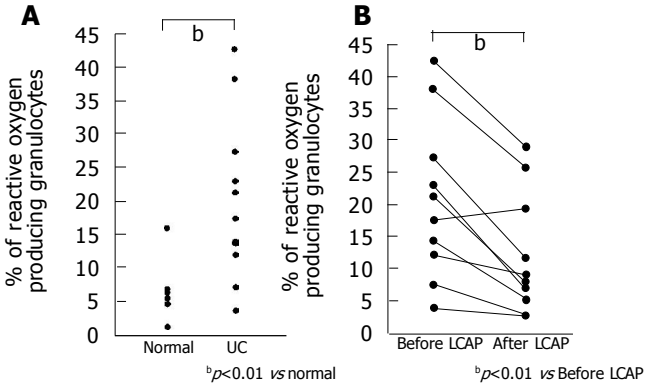

Figure 3 **A**: Percentage of reactive-oxygen-producing granulocytes in normal subjects (n = 6) and UC patients (n = 11); **B**: Percentage of reactive-oxygen-producing granulocytes in the peripheral blood of 10 patients before and after LCAP treatment.

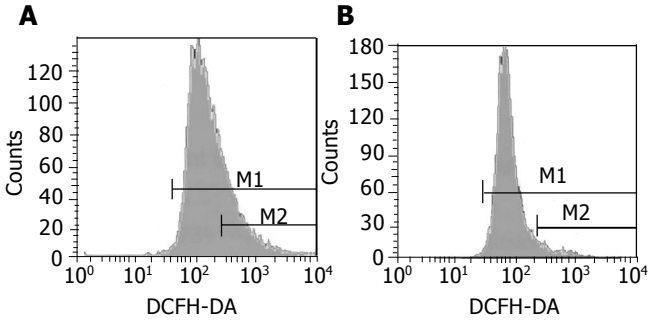

Figure 4 Representative results of FACS analysis in the peripheral blood of one patient before (**A**) and after (**B**) LCAP treatment. The percentages of reactive-oxygen-producing cells in A and B were 22.9% and 7.1%, respectively.

DISCUSSION

A previous clinical trial conducted in Japan revealed that LCAP yielded high therapeutic efficacy, that is, it yielded beneficial effects in 74% of UC patients who were refractory to steroid treatment[9]. In the present study, 73% of active UC patients entered into remission following LCAP treatment, and in the remaining patients also, the treatment was found to have beneficial therapeutic effects. In other words, LCAP was confirmed again to have a high therapeutic efficacy in cases of UC. Another extracorporeal circulation treatment strategy, GMA, has also been reported to exert high therapeutic efficacy in cases of UC (efficacy rate: 80% or higher), similar to LCAP. GMA was reported in one study to yield a beneficial effect in 100% of UC patients, in particular, steroid-naive UC patients[7]. Furthermore, both LCAP and GMA have been confirmed to be associated with only a low frequency of side effects and mild side effects, and high safety[6-9]. The use of these treatment methods has become more widespread since they were approved for reimbursement under the National Health Insurance in Japan, and they have been found to be useful for improving the quality of life of many patients, by inducing remission in a high percentage of patients, minimizing the side effects of steroids associated with high doses, and allowing surgery to be avoided.

However, the mechanisms underlying the therapeutic efficacy of these extracorporeal circulation treatment methods have not yet been clearly elucidated. Some mechanisms have been proposed, as follows: Marked infiltration by neutrophils and lymphocytes is observed at sites of inflammation along the colonic mucosa in UC; many of these leukocytes are activated, and adhere to hemangioendothelial cells via the enhanced surface expression of adhesion molecules, leading to penetration of the mucosa. LCAP has been suggested to cause attenuation of the process of inflammation and exert a therapeutic effect by removing these activated leukocytes from the peripheral blood[17]. In connection with the second mechanism of actions of LCAP treatment, the ability of lymphocytes in peripheral blood to produce cytokines before and after the treatment was investigated. It is shown that LCAP enhances the ability of the peripheral blood lymphocytes to produce IL-4, i.e., an anti-inflammatory cytokine, whereas it does not affect the ability of these cells to produce interferon γ, a pro-inflammatory cytokine[21]. As for the third mechanism, it has been clarified that not only leukocytes, but also platelets are removed by LCAP (ca. 35% of platelets in the peripheral blood are removed during each session of LCAP); it has been reported that platelets induce leukocytes to produce reactive oxygen species[22], and that removal of platelets by LCAP, therefore, indirectly inhibits the production of reactive oxygen species by leukocytes, thereby preventing tissue injury.

Some mechanisms underlying the therapeutic efficacy of GMA have also been proposed. It has been suggested that GMA exerts its therapeutic effects by removing granulocytes and monocytes from the peripheral blood, thereby attenuating inflammation, similar to the mechanism proposed for LCAP[6,16]. Another explanation proposed was based on the observation that leukocytes in the peripheral blood showed decreased expression of membrane LECAM-1 and decreased ability to produce TNF-α, IL-6, and IL-8 under stimulation of LPS following GMA treatment. It has also been suggested that GMA exerts its therapeutic effects by inhibiting leukocyte infiltration at sites of inflammation and inhibiting inflammatory cytokine production[16,23]. Other mechanisms proposed include induction of immature monocytes in the bone marrow following GMA treatment[16].

In the present study, the cytokine levels in the peripheral blood after LCAP were investigated. The level of IL-6, a pro-inflammatory cytokine, was significantly decreased following LCAP treatment. The blood level of IL-10, an inhibitory cytokine, was found to be elevated following LCAP, as compared to the levels measured before treatment. This elevation was particularly marked in the early stages of the treatment, suggesting that the therapeutic efficacy might be closely related to this finding. IL-10 has been reported to functionally inhibit neutrophils and monocytes[20]. In the present study also, the blood levels of IL-6, produced from neutrophils and monocytes, was decreased following LCAP treatment. In other words, the results of the present study suggested that LCAP exerted anti-inflammatory effects by enhancing the production of IL-10, thereby inhibiting the functions of activated leukocytes. LCAP treatment exerts the best therapeutic efficacy when it is carried out once a week for 5-10 wk. It would be of interest to determine the duration of functional inhibition of leukocytes and elevation of IL-10 level following one session of LCAP.

LCAP has also been shown to exert high therapeutic efficacy in cases of CD[24], rheumatoid arthritis (RA)[25], and rapidly-progressive glomerulonephritis[26], in addition to those of UC. Hidaka *et al*[27] who conducted a study of the efficacy of LCAP in RA patients reported that the serum levels of IL-10 increased, whereas those of the pro-inflammatory cytokine IL-15 decreased, following LCAP treatment in RA patients, and that LCAP may influence some chemotactic factors as well. Based on the present results and a review of the literature, LCAP treatment is considered to exert its effects against inflammatory diseases by influencing the cytokine balance through adsorption and removal of activated leukocytes, and causing functional changes of inflammatory cells.

Another report has shown that LCAP removes large numbers of granulocytes and monocytes from the peripheral

blood[17]. It has been revealed by many studies that granulocytes and monocytes are closely associated with the morbid condition in cases of UC[28-32]. Some reports have shown that clustering of these cells at sites of inflammation along the colonic mucosa in cases of UC[10] and the possibility that these activated granulocytes and monocytes induce tissue injury in response to production of various pro-inflammatory cytokines and reactive oxygen species[11-15]. In fact, some reports have shown that the amount of reactive oxygen species is increased at the site of histological inflammation in cases of IBD[33-35]. A report has recently described marked oxidation of actin, which may be caused by the accumulation of reactive oxygen species, at sites of inflammation in IBD[36]. It has also been shown that such oxidation disrupts the cytoskeleton, causing tissue injury. D'Odorico *et al*[14], have also reported that activation of neutrophils in the peripheral blood is associated with chronic intestinal inflammation in IBD. In other words, they indicated that neutrophils in the peripheral blood of UC or CD patients show higher chemiluminescence in response to stimulation, as compared to those of healthy persons, and produce larger amounts of reactive oxygen species. This phenomenon was particularly marked in cases with active UC and ileal CD, strongly suggesting its correlation with the morbid condition in these diseases. Some reports have also shown high levels of nitric oxide metabolites, i.e., one of the reactive oxygen species, in the serum, stool and colonic lumen of IBD patients[37-39]. Based on these observations, it is believed that activated neutrophils and monocytes in the peripheral blood of IBD patients infiltrate the intestinal mucosa to produce reactive oxygen species and cause mucosal injury. There has also been a report discussing the absence of correlation of the amount of reactive oxygen species in the blood with the morbid condition in cases of IBD[40], even though the present study revealed an increase in the percentage of reactive-oxygen-producing cells in the blood in cases of active UC as compared to that in healthy persons, and a decrease in the percentage of these cells with improvement of the morbid condition, showing close involvement of the neutrophils in the peripheral blood with the morbid condition in cases of UC.

In conclusion, LCAP treatment was confirmed to exert high therapeutic efficacy against active UC in the present study, and it was clarified for the first time that LCAP directly decreases the percentage of reactive-oxygen-producing cells in the peripheral blood. The results suggested that the mechanisms underlying the therapeutic effects of LCAP include enhanced production of IL-10 associated with indirect inhibition of the functions of leukocytes, and potent anti-inflammatory effects by the direct removal of reactive-oxygen-producing neutrophils from the peripheral blood. Further studies in the future are proposed to clearly elucidate the underlying mechanisms.

REFERENCES

1 **Moertel CG,** Bargen JA. A critical analysis of the use of salicylazosulfapyridine in chronic ulcerative colitis. *Ann Intern Med* 1959; **51**: 879-889

2 **Schroeder KW,** Tremaine WJ, Ilstrup DM. Coated oral 5-aminosalicylic acid therapy for mildly to moderately active ulcerative colitis. A randomized study. *N Engl J Med* 1987; **317**: 1625-1629

3 **Truelove SC,** Witts LJ. Cortisone and corticotrophin in ulcerative colitis. *Br Med J* 1959; **1**: 387-394

4 **Meyers S,** Sachar DB, Goldberg JD, Janowitz HD. Corticotropin versus hydrocortisone in the intravenous treatment of ulcerative colitis. A prospective, randomized, double blind clinical trial. *Gastroenterology* 1983; **85**: 351-357

5 **Mackay IR,** Wall AJ, Goldstein G. Response to azathioprine in ulcerative colitis. Report of 7 cases. *Am J Dig Dis* 1966; **11**: 536-545

6 **Shimoyama T,** Sawada K, Hiwatashi N, Sawada T, Matsueda K, Munakata A, Asakura H, Tanaka T, Kasukawa R, Kimura K, Suzuki Y, Nagamachi Y, Muto T, Nagawa H, Iizuka B, Baba S, Nasu M, Kataoka T, Kashiwagi N, Saniabadi AR. Safety and efficacy of granulocyte and monocyte adsorption apheresis in patients with active ulcerative colitis: a multicenter study. *J Clin Apher* 2001; **16**: 1-9

7 **Hanai H,** Watanabe F, Takeuchi K, Iida T, Yamada M, Iwaoka Y, Saniabadi A, Matsushita I, Sato Y, Tozawa K, Arai H, Furuta T, Sugimoto K, Bjarnason I. Leukocyte adsorptive apheresis for the treatment of active ulcerative colitis: a prospective, uncontrolled, pilot study. *Clin Gastroenterol Hepatol* 2003; **1**: 28-35

8 **Hanai H,** Watanabe F, Yamada M, Sato Y, Takeuchi K, Iida T, Tozawa K, Tanaka T, Maruyama Y, Matsushita I, Iwaoka Y, Kikuch K, Saniabadi AR. Adsorptive granulocyte and monocyte apheresis versus prednisolone in patients with corticosteroid-dependent moderately severe ulcerative colitis. *Digestion* 2004; **70**: 36-44

9 **Sawada K,** Muto T, Shimoyama T, Satomi M, Sawada T, Nagawa H, Hiwatashi N, Asakura H, Hibi T. Multicenter randomized controlled trial for the treatment of ulcerative colitis with a leukocytapheresis column. *Curr Pharm Des* 2003; **9**: 307-321

10 **Fiocchi C.** Inflammatory bowel disease: etiology and pathogenesis. *Gastroenterology* 1998; **115**: 182-205

11 **Nikolaus S,** Bauditz J, Gionchetti P, Witt C, Lochs H, Schreiber S. Increased secretion of pro-inflammatory cytokines by circulating polymorphonuclear neutrophils and regulation by interleukin 10 during intestinal inflammation. *Gut* 1998; **42**: 470-476

12 **Papadakis KA,** Targan SR. Role of cytokines in the pathogenesis of inflammatory bowel disease. *Annu Rev Med* 2000; **51**: 289-298

13 **Lampinen M,** Carlson M, Sangfelt P, Taha Y, Th?rn M, L??f L, Raab Y, Venge P. IL-5 and TNF-alpha participate in recruitment of eosinophils to intestinal mucosa in ulcerative colitis. *Dig Dis Sci* 2001; **46**: 2004-2009

14 **D'Odorico A,** D'Inca R, Mestriner C, Di Leo V, Ferronato A, Sturniolo GC. Influence of disease site and activity on peripheral neutrophil function in inflammatory bowel disease. *Dig Dis Sci* 2000; **45**: 1594-1600

15 **Oldenburg B,** van Kats-Renaud H, Koningsberger JC, van Berge Henegouwen GP, van Asbeck BS. Chemiluminescence in inflammatory bowel disease patients: a parameter of inflammatory activity. *Clin Chim Acta* 2001; **310**: 151-156

16 **Kashiwagi N,** Sugimura K, Koiwai H, Yamamoto H, Yoshikawa T, Saniabadi AR, Adachi M, Shimoyama T. Immunomodulatory effects of granulocyte and monocyte adsorption apheresis as a treatment for patients with ulcerative colitis. *Dig Dis Sci* 2002; **47**: 1334-1341

17 **Sawada K,** Ohnishi K, Kosaka T, Chikano S, Yokota Y, Egashira A, Izawa H, Yamamura M, Amano K, Satomi M, Shimoyama T. Leukocytapheresis with leukocyte removal filter as new therapy for ulcerative colitis. *Ther Apher* 1997; **1**: 207-211

18 **Rachmilewitz D**. Coated mesalazine (5-aminosalicylic acid) versus sulphasalazine in the treatment of active ulcerative colitis: a randomised trial. *BMJ* 1989; **298**: 82-86

19 **Bass DA,** Parce JW, Dechatelet LR, Szejda P, Seeds MC, Thomas M. Flow cytometric studies of oxidative product formation by neutrophils: a graded response to membrane

stimulation. *J Immunol* 1983; **130**: 1910-1917

20 **Jenkins JK,** Malyak M, Arend WP. The effects of interleukin-10 on interleukin-1 receptor antagonist and interleukin-1 beta production in human monocytes and neutrophils. *Lymphokine Cytokine Res* 1994; **13**: 47-54

21 **Noguchi M,** Hiwatashi N, Hayakawa T, Toyota T. Leukocyte removal filter-passed lymphocytes produce large amounts of interleukin-4 in immunotherapy for inflammatory bowel disease: role of bystander suppression. *Ther Apher* 1998; **2**: 109-114

22 **Suzuki K,** Sugimura K, Hasegawa K, Yoshida K, Suzuki A, Ishizuka K, Ohtsuka K, Honma T, Narisawa R, Asakura H. Activated platelets in ulcerative colitis enhance the production of reactive oxygen species by polymorphonuclear leukocytes. *Scand J Gastroenterol* 2001; **36**: 1301-1306

23 **Hanai H,** Watanabe F, Saniabadi AR, Matsushitai I, Takeuchi K, Iida T. Therapeutic efficacy of granulocyte and monocyte adsorption apheresis in severe active ulcerative colitis. *Dig Dis Sci* 2002; **47**: 2349-2353

24 **Kosaka T,** Sawada K, Ohnishi K, Egashira A, Yamamura M, Tanida N, Satomi M, Shimoyama T. Effect of leukocytapheresis therapy using a leukocyte removal filter in Crohn's disease. *Intern Med* 1999; **38**: 102-111

25 **Hidaka T,** Suzuki K, Matsuki Y, Takamizawa-Matsumoto M, Kataharada K, Ishizuka T, Kawakami M, Nakamura H. Filtration leukocytapheresis therapy in rheumatoid arthritis: a randomized, double-blind, placebo-controlled trial. *Arthritis Rheum* 1999; **42**: 431-437

26 **Furuta T,** Hotta O, Yusa N, Horigome I, Chiba S, Taguma Y. Lymphocytapheresis to treat rapidly progressive glomerulonephritis: a randomised comparison with steroid-pulse treatment. *Lancet* 1998; **352**: 203-204

27 **Hidaka T,** Suzuki K, Kawakami M, Okada M, Kataharada K, Shinohara T, Takamizawa-Matsumoto M, Ohsuzu F. Dynamic changes in cytokine levels in serum and synovial fluid following filtration leukocytapheresis therapy in patients with rheumatoid arthritis. *J Clin Apher* 2001; **16**: 74-81

28 **McCarthy DA,** Rampton DS, Liu YC. Peripheral blood neutrophils in inflammatory bowel disease: morphological evidence of *in vivo* activation in active disease. *Clin Exp Immunol* 1991; **86**: 489-493

29 **Mahida YR.** The key role of macrophages in the immunopathogenesis of inflammatory bowel disease. *Inflamm Bowel Dis* 2000; **6**: 21-33

30 **Meuret G,** Bitzi A, Hammer B. Macrophage turnover in Crohn's disease and ulcerative colitis. *Gastroenterology* 1978; **74**: 501-503

31 **Rugtveit J,** Brandtzaeg P, Halstensen TS, Fausa O, Scott H. Increased macrophage subset in inflammatory bowel disease: apparent recruitment from peripheral blood monocytes. *Gut* 1994; **35**: 669-674

32 **Brannigan AE,** O'Connell PR, Hurley H, O'Neill A, Brady HR, Fitzpatrick JM, Watson RW. Neutrophil apoptosis is delayed in patients with inflammatory bowel disease. *Shock* 2000; **13**: 361-366

33 **Simmonds NJ,** Allen RE, Stevens TR, Van Someren RN, Blake DR, Rampton DS. Chemiluminescence assay of mucosal reactive oxygen metabolites in inflammatory bowel disease. *Gastroenterology* 1992; **103**: 186-196

34 **Keshavarzian A,** Sedghi S, Kanofsky J, List T, Robinson C, Ibrahim C, Winship D. Excessive production of reactive oxygen metabolites by inflamed colon: analysis by chemiluminescence probe. *Gastroenterology* 1992; **103**: 177-185

35 **McKenzie SJ,** Baker MS, Buffinton GD, Doe WF. Evidence of oxidant-induced injury to epithelial cells during inflammatory bowel disease. *J Clin Invest* 1996; **98**: 136-141

36 **Keshavarzian A,** Banan A, Farhadi A, Komanduri S, Mutlu E, Zhang Y, Fields JZ. Increases in free radicals and cytoskeletal protein oxidation and nitration in the colon of patients with inflammatory bowel disease. *Gut* 2003; **52**: 720-728

37 **Oudkerk Pool M,** Bouma G, Visser JJ, Kolkman JJ, Tran DD, Meuwissen SG, Pena AS. Serum nitrate levels in ulcerative colitis and Crohn's disease. *Scand J Gastroenterol* 1995; **30**: 784-788

38 **Roediger WE,** Lawson MJ, Nance SH, Radcliffe BC. Detectable colonic nitrite levels in inflammatory bowel disease – mucosal or bacterial malfunction? *Digestion* 1986; **35**: 199-204

39 **Sasajima K,** Yoshida Y, Yamakado S, Sato J, Miyashita M, Okawa K, Matsutani T, Onda M, Kawano E. Changes in urinary nitrate and nitrite during treatment of ulcerative colitis. *Digestion* 1996; **57**: 170-173

40 **Pavlick KP,** Laroux FS, Fuseler J, Wolf RE, Gray L, Hoffman J, Grisham MB. Role of reactive metabolites of oxygen and nitrogen in inflammatory bowel disease. *Free Radic Biol Med* 2002; **33**: 311-322

Science Editor Guo SY **Language Editor** Elsevier HK

PO Box 2345, Beijing 100023, China
www.wjgnet.com
wjg@wjgnet.com

ELSEVIER

World J Gastroenterol 2005;11(20):3091-3098
World Journal of Gastroenterology ISSN 1007-9327

• *CLINICAL RESEARCH* •

Rabeprazole *vs* esomeprazole in non-erosive gastro-esophageal reflux disease: A randomized, double-blind study in urban Asia

KM Fock, EK Teo, TL Ang, TS Chua, TM Ng, YL Tan

KM Fock, EK Teo, TL Ang, TS Chua, TM Ng, YL Tan, Division of Gastroenterology, Department of Medicine, Changi General Hospital, Singapore
Supported by Eisai Co., Ltd.
Correspondence to: Professor KM Fock, Division of Gastroenterology, Department of Medicine, Changi General Hospital, 2 Simei Street 3, 529889 Singapore. kwong_ming_fock@cgh.com.sg
Telephone: +65-6788-8833 Fax: +65-6260-1692
Received: 2004-12-22 Accepted: 2005-01-05

Abstract

AIM: Gastro-esophageal reflux disease (GERD) is becoming increasingly common in Asia. Data on the efficacy of proton pump inhibitors in patients with non-erosive GERD (NERD) in Asia is lacking. This double-blind study compared the efficacy and safety of rabeprazole with esomeprazole in relief of symptoms in patients with NERD.

METHODS: One hundred and thirty-four patients with reflux symptoms of NERD and normal endoscopy were randomized to receive rabeprazole 10 mg or esomeprazole 20 mg once daily for 4 wk. Symptoms were recorded in a diary and changes in severity of symptoms noted.

RESULTS: At 4 wk of treatment, rabeprazole 10 mg and esomeprazole 20 mg were comparable with regards to the primary endpoint of time to achieve 24-h symptom-free interval for heartburn 8.5 d *vs* 9 d and regurgitation 6 d *vs* 7.5 d. Rabeprazole and esomeprazole were also similarly efficacious in term of patient's global evaluation with 96% of patients on rabeprazole and 87.9% of patients on esomeprazole, reporting that symptoms improved (P = NS). Satisfactory relief of day- and night-time symptoms was achieved in 98% of patients receiving rabeprazole and 81.4% of patients receiving esomeprazole. Adverse events were comparable in both groups (P = NS).

CONCLUSION: Rabeprazole 10 mg has a similar efficacy and safety profile in Asians with NERD as esomeprazole 20 mg. Further study is necessary to investigate whether the small differences between the two drugs seen in this study are related to the improved pharmacodynamic properties of rabeprazole. Both drugs were well tolerated.

Key words: Non-erosive esophageal reflux disease; New proton pump inhibitors

Fock KM, Teo EK, Ang TL, Chua TS, Ng TM, Tan YL. Rabeprazole *vs* esomeprazole in non-erosive gastro-esophageal reflux disease: A randomized, double-blind study in urban Asia. *World J Gastroenterol* 2005; 11(20): 3091-3098
http://www.wjgnet.com/1007-9327/11/3091.asp

INTRODUCTION

Gastro-esophageal reflux disease (GERD) is characterized by recurrent return of gastric contents back into the esophagus, causing heartburn, regurgitation and symptoms, such as chest pain, coughing, hoarseness and dysphagia[1,2]. GERD symptoms can cause significant patient distress and can interfere with everyday life[2].

GERD is a common condition, with an estimated 44% of the adult population in USA experiencing GERD symptoms monthly and about 20% experiencing symptoms weekly[1]. However, prevalence of GERD in Asia is reported to be lower than that in Western countries[3]. A study from Singapore in 1988 reported that the prevalence of monthly reflux symptoms in the community was 1.6%[4]. Recently, a study performed in Hong Kong reported that the monthly and weekly prevalence of GERD symptoms was 8.9% and 2.5%, respectively[5].

GERD can be subdivided into several groups: (1) non-erosive GERD (NERD), (2) erosive GERD, (3) Barrett's esophagus, and GERD-related complications. NERD has been defined as the presence of typical symptoms of GERD caused by intra-esophageal acid in the absence of visible esophageal mucosal injury[1]. In NERD patients the total acid reflux time has been found to be significantly lower than that in patients with erosive esophagitis. Furthermore, as much as 50% of NERD patients have normal 24-h esophageal pH study[6]. It is estimated that up to 70% of patients with typical GERD symptoms in the West have normal endoscopy[7]. In Asia, NERD and endoscopically mild form of erosive esophagitis may account for up to 90% of patients with GERD symptoms[8].

Proton pump inhibitors (PPIs), such as omeprazole, esomeprazole, lansoprazole and rabeprazole, are widely used for the treatment of GERD. PPIs effectively inhibit the duration and extent of gastric acid secretion and provide more complete remission of the symptoms of heartburn than other forms of acid suppression therapy[9,10]. However, the response to PPI in patients with NERD is less efficacious when compared to patients with erosive GERD[1,11].

The goal of treatment is to improve patients' quality of life by providing rapid relief of symptoms and reducing the severity and number of recurrent episodes[8]. Therefore, an important endpoint in clinical trials assessing the efficacy of treatment in NERD patients is time taken for complete

relief of symptoms, especially the pivotal symptoms of heartburn and regurgitation[8]. This can be measured as time to the first 24-h interval free from GERD/NERD symptoms of heartburn or acid regurgitation. Other endpoints include global symptom improvement, satisfactory, and complete relief of day- and night-time symptoms.

Two new PPIs have been introduced in Asia recently: rabeprazole and esomeprazole. Rabeprazole is a PPI that effectively provides symptom relief and healing, and prevents relapse, in patients with erosive GERD[12-14]. One clinical study suggests that rabeprazole effectively relieves the symptoms of heartburn in patients with NERD with significant improvement starting with the dose on 1st d[11]. Esomeprazole, the *s*-enantiomer of omeprazole, has demonstrated superior efficacy over omeprazole in healing and symptom resolution in patients with erosive and non-erosive reflux disease[15,16].

Currently, there is a paucity of clinical data comparing the efficacy and safety of these two PPIs in treating NERD patients let alone in Asian population. We report a randomized, double-blind, parallel-group, 4-wk study designed to investigate the efficacy and safety of rabeprazole 10 mg compared with esomeprazole 20 mg once daily in the treatment of NERD patients. This is the first clinical study directly comparing the efficacy of these two PPIs in NERD patients in Asia.

MATERIALS AND METHODS

The study was conducted in accordance with the Declaration of Helsinki. Ethics committee approval was obtained before the study commenced and all patients gave informed consent.

Study design

In this randomized, double-blind, parallel-group comparative study, patients with NERD received rabeprazole 10 mg once daily or esomeprazole 20 mg once daily for a 4-wk treatment period. Patients recorded their GERD symptoms (heartburn or regurgitation, with or without eructation) daily in the diary provided. Other upper GI symptoms were similarly recorded as well. Patients were screened 7 d prior to enrollment and eligibility was assessed according to the specified inclusion and exclusion criteria. The study consisted of a 1-wk screening phase, followed by endoscopy and a 4-wk, double-blind treatment phase. *Helicobacter pylori* screening was performed using CLO-test and serology.

Inclusion criteria

To be eligible for study entry, patients were required to be aged between 21 and 65 years. GERD symptoms (i.e., heartburn or regurgitation or both) were dominant symptoms. Heartburn or regurgitation was present for at least 3 mo in the previous year, which need not be continuous.

Heartburn was defined as 'substernal burning sensation or pain'. A description like 'a burning sensation behind the breastbone rising up to the throat or neck' or 'a burning pain or discomfort behind the breastbone rising up towards the neck' was accepted as 'heartburn'. Patients who described these symptoms as 'a burning, warm or 'acid' sensation in the epigastrium, substernal area or both' were also accepted as having 'heartburn'. Regurgitation was defined as 'food or fluid coming back up from your stomach'. Eructation was defined as 'belching'.

To qualify for inclusion into the study, subjects need to have experienced at least one period of moderate-to-very severe heartburn or regurgitation in the past 7 d prior to treatment.

In addition, at endoscopy, no esophageal mucosal break was observed, i.e., grade 0 according to the LA Classification. The ability to read and write in either English or Chinese was also a requirement for study entry.

Exclusion criteria

The main exclusion criteria were as follows: known history of gastroduodenal ulcer; infectious or inflammatory conditions of the intestine (including inflammatory bowel disease); malabsorption syndromes; obstruction; gastrointestinal malignancy; gastric or intestinal surgery including vagotomy; Barrett's esophagus; esophageal stricture or pyloric stenosis; scleroderma; erosive esophagitis; positive HIV status and pregnancy. Patients were ineligible if they had: abnormal laboratory tests at the initial visit (including liver enzymes greater than twice the upper limit of normal); GERD treatment refractory to a 2-mo course of H_2-blocker or PPI therapy; taken a PPI within 14 d of screening or a H_2-blocker or prokinetic agent within 7 d of screening; required daily use of NSAIDS, oral steroids, aspirin (>325 mg/d); or were unable to discontinue the use of anticholinergics, cholinergics, spasmolytics, opiates or sucralfate.

Randomization

Patients who qualified were randomized to receive either rabeprazole 10 mg or esomeprazole 20 mg once daily after the morning meal. A computer-generated randomization scheme was used to randomly allocate patients to one of the two treatment groups.

Patients were permitted to take an antacid (Mylanta®) as rescue medication for the relief of heartburn symptom, if necessary. No other medication was allowed.

Blinding

Rabeprazole 10-mg tablets and esomeprazole 20-mg tablets were inserted into identical capsules to ensure double blinding. Patients received 2 wk supply of medication at each study visit.

Study visits

The study consisted of a screening visit and three scheduled visits during the treatment phase: baseline (the end of the screening phase), wk 2 and 4. At each visit, a review of concurrent and disallowed medications was undertaken, completed patient diaries were collected and adverse events were assessed. An upper gastrointestinal endoscopy was conducted 7 d prior to baseline or at the baseline visit. Laboratory analysis was conducted at baseline and at wk 4. Compliance with drug therapy was determined at the scheduled wk 2 and 4 visits.

Symptom severity

Patients recorded the severity of GERD symptoms in a daily diary. Severity was graded on a five-point scale from

none (0), mild (1), moderate (2), severe (3) and very severe (4) for each of the following symptoms: day-time heartburn, night-time heartburn, day-time regurgitation, and night-time regurgitation.

Other upper GI symptoms of belching ('eructation'), early satiety ('the sensation of filling up quickly'), bloating ('feeling like I have a lot of gas in my belly'), nausea and vomiting were also recorded on the five-point scale as explained above.

The symptom severity was defined as follows:

0 = no symptoms	
1 = mild	Symptoms are present occasionally and patients can continue with daily activities.
2 = moderate	Symptoms are present most of the time but patients can perform daily activities.
3 = severe	Symptoms are present continuously. The symptoms are severe and affect daily activities or patient cannot do things that they normally can.
4 = very severe	Symptoms are so severe that patient has to stay in bed and cannot perform activities that they normally could.

Patient informed consent

The Patient Informed Consent was in English; however, identical versions translated into Malay and Mandarin were available to the patients as well. In the development of the Malay and Mandarin versions of the Patient Informed Consent, the original English version was translated, back-translated and checked for accuracy. The Patient Informed Consent was explained in English, Malay or Mandarin according to the subject's first language or preferred language of communication.

Outcome measures

The primary efficacy endpoint was the time (in days) for patients to achieve their first 24-h interval without any symptoms of heartburn or regurgitation. Secondary endpoints were as follows: number of patients who had complete or satisfactory relief of symptoms during wk 1, 2, 3, or 4, symptom severity scores of day-time and night-time heartburn or regurgitation, upper GI symptoms, patients' global evaluation at the end of study and number of antacids used during the study period.

Safety and tolerability were evaluated by recording adverse events (including severity, relationship of the adverse event to the study treatment and outcome and laboratory analysis).

The Case Report Forms were available in English, Malay and Mandarin, according to the subject's first language or preferred language of communication. In the development of the Malay and Mandarin identical versions of the Case Report Form, similar care was taken: the original English version was translated, back-translated and checked for accuracy.

Statistical analysis

Analyses were performed on an intention-to-treat (ITT) basis by an independent statistician. The ITT population was defined as including all randomized patients who received at least one dose of study medication and who had at least one post-baseline assessment for efficacy. The primary outcome, i.e., time taken to achieve 24-h symptom free from heartburn or regurgitation, however, did not include for analysis of patients who did not experience heartburn and/or regurgitation on the day prior to commencement of study medication. Heartburn and regurgitation were analyzed separately.

Subgroup analyses were performed for the subjects who experienced heartburn and/or regurgitation.

Day-time symptoms were those that occur after arising in the morning. Night-time symptoms were those that occur after retiring in the evening. Multiple single episodes experienced during a day-time and/or a night-time period count only as 1 d-time and/or 1 night-time episode.

Differences within or between treatment groups for all tests were considered significant at $P \leqslant 0.05$.

In order to detect a difference in clinical response of 20% or more between the two treatment groups with the use of a two-sided test with 0.80 statistical power and a significant level of 0.05, a sample size of 118 was required. Hence the sample size was determined to be 130, with an allowance of 10% for patients who were lost to follow up. A magnitude of 20% was chosen on the basis that it represented a clinically relevant difference in outcome.

Student's *t*-test and Fischer's exact test were used to compare the patient demographics of the two groups of patients. Subject global evaluation was analyzed using Wilcoxon's test. The primary efficacy parameter was analyzed using log-rank test. The percentage of patients experiencing complete and satisfactory relief of heartburn and regurgitation during the study (day-time and night-time) was analyzed using repeated measurement analysis. The average reflux symptom scores were analyzed using an analysis of covariance (ANCOVA) model between the two PPIs and using paired *t*-test when analyzed between treatment and pre-treatment (baseline). The average weekly antacid tablets consumed were analyzed using an ANCOVA model. The percent of periods without antacids consumption were analyzed using analysis of variance model. Analysis of laboratory data was compared using paired *t*-tests.

Withdrawal criteria

Withdrawal from the study was allowed in the event of a serious adverse event, the detection of intercurrent illness that might invalidate the study or place the patient at risk, concern for patient safety by the investigator, protocol violations or unreliable patient behavior.

RESULTS

Patients studied

One hundred and thirty-four patients were enrolled (67 from each treatment group) in the study and randomly assigned to receive either rabeprazole 10 mg or esomeprazole 20 mg. There were 63 patients in the rabeprazole treatment group and 64 patients in the esomeprazole treatment group with a total of 127 patients eligible for efficacy analysis (ITT)

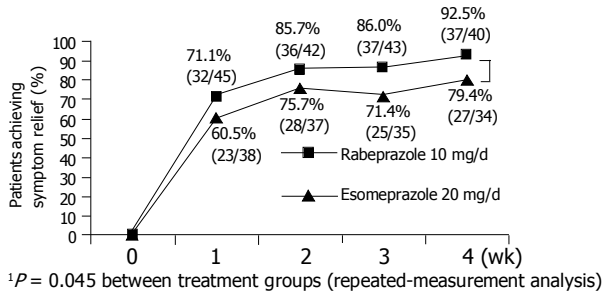

Figure 1 Satisfactory relief of day-time heartburn and regurgitation (in patients who had both heartburn and regurgitation).

(Table 1). Of the seven patients in total excluded from the efficacy analysis (ITT), there were four patients in the rabeprazole and three patients in the esomeprazole group. Of these, four rabeprazole patients and one esomeprazole patient did not take any study medication. One esomeprazole patient withdrew due to persistent headache and another esomeprazole patient withdrew consent after taking study medication for 2 d. Although these latter two patients on esomeprazole did receive at least one dose of study medication, they did not have at least one post-baseline assessment for efficacy (as defined and required in the protocol for ITT analysis). Therefore, they were not included in the ITT analysis for efficacy.

The treatment groups were similar with respect to demographic and clinical characteristics. Although there were more males in the rabeprazole group, this difference was not statistically significant. The mean age of study participants was 38.9 years. The majority of patients were of Chinese descent (79.5%, Table 1).

Efficacy analysis

A summary of the efficacy (and safety) results can be seen in Table 2.

Primary efficacy variable

Time to first 24-h, symptom-free interval The median time to the first 24-h symptom-free interval was similar for patients in both treatment groups; 8.5 d for rabeprazole and 9.0 d for esomeprazole for heartburn (P = NS) and 6.0 d *vs* 7.5 d for regurgitation (P = NS). The proportion of patients achieving these study endpoints during the 4-wk treatment period were higher in rabeprazole group compared with esomeprazole group, but these differences were not statistically significant (24-h heartburn-free for rabeprazole and esomeprazole: 84.4% *vs* 60.9%, 24-h regurgitation-free: 90.0% *vs* 67.9% (P = NS).

Secondary efficacy variables

Satisfactory relief of day-time and night-time symptoms Satisfactory relief of day-time and night-time symptoms (no episode of symptom defined as having moderate or severe in severity during the week) was achieved in 81.4-98.0% of patients of both treatment groups of heartburn or regurgitation after 4-wk treatment.

In a subgroup of patients who had both heartburn and

Table 1 Demographic and baseline characteristics of patients enrolled

Number of subjects enrolled	Total 127	Rabeprazole 63	Esomeprazole 64	P
Gender (%)				
Female	62 (48.8)	25 (39.7)	37 (57.8)	$P = 0.051^1$
Male	65 (51.2)	38 (60.3)	27 (42.2)	
Race (%)				
Chinese	101 (79.5)	52 (82.5)	49 (76.6)	$P = 0.872^1$
Malay	9 (7.1)	4 (6.3)	5 (7.8)	
Indian	15 (11.8)	6 (9.5)	9 (14.1)	
Other	2 (1.6)	1 (1.6)	1 (1.6)	
Age (yr)				
Mean (SD)	38.9 (10.6)	39.3 (11.2)	38.4 (10.0)	$P = 0.629^2$
History of GERD symptoms (yr)				
Mean (SD)	3.6 (4.5)	3.2 (4.2)	3.9 (4.7)	$P = 0.373^2$
Tobacco use, *N* (%)				
Yes	11 (8.7)	4 (6.3)	7 (10.9)	$P = 0.243^1$
No	116 (91.3)	59 (93.7)	57 (89.1)	
Alcohol use, *N* (%)				
Yes	20 (15.7)	9 (14.3)	11 (17.2)	$P = 0.486^1$
No	107 (84.3)	54 (85.7)	53 (82.8)	
Previous medication for reflux disease				
Yes	77 (60.6)	35 (55.6)	42 (65.6)	$P = 0.279^1$
No	50 (39.4)	28 (44.4)	22 (34.4)	
H pylori status				
Positive	50	24 (45.3)	26 (44.0)	
Negative	62	29 (54.7)	33 (56.0)	$P = 0.95^3$
(Not available	15	10	5	

Test[1] Fisher's exact test; Test[2] *t*-test; Test[3] χ^2 test

regurgitation, a statistically significant higher number of patients treated with rabeprazole reported satisfactory relief of day-time symptoms compared to those receiving esomeprazole ($P<0.05$, Figure 1).

Complete relief of day-time and night-time symptoms

Complete relief of day-time heartburn (no episodes of heartburn during the evaluation week) at the 1st wk were 6.9% (14 of 52 patients) in patients treated with rabeprazole and 23.4% (11 out of 52 patients) in those received esomeprazole (P = NS). At the end of wk 4, this increased to 55.3% (26 out of 47) and 41.1% (18 out of 43) for rabeprazole and esomeprazole, respectively (P = NS). Complete relief of night-time heartburn were similar in both patient groups (28.8% (15/62) *vs* 20.9% (9/43)) at wk 1 and (44.4% (20/45) *vs* 41.0% (16/39)) at wk 4 (for rabeprazole and esomeprazole, respectively) (P = NS).

No statistically significant differences were observed in analyses of regurgitation.

Symptom severity score during the first 5 d

Comparing between the two PPIs, there was no statistically significant difference between groups for day- and night-time heartburn or regurgitation within the first 5 d (P = NS, Table 2).

Comparing each individual PPI with treatment *vs* baseline or pre-treatment symptoms severity scores, rabeprazole significantly reduced day- and night-time heartburn scores within 2 d of commencing treatment compared to baseline or pre-treatment ($P<0.01$), and this statistical significance continued up to d 5. However, patients receiving esomeprazole showed a statistically significant improvement in day-time heartburn score from the 3rd to the 5th d, and no significant improvement in night-time heartburn score in the first 5 d (Table 2 and Figure 2).

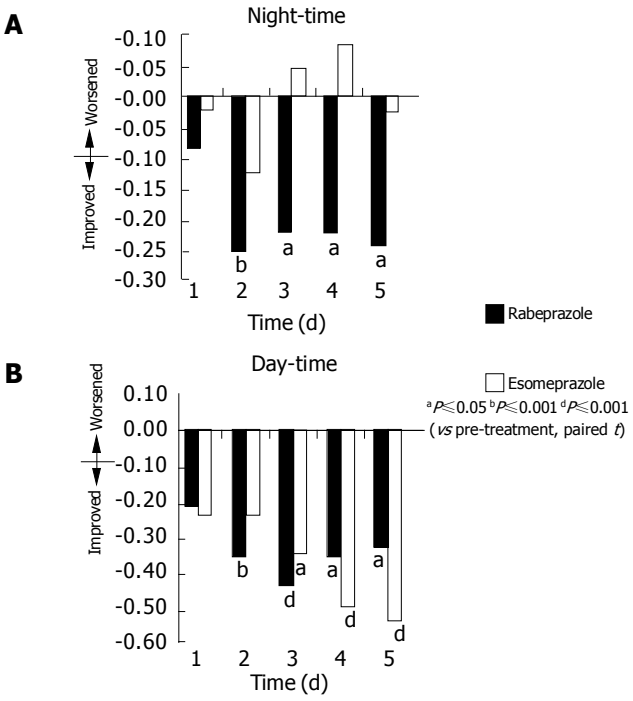

Figure 2 Change in symptom severity score from pre-treatment on d 1 to 5

Table 2 Summary of efficacy and safety results (including important subgroup analyses)

Parameter	Rabeprazole 10 mg (d)	Esomeprazole 20 mg (d)	*P*	Result
Primary efficacy variables				
Time to 24-h symptom-free interval-HB	8.5 d	9 d	0.265	NS
Time to 24-h symptom-free interval-RG	6.0 d	7.5 d	0.405	NS
Secondary efficacy variables				
Time to 48-h symptom-free interval-HB	9.5 d	8.5 d	0.373	NS
Time to 48-h symptom-free interval-RG	8.5 d	11 d	0.271	NS
W1-W4-satisfactory relief DT or NT-HB			>0.05	NS
W1-W4-satisfactory relief DT or NT-RG			>0.05	NS
W1-W4-satisfactory relief DT-HB & RG[4]			0.045[4]	Rabeprazole superior[4]
W1-W4-complete relief DT or NT-HB			>0.05	NS
W1-W4-complete relief DT or NT-RG			>0.05	NS
W1-W4-belching	-0.41	-0.42	0.631	NS
W1-W4-early satiety	-0.26	-0.32	0.178	NS
W1-W4-bloating	-0.46	-0.54	0.608	NS
W1-W4-nausea	-0.23	-0.27	0.319	NS
W1-W4-vomiting	-0.34	-0.21	0.808	NS
Symptom severity score-D1-5-DT HB	$P<0.05$ (D2-5)[1]	$P<0.05$ (D3-5)[1]		NS[2]
Symptom severity score-D1-5-NT HB	$P<0.05$ (D2-5)[1]	NS[1]		NS[3]
Symptom severity score-D1-5-DT RG	$P<0.05$ (D1-5)[1]	$P<0.05$ (D1-5)[1]		NS
Symptom severity score-D1-5-NT RG	$P<0.05$ (D5 only)[1]	$P<0.05$ (D2 only)[1]		NS
Patient's global evaluation (%)	96.4	87.9	0.823	NS
Antacid use-weekly average	0.15	0.16	0.887	NS
Antacid use-% antacid free	85.7	84.9	0.848	NS
Safety				
Adverse events	22	18.2	>0.05	NS

HB-heartburn; RG-regurgitation; DT-day-time; NT-night-time; W1-wk 1; w4-wk 4; [1]Compared to baseline; [2]Rabeprazole statistically superior compared to baseline/pre-treatment from d 2 to 5 and esomeprazole statistically superior compared to baseline/pre-treatment from d 3 to 5; [3]Rabeprazole statistically superior compared to baseline/pre-treatment from d 2 to 5 and esomeprazole not statistically superior compared to baseline/pre-treatment from d 1 to 5; [4]Subgroup analysis.

(heartburn) (ITT).

Antacid use

The use of rescue medication was low in both groups. There was no statistical difference between the two groups for weekly average antacid consumption and percentage antacid free for the duration of the study (P = NS).

Patients' global evaluation

A slightly higher proportion of patients treated with rabeprazole (96.4%, 54 out of 56 patients) reported their symptoms as improved ("slightly improved", "moderately improved" or "markedly improved") at the end of the treatment period compared to those treated with esomeprazole (87.9%, 51 out of 58 patients). The difference was not statistically significant.

Safety analysis

Of the 134 patients enrolled, 129 patients in total were eligible for safety analysis. The five patients excluded from the safety analysis did not take any study medication. Of the five patients, four were from the rabeprazole and one was from the esomeprazole group.

Both drugs were well tolerated during the study. Adverse events considered related to the study medication occurred to a similar extent in patients treated with rabeprazole (22%) and esomeprazole (18.2%) (P = NS). One patient withdrew from the study because of persistent headache from esomeprazole.

Elevation of ALT occurred in one patient taking rabeprazole and four patients receiving esomeprazole. One patient on rabeprazole and two patients on esomeprazole had an increase in AST. These changes were not clinically significant.

There were no obvious differences in tolerability between the treatments. The measurement of laboratory variables and vital signs did not reveal any evidence of deleterious effects of the drugs in either group.

DISCUSSION

One of the problems in defining GERD in Asia is that there is no direct translation of 'heartburn' in most Asian languages, including the Chinese language[7,8] although this gap has been closed since the Asia-Pacific Consensus. Accepted classic symptoms of GERD in Asia include heartburn, regurgitation, dysphagia and odynophagia[7]. The recent Asia-Pacific Consensus on GERD recommends that a 'careful history taking to elicit the classic symptoms of GERD (heartburn and regurgitation) is the cornerstone in the diagnosis of GERD'[8]. In the present study, every effort was made by the investigating physician to ensure that heartburn and/or regurgitation was/were the cardinal presenting symptom(s). In addition, care was taken by the investigators to explain and elicit what the symptom of 'heartburn' meant to the patient. This study was designed to assess the efficacy and rapidity of symptom relief with rabeprazole 10 mg or esomeprazole 20 mg in patients with NERD in urban Asia.

The primary efficacy variable of median time to the first 24-h interval free from heartburn was similar for both drugs being 8.5 d for rabeprazole and 9.0 d for esomeprazole. Results of the primary efficacy variable for relief of regurgitation were similar between the two PPIs as well.

The majority of secondary efficacy variables were similar between the two PPIs as well. Overall, after 4 wk of treatment more patients receiving rabeprazole reported symptom improvement than those receiving esomeprazole (96% *vs* 87%) although this did not reach statistical significance. Complete relief of day-time symptoms after 4 wk of treatment was reported in 41.9% and 58.0%, whilst complete relief of night-time symptoms was lower at 41.0% *vs* 52.3%. Satisfactory relief of symptoms, defined as not having any episode greater than moderately severe, was reported in 73% (esomeprazole) to 96% (rabeprazole) of patients treated. In real-life situation, most patients would find satisfactory relief of symptoms as an acceptable treatment outcome. Further studies, however, are needed to confirm these observations. Our observations do support the clinical phar-macokinetics studies currently available on the two PPIs.

Pharmacodynamic studies involving rabeprazole and esomeprazole in healthy subjects showed that 40 mg of esomeprazole was more effective than 20 mg rabeprazole on d 5 of treatment in maintaining intragastric pH above 4.0, suggesting that, by d 5, 40 mg esomeprazole had more profound acid suppression than 20 mg rabeprazole[17]. On the other hand, 20 mg of rabeprazole increased intragastric pH more than 20 mg esomeprazole with a higher mean AUC (area under the plasma concentration-time curve) intragastric pH on d 1 of treatment[18]. On d 5 that difference remained except 11-14 h after dosing[18]. A study comparing rabeprazole 20 mg and esomeprazole 40 mg demonstrated rabeprazole 20 mg to produce a greater or equivalent acid suppression on day 1 (i.e., from the first dose), with rabeprazole showing significant superiority at night[19,20]. These studies demonstrate that rabeprazole have a faster onset of acid inhibitory action than other PPIs including esomeprazole from d 1 of dosing[18-20], with esomeprazole the superiority is seen over other PPIs from day 5 of dosing[17].

There was no statistically significant difference between the two groups for reduction in symptom severity scores for the first 5 d during day-time and night-time regurgitation. Nevertheless, rabeprazole effectively reduced the severity of day-time and night-time heartburn in patients with NERD compared to pre-treatment, improving symptom scores compared with baseline scores from as early as the 2nd d (P<0.05) following dosing. In contrast, esomeprazole produced significant improvement only in the symptom score of day-time heartburn from 3rd d onwards and no statistically significant change in symptom score in night-time heartburn in the first 5 d.

Several reports have suggested that patients with NERD are less responsive to PPIs[21-23]. Our study showed that after 4-wk treatment, both PPIs produced satisfactory relief of day-time heartburn in 91% of patients with non-erosive reflux disease (91% rabeprazole and 79% esomeprazole). This response rate is higher than that seen in Miner's study in USA, where only 56% of NERD patients responded to PPI after 4 wk[11]. Complete relief of day-time heartburn

was also higher in our study being reported in 45.6% (rabeprazole) and 41% (esomeprazole) of the patients treated compared with 29% in Miner's study[11]. This could be due to selection of a less severely symptomatic patient population. Patients were required to have had only one episode of moderate-to-severe GERD in the 7 d prior to study entry, whereas entry into the Miner study required patients to have had a minimum of five episodes in the week prior to entry[11]. Nevertheless, there are about 20% of our NERD patients who did not attain satisfactory relief of symptoms after 4 wk of treatment. Our data has shown that more patients respond to PPIs at wk 4 than at wk 1. Hence, by extending the duration of therapy beyond 4 wk, it may be possible that more patients would have symptom relief. Clinical studies with longer treatment periods are needed to determine if this hypothesis is true. Recent investigations have demonstrated the presence of highly acidic 'pocket' high in the fundus below the cardio-esophageal junction during the post-prandial period[24]. Dosing with acid suppressing agents will have to be tailored to neutralize this post-prandial acid 'pocket'.

Although there was rapid onset of action, the median time to the first 24-h period symptom free from heartburn was 8.5 d with rabeprazole and 9.0 d with esomeprazole. This was higher than the 2.5 d observed in Miner's study[11]. This difference could be explained by the fact that, in our study, patients who did not experience reflux symptoms 24 h prior to study were excluded from the analysis whereas they were included in Miner's study[11]. As these patients were excluded from analysis, the median reported in the study would overestimate the actual time taken to reach the first 24-h interval free from heartburn. The rapid action of these newer PPIs could be clinically relevant when treating NERD patients with "on-demand therapy", as these newer PPIs could produce symptom relief from d 2 or 3 onwards. This would translate into a shorter period of 'on-demand' therapy. This is consistent with the results seen in earlier report regarding on-demand treatment with rabeprazole 10 mg[25]. In that study, use of rabeprazole was required in only 26% of the total study period, indicating an average intake of only one tablet in 4 d[25].

In summary, our study demonstrates that once-daily therapy with the newer PPIs rabeprazole 10 mg or esomeprazole 20 mg produce improvement in majority of NERD patients. Relief from the symptoms of heartburn and regurgitation in a predominantly Chinese population with NERD can occur after 2 d of treatment. Further studies are needed to determine the optimum treatment period and symptom relapse rate on cessation of treatment.

REFERENCES

1 **Fass R.** Epidemiology and pathophysiology of symptomatic gastroesophageal reflux disease. *Am J Gastroenterol* 2003; **98**: S2-S7

2 **Damiano A,** Siddique R, Xu X, Johanson J, Sloan S. Reductions in symptom distress reported by patients with moderately severe, nonerosive gastroesophageal reflux disease treated with rabeprazole. *Dig Dis Sci* 2003; **48**: 657-662

3 **Holtmann G.** Reflux disease: the disorder of the third millennium. *Eur J Gastroenterol Hepatol* 2001; **13 Suppl 1**: S5-11

4 **Ho KY,** Kang JY, Seow A. Prevalence of gastrointestinal symptoms in a multiracial Asian population, with particular reference to reflux-type symptoms. *Am J Gastroenterol* 1998; **93**: 1816-1822

5 **Wong WM,** Lai KC, Lam KF, Hui WM, Hu WH, Lam CL, Xia HH, Huang JQ, Chan CK, Lam SK, Wong BC. Prevalence, clinical spectrum and health care utilization of gastro-oesophageal reflux disease in a Chinese population: a population-based study. *Aliment Pharmacol Ther* 2003; **18**: 595-604

6 **Martinez SD,** Malagon IB, Garewal HS, Cui H, Fass R. Non-erosive reflux disease (NERD)-acid reflux and symptom patterns. *Aliment Pharmacol Ther* 2003; **17**: 537-545

7 **Goh KL,** Chang CS, Fock KM, Ke M, Park HJ, Lam SK. Gastro-oesophageal reflux disease in Asia. *J Gastroenterol Hepatol* 2000; **15**: 230-238

8 **Fock KM,** Talley N, Hunt R, Fass R, Nandurkar S, Lam SK, Goh KL, Sollano J. Report of the Asia-Pacific consensus on the management of gastroesophageal reflux disease. *J Gastroenterol Hepatol* 2004; **19**: 357-367

9 **Holtmann G,** Bytzer P, Metz M, Loeffler V, Blum AL. A randomized, double-blind, comparative study of standard-dose rabeprazole and high-dose omeprazole in gastro-oesophageal reflux disease. *Aliment Pharmacol Ther* 2002; **16**: 479-485

10 **Galmiche JP,** Zerbib F, Ducrottè P, Fournet J, Rampal P, Avasthy N, Humphries TJ. Decreasing oesophageal acid exposure in patients with GERD: a comparison of rabeprazole and omeprazole. *Aliment Pharmacol Ther* 2001; **15**: 1343-1350

11 **Miner P,** Orr W, Filippone J, Jokubaitis L, Sloan S. Rabeprazole in nonerosive gastroesophageal reflux disease: a randomized placebo-controlled trial. *Am J Gastroenterol* 2002; **97**: 1332-1339

12 **Cloud ML,** Enas N, Humphries TJ, Bassion S. Rabeprazole in treatment of acid peptic diseases: results of three placebo-controlled dose-response clinical trials in duodenal ulcer, gastric ulcer, and gastroesophageal reflux disease (GERD). The Rabeprazole Study Group. *Dig Dis Sci* 1998; **43**: 993-1000

13 **Dekkers CP,** Beker JA, Thjodleifsson B, Gabryelewicz A, Bell NE, Humphries TJ. Double-blind comparison [correction of Double-blind, placebo-controlled comparison] of rabeprazole 20 mg vs. omeprazole 20 mg in the treatment of erosive or ulcerative gastro-oesophageal reflux disease. The European Rabeprazole Study Group. *Aliment Pharmacol Ther* 1999; **13**: 49-57

14 **Thjodleifsson B,** Rindi G, Fiocca R, Humphries TJ, Morocutti A, Miller N, Bardhan KD. A randomized, double-blind trial of the efficacy and safety of 10 or 20 mg rabeprazole compared with 20 mg omeprazole in the maintenance of gastro-oesophageal reflux disease over 5 years. *Aliment Pharmacol Ther* 2003; **17**: 343-351

15 **Kahrilas PJ,** Falk GW, Johnson DA, Schmitt C, Collins DW, Whipple J, D'Amico D, Hamelin B, Joelsson B. Esomeprazole improves healing and symptom resolution as compared with omeprazole in reflux oesophagitis patients: a randomized controlled trial. The Esomeprazole Study Investigators. *Aliment Pharmacol Ther* 2000; **14**: 1249-1258

16 **Lind T,** Rydberg L, Kylebäck A, Jonsson A, Andersson T, Hasselgren G, Holmberg J, Rohss K. Esomeprazole provides improved acid control *vs* omeprazole In patients with symptoms of gastro-oesophageal reflux disease. *Aliment Pharmacol Ther* 2000; **14**: 861-867

17 **Wilder-Smith CH,** Rohss K, Nilsson-Pieschl C, Junghard O, Nyman L. Esomeprazole 40 mg provides improved intragastric acid control as compared with lansoprazole 30 mg and rabeprazole 20 mg in healthy volunteers. *Digestion* 2003; **68**: 184-188

18 **Warrington S,** Baisley K, Boyce M, Tejura B, Morocutti A, Miller N. Effects of rabeprazole, 20 mg, or esomeprazole, 20 mg, on 24-h intragastric pH and serum gastrin in healthy subjects.

Aliment Pharmacol Ther 2002; **16**: 1301-1307

19 **Baisley K,** Warrington S, Tejura B, Morocutti A, Miller N. Rabeprazole 20 mg compared with esomeprazole 40 mg in the control of intragastric pH in healthy volunteers. *Gut* 2002; 50 (Suppl 2): A63

20 **Pantoflickova D,** Dorta G, Ravic M, Jornod P, Blum AL. Acid inhibition on the first day of dosing: comparison of four proton pump inhibitors. *Aliment Pharmacol Ther* 2003; **17**: 1507-1514

21 **Carlsson R,** Dent J, Watts R, Riley S, Sheikh R, Hatlebakk J, Haug K, de Groot G, van Oudvorst A, Dalvag A, Junghard O, Wiklund I. Gastro-oesophageal reflux disease in primary care: an international study of different treatment strategies with omeprazole. International GORD Study Group. *Eur J Gastroenterol Hepatol* 1998; **10**: 119-124

22 **Galmiche JP,** Barthelemy P, Hamelin B. Treating the symptoms of gastro-oesophageal reflux disease: a double-blind comparison of omeprazole and cisapride. *Aliment Pharmacol Ther* 1997; **11**: 765-773

23 **Venables TL,** Newland RD, Patel AC, Hole J, Wilcock C, Turbitt ML. Omeprazole 10 milligrams once daily, omeprazole 20 milligrams once daily, or ranitidine 150 milligrams twice daily, evaluated as initial therapy for the relief of symptoms of gastro-oesophageal reflux disease in general practice. *Scand J Gastroenterol* 1997; **32**: 965-973

24 **Fletcher J,** Wirz A, Young J, Vallance R, McColl KE. Unbuffered highly acidic gastric juice exists at the gastroesophageal junction after a meal. *Gastroenterology* 2001; **121**: 775-783

25 **Bytzer P,** Blum A, De Herdt D, Dubois D. Six-month trial of on-demand rabeprazole 10 mg maintains symptom relief in patients with non-erosive reflux disease. *Aliment Pharmacol Ther* 2004; **20**: 181-188

Science Editor Guo SY **Language Editor** Elsevier HK

PO Box 2345, Beijing 100023, China
www.wjgnet.com
wjg@wjgnet.com

ELSEVIER

World J Gastroenterol 2005;11(20):3099-3104
World Journal of Gastroenterology ISSN 1007-9327

• *CLINICAL RESEARCH* •

MELD *vs* Child-Pugh and creatinine-modified Child-Pugh score for predicting survival in patients with decompensated cirrhosis

George V. Papatheodoridis, Evangelos Cholongitas, Eleni Dimitriadou, Giota Touloumi, Vassilios Sevastianos, Athanasios J. Archimandritis

George V. Papatheodoridis, Evangelos Cholongitas, Vassilios Sevastianos, Athanasios J. Archimandritis, 2nd Department of Internal Medicine, National University of Athens Medical School, Hippokration General Hospital, Athens, Greece
Eleni Dimitriadou, Giota Touloumi, Department of Epidemiology, National University of Athens Medical School, Athens, Greece
Correspondence to: George V. Papatheodoridis, MD, Assistant Professor in Medicine and Gastroenterology, 2nd Department of Internal Medicine, Medical School of Athens University, Hippokration General Hospital of Athens, 114 Vas. Sophias Ave., 115 27 Athens, Greece. gpapath@cc.uoa.gr
Telephone: +30-210-7774742 Fax: +30-210-7706871
Received: 2004-10-19 Accepted: 2005-01-05

Abstract

AIM: Model of End-stage Liver Disease (MELD) score has recently gained wide acceptance over the old Child-Pugh score in predicting survival in patients with decompensated cirrhosis, although it is more sophisticated. We compared the predictive values of MELD, Child-Pugh and creatinine-modified Child-Pugh scores in decompensated cirrhosis.

METHODS: A cohort of 102 patients with decompensated cirrhosis followed-up for a median of 6 mo was studied. Two types of modified Child–Pugh scores estimated by adding 0-4 points to the original score using creatinine levels as a sixth categorical variable were evaluated.

RESULTS: The areas under the receiver operating characteristic curves did not differ significantly among the four scores, but none had excellent diagnostic accuracy (areas: 0.71-0.79). Child-Pugh score appeared to be the worst, while the accuracy of MELD was almost identical with that of modified Child-Pugh in predicting short-term and slightly better in predicting medium-term survival. In Cox regression analysis, all four scores were significantly associated with survival, while MELD and creatinine-modified Child-Pugh scores had better predictive values (c-statistics: 0.73 and 0.69-0.70) than Child-Pugh score (c-statistics: 0.65). Adjustment for gamma-glutamate transpeptidase levels increased the predictive values of all systems (c-statistics: 0.77-0.81). Analysis of the expected and observed survival curves in patients subgroups according to their prognosis showed that all models fit the data reasonably well with MELD probably discriminating better the subgroups with worse prognosis.

CONCLUSION: MELD compared to the old Child-Pugh and particularly to creatinine-modified Child-Pugh scores does not appear to offer a clear advantage in predicting survival in patients with decompensated cirrhosis in daily clinical practice.

Key words: Child-Pugh; MELD; Cirrhosis; Decompensated cirrhosis

Papatheodoridis GV, Cholongitas E, Dimitriadou E, Touloumi G, Sevastianos V, Archimandritis AJ. MELD *vs* Child-Pugh and creatinine-modified Child-Pugh score for predicting survival in patients with decompensated cirrhosis. *World J Gastroenterol* 2005; 11(20): 3099-3104
http://www.wjgnet.com/1007-9327/11/3099.asp

INTRODUCTION

The poor survival of patients with decompensated cirrhosis has driven physicians to a constant search for good prognostic markers[1,2]. The need for improvement in the accuracy of prognosis in this setting has increased in the current era of the expansion of orthotopic liver transplantation (OLT) and the parallel increasing discrepancy between the numbers of OLT candidates and the numbers of available donor livers[2,3]. Indeed, patients with decompensated cirrhosis who are potential OLT candidates should enter into the transplant waiting lists neither too early nor too late, since early OLTs take away livers from candidates who are very sick and with more urgent indications and late OLTs are associated with worse outcomes[4].

The old Child-Turcotte classification[5] and the subsequently modified Child-Pugh score (CP score)[6] have been the most widely applied prognostic markers in patients with decompensated cirrhosis mainly due to their simplicity for use in daily clinical practice[2,7,8]. The determination of CP score, which may range from 5 to 15, is based on the presence and severity of ascites and hepatic encephalopathy, the prolongation of prothrombin time, and the levels of serum bilirubin and albumin. According to their CP scores, patients are classified into three classes (Child class A, B, and C with CP scores 5-6, 7-9, and 10-15, respectively)[6]. The predictive value of the CP score has been shown in many studies in the past[2,9], but the inclusion of two subjective variables (ascites and encephalopathy) with the inevitable interobserver variation and the need for even better prognosis have prompted the search for more objective and more accurate prognostic markers in this setting[2].

During the last two decades, several scoring systems or prognostic instruments have been proposed for predicting survival in patients with decompensated cirrhosis[10-13], but none gained wide acceptance until the recent development of the Mayo Clinic Model of End-stage Liver Disease (MELD)[2,14,15]. MELD score[16], which was initially developed for predicting survival in patients undergoing transjugular intrahepatic portosystemic shunts (TIPS)[17], has been suggested to provide more accurate prognosis than CP score in patients with decompensated cirrhosis and therefore to improve the estimation of priority for liver grafts allocation[2,16]. MELD score calculation is based on the etiology of cirrhosis and three simple and objective laboratory variables, serum bilirubin, serum creatinine and prothrombin time expressed as international normalized ratio (INR), but it includes logarithmic transformations and multiplication by several factors being substantially more sophisticated than that of the CP score[6,17]. Moreover, it has been suggested that it may be difficult to reconcile clinical impression with MELD score[8]. Recently, a modified CP score taking into account serum creatinine levels was also evaluated in patients undergoing TIPS[18], since renal function in patients with decompensated cirrhosis has been shown to affect post-TIPS or post-transplant survival[19-21] and no renal parameter was included in the original CP score.

The aim of this study was to compare the accuracy of MELD, CP, and modified CP score for predicting short-term and medium-term survival in patients with decompensated cirrhosis.

MATERIALS AND METHODS

We retrospectively studied 102 patients with decompensated cirrhosis, who were admitted to our department between June 1998 and May 2000. Patients with hepatocellular carcinoma, severe primary cardiopulmonary failure or intrinsic kidney disease were excluded, while patients with more than one admission during the study period were evaluated in the analysis only at their first admission.

The diagnosis of decompensated cirrhosis was based on clinical, laboratory, previous histological, and radiological signs of cirrhosis with at least one sign of liver decompensation (ascites, variceal bleeding, hepatic encephalopathy, non-obstructive jaundice). The cause of cirrhosis was considered to be chronic hepatitis B virus infection in cases with long-standing (>6 mo) HBsAg positivity; chronic hepatitis C virus (HCV) infection in cases with detectable both antibodies against HCV (anti-HCV) and serum HCV-RNA; alcohol abuse in cases with a compatible history and absence of other causes of liver injury; primary biliary cirrhosis in cases with elevated alkaline phosphatase, positive antimitochondrial antibodies and/or compatible previous histological findings; primary sclerosing cholangitis in cases with elevated alkaline phosphatase and compatible radiological and/or histological findings.

According to our routine clinical practice, detailed medical history, complete physical examination, and a battery of laboratory tests were performed in all patients with decompensated cirrhosis on the day of admission. Moreover, diagnostic paracentesis and ascitic fluid culture were performed in all admitted cirrhotic patients with ascites. The age, sex, cause of cirrhosis, cause of admission, first and previous complications of decompensated cirrhosis including spontaneous bacterial peritonitis (SBP) as well as complete blood count including platelet count, prothrombin time and INR, serum urea and creatinine, total, and direct bilirubin, alanine aminotransferase (ALT) and aspartate aminotransferase (AST), alkaline phosphatase, gamma-glutamate transpeptidase (GGT), serum albumin and globulins and ascitic fluid characteristics and culture were retrospectively recorded for all patients. In June 2002, the date of last available information as well as the final status (alive, death from liver disease, OLT, and death from liver unrelated causes) were recorded.

Based on the admission data, the CP score (range: 5-15) and Child class were estimated for each patient according to the suggestion by Pugh *et al*[6], while the MELD score (range: 6-40) was calculated according to the formula proposed by Kamath *et al*[16], which was a slight modification of the risk score used in the original TIPS model[17]. In addition, two types of modified CP score (CP score-I and CP score-II) with serum creatinine as a sixth variable were also calculated: CP score-I (range: 5-19) derived from the original CP score by adding 0 points for creatinine <1.3 mg/dL and 4 points for creatinine ≥1.3 mg/dL according to what was reported by Angermayr *et al*[18], while CP score-II (range: 5-19) derived from the original CP score by adding 0 points for creatinine <1.3 mg/dL, 2 points for creatinine 1.3-1.8 mg/dL and 4 points for creatinine >1.8 mg/dL.

Statistical analysis

All data were analyzed using the statistical program STATA. Results were expressed as mean values (SD) or as median values (range). Qualitative variables were compared by corrected χ^2 test and quantitative variables by *t*-test or Wilcoxon signed rank test. The accuracy of the different score systems for predicting short-term survival was evaluated through the urea under the receiver operating characteristic (ROC) curve, whereas the different areas were compared by the non-parametric method proposed by DeLong *et al*[22].

Cox proportional hazards models were used to determine variables associated with overall survival. Multivariate models were constructed to identify independent variables from the score systems factors. For each Cox model, a predictive score was calculated for each patient as: $P=\beta_1X_1+\beta_2X_2+\ldots+\beta_kX_k$, where X_1, X_2,…, X_k are the levels of k prognostic factors and β_1, β_2,…, β_k are the corresponding regression coefficients. Higher predictive scores correspond to poorer prognosis. The accuracy of the different models as predictors of survival was evaluated by the concordance (c)-statistics (equivalent to the area under the ROC curve). Each model was considered to have diagnostic accuracy in case of a c-statistics >0.70 and excellent diagnostic accuracy in case of a c-statistics >0.80.

To assess how well the models fit the data predicted by the models and actual survival curves were graphically compared. For that, patients were ranked according to their predictive score and divided into three groups with roughly equal numbers of patients' deaths in each group. Actual survival curve for each group was calculated using the Kaplan-Meier method.

RESULTS

The patient baseline characteristics are presented in Table 1. During a median follow-up of 16 mo (0.5-42 mo), 19 (19%) of the 102 patients died and another 5 (5%) underwent OLT. No patient died from liver unrelated causes. The 3-, 6-, 12-, and 24-mo survival rates were 91%, 86%, 84%, and 76%, respectively.

Table 1 Baseline characteristics of 102 patients with decompensated cirrhosis

Age (yr)	61 (27-89)
Sex, males	69 (68%)
Cause of cirrhosis	
HBV	24 (23%)
HCV	17 (17%)
Alcohol	39 (38%)
PBC/PSC	7 (7%)
Unknown	15 (15%)
Cause of admission	
Tense ascites	37 (36%)
Encephalopathy	17 (17%)
Variceal bleeding	16 (16%)
Jaundice	5 (5%)
Fever	11 (11%)
Other	16 (16%)
SBP on admission	9 (9%)
First sign of decompensation	
Ascites	66 (65%)
Variceal bleeding	30 (29%)
Encephalopathy	5 (5%)
Jaundice	1 (1%)
Hematocrit (%)	33 (17-48)
Hemoglobin (g/dL)	11 (5-16)
White blood count ($\times 10^9$/L)	5.7 (1.2-23.9)
Platelet count ($\times 10^9$/L)	105 (19-394)
Prothrombin time (s)	16 (11-35)
INR	1.3 (0.9-3.3)
Creatinine (mg/dL)	1.1 (0.5-3.7)
Bilirubin (mg/dL)	2.6 (0.3-33.9)
AST (IU/L)	72 (20-610)
ALT (IU/L)	44 (11-433)
Alkaline phosphatase (U/L)	101 (42-487)
GGT (U/L)	70 (10-1 165)
Albumin (g/dL)	3.2 (1.9-4.3)
Child class	
A	13 (13%)
B	42 (41%)
C	47 (46%)
Child–Pugh score	9 (5-15)
Modified Child–Pugh score-I	10 (5-19)
Modified Child–Pugh score-II	10 (5-17)
MELD score	12 (-10-45)

HBV: hepatitis B virus, HCV: hepatitis C virus, PBC: primary biliary cirrhosis, PSC: primary sclerosing cholangitis, SBP: spontaneous bacterial peritonitis, INR: international normalized ratio, AST: aspartate aminotransferase, ALT: alanine aminotransferase, GGT: gamma-glutamyl-transpeptidase, MELD: Model for End-stage Liver Disease. All quantitative variables are expressed as median values (range).

Predictive models for 3-, 6-, 12-, and 24-mo survival

The ROC curves of all four scoring systems for 3-, 6-, 12-, and 24-mo survival are shown in Figure 1. Comparison of the areas under the ROC curves among the four scoring systems did not reveal any statistical significant difference. All scoring systems were found to have diagnostic accuracy in predicting survival, perhaps with the marginal exception of CP score for predicting 12-mo survival. However, none of the scores had excellent diagnostic accuracy (area >0.80). MELD score appeared to have better predictive accuracy compared to the CP scores. Among the rest of the scores, modified CP-I was associated with better area under the ROC curve than the CP score, whereas modified CP-II score was relatively more accurate in predicting short-term survival than the modified CP-I score. The area under the ROC curve for MELD and CP-II scores were almost identical for 3-mo (0.79 and 0.78) and 6-mo (0.77 and 0.76) survival, while there was a slight decrease in the predictive value of CP-II score during further follow-up. Thus, MELD appear to have a slight advantage in predicting 12- and 24-mo survival (0.78 and 0.79) compared with CP-II score (0.74 and 0.76), which ranked second (Table 2). In general, there was a tendency for decreasing accuracy of the CP scoring systems for predicting longer survival.

Table 2 Comparisons of the areas under the ROC curve of Child-Pugh, modified Child-Pugh-I, modified Child-Pugh-II and MELD scores for 3-, 6-, 12-, and 24-mo survival

Survival (mo)	Predictive scores	Area under ROC	P (χ^2)
3	Child-Pugh	0.73	0.19
	Modified Child-Pugh-I	0.76	0.58
	Modified Child-Pugh-II	0.78	0.73
	MELD	0.79	
6	Child-Pugh	0.71	0.18
	Modified Child-Pugh-I	0.73	0.49
	Modified Child-Pugh-II	0.76	0.85
	MELD	0.77	
12	Child-Pugh	0.68	0.09
	Modified Child-Pugh-I	0.73	0.38
	Modified Child-Pugh-II	0.74	0.51
	MELD	0.78	
24	Child-Pugh	0.70	0.27
	Modified Child-Pugh-I	0.75	0.48
	Modified Child-Pugh-II	0.76	0.64
	MELD	0.79	

P for comparison with MELD score.

Predictive models for overall survival

Univariate analysis using Cox proportional hazards models showed that ascites as first sign of liver decompensation ($P = 0.017$), presence of SBP on admission ($P = 0.010$), serum levels of bilirubin ($P<0.001$), AST ($P = 0.018$), ALT ($P = 0.039$), GGT ($P = 0.019$), and creatinine ($P = 0.002$) were significantly associated with survival (Table 3).

MELD, CP, and modified CP-I and CP-II scores were all significantly associated with survival in univariate analysis. Multivariate Cox regression analysis including all significant baseline characteristics together with each predictive score showed that the only factor that remained consistently statistically significant for all scores was GGT (log-transformed).

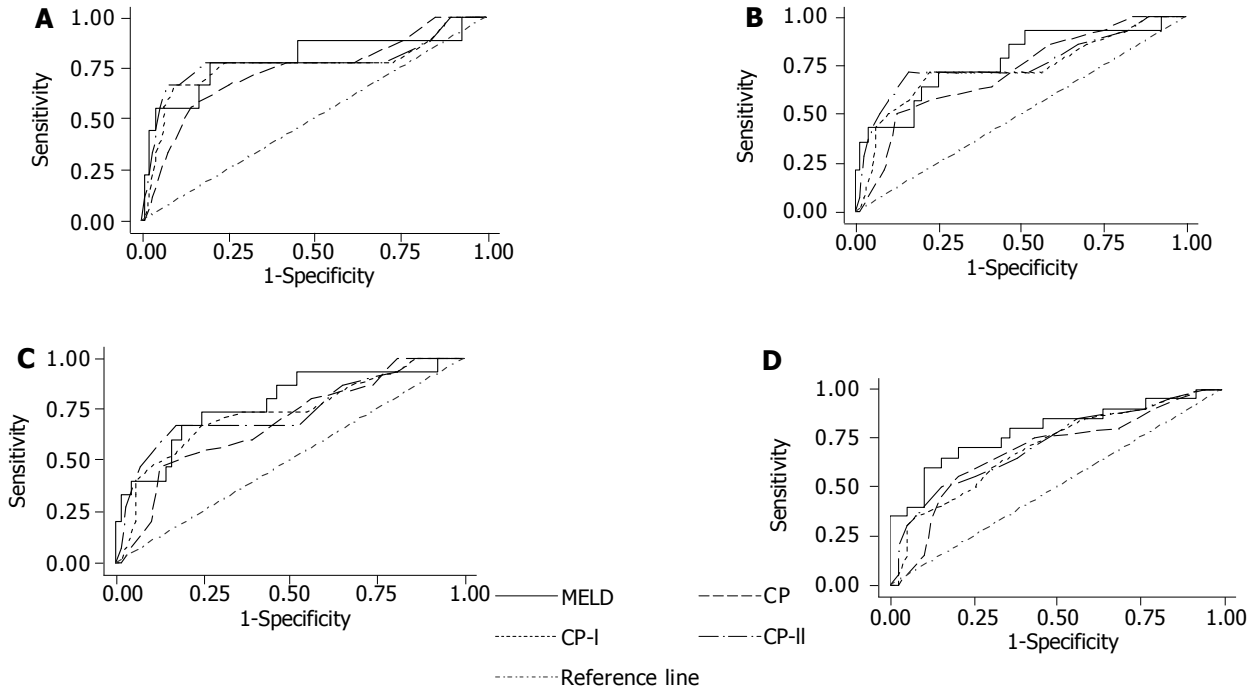

Figure 1 ROC curves of MELD, Child-Pugh (CP), modified Child-Pugh-I (CP-I) and modified Child-Pugh-II (CP-II) score for 3-mo (**A**), 6-mo (**B**), 12-mo (**C**) and 24-mo (**D**) survival.

Table 4 shows the crude and the adjusted for GGT results for all scoring systems as well as the corresponding c-statistics. MELD and modified CP-II scores were again found to have the better predictive value for overall survival than CP score. Including GGT in the model increased substantially the value of the c-statistics.

The expected and observed survival curves for each score in the three patient subgroups divided according to the patient respective predictive degree *P* are shown in Figure 2. The models fit the data reasonably well. MELD score appeared to discriminate better than the rest of the scores the subgroup of patients with the worse prognosis had.

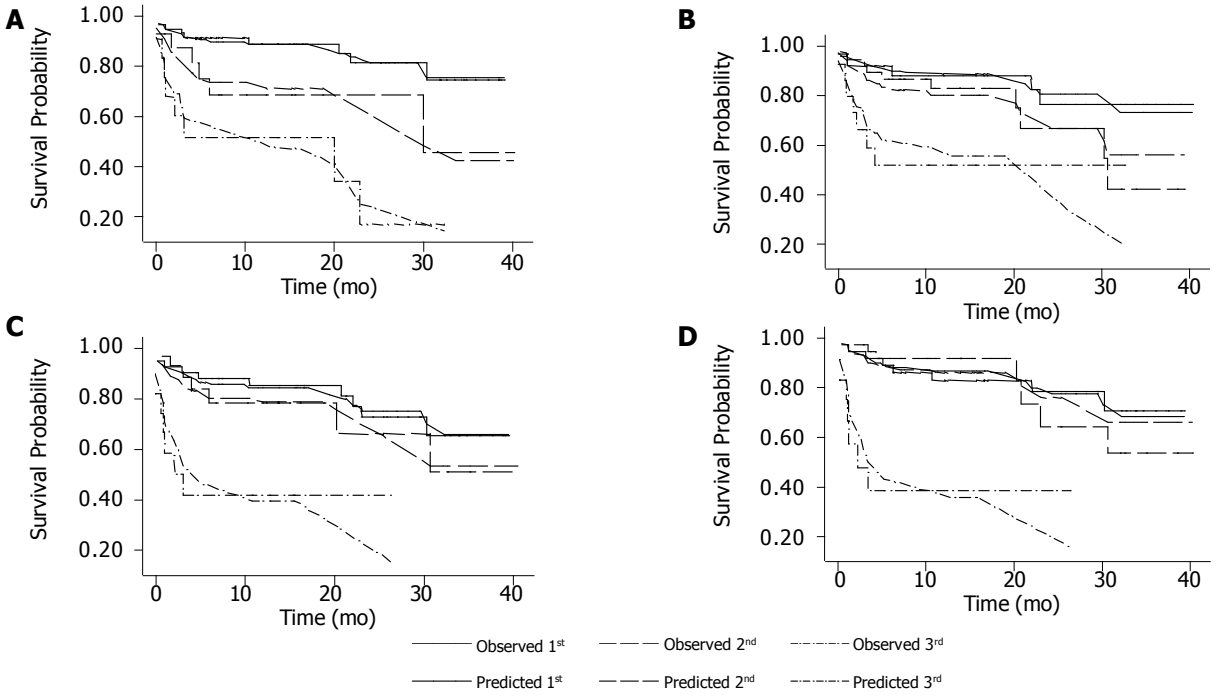

Figure 2 Expected and observed survival curves for MELD (**A**), Child-Pugh (CP) (**B**), modified Child-Pugh-I (CP-I) (**C**) and modified Child-Pugh-II (CP-II) (**D**) score in three patient subgroups (1st, 2nd, 3rd) with roughly equal numbers of patients deaths in each subgroup.

Table 3 Association of baseline characteristics with survival in 102 patients with decompensated cirrhosis (results from univariate Cox proportional hazards models)

Patient characteristic	Hazard ratio	95%CI	*P*
Age (per yr)	0.99	0.90-1.03	0.72
Sex (male)	0.68	0.27-1.72	0.92
Cause of cirrhosis (unknown)			
HBV	0.41	0.12-1.58	0.21
HCV	1.21	0.35-4.17	0.77
Alcohol	0.72	0.27-1.93	0.51
PBC/PSC	0.97	0.47-3.85	0.68
SBP on admission	4.25	1.41-12.84	0.01
White blood count ($\times 10^9$/L)	1.12	0.43-3.68	0.90
Platelet count ($\times 10^9$/L)	1.06	0.52-2.15	0.87
Prothrombin time (s)	2.48	0.50-12.19	0.26
INR	4.22	0.98-18.19	0.052
Creatinine (mg/dL)	4.62	1.76-12.13	0.012
Bilirubin (mg/dL)	2.25	1.5-3.38	<0.001
AST (IU/L)	1.95	1.12-3.4	0.018
ALT (IU/L)	1.70	1.03-2.8	0.039
Alkaline phosphatase (U/L)	0.83	0.38-1.86	0.66
GGT (U/L)	1.64	1.09-2.46	0.019
Albumin (g/dL)	0.53	0.07-3.84	0.53
Child class (A)			
B	2.11	0.46-9.77	0.34
C	3.71	0.78-17.61	0.10

CI: confidence interval, HBV: hepatitis B virus, HCV: hepatitis C virus, PBC: primary biliary cirrhosis, PSC: primary sclerosing cholangitis, SBP: spontaneous bacterial peritonitis, INR: international normalized ratio, AST: aspartate aminotransferase, ALT: alanine aminotransferase, GGT: gamma-glutamyl-transpeptidase, MELD: Model for End-stage Liver Disease. Hazard ratios (95%CI) for quantitative variables are expressed for 1 relevant unit increase of $\log_e$.

DISCUSSION

Although the relatively new MELD score has already been instituted by some transplant programs, such as UNOS, to be the score of choice for stratification of liver transplant candidates on the waiting lists for allocation of donor livers[23], its superiority over the old CP score in predicting actual survival in patients with decompensated cirrhosis has not been documented. MELD score has been proven to be a reliable measure of short-term mortality risk in patients with end-stage liver disease and a suitable marker for allocation of donor livers[16,24], but the results in studies comparing MELD with CP score appear to be unclear. For prediction of survival in patients undergoing TIPS, MELD compared to CP score was found to be superior in the original MELD model study[17] and in a study from Italy[25], slightly superior in a subsequent study from Germany[26] and equally accurate in a study from Austria[19]. In patients with liver cirrhosis, however, both MELD and CP scores have been found to represent equally good predictors of survival without significant differences in the accuracy of their predictive values in all but one study population. Finally, MELD was found to be equivalent to CP score for predicting in-hospital and 12-mo mortality in patients with acute variceal bleeding.

Our data further support that MELD score is not significantly superior to CP score in predicting survival in patients with decompensated liver disease. The c-statistics for prediction of 3-, 6-, 12-, and 24-mo survival by the MELD score ranged from 0.75 to 0.79 being compatible with previous findings in other retrospectively evaluated cohorts of patients with decompensated cirrhosis[16]. Although no significant difference between MELD and CP score was observed in our study, the predictive accuracy of MELD score was always superior offering the greatest benefit in the prediction of 12- and 24-mo survival. The modified CP-I score with the addition of serum creatinine levels as a dichotomous categorical variable (0 points for creatinine <1.3 mg/dL and 4 points for creatinine ⩾1.3 mg/dL) according to what was recently proposed by Angermayr *et al*[18], did not offer a clear benefit over the old CP score (c-statistics: 0.68-0.77 and 0.68-0.73, respectively). In contrast, the modified CP-II score with the addition of serum creatinine levels as a trichotomous categorical variable (0 points for creatinine <1.3 mg/dL, 2 points for creatinine = 1.3-1.8 mg/dL and 4 points for creatinine >1.8 mg/dL) was found to be slightly superior than the CP score, since its c-statistics (0.71-0.78) were always better than those of the CP score and very close to the c-statistics of the MELD score.

If two or more scoring systems offer similar accuracy in predicting survival, then other characteristics should be taken into account for adopting one of them into clinical practice. The main drawbacks of the old CP score are the inclusion of two subjective parameters, such as ascites and encephalopathy, and the estimation of three objective parameters, prothrombin time, serum bilirubin and albumin levels, as categorical variables[6]. Thus, in the CP score, there may be significant interobserver variation in the assessment of the severity of ascites and encephalopathy, which may easily change by medical interventions, while an extended range of values of prothrombin time, bilirubin and albumin levels take the same points even if they may reflect different degrees of liver failure. Moreover, CP score does not take into account the patient's renal function, which appears to be strongly associated with survival[21].

MELD score is undoubtedly more objective than the CP score, since its calculation is based on the etiology of cirrhosis and three simple and reproducible laboratory parameters, INR, serum creatinine and bilirubin levels[16]. Moreover, the dynamic nature of MELD score, which is expressed within a continuous scale of 34 points taking into account the exact value of its laboratory parameters, offers

Table 4 Crude and adjusted for GGT hazard ratio (HR) of death and 95%CI for the four scoring systems

Scoring system	Unadjusted		Adjusted	
	HR (95%CI)	c-statisticsHR	(95%CI)	c-statistics
Child-Pugh score	1.23 (1.04-1.45)	0.65	1.38 (1.14-1.68)	0.77
Modified Child-Pugh-I score	1.21 (1.09-1.36)	0.69	1.30 (1.13-1.50)	0.79
Modified Child-Pugh-II score	1.30 (1.13-1.48)	0.70	1.38 (1.18-1.62)	0.78
MELD score	1.11 (1.06-1.15)	0.73	1.10 (1.06-1.15)	0.81

MELD: Model for End-stage Liver Disease. HR (95%CI) are expressed for 1 unit increase.

an advantage in the determination of priorities of liver organs allocation[2,8]. On the other hand, MELD score cannot be calculated at the bedside and is much more complex than the easy to calculate CP score, since it includes logarithmic transformations and multiplication by several factors[16]. In addition, changes in several parameters of the MELD score may not be directly related to changes of the severity of liver disease, such as a creatinine increase due to extensive use of diuretics or other iatrogenic factors. Finally, it has been suggested that MELD score may underestimate the severity of liver disease in patients with decompensated cirrhosis and predominant complications of portal hypertension, since it does not include any parameter related to portal hypertension[8].

In conclusion, both MELD and CP score can accurately predict short-term (3- and 6-mo) survival in patients with decompensated cirrhosis, while MELD appears to have a slight advantage in predicting medium-term (12- and 24-mo) survival. The modified CP score with the addition of serum creatinine as a categorical parameter was found to improve the predictive accuracy of CP score being equivalent with the MELD score in predicting short- and medium-term survival. Thus, the creatinine-modified Child-Pugh scores seem to deserve further evaluation, since they are simpler than and of similar predictive accuracy with the MELD score and have higher predictive accuracy than the old Child-Pugh score. Taking into consideration the drawbacks of the MELD and CP scoring systems, we do not see a clear advantage in daily clinical practice for MELD score over the familiar and more easily calculated CP score or creatinine-modified CP score for predicting survival in patients with decompensated cirrhosis. Perhaps, the situation is different in the liver transplant waiting lists, since the dynamic range of the MELD score may allow better determination of priorities for organ allocation.

REFERENCES

1 **D'Amico G,** Morabito A, Pagliaro L, Marubini E. Survival and prognostic indicators in compensated and decompensated cirrhosis. *Dig Dis Sci* 1986; **31**: 468-475
2 **Forman LM,** Lucey MR. Predicting the prognosis of chronic liver disease: an evolution from child to MELD. Mayo End-stage Liver Disease. *Hepatology* 2001; **33**: 473-475
3 **Lucey MR,** Brown KA, Everson GT, Fung JJ, Gish R, Keeffe EB, Kneteman NM, Lake JR, Martin P, McDiarmid SV, Rakela J, Shiffman ML, So SK, Wiesner RH. Minimal criteria for placement of adults on the liver transplant waiting list: a report of a national conference organized by the American Society of Transplant Physicians and the American Association for the Study of Liver Diseases. *Liver Transpl Surg* 1997; **3**: 628-637
4 **Freeman RB Jr,** Edwards EB. Liver transplant waiting time does not correlate with waiting list mortality: implications for liver allocation policy. *Liver Transpl* 2000; **6**: 543-552
5 **Child CG3,** Turcotte JG. Surgery and portal hypertension. In: Child CG3, ed. The Liver and Portal Hypertension. *Philadelphia: Saunders* 1964: 1-85
6 **Pugh RN,** Murray-Lyon IM, Dawson JL, Pietroni MC, Williams R. Transection of the oesophagus for bleeding oesophageal varices. *Br J Surg* 1973; **60**: 646-649
7 **Conn HO.** A peek at the Child-Turcotte classification. *Hepatology* 1981; **1**: 673-676
8 **Reuben A.** Child comes of age. *Hepatology* 2002; **35**: 244-245
9 **Infante-Rivard C,** Esnaola S, Villeneuve JP. Clinical and statistical validity of conventional prognostic factors in predicting short-term survival among cirrhotics. *Hepatology* 1987; **7**: 660-664
10 **Schlichting P,** Christensen E, Andersen PK, Fauerholdt L, Juhl E, Poulsen H, Tygstrup N. Prognostic factors in cirrhosis identified by Cox's regression model. *Hepatology* 1983; **3**: 889-895
11 **Villeneuve JP,** Infante-Rivard C, Ampelas M, Pomier-Layrargues G, Huet PM, Marleau D. Prognostic value of the aminopyrine breath test in cirrhotic patients. *Hepatology* 1986; **6**: 928-931
12 **Adler M,** Verset D, Bouhdid H, Bourgeois N, Gulbis B, Le Moine O, Van de Stadt J, Gelin M, Thiry P. Prognostic evaluation of patients with parenchymal cirrhosis. Proposal of a new simple score. *J Hepatol* 1997; **26**: 642-649
13 **Cooper GS,** Bellamy P, Dawson NV, Desbiens N, Fulkerson WJ, Goldman L, Quinn LM, Speroff T, Landefeld CS. A prognostic model for patients with end-stage liver disease. *Gastroenterology* 1997; **113**: 1278-1288
14 **Wiesner RH,** McDiarmid SV, Kamath PS, Edwards EB, Malinchoc M, Kremers WK, Krom RA, Kim WR. MELD and PELD: application of survival models to liver allocation. *Liver Transpl* 2001; **7**: 567-580
15 **McCaughan GW,** Strasser SI. To MELD or not to MELD? *Hepatology* 2001; **34**: 215-216
16 **Kamath PS,** Wiesner RH, Malinchoc M, Kremers W, Therneau TM, Kosberg CL, D'Amico G, Dickson ER, Kim WR. A model to predict survival in patients with end-stage liver disease. *Hepatology* 2001; **33**: 464-470
17 **Malinchoc M,** Kamath PS, Gordon FD, Peine CJ, Rank J, ter Borg PC. A model to predict poor survival in patients undergoing transjugular intrahepatic portosystemic shunts. *Hepatology* 2000; **31**: 864-871
18 **Angermayr B,** Koenig F, Cejna M, Karnel F, Gschwantler M, Ferenci P, Gangl A, Peck-Radosavljevic M. Creatinine-modifies Child-Pugh score (CPSC) compared with MELD-score to predict survival in patients undergoing TIPS. *Hepatology* 2002; **36**: 378A
19 **Angermayr B,** Cejna M, Karnel F, Gschwantler M, Koenig F, Pidlich J, Mendel H, Pichler L, Wichlas M, Kreil A, Schmid M, Ferlitsch A, Lipinski E, Brunner H, Lammer J, Ferenci P, Gangl A, Peck-Radosavljevic M. Child-Pugh versus MELD score in predicting survival in patients undergoing transjugular intrahepatic portosystemic shunt. *Gut* 2003; **52**: 879-885
20 **Moreau R,** Lebrec D. Acute renal failure in patients with cirrhosis: perspectives in the age of MELD. *Hepatology* 2003; **37**: 233-243
21 **Nair S,** Verma S, Thuluvath PJ. Pretransplant renal function predicts survival in patients undergoing orthotopic liver transplantation. *Hepatology* 2002; **35**: 1179-1185
22 **DeLong ER,** DeLong DM, Clarke-Pearson DL. Comparing the areas under two or more correlated receiver operating characteristic curves: a nonparametric approach. *Biometrics* 1988; **44**: 837-845
23 **Everson GT.** MELD: the answer or just more questions? *Gastroenterology* 2003; **124**: 251-254
24 **Wiesner R,** Edwards E, Freeman R, Harper A, Kim R, Kamath P, Kremers W, Lake J, Howard T, Merion RM, Wolfe RA, Krom R. Model for end-stage liver disease (MELD) and allocation of donor livers. *Gastroenterology* 2003; **124**: 91-96
25 **Salerno F,** Merli M, Cazzaniga M, Valeriano V, Rossi P, Lovaria A, Meregaglia D, Nicolini A, Lubatti L, Riggio O. MELD score is better than Child-Pugh score in predicting 3-month survival of patients undergoing transjugular intrahepatic portosystemic shunt. *J Hepatol* 2002; **36**: 494-500
26 **Schepke M,** Roth F, Fimmers R, Brensing KA, Sudhop T, Schild HH, Sauerbruch T. Comparison of MELD, Child-Pugh, and Emory model for the prediction of survival in patients undergoing transjugular intrahepatic portosystemic shunting. *Am J Gastroenterol* 2003; **98**: 1167-1174

Science Editor Guo SY **Language Editor** Elsevier HK

PO Box 2345, Beijing 100023, China
www.wjgnet.com
wjg@wjgnet.com

ELSEVIER

World J Gastroenterol 2005;11(20):3105-3111
World Journal of Gastroenterology ISSN 1007-9327

• *CLINICAL RESEARCH* •

Oral immune regulation using colitis extracted proteins for treatment of Crohn's disease: Results of a phase I clinical trial

Eran Israeli, Eran Goldin, Oren Shibolet, Athalia Klein, Nilla Hemed, Dean Engelhardt, Elazar Rabbani, Yaron Ilan

Eran Israeli, Eran Goldin, Oren Shibolet, Athalia Klein, Nilla Hemed, Yaron Ilan, Gastroenterology and Liver Units, Department of Medicine, Hebrew University-Hadassah Medical Center, Jerusalem, Israel
Dean Engelhardt, Elazar Rabbani, Enzo Biochem, New York, NY, USA
Supported by the Enzo Therapeutics Inc., NY, USA
Correspondence to: Yaron Ilan, MD, Liver Unit, Department of Medicine, Hadassah University Hospital, POB 12000, Jerusalem IL-91120, Israel. ilan@hadassah.org.il
Telephone: +972-2-6777816 Fax: +972-2-6431021
Received: 2003-12-28 Accepted: 2004-02-12

Abstract

AIM: To evaluate safety and possible efficacy of induction of oral immune regulation using colitis extracted proteins (CEP) in Crohn's disease (CD) subjects.

METHODS: Ten CDs were treated orally with autologous CEP thrice weekly for 16 wk. Subjects were monitored for CDAI and IBDQ. Immune modulatory effect was assessed by T-lymphocyte FACS analysis, CEP-specific IFNγ ELISPOT assay and cytokine levels.

RESULTS: Induction of oral immune regulation significantly ameliorated disease activity. All (10/10) subjects had clinical response (CDAI $\leqslant$ 70) and 7/10 achieved clinical remission (CDAI $\leqslant$ 150). Significant increase in mean IBDQ score was noted (134±9 *vs* 164±12). No treatment-related adverse events were noted. High levels of CEP-specific IFNγ spot forming colonies were detected in five subjects prior to treatment and in all five, a marked decrease was observed. The CD4+/CD8+ lymphocyte ratio and peripheral NKT cell numbers increased significantly, in 7/10 and in 5/10 subjects, respectively. Significant increase in serum IL-10 and IL-4 levels was observed in 7/10 subjects during treatment period.

CONCLUSION: Immune regulation via oral administration of CEP is a safe and possibly effective treatment for subjects with moderate CD and may provide means of antigen-specific immune modulation.

Key words: Crohn's disease; Colitis extracted proteins

Israeli E, Goldin E, Shibolet O, Klein A, Hemed N, Engelhardt D, Rabbani E, Ilan Y. Oral immune regulation using colitis extracted proteins for treatment of Crohn's disease: Results of a phase I clinical trial. *World J Gastroenterol* 2005; 11(20): 3105-3111
http://www.wjgnet.com/1007-9327/11/3105.asp

INTRODUCTION

Crohn's disease (CD) is an immune mediated disorder. Both an appropriate response to an injurious, exogenous agent, or abnormal host responses to ubiquitous agents were suggested to play a role in the pathogenesis of the disease[1,2]. Abnormalities of T-cell-mediated immunity, including cutaneous anergy, and changes in T-cell subsets were described in these patients[1]. In addition, patients with CD have antibodies against components of colon cells and several different bacterial antigens. Changes in mucosal-cell-mediated immunity were identified, including alterations in mucosal T-cell subsets and concentrations of mucosal IgG cells, suggesting chronic antigen stimulation. Exposure of target antigens after infectious, immune, or toxic damage leads to activation of mucosal immune cells, resulting in cytokines that lead to mucosal inflammatory response[3-5]. An imbalance between Th1-pro-inflammatory and Th2-anti-inflammatory subtype of immune response plays a role in the pathogenesis of CD[6]. In both experimental colitis and in patients with CD, the disease is a Th1-mediated immune disorder resulting in a life-long inflammatory response against gut epitopes. Anti-inflammatory cytokines such as IL-10 downregulate the pro-inflammatory effects of Th1-mediated cytokines, thereby alleviating the disease[7-11].

Current treatments of CD, similar to that of other immune-mediated disorders, require overcoming the immune response towards disease-associated target antigens[12]. This involves systemic immunosuppression. New modes of immune modulatory treatments are not antigen specific, and therefore are either not effective in a large number of patients, or associated with unwanted side effects[12].

Oral immune regulation is a recognized procedure alteration of the host immune response towards orally administered antigens[13-15]. It was previously shown effective in preventing immune-mediated disorders in animal models[16-20]. This method was also tested in humans with various immune-mediated disorders[21]. Recently it has been shown by us and others that oral immune regulation can be used to alleviate experimental colitis in a model system using mice treated with 2,4,6-trinitrobenzene sulfonic acid (TNBS)[9,22-26]. TNBS induces an autoimmune response resembling CD in humans[22]. Oral administration of low doses of colitis-extracted proteins to mice with experimental colitis significantly decreased the inflammatory response.

The aims of the present study were to determine the safety and tolerability of oral administration of autologous colonic mucosal cells from CD patients, and to determine the efficacy of this mode of treatment in patients with CD. The effects of oral immune regulation towards colonic

proteins on the immune system were studied. The results show that immune regulation via oral administration of proteins extracted from colonic mucosa was a safe and possibly an effective treatment for subjects with moderate to severe CD.

MATERIALS AND METHODS

Patients

Patient population One group of 10 patients was followed up in an open-labeled, non-randomized, one-center prospective trial. All experiments were carried out in accordance with the guidelines of the Hebrew-University-Hadassah Institutional Committee for Human Clinical Trials and Good Clinical Practice regulations. The Israel Ministry of Health Committee for Human Trials approved all experiments.

Inclusion criteria Eligible participants (men and women >18 years) signed a written informed consent. The diagnosis of CD with clinical evidence of active (symptomatic) disease was based on clinical history, blood tests and/or histology, or X-ray, or endoscopy, with a CDAI score >200 and <350. Subjects receiving oral steroid therapy were requested to have received a dose equivalent to or <25 mg of prednisone per day, and to have been on a stable dose for 2 wk prior to their first visit.

Exclusion criteria Subjects who had undergone bowel surgery within the last 3 mo; subjects who had a prior colostomy, ileostomy, or colectomy with ileorectal anastomosis; subjects likely to require emergency surgery for persistent intestinal obstruction, bowel perforation, uncontrolled bleeding or abdominal abscess or infection, toxic megacolon; subjects whose symptoms were believed to be largely due to the presence of fibrotic strictures; subjects with other infectious or neoplastic diseases of the bowel; subjects with an acute infectious disease; subjects receiving oral prednisone at a dose of >25 mg/d (or equivalent); subjects who were receiving an elemental diet or parenteral nutrition; subjects who were receiving immunosuppressive drugs such as azathioprine or 6-mercaptopurine; subjects who had either received methotrexate or cyclosporine or anti-TNFα or who had participated in another clinical trial within the last 3 mo; subjects with a history of major psychiatric disturbance, or who were drug or alcohol abusers; subjects with a history of GI tract malignancy or IBD-associated malignant changes in the intestine; subjects with a history of coagulopathy; women with child-bearing potential unless surgically sterile or using adequate contraception (either IUD, oral or depot contraceptive, or barrier plus spermicide); pregnant or breastfeeding mothers were excluded from the study.

Oral antigen preparation and administration Subjects who fulfilled the inclusion/exclusion criteria for participation in the study were scheduled for a colonoscopy during which time colon biopsies were taken from the subject for preparation of the colon-specific protein (study drug). The containing extract was prepared according to Enzo Therapeutics, Inc., Specification Number L0060-00-0109, "Preparation of Autologous Colon-Specific Antigen for Oral Immune Regulation for IBD: Crohn's Disease". Additional tissue samples were used for pathological analysis. Preliminary tests showed that each intestinal biopsy yielded approximately 300 μg protein. Thus, six biopsies produced approximately 1 800 μg protein, which provided a supply of protein for the entire study. The administered dose based on previous studies in human subjects was between 18 and 30 μg/dose. Protein extract was divided into 50 doses in 5 mL of normal saline and stored at a temperature of -70 ℃. All subjects were fed with antigen extracted from their own intestinal mucosa. A 2-wk supply was given to the subject who at each visit was instructed to maintain the vials in a refrigerator at home. Each subject ingested 3 doses per week for 16 wk, a total of 48 doses. Two of the five milliliters of vial doses were kept as retained.

Clinical and laboratory follow-up Study individuals were monitored with a variety of safety, biologic and efficacy parameters during the baseline, feeding, and post-feeding periods. The safety parameters included general clinical safety parameters to monitor the individual's overall status as well as specific organ systems, and antigen-specific parameters relevant to the administration of the study drugs.

Safety and tolerability of oral administration of the study drugs were determined by evaluation of clinical parameters as detailed by the subject in his/her diary entries; by biweekly physical examinations and medical history, and biweekly laboratory evaluations. A designated physician involved in the study was accountable for interim history, vital signs, body weight, adverse event assessment and physical examination. Complete blood counts (CBC), sedimentation rate (ESR) and standard chemistries (SMA) were performed every 2 wk throughout the study. Evaluation of the effect of oral administration of the study drug on amelioration of the immune-mediated intestinal and extraintestinal injury in subjects with CD was assessed by following the biweekly CDAI score. IBDQ was evaluated at baseline and at the end of treatment period (16 wk). Response was determined if any of the following occurred: a decrease in CDAI score from time 0 by 70 points, or a decrease to a level ⩽150 points, which defines clinical remission.

Evaluation of the ability to induce immune regulation by oral administration of the study drug was assessed by monthly serum cytokine levels, and by analysis of T-cell subpopulations biweekly, as described below. IFNγ ELISPOT assay was performed at wk 0 and 32.

Flow cytometry analysis for determination of the effect of oral immune regulation on CD4, CD8, NKT, CD3+/45RA, CD3+/45RO, CD19+/45RA, CD25+/45RO, CD4+/45RO, CD8+/45RO, CD44+/45RO, and CD16+/56+ lymphocytes in peripheral blood Blood samples were collected throughout the study period. Immediately after lymphocyte isolation, duplicates of 2-5×10^4 cells/500 μL PBS were deposited into Falcon 2052 tubes incubated with 4 mL of 1% BSA for 10 min, and centrifuged at 1 400 r/min for 5 min. Cells were resuspended in 10 μL FCS with 1:20 FITC-antihuman CD4, CD8, NKT, CD3+/45RA, CD19+/45RA, CD25+/45RO, CD3+/45RO, CD4+/45RO, CD8+/45RO, CD44+/45RO, or CD16+/56+ antibodies (Pharmingen, and R&D, USA), and mixed every 10 min for 30 min. Cells were washed twice in 1% BSA, 0.5 mL 1% paraformaldehyde was added, and kept at 4 ℃ until reading. For the control group, only 5 μL of 1% BSA was added. Analytical cell sorting was performed on 1×10^4

cells from each group with a fluorescence-activated cell sorter (FACSTAR plus, Becton Dickinson). Only live cells were counted and background fluorescence from non-antibody-treated lymphocytes was deducted from levels obtained.

IFNγ ELISPOT assays IFNγ spot forming cells (SFC) were determined using a colitis extracted protein (CEP)-specific ELISPOT assay (Mabtech, Nacka, Sweden) as described with the following modifications[27]. In brief, 96-well filtration plates coated with high protein binding hydrophobic PVDF membrane (polyvinylidene disulfide) were used (Millipore Corp., Bedford, MA, USA). Plates were coated with 1-D1K anti-IFNγ coating antibody (15 mg/mL, Mabtech) for 24 h at 4 ℃. Peripheral blood mononuclear cells (PBMCs) were isolated by Ficoll gradient separation from 20 mL blood samples, collected in acid citrate dextrose tubes, and processed within 1 h. PBMCs were washed twice in RPMI 1640 with 10% fetal calf serum. Cells were cultured in 96-well plates (1×10^5 cells/well) with RPMI 1640 and 10% FCS. Three triplicates were prepared with CEP from each patient (50 μg/mL), phytohemagglutinin (PHA, 2.5 μg/mL), or RPMI without antigen. Plates were incubated for 48 h at 37 ℃ and 50 mL/L CO_2. Following washing, dilute biotinylated antibodies (7-B6-1-biotin, Mabtech) were added in filtered PBS with 0.5% FCS to 1 μg/mL, in a total volume of 100 μL/well. Plates were incubated for 3 h at room temperature. Following washing, 100 mL of streptavidin-alkaline phosphatase was added, and plates were incubated for 90 min at room temperature. After washing, a substrate was added (BCIP/NBT, BioRad, Richmond, USA) for 30 min until dark red purple spots emerged. Using a dissection microscope, two independent investigators counted dark spots, reflecting IFNγ-secreting clones. Results are expressed as means of triplicate IFNγ-secreting cells per 10^5 PBMCs, after subtracting the mean spots from wells without viral antigens.

IFNγ and IL-4 serum levels IL-4, IL-10, and IFNγ serum levels were measured by a "sandwich" ELISA, using Genzyme Diagnostics kits (Genzyme Diagnostics, MA, USA) according to the manufacturer's instructions.

Statistical analysis

Summary statistics by time point of all clinical and laboratory variables were calculated, and statistical significance of changes from baseline was assessed by Student's *t*-test at each time point.

RESULTS

Patient characteristics

One group of 10 patients was studied. They included six males and four females with a mean age of 37 years (range 19-59 years). Mean duration of disease was 11 years (range 2-37 years). Disease site was the ileum in six patients, the ileocolon in two patients, and the colon in two patients. Two patients underwent prior intestinal resection; two suffered from fistulae. Concomitant medications: Five patients were treated with 5-ASA and five were treated with corticosteroids. Steroid treatment was discontinued in two patients and significantly reduced in one patient throughout the study period.

Effect of oral immune regulation towards autologous colitis extracted proteins on CDAI score

Administration of the study drug significantly ameliorated disease activity. During the course of treatment, 10/10 subjects had a clinical response (CDAI decrease of at least 70 points), and 7/10 subjects achieved clinical remission (CDAI ⩽ 150). Median time to response was 5 wk (Figures 1A and B). The median decrease of CDAI was -102 points in 6 wk (from 264 to 162 points, $P = 0.003$), and -129 points in 14 wk (135 points, $P = 0.0001$). At the end of the non-treatment 16-wk follow-up period, CDAI score increased to 206 points.

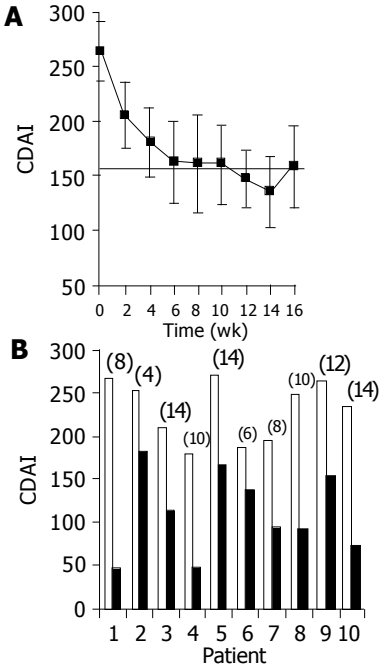

Figure 1 Effect of the study drug on CDAI score. **A**: mean±SE CDAI scores over time during the treatment period; **B**: CDAI scores of individual patients: Baseline score (wk 0, open bars) as compared with score at time of maximal decrease (black bars, no. of week appears for each patient in parenthesis above bar).

Effect of oral immune regulation towards autologous colitis extracted proteins on IBDQ score

Administration of the study drug significantly ameliorated disease activity as measured by IBDQ score. A significant increase in mean IBDQ score was noted at wk 16 as compared to baseline (134±9 *vs* 164±12, $P<0.05$, Figures 2A and B).

Effect of oral immune regulation towards autologous colitis extracted proteins on subpopulations of T lymphocytes

Administration of the study drug significantly induced a significant increase in the CD4+/CD8+ lymphocyte ratio, in 7/10 subjects (Figure 3). The peripheral NKT cell number increased significantly in 5/10 subjects (Figure 4). A significant increase in the CD3+/45RA (Figure 5), CD19+/45RA (Figure 6), and CD25+/45RO (Figure 7) lymphocytes was noted in the majority of treated subjects (Figure 5). No major changes occurred in CD3+/45RO, CD4+/45RO, CD8+/45RO, CD44+/45RO, and CD16+/56+ lymphocytes subpopulations.

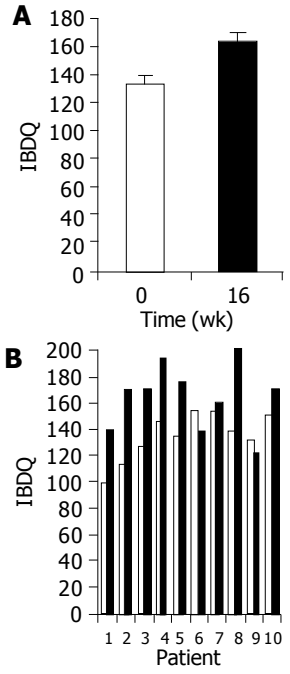

Figure 2 Effect of the study drug on IBDQ scores. **A**: Mean IBDQ scores (±SE) at baseline (wk 0, open bars) as compared to end of treatment (wk 16, black bars); **B**: IBDQ score of individual patients at baseline as compared to wk 16.

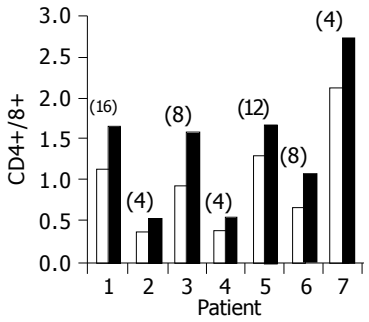

Figure 3 Peripheral $CD4^+/CD8^+$ lymphocyte ratio in 7/10 patients in whom a significant increase was observed. Baseline ratio (open bars) as compared to level of maximal increase (black bars, no. of week shown in parenthesis above each bar).

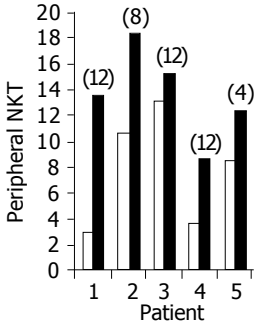

Figure 4 Peripheral NKT lymphocyte percent in 5/10 patients in whom a significant increase was observed during treatment. Baseline ratio (open bars) as compared to level of maximal increase (black bars, no. of week shown in parenthesis above each bar).

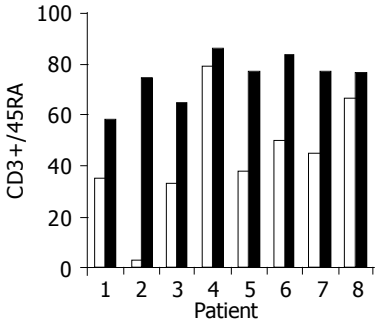

Figure 5 Peripheral $CD3^+$/45RA lymphocyte ratio in 8/10 patients in whom a significant increase was observed during treatment. Baseline ratio (open bars) as compared to level of maximal increase (black bars).

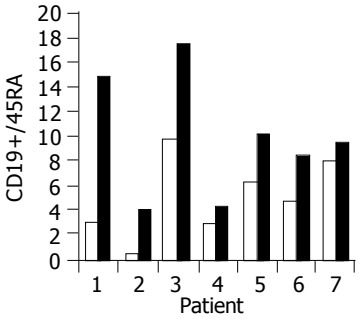

Figure 6 Peripheral $CD19^+$/45RA lymphocyte ratio in 7/10 patients in whom a significant increase was observed during treatment. Baseline ratio (open bars) as compared to level of maximal increase (black bars).

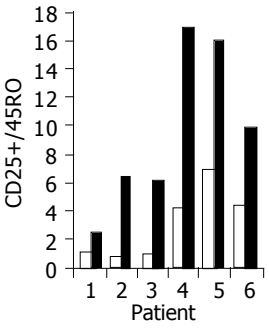

Figure 7 Peripheral $CD25^+$/45RO lymphocyte ratio in 6/10 patients in whom a significant increase was observed during treatment. Baseline ratio (open bars) as compared to level of maximal increase (black bars).

Effect of oral immune regulation towards autologous colitis extracted proteins on antigen specific IFNγ-producing T cell clones

The antigen-specific effect of oral immune regulation on IFNγ SFC was determined using a CEP-specific ELISPOT assay. In five patients, positive T-cell clones were detected prior to oral protein administration. In all five, a significant decrease in the number of IFN-positive SFC was noted (0.2-3.6 to 0-0.2 SFC).

Effect of oral immune regulation towards autologous colitis extracted proteins on serum cytokine levels

A significant increase in IL-4 (from 0.17±0.1 to 0.63±0.15

pg/mL, $P<0.05$), and IL-10 (from 1.7±0.61 to 3.5±1.02 pg/mL, $P<0.05$) serum levels was observed in 7/10 subjects during treatment period (Figures 8 and 9). No significant changes in serum IFNγ levels were observed.

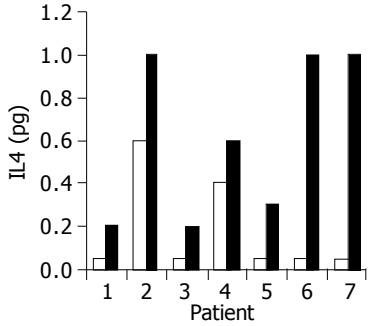

Figure 8 Effect of the study drug on serum IL-4 levels in 7/10 patients in whom a significant increase was observed during treatment. Baseline ratio (open bars) as compared to level of maximal increase (black bars).

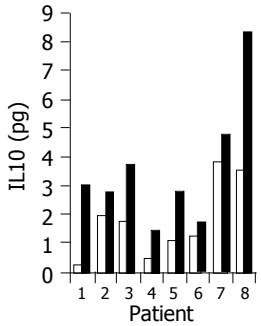

Figure 9 Effect of the study drug on serum IL-10 levels in 8/10 patients in whom a significant increase was observed during treatment. Baseline ratio (open bars) as compared to level of maximal increase (black bars).

Safety measures

Treatment was well tolerated by all patients. All 10 patients completed the study and no major treatment-related adverse reactions were noted. A physician followed up the interim history, vital signs, body weight, adverse event assessment and performed a physical examination. CBC, ESR and standard chemistries (SMA) were performed every 2 wk throughout the study. No major treatment-related adverse events were reported or observed in any of the treated patients during the feeding and follow-up periods. No major changes in any of the extraintestinal systems monitored were reported in any of the patients.

DISCUSSION

The results of the present study suggest that induction of oral immune regulation via oral administration of an autologous colon-specific protein-containing extract is a safe and could possibly be an effective treatment for subjects with mild to moderate CD. Induction of oral immune regulation towards CEP appeared to significantly ameliorate disease activity. During the course of treatment period, 10/10 subjects had a favorable clinical response (CDAI≤70), and 7/10 subjects achieved clinical remission (CDAI≤150). Median time to response was 5 wk. A significant increase in mean IBDQ score was noted at wk 16 as compared to baseline. No treatment-related adverse events were noted in any of the subjects.

The data of the present study provide a clue to the mechanism associated with the clinical effects. High levels of CEP-specific IFNγ spot forming colonies were detected in five subjects prior to treatment. In all five, a marked decrease was observed. A significant increase in IL-10 and IL-4 serum levels was observed in 7/10 subjects during the treatment period. These results suggest that immune regulation by the study drug could alter bowel-associated antigen-specific immunity, and may induce a systemic Th1 to Th2 immune shift.

Successful treatment of IBD, similar to that of other immune-mediated disorders, requires mitigation of the immune response towards disease-associated target antigens. This involves generalized immunosuppression, which may bring undesirable side effects[1,12]. Several new immunomodulatory treatments were tested in patients with IBD over the last few years. These treatments are all non-antigen specific[12]. This lack of disease-associated antigens' specificity may explain the relatively low response rate, as well as the relatively high levels of unwanted side effects. In contrary, induction of antigen-specific oral immune regulation towards autologous colon specific protein-containing extracts could potentially enable long-term alleviation of the disease, while leaving the general immunological defense of the recipient intact[9,22-26]. In addition, as all of the new immune modulatory agents involve systemic immune suppression, their long-term effects are yet to be tested. On the contrary, antigen-specific oral immune regulation is unlikely to have long-term effects in other systems.

Induction of oral immune regulation has been used to alleviate several immune-mediated disorders in animals, including collagen-induced arthritis, experimental colitis, chronic graft *vs* host disease, and experimental encephalomyelitis[13-20]. We have previously shown that oral immune regulation towards adenoviral antigens can abrogate the humoral and cellular components of the anti-viral immunity[18,27]. It was also shown that oral administration of low-dose HBV-envelope proteins (BioHepB) induced peripheral humoral immune tolerance towards HBV epitopes in naive animals. In addition, tolerance induction downregulated any pre-existing anti-HBV immune response, and inhibited anti-HBs antibody production in mice with secondary anti-viral immunity[27]. This mode of treatment was tested in patients with rheumatoid arthritis, autoimmune uveitis, type I diabetes mellitus, and multiple sclerosis[21,28-31]. We have recently shown that this method is effective in patients with chronic HBV infection[32]. The results of these studies showed that HBV-specific T-cell immune modulation can be elicited via oral administration of HBV envelope proteins to chronically infected individuals. In the experimental colitis model, induction of oral immune regulation was shown by several groups to alleviate the disease[22]. This response was associated with a reverse of the cytokine secretion paradigm with increased secretion of IL-4 and decreased secretion of IFNγ. Adoptive transfer of tolerance by transplantation of immune cells from orally-tolerized donors to sublethally

irradiated recipients supports the existence of suppressor cells in this setting[22].

As the intestinal damage in CD patients results mostly from the host immune response, two explanations may elucidate these results, the first being the principle of induction of immune tolerization. Oral immune regulation towards colitis proteins may have altered the immune deviation, thereby removing a deleterious T-cell population (such as those that secrete IFNγ), thus uncovering a more efficacious sub-dominant response (secreting anti-inflammatory cytokines such as IL-4 and IL-10). The second possible explanation is induction of immunity. Oral immune regulation may have enhanced the effect of a beneficial subset of T cells towards the fed antigens in these patients, or of a regulatory subtype of T lymphocytes that reintroduce the required immunological balance in this setting. Correction of an immunological imbalance can lead to an enhanced effect on the part of T-cell subtypes, rather than a clearance or irreversible suppression of "unwanted" T cells. It is possible that simultaneous downregulation of one subset of T cells and augmentation of another occurs. Similar approaches were recently described towards *Schistosoma mansoni* and HBV infections, in which the immune response was responsible for the disease[32,33]. Inherent in this concept is the understanding that pathology is not essential for the development of a protective response. As it is not always possible to separate pathology from "excessive" immune protection, it might not always be possible to determine the role of different antigens and/or subsets of T cells in the induction of each response.

The data of the present study showed a significant increase in the peripheral CD4+/CD8+ lymphocyte ratio in 7/10 patients, and of the peripheral NKT cell numbers in 5/10 subjects. Interestingly, in the experimental colitis model, tolerance induction led to a significant increase in NKT numbers[26,34-36]. The peripheral CD4+/CD8+ ratio increased threefold in tolerized *vs* non-tolerized mice. An opposite effect was observed in the intrahepatic CD4+/CD8+. T lymphocytes expressing NK cell markers (NKT cells) exist in low numbers in the peripheral blood and most other tissues, but are abundant in the liver and bone marrow[37]. They are typified as CD4+ or CD4-CD8- and CD16-, and express $\alpha\beta$ TCR^{int}. Upon *in vivo* and *in vitro* stimulations, they produce large amounts of both IL-4 and IFNγ, exhibit enhanced cytolytic activity, and have a regulatory role in helper T (Th) cell differentiation[38-40]. NKT lymphocytes were shown to play a regulatory role in immune-mediated disorders. Others and we have recently shown that this subset of lymphocytes may have a role in peripheral tolerance induction. Induction of peripheral tolerance via oral administration of an antigen, or FK506 treatment, was associated with significant increases in intrahepatic NKT lymphocyte proportions and cytotoxicity function[36]. Depletion of NKT lymphocytes prevented the Th1 to Th2 immune shift, hindering the ability to induce immune tolerance in experimental colitis[26]. The results of the present study suggest that oral immune regulation induces a systemic immune shift in subpopulations of T cells. However, based on the present data it is difficult to draw conclusions on the exact role of subtypes of T lymphocytes in the pathogenesis of CD, as well as on the regulatory role of NKT cells in this setting.

Application of oral tolerance in some patients with IBD may require the use of surrogate antigens. A similar approach has been used in trials involving patients with multiple sclerosis, diabetes, and rheumatoid arthritis[41-45]. A bystander effect is known to play a role in oral immune regulation[44]. It involves regulatory cells secreting non-antigen-specific cytokines that suppress inflammation in the microenvironment, where the fed antigen is localized. Mucosal Th2/Th3 cells, secreting TGFβ generated by intermittent feeding of a low-dose antigen, may play a role in bystander tolerance[13]. We have previously shown that surrogate antigens derived from normal colonic wall and those derived from other species induced a beneficial effect in experimental colitis[35]. These results suggest that surrogate antigens, related to the disease-target epitopes, may have a similar immune modulating effect. They imply that closely related proteins are being presented and processed by gut-associated lymphoid tissue in a similar way. Both administration of an antigenitically similar epitope, or of an epitope distinct from the disease-target antigen but found in the target organ, can regulate peripheral immune activation. Geographical proximity and/or antigenic similarity to the disease-target antigen may be held responsible for these effects. In the present study, biopsies were taken preferentially from inflamed areas in the colon, or the terminal ileum. In some of the patients, however, biopsies were taken from mucosa of a normal appearance. In both, a clinical effect was noted.

During the periods of follow-up, 5 of the 10 patients experienced a relapse of their symptoms. This loss of effect may be due to the partial effect of oral immune regulation on subtypes of regulatory T lymphocytes in this setting. It may suggest that long-term treatment, and even continuous exposure of the disease-associated antigens, are required in these settings.

In summary, induction of oral immune regulation towards colitis-extracted proteins is a safe and perhaps effective new mode of therapy in patients with mild to moderate CD. This novel method significantly alleviated the disease while altering the antigen-specific immune response. It had no undesirable effects in other systems. As the present study was an open non-randomized trial, large-scale double blind placebo trials would be required in order to evaluate this new mode of treatment for CD patients.

REFERENCES

1 **Podolsky DK**. Inflammatory bowel disease. *N Engl J Med* 2002; **347**: 417-429
2 **Su C**, Lichtenstein GR. Recent developments in inflammatory bowel disease. *Med Clin North Am* 2002; **86**: 1497-1523
3 **Rimm DL**, Holland TE, Morrow JS, Anderson JM. Autoantibodies specific for villin found in patients with colon cancer and other colitides. *Dig Dis Sci* 1995; **40**: 389-395
4 **Hibi T**, Aiso S, Ishikawa M, Watanabe M, Yoshida T, Kobayashi K, Asakura H, Tsuru S, Tsuchiya M. Circulating antibodies to the surface antigens on colon epithelial cells in ulcerative colitis. *Clin Exp Immunol* 1983; **54**: 163-168
5 **Das KM**, Vecchi M, Sakamaki S. A shared and unique epitope (s) on human colon, skin and biliary epithelium detected by a monoclonal antibody. *Gastroenterology* 1990; **98**: 464-469
6 **Strober W**, Nourish MF. Immunological diseases of the gastrointestinal tract. In: RR Rich, Ed. Clinical Immunology. St. Louis: Mosey 1995: 1401-1428

7 **Mizoguchi A**, Mizoguchi E, Chiba C, Spiekermann GM, Tonegawa S, Nagler-Anderson C, Bhan AK. Cytokine imbalance and autoantibody production in T cell receptor-alpha mutant mice with inflammatory bowel disease. *J Exp Med* 1996; **183**: 847-856

8 **Strober W**, Kelsall B, Fuss L, Marth T, Ludviksson B, Ehrhardt R, Neurath M. Reciprocal IFN-gamma and TGF-beta responses regulate the occurrence of mucosal inflammation. *Immunol Today* 1997; **18**: 61-64

9 **Neurath MF**, Fuss I, Kelsall BL, Presky DH, Waegell W, Strober W. Experimental granulomatous colitis in mice is abrogated by induction of TGF-beta-mediated oral tolerance. *J Exp Med* 1996; **183**: 2605-2616

10 **Madsen KL**, Lewis SA, Tavernini MM, Hibbard J, Fedorak RN. Interleukin 10 prevents cytokine-induced disruption of T84 monolayer barrier integrity and limits chloride secretion. *Gastroenterology* 1997; **113**: 151-159

11 **van Deventer SJ,** Elson CO, Fedorak RN. Multiple doses of intravenous interleukin 10 in steroid-refractory Crohn's disease. Crohn's Disease Study Group. *Gastroenterology* 1997; **113**: 383-389

12 **Sandborn WJ**, Targan SR. Biologic therapy of inflammatory bowel disease. *Gastroenterology* 2002; **122**: 1592-1608

13 **Weiner HL**. Oral tolerance: immune mechanisms and treatment of autoimmune diseases. *Immunol Today* 1997; **18**: 335-343

14 **Strobel S**, Mowat AM. Immune responses to dietary antigens: oral tolerance. *Immunol Today* 1998; **19**: 173-181

15 **Ilan Y**. Immune downregulation leads to upregulation of an antiviral response: a lesson from the hepatitis B virus. *Microbes Infect* 2002; **4**: 1317-1326

16 **Miller A**, Lider O, Roberts AB, Sporn MB, Weiner HL. Suppressor T cells generated by oral tolerization to myelin basic protein suppress both in vitro and in vivo immune responses by the release of transforming growth factor beta after antigen-specific triggering. *Proc Natl Acad Sci USA* 1992; **89**: 421-425

17 **von Herrath MG,** Dyrberg T, Oldstone MB. Oral insulin treatment suppresses virus-induced antigen-specific destruction of beta cells and prevents autoimmune diabetes in transgenic mice. *J Clin Invest* 1996; **98**: 1324-1331

18 **Ilan Y**, Prakash R, Davidson A, Jona G, Horwitz MS, Chowdhury NR, Chowdhury JR. Oral tolerization to adenoviral antigens permits long term gene expression using recombinant adenoviral vectors. *J Clin Invest* 1997; **99**:1098-1106

19 **Nagler A**, Pines M, Abadi U, Pappo O, Zeira M, Rabbani E, Engelhardt D, Ohana M, Chowdhury NR, Chowdhury JR, Ilan Y. Oral tolerization ameliorates liver disorders associated with chronic graft versus host disease in mice. *Hepatology* 2000; **31**: 641-648

20 **Ilan Y**, Gotsman I, Pines M, Beinart R, Zeira M, Ohana M, Rabbani E, Engelhardt D, Nagler A. Induction of oral tolerance in splenocyte recipients toward pretransplant antigens ameliorates chronic graft versus host disease in a murine model. *Blood* 2000; **95**: 3613-3619

21 **Garside P**, Mowat AM. Oral tolerance. *Semin Immunol* 2001; **13**: 177-185

22 **Ilan Y**, Weksler-Zangen S, Ben-Horin S, Sestiere M, Diment J, Sauter B, Roy Chowdhury N, Roy Chowdhury J, Goldin E. Weksler-Zangen S, Ben-Horin S, Diment J, Sauter B, Rabbani E, Engelhardt D, Chowdhury NR, Chowdhury JR, Goldin E. Treatment of experimental colitis by oral tolerance induction: a central role for suppressor lymphocytes. *Am J Gastroenterol* 2000; **95**: 966-973

23 **Galliaerde V**, Desvignes C, Peyron E, Kaiserlian D. Oral tolerance to haptens: intestinal epithelial cells from 2,4-dinitrochlorobenzene-fed mice inhibit hapten-specific T-cell activation *in vitro*. *Eur J Immunol* 1995; **25**: 1385-1390

24 **Dasgupta A**, Ramaswamy K, Giraldo J, Taniguchi M, Amenta PS, Das KM. Colon epithelial cellular protein induces oral tolerance in the experimental model of colitis by trinitrobenzene sulfonic acid. *J Lab Clin Med* 2001; **138**: 257-269

25 **Dasgupta A**, Kesari KV, Ramaswamy KK, Amenta PS, Das KM. Oral administration of unmodified colonic but not small intestinal antigens protects rats from hapten-induced colitis. *Clin Exp Immunol* 2001; **125**: 41-47

26 **Trop S**, Samsonov D, Gotsman I, Alper R, Diment J, Ilan Y. Liver associated lymphocytes expressing NK1.1 are essential for oral immune tolerance induction in a murine model. *Hepatology* 1999; **29**: 746-755

27 **Gotsman I**, Beinart R, Alper R, Rabbani E, Engelhardt D, Ilan Y. Induction of oral tolerance towards hepatitis B envelope antigens in a murine model. *Antiviral Res* 2000; **48**: 17-26

28 **Weiner HL,** Friedman A, Miller A, Khoury SJ, al-Sabbagh A, Santos L, Sayegh M, Nussenblatt RB, Trentham DE, Hafler DA. Oral tolerance: immunologic mechanisms and treatment of animal and human organ-specific autoimmune diseases by oral administration of autoantigens. *Annu Rev Immunol* 1994; **12**: 809-837

29 **Weiner HL**, Mackin GA, Matsui M, Orav EJ, Khoury SJ, Dawson DM, Hafler DA. Double blind pilot trial of oral tolerization with myelin antigens in multiple sclerosis. *Science* 1993; **259**: 1321-1324

30 **Trentham DE**. Oral tolerization as a treatment of rheumatoid arthritis. *Rheum Dis Clin North Am* 1998; **24**: 525-536

31 **Husby S**, Mestecky J, Moldoveanu Z, Holland S, Elson CO. Oral tolerance in humans. T cell but not B cell tolerance after antigen feeding. *J Immunol* 1994; **152**: 4663-4670

32 **Safadi R**, Israeli E, Papo O, Shibolet O, Melhem A, Bloch A, Rowe M, Alper R, Klein A, Hemed N, Segol O, Thalenfeld B, Engelhardt D, Rabbani E, Ilan Y. Treatment of chronic hepatitis B virus infection via oral immune regulation toward hepatitis B virus proteins. *Am J Gastroenterol* 2003; **98**: 2505-2515

33 **McSorley SJ**, Garside P. Vaccination by inducing oral tolerance? *Immunol Today* 1999; **20**: 555-560

34 **Gotsman I**, Shlomai A, Alper R, Rabbani E, Engelhardt D, Ilan Y. Amelioration of immune-mediated experimental colitis: tolerance induction in the presence of preexisting immunity and surrogate antigen bystander effect. *J Pharmacol Exp Ther* 2001; **297**: 926-932

35 **Shlomai A**, Trop S, Gotsman I, Jurim O, Diment J, Alper R, Rabbani E, Engelhardt D, Ilan Y. Immunomodulation of experimental colitis: the role of NK1.1 liver lymphocytes and surrogate antigens--bystander effect. *J Pathol* 2001; **195**: 498-507

36 **Samsonov D**, Trop S, Alper R, Diment J, Ilan Y. Enhancement of immune tolerance via induction of NK1.1 positive liver-associated-lymphocytes under immunosuppressive conditions. *J Hepatol* 2000; **32**: 812-820

37 **MacDonald HR**. NK1.1+ T cell receptor-alpha/beta+ cells: new clues to their origin, specificity, and function. *J Exp Med* 1995; **182**: 633-638

38 **Bendelac A**. Mouse NK1+ T cells. *Curr Opin Immunol* 1995; **7**: 367-374

39 **Godfrey DI,** Hammond KJ, Poulton LD, Smyth MJ, Baxter AG. NKT cells: facts, functions and fallacies. *Immunol Today* 2000; **21**: 573-583

40 **Abo T**, Kawamura T, Watanabe H. Physiological responses of extrathymic T cells in the liver. *Immunol Rev* 2000; **174**:135-149

41 **Zhang ZY**, Lee CS, Lider O, Weiner HL. Suppression of adjuvant arthritis in Lewis rats by oral administration of type II collagen. *J Immunol* 1990; **145**: 2489-2493

42 **von Herrath MG**. Bystander suppression induced by oral tolerance. *Res Immunol* 1997; **148**: 541-554

43 **Karpus WJ**, Kennedy KJ, Smith WS, Miller SD. Inhibition of relapsing experimental autoimmune encephalomyelitis in SJL mice by feeding the immunodominant PLP139-151 peptide. *J Neurosci Res* 1996; **45**: 410-423

44 **Miller A**, Lider O, Weiner HL. Antigen-driven bystander suppression after oral administration of antigens. *J Exp Med* 1991; **174**: 791-798

45 **Lundin BS**, Dahlgren UI, Hanson LA, Telemo E. Oral tolerization leads to active suppression and bystander tolerance in adult rats while anergy dominates in young rats. *Scand J Immunol* 1996; **43**: 56-63

Science Editor Zhu LH and Guo SY **Language Editor** Elsevier HK

PO Box 2345, Beijing 100023, China
www.wjgnet.com
wjg@wjgnet.com

ELSEVIER

World J Gastroenterol 2005;11(20):3112-3117
World Journal of Gastroenterology ISSN 1007-9327

• *CLINICAL RESEARCH* •

Esomeprazole tablet *vs* omeprazole capsule in treating erosive esophagitis

Chih-Yen Chen, Ching-Liang Lu, Jiing-Chyuan Luo, Full-Young Chang, Shou-Dong Lee, Yung-Ling Lai

Chih-Yen Chen, Ching-Liang Lu, Jiing-Chyuan Luo, Full-Young Chang, Shou-Dong Lee, Division of Gastroenterology, Department of Medicine, Taipei Veterans General Hospital and School of Medicine, National Yang-Ming University, Taipei, Taiwan, China
Yung-Ling Lai, AstraZeneca Taiwan Limited, Taipei, Taiwan, China
Supported by the Research Foundation of Digestive Medicine, Taiwan, China
Correspondence to: Full-Young Chang, MD, Chief, Division of Gastroenterology, Taipei Veterans General Hospital, No. 201, Sec. 2, Shih-Pai Road, Taipei 112, Taiwan, China. changfy@vghtpe.gov.tw
Telephone: +886-2-28757308 Fax: +886-2-28739318
Received: 2004-05-12 Accepted: 2004-06-29

Abstract

AIM: Esomeprazole, an oral S-form of omeprazole, has been a greater acid inhibitor over omeprazole in treating acid-related diseases. Only less published data is available to confirm its efficacy for Asian people. Therefore, a perspective, double-blind, randomized comparison of esomeprazole tablets 40 mg (Nexium®) *vs* omeprazole capsules 20 mg (Losec®) in treating Chinese subjects with erosive/ulcerative reflux esophagitis (EE) was conducted.

METHODS: A total of 48 EE patients were enrolled and randomized into two treatment groups under 8-wk therapy: 25 receiving esomeprazole, while another 23 receiving omeprazole treatment. Finally, 44 completed the whole 8-wk therapy.

RESULTS: The difference in healing EE between two groups was 22.7% (72.7% *vs* 50.0%), not reaching significant value (P = 0.204). The median of the first time needed in relieving heartburn sensation was 1 d for both groups and the remission rates for heartburn on the 1st d after treatment were 77.3% and 65%, respectively (NS). The scores of various reflux relieving symptoms evaluated either by patients or by investigators were not different. Regarding drug safety, 28% of esomeprazole group and 26.1% of omeprazole group reported at least one episode of adverse effects, while constipation and skin dryness were the common side effects in both groups (NS).

CONCLUSION: Esomeprazole 40 mg is an effective and safe drug at least comparable to omeprazole in treating Chinese EE patients.

Key words: Esomeprazole; Someprazole; Esophagitis

Chen CY, Lu CL, Luo JC, Chang FY, Lee SD, Lai YL. Esomeprazole tablet *vs* omeprazole capsule in treating erosive esophagitis. *World J Gastroenterol* 2005; 11(20): 3112-3117
http://www.wjgnet.com/1007-9327/11/3112.asp

INTRODUCTION

The reflux of gastric acid and duodenal contents into esophagus is a normal physiological phenomenon. However, the sustained esophageal mucosal damage, e.g., erosive/reflux esophagitis induced by this kind of reflux, may happen when the normal esophageal clearance and mucosal protection ability are impaired[1]. Gastroesophageal reflux disease (GERD) refers to individuals who are exposed to the physical complications from this reflux, or who experience clinically significant impairment of healthy well-being and quality of life due to reflux-related symptoms[2]. Today, prompt and effective relief of GERD symptoms is the primary goal for these patients. Since acid has been the major pathogen leading to reflux-associated symptoms, current GERD treatment is mainly aimed to reduce the acid exposure to esophagus[3,4]. For example, omeprazole (Losec®), the first proton pump inhibitor (PPI) showing an effective acid inhibitory ability, provides the satisfactory therapy either in GERD symptom relief or in healing of erosive esophagitis[5-7]. The modified formulation of omeprazole, multiple unit pellet system, remains effective in healing and relieving symptoms in GERD patients[8]. Up to date, omeprazole efficacy and safety are well established in many trials because more than 600 million patients have used omeprazole capsules worldwide including Taiwan[9,10].

Esomeprazole (Nexium®), the new S-isomer of omeprazole, is introduced to reduce gastric acid secretion more efficiently[9]. Unlike omeprazole, pharmacodynamic data suggest that the metabolism of esomeprazole in human liver microsomes is less dependent on CYP2C19 but mainly via CYP3A4[11]. Based on this observation, perhaps the inter-individual variation of esomeprazole metabolism is less compared to omeprazole[12]. In addition, studies have pointed out that esomeprazole exhibits significantly higher bioavailability, leading to the greater inhibition of gastric acid secretion compared to omeprazole[11,13]. Accordingly, many studies conducted in Western countries have confirmed the superior efficacy of esomeprazole over omeprazole in treating GERD patients[9,14].

GERD appears less common in East Asian countries compared to Western ones[15,16]. It is of interest to know the reason for the efficacy of esomeprazole in Asian GERD patients. Kao *et al*[17], indicated that esomeprazole achieved

68-73.9% sustained symptomatic response rate for GERD patients in an on-demand therapy trial. Based on the study design of a double-blind, randomized and controlled trial, the purpose of our study was to compare the efficacy and safety of esomeprazole tablet 40 mg and omeprazole capsule 20 mg in treating patients with endoscopically confirmed reflux esophagitis (EE) enrolled in a single center. Our primary objective was to assess the EE healing rate using both agents by an 8-wk treatment period. While the secondary objectives were to compare the response of reflux symptoms and general well-being by both agents at wk 4 and 8, respectively, to compare the time needed to relieve heartburn by both agents, and to evaluate the tolerability and safety of both agents.

MATERIALS AND METHODS

Design and study population

This was an active-controlled, double-blinded, double-dummy, randomized, single-center study with a parallel group designed to enroll 48 EE patients. Forty-eight outpatients (M/F: 38/10, age: 54.1±17.8 years), who sought medical care because of typical GERD symptoms for at least 1 mo, were consecutively enrolled in the study. They all received an endoscopy to confirm the EE diagnosis according to Los Angeles (LA) grading system[18], and met an inclusion criterion for an 8-wk treatment period with either esomeprazole tablet 40 mg or omeprazole capsule 20 mg (AstraZeneca, Gothenburg, Sweden). While endoscopy specimens were simultaneously obtained from stomach antrum and body for a rapid urease test to determine *Helicobacter pylori* (*H pylori*) infection. Those subjects with the following conditions were excluded: coexistence of healed or active peptic ulcer, gastrointestinal malignancy, esophago-gastric surgical history, esophagitis obviously resulted from systemic diseases, infections, drugs, burn, radiotherapy or physical deformity, severe esophageal stricture requiring dilatation at first endoscopy or expectation of requiring dilatation during the study, recent PPI treatment within 8 d prior to endoscopy, or using PPIs for more than 5 d in the last 28 d prior to endoscopy, with *H pylori* eradication therapy within the last 28 d prior to randomization or at any time during the study, using other antisecretory or prokinetic agents between endoscopy and randomization or at any time during the study, or with any investigational (non-approved) drug during the last 30 d prior to randomization. In addition, those with severe concurrent diseases judged by the investigators to complicate the evaluation of the trial, pregnancy, lactation or child-bearing potential without adequate contraception (contraceptive pill or intrauterine device), chronic alcoholism, drug abuse or any other conditions associated with poor patient compliance including expected non-co-operation, previous randomization in the study, and patients who needed continuously concomitant therapy with anticholinergics, cisapride, prostaglandin analogs, non-steroidal anti-inflammatory drugs (including COX-II) and aspirin (excluding low-dose aspirin e.g., 100 mg, as anti-platelet) were also excluded from this study. This study was approved by the Ethical Committee of Taipei Veterans General Hospital and carried out in accordance with the World Medical Association Helsinki Declaration. Written informed consent was obtained before any study-related procedures were performed.

The GERD symptoms such as heartburn, acid regurgitation, epigastric/chest pain, belching, nausea, vomiting and global well-being were assessed based on a standard visual analog scaled (VAS) questionnaire. Study medication was administered only to those subjects included in this study, following the procedures set out in the clinical study protocol. A sequence of patient numbers was assigned to the study center. All subjects entering the study received a patient number. This patient number was printed on the case report form and was used to identify the subject throughout the study. A randomization schedule was generated by the AstraZeneca using a validated system that automated the random assignment of treatment groups according to the randomization numbers. This schedule linked sequential numbers to treatment codes allocated at random. The schedule was prepared with a 1:1 randomization ratio in block size of 4. The study medication was labeled with the randomization numbers (medication numbers). At the end of baseline visit, eligible patients were randomized to the study medication in accordance with the randomization schedule. The next eligible subject received the study medication with the lowest available randomization number. Each subject was given only the study medication carrying his/her randomization number. The investigator documented the randomization number by sticking the label provided on the appropriate case report form. Subjects who permanently discontinued from the study were to retain their subject number and their randomization number, if already given. New subjects were always allotted a new subject number and, if applicable, a new randomization number.

Patients were asked to come back to the study office on three occasions (baseline, wk 4 and 8, respectively) during the trial. All doses were taken by mouth once daily in the morning before breakfast. During the study period, the patients were instructed to take one tablet of esomeprazole or matching placebo and one capsule of omeprazole or matching placebo in the morning with a glass of water. The first dose of study medication was taken on the morning after randomization. This was considered as d 1 of treatment. After the whole course of treatment, they were asked to come back on the last day of medication. At that time, they received the 2nd endoscopy to assess the EE status again. Meanwhile GERD symptoms based on VAS after treatment were scored again. All the endoscopic EE diagnoses and their follow-up according to LA grading were initially performed by an experienced endoscopist (Chang), while all the endoscopic findings including EE were recorded by Polaroid films. When all the studies were completed, the recorded films assigned to their study codes were reviewed independently by another two endoscopists (Lu and Chen) who were blind to the order and code of endoscopy for each patient. If three readings in each film were dissimilar, this film was discussed by the above three investigators together to obtain the final endoscopic assessment. Healing was defined as no EE evidence.

Efficacy data

The primary endpoint of this trial was the percentage of enrolled patients whose EE was healed by wk-8 visit. The

secondary efficacy variables included for the first time the relief of heartburn symptoms, changes of reflux symptom scores (based on VAS score) and overall therapeutic effects judged via either subjective (patient) or objective (investigator) assessment.

Safety data

The safety assessments included observed and reported adverse events (AE) and clinical laboratory evaluations (hematology and serum chemistry).

Study duration and dates

The study took place between 28 March, 2001 and 26 October, 2001.

Statistical procedures

For the primary efficacy parameter, the healing rate for each group was calculated with 95%CI. The difference between the two treatment groups and the corresponding 95%CI were also provided and compared by using Fisher's exact test. The cumulative percentage of patients who exhibited the first relief of their diary-recorded symptom of heartburn was compared using Fisher's exact test on d 1, 7, and 28, respectively. The median first time to relieve heartburn symptom between the two groups were compared using log-rank test. For reflux symptoms, Wilcoxon rank sum test was used to assess patient VAS score, and Fisher's exact test was used to assess investigator scores as well as the overall therapeutic effect.

AE were summarized according to coding symbols for thesaurus of adverse reaction terms. The number of patients who reported a particular event and the number of events were summarized. Comparative incidence of AE was evaluated using Fisher's exact test. Each laboratory parameter was listed with values outside the reference range identified. For each laboratory parameter, changes in abnormality/normality status from pre- to post-treatment were summarized in shift tables and assessed using McNemar test.

Interim analysis

No interim analysis was performed in this study.

RESULTS

Study subjects and conduct

Finally, 48 eligible EE patients were enrolled and randomized according to the protocol. Their demographics and baseline characteristics are summarized in Table 1. Of them, 25 patients were distributed into esomeprazole group whereas 23 patients were on omeprazole treatment. Table 1 illustrates that both groups were comparable in their demographic characteristics and basal clinical manifestations except the subjects of esomeprazole group had a higher chance of belching ($P<0.05$). Among the 48 randomized patients, only 44 (esomeprazole: 24; omeprazole: 20) completed the whole study course. The reasons why four of them did not finish the trial were as follows: two lost their follow-up and another two discontinued the study medication. In addition, 2 (all were esomeprazole) of 44 who finished the study refused endoscopy follow-up at wk-8 visit were excluded from per protocol analysis.

Efficacy

The EE healing rates of esomeprazole and omeprazole treatment judged at the end of 8-wk trial [per-protocol (PP)] were 72.7% (16/22, 95%CI: 49.8-89.3%) and 50.0% (10/20, 27.2-72.8%) respectively [intent-to-treat (ITT): 64% (16/25, 95%CI: 44.3-83.8%) *vs* 45.5% (10/22, 95%CI: 22.7-68.3%), $P = 0.2481$], while the odds ratio was 2.667 (PP: 95%CI: 0.739-9.63, $P = 0.2040$) for esomeprazole over omeprazole.

In order to understand whether esomeprazole was effective in reducing LA-based EE grading, we further analyzed their extent of changed grading for both groups, e.g., 0 (no change), -1 (A to healed, B to A, C to B and D to C), -2 (B to healed, C to A and D to B) and -3 (C to healed, D to A), respectively (Figure 1). Although esomeprazole showed a better healing ability, however, no significant difference was found.

Table 1 Demographics and baseline characteristics of erosive esophagitis patients treated with esomeprazole or omeprazole (mean±SE)

	Esomeprazole 40 mg $n = 25$	Omeprazole 20 mg $n = 23$	P
Age (yr)	49.2±3.7	59.0±3.4	0.0596
Sex (male%)	20 (80)	18 (78.3)	1.0000
Body weight (kg)	68.4±2.4	70.9±2.5	0.4779
Height (cm)	166.7±1.3	169.0±1.4	0.2096
Basal reflux symptoms (VAS)			
Heartburn	29.4±5.7	23.6±5.9	0.2683
Nausea	18.7±5.5	13.8±5.8	0.8520
Regurgitation	29.8±6.1	24.5±6.4	0.3365
Vomiting	14.0±4.7	8.8±4.9	0.5702
Belching	47.0±6.0	25.2±6.3	0.0121
Dysphagia	7.5±5.0	14.7±5.2	0.7421
Epigastric pain	15.8±5.5	16.7±5.8	0.9223
LA grade of erosive esophagitis [n (%)]			0.6617
A	15 (60)	11 (47.8)	
B	7 (28)	7 (30.4)	
C	2 (8)	2 (8.7)	
D	1 (4)	3 (13.0)	
Hp infection status	10 (40)	11 (47.8)	0.5643

VAS: visual analog scale, scored from 0 (none) to 100 (most severe); *Hp*: *Helicobacter pylori*; LA: Los Angeles.

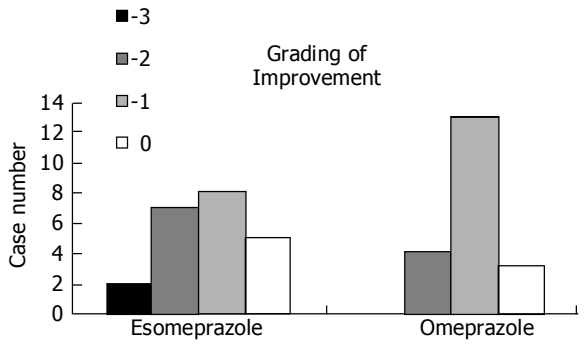

Figure 1 Histogram showing endoscopic assessment for the improved LA grading in erosive esophagitis patients after esomeprazole or omeprazole treatment. Grade of improvement: -3 means D to A or C to healed, -2 means D to B, C to A, or B to healed, -1 means D to C, C to B, B to A, or A to healed.

The median time to the first relief of heartburn between esomeprazole and omeprazole groups was similar on d 1 after treatment. On d 1, 77.3% and 65% of EE patients recorded the first relief of heartburn, respectively (Figure 2). Table 2 denotes that esomeprazole treatment was not significantly different from omeprazole in any of improved GERD symptom scores evaluated by patients themselves based on VAS except belching improvement was marked in patients undergoing esomeprazole treatment ($P<0.05$). Table 3 illustrates that the therapeutic symptomatic response scores of both treatments were similar (NS).

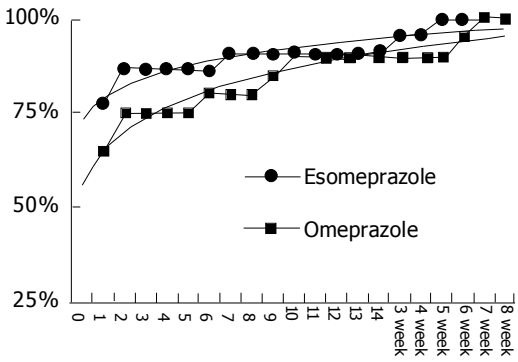

Figure 2 No cumulative percentage difference in relieving heartburn between erosive esophagitis patients after esomeprazole or omeprazole treatment illustrated by scattering plot.

Safety

In general, EE patients receiving esomeprazole (28.0%) and omeprazole (26.1%) treatment reported AE at least once during the trial (NS). Among them, constipation, dry skin sensation, diarrhea, headache, somnolence, *etc.*, were the recorded AE in both groups (Table 4). Their distributions were also not different. Only one patient in omeprazole group reported a serious adverse event of cellulites during the treatment period, this causal relationship to treatment was judged to be unrelated. In addition, there were no clinically meaningful differences between treatment groups in terms of changed laboratory values or physical examinations.

Table 2 Changes of reflux symptoms assessed on visual analog scale of studied patients 8 wk after esomeprazole or omeprazole treatment (mean±SE)

Reflux symptoms	Esomeprazole $n=22$	Omeprazole $n=22$	*P*
Heartburn	-22.3±2.1	-21.4±2.2	0.5453
Nausea	-11.9±2.2	-12.7±2.4	0.8867
Regurgitation	-22.4±2.2	-20.4±2.3	0.8598
Vomiting	-9.1±1.61	-8.8±1.7	0.4438
Belching	-24.1±4.3	-17.9±4.6	0.0113
Dysphagia	-8.4±1.4	-6.5±1.5	0.8044
Epigastric pain	-10.6±2.0	-11.1±2.1	0.1747

VAS was scored from 0 (none) to 100 (most severe).

Table 3 Changed reflux symptoms of studied patients 8 wk after esomeprazole or omeprazole treatment (%)

		Esomeprazole ($n=22$)	Omeprazole ($n=20$)	*P*
Heartburn	Improved	50.0	65.0	0.0993
	Nochange	50.0	25.0	
	Worse	0.0	10.0	
Regurgitation	Improved	77.3	85.0	1.0000
	Nochange	18.2	15.0	
	Worse	4.5	0.0	
Dysphagia	Improved	36.4	35.0	0.8697
	No change	63.6	60.0	
	Worse	0.0	5.0	
Epigastric pain	Improved	27.3	50.0	0.1895
	Nochange	63.6	50.0	
	Worse	9.1	0.0	
Nausea	Improved	22.7	35.0	0.5036
	Nochange	68.2	65.0	
	Worse	9.1	0.0	
Vomiting	Improved	22.7	40.0	0.3200
	Nochange	77.3	60.0	
	Worse	0.0	0.0	
Belching	Improved	54.5	45.0	0.8999
	Nochange	36.4	45.0	
	Worse	9.1	10.0	

DISCUSSION

Our study mainly indicated that both esomeprazole and omeprazole were similarly effective in healing EE, relieving reflux symptoms for the Chinese EE patients in Taiwan. Gastro-esophageal reflux-induced EE is one of the GERDs, which ranges from endoscopy negative reflux to severe complications of Barrett's esophagus as either high-grade dysplasia or adenocarcinoma[19,20]. Unlike endoscopy negative reflux, EE is very easily identified in GERD subjects based on experienced endoscopy. Until now, EE treatment is similar to any kind of GERD, e.g., reducing acid reflux, healing erosive lesions and preventing future relapse[2].

The EE severity is usually related to the extent and time of esophageal acid exposure[22]. It means the greater the acid exposure the severe the mucosal damage. Among the refluxed contents, acid is the most important pathogen leading to GERD, while effective acid reduction remains the only available method to treat GERD at this moment[2,22,23]. Accordingly, effective acid control for GERD subjects likely results in faster resolution of reflux symptoms, healing of reflux lesions quickly, better response of those with severe lesions and less frequent relapse. Symptom relief is indeed

Table 4 AE in studied patients 8 wk after esomeprazole or omeprazole treatment (ITT)

	Esomeprazole (n = 25) n (%)	Omeprazole (n = 23) n (%)	P
Patient with at least one AE	7 (28.0)	6 (26.1)	1.0000
Constipation	2 (8.0)	1 (4.4)	1.0000
Dry skin	1 (4.0)	3 (13.0)	0.3381
Diarrhea	1 (4.0)	1 (4.4)	1.0000
Headache	1 (4.0)	1 (4.4)	1.0000
Somnolence	1 (4.0)	1 (4.4)	1.0000
Cellulites	0 (0.0)	1 (4.4)	0.4792
Bronchitis	0 (0.0)	1 (4.4)	0.4792

very important to all GERD patients because these symptoms usually bother their daily quality of life. Now step down treatment for GERD patients beginning with an effective PPI was recommended by the Genval consensus[2]. Although many of our studied GERD patients had mild EE, however, they still complained of cardinal reflux symptoms and other reflux-related symptoms. After 1 d of active esomeprazole and omeprazole treatment, 77.3% and 65% of patients recorded their first relief of heartburn. After 8-wk treatment, the VAS scores of many reflux symptoms were improved in both groups. In addition, the objective ranking of overall therapeutic effect showed a favorable and comparable result in both groups. We thus confirmed that 40 mg esomeprazole and 20 mg omeprazole daily for 8 wk could offer a sufficient acid suppression leading to the effective symptomatic relief for Asian EE patients without serious AE.

Benefits have been demonstrated in studies of esomeprazole *vs* omeprazole and lansoprazole[15,25-27]. Our study was to compare the therapeutic efficacy of a single isomer PPI, esomeprazole and omeprazole in treating EE patients in Taiwan. In fact, we found that EE was finally healed in more than half of our enrolled patients after 8-wk treatment. This EE healing rate was obviously lower than that in previous reports (67-85%) using PPI for a similar duration[5-7,28-33]. It has been pointed out that EE is usually less commonly presented and milder in nature among the Orientals in comparison with Occidentals[28-35]. In our study, the EE severity scored via LA grading system among the 48 consecutively enrolled patients was mainly classified as LA grade A, whereas previous reports from Western studies often included EE patients with an advanced grade[5-7,15-18,22-24]. Theoretically, our study should provide a better efficacy since many of the enrolled subjects had mild EE in nature. Surprisingly, we obtained a lower EE healing efficacy based on the similar PPI for a similar therapeutic duration. It is unknown whether the ethnic factor compromises the therapeutic efficacy. For example, PPI treatment for GERD patients only achieved 57.7% and 77% healing rates in two Japanese group studies, respectively[36,37]. Because our study was a single center trial and only enrolled a limited number of eligible EE patients, we believe that the lower and indistinguishable efficacy of esomeprazole *vs* omeprazole treatment was most likely originated from a type II error of inadequate study power, which was common in many drug trial studies[38,39]. In addition, long-term management of EE patients with PPI maybe more meaningful since initial management of EE patients to achieve healing has been overemphasized[40].

In summary, esomeprazole is at least similar to omeprazole in healing EE and removing reflux-related symptoms. Both esomeprazole and omeprazole are safe and well tolerated by Asian EE patients.

ACKNOWLEDGMENTS

The authors thank Jack Chai, MS, for his secretarial assistance.

REFERENCES

1 **Dodds WJ,** Hogan WJ, Helm JF, Dent J. Pathogenesis of reflux esophagitis. *Gastroenterology* 1981; **81**: 376-394
2 **An evidence-based appraisal of reflux disease management--the Genval Workshop Report**. *Gut* 1999; **44** (Suppl 2): S1-S16
3 **Tytgat GN,** Nio CY. The medical therapy of reflux oesophagitis. *Baillieres Clin Gastroenterol* 1987; **1**: 791-807
4 **Bell NJ,** Hunt RH. Role of gastric acid suppression in the treatment of gastro-oesophageal reflux disease. *Gut* 1992; **33**: 118-124
5 **Bate CM,** Green JR, Axon AT, Murray FE, Tildesley G, Emmas CE, Taylor MD. Omeprazole is more effective than cimetidine for the relief of all grades of gastro-oesophageal reflux disease-associated heartburn, irrespective of the presence or absence of endoscopic oesophagitis. *Aliment Pharmacol Ther* 1997; **11**: 755-763
6 **Galmiche JP,** Barthelemy P, Hamelin B. Treating the symptoms of gastro-oesophageal reflux disease: a double-blind comparison of omeprazole and cisapride. *Aliment Pharmacol Ther* 1997; **11**: 765-773
7 **Hallerback B,** Unge P, Carling L, Edwin B, Glise H, Havu N, Lyrenas E, Lundberg K. Omeprazole or ranitidine in long-term treatment of reflux esophagitis. The Scandinavian Clinics for United Research Group. *Gastroenterology* 1994; **107**: 1305-1311
8 **Lu CL,** Chen TS, Chen CY, Chang FY, Kang LJ, Lee SD. Treatment of erosive oesophagitis with omeprazole: a comparison with different delivery system. *Dig Liver Dis* 2001; **33**: 731
9 **Lindberg P,** Keeling D, Fryklund J, Andersson T, Lundborg P, Carlsson E. Review article: Esomeprazole-enhanced bioavailability, specificity for the proton pump and inhibition of acid secretion. *Aliment Pharmacol Ther* 2003; **17**: 481-488
10 **Sjovall H,** Bjornsson E, Holmberg J, Hasselgren G, Rohss K, Hassan-Alin M. Pharmacokinetic study of esomeprazole in patients with hepatic impairment. *Eur J Gastroenterol Hepatol* 2002; **14**: 491-496
11 Investigator's brochure on esomeprazole for oral use. 1999
12 **Lind T,** Rydberg L, Kyleback A, Jonsson A, Andersson T, Hasselgren G, Holmberg J, Rohss K. Esomeprazole provides improved acid control vs. omeprazole In patients with symptoms of gastro-oesophageal reflux disease. *Aliment Pharmacol Ther* 2000; **14**: 861-867
13 **Andersson T,** Hassan-Alin M, Hasselgren G, Rohss K, Weidolf L. Pharmacokinetic studies with esomeprazole, the (S)-isomer of omeprazole. *Clin Pharmacokinet* 2001; **40**: 411-426
14 **Kahrilas PJ,** Falk GW, Johnson DA, Schmitt C, Collins DW, Whipple J, D'Amico D, Hamelin B, Joelsson B. Esomeprazole improves healing and symptom resolution as compared with omeprazole in reflux oesophagitis patients: a randomized controlled trial. The Esomeprazole Study Investigators. *Aliment Pharmacol Ther* 2000; **14**: 1249-1258
15 **Chang CS,** Poon SK, Lien HC, Chen GH. The incidence of reflux esophagitis among the Chinese. *Am J Gastroenterol* 1997; **92**: 668-671
16 **Goh KL,** Chang CS, Fock KM, Ke M, Park HJ, Lam SK. Gastro-oesophageal reflux disease in Asia. *J Gastroenterol Hepatol* 2000; **15**: 230-238
17 **Kao AW,** Sheu BS, Sheu MJ, Chang YM, Huang SF, Chuang

CH, Lai YL, Kao YH. On-demand therapy for Los Angeles grade A and B reflux esophagitis: esomeprazole versus omeprazole. *J Formos Med Assoc* 2003; **102**: 607-612
18 **Armstrong D,** Bennett JR, Blum AL, Dent J, De Dombal FT, Galmiche JP, Lundell L, Margulies M, Richter JE, Spechler SJ, Tytgat GN, Wallin L. The endoscopic assessment of esophagitis: a progress report on observer agreement. *Gastroenterology* 1996; **111**: 85-92
19 **Jankowski JA,** Provenzale D, Moayyedi P. Esophageal adenocarcinoma arising from Barrett's metaplasia has regional variations in the west. *Gastroenterology* 2002; **122**: 588-590
20 **Jankowski JA,** Harrison RF, Perry I, Balkwill F, Tselepis C. Barrett's metaplasia. *Lancet* 2000; **356**: 2079-2085
21 **Whittles CE,** Biddlestone LR, Burton A, Barr H, Jankowski JA, Warner PJ, Shepherd NA. Apoptotic and proliferative activity in the neoplastic progression of Barrett's oesophagus: a comparative study. *J Pathol* 1999; **187**: 535-540
22 **Richter JE.** Gastroesophageal reflux disease in the older patient: presentation, treatment, and complications. *Am J Gastroenterol* 2000; **95**: 368-373
23 **Dent J.** Gastro-oesophageal reflux disease. *Digestion* 1998; **59**: 433-445
24 **Pope CE.** Acid-reflux disorders. *N Engl J Med* 1994; **331**: 656-660
25 **Castell DO,** Kahrilas PJ, Richter JE, Vakil NB, Johnson DA, Zuckerman S, Skammer W, Levine JG. Esomeprazole (40 mg) compared with lansoprazole (30 mg) in the treatment of erosive esophagitis. *Am J Gastroenterol* 2002; **97**: 575-583
26 **Lauritsen K,** Deviere J, Bigard MA, Bayerdorffer E, Mozsik G, Murray F, Kristjansdottir S, Savarino V, Vetvik K, De Freitas D, Orive V, Rodrigo L, Fried M, Morris J, Schneider H, Eklund S, Larko A. Esomeprazole 20 mg and lansoprazole 15 mg in maintaining healed reflux oesophagitis: Metropole study results. *Aliment Pharmacol Ther* 2003; **17**: 333-341
27 **Vakil NB,** Shaker R, Johnson DA, Kovacs T, Baerg RD, Hwang C, D'Amico D, Hamelin B. The new proton pump inhibitor esomeprazole is effective as a maintenance therapy in GERD patients with healed erosive oesophagitis: a 6-month, randomized, double-blind, placebo-controlled study of efficacy and safety. *Aliment Pharmacol Ther* 2001; **15**: 927-935
28 **Gough AL,** Long RG, Cooper BT, Fosters CS, Garrett AD, Langworthy CH. Lansoprazole versus ranitidine in the maintenance treatment of reflux oesophagitis. *Aliment Pharmacol Ther* 1996; **10**: 529-539
29 **Hatlebakk JG,** Berstad A, Carling L, Svedberg LE, Unge P, Ekstrom P, Halvorsen L, Stallemo A, Hovdenak N, Trondstad R. Lansoprazole versus omeprazole in short-term treatment of reflux oesophagitis. Results of a Scandinavian multicentre trial. *Scand J Gastroenterol* 1993; **28**: 224-228
30 **Castell DO,** Richter JE, Robinson M, Sontag SJ, Haber MM. Efficacy and safety of lansoprazole in the treatment of erosive reflux esophagitis. The Lansoprazole Group. *Am J Gastroenterol* 1996; **91**: 1749-1757
31 **Mee AS,** Rowley JL. Rapid symptom relief in reflux oesophagitis: a comparison of lansoprazole and omeprazole. *Aliment Pharmacol Ther* 1996; **10**: 757-763
32 **Robinson M,** Sahba B, Avner D, Jhala N, Greski-Rose PA, Jennings DE. A comparison of lansoprazole and ranitidine in the treatment of erosive oesophagitis. Multicentre Investigational Group. *Aliment Pharmacol Ther* 1995; **9**: 25-31
33 **Mössner J,** Hölscher AH, Herz R, Schneider A. A double-blind study of pantoprazole and omeprazole in the treatment of reflux oesophagitis: a multicentre trial. *Aliment Pharmacol Ther* 1995; **9**: 321-326
34 **Xia HH,** Talley NJ. *Helicobacter pylori* infection, reflux esophagitis, and atrophic gastritis: an unexplored triangle. *Am J Gastroenterol* 1998; **93**: 394-400
35 **Bercík P,** Verdú EF, Armstrong D. *H pylori* related increase in omeprazole (ome) effect is associated with ammonia production (abstr). *Gastroenterology* 1996; **110**: A64
36 **Endo M,** Sugihara K. Long-term maintenance treatment of reflux esophagitis resistant to H2-RA with PPI (lansoprazole). *Nihon Rinsho* 2000; **58**: 1865-1870
37 **Umeda N,** Miki K, Hoshino E. Lansoprazole versus famotidine in symptomatic reflux esophagitis: a randomized, multicenter study. *J Clin Gastroenterol* 1995; **20** Suppl 1: S17-S23
38 **Talley N.** Managing reflux disease-Critically reviewing the evidence in 2003. International Symposium, Marbella, Spain, January 18, 2003
39 **Al MJ,** van Hout BA, Michel BC, Rutten FF. Sample size calculation in economic evaluations. *Health Econ* 1998; **7**: 327-335
40 **Dent J,** Talley NJ. Overview: initial and long-term management of gastro-oesophageal reflux disease. *Aliment Pharmacol Ther* 2003; **17** Suppl 1: 53-57

Science Editor Wang XL **Language Editor** Elsevier HK

PO Box 2345, Beijing 100023, China
www.wjgnet.com
wjg@wjgnet.com

ELSEVIER

World J Gastroenterol 2005;11(20):3118-3121
World Journal of Gastroenterology ISSN 1007-9327

• *BRIEF REPORTS* •

Clinical significance of granuloma in Crohn's disease

Tamás Molnár, László Tiszlavicz, Csaba Gyulai, Ferenc Nagy, János Lonovics

Tamás Molnár, Ferenc Nagy, János Lonovics, First Department of Medicine Faculty of Medicine, University of Szeged, H-6720 Szeged, Korányi fasor 8., Hungary
László Tiszlavicz, Department of Pathology, Faculty of Medicine, University of Szeged, H-6720 Szeged, Korányi fasor 8., Hungary
Csaba Gyulai, Department of Radiology, Faculty of Medicine, University of Szeged, H-6720 Szeged, Korányi fasor 8., Hungary
Correspondence to: Tamás Molnár, First Department of Medicine Faculty of Medicine, University of Szeged, H-6720 Szeged, Korányi fasor 8., Hungary. mot@in1st.szote.u-szeged.hu
Telephone: +36-62-545186 Fax: +36-62-545185
Received: 2004-10-09 Accepted: 2004-10-18

Abstract

AIM: Granuloma is considered the hallmark of microscopic diagnosis in Crohn's disease (CD), but granulomas can be detected in only 21-60% of CD patients. The aim of this study was to evaluate the frequency of granulomas by multiple endoscopic biopsies in patients with CD and to examine whether group of patients with or without granuloma exhibit a different clinical course.

METHODS: Fifty-six patients with newly diagnosed CD were included in the study. Jejunoscopy, enteroclysis and ileo-colonoscopy were performed in all patients. At least two biopsy specimens from each examined gastrointestinal segment were examined microscopically searching granuloma. The clinical course was followed in all patients, and extraintestinal manifestations as well as details of any immunosuppressive therapy and surgical intervention were noted.

RESULTS: Granuloma was found in 44.6% of the cases (25 patients). Patients with granuloma had higher activity parameters at the time of the biopsies. Extraintestinal manifestations were observed and surgical interventions were performed more often in the granuloma group. The need of immunosuppressive therapy was significantly more frequent in the patients with granuloma. Granuloma formation is more often seen in younger patients, and mainly in the severe, active penetrating disease.

CONCLUSION: The significantly higher frequency of surgical interventions and immunosuppressive therapy suggests that granuloma formation is associated with a more severe disease course during the first years of CD.

Key words: Crohn's disease; Granuloma; Activity; Complication

Molnár T, Tiszlavicz L, Gyulai C, Nagy F, Lonovics J. Clinical significance of granuloma in Crohn's disease. *World J Gastroenterol* 2005; 11(20): 3118-3121
http://www.wjgnet.com/1007-9327/11/3118.asp

INTRODUCTION

Crohn's disease (CD) is a chronic transmural inflammatory bowel disease of unknown etiology. Granuloma is considered the hallmark of microscopic diagnosis in CD, but granulomas can be detected in only 40-60% of surgically resected bowel segments in CD patients[1]. The frequency of granuloma in bioptic samples varies in 15-36% according to different authors[2]. The severity of the disease shows a great variability as well. Several factors (e.g., localization of the disease, maximum extent of involvement, the behavior type: inflammatory, stricturing or penetrating) make influence on the clinical course of the disease. There are inconsistent data in the literature about the prognostic significance of the granuloma in CD. Our aim was to divide our newly diagnosed CD patients into two subgroups on the basis of the presence or absence of granuloma at the time of diagnosis. We have been accomplishing follow-up studies for at least 3 years in order to get information about these two different groups (patients with or without granuloma), whether they show any difference in the clinical course.

MATERIALS AND METHODS

Patients

Fifty-six patients with newly diagnosed CD were included in this prospective study during the period from January 1997 to September 2000. Their CD was diagnosed on the basis of the standard clinical, radiological, endoscopic and histologic criteria. The female/male ratio was 31/25, the median age of the patients was 36.29 years (ranging: 18-65 years). Positive family history was observed only in one new case; this female patient with granuloma had a brother with diagnosed CD. The localization of CD was as follows: in 33 patients (59%) both small and large bowels were involved (among them in 6 patients upper gastrointestinal tract (UGT) involvement-esophageal/gastric/duodenal was also observed), in 18 patients (32%) the large bowel only, in 5 (9%) the terminal ileum alone was inflamed. The ethical committee of our department approved the study. Informed oral consent was obtained from the patients.

Diagnostic methods to determine the frequency of granuloma and the activity of CD at the beginning of the study

Clinical parameters Blood samples were taken from all patients on each visit to determine the hemoglobin and

hematocrit, as well as the C reactive protein (CRP) values. The Crohn's disease activity index (CDAI) (Best)[3] was calculated to measure the clinical disease activity.

Localization of CD, endoscopic activity index To determine the severity of CD and the extent of the involved bowel segments, physical examination, abdominal ultrasound, jejunoscopy, small bowel enteroclysis, ileo-colonoscopy were performed in all patients at the time of the first admission, when the study started. Four large bowel segments (the caecum and ascending colon, the transverse colon, the descending colon, and the sigmoid colon and rectum) and the ileum were examined by colonoscopy and scored according to the findings. The proximal small bowel segment alterations (jejunum together with the duodenum) were detected by jejunoscopy. Each segment were scored by using the protocol of Mary and Modigliani with some modification (0 = normal mucosa, 1 = edema, erythema, granularity of the mucosa, and aphthous lesions, 2 = sporadic or superficial ulcerations, and 3 = extensive deep ulcerations, and stenosis). This way these diagnostic methods could produce quantifiable data about the severity of the inflammation in each part of the gastrointestinal tract[4]. At least two biopsy specimens from each examined gastrointestinal segment (esophagus, body and antral region of the stomach, bulb, distal part of duodenum, jejunum, ileum, ascending colon, transverse colon, descending colon, sigmoid colon and rectum) were examined microscopically searching granuloma by one pathologist using the standard methods.

Follow up Two gastroenterologists (T.M. and F.N.) followed all the patients. They were unaware of the presence of granuloma during the study.

Disease behavior

According to the behavior of the inflammation (Vienna Classification)[5] patients were divided into three subgroups at the end of the study. Twenty-three patients were in the inflammatory (non-stricturing, non-penetrating) type, 15 patients in the stricturing and 18 patients in the penetrating-fistulizing type of CD.

Severity of CD

Scheduling of follow-up visits depended on the actual severity of CD. The completely symptoms-free patients were supervised by every 3 mo, and naturally, patients with active disease were observed more frequently. The following parameters were recorded during the follow-up period to determine the severity of CD: frequency of relapses (definition of relapse: CDAI above 150), frequency of extraintestinal manifestations (arthritis, sacroileitis, pyoderma gangrenosum, erythema nodosum, cutaneous vasculitis, episcleritis, uveitis, aphtous stomatitis), fistulas, need of immunosuppressive therapy, number of surgical intervention, as well as total number of hospitalization.

Statistical analysis

Data are expressed as mean±SD. Correlation coefficients were calculated by using *t*- and χ^2-tests.

RESULTS

Granuloma was found in at least one tissue sample in 44.6% of the cases (25 patients). The average years of age of the patients in group I (patients with granuloma) and group II (patients without granuloma) was 29.6 and 36.4 years, respectively. The proportion of the female patients was moderately higher in the group with granuloma (60 *vs* 51.3%). Similar smoking status was observed in the two groups: 60 and 61.2% of the patients were smoker in group I and II, respectively. Involvement of the upper GI tract was about 2.5 times more frequent (16.0 *vs* 6.4%, $P<0.05$) in the granuloma group. Penetrating disease behavior was slightly more often associated with granuloma (44% *vs* 23%). The clinical characteristics of the two groups of patients are summarized in Table 1. Patients with granuloma had higher activity parameters at the time of the biopsies (CDAI: 218.9±108.2 *vs* 144.1±92.5, $P = 0.01$; CRP level: 62.7±84.9 *vs* 48.5±87.8). The overall endoscopic scores tended to be higher in group I than those in group II, but it did not reach the level of significance. The average follow-up times were similar in the two groups: 38.5±7.34 and 36.8±3.83 mo. The appearance of the extraintestinal manifestations was observed more often in the granuloma group, but there was no significant difference between the two groups. Arthritis occurred most frequently in both groups, sacroileitis and seronegative peripheral arthritis were the two most common disorders. Aphtous stomatitis was associated with

Table 1 Clinical characteristics of patients (mean±SD)

	Patients with granuloma Group I	Patients without granuloma Group II	Significance
Number of patients	25	31	NS
Female/male ratio (No.)	15/10	16/15	NS
Median age (yr)	29.60±11.32	36.46±12.94	NS
Localization			
Small bowel only	1 (4%)	4 (12.9%)	NS
Large bowel only	10 (40%)	8 (25.8%)	NS
Small and large bowel	10 (40%)	17 (54.8%)	NS
UGT involvement	4 (16%)	2 (6.4%)	$P<0.05$
Disease behavior type			
Inflammatory	8 (32%)	15 (48.4%)	NS
Stricturing	6 (24%)	9 (29.0%)	NS
Penetrating	11 (44%)	7 (22.6%)	NS
Activity of CD			
CDAI	218.9±108.2	144.1±92.5	$P = 0.01$
Endoscopic scores	6.60±3.53	5.35±4.20	NS

UGT = upper gastrointestinal tract.

Table 2 Frequency of different extraintestinal manifestations in patients with or without granuloma

	Patients with granuloma (%)	Patients without granuloma (%)	Significance
Number of extraintestinal manifestations	10/25 (40)	7/31 (22.6)	*P* = NS
Arthritis	6/25 (24)	4/31 (12.9)	*P* = NS
Eye manifestation	0/25	1/31 (3.2)	*P* = NS
Cutan manifestation	2/25 (8)	0/31	*P* = NS
Aphtous stomatitis	2/25 (8)	2/31 (6.4)	*P* = NS

NS = non-significant.

Table 3 Frequency of relapses in the two groups

Number of relapse after the succesful treatment of fist attack	Patients with granuloma (25) (%)	Patients without granuloma (31) (%)
0	5 (20)	12 (38.7)
1	10 (40)	15 (48.4)
2	7 (28)	4 (12.9)
3	3 (12)	0 (0)

Trend -$P = 0.06$, χ^2 test.

CD in about 7% of all patients. Noticeably every aphtous stomatitis started simultaneously with the first symptoms of the CD. Iridocyclitis, cutaneous vasculitis and metastatic CD were the other extraintestinal manifestations (Table 2). There was a strong trend towards significantly increased frequency of relapses in the granuloma positive group ($P = 0.06$, χ^2 test) (Table 3). The number of hospitalization was significantly higher in granuloma group (20 *vs* 12, $P<0.05$). Surgical interventions were performed more often in the granuloma group (48% *vs* 22.5%, $P<0.05$). Stenosis, abscess, fistula and perforation were the indications for surgery. The use of immunosuppressive drugs was significantly more frequent in the patients with granuloma (60% *vs* 32.2%, $P<0.05$). The most frequent indication of immunosuppressive therapy was the prevention of postoperative relapse in both groups (10/15 in group I, 7/10 in group II); steroid dependency was the other cause (5 *vs* 3 in group I *vs* II). As the follow-up periods after the start of the immunosuppression were mainly short and different between the cases and groups, the response rate to immunosuppressive therapy was incomparable between the groups.

DISCUSSION

The granuloma formation is a host response reaction by the localized accumulation of epitheloid cells, macrophages and lymphocytes. Granulomas can be found in many infectious, allergic and neoplastic disorders[6]. Although the first description of granuloma in CD was in 1913 by Dalziel[7], the exact role and significance of this "specific" histologic lesion remain a puzzle. It is a plausible idea that the granuloma is the site where the etiological agent resides, the antigen specification occurs and the T cells differentiation into Th1 cells starts[8], but there is no evidence to confirm this theory. The pathological host response is one of the important basic concepts in the development of CD besides the genetic predisposition and the environmental factors. The different individual host response may explain the presence or absence of granuloma.

The first publication which tried to examine whether the presence of granuloma is associated with good or poor prognosis was printed more than forty years ago[9]. A few studies have been published since then which examine the prognostic role of the granuloma, although, their results are controversial. The most studied topic was the postsurgical recurrence of CD. Anseline *et al* examined several factors that might predict recurrence after the operation in 130 patients over a 24-year period. A highly significant positive association was revealed between the presence of the granuloma and the likelihood of recurrence ($P = 0.003$) on the basis of the multivariate regression analysis[10]. A similar tendency was published by Trnka *et al*[11]; they found that there was an increasing chance for the recurrence in a subgroup of patients with ileocolonic disease. On the other hand, some studies suggest just the opposite[12-14]. These publications suggest that patients with granuloma have less frequent postoperative recurrence and/or have a better prognosis. These studies were the pioneers in this topic, therefore the selection of patients, the diagnostic and the statistical methods might have been less accurate than the ones in the latest publication. There has been only some studies so far where the presence of granuloma was determined by endoscopic biopsies[15]. Markowitz *et al*, examined a pediatric population, and rectosigmoid biopsies were taken from 58 subjects. All biopsies had been obtained from newly diagnosed patients before any therapies were started and the children were followed for at least one year. The frequency of granuloma was 32.7%. More severe perianal complications, a higher frequency of surgery and more extensive inflammatory involvement were observed in patients with granuloma. The medical treatment and the need of hospitalization were similar in both groups. Ramzan *et al*[16], published a paper recently in the Inflammatory Bowel Diseases, in which they performed a study with a similar goal like us. Although the granuloma was seeked not only in bioptic samples but also in resected bowel, they found a surprisingly low prevalence (25.6% *vs* our 44.6%), but we do not know how many biopsies were taken from how many and which gastrointestinal segment. The other weak point of this study is the retrospective way of the analysis. Although the crucial point of the study is the frequency of relapse, the authors did not give a definition of the relapse, and it is not very

easy to calculate the number of relapses retrospectively. We have found a higher frequency of granuloma in the biopsies of our patients than Markowitz and Ramzan, however, we took biopsies from more (even intact) segments of the entire gastrointestinal tract. We have examined newly diagnosed patients, and we have also found a more severe clinical course like Markowitz in the first two years of the disease in patients having granuloma in any part of the gastrointestinal tract. As the smoking status of the groups was similar, this environmental factor did not influence our result. Considering that these were the first symptoms and the first examinations of the patients, we can conclude that the onset of CD was also more severe in the granuloma group. Our results, naturally, with small number of cases are not capable to solve the controversy about the prognostic significance of epitheloid granuloma in CD, but suggest that being aware of the fact whether the patient has or has not granuloma is a useful prognostic marker. We propose that all endoscopically available parts of the gastrointestinal tract should be examined histologically as well at the time of the first examination of the patient to search granuloma. The presence of granuloma may suggest a more aggressive form of inflammatory bowel disease and this fact has to influence the management of patients.

REFERENCES

1 **Wolfson DM,** Sachar DB, Cohen A, Goldberg J, Styczynski R, Greenstein AJ, Gelernt IM, Janowitz HD. Granulomas do not affect postoperative recurrence rates in Crohn's disease. *Gastroenterology* 1982; **83**: 405-409

2 **Keller KM,** Bender SW, Kirchmann H, Ball F, Schmitz-Moormann P, Wirth S, Baumann W. Diagnostic significance of epithelioid granulomas in Crohn's disease in children. Multicenter Paediatric Crohn's Disease Study Group. *J Pediatr Gastroenterol Nutr* 1990; **10**: 27-32

3 **Best WR,** Becktel JM, Singleton JW, Kern F. Development of a Crohn's disease activity index. National Cooperative Crohn's Disease Study. *Gastroenterology* 1976; **70**: 439-444

4 **Molnar T,** Papos M, Gyulai C, Ambrus E, Kardos L, Nagy F, Palko A, Pavics L, Lonovics J. Clinical value of technetium-99m-HMPAO-labeled leukocyte scintigraphy and spiral computed tomography in active Crohn's disease. *Am J Gastroenterol* 2001; **96**: 1517-1521

5 **Gasche C,** Scholmerich J, Brynskov J, D'Haens G, Hanauer SB, Irvine EJ, Jewell DP, Rachmilewitz D, Sachar DB, Sandborn WJ, Sutherland LR. A simple classification of Crohn's disease: report of the Working Party for the World Congresses of Gastroenterology, Vienna 1998. *Inflamm Bowel Dis* 2000; **6**: 8-15

6 **Tsai HH**. Other granulomatosus diseases of the bowel. In: Inflammatory bowel diseases. *Churchill Livingstone* 1997: 379-385

7 **Smith MS,** Wakefield AJ. Viral association with Crohn's disease. *Ann Med* 1993; **25**: 557-561

8 **Kakazu T,** Hara J, Matsumoto T, Nakamura S, Oshitani N, Arakawa T, Kitano A, Nakatani K, Kinjo F, Kuroki T. Type 1 T-helper cell predominance in granulomas of Crohn's disease. *Am J Gastroenterol* 1999; **94**: 2149-2155

9 **Antonius JI,** Gump FE, Lattes R, Lepore M. A study of certain microscopic features in regional enteritis, and their possible prognostic significance. *Gastroenterology* 1960; **38**: 889-905

10 **Anseline PF,** Wlodarczyk J, Murugasu R. Presence of granulomas is associated with recurrence after surgery for Crohn's disease: experience of a surgical unit. *Br J Surg* 1997; **84**: 78-82

11 **Trnka YM,** Glotzer DJ, Kasdon EJ, Goldman H, Steer ML, Goldman LD. The long-term outcome of restorative operation in Crohn's disease: influence of location, prognostic factors and surgical guidelines. *Ann Surg* 1982; **196**: 345-355

12 **Glass RE,** Baker WN. Role of the granuloma in recurrent Crohn's disease. *Gut* 1976; **17**: 75-77

13 **Chambers TJ**, Morson BC. The granuloma in Crohn's disease. *Gut* 1979; **20**: 269-274

14 **Wolfson DM,** Sachar DB, Cohen A, Goldberg J, Styczynski R, Greenstein AJ, Gelernt IM, Janowitz HD. Granulomas do not affect postoperative recurrence rates in Crohn's disease. *Gastroenterology* 1982; **83**: 405-409

15 **Markowitz J,** Kahn E, Daum F. Prognostic significance of epithelioid granulomas found in rectosigmoid biopsies at the initial presentation of pediatric Crohn's disease. *J Pediatr Gastroenterol Nutr* 1989; **9**: 182-186

16 **Ramzan NN,** Leighton JA, Heigh RI, Shapiro MS. Clinical significance of granuloma in Crohn's disease. *Inflamm Bowel Dis* 2002; **8**: 168-173

Science Editor Guo SY **Language Editor** Elsevier HK

PO Box 2345, Beijing 100023, China
www.wjgnet.com
wjg@wjgnet.com

ELSEVIER

World J Gastroenterol 2005;11(20):3122-3126
World Journal of Gastroenterology ISSN 1007-9327

• *BRIEF REPORTS* •

Maximum tolerated volume in drinking tests with water and a nutritional beverage for the diagnosis of functional dyspepsia

Aldo Montaño-Loza, Max Schmulson, Sergio Zepeda-Gómez, Jose Maria Remes-Troche, Miguel Angel Valdovinos-Diaz

Aldo Montaño-Loza, Max Schmulson, Sergio Zepeda-Gómez, Jose Maria Remes-Troche, Miguel Angel Valdovinos-Diaz, Department of Gastroenterology, Instituto Nacional de Ciencias Medicas y Nutricion, Salvador Zubiran, Vasco de Quiroga # 15, Tlalpan. CP 14000, México DF
Co-first-authors: Aldo Montaño-Loza and Max Schmulson
Co-correspondents: Aldo Montaño-Loza
Correspondence to: Dr. Miguel Angel Valdovinos-Diaz, Department of Gastroenterology, Instituto Nacional de Ciencias Medicas y Nutricion, Salvador Zubiran, Vasco de Quiroga # 15, Tlalpan. PC 14000, Mexico City, Mexico. mavaldo@quetzal.innsz.mx
Telephone: +5573-34-18 Fax: +56550942
Received: 2004-10-09 Accepted: 2004-12-20

Abstract

AIM: Recently, drinking load tests with water or nutritional beverages have been proposed as diagnostic tools for functional dyspepsia (FD), therefore we sought to reproduce if these tests can discriminate between FD patients and controls in a Mexican population.

METHODS: Twenty FD-Rome II patients were matched by age and gender with 20 healthy controls. All underwent both drinking tests at a 15 mL/min rate, randomly, 7 d apart. Every 5 min within each test, four symptoms were evaluated (satiety, bloating, nausea and pain) by Likert scales. Maximum tolerated volume (MTV) was defined as the ingested volume when a score of 5 was reached for any symptom or when the test had to be stopped because the patients could not tolerate more volume. Sensitivity and specificity were analyzed.

RESULTS: FD patients had higher symptom scores for both tests compared to controls (water: $t = 4.1$, $P = 0.001 < 0.01$; Nutren®: $t = 5.2$, $P = 0.001 < 0.01$). The MTV for water and Nutren® were significantly lower in FD (water: 1014±288 *vs* 1749±275 mL; $t = 7.9$, $P = 0.001 < 0.01$; Nutren®: 652±168 *vs* 1278±286 mL; $t = 6.7$, $P = 0.001 < 0.01$). With the volume tolerated by the controls, the percentile 10 was determined as the lower limit for tolerance. Sensitivity and specificity were 0.90, 0.95 for water and 0.95, 0.95 for Nutren® tests.

CONCLUSION: A drinking test with water or a nutritional beverage can discriminate between FD patients and healthy subjects in Mexico, with high sensitivity and specificity. These tests could be used as objective, noninvasive, and safe diagnostic approaches for FD patients.

Key words: Functional dyspepsia; Water and nutrient drinking load tests; Maximum tolerated volume

Montaño-Loza A, Schmulson M, Zepeda-Gomez S, Remes-Troche JM, Valdovinos-Diaz MA. Maximum tolerated volume in drinking tests with water and a nutritional beverage for the diagnosis of functional dyspepsia. *World J Gastroenterol* 2005; 11(20): 3122-3126
http://www.wjgnet.com/1007-9327/11/3122.asp

INTRODUCTION

Functional dyspepsia (FD) is the second most common functional gastrointestinal disorder, after irritable bowel syndrome[1]. This condition is characterized by chronic, recurrent pain or discomfort in the upper abdomen in the absence of any organic or structural disorder[2]. Its prevalence ranges between 5% and 20% in the general population worldwide[3-7]. The pathogenesis of this entity is complex and it has been related to alterations in gastric motility[8,9] visceral hypersensitivity[10,11] and psychological factors[12]. A significant number of FD patients have a diminished or absent gastric fundic accommodation and this is related with satiety and weight loss[6,7,13]. Also, about 40% of patients with FD have hypersensitivity to mechanical distention that may cause pain, abdominal discomfort, bloating and satiety[14]. Methods to evaluate gastric accommodation and hypersensitivity such as a barostat[15] are invasive, expensive and not readily available, as well as imaging studies to evaluate accommodation such as ultrasound[16,17], SPECT imaging[18] and nuclear medicine studies which also require expertise[19,20]. Yet, the diagnosis of FD is based on symptoms and "lack of organic disease", including a normal upper endoscopy. Therefore the absence of an objective finding increases uncertainty in these patients[21]. Recently, a rapid liquid drinking test with water or a nutritional beverage (Nutridrink) have been used to discriminate FD patients from normal subjects and to identify the presence of hypersensitivity and diminished gastric accommodation[18,22]. These tests can be performed in a short period of time, are of low cost and have no adverse effects. Therefore we sought to reproduce the clinical usefulness of the drinking tests with water and a nutritional beverage to discriminate FD patients from healthy controls and to investigate their sensitivity and specificity.

MATERIALS AND METHODS

Patients

In a prospective controlled study, 20 consecutive patients

with FD fulfilling the Rome II[2] diagnostic criteria (pain or abdominal discomfort centered in the upper abdomen, at least for 12 wk, not necessarily consecutive, in the last 12 mo, with a normal upper gastrointestinal endoscopic examination and absence of any other systemic disease), who consulted a Functional Bowel Disorders and Motility Clinic were included. Upper endoscopies were performed within 3 mo prior to the study. The patients suspended all antisecretory medications including H_2 blockers and proton pump inhibitors, antacids, prokinetics or visceral analgesics, 1 wk prior to the protocol. All patients signed an informed consent and the protocol was approved by the Institutional Committee for Human Research.

Controls

Patients were matched by gender and age (±5 years) with 20 healthy volunteers (controls), recruited from advertisement, without any digestive symptoms and not fulfilling the Rome II criteria for FD, nor any past history of systemic diseases, gastrointestinal surgeries, erosions or ulcers seen on previous upper endoscopic examination or any other imaging study, and who were not taking any medications.

Methods

Drinking tests with water and a nutritional beverage: After an overnight fast of 8 h, patients arrived at the Motility Unit of the Instituto Nacional de Ciencias Medicas y Nutricion, Salvador Zubiran of Mexico City, an academic referral center. They were randomized to begin either with water or the nutritional beverage (Nutren®, Nestle; 1.5 kcal/mL, 51% carbohydrates, 33% lipids, and 16% proteins). Water and Nutren® were ingested at a predetermined rate of 15 mL/min as reported elsewhere[15]. Every 5 min within each drinking test symptoms such as satiety, bloating, nausea and epigastric pain were evaluated by using Likert scales from 0 to 5: 0 = without sensation, 1 = very mild, 2 = mild, 3 = moderate, 4 = severe and 5 = very severe. When a score of 5 was reached for any of the symptoms, or when the subjects could not tolerate any more volume, the tests were stopped and the total ingested volume (mL) was recorded. The maximum tolerated volume (MTV) was defined as the total ingested volume, after the test was stopped. All subjects were asked to score the same symptoms, 1 and 2 h after the tests were completed. Sensitivity and specificity for the drinking tests to discriminate FD from healthy controls were analyzed, considering the Rome II criteria for FD (symptom criteria and a normal endoscopy) as the gold standard for FD diagnosis.

Statistical analysis

The ratings within each 5 min during the test and at the two follow-up periods were analyzed. For each symptom, a score was obtained by the summation of all the ratings within each test divided by the time in minutes of the length of the drinking test and multiplied by 100 (to correct for those who drank longer and had more scores to add up). A total score was obtained by adding all the individual symptom scores. Also, the ratings for each symptom at the follow-up periods were added to obtain the 1 and 2 h scores for water and Nutren®.

Frequencies were expressed in percentages and compared by using Fisher exact test. Symptoms scores and volumes were expressed as mean±SD for each group (FD patients and controls) and comparisons were done by using the *t* test. A $P \leqslant 0.05$ was considered statistically significant. The Pearson (*r*) test was used to establish correlations of the MTV between both drinking tests. The SPSS version 10.0 for Windows was used for the data analysis.

RESULTS

Table 1 depicts age, gender and body mass index (BMI) characteristics of FD patients and controls. There was no statistical difference between the two groups in relation to the BMI.

Table 1 Baseline characteristics

	FD patients (n = 20)	Controls (n = 20)	P
Age (yr)	34±15	31±9	NS
Gender (M/F)	4/16	4/16	NS
BMI (kg/m^2)	23±2.8	23±2.3	NS

BMI: body mass index.

Symptoms

During both tests, the most frequent symptoms reported by FD patients and controls were bloating and satiety. The frequency of symptoms reported during the water test was (FD patients and controls, %): satiety 100 and 65 ($\chi^2 = 5.5$, $P = 0.02<0.05$), bloating 90 and 55 ($\chi^2 = 4.5$, $P = 0.03<0.05$), nausea 65 and 25 ($\chi^2 = 4.9$, $P = 0.02<0.05$), and epigastric pain 45 and 15 ($\chi^2 = 2.9$, $P = 0.08$, NS). Similarly, the frequency of symptoms for the Nutren® test was: satiety 100 and 90 ($\chi^2 = 0.35$, $P = 0.5$, NS), bloating 100 and 70 ($\chi^2 = 4.2$, $P = 0.03<0.05$), nausea 75 and 25 ($\chi^2 = 8.1$, $P = 0.004<0.01$), and epigastric pain 55 and 15 ($\chi^2 = 5.3$, $P = 0.02<0.05$).

FD patients had significantly higher scores for satiety, bloating and pain in the water test, and also significantly higher scores for satiety, bloating, nausea and pain in the Nutren® test (Tables 2 and 3).

Table 2 Symptom scores for the water test

	Bloating	Nausea	Satiety	Pain	Total
FD patients	31.1±16.9	17.8±22.5	41.5±20.5	26.1±27	90.4±11.8
Controls	6.8±7.7	7.5±5.2	12.5±11.1	2.0±2.8	28.8±3.7
P	<0.001	NS	<0.001	<0.001	<0.001

Note: symptoms are shown as mean ± SD.

Table 3 Symptom scores for the Nutren® test

	Bloating	Nausea	Satiety	Pain	Total
FD patients	51.5±18.8	45.5±23.4	76.9±47.1	13.2±14.7	186.7±26.1
Controls	19.4±7.4	15.3±8.6	25.2±9.2	4.2±2.9	64.1±8.9
P	<0.001	<0.001	<0.001	<0.01	<0.001

Note: symptoms are shown as mean ± SD.

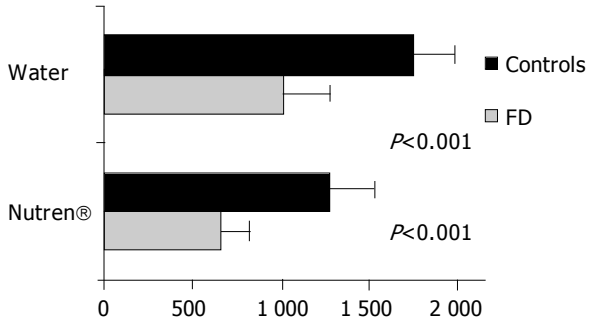

Figure 1 Maximum tolerated volumes of water and Nutren® in healthy controls and FD patients. FD: Functional Dyspepsia.

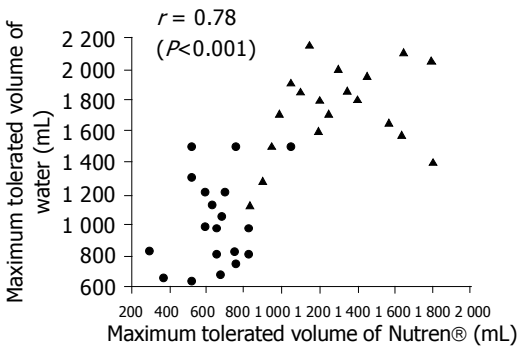

Figure 2 Correlation of maximum tolerated volume (MTV) between water and Nutren® tests in FD patients (●) and healthy controls (▲).

At the 1 h follow-up evaluation for the water test, the symptom scores reported by the FD patients were higher than those reported by controls (9.1±3.2 *vs* 2.9 ± 1.5, $t = 5.6$, $P = 0.001<0.01$). At the 2 h follow-up evaluation, FD patients reported a symptom score of 4.5±4.2, while none of the controls reported any symptoms ($t = 4.9$, $P = 0.001<0.01$). For the Nutren® test, FD patients had significantly higher scores than controls at the 1 and 2 h follow-ups (1 h: 14.3±2.5 *vs* 2.3±0.58, $t = 3.1$, $P = 0.001<0.01$; 2 h: 5.9±1.9 *vs* 1.4±0.84, $t = 2.7$, $P = 0.01<0.05$).

Maximum tolerated volume (MTV)

There were no statistically significant differences in the MTV according to gender both for water (males: 1587±466 mL *vs* females: 1 380±472 mL) and the Nutren® test (males: 1 125±577 mL *vs* females: 935±352 mL).

The MTV for water and Nutren® was significantly lower in FD patients (water: 1 014±288 *vs* 1 749±275 mL; $t = 7.9$, $P = 0.001<0.01$; Nutren®: 652±168 *vs* 1 278±286 mL; $t = 6.7$, $P = 0.001<0.01$; Figure 1). With the volume tolerated by healthy controls, we determined the percentile 10 as the lower limit of the normal range for drinking tolerance. That is ⩾1 200 mL for females and ⩾1 400 mL for males in the water test, and ⩾900 mL for females and ⩾1 200 mL for males in the Nutren®.

Considering these limits, 18 out of 20 patients with FD had abnormal results (lower tolerated volume) for the water test compared to only one control, and 19 FD patients had lower tolerated volumes in the Nutren® test compared to one of the healthy controls. The sensitivity and specificity of the drinking test with water was 0.90 (CI 95% 0.69-0.97) and 0.95 (CI 95% 0.76-0.99), respectively. For the Nutren® test, sensitivity and specificity was 0.95 (CI 95% 0.76-0.99), and 0.95 (CI 95% 0.76-0.99), respectively.

Correlation between both drinking tests

There was a significant correlation in the MTV between the water and the Nutren® tests ($r = 0.78$, $P = 0.001<0.01$; Figure 2).

DISCUSSION

In the current study we evaluated two drinking load tests [water and a nutritional beverage (Nutren®)] in Mexican patients with FD and healthy controls, and we have shown that more than 85% of the patients have a decreased tolerance for drinking capacity. In addition, we found that both tests induced dyspeptic symptoms such as bloating, nausea, satiety and epigastric pain more frequently in patients than in controls, and the first ones reported the symptoms earlier and with lower ingested volumes. Also, when compared to the Rome II criteria (symptom criteria and negative upper endoscopy) as the gold standard for diagnosing FD, the sensitivity and specificity for the water and Nutren® drinking tests have shown that both are useful tools to discriminate patients from healthy subjects. These results reproduced the data reported by other groups. In an Italian study using a water load test, the maximum tolerated volume was significantly lower in FD patients than controls and scores for satiety, pain, nausea, fullness and bloating were higher for the latter ones[19]. Another study found that a caloric drinking test distinguished FD patients with or without early satiety[23]. Using mineral water at a rate of 100 mL/min in a Nordic population, maximal water intake was significantly lower in FD patients than healthy controls[22].

Several possibilities can explain the above findings. Using transabdominal ultrasound, Gilja *et al*[16], reported that in response to a soup meal, FD patients had smaller sizes and higher emptying fractions of the proximal stomach and they reported more symptoms than controls. Tack *et al*[15], reported that this impaired gastric accommodation to a meal was found in 40% of patients with FD and was associated with symptoms of early satiety in a multivariate analysis. Previously, Boeckxstaens *et al*[23], reported that FD patients had a lower drinking capacity for both water and a caloric liquid, compared to healthy volunteers or patients with mild dyspeptic symptoms, and that FD patients developed significantly more symptoms than the healthy volunteers after both tests. In contrast to our findings, they also reported that compared to women, men consumed significantly more water and Nutridrink®, a nutritional beverage with the same composition as the Nutren® used in our study. Finally, in their study, drinking capacity did not predict impaired fundic accommodation or visceral hypersensitivity.

The speed of liquid ingestion in the oral load tests is controversial and may explain the differences among the studies. Boeckxstaens *et al*[23], tested water and Nutridrink® at a fast ingestion rate of 100 mL/min, and showed a diminished tolerance for liquid ingestion only in 50% of FD patients. In a more recent study, Tack *et al*[11], showed that a

liquid ingestion of a caloric drink at a speed of 15 mL/min induced symptoms of satiety in FD patients, and a significant correlation existed between the amount of calories ingested during the satiety testing and the amplitude of the gastric accommodation. The same group of researchers found that the gastric accommodation is a slow-onset reflex presenting in a gradual manner and reaching its maximal relaxation 15 min after ingestion of a meal[14].

The duration of the rapid drinking test is clearly lower than the time required for full development of the accommodation reflex[24].

Based on the above data, in the current study we used the predetermined speed of liquid ingestion of 15 mL/min. The maximum ingested volume of a nutritional drink depends on the balance between mechanisms that increase the gastric volume (fundic relaxation) and the negative feedback that slows gastric emptying and induces symptoms after a meal. In the absence of nutrients, other mechanisms that limit liquid ingestion in FD patients should be considered. The gastric and duodenal distention may trigger vaso-vagal reflexes that result in proximal gastric relaxation and induction of satiety and fullness[25-27]. The vaso-vagal reflexes could also be activated during a test with water. In our study, the finding of a greater tolerance of water volume ingestion than that of a nutritional drink by healthy volunteers suggests that the feedback mechanisms induced by nutrients are activated before the reflexes are induced by distention[28-30]. Interestingly, our patients with FD had similarly low water and nutritional beverage tolerated volumes, suggesting a decreased threshold for the activation for both reflexes[31,32].

The gastric accommodation disturbances[11,33,34] and proximal gastric mechanical distention hypersensitivity[35,36] are recognized as the most important pathogenic mechanisms in FD. The gastric barostat test is considered the "gold standard" for the evaluation of the proximal gastric accommodation in response to a meal; however, this is an invasive, time-consuming, and not readily available test. There is a need of less expensive, non-invasive and highly available diagnostic tests for FD that can provide an objective diagnosis to the patients. Whether an abnormal fundic relaxation in response to a meal, an abnormal distribution of the gastric contents, or gastric hypersensitivity are the causes of dyspeptic symptoms in response to a drinking load test, is unknown. Furthermore, hypersensitivity in functional dyspepsia is associated with abnormal gastric accommodation[18-22] and hyperalgesia, and cofactors of this hypersensitivity are likely to be wall tension and the function of visceral afferents[10,32,35]. The high percentage of FD patients with impaired drinking capacity in our study, supports a multifactorial component in symptoms generation, and together with the high sensitivity and specificity, for discriminating FD from healthy controls by using the Rome II criteria, including symptoms and a negative endoscopy as the gold standard for diagnosis, provides a simple test for patients with a disease where the absence of an objective diagnosis, creates anxiety and a continuous search for an answer.

In Mexico, functional gastrointestinal disorders are the main reason for consulting a gastroenterologist, with FD being the second most frequent disorder following IBS[4]. Lydeard and Jones have reported that FD patients seeking health care are more preoccupied that their symptoms might be related to cancer compared to those who do not consult[37]. Effective well-founded reassurance that no serious disease is present is an important outcome of medical intervention, but patients consider that medical explanations are not sufficient to clarify the nature of their condition and negative results of paraclinical investigations may be taken as "bad news" driving patients to keep consulting in search of an objective diagnosis. Anxiety has been found to be an independent factor associated with health-care seeking in FD[38]. Other psychosocial factors including abnormal illness attitudes and beliefs have been found to characterize those patients who seek help versus those that do not[39]. Furthermore, physicians also lack confidence in their functional diagnosis. In a British study, clinicians reported confidence in 63-91% of their organic diagnosis compared to only 48% of FD diagnosis[40]. This difference was related to the possibility of an objective confirmation of organic disease by using paraclinical investigations. The absence of confidence in functional diagnosis may drive clinicians to order more investigations that may increase the anxiety and the fear of a more serious disorder in functional patients. Therefore, a drinking loading test may be a potential tool for an objective diagnosis in patients consulting for FD.

Both drinking tests caused more symptoms in patients with FD than in healthy controls. In the future, it would be useful to find which test (water or nutritional beverage) has a more diagnostic importance. Meanwhile, we considered that both are easy to perform, available, safe, non-invasive and useful to discriminate FD patients from healthy volunteers. Furthermore, these tests could be used in future studies to evaluate the effect of new treatments in the management of postprandial symptoms in patients with FD.

In conclusion, a drinking load test with water or a nutritional beverage at a slow drinking rate of 15 mL/min, can discriminate FD patients from controls in a simple, non-invasive, safe and available manner. Our findings in a group of Mexican patients with FD, are in accordance with previously reported studies. The gastric distention produced by the volume of water or nutritional beverage reproduces the symptoms of FD and suggests a multifactorial origin for symptom generation, including impairment in gastric sensitivity and proximal accommodation. The current data supports the potential usefulness of liquid loading tests to provide FD patients with an objective diagnosis in a disease with otherwise no objective diagnostic data rather than clinical criteria, and with a potential use in the evaluation of future treatments.

REFERENCES

1 **Chang L.** Review article: epidemiology and quality of life in functional gastrointestinal disorders. *Aliment Pharmacol Ther* 2004; **20** Suppl 7: 31-39
2 **Talley NJ,** Stanghellini V, Heading RC, Koch KL, Malagelada JR, Tytgat GN. Functional gastroduodenal disorders. *Gut* 1999; **45** Suppl 2: II37-II42
3 **Agréus L**. The epidemiology of functional gastrointestinal disorders. *Eur J Surg Suppl* 1998; **583**: 60-66
4 **Huerta I,** Valdovinos MA, Schmulson M. Irritable bowel syn-

drome in Mexico. *Dig Dis* 2001; **19**: 251-257
5 **Gschossmann JM,** Haag S, Holtmann G. Epidemiological trends of functional gastrointestinal disorders. *Dig Dis* 2001; **19**: 189-194
6 **Locke GR.** Prevalence, incidence and natural history of dyspepsia and functional dyspepsia. *Baillieres Clin Gastroenterol* 1998; **12**: 435-442
7 **Kawamura A,** Adachi K, Takashima T, Yuki M, Ono M, Kinoshita Y. Prevalence of irritable bowel syndrome and its relationship with Helicobacter pylori infection in a Japanese population. *Am J Gastroenterol* 2001; **96**: 1946
8 **Talley NJ,** Silverstein MD, Agréus L, Nyrén O, Sonnenberg A, Holtmann G. AGA technical review: evaluation of dyspepsia. American Gastroenterological Association. *Gastroenterology* 1998; **114**: 582-595
9 **Bredenoord AJ,** Chial HJ, Camilleri M, Mullan BP, Murray JA. Gastric accommodation and emptying in evaluation of patients with upper gastrointestinal symptoms. *Clin Gastroenterol Hepatol* 2003; **1**: 264-272
10 **Feinle-Bisset C,** Vozzo R, Horowitz M, Talley NJ. Diet, food intake, and disturbed physiology in the pathogenesis of symptoms in functional dyspepsia. *Am J Gastroenterol* 2004; **99**: 170-181
11 **Tack J,** Caenepeel P, Fischler B, Piessevaux H, Janssens J. Symptoms associated with hypersensitivity to gastric distention in functional dyspepsia. *Gastroenterology* 2001; **121**: 526-535
12 **Fischler B,** Tack J, De Gucht V, Shkedy ZI, Persoons P, Broekaert D, Molenberghs G, Janssens J. Heterogeneity of symptom pattern, psychosocial factors, and pathophysiological mechanisms in severe functional dyspepsia. *Gastroenterology* 2003; **124**: 903-910
13 **Tack J,** Bisschops R, Sarnelli G. Pathophysiology and treatment of functional dyspepsia. *Gastroenterology* 2004; **127**: 1239-1255
14 **Tack J,** Demedts I, Dehondt G, Caenepeel P, Fischler B, Zandecki M, Janssens J. Clinical and pathophysiological characteristics of acute-onset functional dyspepsia. *Gastroenterology* 2002; **122**; 1738-1747
15 **Tack J,** Piessevaux H, Coulie B, Caenepeel P, Janssens J. Role of impaired gastric accommodation to a meal in functional dyspepsia. *Gastroenterology* 1998; **115**: 1346-1352
16 **Gilja OH,** Hausken T, Wilhelmsen I, Berstad A. Impaired accommodation of proximal stomach to a meal in functional dyspepsia. *Dig Dis Sci* 1996; **41**: 689-696
17 **De Schepper HU,** Cremonini F, Chitkara D, Camilleri M. Assessment of gastric accommodation: overview and evaluation of current methods. *Neurogastroenterol Motil* 2004; **16**: 275-285
18 **Kim DY,** Delgado-Aros S, Camilleri M, Samsom M, Murray JA, O'Connor MK, Brinkmann BH, Stephens DA, Lighvani SS, Burton DD. Noninvasive measurement of gastric accommodation in patients with idiopathic nonulcer dyspepsia. *Am J Gastroenterol* 2001; **96**: 3099-3105
19 **Tossetti C,** Salvioli B, Stanghellini V, Cogliandro L, Cogliandro R, Marra MG, De Giorgio R, Mazzotta E, Zamboni P, Corinaldesi R. Reproducibility of a water load test in healthy subject's symptom profile compared to patients with functional dyspepsia. *Gastroenterology* 1999; **116**(S): A 336
20 **Cuommo R,** Sarnelli G, Grasso R, Alfieri M, Niccolai E. Early satiety in functional dyspepsia: validity of a caloric drinking test and relation to gastric emptying dyspepsia. *Gastroenterology* 1999; **116**(S): A142
21 **Simrén M,** Tack J. Functional dyspepsia: evaluation and treatment. *Gastroenterol Clin North Am* 2003; **32**: 577-599
22 **Strid H,** Norstrom M, Sjober J, Simren M, Svedlund J, Abrahamsson H, Bjornsson ES. Impact of sex and psychological factors on the water loading test in functional dyspepsia. *Scand J Gastroenterol* 2001; **36**: 725-730
23 **Boeckxstaens GE,** Hirsch DP, van den Elzen BD, Heisterkamp SH, Tytgat GN. Impaired drinking capacity in patients with functional dyspepsia: relationship with proximal stomach function. *Gastroenterology* 2001; **121**: 1054-1063
24 **Tack J.** Drink tests in functional dyspepsia. *Gastroenterology* 2002; **122**: 2093-2094; author reply 2094-2095
25 **Azpiroz F,** Malagelada JR. Perception and reflex relaxation of the stomach in response to gut distention. *Gastroenterology* 1990; **98**: 1193-1198
26 **Ladabaum U,** Koshy SS, Woods ML, Hooper FG, Owyang C, Hasler WL. Differential symptomatic and electrogastrographic effects of distal and proximal human gastric distension. *Am J Physiol* 1998; **275**: G418-G424
27 **Coffin B,** Azpiroz F, Guarner F, Malagelada JR. Selective gastric hypersensitivity and reflex hyporeactivity in functional dyspepsia. *Gastroenterology* 1994; **107**: 1345-1351
28 **Barbera R,** Feinle C, Read NW. Abnormal sensitivity to duodenal lipid infusion in patients with functional dyspepsia. *Eur J Gastroenterol Hepatol* 1995; **7**: 1051-1057
29 **Feinle C,** Meier O, Otto B, D'Amato M, Fried M. Role of duodenal lipid and cholecystokinin A receptors in the pathophysiology of functional dyspepsia. *Gut* 2001; **48**: 347-355
30 **Samsom M,** Verhagen MA, vanBerge Henegouwen GP, Smout AJ. Abnormal clearance of exogenous acid and increased acid sensitivity of the proximal duodenum in dyspeptic patients. *Gastroenterology* 1999; **116**: 515-520
31 **Vingerhagen S,** Hausken T, Gilja OH, Berstad A. Influence of a 5HT1 receptor agonist on gastric accommodation and initial transpyloric flow in healthy subjects. *Neurogastroenterol Motil* 2000; **12**: 95-101
32 **Koch KL,** Hong SP, Xu L. Reproducibility of gastric myoelectrical activity and the water load test in patients with dysmotility-like dyspepsia symptoms and in control subjects. *J Clin Gastroenterol* 2000; **31**: 125-129
33 **Thumshirn M,** Camilleri M, Saslow SB, Williams DE, Burton DD, Hanson RB. Gastric accommodation in non-ulcer dyspepsia and the roles of *Helicobacter pylori* infection and vagal function. *Gut* 1999; **44**: 55-64
34 **Salet GA,** Samsom M, Roelofs JM, van Berge Henegouwen GP, Smout AJ, Akkermans LM. Responses to gastric distension in functional dyspepsia. *Gut* 1998; **42**: 823-829
35 **Mertz H,** Fullerton S, Naliboff B, Mayer EA. Symptoms and visceral perception in severe functional and organic dyspepsia. *Gut* 1998; **42**: 814-822
36 **Lemann M,** Dederding JP, Flourie B, Franchisseur C, Rambaud JC, Jian R. Abnormal perception of visceral pain in response to gastric distension in chronic idiopathic dyspepsia. The irritable stomach syndrome. *Dig Dis Sci* 1991; **36**: 1249-1254
37 **Lydeard S,** Jones R. Factors affecting the decision to consult with dyspepsia: comparison of consulters and non-consulters. *J R Coll Gen Pract* 1989; **39**: 495-498
38 **Hu WH,** Wong WM, Lam CL, Lam KF, Hui WM, Lai KC, Xia HX, Lam SK, Wong BC. Anxiety but not depression determines health care-seeking behaviour in Chinese patients with dyspepsia and irritable bowel syndrome: a population-based study. *Aliment Pharmacol Ther* 2002; **16**: 2081-2088
39 **Koloski NA,** Talley NJ, Boyce PM. Predictors of health care seeking for irritable bowel syndrome and nonulcer dyspepsia: a critical review of the literature on symptom and psychosocial factors. *Am J Gastroenterol* 2001; **96**: 1340-1349
40 **Cann PA,** Gleeson MH, Robinson TJ, Wicks AC. Assessing dyspepsia in general practice. *Br J Clin Pract* 1994; **48**: 263-267

Science Editor Guo SY **Language Editor** Elsevier HK

PO Box 2345, Beijing 100023, China
www.wjgnet.com
wjg@wjgnet.com

ELSEVIER

World J Gastroenterol 2005;11(20):3127-3130
World Journal of Gastroenterology ISSN 1007-9327

• *BRIEF REPORTS* •

Portal hypertensive colopathy in patients with liver cirrhosis

Keiichi Ito, Katsuya Shiraki, Takahisa Sakai, Hitoshi Yoshimura, Takeshi Nakano

Keiichi Ito, Katsuya Shiraki, Takahisa Sakai, Hitoshi Yoshimura, Takeshi Nakano, First Department of Internal Medicine, Mie University School of Medicine, 2-174 Edobashi, Tsu, Mie 514-8507, Japan
Correspondence to: Katsuya Shiraki, MD, PhD, First Department of Internal Medicine, Mie University School of Medicine, 2-174 Edobashi, Tsu, Mie 514-8507, Japan. katsuyas@clin.medic.mie-u.ac.jp
Telephone: +81-592-31-5015 Fax: +81-592-31-5201
Received: 2004-06-19 Accepted: 2004-11-04

Abstract

AIM: In patients with liver cirrhosis and portal hypertension, portal hypertensive colopathy is thought to be an important cause of lower gastrointestinal hemorrhage. In this study, we evaluated the prevalence of colonic mucosal changes in patients with liver cirrhosis and its clinical significance.

METHODS: We evaluated the colonoscopic findings and liver function of 47 patients with liver cirrhosis over a 6-year period. The main cause of liver cirrhosis was post-viral hepatitis (68%) related to hepatitis B (6%) or C (62%) infection. All patients underwent upper gastrointestinal endoscopy to examine the presence of esophageal varices, cardiac varices, and congestive gastropathy, as well as a full colonoscopy to observe changes in colonic mucosa. Portal hypertensive colopathy was defined endoscopically in patients with vascular ectasia, redness, and blue vein. Vascular ectasia was classified into two types: type 1, solitary vascular ectasia; and type 2, diffuse vascular ectasia.

RESULTS: Overall portal hypertensive colopathy was present in 31 patients (66%), including solitary vascular ectasia in 17 patients (36%), diffuse vascular ectasia in 20 patients (42%), redness in 10 patients (21%) and blue vein in 6 patients (12%). As the Child-Pugh class increased in severity, the prevalence of portal hypertensive colopathy rose. Child-Pugh class B and C were significantly associated with portal hypertensive colopathy. Portal hypertensive gastropathy, esophageal varices, ascites and hepatocellular carcinoma were not related to occurrence of portal hypertensive colopathy. Platelet count was significantly associated with portal hypertensive colopathy, but prothrombin time, serum albumin level, total bilirubin level and serum ALT level were not related to occurrence of portal hypertensive colopathy.

CONCLUSION: As the Child-Pugh class worsens and platelet count decreases, the prevalence of portal hypertensive colopathy increases in patients with liver cirrhosis. A colonoscopic examination in patients with liver cirrhosis is indicated, especially those with worsening Child-Pugh class and/or decreasing platelet count, to prevent complications such as lower gastrointestinal bleeding.

Key words: Portal hypertensive colopathy; Liver cirrhosis

Ito K, Shiraki K, Sakai T, Yoshimura H, Nakano T. Portal hypertensive colopathy in patients with liver cirrhosis. *World J Gastroenterol* 2005; 11(20): 3127-3130
http://www.wjgnet.com/1007-9327/11/3127.asp

INTRODUCTION

Liver cirrhosis causes multiple complications, including esophageal varices due to portal hypertension. In comparison with alcohol-related etiologies of liver cirrhosis in Europe and America, liver cirrhosis due to post-viral infection, especially HCV infection, is more predominant in Japan. In patients with liver cirrhosis and portal hypertension, varices of the esophagus, stomach and portal hypertensive gastropathy are well described[1-3]. These complications are the most common causes of gastrointestinal hemorrhage. Recently, colorectal mucosal lesions in patients with liver cirrhosis were reported as portal hypertensive colopathy[4-7]. These are thought to be important causes of lower gastrointestinal hemorrhage[8], although the clinical importance of these lesions in patients with portal hypertensive colopathy is not well established. In this study, we evaluated the prevalence of colonic mucosal changes in patients with liver cirrhosis, especially that due to post-viral infection HCV, and its clinical significance.

MATERIALS AND METHODS

Patients

We evaluated the liver function and colonoscopic findings in 47 patients with liver cirrhosis over a 6-year period. Liver cirrhosis was confirmed by histology or by compatible physical findings, laboratory data, and radiographic features. The etiologies of cirrhosis are shown in Table 1. The main cause of liver cirrhosis was post-viral hepatitis (68%) related to hepatitis B (6%) or C (62%) infection. In addition, 13 patients (27%) had hepatocellular carcinoma.

Methods

An upper gastrointestinal endoscopy was performed in all patients to evaluate the presence of esophageal varices, cardiac varices, and congestive gastropathy. Liver disease

severity was assessed according to Child-Pugh's classification. All patients underwent a full colonoscopy with anti-cholinergic drugs, after preparation with polyethylene glycol electrolyte solution. Noted changes in colonic mucosa included the number, size, and location of vascular lesions. Portal hypertensive colopathy was defined endoscopically in patients with vascular ectasia, redness (Figure 1), and blue vein (Figure 2). Vascular ectasia was further classified into two types: type 1, solitary vascular ectasia (Figure 3); and type 2, diffuse vascular ectasia (Figure 4). Results from multiple, independent observers were compiled to determine the prevalence of portal hypertensive colopathy.

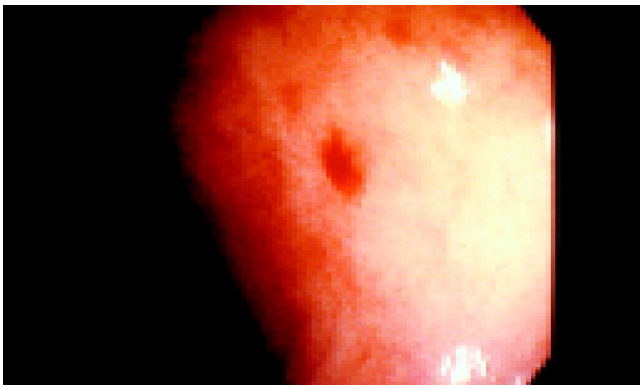

Figure 1 Colonoscopic examination shows redness.

Figure 2 Colonoscopic examination shows a blue vein.

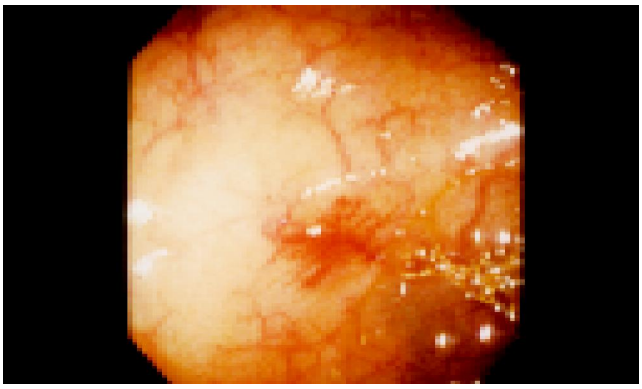

Figure 3 Colonoscopic examination shows a solitary vascular ectasia.

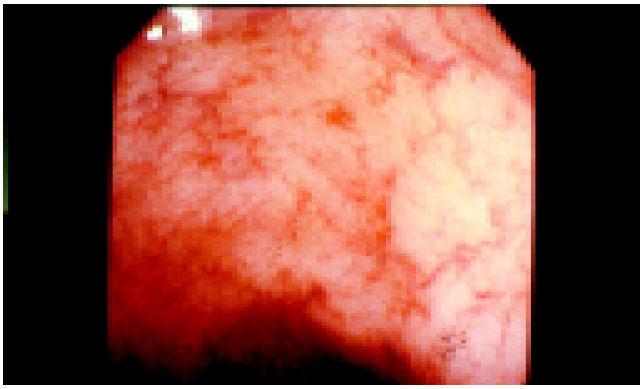

Figure 4 Colonoscopic examination shows diffuse vascular ectasia.

Table 1 Etiologies of liver cirrhosis

Diagnosis	Patients(*n*)
HCV	29
HBV	3
Non-Bnon-C	5
Alcohol	5
AIH	3
PBC	2

AIH: autoimmune hepatitis, PBC: primary biliary cirrhosis.

Statistical analyses

Data are expressed as mean±SD. Statistical comparisons were made with the χ^2 test. A P value less than 0.05 was considered significant.

RESULTS

In our cirrhotic patients, the primary indications for colonoscopy included a positive fecal occult blood test in 16 (34%), melena in 11 (23%), iron deficiency anemia in 5 (10%), diarrhea in 2 (4%), abdominal pain in 2 (4%), high level of serum CEA in 2 (4%), and screening in 5 (10%) patients. Overall portal hypertensive colopathy was present in 31 patients (66%), whereas vascular ectasia was observed in 17 (36%), diffuse vascular ectasia in 20 (42%), redness in 10 (21%) and blue vein in 6 (12%) patients.

The clinical characteristics of the cirrhotic patients with or without portal hypertensive colopathy are shown in Table 2. As the Child-Pugh class worsened, the prevalence of portal hypertensive colopathy increased. Child-Pugh class B and C were significantly associated with portal hypertensive colopathy. Portal hypertensive gastropathy, esophageal varices, hepatocellular carcinoma, and presence of ascites were not related to occurrence of portal hypertensive colopathy.

The laboratory data of these patients are shown in Table 3. Platelet count but not serum ALT level was significantly associated with portal hypertensive colopathy. The prothrombin time as well as serum albumin and total bilirubin levels were not related to the occurrence of portal hypertensive colopathy.

Table 2 Characteristics of the 47 patients

		PHC-positive $n = 31$ (%)	PHC-negative $n = 16$ (%)	*P*
Age (yr)		62.5±7.3	61.6±9.7	NS
Sex	(M:F)	18:13	13:3	NS
Child–Pugh	(A:B+C)	11:20	12:4	$P<0.05$
PHG	None	23 (76.7)	10 (62.5)	NS
	Mild	5	5	NS
	Severe	2	1	NS
Ascites		3 (9.7)	1 (6.3)	NS
Splenomegaly		24 (77.4)	11 (68.8)	NS
Alcohol		4 (12.9)	3 (18.8)	NS
HCC		7 (22.6)	6 (37.5)	NS
EG varices		17 (54.8)	5 (31.3)	NS

PHC: portal hypertensive colopathy, PHG: portal hypertensive gastropathy, HCC: hepatocellular carcinoma, EG varices: esophago-gastric varices.

Table 3 Laboratory data of the 47 patients

	PHC-positive $n = 31$	PHC-negative $n = 16$	*P*
Prothrombin time (%)	74.0±15.7	81.4±21.7	NS
ALT (IU/L)	51.1±33.8	55.9±41.8	NS
Platelet ($\times 10^4/mm^3$)	8.3±4.3	12.1±5.1	$P<0.05$
Serum albumin (g/dL)	3.2±0.6	3.4±0.5	NS
Total bilirubin (mg/dL)	1.55±0.94	1.08±0.73	NS
Cholinesterase (△pH)	0.48±0.27	0.55±0.21	NS
ICG R15	30.5±15.4	25.0±9.6	NS

ICG R15: indocyanine green retention rate at 15 min.

DISCUSSION

Various vascular abnormalities have been observed in the mucosa of upper gastrointestinal tract of cirrhotic patients, including gastroesophageal varices and gastric antral vascular ectasia[1-3]. These vascular lesions account for most of the upper gastrointestinal bleeding in cirrhotic patients. Similarly, vascular ectasias and varices may occur in the colonic mucosa of cirrhotic patients, and bleeding from these vascular lesions was reported[4,5]. In the present study, portal hypertensive colopathy was present in 66% (31/47) of the cirrhotic patients. Several studies have described the colonic findings associated with cirrhosis and portal hypertension was observed in 50-84% patients with liver cirrhosis[6-15]. Histologic examination of rectal mucosal lesions in patients with liver cirrhosis revealed dilatation of blood vessels in the mucosa, increased lymphocytes and plasma cells in the lamina propria, and edema of the mucosa[4,7]. In our study, portal hypertensive colopathy was found in 23% of patients in rectosigmoid colon, 11% in the descending colon, 24% in the transverse colon, 23% in the ascending colon and 16% in the cecum.

We classified the portal hypertensive colopathy into four types. Solitary vascular ectasias were found predominantly in the transverse and ascending colon (55%). Diffuse vascular ectasias were found predominantly in the right side colon (45%). Redness was found in the overall colon and blue vein in the rectum. In contrast to prior studies[4,6-10,12-14]. Our data demonstrated that the prevalence of portal hypertensive colopathy increased with worsening Child-Pugh class. The association with Child-Pugh class may be a result of increased hemodynamic dysfunction in those with more advanced liver disease. A decreased platelet count was also related to occurrence of portal hypertensive colopathy, which to our knowledge has not been reported previously. It is possible that the concurrent low platelet count and portal hypertensive colopathy may be due to a relatively high number of patients with post-viral infection in this Japanese cohort as post-viral liver cirrhosis decreases platelet count more than alcoholic liver cirrhosis does.

Child-Pugh class A, presence of ascites, prothrombin time, serum albumin level, and total bilirubin level were not related to occurrence of portal hypertensive colopathy. However, as Child-Pugh class worsened, the prevalence of portal hypertensive colopathy correspondingly increased. Synthetic liver function is important for the prevalence of portal hypertensive colopathy. Similar to the prior studies[16-18], we also observed that esophageal varices were not related to portal hypertensive colopathy. Portal hypertensive colopathy may not be a distinct entity but, rather, a regional manifestation of portal hypertension[15]. Lower gastrointestinal bleeding is the major complication of portal hypertensive colopathy. In our study, active oozing colonic lesions were found in two cases of 11 cirrhotic patients with melena. These patients underwent endoscopic clipping for treatment of active bleeding, but bleeding recurred. Each case was Child-Pugh class B and had decreasing platelet count. Therefore, we suggest that a colonoscopic examination should be performed in patients with liver cirrhosis, especially those with worsening Child-Pugh class and decreasing platelet count.

In conclusion, as the Child-Pugh class worsens and platelet count decreases, the prevalence of portal hypertensive colopathy increases in patients with liver cirrhosis. Colonoscopic examination is needed in these patients, especially those with worsening Child-Pugh class and decreasing platelet count, to prevent complications, such as lower gastrointestinal bleeding.

REFERENCES

1 **Viggiano TR**, Gostout CJ. Portal hypertensive intestinal vasculopathy: a review of the clinical, endoscopic, and histopathologic features. *Am J Gastroenterol* 1992; **87**: 944-954
2 **Arendt T**, Barten M, Lakner V, Arendt R. Diffuse gastric antral vascular ectasia: cause of chronic gastrointestinal blood loss. *Endoscopy* 1987; **19**: 218-220
3 **Gostout CJ**, Viggiano TR, Balm RK. Acute gastrointestinal bleeding from portal hypertensive gastropathy: prevalence and clinical features. *Am J Gastroenterol* 1993; **88**: 2030-2033
4 **Kozarek RA**, Botoman VA, Bredfeldt JE, Roach JM, Patterson DJ, Ball TJ. Portal colopathy: prospective study of colonoscopy in patients with portal hypertension. *Gastroenterology* 1991; **101**: 1192-1197
5 **Naveau S**, Bedossa P, Poynard T, Mory B, Chaput JC. Portal hypertensive colopathy. A new entity. *Dig Dis Sci* 1991; **36**: 1774-1781
6 **Tam TN**, NG WW, Lee SD. Colonic mucosal changes in patients with liver cirrhosis. *Gastrointest Endosc* 1995; **42**: 408-412
7 **Bini EJ**, Lascarides CE, Micale PL, Weinshel EH. Mucosal abnormalities of the colon in patients with portal hypertension: an endoscopic study. *Gastrointest Endosc* 2000; **52**: 511-516
8 **Weinshel E**, Chen W, Falkenstein DB, Kessler R, Raicht RF.

Hemorrhoids or rectal varices: defining the cause of massive rectal hemorrhage in patients with portal hypertension. *Gastroenterology* 1986; **90**: 744-747

9 **Wang M**, Desigan G, Dunn D. Endoscopic sclerotherapy for bleeding rectal varices: a case report. *Am J Gastroenterol* 1985; **80**: 779-780

10 **Wilson SE**, Stone RT, Christie JP, Passaro E. Massive lower gastrointestinal bleeding from intestinal varices. *Arch Surg* 1979; **114**: 1158-1161

11 **Chen LS**, Lin HC, Lee FY, Hou MC, Lee SD. Portal hypertensive colopathy in patients with cirrhosis. *Scand J Gastroenterol* 1996; **31**: 490-494

12 **Rabinovitz M**, Schade RR, Dindzans VJ, Belle SH, Van Thiel DH, Gavaler JS. Colonic disease in cirrhosis. An endoscopic evaluation in 412 patients. *Gastroenterology* 1990; **99**: 195-199

13 **Scandalis N**, Archimandritis A, Kastanas K, Spiliadis C, Delis B, Manika Z. Colonic findings in cirrhotics with portal hypertension. A prospective colonoscopic and histological study. *J Clin Gastroenterol* 1994; **18**: 325-328; discussion 329

14 **Goenka MK**, Kochhar R, Nagi B, Mehta SK. Rectosigmoid varices and other mucosal changes in patients with portal hypertension. *Am J Gastroenterol* 1991; **86**: 1185-1189

15 **Ganguly S**, Sarin SK, Bhatia V, Lahoti D. The prevalence and spectrum of colonic lesions in patients with cirrhotic and noncirrhotic portal hypertension. *Hepatology* 1995; **21**: 1226-1231

16 **Misra SP**, Dwivedi M, Misra V. Prevalence and factors influencing hemorrhoids, anorectal varices, and colopathy in patients with portal hypertension. *Endoscopy* 1996; **28**: 340-345

17 **Bresci G**, Gambardella L, Parisi G, Federici G, Bertini M, Rindi G, Metrangolo S, Tumino E, Bertoni M, Cagno MC, Capria A. Colonic disease in cirrhotic patients with portal hypertension: an endoscopic and clinical evaluation. *J Clin Gastroenterol* 1998; **26**: 222-227

18 **Yamakado S**, Kanazawa H, Kobayashi M. Portal hypertensive colopathy: endoscopic findings and the relation to portal pressure. *Intern Med* 1995; **34**: 153-157

Science Editor Zhu LH and Guo SY **Language Editor** Elsevier HK

PO Box 2345, Beijing 100023, China
www.wjgnet.com
wjg@wjgnet.com

ELSEVIER

World J Gastroenterol 2005;11(20):3131-3134
World Journal of Gastroenterology ISSN 1007-9327

• *BRIEF REPORTS* •

High level of hepatitis B virus DNA after HBeAg-to-anti-HBe seroconversion is related to coexistence of mutations in its precore and basal core promoter

Xiao-Mou Peng, Gui-Mei Huang, Jian-Guo Li, Yang-Su Huang, Yong-Yu Mei, Zhi-Liang Gao

Xiao-Mou Peng, Gui-Mei Huang, Jian-Guo Li, Yang-Su Huang, Yong-Yu Mei, Zhi-Liang Gao, Department of Infectious Diseases, the Third Affiliated Hospital, Sun Yat-Sen University, Guangzhou 510630, Guangdong Province, China
Supported by the Science Foundation of Guangdong Province, No. 99M04801G
Correspondence to: Xiao-Mou Peng, Department of Infectious Diseases, the Third Affiliated Hospital, Sun Yat-Sen University, Guangzhou 510630, Guangdong Province, China. xiaomoupeng@hotmail.com
Telephone: +86-20-85516867-2019 Fax: +86-20-85515940
Received: 2004-07-09 Accepted: 2004-09-24

Abstract

AIM: G1896A mutation in precore or A1762T/G1764A mutations in basal core promoter are suspected to be responsible for patients with detectable level of HBV DNA in serum after seroconversion from HBeAg to anti-HBe. However, G1896A variant has impaired, while A1762T/G1764A variant may have intact replication ability. They themselves or their coexistence status may play different roles in such meaningless seroconversion. For these reasons, the significances of these two types of mutations were comparatively investigated in this study.

METHODS: One hundred and sixty-five sera with positive anti-HBe and HBV DNA were collected from different patients. Mutations of G1896A and A1762T/G1764A among these serum samples were detected using competitively differentiated PCR. HBV DNA was demonstrated using real-time quantitative PCR.

RESULTS: G1896A and/or A1762T/G1764A mutations were detected in 89.1% (147/165) out of patients with detectable HBV DNA in serum after HBeAg-to-anti-HBe seroconversion. The positive rate of G1896A variants was significantly higher than that of A1762T/G1764A mutations (77.6% *vs* 50.3%, $\chi^2 = 26.61$, $P<0.01$). The coexistence positive rate of these two types of mutations was 38.8% (64/165). Coexistence mutations were found in 77.1% (64/83) out of sera with A1762T/G1764A mutations, and in 50.0% (64/128) out of sera with G1896A mutation. Compared with variants with G1896A mutation only, the coexistence mutations were predominant in patients with high level of serum HBV DNA, and related to higher total bilirubin, lower serum albumin and progressive liver diseases.

CONCLUSION: The coexistence of G1896A mutation and A1762T/G1764A mutations is very common, and responsible for the major cases with high level of HBV DNA in serum and progressive liver diseases after HBeAg-to-anti-HBe seroconversion. This coexistence mutation variant may have higher pathogenicity and replication ability.

Key words: Hepatitis B; Hepatitis B virus; Viral load; Mutant

Peng XM, Huang GM, Li JG, Huang YS, Mei YY, Gao ZL. High level of hepatitis B virus DNA after HBeAg-to-anti-HBe seroconversion is related to coexistence of mutations in its precore and basal core promoter. *World J Gastroenterol* 2005; 11(20): 3131-3134
http://www.wjgnet.com/1007-9327/11/3131.asp

INTRODUCTION

In the natural history or during the antiviral therapy of chronic HBV infection, seroconversion from HBeAg to anti-HBe is usually accompanied by a decrease in viral replication and remission of liver disease[1-4]. However, viral replication and liver damage persist in about 10% of patients after seroconversion[5-8]. The characteristic laboratory findings of these patients are that there are detectable levels of HBV DNA, and HBV variants with mutations in precore, core or basal core promoter (BCP) regions[5,6,9,10]. Among these mutations, HBV variants with a G-to-A mutation at nucleotide 1 896 (G1896A) or double-point mutation in BCP, A-to-T mutation at nucleotide 1 762 and G-to-A mutation at nucleotide 1 764 (A1762T/G1764A) are the commonest[9-14], and may be responsible for these meaningless seroconversions. However, G1896A variant has impaired, while A1762T/G1764A variant may have intact replication ability[15-17]. They themselves or their coexistence status may play different roles in such meaningless seroconversions. For these reasons, G1896A mutation and A1762T/G1764A mutations were detected using competitively differentiated polymerase chain reaction (CD-PCR) in this study, and the serum viral loads of patients with infections of G1896A variant, A1762T/G1764A variant or coexistence mutation variant of these two types of mutations were comparatively studied.

MATERIALS AND METHODS

Samples

One hundred and sixty-five serum samples with positive

anti-HBe were selected out from 300 continuous serum samples with positive HBsAg and HBV DNA from different patients in the Department of Infectious Diseases, the Third Affiliated Hospital, Sun Yat-Sen University. The serum markers of HBV were demonstrated by ELISA. The HBV DNA level was quantified using fluorescein quantitative PCR (Taqmen, Roche). These samples were divided into three groups according to the level of HBV DNA in serum, low-level group ($\geqslant 10^3$ to $<10^5$ copies/mL), median level group ($\geqslant 10^5$ to $<10^7$ copies/mL) and high-level group ($\geqslant 10^7$ copies/mL). There were 61 samples in the low-level group, 58 samples in median level group and 46 samples in the high-level group.

Reagents

Mutant-type control for CD-PCR, recombinant plasmids pG1896A and pHB-BCP2 were constructed before. Wild-type control for CD-PCR, pTZ19U-HBV that contained double copies of HBV DNA (adw) were presented by Professor Huang Zhimin, Sun Yat-Sen University. T4 DNA ligase and pfu DNA polymerase were purchased form Promega Company (USA). Anti-digoxigenin (anti-DIG) and anti-fluorescein (anti-FITC) labeled with horseradish peroxidase were purchased from Roche Company (USA). Primers shown in Table 1 were designed with the Omega 2 software and synthesized in Bioasia Biological Engineering Company (Shanghai, China).

Table 1 Primers and probes for detections of G1896A or A1762T/G1764A mutations

Denomination	Sequences (5′→3′)
PCP	BIO-GAGAC TCTAA GGCTT CTCGA TACAG AGCTG AGG
PCMd	DIG-CTCAC GCTAC ATTGT GTGCC TTGGG TGGCT TCA
PCWd	FITC-GTCCG TAGTC TCGTT GTGCC TTGGG TGGCT TGG
BCP1-M	DIG-GCTGA CGATG CGATG GGGAG GAGAT TAGGT TAATG A-3′
BCP1-W	FITC-CGTCC GTAGT GCCGA GGGAG GAGAT TAGGT TAAAG G-3′
PCA	CCCAG CAGAG AATGG CTTGC CTGAG TGCAG TATG
PCSc	CCCGA ATTCC ACCGT GAACG CCCAT CAG
PCAc	CCCAA GCTTG CAGTA TGGTG AGGTG AGCAA TG

BIO: the abbreviation of biotin; DIG: the abbreviation of digoxigenin; FITC: the abbreviation of fluorescein isothiocyanate. The underlined nucleotides had no relationship with HBV.

G1896A mutation detection

The method of CD-PCR was described in detail in previous paper. G1896A mutation was detected using CD-PCR with a few modifications. Briefly here, a 30-μL PCR reaction was performed. The reaction mixture contained 10 mmol/L Tris-HCl, pH 8.5, 50 mmol/L KCl, 1.5 mmol/L $MgCl_2$, 20 μmol/L dNTPs, 2 U pfu DNA polymerase, 20 pmoL FLU-PCWd, 20 pmoL DIG-PCMd, 10 pmoL PCA and 5 μL plasmid or extracted DNA. The cycling conditions were as follows: 2 cycles (first set) of 94 ℃ for 60 s, 53 ℃ for 120 s and 72 ℃ for 120 s, followed by 35 cycles (second set) of 94 ℃ for 30 s, 65 ℃ for 30 s, 94 ℃ for 40 s and 72 ℃ for 60 s. The PCR products were then hybridized with solidified biotin-labeled probe PCP in two different holes of microtiter plate. The color reaction was obtained after the captured PCR products reacted with horseradish peroxidase-labeled anti-DIG or anti-FITC respectively. Wild-type and G1896A mutant-type plasmids were used as positive control and negative control.

A1762T/G1764A mutation detection

A1762T/G1764A mutation was detected using CD-PCR just like G1896A mutation. The main differences were that BCP1-M and BCP1-W were used as competitive primers and recombinant plasmid pHB-BCP2 was used as positive control.

DNA sequencing

To confirm the results of CD-PCR, three samples of each group, the G1896A mutation group, A1762T/G1764A mutation group and the groups with positive or negative for both types of mutation were selected for DNA sequence analysis. Fragments of HBV BCP, precore and core regions were analyzed using DNA sequencing after they were amplified using primer PCSc and PCAc, and cloned into plasmid pUC19.

Statistical analysis

For statistical analysis, *t* tests, χ^2 examination or Fisher exact probability analysis was used. SPSS 10.0 for Windows was used for all statistical analysis. $P<0.05$ was considered statistically significant.

RESULTS

Detections of G1896A and A1762T/G1764A mutations

G1896A and A1762T/G1764A mutations in patients with positive HBV DNA in serum after seroconversion were very common. HBV strains with G1986A and/or A1762T/G1764A mutations were predominant (89.1%, 147/165). Compared with A1762T/G1764A mutations, the positive rates of G1896A variants were significantly higher (77.6% *vs* 50.3%, $\chi^2 = 26.61$, $P<0.01$) in these patients. The coexistence positive rate of these two types of mutations was 38.8% (64/165). Coexistence mutations were found in 77.1% (64/83) out of sera with A1762T/G1764A mutations, and in 50.0% (64/128) out of sera with G1896A mutation.

Confirmation analysis of G1896A and A1762T/G1764A mutations

The CD-PCR results of 12 selected samples were confirmed as expected by DNA sequence analysis. It suggests that the results of CD-PCR are believable.

Relationship of mutations with serum HBV DNA level

The relationship of G1896A and A1762T/G1764A mutations to serum HBV DNA level in these patients is shown in Table 2. From low, median to high level of HBV DNA, the total positive rates of G1896A mutation decreased in turn, while the total positive rates of A1762T/G1764A mutations increased. Since coexistence of G1896A and A1762T/G1764A mutations were very common in these patients, the mutations of G1896A only, A1762T/G1764A only and their coexistence were separately considered (Table 2). The status of mutations of G1896A only was the same as that of total G1896A mutation. The status of

Table 2 Relationship between CD-PCR results and serum HBV DNA load in 165 serum samples with detectable HBV DNA in serum after HBeAg-to-anti-HBe seroconversion

	No. (%) of CD-PCR results				
	Total G1896A	Total A1762T/G1764A	G1896A only	A1762T/G1764A only	Coexistence
Low-level group (n = 61)	53 (86.9)[b]	20 (32.8)	35 (57.4)[d]	2 (3.3)	18 (29.5)
Median level group (n = 58)	45 (77.6)	32 (55.2)[e]	23 (39.6)	10 (17.3)	22 (37.9)
High-level group (n = 46)	30 (65.2)	31 (67.4)[f]	6 (13.0)	7 (15.2)	24 (52.2)[g]

[1]χ^2 = 7.08, [b]P<0.01, [2]χ^2 = 21.81, [d]P<0.01, compared with high-level group. [3]χ^2 = 6.06, [e]P<0.05, compared with low-level group. [4]χ^2 = 8.20, [f]P<0.01, compared with median level group. [5]χ^2 = 5.65, [g]P<0.05, compared with low-level group.

Table 3 Main clinical data of 147 serum samples with G1896A and/or A1762T/G1764A mutations

	G1896A only (n = 64)	A1762T/G1764A only (n = 19)	Coexistence (n = 64)
Age (yr)	40.5±12.8	43.2±14.2	40.7±12.8
Sex (no. male/no. female)	55/9	18/1	59/5
Alanine aminotransferase (IU/L)	101.9±158.3	121.8±183.1	116.7±137.3
Total bilirubin (μmol/L)	25.2±39.2	24.8±40.6	32.5±55.2[b]
Serum albumin (g/L)	38.4±5.3	39.1±5.8	37.7±5.3[d]
Clinical diagnosis			
Chronic hepatitis Mild (n)	23	3	13
Median (n)	20	10	14
Gravies (n)	12	4	22[f]
Liver cirrhosis	9	2	15[g]

[1]t = –2.85, [b]P<0.01, [2]t = 6.37, [d]P<0.01, compared with group of G1896A only. [3]χ^2 = 18.3, [f]P<0.01, [4]χ^2 = 4.03, [g]P<0.05, compared with group of mild type of chronic hepatitis B.

mutations of A1762T/G1764A only could not be analyzed because of the limited case numbers. The status of coexistence was the same as that of total A1762T/G1764A mutations. In high-level group, HBV variants with coexistence of G1896A mutation and A1762T/G1764A mutations were predominant.

Relationship of mutations with main clinical data

The main clinical data of 147 serum samples with G1896A mutation and/or A1762T/G1764A are shown in Table 3. The patients with coexistence mutation variant infections were related with higher total bilirubin and lower serum albumin as compared with patients who were infected by HBV variants of G1896A mutation only. For clinical diagnosis, coexistence mutations were more often to be found in progressive liver diseases (gravies type of chronic hepatitis B and liver cirrhosis), while G1896A mutation only is found more often in benign liver diseases (mild or median type of chronic hepatitis B).

DISCUSSION

CD-PCR is a rapid method for point mutation screening, and can detect mutations with high specificity, efficiency and rapidity. Using this technique in this study, G1896A and/or A1762T/G1764A mutations were detected in 89.1% out of patients with detectable HBV DNA in serum after HBeAg-to-anti-HBe seroconversion. It suggests that G1896A and/or A1762T/G1764A mutations are major causes of this meaningless seroconversion. G1896A mutation was detected in up to 77.6% of such patients. However, the variant with G1896A mutation is usually accompanied by a decrease in HBV replication and remission of liver disease[9,15,18-22], and can be considered as favorable factor of response to interferon treatment[23]. That means G1896A mutation may not be responsible for the meaningless seroconversion, especially for patients with progressive liver diseases. This view is further supported by those variants with G1896A mutation only which were closely related to low level of HBV DNA and benign liver diseases, when HBV DNA level and clinical data were taken into account in this study.

The A1762T/G1764A variant is usually accompanied by increase in HBV replication and decrease in HBeAg secretion, and may be related to liver deterioration[9,24-28], or at least not to affect HBV DNA level[18]. A1762T/G1764A mutations were detected in half of the patients, and coexisted with G1896A mutation in 77.1% out of all A1762T/G1764A mutations in this study. The coexistence mutation variant was also found to be related to high level of HBV DNA in serum. These results suggest that A1762T/G1764A mutations, especially the coexistence mutations, may play more important roles in the meaningless seroconversion than G1896A mutation. Other data show that A1762T/G1764A mutations take place years early than G1896A before seroconversion[13]. Thus, these results suggest that, when it subsequently occurs in the genome, G1896A mutation can decrease the replication of wild-type HBV but A1762T/G1764A variant. The reason may be that the transcription of A1762T/G1764A variant is regulated in a different manner and by different transcriptional factors[16,17,29].

The coexistence of G1896A mutation and A1762T/G1764A mutations are very common[25], have a clear link with chronic active hepatitis[26], are associated with the degree of histological injury[30] and are found to be related to high level of HBV DNA, higher total bilirubin, lower serum albumin and progressive liver diseases in this study. Thus, this coexistence mutation variant might have higher pathogenicity and replication ability. However, some research demonstrated that the dual mutations occurred less frequently in patients with high level of serum HBV DNA[5]. For these reasons, the coexistence of G1896A

mutation and A1762T/G1764A mutations is worth some further extensive investigations.

REFERENCES

1 **van Zonneveld M**, Honkoop P, Hansen BE, Niesters HG, Darwish Murad S, de Man RA, Schalm SW, Janssen HL. Long-term follow-up of alpha-interferon treatment of patients with chronic hepatitis B. *Hepatology* 2004; **39**: 804-810

2 **Ganem D**, Prince AM. Hepatitis B virus infection--natural history and clinical consequences. *N Engl J Med* 2004; **350**: 1118-1129

3 **Hoofnagle JH**, Dusheiko GM, Seeff LB, Jones EA, Waggoner JG, Bales ZB. Seroconversion from hepatitis B e antigen to antibody in chronic type B hepatitis. *Ann Intern Med* 1981; **94**: 744-748

4 **Liaw YF**, Chu CM, Su IJ, Huang MJ, Lin DY, Chang-Chien CS. Clinical and histological events preceding hepatitis B e antigen seroconversion in chronic type B hepatitis. *Gastroenterology* 1983; **84**: 216-219

5 **Lin CL**, Liao LY, Liu CJ, Chen PJ, Lai MY, Kao JH, Chen DS. Hepatitis B genotypes and precore/basal core promoter mutants in HBeAg-negative chronic hepatitis B. *J Gastroenterol* 2002; **37**: 283-287

6 **Schiefke I**, Klecker C, Maier M, Oesen U, Etzrodt G, Tannapfel A, Liebert UG, Berr F. Sequential combination therapy of HBe antigen-negative/ virus-DNA-positive chronic hepatitis B with famciclovir or lamivudine and interferon-alpha-2a. *Liver Int* 2004; **24**: 98-104

7 **Bonino F**, Rosina F, Rizzetto M, Rizzi R, Chiaberge E, Tardanico R, Callea F, Verme G. Chronic hepatitis in HBsAg carriers with serum HBV-DNA and anti-HBe. *Gastroenterology* 1986; **90**: 1268-1273

8 **Chu CM**, Karayiannis P, Fowler MJ, Monjardino J, Liaw YF, Thomas HC. Natural history of chronic hepatitis B virus infection in Taiwan: studies of hepatitis B virus DNA in serum. *Hepatology* 1985; **5**: 431-434

9 **Yotsuyanagi H**, Hino K, Tomita E, Toyoda J, Yasuda K, Iino S. Precore and core promoter mutations, hepatitis B virus DNA levels and progressive liver injury in chronic hepatitis B. *J Hepatol* 2002; **37**: 355-363

10 **Yuen MF**, Sablon E, Yuan HJ, Hui CK, Wong DK, Doutreloigne J, Wong BC, Chan AO, Lai CL. Relationship between the development of precore and core promoter mutations and hepatitis B e antigen seroconversion in patients with chronic hepatitis B virus. *J Infect Dis* 2002; **186**: 1335-1338

11 **Knoll A**, Rohrhofer A, Kochanowski B, Wurm EM, Jilg W. Prevalence of precore mutants in anti-HBe-positive hepatitis B virus carriers in Germany. *J Med Virol* 1999; **59**: 14-18

12 **Chu CM**, Yeh CT, Lee CS, Sheen IS, Liaw YF. Precore stop mutant in HBeAg-positive patients with chronic hepatitis B: clinical characteristics and correlation with the course of HBeAg-to-anti-HBe seroconversion. *J Clin Microbiol* 2002; **40**: 16-21

13 **Yamaura T**, Tanaka E, Matsumoto A, Rokuhara A, Orii K, Yoshizawa K, Miyakawa Y, Kiyosawa K. A case-control study for early prediction of hepatitis B e antigen seroconversion by hepatitis B virus DNA levels and mutations in the precore region and core promoter. *J Med Virol* 2003; **70**: 545-552

14 **Kajiya Y**, Hamasaki K, Nakata K, Miyazoe S, Takeda Y, Higashi S, Ohkubo K, Ichikawa T, Nakao K, Kato Y, Eguchi K. A long-term follow-up analysis of serial core promoter and precore sequences in Japanese patients chronically infected by hepatitis B virus. *Dig Dis Sci* 2001; **46**: 509-515

15 **Lamberts C**, Nassal M, Velhagen I, Zentgraf H, Schroder CH. Precore-mediated inhibition of hepatitis B virus progeny DNA synthesis. *J Virol* 1993; **67**: 3756-3762

16 **Tang H**, Raney AK, McLachlan A. Replication of the wild type and a natural hepatitis B virus nucleocapsid promoter variant is differentially regulated by nuclear hormone receptors in cell culture. *J Virol* 2001; **75**: 8937-8948

17 **Buckwold VE**, Xu Z, Chen M, Yen TS, Ou JH. Effects of a naturally occurring mutation in the hepatitis B virus basal core promoter on precore gene expression and viral replication. *J Virol* 1996; **70**: 5845-5851

18 **Gandhe SS**, Chadha MS, Walimbe AM, Arankalle VA. Hepatitis B virus: prevalence of precore/core promoter mutants in different clinical categories of Indian patients. *J Viral Hepat* 2003; **10**: 367-382

19 **Akahane Y**, Yamanaka T, Suzuki H, Sugai Y, Tsuda F, Yotsumoto S, Omi S, Okamoto H, Miyakawa Y, Mayumi M. Chronic active hepatitis with hepatitis B virus DNA and antibody against e antigen in the serum. Disturbed synthesis and secretion of e antigen from hepatocytes due to a point mutation in the precore region. *Gastroenterology* 1990; **99**: 1113-1119

20 **Carman WF**, Jacyna MR, Hadziyannis S, Karayiannis P, McGarvey MJ, Makris A, Thomas HC. Mutation preventing formation of hepatitis B e antigen in patients with chronic hepatitis B infection. *Lancet* 1989; **2**: 588-591

21 **Tong SP**, Li JS, Vitvitski L, Trepo C. Active hepatitis B virus replication in the presence of anti-HBe is associated with viral variants containing an inactive pre-C region. *Virology* 1990; **176**: 596-603

22 **Okamoto H**, Yotsumoto S, Akahane Y, Yamanaka T, Miyazaki Y, Sugai Y, Tsuda F, Tanaka T, Miyakawa Y, Mayumi M. Hepatitis B viruses with precore region defects prevail in persistently infected hosts along with seroconversion to the antibody against e antigen. *J Virol* 1990; **64**: 1298-1303

23 **Zampino R**, Marrone A, Cirillo G, del Giudice EM, Utili R, Karayiannis P, Liang TJ, Ruggiero G. Sequential analysis of hepatitis B virus core promoter and precore regions in cancer survivor patients with chronic hepatitis B before, during and after interferon treatment. *J Viral Hepat* 2002; **9**: 183-188

24 **Laras A**, Koskinas J, Hadziyannis SJ. *In vivo* suppression of precore mRNA synthesis is associated with mutations in the hepatitis B virus core promoter. *Virology* 2002; **295**: 86-96

25 **Nakashima H**, Furusyo N, Kubo N, Kashiwagi K, Etoh Y, Kashiwagi S, Hayashi J. Double point mutation in the core promoter region of hepatitis B virus (HBV) genotype C may be related to liver deterioration in patients with chronic HBV infection. *J Gastroenterol Hepatol* 2004; **19**: 541-550

26 **Mayerat C**, Mantegani A, Spertini F, Frei PC. Mutations in the basal core promoter and precore/core gene of hepatitis B virus in patients with chronic active but not acute hepatitis B. *Eur J Clin Microbiol Infect Dis* 1999; **18**: 871-878

27 **Gerner P**, Lausch E, Friedt M, Tratzmuller R, Spangenberg C, Wirth S. Hepatitis B virus core promoter mutations in children with multiple anti-HBe/HBeAg reactivations result in enhanced promoter activity. *J Med Virol* 1999; **59**: 415-423

28 **Kramvis A**, Kew MC. The core promoter of hepatitis B virus. *J Viral Hepat* 1999; **6**: 415-427

29 **Buckwold VE**, Xu Z, Yen TS, Ou JH. Effects of a frequent double-nucleotide basal core promoter mutation and its putative single-nucleotide precursor mutations on hepatitis B virus gene expression and replication. *J Gen Virol* 1997; **78** (Pt 8): 2055-2065

30 **Jardi R**, Rodriguez F, Buti M, Costa X, Valdes A, Allende H, Schaper M, Galimany R, Esteban R, Guardia J. Mutations in the basic core promoter region of hepatitis B virus. Relationship with precore variants and HBV genotypes in a Spanish population of HBV carriers. *J Hepatol* 2004; **40**: 507-514

Science Editor Guo SY **Language Editor** Elsevier HK

PO Box 2345, Beijing 100023, China
www.wjgnet.com
wjg@wjgnet.com

ELSEVIER

World J Gastroenterol 2005;11(20):3135-3138
World Journal of Gastroenterology ISSN 1007-9327

• *BRIEF REPORTS* •

Nerve-pathways of acupoint Fengch'ih in rat by anterograde transport of HRP

Gang-Ming Xi, Hua-Qiao Wang, Guo-Hou He, Chao-Feng Huang, Qun-Fang Yuan, Guo-Yao Wei, Hua Li, Wen-Wen Liu, Hua-Yan Fan

Gang-Ming Xi, Department of Neurology, Shiyan Renmin Hospital Affiliated to Yunyang Medical College, Shiyan 442000, Hubei Province, China
Guo-Hou He, Chao-Feng Huang, Guo-Yao Wei, Hua Li, Wen-Wen Liu, Hua-Yan Fan, Department of Neurology, Taihe Hospital Affiliated to Yunyang Medical College, Shiyan 442000, Hubei Province, China
Hua-Qiao Wang, Qun-Fang Yuan, Department of Anatomy & Brain Research, Preclinical Medicine School, Sun Yat-Sen University, Guangzhou 510080, Guangdong Province, China
Supported by the Science Research Fund of Hubei Province, No. WZ1539
Correspondence to: Professor Hua-Qiao Wang, Department of Anatomy & Brain Research, Preclinical Medicine School, Sun Yat-Sen University, Guangzhou 510080, Guangdong Province, China. zhxwwk@gzsums.edu.cn
Telephone: +86-20-87331962-111
Received: 2004-07-17 Accepted: 2004-09-04

Abstract

AIM: To study the nervous-pathways of Fengch'ih acupuncture by means of anterograde transport of aqueous solution of horseradish peroxidase (HRP).

METHODS: Fifty Wistar rats were randomly divided into 1, 2, 3, 4, and 5 d groups, and every group had 10 animals. HRP (30% aqueous solution) was injected into a Fengch'ih. Serial, transverse or capital, 40 μm sections of the cervical spinal ganglia, cervical and thoracic spinal cord segment and brain were cut on a cryotome. Sections were incubated for HRP histochemistry according to the tetramethylbenzidine (TMB). Part of the sections were counterstained with neutral red.

RESULTS: After 1 d of survival times, many labeled cell bodies were found in 1-4 cervical spinal ganglia, anterior horn of 1-4 cervical spinal cord, ventromedial division of facial nucleus, accessory facial nucleus ipsilaterally. With increasing survival times, the intensity of labeled cells were slightly decreased.

CONCLUSION: Fengch'ih may bring into full play its effect by correlation of posterior ear branch of facial nerve and anterior branch of 2-3 cervical nerve with 1-4 cervical the anterior horn of the spinal cord, ventromedial division of facial nucleus, accessory facial nucleus.

Key words: Point Fengch'ih; Acupuncture; Horseradish peroxidase

Xi GM, Wang HQ, He GH, Huang CF, Yuan QF, Wei GY, Li H, Liu WW, Fan HY. Nerve-pathways of acupoint Fengch'ih in rat by anterograde transport of HRP. *World J Gastroenterol* 2005; 11(20): 3135-3138
http://www.wjgnet.com/1007-9327/11/3135.asp

INTRODUCTION

The acupoint of Fengch'ih, also known as Refu, is derived from the medical literature *Miraculous Pivot: Febrile Disease*, and held to be on the Gallbladder Channel of foot-Shaoyang, including hand- and foot-Shaoyang, Yangwei and Yanghui, one of the most commonly used acupoints in clinical treatment. As is documented, Fengch'ih can be used to treat many diseases, especially those resulting from pathogenic wind. Its clinical application is also extensive in modern time for treating such diseases as dyspepsia, stomach-ache, gastric ulcer, common cold, headache, cervical spondylosis, trigeminal neuralgia, hypertension, apoplexia, epilepsia, optic atrophy, myopia, tinnitus, painful heels[1]. However, little is known about its nerve-pathway. In the present study, we aim to illustrate the nerve-pathways and therapeutic mechanisms of Fengch'ih acupuncture, by means of anterograde transport of aqueous solution of horseradish peroxidase (HRP).

MATERIALS AND METHODS

A total of 50 adult Wistar rats in good condition, each body weighing 250-300 g, were divided randomly into control and acupuncture group regardless of the sex, and each group subdivided into 1, 2, 3, 4, and 5 d with 10 rats in each subgroup. The animals were anesthetized with 10% chloral hydrate (0.3 mL/100 g) intraperitoneally to surgery.

The animals were fixed in prone position on the table. Fengch'ih was ascertained at the intersection of sternocleidomastoid muscle and trapezius muscle. After conventional sterilization, 30% HRP50 μL was injected into a Fengch'ih acupoint. As for the controls, equal quantity of HRP was injected into Fengch'ih.

After survival times of 1-5 d, the animals were deeply anesthetized with 10% chloral hydrate, and thoracotomy was done quickly, and intubation was performed via left ventricle to aorta, and perfused with 50-150 mL 0.9% NaCl (till the liver whitened), followed by 4 ℃ 1.0% paraformaldehyde-1.25% glutaraldehyde in 0.1 mol/L phosphate

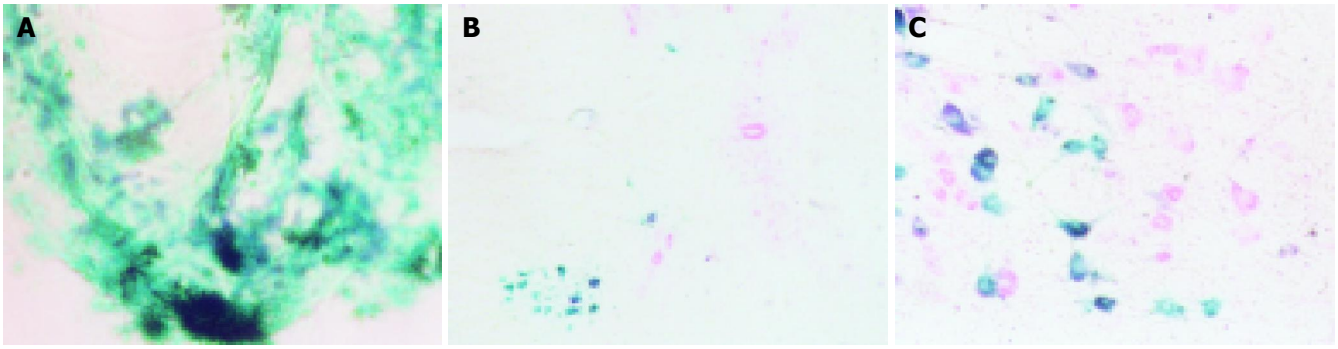

Figure 1 The distribution of HRP-positive neurons of cervical dorsal root ganglia, the anterior horn cervical spinal cord, the ventromedial division of the facial nucleus. **A**: Photomicrograph of the longitudinal sections of the second cervical dorsal root ganglion showed an intense and homogeneous distribution of HRP reaction product within the cell bodies and their processes. The labeled neurons were green and their processes arranged as pine needle stained with Gu YM's technique. ×400. **B**: Photomicrograph of horizontal sections of second cervical spinal cord. The labeled neurons were located in the anterior horn. The dark green cells were the HRP-positive neurons and the red cells were the negative neurons stained with Gu YM's technique and counterstained by neutral red. ×40. **C**: Photomicrograph of the facial nucleus showed the labeled neurons in the ventromedial division nucleus.The labeled neurons were dark green and the negative neurons were red stained with Gu YM's technique and counterstained by neutral red. ×100.

buffer, pH 7.4, of 500 mL, first rapidly and then slowly, lasting no less than 30 min. Soon, the brainstem with attached cerebellum, cervical and upper thoracic spinal cord, and the first to eighth bilateral cervical dorsal root ganglia were removed quickly and stored overnight in 0.1 mol/L phosphate buffer containing 30% sucrose.

In order to locate the positive nuclear groups, serial, capital or transverse (brainstem and spinal cord) or longitudinal (dorsal root ganglion) 40-μm sections were cut on a cryotome. Sections were incubated for HRP histochemistry according to the tetramethylbenzidine-sodium tungstate (TMB-ST) protocol[2], and mounted on neutral gum-coated slides. Part of the sections was counterstained with neutral red. The sections were examined with bright field microscopy. All photomicrographs (Figures 1A-C) were taken with a photomic-roscope (Olympus microscope) on panchromatic film (made in Japan). Magnified multiples of microscope and photograph were 20×, 10×, and 12.15×, respectively. The finally magnified multiple of the neurons was 2 430.

To count numerical density on volume (N_v), numerical density on area (N_a) and mean volume ($\bar{v}$) of the HRP-positive neurons in the photograph of cervical dorsal root ganglia, anterior horn of spinal cord and facial nucleus of nerve, a square-net-test-system with 2 500 counting grid was applied. The border length of the counting grid was 2 mm, and its area was 4 mm^2. The value of area divided by magnified multiple was named practice value. The section number of the HRP-positive neurons, the crossing number falling on the section and reference testing crossing number were counted. And then, the Novena and $\bar{v}$ were computed according to stereological formula[3]. Every stereological parameter was expressed by mean±SD.

RESULTS

HRP positive neurons were green when they were not counterstained, and changed into dark green after being counterstained. In cytoplasm and processes many HRP positive particles were found, and those in the processes were in the pattern of a pearl string. One day after injection, the HRP positive neurons began to appear in 1-4 homolateral cervical dorsal root ganglia, the anterior horn of the 1-4 cervical spinal cord (layer VIII and IX), the ventromedial division of the facial nucleus, the accessory facial nucleus (Figure 1). The HRP positive particles in the HRP neurons of the above-mentioned regions declined with the increase of survival time, and those HRP positive particles in the cytoplasm and the process faded away on the 5th d. The N_v, Na, $\bar{v}$ of the HRP-positive neurons in cervical dorsal root ganglia, anterior horn of the 1-4 cervical spinal cords, and the ventromedial division of the facial nucleus referred to in Table 1.

Table 1 N_v, Na, $\bar{v}$ of HRP-positive neurons in cervical dorsal root ganglia, anterior horn of the cervical spinal cord and the facial nucleus (mean±SD)

	Nv (×10^3 mm^{-3})	Na (mm^{-2})	$\bar{v}$ (×10^{-5} mm^3)
Dorsal root ganglia	2.65±2.39	31.85±20.46	5.12±3.27
Anterior horn	2.06±1.30	88.00±54.53	5.96±2.38
Facial nucleus	2.43±0.09	91.49±11.08	2.91±1.19

DISCUSSION

Acupunctures on the Fengch'ih acupoint can be categorized as: (1) the superficial needling, the most common one, with the needlepoint slanted toward the apex of nose, for treating many diseases; (2) deep needling, the special one, with the needle pointed straight toward homolateral nose for treating sequelae of apoplexy, toward the bottom of homolateral angularis for treating diseases in trunk, neck, limbs, throat, and trachea, toward throat for treating pseudobulbar paralysis, or slightly toward temporal for hemicrania, and (3) penetration needling, toward opposite side of Fengch'ih (Fengfu), mainly for cervical spondylosis. Then, what is the functioning of Fengch'ih? The following is an illustration of its nerve pathway based on the anatomy of Fengch'ih and the findings of the present experiment.

The acupoint of Fengch'ih is located at the intersection of trapeziums muscle and the upper end of sternocleidomastoid muscle, under the superior nuchal line pitting of inside the hairline. The sensory fibers of its skin and subcutaneous fascia come from the posterior branch of the 3rd cervical nerve

and the branches of lesser occipital nerve. The sympathetic fibers originates from 8 and 1-2 thoracic lateral horn cells. At the acupoint is located lesser occipital nerve trunk, and deeper are lateral suboccipital triangle, occipital artery and vein, vertebral artery, and the posterior branch of the 1st cervical nerve. Lesser occipital nerve originates either from the anterior branch of the 2nd and the 3rd cervical nerve, or from the nerve loop between the two, then, along the posterior border of the end of sternocleidomastoid muscle, extends to the lateral scalp, and distributes behind auricle and in the lateral skin of occipital nerve. Its ramie communicates with the branches of greater occipital nerve and auriculotemporal nerve[4,5].

In addition, facial nerve branches off the stylomastoid foramen. Posterior auricular nerve controls occipital muscle, periauricular muscles, posterior belly of digastrics muscles and stylohyoid muscle[5].

In the present study, after the injection of HRP into Fengch'ih acupoint, HRP positive neurons were found in the regions of bilateral or homonymous 1st-4th cervical dorsal root ganglia and their corresponding anterior horns (layers VIII–IX) of the spinal cord, ventromedial division of the facial nucleus and the accessory facial nucleus. Based on the anatomical structure of Fengch'ih acupoint, it is assumed that HRP is carried through the branches of the 1st-4th cervical nerve to dorsal root ganglia directly, or straight to the motoneurons of the anterior horn of the 1st-4th spinal cord. After HRP was injected into the sternocleidomastoid and trapezius muscles, all labeling were found ipsilaterally; retrogradely labeled cells were located in the C_2-C_4 dorsal root ganglia, and transganglionic labelings in the C_1 to the rostral C_6 spinal segments and in the medulla oblongata. Labeled terminal fields were the lamina VI, the central cervical nucleus and the ventral horn in the cervical spinal cord[6]. Injections of WGA-HRP or free HRP into rostral cervical dorsal root ganglia and HRP application to C_2 and C_3 dorsal rami produced labeling in dorsal and ventral horns at the level of entrance[7]. Injections of WGA-HRP into the second cervical dorsal root ganglion produced labeling in the dorsal and ventral horns. Injections of aqueous HRP into the suboccipital muscles produced heavy transganglionic label within the central cervical nucleus[8]. After injection of HRP into ganglia (C_3) without involvement of the ventral roots and spinal nerves, a few ipsilateral spinal ventral horn neurons (C_3) were retrogradely labeled with HRP. Subsequent to an HRP and wheat germ agglutinin WGA-HRP-mixture injection into the dorsal neck or suboccipital muscles, many spinal motoneurons (C_3) were labeled retrogradely with an HRP mixture. These findings strongly suggest that some spinal motoneurons send their axon collaterals to the dorsal root ganglia, in which the terminals of the axon collaterals directly synapse with the dorsal root ganglion cells[9].

The neurons of the ventromedial division of facial nucleus were labeled retrogradely with an HRP through the posterior auricular nerve of the facial nerve. The facial nerve were six main branches which were the zygomatico-orbital, cervical, posterior auricular, anterior auricular, superior labial, and inferior labial branches[10]. The facial nucleus of a variety of species was divided cytoarchitectonically into the ventral, medial, intermediate, dorsal and lateral divisions. When horseradish peroxidase (HRP) was applied to the inferior labial, cervical or posterior auricular branch of the facial nerve, HRP-labeled neurons were seen in the lateral, ventral or medial division of the facial nucleus, respectively. After applying HRP to the anterior auricular-zygomatico-orbital branch, labeled neurons were observed mainly in the intermediate and dorsal divisions. HRP applied to the superior labial branch labeled neurons within the dorsal and lateral divisions[11-14]. The neurons of the accessory facial nucleus were labeled retrogradely with an HRP through the nerve supplying the posterior belly of the digastrics muscle in the accessory facial nucleus[15]. These results are consistent with those of ours.

The absence of HRP in the posterior horn of spinal cord, the cuneate nucleus, the gracile nucleus, the ambiguous nucleus, the nucleus of solitary tract, and the trigeminal nerve nucleus indicates that Fengch'ih functions without these nuclei. It is still uncertain whether the 1st-4th cervical nerve is directly related to facial nucleus and accessory facial nucleus, or to the anterior horn of spinal cord, whether facial nucleus and accessory facial nucleus are related to the anterior horn of the 1st-4th cervical spinal cord, which deserves further investigation.

ACKNOWLEDGMENTS

This study would not have been possible without the Scientific Research Fund supported by the Health Department of Hubei Province. We gratefully thank accessory director physician, Yan WQ, for purchasing chemical reagent and accessory professor, Zhang XJ, for improving the paper. Lastly, we would like to express our gratitude to the help of all doctors and nurses of the Department of Neurology of Taihe Hospital Affiliated to Yunyang Medical College.

REFERENCES

1 **Sun X,** Li XW. Acupuncture manipulation of the acupoint "Fengch'ih". *Beijing Zhongyiyao Daxue Xuebao* 1999; **22**: 75-76

2 **Gu YM,** Chen YC, Ye LM. A new highly sensitive HRP-TMB method using sodium tungstate as a stabilizer, I Light microscopic study. *Shenjing Jiepouxue Zazhi* 1990; **6**: 121-127

3 **Xi GM,** Wang HQ, Tang TY, Zhou LH, Yuan YW, Fan HY, Ye TX. Development of the excitability amino acid neurons in hippocampal formation of postnatal rat. *Shenjing Jiepouxue Zazhi* 1999; **2**: 165-170

4 **Wu ZS.** Investigation on form and structure of the acupoint "ShangTian Zhu and Fengch'ih". *Shanghai Zhenjiu Zazhi* 1987; **6**: 28-30

5 **Li WD,** Du Z, Fang ZQ, Wang LH. Investigation on anatomical structure and safety acupuncture. *Zhongguo Zhenjiu* 1997; **17**: 505-506

6 **Ishii Y.** Central afferent projections from the rat sternocleidomastoid and trapezius muscles. A study using transganglionic transport of horseradish peroxidase. *Osaka Daigaku Shigaku Zasshi* 1989; **34**: 193-212

7 **Neuhuber WL,** Zenker W. Central distribution of cervical primary afferents in the rat, with emphasis on proprioceptive projections to vestibular, perihypoglossal, and upper thoracic spinal nuclei. *J Comp Neurol* 1989; **280**: 231-253

8 **Prihoda M,** Hiller MS, Mayr R. Central projections of cervical primary afferent fibers in the guinea pig: an HRP and WGA/HRP tracer study. *J Comp Neurol* 1991; **308**: 418-431

9 **Kayahara T.** Synaptic connections between spinal motoneu-

rons and dorsal root ganglion cells in the cat. *Brain Res* 1986; **376**: 299-309

10 **Uemura-Sumi M,** Manabe Y, Matsushima R, Mizuno N. Correlation of the main peripheral branches of the facial nerve with the cytoarchitectonic subdivisions of the facial nucleus in the guinea pig. *Anat Embryol (Berl)* 1986; **174**: 161-166

11 **Hinrichsen CF,** Watson CD. The facial nucleus of the rat: representation of facial muscles revealed by retrograde transport of horseradish peroxidase. *Anat Rec* 1984; **209**: 407-415

12 **Populin LC,** Yin TC. Topographical organization of the motoneuron pools that innervate the muscles of the pinna of the cat. *J Comp Neurol* 1995; **363**: 600-614

13 **Satoda T,** Takahashi O, Tashiro T, Matsushima R, Uemura-Sumi M, Mizuno N. Somatotopic organization of facial nucleus of rabbit. With particular reference to intranuclear representation of perioral branches of the facial nerve. *Anat Anz* 1988; **165**: 83-90

14 **Watson CR,** Sakai S, Armstrong W. Organization of the facial nucleus in the rat. *Brain Behav Evol* 1982; **20**: 19-28

15 **Terashima T,** Kishimoto Y, Ochiishi T. Musculotopic organization of the facial nucleus of the reeler mutant mouse. *Brain Res* 1993; **617**: 1-9

Science Editor Guo SY **Language Editor** Elsevier HK

PO Box 2345, Beijing 100023, China
www.wjgnet.com
wjg@wjgnet.com

ELSEVIER

World J Gastroenterol 2005;11(20):3139-3143
World Journal of Gastroenterology ISSN 1007-9327

• *BRIEF REPORTS* •

Expression of E-cadherin in gastric carcinoma and its correlation with lymph node micrometastasis

Ze-Yu Wu, Wen-Hua Zhan, Jing-Hua Li, Yu-Long He, Jian-Ping Wang, Ping Lan, Jun-Sheng Peng, Shi-Rong Cai

Ze-Yu Wu, Wen-Hua Zhan, Yu-Long He, Jian-Ping Wang, Ping Lan, Jun-Sheng Peng, Shi-Rong Cai, Department of Gastrointestinal and Pancreatic Surgery, the First Affiliated Hospital, Sun Yat-Sen University, Guangzhou 510080, Guangdong Province, China
Jing-Hua Li, Department of Parasitology, Zhong Shan Medical College, Sun Yat-Sen University, Guangzhou 510089, Guangdong Province, China
Supported by the National Natural Science Foundation of China, No. 30271276
Correspondence to: Dr. Wen-Hua Zhan, Department of Gastrointestinal and Pancreatic Surgery, the First Affiliated Hospital, Sun Yat-Sen University, Guangzhou 510080, Guangdong Province, China. wenhuazh@21cn.com
Telephone: +86-20-87755766-8211 Fax: +86-20-87335945
Received: 2004-07-28 Accepted: 2004-09-30

Abstract

AIM: To examine the expression of E-cadherin in the primary tumor and to evaluate its relationship with lymph node micrometastasis (LNM).

METHODS: The authors studied 850 lymph nodes resected from 30 patients with gastric carcinoma who underwent gastrectomy with lymphadenectomy using reverse transcription polymerase chain reaction (RT-PCR) assay in addition to H&E staining. Cytokeratin-20 (CK-20) gene marker was used in this assay. The level of E-cadherin expression in the primary tumor was examined by immunochemical technique (EliVision™ plus).

RESULTS: LNM was detected in 77 (12.5%) lymph nodes of 14 patients (46.7%) with gastric carcinoma. The incidence of LNM was significantly higher in the diffuse type (12 of 19 cases, 63.2%) than in the intestinal type of gastric carcinoma (2 of 11 cases, 18.2%, $P = 0.026$). The incidence of LNM also increased in accordance with the depth of tumor invasion. The loss of expression of E-cadherin in primary tumors was found in 14 (46.7) of 30 tumors. The absence of E-cadherin expression was significantly associated with the Lauren classification ($P = 0.026$), lymph node metastasis ($P = 0.011$), the grade of differentiation ($P = 0.004$) and the lymphatic invasion ($P = 0.001$). Expression of E-cadherin was negative in 10 (71.4%) of the 14 patients with LNM, and in 4 (25%) of the 16 patients without LNM ($P = 0.026$).

CONCLUSION: The current results indicate that the RT-PCR assay is useful for the detection of LNM and can significantly increase the detection rate of lymph node metastasis in patients with gastric carcinoma. The Lauren classification and depth of tumor invasion are significantly associated with lymph node micrometastases. Our findings also indicate that E-cadherin may play an important role in determining the growth type and differentiation of gastric carcinoma. The loss of E-cadherin expression may contribute to LNM.

Key words: Gastric carcinoma; Lymph node micrometastasis; Cytokeratin-20; E-cadherin; Reverse transcription polymerase chain reaction; Immunohistochemistry

Wu ZY, Zhan WH, Li JH, He YL, Wang JP, Lan P, Peng JS, Cai SR. Expression of E-cadherin in gastric carcinoma and its correlation with lymph node micrometastasis. *World J Gastroenterol* 2005; 11(20): 3139-3143
http://www.wjgnet.com/1007-9327/11/3139.asp

INTRODUCTION

Lymph node metastasis is one of the most important prognostic factors in gastric carcinoma[1-3]. Histopathological examination of resected lymph nodes using H&E staining has been the gold standard for diagnosis of lymph node metastasis; however, the incidence of LNM is often overlooked by the routine histologic method. Recent advances in immunohistochemical and molecular biologic techniques have made it possible to detect LNM not evidenced by routine H&E evaluation. Cytokeratin is a component of the cytoskeleton of epithelial cells that is not present in normal lymph nodes[4]. Several investigators have reported that cytokeratin immunostaining can identify lymph node micrometastases missed by routine H&E staining in patients with gastric carcinoma[5-7]. However, it has been reported that the immunohistochemical technique might still generate false-negative results from overlooking possible micrometastases localized outside the cutting slice or false-positive results due to antibody cross-reactivity with host stromal or inflammatory cells[8]. In the current study, to overcome these problems, we applied RT-PCR assay to detect micrometastasis in the lymph nodes resected from 30 cases of stage I-IV gastric carcinomas, and examined the relationship between LNM and clinicopathologic characteristics. Moreover, the mechanism of LNM is still not completely known presently. E-cadherin is an adhesive molecule of epithelial cells and plays an important role in the formation and maintenance of epithelia architecture. It has been reported that reduced expression of E-cadherin is

closely associated with lymph node metastasis[9,10]. However, the relationship between E-cadherin expression in the primary tumor and LNM has not been extensively discussed. Therefore, the main objective of this study was to explore E-cadherin expression in the primary tumor and its relationship with LNM in patients with gastric carcinoma. The relationship between E-cadherin expression and clinicopathologic features of gastric carcinoma was also investigated.

MATERIALS AND METHODS

Patients and specimens

A total of 850 lymph nodes resected from 30 patients with gastric carcinoma who underwent gastrectomy at the Department of Gastrointestinal Pancreatic Surgery at Sun Yat-Sen University of Medical Sciences were studied. There were 17 men and 13 women, ranging in age from 26 to 82 years, with a mean age of 56.8 years. None of these patients had received preoperative chemotherapy or radiotherapy. Total gastrectomy was performed in 16 patients, distal subtotal gastrectomy in 13 patients, and proximal subtotal gastrectomy in one patient. One patient underwent D1 lymphadenectomy, 22 patients underwent D2 lymphadenectomy, four patients underwent D3 lymphadenectomy, and three patients underwent palliative resection. According to the Lauren' criteria[11], 19 tumors were classified as diffusive type carcinomas, and 11 tumors were classified as intestinal type carcinomas. Depth of tumor invasion and extent of lymph node metastasis were classified according to UICC TNM classification published in 1997.

Half of each resected lymph node was fixed in 40 g/L formaldehyde and embedded in paraffin for routine histopathological examination. The other half was stored in 1 mL RNA later (Sigma, USA) at 4 ℃ overnight, then transferred to a clean freezing tube and stored at 70 ℃ for RNA extraction. The resected primary tumors were also fixed in 40 g/L formaldehyde and embedded in paraffin. Two consecutive sections, each 4 μm-thick, were examined by ordinary H&E staining and immunostaining with anti-E-cadherin antibody, respectively.

RNA extraction

Lymph node samples were homogenized in 1 mL of TRIzol Reagent (Invitrogen) per 50-100 mg of tissue using power homogenizer. RNA extraction was carried out according to the protocol recommended by the manufacturer. Total RNA was dissolved in diethylpyrocarbonate-treated water and the volume and quality of the RNA then assessed by the ultraviolet spectrophotometer.

The Access RT-PCR

Complementary DNA (cDNA) was synthesized and amplified from total RNA using the Access RT-PCR system (Promega). The primer sequences used for CK-20 detection were 5'-ggtcgcgactacagtgcatattaca-3' (sense) and 5'-cctcagcagccagtttagcattatc-3' (anti-sense)[12]. cDNA synthesis was monitored by beta-actin RT-PCR using the following primers: 5'-caaatgcttctaggcggact-3' (sense) and 5'-atgctatc-acctcccctgtg-3' (anti-sense). The RT-PCR was performed in a 25-μL reaction mixture containing nuclease-free water 11 μL, 5×Reacton Buffer 5 μL, dNTP (10 mmol/L) 0.5 μL, each of beta-actin primers (20 μmol/L) 0.5 μL, each of CK-20 primers (10 μmol/L) 1.25 μL, $MgSO_4$ (25 mmol/L) 1 μL, AMV reverse transcriptase (5 U/μL) 0.5 μL, Tfl DNA polymerase (5 U/μL) 0.5 μL, and RNA sample 3 μL. The Access RT-PCR condition was set up as follows: 1 cycle at 48 ℃ for 45 min (reverse transcription), 1 cycle at 94 ℃ for 2 min (AMV RT inactivation), followed by 40 cycles at 94 ℃ for 30 s (denaturation) and at 62 ℃ for 1 min (annealing) and at 68 ℃ for 1.5 min (extension), followed by a final extension at 68 ℃ for 7 min. The resultant cDNA products of CK-20 and beta-actin were 121 and 381 base pairs, respectively. The RT-PCR products were analyzed by electrophoresis on 2% agarose gels stained with ethidium bromide. In this report, "micrometastasis" in the regional lymph nodes was defined as metastasis that was detected only by the RT-PCR assay but not by ordinary H&E staining (Figure 1).

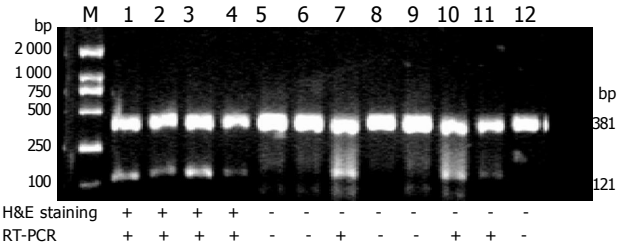

Figure 1 Comparison of the results of RT-PCR and H&E staining. M: DL2000Marker; lanes 1-12: dissected lymph nodes. The estimated size of the amplified products in base pairs (bp) appears on the right. Lymph nodes of lanes 7, 10, and 11 were diagnosed LNM.

Immunohistochemistry

The dissected primary tumors were fixed in 40 g/L formaldehyde and embedded in paraffin. Specimens from the paraffin embedded block were cut into 4 μm sections and then placed on slides. E-cadherin immunohistochemical staining was performed using EliVision™ plus IHC Kit (Maixin Biological, Fuzhou, China). After the slides were deparaffinized with xylene and dehydrated with ethanol, they were placed in 10 mmol/L citrate buffer and heated in a microwave at 700 W for 5 min for the retrieval of antigens in the specimens. Endogenous peroxidase activity was blocked by incubation of the slides in 3% hydrogen peroxide in absolute methanol at room temperature for 10 min. The slides were then incubated sequentially with 50 μL of mouse monoclonal antibody against human E-cadherin (Maixin Biological, Fuzhou, China) overnight at 4 ℃, with 50 μL of polymer enhancer for 20 min, and 50 μL of polymerized HRP-anti mouse IgG for 30 min. The reaction products were visualized with diaminobenzidine (DAB Kit, Maixin Biological, Fuzhou, China), and slides were counterstained with hematoxylin, dehydrated, and evaluated by light microscopy. Tris-buffered saline (TBS) solution was used instead of the primary antibody for negative controls.

For the purpose of data analysis, the expression level

of E-cadherin in the primary tumor was graded according to the proportion of positive tumor cells. If more than 25% of the tumor cells were positively stained for E-cadherin, the tumor was classified as having preserved E-cadherin expression. In contrast, if 25% or less of the tumor cells were positively stained, the tumor was classified as having the loss of E-cadherin expression. The stained slides were observed independently by two pathologists who had no knowledge of the clinicopathological data. All the staining results for E-cadherin were examined in relation to the clinicopathological parameters of the tumors.

Statistical analysis

Statistical analysis was performed by Fisher's exact test to examine the association of LNM and the expression of E-cadherin in the primary tumor with the clinicopathologic characteristics of the primary tumor, and examine the relationship between the expression of E-cadherin in the primary tumor and LNM. Statistical significance was defined as $P<0.05$.

RESULTS

Correlation between LNM and clinicopathologic characteristics

Routine examination by H&E staining confirmed metastasis in 233 lymph nodes from 20 patients. All these 233 lymph nodes were cytokeratin-20 positive; moreover, LNM was detected in an additional 67 lymph nodes in 12 cases of these 20 patients. LNM was also detected in 10 lymph nodes from two cases of 10 patients who had no obvious metastases identified by H&E staining. Totally, LNM was identified only by the RT-PCR assay in 77 (12.5%) lymph nodes of 14 patients (46.7%) with gastric carcinoma. From Table 1, we also found that the incidence of LNM was significantly higher in the diffuse type (12 of 19 cases, 63.2%) than in the intestinal type of gastric carcinoma (2 of 11 cases, 18.2%, $P = 0.026$). Micrometastases increased in accordance with the depth of tumor invasion. Seven of 21 cases that had lesions within submucosa layer were detected to have micrometastases in the lymph nodes; in contrast, seven of nine cases with invasion reaching the muscularis propria and deeper invasion had micrometastases ($P = 0.046$). Other clinicopathologic findings including gender, age, location, diameter, histologic differentiation, lymphatic invasion and vascular invasion had no statistically significant correlation with the incidence of LNM ($P>0.05$).

Table 1 Correlation between LNM and clinicopathologic characteristics

Variable	Patients (*n*)	LNM		
		Negative (%)	Positive (%)	*P*
Gender				
Male	17	9 (52.9)	8 (47.1)	
Female	13	7 (53.8)	6 (46.2)	$P = 1.000$
Age				
<50 yr	10	4 (40)	6 (60)	
≥R50 yr	20	12 (60)	8 (40)	$P = 0.442$
Superficial diameter				
<5 cm	17	9 (52.9)	8 (47.1)	
≥R5 cm	13	7 (53.8)	6 (46.2)	$P = 1.000$
Tumor location				
Upper/middle third	17	8 (47.1)	9 (52.9)	
Lower third	13	8 (61.5)	5 (38.5)	$P = 0.484$
Histologic type				
Intestinal	11	9 (81.8)	2 (18.2)	
Diffuse	19	7 (36.8)	12 (63.2)	$P = 0.026$
Depth of invasion				
T1/T2	21	14 (66.7)	7 (33.3)	
T3/T4	9	2 (22.2)	7 (77.8)	$P = 0.046$
Histologic differentiation				
Well/moderate	13	9 (69.2)	4 (30.8)	
Poor	17	7 (58.8)	10 (41.2)	$P = 0.159$
Lymphatic invasion				
Positive	18	7 (38.9)	11 (61.1)	
Negative	12	9 (75)	3 (25)	$P = 0.072$
Vascular invasion				
Positive	5	3 (60)	2 (40)	
Negative	25	13 (52)	12 (48)	$P = 1.000$

Expression of E-cadherin

The loss of expression of E-cadherin in primary tumors was found in 14 (46.7) of 30 tumors. From Table 2, we found that the absence of E-cadherin expression was significantly associated with The Lauren classification ($P = 0.026$), lymph node metastasis ($P = 0.011$), the grade of differentiation ($P = 0.004$) and the lymphatic invasion ($P = 0.001$), but not correlated with age, gender, location, diameter and depth of tumor invasion ($P>0.05$).

Table 2 Correlation between the expression of E-cadherin in primary tumors and clinicopathologic characteristics

Variable	Patients (*n*)	Expression of E-cadherin		
		Negative (%)	Positive (%)	*P*
Gender				
Male	17	7 (41.2)	10 (58.8)	
Female	13	7 (53.8)	6 (46.2)	$P = 0.713$
Age				
<50 yr	10	3 (30)	7 (70)	
≥R50 yr	20	11 (55)	9 (45)	$P = 0.260$
Superficial diameter				
<5 cm	17	7 (41.2)	10 (58.8)	
≥R5 cm	13	7 (53.8)	6 (46.2)	$P = 0.713$
Tumor location				
Upper/middle third	17	8 (47.1)	9 (52.9)	
Lower third	13	6 (46.2)	7 (53.8)	$P = 1.000$
Histologic type				
Intestinal	11	2 (18.2)	9 (81.8)	
Diffuse	19	12 (63.2)	7 (36.8)	$P = 0.026$
Depth of invasion				
T1/T2	21	8 (38.1)	13 (61.9)	
T3/T4	9	6 (66.7)	3 (33.3)	$P = 0.236$
Histologic differentiation				
Well/moderate	13	2 (15.4)	11 (84.6)	
Poor	17	12 (70.6)	5 (29.4)	$P = 0.004$
Lymph node metastasis				
Positive	18	12 (66.7)	6 (33.3)	
Negative	12	2 (16.7)	10 (83.3)	$P = 0.011$
Lymphatic invasion				
Positive	18	13 (72.2)	5 (27.8)	
Negative	12	1 (8.3)	11 (91.7)	$P = 0.001$

Correlation between LNM and the expression of E-cadherin

From Table 3, we found that expression of E-cadherin was negative in 10 (71.4%) of the 14 patients with LNM, and in 4 (25%) of the 16 patients without LNM. The difference between these two groups was statistically significant ($P = 0.026$).

Table 3 Correlation between LNM and the expression of E-cadherin

LNM	Patients (*n*)	Expression of E-cadherin		
		Negative (%)	Positive (%)	*P*
Positive	14	10 (71.4)	4 (28.6)	
Negative	16	4 (25)	12 (75)	*P* = 0.026

DISCUSSION

It is well known that lymph node metastasis is the most important prognostic factor for patients with gastric carcinoma. However, even after undergoing radical resection of primary tumors and lymph nodes, about 20% of patients with gastric carcinoma reportedly die of recurrence[13], and about 3% of patients with early-stage gastric carcinoma also reportedly die of recurrence[14]. These findings suggest the existence of LNM that cannot be identified by routine H&E staining. Several investigators have demonstrated the usefulness of immunohistochemical technique for detection of micrometastases in lymph nodes of gastric carcinoma patients[5-7,15,16]. In the present study, RT-PCR assay was applied to detect micrometastsis in the lymph nodes resected from 30 cases of stage I-IV gastric carcinomas. Totally, LNM was detected by the RT-PCR assay in 77 (12.5%) lymph nodes of 14 patients (46.7%) with gastric carcinoma. The incidence of LNM was significantly higher in the diffuse type (12 of 19 cases, 63.2%) than in the intestinal type of gastric carcinoma (2 of 11 cases, 18.2%, $P = 0.026$). Similar to our results, Ishida *et al*, studied 2 446 lymph nodes removed during surgery for 109 cases of gastric carcinoma, including Stages I-IV. Metastases were confirmed in 230 lymph nodes (9.4%) stained with H&E, and an additional 201 lymph nodes (17.6%) had micrometastases identified only by immunostaining. They also demonstrated that the diffuse type had more micrometastases than the intestinal type[5].

In addition, we also found that there was a significant correlation between LNM and depth of tumor invasion. Seven of 21 cases that had lesions within submucosa layer were detected to have micrometastases in the lymph nodes; in contrast, seven of nine cases with invasion reaching the muscularis propria and deeper invasion had micrometastases ($P = 0.046$). Micrometastases increased in accordance with the depth of tumor invasion. Tsujitani *et al*, obtained almost the same results as ours. They reported that micrometastases in the lymph nodes were found in 18% of mucosal cancer, 25% of submucosal cancer, and 65% of T3 (serosal) cancer specimens, with cancer-free nodes examined by H&E staining[17].

These results indicate that RT-PCR assay is clearly more sensitive than routine histopathological examination for detection of micrometastases in lymph nodes of gastric carcinoma patients. Lymph node micrometastases are significantly associated with the Lauren classification and depth of tumor invasion.

E-cadherin is a 120-ku transmembrane glycoprotein that is responsible for calcium-dependent intercellular adhesion by homotypic interactions. E-cadherin plays an important role in maintaining cell polarity and tissue morphology[18]. Previous studies showed that 43.5-72% of gastric carcinoma had reduction or loss of E-cadherin expression[19,20]. In our study, the loss of E-cadherin expression was observed in 46.7% (14 of 30 cases) of gastric carcinoma. We also found the absence of E-cadherin expression was significantly related with the histologic type and the grade of tumor differentiation. In 19 gastric carcinomas with diffuse type of growth 12 showed negative E-cadherin expression, while in 11 gastric carcinomas with intestinal type of growth only two showed negative E-cadherin expression. The difference was statistically significant ($P = 0.026$). In 17 poorly-differentiated gastric carcinomas 12 showed negative E-cadherin expression, while in 13 well- or moderately-differentiated gastric carcinomas only two showed negative E-cadherin expression. The difference was also statistically significant ($P = 0.004$). Recently, several scholars also reported that the reduction or absence of E-cadherin expression occurred more frequently in diffuse than intestinal type of gastric carcinoma, and correlated with poor differentiation[21,22]. These findings indicate that E-cadherin may play an important role in determining the growth type and differentiation of gastric carcinoma.

The E-cadherin gene has generally been recognized as an invasion-suppressor gene[23,24]. Chen *et al*[22], reported that the loss of E-cadherin expression was significantly associated with tumor invasion. Yonemura *et al*[20], also reported that reduced E-cadherin expression showed a strong relationship with positive serosal involvement and infiltrating type. In the present study, the absence of E-cadherin expression was more frequent in T3 or T4 tumors (six of nine tumors, 66.7%), compared with T1 or T2 tumors (8 of 21 tumors, 38.1%), but this difference was not statistically significant ($P = 0.236$). This may be explained by the fact that the cases in our study were comparatively few. To draw a further conclusion, larger sample investigations on gastric carcinoma are needed.

It has been reported that reduced expression of E-cadherin plays an important role in the development of lymph node metastases in patients with gastric carcinoma. However, the relationship between E-cadherin expression in the primary tumor and LNM has not been extensively discussed. In our study, we found that expression of E-cadherin was negative in 10 (71.4%) of the 14 patients with LNM, and in 4 (25%) of the 16 patients without LNM. The difference between these two groups was statistically significant ($P = 0.026$). The result indicates the loss of E-cadherin expression may contribute to LNM.

REFERENCES

1 **Maruyama K,** Gunven P, Okabayashi K, Sasako M, Kinoshita T. Lymph node metastases of gastric cancer. General pattern in 1931 patients. *Ann Surg* 1989; **210**: 596-602
2 **Roder JD,** Bottcher K, Siewert JR, Busch R, Hermanek P, Meyer HJ. Prognostic factors in gastric carcinoma. Results of the German Gastric Carcinoma Study 1992. *Cancer* 1993; **72**: 2089-2097
3 **Shen KH,** Wu CW, Lo SS, Hsieh MC, Hsia CY, Chiang SC, Lui WY. Factors correlated with number of metastatic lymph nodes in gastric cancer. *Am J Gastroenterol* 1999; **94**: 104-108
4 **Moll R,** Franke WW, Schiller DL, Geiger B, Krepler R. The catalog of human cytokeratins: patterns of expression in normal epithelia, tumors and cultured cells. *Cell* 1982; **31**: 11-24
5 **Ishida K,** Katsuyama T, Sugiyama A, Kawasaki S. Immu-

nohistochemical evaluation of lymph node micrometastases from gastric carcinomas. *Cancer* 1997; **79**: 1069-1076
6 **Cai J,** Ikeguchi M, Maeta M, Kaibara N. Micrometastasis in lymph nodes and microinvasion of the muscularis propria in primary lesions of submucosal gastric cancer. *Surgery* 2000; **127**: 32-39
7 **Fukagawa T,** Sasako M, Mann GB, Sano T, Katai H, Maruyama K, Nakanishi Y, Shimoda T. Immunohistochemically detected micrometastases of the lymph nodes in patients with gastric carcinoma. *Cancer* 2001; **92**: 753-760
8 **Xu X,** Roberts SA, Pasha TL, Zhang PJ. Undesirable cytokeratin immunoreactivity of native nonepithelial cells in sentinel lymph nodes from patients with breast carcinoma. *Arch Pathol Lab Med* 2000; **124**: 1310-1313
9 **Mayer B,** Johnson JP, Leitl F, Jauch KW, Heiss MM, Schildberg FW, Birchmeier W, Funke I. E-cadherin expression in primary and metastatic gastric cancer: down-regulation correlates with cellular dedifferentiation and glandular disintegration. *Cancer Res* 1993; **53**: 1690-1695
10 **Kinsella AR,** Green B, Lepts GC, Hill CL, Bowie G, Taylor BA. The role of the cell-cell adhesion molecule E-cadherin in large bowel tumour cell invasion and metastasis. *Br J Cancer* 1993; **67**: 904-909
11 **Lauren P.** The two histological main types of gastric carcinoma: diffuse and so-called intestinal–type carcinoma. An attempt at a histo-clinical classification. *Acta Pathol Microbiol Scand* 1965; **64**: 31-49
12 **Okada Y,** Fujiwara Y, Yamamoto H, Sugita Y, Yasuda T, Doki Y, Tamura S, Yano M, Shiozaki H, Matsuura N, Monden M. Genetic detection of lymph node micrometastases in patients with gastric carcinoma by multiple-marker reverse transcriptase-polymerase chain reaction assay. *Cancer* 2001; **92**: 2056-2064
13 **Tsushima K,** Sakata Y. Treatment of recurrent gastric cancer. *Gan To Kagaku Ryoho* 1998; **25**: 321-326
14 **Ohgaki M,** Toshio T, Akeo H, Yamasaki J, Togawa T. Effect of extensive lymph node dissection on the survival of early gastric cancer. *Hepatogastroenterology* 1999; **46**: 2096-2099
15 **Lee E,** Chae Y, Kim I, Choi J, Yeom B, Leong AS. Prognostic relevance of immunohistochemically detected lymph node micrometastasis in patients with gastric carcinoma. *Cancer* 2002; **94**: 2867-2873
16 **Choi HJ,** Kim YK, Kim YH, Kim SS, Hong SH. Occurrence and prognostic implications of micrometastases in lymph nodes from patients with submucosal gastric carcinoma. *Ann Surg Oncol* 2002; **9**: 13-19
17 **Tsujitani S,** Kaibara N. Clinical significance of molecular biological detection of micrometastases in gastric carcinoma. *Nihon Geka Gakkai Zasshi* 2001; **102**: 741-744
18 **Takeichi M.** Cadherin cell adhesion receptors as a morphogenetic regulator. *Science* 1991; **251**: 1451-1455
19 **Joo YE,** Rew JS, Choi SK, Bom HS, Park CS, Kim SJ. Expression of e-cadherin and catenins in early gastric cancer. *J Clin Gastroenterol* 2002; **35**: 35-42
20 **Yonemura Y,** Endou Y, Kimura K, Fushida S, Bandou E, Taniguchi K, Kinoshita K, Ninomiya I, Sugiyama K, Heizmann CW, Schafer BW, Sasaki T. Inverse expression of S100A4 and E-cadherin is associated with metastatic potential in gastric cancer. *Clin Cancer Res* 2000; **6**: 4234-4242
21 **Joo YE,** Rew JS, Kim HS, Choi SH, Park CS, Kim SJ. Changes in the E-cadherin-catenin complex expression in early and advanced gastric cancers. *Digestion* 2001; **64**: 111-119
22 **Chen HC,** Chu RY, Hsu PN, Hsu PI, Lu JY, Lai KH, Tseng HH, Chou NH, Huang MS, Tseng CJ, Hsiao M. Loss of E-cadherin expression correlates with poor differentiation and invasion into adjacent organs in gastric adenocarcinomas. *Cancer Lett* 2003; **201**: 97-106
23 **Mareel M,** Vleminckx K, Vermeulen S, Yan G, Bracke M, van Roy F. Downregulation *in vivo* of the invasion-suppressor molecule E-cadherin in experimental and clinical cancer. *Princess Takamatsu Symp* 1994; **24**: 63-80
24 **Yonemura Y,** Ninomiya I, Kaji M, Sugiyama K, Fujimura T, Tsuchihara K, Kawamura T, Miyazaki I, Endou Y, Tanaka M. Decreased E-cadherin expression correlates with poor survival in patients with gastric cancer. *Anal Cell Pathol* 1995; **8**: 177-190

Science Editor Li WZ **Language Editor** Elsevier HK

PO Box 2345, Beijing 100023, China
www.wjgnet.com
wjg@wjgnet.com

ELSEVIER

World J Gastroenterol 2005;11(20):3144-3146
World Journal of Gastroenterology ISSN 1007-9327

• *BRIEF REPORTS* •

HMLH1 gene mutation in gastric cancer patients and their kindred

Jian-Hua Li, Xian-Zhe Shi, Shen Lü, Min Liu, Wan-Ming Cui, Li-Na Liu, Jing Jiang, Guo-Wang Xu

Jian-Hua Li, Shen Lü, Min Liu, Laboratory of Molecular Biology, the Second Hospital of Dalian Medical University, Dalian 116027, Liaoning Province, China
Xian-Zhe Shi, Guo-Wang Xu, National Chromatographic Research and Application Center, Dalian Institute of Chemical Physics, the Chinese Academy of Sciences, Dalian 116011, Liaoning Province, China
Wan-Ming Cui, Li-Na Liu, Department of Gastroenterology, the First Hospital of Dalian Medical University, Dalian 116001, Liaoning Province, China
Jing Jiang, Department of Material Engineering, Dalian Science and Technology University, Dalian 116027, Liaoning Province, China
Supported by the Knowledge Innovation Program of the Chinese Academy of Sciences, No. DICP K2001A4
Correspondence to: Shen Lü, Professor, PhD, Laboratory Center of Molecular Biology, The Second Hospital of Dalian Medical University, Dalian 116027, Liaoning Province, China. ljhsxw@pa18.com
Telephone: +86- 411-84687554
Received: 2004-04-15 Accepted: 2004-05-09

Abstract

AIM: To study the status of hMLH1 gene point mutations of gastric cancer kindreds and gastric cancer patients from northern China, and to find out gene mutation status in the population susceptible to gastric cancer.

METHODS: Blood samples of 120 members from five gastric cancer families, 56 sporadic gastric cancer patients and control individuals were collected. After DNA extraction, the mutations of exon 8 and exon 12 of hMLH1 gene were investigated by PCR-SSCP-CE, followed by DNA sequencing.

RESULTS: In the five kindreds, the mutation frequency was 25% (5/16) for the probands and 18% (19/104) for the non-cancerous members, which were significantly higher than the controls ($P<0.01$ $\chi^2=7.71$, $P<0.01$ $\chi^2=8.65$, respectively). In the sporadic gastric cancer, the mutation frequency was 7% (4/56), which was similar to that (5/100) in the healthy controls. The mutation point of exon 8 was at 219 codon of hMLH1 gene (A-G), resulting in a substitution of Ile-Val (ATC-GTC), whereas the mutation of exon 12 was at 384 codon of hMLH1 gene (T-A) resulting in a substitution of Asp-Val (GTT-GAT), which were the same as previously found in hereditary nonpolyposis colorectal carcinoma.

CONCLUSION: The members of gastric cancer families from northern China may have similar genetic background of hMLH1 gene mutation as those of hereditary nonpolyposis colorectal carcinoma.

Key words: Gastric cancer kindred; Mismatch repair; Mutation; HNPCC

Li JH, Shi XZ, Lü S, Liu M, Cui WM, Liu LN, Jiang J, Xu GW. HMLH1 gene mutation in gastric cancer patients and their kindred. *World J Gastroenterol* 2005; 11(20): 3144-3146
http://www.wjgnet.com/1007-9327/11/3144.asp

INTRODUCTION

Gastric cancer is one of the most common cancers and a leading cause of cancer death in China. Although the molecular biological mechanism involved in the gastric tumorigenesis remains unclear, clinical and epidemic studies have shown that gastric cancer occurrence has a tendency of familial accumulation. Several members can be attacked by gastric cancer just in one family. Moreover, the younger generations of these families are found to develop colorectal cancer at a high frequency in recent years because of the change of food habit. So we imagine that individuals susceptible to gastric cancer may have the similar genetic background as those of colorectal cancer. Hereditary nonpolyposis colorectal carcinoma (HNPCC) is a kind of colorectal cancer that has been well studied[1,2]. One of the reasons why HNPCC emerges is germline mutation in mismatch repair genes[3,4], most commonly in hMLH1 (human MutL homolog1) and hMSH2 (human MutS homolog2)[5]. Therefore, we selected the hot mutant sequences exon 8 and exon 12 of hMLH1 gene to detect gene mutation status in the population susceptible to gastric cancer.

MATERIALS AND METHODS

Sample collection

Peripheral blood samples of 120 members in five gastric cancer families, 56 sporadic gastric cancer patients and control individuals were collected from the southern district of Liaoning Province, northeast of China. All blood samples were stored at -20 ℃ until used. Of the 120 familial samples, 16 were from gastric cancer patients (all were adenocarcinomas) aged 36-58 years, nine male and seven female and 104 were from non-cancerous members aged 9-70 years, 59 male and 45 female. All the five gastric cancer families met the following standards: three or more cases were affected by gastric cancer in two successive generations, two or more of them were first-degree relatives and at least one diagnosed to have had gastric cancer before the age of 50, whereas

there was no first-degree relative affected by gastric cancer in those sporadic patients (all were adenocarcinomas) aged 42-64 years, 36 male and 20 female and healthy controls aged 18-60 years, 60 male and 40 female.

DNA extraction

Genomic DNA was extracted from blood using the DNA extraction kit (Huashun Co., Ltd, Shanghai).

PCR of hMLH1 gene in exon 8 and exon 12

Primer sequences used were as follows: for exon 8, 5'-AM-ACAGACTTTGCTACCAGGACTTG-3' (Forward) and 5'-FAM-TGTCTTATCCTCTGTGACAATGG-3' (Reverse) and for exon 12, 5'-FAM-CTCAGCCATGAGAC-AATAAATCC-3' (Forward) and 5'-FAM-GGTTCCCAAA-TAATGTGATGG-3' (Reverse). Fluorescence-labeled primers and PCR amplification kits were obtained from TaKaRa Biotechnology (Dalian, China). The reaction mixture contained 10 mmol/L Tris-HCl (pH 9.0), 50 mmol/L KCl, 1.5 mmol/ L $MgCl_2$, 200 μmol/L dNTPs, 1 mmol/L each primer, 100-200 ng of the extracted genomic DNA and 1.25 U Taq DNA polymerase in a total volume of 25 μL. PCR was performed with a Perkin-Elmer Model 2700 PCR system (Foster City, CA, USA) with the following polymerase chain reaction (PCR) program: initial denaturation at 94 ℃ for 5 min, followed by 35 cycles of denaturation at 94 ℃ for 40 s, annealing at 55 ℃ for 40 s, extension at 72 ℃ for 1 min, and a final elongation step at 72 ℃ for 5 min.

SSCP analysis by capillary electrophoresis

Single-strand conformation polymorphism (SSCP) of DNA was analyzed by the method of capillary electrophoresis (CE). A P/ACE MDQ capillary electrophoresis instrument (Beckman, Palo Alto, CA, USA) with argon ion LIF detector (λ_{ex} = 488 nm, λ_{em} = 520 nm) was employed. The capillary was coated with linear polyacrylamide with an inner diameter of 75 μm and an effective length of 30 cm. Prior to electrophoresis, the PCR products were diluted 20-folds with water, and heated at 95 ℃ for 10 min, then immediately put into ice water and kept for 5 min. The samples were injected at reverse polarity of 5 kV for 5 s, and separation was carried out under constant voltage. Single-strand DNA fragments were detected by LIF detector and the data were collected and analyzed by MDQ software.

CE-sequencing

The samples suspected to be mutant by CE-SSCP were sequenced. The PCR for sequencing was performed using nonfluorescent forward primer and the Big Dye terminator cycle sequencing ready reaction kit (Perkin-Elmer, ABI Prism) under the following conditions: initial denaturation at 96 ℃ for 2 min, 25 cycles at 96 ℃ for 10 s, annealing at 50 ℃ for 5 s, extension at 60 ℃ for 2 min, and a final elongation step at 60 ℃ for 7 min, in a 2 700 thermal cycler (Perkin-Elmer). The products were purified by an ethanol/NaAc method, and then CE-sequencing was conducted using ABI Prism 310 (Perkin-Elmer, ABI Prism).

RESULTS

Of the 16 probands in the five kindreds, two cases were found mutant at exon 8, two cases were found mutant at exon 12 and the total mutation frequency was 25% (5/16). Meanwhile 12 cases were found mutant at exon 8, seven cases were found mutant at exon 12 and the total mutation frequency was 18% (19/104) in the familial noncancerous members. In the 56 cases of sporadic gastric cancer, two cases were found mutant at exon 8, two cases were found mutant at exon 12 and the total mutation frequency was 7% (4/56), which was similar to the healthy control individuals but being significantly lower than both the probands and familial members in the kindreds (Table 1). The mutation point of exon 8 was at 219 codon of hMLH1 gene (A-G), resulting in a substitution of Ile-Val (ATC-GTC) (Figures 1A and 2A), whereas the mutation of exon 12 was at 384 codon of hMLH1 gene (T-A), resulting in a substitution of Asp-Val (GTT-GAT) (Figures 1B and 2B), which was the same as previously found in HNPCC.

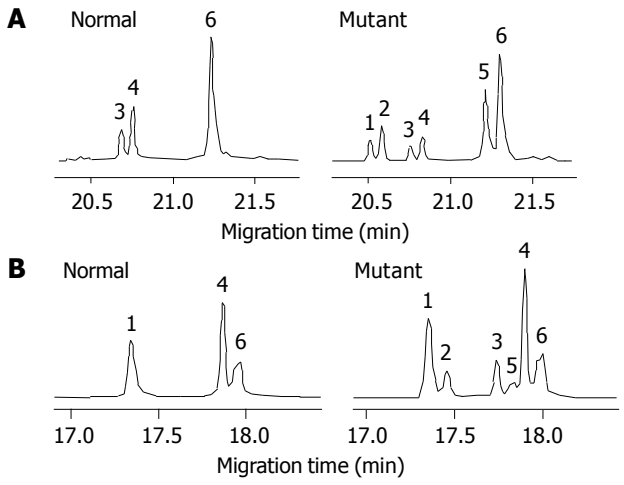

Figure 1 SSCP analysis of the normal and mutant samples of hMLH1 gene exon 8 (**A**) and exon 12 (**B**). Peaks 3, 4, 6- wild type ssDNA and peaks 1, 2, 5-mutant ssDNA for exon 8 (A); Peaks 1, 4-wild type ssDNA, peaks 2, 3-mutant ssDNA and peaks 5, 6-primer ssDNA for exon 12 (B).

Table 1 Comparison of hMLH1mutation among the gastric cancer kindreds, sporadic gastric cancer patients, and control individuals

Groups	Cases	HMLH1 mutation		Mutation rate (%)
		Exon 8	exon 12	
Probands of kindreds	16	2	2	25[b]
Non-cancerous members of kindreds	104	12	7	18[d]
Sporadic gastric cancer patients	56	2	2	7
Control individuals	100	2	3	5

[b]$P<0.01$ $\chi^2 = 7.71$, [d]$P<0.01$ $\chi^2 = 8.65$ *vs* control individuals.

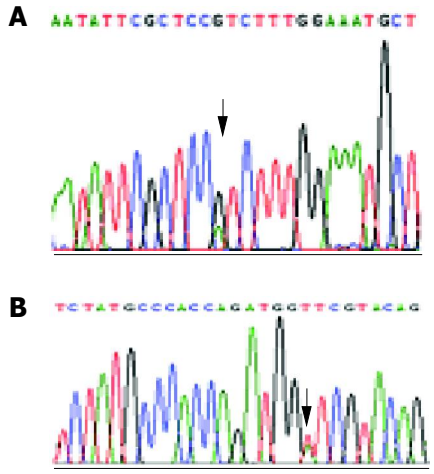

Figure 2 Electrophorogram section of CE-sequencing of hMLH1 gene exon 8 (**A**) and exon 12 (**B**). Arrow: substitution of A-G (A) and T-A (B).

DISCUSSION

Mismatch repair (MMR) plays a central role in maintaining genomic stability by repairing DNA replication errors and inhibiting recombination between non-identical sequences[7,8]. Loss of mismatch repair causes destabilization of the genome and results in high mutation frequency[9]. HMLH1 gene is a prominent component in the human mismatch repair system and its dysfunction is involved in a number of patients with HNPCC[10,11]. It has been reported that germline mutations of MMR are identified in nearly 80% of the patients with HNPCC and almost 60% of the mutations are in hMLH1[5].

According to statistics, about 8-10% of gastric cancer cases are related to an inherited familial genetic factor[12]. Up to 3-fold increases in risk for gastric cancer among relatives of gastric cancer patients are consistent[13]. The gene background of gastric cancer susceptibility is not sufficiently known to us, especially in China, although the hereditary tendency is even higher.

We primarily detected exon 8 and exon 12 of the hMLH1 gene in 16 probands' peripheral blood sample of five gastric cancer kindreds and found the same mutations that had previously been discovered in HNPCC. The mutation frequency was significantly higher than that of the control individuals and it was true of those familial members. It was proposed that the gene background is characterized by hMLH1 mutation in gastric cancer kindreds and that the presence of hMLH1 mutation is associated with an increased risk of developing gastric cancer and those carrying mutant hMLH1 gene are prone to develop gastric cancer even at an early age. What about sporadic gastric cancer? To answer this question, we extended the samples by analyzing 56 sporadic gastric cancer patients with their blood samples. To our surprise, the mutation frequency in the blood samples were similar to control individuals, which was significantly lower than both the probands and noncancerous members in the five kindreds' blood samples. It seems that hMLH1 gene mutation is not a characteristic of sporadic gastric cancer.

From the above-mentioned, it can be concluded that there may be similar hMLH1 gene mutation as HNPCC in somatic cells in gastric cancer kindreds, but not in those in sporadic gastric cancer patients. The mutations of hMLH1 gene may be involved in tumorigenesis of hereditary gastric cancer in northern China.

REFERENCES

1 **Park JG,** Vasen HF, Park KJ, Peltomaki P, Ponz de Leon M, Rodriguez-Bigas MA, Lubinski J, Beck NE, Bisgaard ML, Miyaki M, Wijnen JT, Baba S, Lynch HT. Suspected hereditary nonpolyposis colorectal cancer: International Collaborative Group on Hereditary Non-Polyposis Colorectal Cancer (ICG-HNPCC) criteria and results of genetic diagnosis. *Dis Colon Rectum* 1999; **42**: 710-715; discussion 715-716

2 **Lynch HT,** Watson P, Shaw TG, Lynch JF, Harty AE, Franklin BA, Kapler CR, Tinley ST, Liu B, Lerman C. Clinical impact of molecular genetic diagnosis, genetic counseling, and management of hereditary cancer. Part II: Hereditary nonpolyposis colorectal carcinoma as a model. *Cancer* 1999; **86**: 2457-2463

3 **Dieumegard B,** Grandjouan S, Sabourin JC, Le Bihan ML, Lefrere I, Bellefqih JP, Rougier P, Lasser P, Benard J, Couturier D, Bressac-de Paillerets B. Extensive molecular screening for hereditary non-polyposis colorectal cancer. *Br J Cancer* 2000; **82**: 871-880

4 **Wang Q,** Lasset C, Desseigne F, Saurin JC, Maugard C, Navarro C, Ruano E, Descos L, Trillet-Lenoir V, Bosset JF, Puisieux A. Prevalence of germline mutations of hMLH1, hMSH2, hPMS1, hPMS2, and hMSH6 genes in 75 French kindreds with nonpolyposis colorectal cancer. *Hum Genet* 1999; **105**: 79-85

5 **Peltomaki P,** Vasen HF. Mutations predisposing to hereditary nonpolyposis colorectal cancer: database and results of a collaborative study. The International Collaborative Group on Hereditary Nonpolyposis Colorectal Cancer. *Gastroenterology* 1997; **113**: 1146-1158

6 **Peltomaki P.** Deficient DNA mismatch repair: a common etiologic factor for colon cancer. *Hum Mol Genet* 2001; **10**: 735-740

7 **Jacob S,** Praz F. DNA mismatch repair defects: role in colorectal carcinogenesis. *Biochimie* 2002; **84**: 27-47

8 **Duval A,** Hamelin R. Genetic instability in human mismatch repair deficient cancers. *Ann Genet* 2002; **45**: 71-75

9 **Loukola A,** Eklin K, Laiho P, Salovaara R, Kristo P, Jarvinen H, Mecklin JP, Launonen V, Aaltonen LA. Microsatellite marker analysis in screening for hereditary nonpolyposis colorectal cancer (HNPCC). *Cancer Res* 2001; **61**: 4545-4549

10 **Han HJ,** Maruyama M, Baba S, Park JG, Nakamura Y. Genomic structure of human mismatch repair gene, hMLH1, and its mutation analysis in patients with hereditary nonpolyposis colorectal cancer (HNPCC). *Hum Mol Genet* 1995; **4**: 237-242

11 **Hutter P,** Couturier A, Membrez V, Joris F, Sappino AP, Chappuis PO. Excess of hMLH1 germline mutations in Swiss families with hereditary non-polyposis colorectal cancer. *Int J Cancer* 1998; **78**: 680-684

12 **La Vecchia C,** Negri E, Franceschi S, Gentile A. Family history and the risk of stomach and colorectal cancer. *Cancer* 1992; **70**: 50-55

13 **Zanghieri G,** Di Gregorio C, Sacchetti C, Fante R, Sassatelli R, Cannizzo G, Carriero A, Ponz de Leon M. Familial occurrence of gastric cancer in the 2-year experience of a population-based registry. *Cancer* 1990; **66**: 2047-2051

Science Editor Zhang JZ, Ma JY and Guo SY **Language Editor** Elsevier HK

PO Box 2345, Beijing 100023, China
www.wjgnet.com
wjg@wjgnet.com

ELSEVIER

World J Gastroenterol 2005;11(20):3147-3150
World Journal of Gastroenterology ISSN 1007-9327

• *BRIEF REPORTS* •

Effect of emodin on small intestinal peristalsis of mice and relevant mechanism

Hong-Quan Zhang, Cheng-Hua Zhou, Yu-Qing Wu

Hong-Quan Zhang, Cheng-Hua Zhou, Yu-Qing Wu, Medical and Pharmacological Institute, Yangzhou University, Yangzhou 225001, Jiangsu Province, China
Correspondence to: Professor Hong-Quan Zhang, Medical and Pharmacological Institute, Yangzhou University, Yangzhou 225001, Jiangsu Province, China. lixin2001@sohu.com
Telephone: +86-514-7978821 Fax: +86-514-7978821
Received: 2004-07-05 Accepted: 2004-09-04

Abstract

AIM: To investigate the effect of emodin on small intestinal peristalsis of mice and to explore its relevant mechanisms.

METHODS: The effect of emodin on small intestinal peristalsis of mice was observed by charcoal powder propelling test of small intestine. The contents of motilin and somatostatin in small intestine of mice were determinated by radioimmunoassay. The electrical potential difference (PD) related to Na^+ and glucose transport was measured across the wall of reverted intestinal sacs. Na^+–K^+-ATPase activity of small intestinal mucosa was measured by spectroscopic analysis.

RESULTS: Different dosages of emodin can improve small intestinal peristalsis of mice. Emodin increased the content of motilin, while reduced the content of somatostatin in small intestine of mice significantly. Emodin 0.2, 0.4, 0.8, and 1.6 g/L decreased PD when there was glucose. However, emodin had little effect when glucose was free. The Na^+–K^+-ATPase activity of small intestinal mucosa of mice in emodin groups was inhibited obviously.

CONCLUSION: Emodin can enhance the function of small intestinal peristalsis of mice by mechanisms of promoting secretion of motilin, lowering the content of somatostatin and inhibiting Na^+–K^+-ATPase activity of small intestinal mucosa.

Key words: Emodin; Small intestinal; Motilin; Somatostatin; Na^+–K^+-ATPase

Zhang HQ, Zhou CH, Wu YQ. Effect of emodin on small intestinal peristalsis of mice and relevant mechanism. *World J Gastroenterol* 2005; 11(20): 3147-3150
http://www.wjgnet.com/1007-9327/11/3147.asp

INTRODUCTION

Rhubarb has been used to treat gastrointestinal disorders for hundreds of years. The effective components of rhubarb are anthraquinone derivatives, emodin being the most important. Traditional viewpoints hold that emodin primarily acts on the large intestine and it can enhance the excitability of smooth muscles of the large intestine[1,2]. We have obtained more than 95% pure emodin from China Pharmaceutical University In this study, we evaluated whether emodin had any effects on small intestinal peristalsis of mice and explored its relevant mechanisms.

MATERIALS AND METHODS

Animals and treatment[3]

Fifty healthy ICR mice (weighing 18-22 g) were randomly divided into five groups: normal control, model, low dose of emodin, medium dose of emodin and high dose of emodin. The animals in emodin treatment groups and model group were put through intragastric gavage (IG) with compound diphenoxylate 0.2 mL/10 g. Those in normal control were treated with NS. Thirty minutes later different medications were given: mice in normal control and model group were given NS, and those in emodin treatment groups were given emodin 0.1, 0.2, and 0.4 g/kg respectively. All of the animals were administered as above for 1 wk and were fasted for 12 h before the last administration.

Charcoal powder propelling test of small intestine[4]

Thirty minutes after the last administration, all animals were IG charcoal powder suspended liquid 0.2 mL/10 g. Twenty minutes later the mice were killed by exarticulation. The small intestine from pylorus to the boundary of ileum and cecum was isolated and its length was "total length of small intestine". The length from pylorus to the foreland of charcoal powder was "charcoal powder propelling length".

Charcoal powder propelling ratio=[charcoal powder propelling length (cm)/total length of small intestine(cm)] ×100%.

Determination of motilin and somatostatin

Fifty mice were administered as above. Thirty minutes after the last administration, the small intestinal tissues were treated according to Sun *et al*[5]. The contents of motilin and somatostatin in small intestine of mice were determined by radioimmunoassay according to the protocols of the kit.

Determination of Na^+–K^+-ATPase activity

After isolating small intestinal tissues, the mice above were intercepted between 5 cm intestinal segments below the Treitz ligament. The intestines were rinsed repeatedly by

NS and made into homogenates of small intestinal mucosa. The Na^+–K^+-ATPase activity of small intestinal mucosa was measured by spectroscopic analysis according to the protocols of the kit. The protein was determined by Coomassie Brilliant Blue Method. The unit of Na^+–K^+-ATPase activity was μmol pi/mg Pro/h.

Potential difference (PD) of isolated small intestine[6,7]

About 8 cm of jejunum was taken, and cleaned with K-H solution. The wall of intestinal sacs was reverted. We ligated one end, and the other end was tied with tubuliform glass-tube. The reverted intestinal sac full of K-H solution was put in a tube full of 25 mmol/L glucose K-H solution (glucose K-H) or glucose-free K-H (at 37 ℃). The mixed gas including 50 mL/L CO_2 and 95% O_2 was injected. The electrical potential difference (PD) was measured across the wall of reverted intestinal sacs. The drugs in experiment were dissolved by glucose-free KH or glucose KH, PH was regulated and the osmotic pressure was modulated with mannitol. PD was recorded every 2.5 min and observed 15 min continuously.

Statistical analysis

All data were expressed as mean±SD. Statistical analysis was performed using unpaired *t* test. Differences were considered significant when $P \leqslant 0.05$.

RESULTS

Effect of emodin on charcoal powder propelling movement of small intestine in mice

The charcoal powder propelling ratio in normal control was 56.4±4.9%, while it greatly decreased to 44.7±10.3% in model group. Comparing with model group, emodin 0.1, 0.2, and 0.4 g/kg induced obvious increase of the charcoal powder propelling ratio of small intestine, and reached 54.6±6.6%, 67.2±18.4%, and 70.6±10.1%, respectively (Table 1).

Table 1 Effect of emodin on charcoal powder propelling movement of small intestine in mice (mean±SD, *n* = 10)

Group	Dose (g/kg)	Charcoal powder propelling ratio (%)
Normal control	–	56.4±4.9
Model	–	44.7±10.3[d]
Emodin low dose	0.1	54.6±6.6[a]
Emodin medium dose	0.2	67.2±18.4[b]
Emodin high dose	0.4	70.6±10.1[b]

[a]P<0.05 *vs* model; [b]P<0.01 *vs* model; [d]P<0.01 *vs* normal control.

Effect of emodin on the contents of motilin and somatostatin in small intestine of mice

Comparing with normal control, the content of motilin was lower while the content of somatostatin was higher in model group (P<0.01). After treatment with different doses of emodin, the content of motilin increased (P<0.05, P<0.01), while that of somatostatin decreased significantly (P<0.05, P<0.01) (Figure 1).

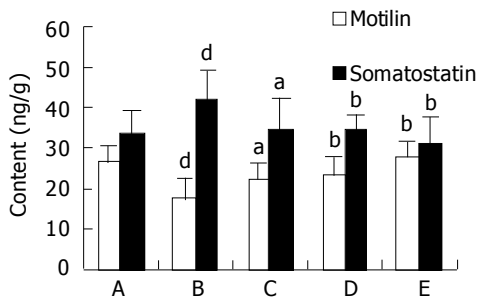

Figure 1 Effect of emodin on the contents of motilin and somatostatin in small intestine of mice (mean±SD, *n* = 10). A. Normal control; B. Model; C. Emodin low dose; D. Emodin medium dose; E. Emodin high dose. [a]P<0.05 *vs* model; [b]P<0.01 *vs* model; [d]P<0.01 *vs* normal control.

Effect of emodin on PD of isolated small intestine

Effect of glucose K-H and different concentrations of emodin on PD of isolated small intestine Before administration *vs* after administration: Fifteen minutes after administration of 0.2, 0.4, 0.8, and 1.6 g/L of emodin can lower PD of isolated small intestine of mice significantly (P<0.01) (Figure 2); compared between different groups: there was no significant difference between every group before administration. Fifteen minutes after administration of 0.2, 0.4, 0.8, and 1.6 g/L of emodin can lower PD of isolated small intestine of mice significantly, compared to K-H solution group, there were significant differences (P<0.01), which indicated that 0.2, 0.4, 0.8, and 1.6 g/L of emodin can lower PD of isolated small intestine of mice significantly, and, the inhibitory effect enhanced with increasing concentration (Figure 3).

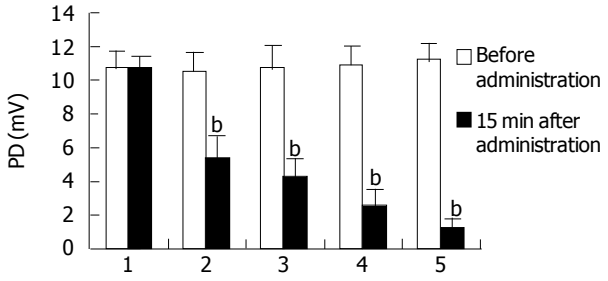

Figure 2 Effect of emodin on transmural PD (glucose K-H) of mice *in vitro*: comparison of the same group before administration and 15 min after administration. mean±SD, *n* = 10 1.K-H solution; 2.emodin (0.2 g/L); 3. emodin (0.4 g/L); 4. emodin (0.8 g/L); 5. emodin (1.6 g/L); [b]P<0.01 *vs* before administration.

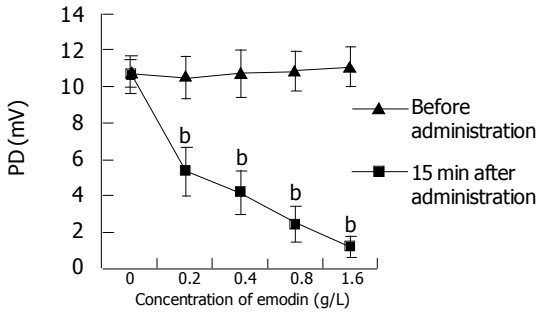

Figure 3 Effect of emodin on transmural PD (glucose K-H) of mice *in vitro*: comparison of different group before administration and 15 min after administration. mean±SD, *n* = 100. K-H solution; [b]P<0.01 *vs* K-H solution.

Effect of glucose-free K-H and different concentration of emodin on PD of isolated small intestine There are no significant differences in comparison between the same group before administration and 15 min after administration. The results indicated that emodin dissolved by glucose-free K-H had no evident inhibitory effect on PD of isolated small intestine (Table 2).

Table 2 Effect of emodin (glucose-free K-H) on transmural potential difference (PD) of mice *in vitro* (mean±SD, n = 10)

Group	Concentration (g/L)	PD (mV)	
		Before administration	15 min after administration
K-H solution		2.43±0.43	2.25±0.39
Emodin	0.2	2.15±0.58	2.02±0.50
	0.4	2.42±0.40	2.28±0.52
	0.8	2.55±0.34	2.52±0.32
	1.6	2.38±0.21	2.23±0.27

Effect of emodin on the activity of Na^+–K^+-ATPase in small intestinal mucosa of mice The activity of Na^+–K^+-ATPase in small intestinal mucosa of mice was higher significantly in model group than that in normal control (P<0.01). In emodin treatment groups the activity of Na^+–K^+-ATPase in small intestinal mucosa of mice decreased prominently (P<0.05, P<0.01) (Table 3).

Table 3 Effect of emodin on the activity of Na^+–K^+-ATPase in small intestinal mucosa of mice (mean±SD, n = 10)

Group	Dose (mg/kg)	Activity of Na^+–K^+-ATPase (μmol pi/mg Pro/h)
Normal control	–	15.82±3.29
Model	–	20.84±4.29[d]
Emodin low dose	0.1	17.41±2.56[a]
Emodin medium dose	0.2	16.57±1.74[b]
Emodin high dose	0.4	16.20±2.09[b]

[a]P<0.05, [b]P<0.01 *vs* model; [d]P<0.01 *vs* normal control.

DISCUSSION

Rhubarb is one of the most frequently used evacuants in clinic. Emodin is one of the primary components of rhubarb. Emodin is thought to be acting mainly on the large intestine[8-11]. In this study, we have attempted to investigate the effect of emodin on small intestinal peristalsis of mice and to explore its relevant mechanisms.

We observed the effect of emodin on charcoal powder propelling movement of small intestine in mice. The result showed that emodin increased the charcoal powder propelling ratio of small intestine, which indicates that emodin can enhance the function of small intestinal peristalsis of mice.

Motilin, which is made up of 22 amino acids, has long been recognized as an important endogenous peptide regulator of gastrointestinal motor function. Motilin is secreted by M_0 cells distributing in the recess of mucosa in duodenum and jejunum[12-14]. In the interphase of digestion, motilin is secreted with periodicity. Motilin can touch off the occurrence of three phases of migrating motor complex (MMC) through acting on the motilin nerve cells in the nervous system of intestinal tract, which arouses the intense constriction of stomach and segmentation contraction of small intestine. The punchy contractive wave of three phases of MMC extended to a distance along the small intestine at the rate of 5-10 cm/min. And when it passes through the gastrointestinal tract, it can clean up the contents of gastrointestine including the alimentary residue of last diet, cellular fragment falling off and bacteria. So motilin is a street sweeper[15]. Motilin plays an important role in regulation of gastrointestinal movement by touching off the occurrence of three phases of MMC. In our study we found that the content of motilin in small intestine of mice in model group was lower than that in normal control, and after treatment with emodin, the content of motilin was increased at different degree. So emodin can enhance the function of small intestinal peristalsis of mice by promoting secretion of motilin.

Somatostatin distributed in the gastrointestinal tract diffusely. Somatostatin can inhibit gastrointestinal function by two ways: one is by inhibiting the activity of adenylyl cyclase through inhibitory G protein; the other is by inhibiting the release of cholinergic neurotransmitter[16-19]. The result of this study showed that the content of somatostatin in small intestine of mice was increased significantly comparing with normal control. Different dosages of emodin could inhibit the secretion of the somatostatin prominently. This may be another mechanism of emodin to promote the movement of small intestine.

Some electrolyte can get across the epithelium of small intestine by active transport or passive transport, which leads to electrical potential difference (PD) between mucous membrane and chorion of small intestine. When it was adjusted to zero, passive transport of electrolyte was inhibited, while active transport continued. Then the change of PD between mucous membrane and chorion of small intestine reflected the change of active transport[20]. Glucose absorption in small intestine mucous membrane was completed by active transport. Active transport needs to consume energy, the main substance supplying energy is Na^+–K^+-ATPase[21,22]. So the decrease of active transport of ion indicated that Na^+–K^+-ATPase may be inhibited.

In this study we used high glucose K-H solution in order to study the role of glucose accompanied Na^+-transportation, which leads to PD maintaining a steady high level, contributing to eliminate interference of organic component in drugs to PD. In order to study glucose-non-dependent Na^+-transportation, we used glucose-free K-H to observe the change of simple Na^+-transportation PD. We found that when glucose existed, different doses of emodin could lower PD significantly. On the contrary, when glucose was absent, emodin had no evident effect on PD. The above results indicated that emodin had no significant effect on simple Na^+-transportation PD, it mainly inhibited the active transportation of Na^+, especially inhibited glucose-dependent Na^+-transportation.

Sodium pump is Na^+–K^+-ATPase in substance. One ATP molecule breaking down, there are three sodium ions moving out of the cell membrane and two potassium ions

moving into the cell membrane at the same time. By this way a potential energy reservoir is established, which is in favor of the transmembrane transportation. The absorption of glucose and amino acid by intestinal mucosa is just through this secondary active transport[23-25]. When the activity of Na^+–K^+-ATPase in intestinal mucosa is reduced, the potential energy reservoir is lessened. And the absorption of glucose, amino acid and sodium ions by intestinal tract is decreased too, which results in the enhancement of the osmotic pressure in enteric cavity and the peristalsis of intestinal tract which is fortified and quickened subsequently[22]. Our study indicated that the the activity of Na^+–K^+-ATPase in intestinal mucosa in emodin treatment groups was decreased prominently comparing with that in model group. The decrease of the activity of Na^+–K^+-ATPase in intestinal mucosa may be also one of the mechanisms for emodin to accelerate the movement of small intestine.

In conclusion, emodin can enhance the function of small intestinal peristalsis of mice and its mechanisms may be relevant to promoting secretion of motilin, lowering the content of somatostatin and inhibiting Na^+–K^+-ATPase activity of small intestinal mucosa.

REFERENCES

1 **Shen YJ**. Pharmacology of traditional Chinese medicine.1th ed. *Beijing: People's health publication* 2002: 329-330
2 **Kai M**, Hayashi K, Kaida I, Aki H, Yamamoto M. Permeation-enhancing effect of aloe-emodin anthrone on water-soluble and poorly permeable compounds in rat colonic mucosa. *Biol Pharm Bull* 2002; **25**: 1608-1613
3 **Wan JZ**. One kind of simple constipation model of mice. *Chin Pharmacol Bull* 1994; **10**: 71-72
4 **Chen Q**. Methodology of pharmacology of traditional Chinese medicine.1th ed. *Beijing: People's health publication* 1993: 331-335
5 **Sun WF**, Xu W, Wang XC, Wei S, Luo XY, Xiao DY. Effect of Shengjiang Decoctinon on gastrointestinal peristalsis and gastrointestinal hormones of mice. *J Anhui TCM College* 2002; **21**: 45-47
6 **Jia B**, Gu XL, Zhang SQ. The effect of chinese traditional medicine additive on glucose absorption of isolated small intestine. *Livestock And Poultry Industry* 1998; **12**: 15-16
7 **Cui ZQ**, Guo SD, Ye B, Zhang HR. The effect of taurine on transmural potential of mouse small intestine *in vitro*. *Chinese Pharmacol Bulletin* 1995; **11**: 288-290
8 **Iizuka A**, Iijima OT, Kondo K, Itakura H, Yoshie F, Miyamoto H, Kubo M, Higuchi M, Takeda H, Matsumiya T. Evaluation of Rhubarb using antioxidative activity as an index of pharmacological usefulness. *J Ethnopharmacol* 2004; **91**: 89-94
9 **Ding M**, Ma S, Liu D. Simultaneous determination of hydroxyanthraquinones in rhubarb and experimental animal bodies by high-performance liquid chromatography. *Anal Sci* 2003; **19**: 1163-1165
10 **Zhao J**, Chang JM, Du NS. Studies on the chemical constituents in root of Rheum rhizastachyum. *Zhongguo Zhongyao Zazhi* 2002; **27**: 281-282
11 **Shang XY**, Yuan ZB. Determination of six effective components in Rheum by cyclodextrin modified micellar electrokinetic chromatography. *Yaoxue Xuebao* 2002; **37**: 798-801
12 **Peeters TL**. Central and peripheral mechanisms by which ghrelin regulates gut motility. *J Physiol Pharmacol* 2003; **54** Suppl 4: 95-103
13 **Delinsky DC**, Hill KT, White CA, Bartlett MG. Quantitative determination of the polypeptide motilin in rat plasma by externally calibrated liquid chromatography/electrospray ionization mass spectrometry. *Rapid Commun Mass Spectrom* 2004; **18**: 293-298
14 **Qi QH**, Wang J, Hui JF. Effect of dachengqi granule on human gastrointestinal motility. *Zhongguo Zhong Xiyi Jiehe Zazhi* 2004; **24**: 21-24
15 **Yao T**. Physiology. 5th ed. *Beijing: People's Health Publication* 2002: 188-190
16 **Peeters TL**, Muls E, Janssens J, Urbain JL, Bex M, Van Cutsem E, Depoortere I, De Roo M, Vantrappen G, Bouillon R. Effect of motilin on gastric emptying in patients with diabetic gastroparesis. *Gastroenterology* 1992; **102**: 97-101
17 **Leandros E**, Antonakis PT, Albanopoulos K, Dervenis C, Konstadoulakis MM. Somatostatin versus octreotide in the treatment of patients with gastrointestinal and pancreatic fistulas. *Can J Gastroenterol* 2004; **18**: 303-306
18 **de Franchis R**. Somatostatin, somatostatin analogues and other vasoactive drugs in the treatment of bleeding oesophageal varices. *Dig Liver Dis* 2004; **36** Suppl 1: S93-100
19 **Konturek PC**, Konturek SJ. The history of gastrointestinal hormones and the Polish contribution to elucidation of their biology and relation to nervous system. *J Physiol Pharmacol* 2003; **54** Suppl 3: 83-98
20 **Kitaoka S**, Hayashi H, Yokogoshi H, Suzuki Y. Transmural potential changes associated with the *in vitro* absorption of theanine in the guinea pig intestine. *Biosci Biotechnol Biochem* 1996; **60**: 1768-1771
21 **Cereijido M**, Shoshani L, Contreras RG. The polarized distribution of Na^+, K^+-ATPase and active transport across epithelia. *J Membr Biol* 2001; **184**: 299-304
22 **Zhou XM**, Chen QH. Biochemical study of Chinese rhubarb. XXII. Inhibitory effect of anthraquinone derivatives on Na^+-K^+-ATPase of the rabbit renal medulla and their diuretic action. *Yaoxue Xuebao* 1988; **23**: 17-20
23 **Laughery M**, Todd M, Kaplan JH. Oligomerization of the Na, K-ATPase in cell membranes. *J Biol Chem* 2004; **279**: 36339-36348
24 **Ukkola O**, Joanisse DR, Tremblay A, Bouchard C. Na+-K+-ATPase alpha 2-gene and skeletal muscle characteristics in response to long-term overfeeding. *J Appl Physiol (1985)* 2003; **94**: 1870-1874
25 **Horvath G**, Agil A, Joo G, Dobos I, Benedek G, Baeyens JM. Evaluation of endomorphin-1 on the activity of Na(+),K(+)-ATPase using *in vitro* and *in vivo* studies. *Eur J Pharmacol* 2003; **458**: 291-297

Science Editor Guo SY **Language Editor** Elsevier HK

PO Box 2345, Beijing 100023, China
www.wjgnet.com
wjg@wjgnet.com

ELSEVIER

World J Gastroenterol 2005;11(20):3151-3155
World Journal of Gastroenterology ISSN 1007-9327

• *CASE REPORT* •

An uncommon clinical presentation of retroperitoneal non-Hodgkin lymphoma successfully treated with chemotherapy: A case report

Chiara Fulignati, Pietro Pantaleo, Greta Cipriani, Marianna Turrini, Rosalia Nicastro, Roberto Mazzanti, Bruno Neri

Chiara Fulignati, Pietro Pantaleo, Greta Cipriani, Marianna Turrini, Rosalia Nicastro, Roberto Mazzanti, Bruno Neri, Department of Internal Medicine, Centre of Experimental and Clinical Oncology, University of Florence, School of Medicine, Viale Morgagni, 85, I-50134 Firenze, Italy
Correspondence to: Bruno Neri, Department of Internal Medicine, Centre of Experimental and Clinical Oncology, University of Florence, School of Medicine, Viale Morgagni, 85, I-50134 Firenze, Italy. brunoneri@unifil.it
Telephone: +39-554-29611
Received: 2004-06-29 Accepted: 2004-08-31

Abstract

We report the case of a patient affected by an extra-nodal non-Hodgkin lymphoma presenting as a unique, large retroperitoneal mass with an unusual clinical presentation mimicking gastric peptic or neoplastic disease. The patient was successfully treated with a first generation therapy, CHOP modified regimen (cyclophosphamide 600 mg/m^2 intravenously on d 1, epirubicin 55 mg/m^2 intravenously on d 1, vincristine 1.2 mg/m^2 intravenously on d 1, prednisone 60 mg/m^2 on d 1-5), and a complete response was achieved. The (18)F-fluorodeoxyglucose positron emission tomography was used to assess the therapy outcome. A brief review of literature is provided.

Key words: Lymphoma; Grastric disease

Fulignati C, Pantaleo P, Cipriani G, Turrini M, Nicastro R, Mazzanti R, Neri B. An uncommon clinical presentation of retroperitoneal non-Hodgkin lymphoma successfully treated with chemotherapy: A case report. *World J Gastroenterol* 2005; 11(20): 3151-3155
http://www.wjgnet.com/1007-9327/11/3151.asp

INTRODUCTION

Non-Hodgkin lymphoma (NHL) causes many deaths worldwide, and its incidence is increasing[1]. It represents a heterogeneous group of neoplasms originating from lymphocytes[1-3]. In Western countries, 80% of NHL consists of a neoplastic growth originating from B lymphocytes[4]. The etiology of this disease is still partially unclear[1]. Some infectious agents have been associated more or less strictly with the development of a NHL as i.e., the Epstein-Barr virus, the human herpesvirus 8, and the human T-cell lymphotropic virus type I[1]. Also the *Helicobacter pylori* (*H pylori*) chronic infection has been strictly implicated in the pathogenesis of gastric lymphomas[5]. Several other environmental factors have been linked with the increasing incidence of NHL with conflicting evidence[6].

Also the disease classification is still complex and debated. The older classification systems, such as the Kiel classification and the Working Formulation, were based on NHL morphology[7]. Only recently, a new system was developed by the International Lymphoma Study Group, the Revised European and American Classification of Lymphoid Neoplasms that incorporate all available information to define the disease such as clinical features, morphology, immunophenotype as well as genetic features[8]. The stage of the disease is classified according to the Ann Arbor staging system[6].

Nearly 70% of lymphomas present a generally multi-localized, single or multiple lymphoadenomegaly without pain, with involvement in almost 30-40% of latero-cervical lymphnodes. In 30% of patients an extranodal localization is reported in Waldeyer's ring, in the stomach and generally in the gastro-intestinal tract. The retro-peritoneal localization is extremely rare and its diagnosis is often difficult. It often requires a time consuming and costly diagnostic workup.

Indolent NHL is generally considered incurable. Several regimens have been commonly used; however, treatment has never been shown to extend overall survival[9].

The poly-chemotherapy with CHOP regimen has been so far considered as the standard first-line treatment for advanced large B-cell lymphoma but upcoming therapies seem to promise a relevant improvement in patients' outcomes[10].

Several efforts have been made also to enhance the pre- and post-treatment disease assessment. This evaluation relies mainly on a CT scan performed after three or four conventional cycles of treatment[11,12]. The current evidence for the ability of (18)F-fluorodeoxyglucose positron emission tomography (FDG-PET) to detect disease not suspected from conventional staging is still equivocal, although an increased number of sites of disease are reported to be found in many patients by the means of FDG-PET but whether this is an independent prognostic factor remains to be seen[13,14].

The role of FDG-PET in NHL follow-up has not been widely investigated but there is some evidence that an early negative FDG-PET scan after completion of treatment is a strong predictor for patients who will be cured, and in this group of patients the follow-up could be minimized. Therapy also, in the case of aggressive disease, could be tailored[15]. In this article we report the case of an uncommon clinical presentation of a large B-cell lymphoma in a male patient

treated by a standard CHOP regimen in which a complete remission was achieved. Besides the uncommon presentation, this article emphasizes the role and the good sensitivity of FDG-PET in assessing response to therapy.

CASE REPORT

At the beginning of May 2002, a 56-year-old man, a hard smoker (30 packs/year) with hypertension, referred to the outpatient section of the Day-Hospital Unit of the Centre of Experimental and Clinical Medicine (Department of Internal Medicine, University of Florence) with recurrent epigastric burning pain following meals. Anorexia and asthenia associated with a marked loss of weight (a 7 kg reduction in 6 wk) were also present. The patient was referred to us by the general practitioner since he suspected from the symptom, the presence of a gastric neoplasia. In the past clinical history of the patient, no relevant disease was present and he underwent surgery at the age of 51 because of renal gallstones. No familiar history of gastric or esophageal cancer was reported.

Physical examination was normal and an accurate cardiological examination and electrocardiogram ruled out any cardiological origin of the pain. No alteration was found in the standard hematochemical determinations, in the hemachrome and in the differential blood count.

He firstly underwent an ultrasound (US) abdominal tomography on May 29, 2002 that did not show any relevant finding.

An esophago-gastro-duodenoscopy (EGDS) was performed just few days later, on June 4, 2002, and a biopsy during the procedure was performed in a erythematous area of the gastric antrum. No evidence of esophagitis was present. The histopathological examination performed on the gastric mucosal samples showed the presence of a superficial gastritis. Both the histopathological examination and urea breath test for *H pylori* were positive for the presence of this bacterium and the specific therapy with antibiotics and a proton pump inhibitor was immediately begun (amoxicillin 1 000 mg along with clarithromicin 500 mg b.i.d. for a week and omeprazole 40 mg for the 1st wk and thereafter 20 mg for 3 wk once a day).

A further abdominal US examination performed by a different examiner from that of the first one did not reveal any pathological finding. However, despite the therapy, after 2 wk, the patient reported an increase of the epigastric pain and a posterior irradiation was associated in that occasion.

On July 19, 2002 an abdominal contrast-enhanced CT scan demonstrated the presence of a solid mass in the retroperitoneal space. Its size was 9.5 cm×6.5 cm×12 cm and was located superiorly between the left hepatic lobe and the stomach. The gastric corpus was displaced to the left, while the antro-pyloric region forward. No cleavage limits were observed at the contrast-enhanced CT scans between the mass, the kidneys and the pancreas. Some lymphadenopathies were present at pre- and para-aortic levels (Figure 1). Few days later the patient was referred to the Surgery Department because of a further increase of the pain. A port-a-cath catheter was placed in the right subclavian vein and an intravenous therapy for the pain with morphine chlorhydrate (up to 60 mg/d) and ketorolac salt of trometamol (40 mg/d) was started.

Figure 1 Basal contrast-enhanced abdominal CT scan. The large retroperitoneal mass is indicated by the white arrow.

Since it did not appear to be possible to obtain a sample of the mass percutaneously both under US or CT guidance, the patient underwent an explorative laparotomy and a biopsy of the mass that appeared as a solid mass in the retroperitoneal space was taken. The histopathological examination revealed the presence of a B large-cell lymphoma. The immunohistochemical staining was positive for the following antigens: CD-45, CD-20, Bcl, Bcl-6, and MIB-1. Based on these data the disease was staged IV according to the Ann Arbor classification[5].

On August 29, 2002, the patient was eventually referred to our Day-Hospital Unit and was started on a treatment with CHOP modified regimen (cyclophosphamide 600 mg/m^2 intravenously on d 1, epirubicin 55 mg/m^2 intravenously on d 1, vincristine 1.2 mg/m^2 intravenously on d 1, prednisone 60 mg/m^2 on d 1-5). He was scheduled to receive seven administrations of this regimen starting from August 29, 2002 until March 10, 2003. The patient tolerated the therapy well. No major toxicity, as assessed by the CTC criteria[16], was observed during the whole period of the therapy administration.

The general condition improved just after the administration of the first course of treatment and continued to improve with the further courses of therapy. The Karnofsky performance status was 40% before treatment and improved to 100% after the fourth cycle. The pain was controlled during the treatment period with the administration of fentanyl via a transdermal device. The dosage was 75 μg/h at the beginning and it was reduced to 50 μg/h and finally to 25 μg/h during the second course of the treatment and completely discontinued after the third one. Anorexia and asthenia disappeared and the patient's body mass index rose from 20 to 24 in about 6 mo.

A contrast-enhanced CT scan of the abdomen was performed after the third treatment and it demonstrated a reduction of the mass with residual disease of about 1 cm localized at celiac trunk and it was considered as a partial response according to the SWOG criteria (Figure 2)[17]. The lymphoadenomegalies observed in the prior examination were still present. After the seventh course of treatment a total-body FDG-PET was performed and it did not show any pathological finding (Figure 3). However, 4 mo after

the completion of the treatment (July 2003), a contrast-enhanced CT showed a minimal residual disease localized at the celiac tripod (Figure 4). Finally a further FDG-PET performed in October 2003 showed the complete remission of the disease (Figure 5).

Two months later the port-a-cath catheter was removed.

At the moment of writing this case report (April 4, 2004), the patient is alive and no evidence of a relapse of the disease is observed. His general condition is good and he entered the follow-up program.

Figure 2 Contrast-enhanced abdominal CT scan performed. The large retroperitoneal mass is reduced in size but a residual disease of about 1 cm is localized at celiac trunk (white arrow).

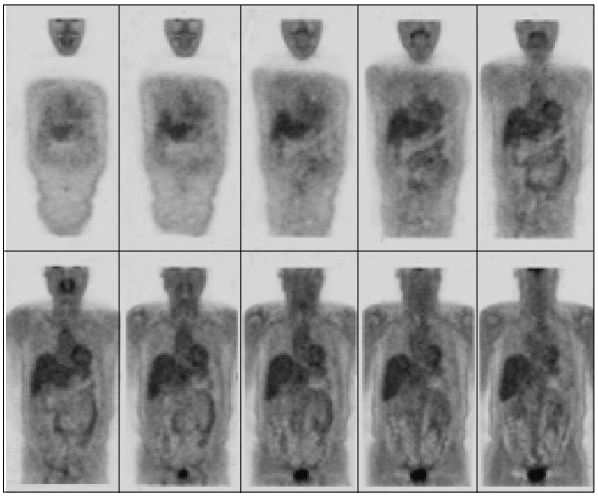

Figure 3 Total-body FDG-PET performed after the seventh course of treatment.

Figure 4 Contrast-enhanced CT performed 4 mo after the completion of the treatment. A minimal residual disease is localized at the celiac tripod.

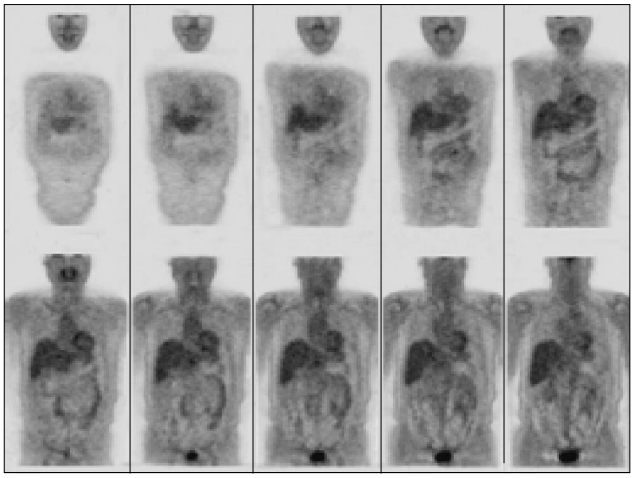

Figure 5 FDG-PET performed in October 2003: a complete remission of the disease is showed.

DISCUSSION

A primary and unique retroperitoneal localization of NHL is quite rare and, according to our knowledge, only case that has been described yet[18], and a clinical presentation with an epigastric pain and ulcer-like dyspepsia mimicking a peptic disease is extremely rare. Abdominal NHL typically present themselves as a solid mass and they cause abdominal pain due to compression or infiltration of nerves and its pain is often referred as a diffuse pain[19]. Abdominal lymphomas often belong to the sclerosant variety of follicle centre lymphomas[19].

The symptoms presented in this case were very similar to that of esophagitis and gastric ulcer and the relationship with meals suggested to the general practitioner, the presence at least of a peptic-related disease or a gastric neoplasia since the patient had a previously known risk factor for gastric cancer (cigarette smoking) and the presence of asthenia, anorexia and the weight loss prompted the general practitioner to start a diagnostic workup oriented to gastric cancer. The negative result of the first abdominal US scan prompted us to perform a further US and a EGDS. This last examination was negative for gastric cancer and resulted only with the presence of a mild gastritis associated with *H pylori* infection. Even the second US resulted negative. Therefore, since the data obtained from the first investigations were in some way contradictory, further assessments were planned. Contrast-enhanced CT scans identified the mass, but no indication on the nature was obtained. A laparoscopic examination of the retroperitoneal space was thereafter planned and performed. So, the patient underwent several expensive investigations to achieve the diagnosis. The complexity of this clinical workup is probably due to the rarity of the disease by itself and also because of the uncommon clinical presentation. Most probably, the presence of a marked weight loss is the only symptom that could have oriented the diagnostic workup towards the suspicion of a neoplastic disease.

Indolent NHL is generally considered incurable. The CHOP, a first generation chemotherapy regimen, still

represents the standard chemotherapy regimen for NHL treatment[20]. It obtains a complete response in about 45-53% of cases, with a long-term survival of 30-37%, and few and acceptable side-effects. The disease localization affects treatment choice, but generally the correct therapeutic approach to the extra-nodal NHL requires the integration of chemotherapy, radiotherapy and surgery.

Several regimens have been commonly so far used in the therapy of nodal and extra-nodal NHL. The response rate to the treatment is initially greater than 50% but the response and its duration decrease with subsequent chemotherapy. However, treatment has never been shown to extend overall survival.

The poly-chemotherapy with CHOP regimen has been considered as the standard first-line treatment for advanced large B-cell lymphoma[21] as no improvement in failure-free survival or overall survival, but increased toxic effects with newer regimens were shown with the less complicated and less expensive regimen of CHOP[24]. New strategies are being developed to improve the prognosis of these patients and the association of the CHOP regimen with rituximab, a human-mouse chimeric monoclonal anti-CD20 antibody that kills CD20-positive cells by activation of complement-dependent and antibody-dependent cell-mediated cytotoxicity, has been recently proposed[22-24].

In our case the choice of the CHOP regimen was funded and we obtained a complete remission. The use of the CHOP, a first generation regimen, should not be discontinued, since there is no improvement from the use of newer regimens[21]. However, the association of CHOP with mechanism-based drugs such as rituximab may further improve treatment outcomes especially in aggressive disease[22].

In this setting it appears clear that a correct pre- and post-treatment evaluation is mandatory to assess patient outcome, to evaluate the relapse risk and to establish the prognosis and in predicting survival and eventually to plan the follow-up[25]. Thus, it seems necessary to use more than one tool to evaluate disease extension and after the therapy residual disease.

The role of the functional metabolic imaging through FDG-PET has gained relevance in the staging and evaluation of response of various solid and hematologic malignancies. FDG-PET has recently emerged as an useful prognostic tool also in patients with aggressive lymphomas[13,14,26]. This kind of investigation performed few cycles after the chemotherapy can predict relapse risk[27,28]. The vast majority of patients with positive FDG-PET scans present poorer clinical outcomes as compared to patients with negative scans[28]. In patients where FDG-PET showed residual disease after treatment, relapses were reported in 100% of the cases, whereas a long-term survival was seen in more than 80% of patients with negative PET results[28].

Providing that these observations will obtain a confirmation, by FDG-PET we would be able to customize for the single patient with aggressive lymphoma, the appropriate treatment and follow-up. The patient of this case report underwent two FDG-PET and in both cases the negative result corresponded to a remission of the disease.

Besides its rarity and complexity, this case suggests that the use of FDG-PET in assessing the response to chemotherapy of extra-nodal NHL must be implemented and that FDG-PET could be the most useful predictive tool in assessing patient outcome. The use of morphologic tools (contrast-enhanced CT or magnetic resonance) in association with a functional metabolic imaging test appears to be mandatory also in the evaluation of extra-nodal aggressive NHL.

REFERENCES

1 **Hennessy BT**, Hanrahan EO, Daly PA. Non-Hodgkin lymphoma: an update. *Lancet Oncol* 2004; **5**: 341-353
2 **Rossi D**, Gaidano G. Molecular heterogeneity of diffuse large B-cell lymphoma: implications for disease management and prognosis. *Hematology* 2002; **7**: 239-252
3 **Pileri SA**, Zinzani PL, Went P, Pileri A, Bendandi M. Indolent lymphoma: the pathologist's viewpoint. *Ann Oncol* 2004; **15**: 12-18
4 **Chiu BC**, Weisenburger DD. An update of the epidemiology of non-Hodgkin's lymphoma. *Clin Lymphoma* 2003; **4**: 161-168
5 **Wotherspoon AC**. Gastric lymphoma of mucosa-associated lymphoid tissue and *Helicobacter pylori*. *Annu Rev Med* 1998; **49**: 289-299
6 **DeVita VT**, Hellman S, Rosenberg SA, eds. Cancer: principles and practice of oncology, 6th edn. Philadelphia, PA: *Lippincott Williams & Wilkins* 2001
7 **Jaffe ES**, Harris NL, Diebold J, Muller-Hermelink HK. World Health Organization classification of neoplastic diseases of the hematopoietic and lymphoid tissues. A progress report. *Am J Clin Pathol* 1999; **111**: S8-12
8 **Armitage JO**, Weisenburger DD. New approach to classifying non-Hodgkin's lymphomas: clinical features of the major histologic subtypes. Non-Hodgkin's Lymphoma Classification Project. *J Clin Oncol* 1998; **16**: 2780-2795
9 **Marcus R**. Current treatment options in aggressive lymphoma. *Leuk Lymphoma* 2003; **44** Suppl 4: S15-S27
10 **Fisher RI**, Gaynor ER, Dahlberg S, Oken MM, Grogan TM, Mize EM, Glick JH, Coltman CA, Miller TP. Comparison of a standard regimen (CHOP) with three intensive chemotherapy regimens for advanced non-Hodgkin's lymphoma. *N Engl J Med* 1993; **328**: 1002-1006
11 **Rankin SC**. Assessment of response to therapy using conventional imaging. *Eur J Nucl Med Mol Imaging* 2003; **30** Suppl 1: S56-S64
12 **Vinnicombe SJ**, Reznek RH. Computerised tomography in the staging of Hodgkin's disease and non-Hodgkin's lymphoma. *Eur J Nucl Med Mol Imaging* 2003; **30** Suppl 1: S42-S55
13 **Otsuka H**, Graham M, Kubo A, Nishitani H. Clinical utility of FDG PET. *J Med Invest* 2004; **51**: 14-19
14 **Rohren EM**, Turkington TG, Coleman RE. Clinical applications of PET in oncology. *Radiology* 2004; **231**: 305-332
15 **Kasamon YL**, Wahl RL, Swinnen LJ. FDG PET and high-dose therapy for aggressive lymphomas: toward a risk-adapted strategy. *Curr Opin Oncol* 2004; **16**: 100-105
16 **Arbuck SG**, Ivy SP, Setser A. The Revised Common Toxicity Criteria: Version 2.0. CTEP Website. Available from: http://ctep.info.nih.gov
17 **Green S**, Weiss GR. Southwest Oncology Group standard response criteria, endpoint definitions and toxicity criteria. *Invest New Drugs* 1992; **10**: 239-253
18 **Waldron JA**, Magnifico M, Duray PH, Cadman EC. Retroperitoneal mass presentations of B-immunoblastic sarcoma. *Cancer* 1985; **56**: 1733-1741

19 **Crump M**, Gospodarowicz M, Shepherd FA. Lymphoma of the gastrointestinal tract. *Semin Oncol* 1999; **26**: 324-337
20 **Seymour JF.** New treatment approaches to indolent non-Hodgkin's lymphoma. *Semin Oncol* 2004; **31**: 27-32
21 **Fisher RI**, Shah P. Current trends in large cell lymphoma. *Leukemia* 2003; **17**: 1948-1960
22 **Coiffier B.** Effective immunochemotherapy for aggressive non-Hodgkin's lymphoma. *Semin Oncol* 2004; **31**: 7-11
23 **Davis TA**, Grillo-Lopez AJ, White CA, McLaughlin P, Czuczman MS, Link BK, Maloney DG, Weaver RL, Rosenberg J, Levy R. Rituximab anti-CD20 monoclonal antibody therapy in non-Hodgkin's lymphoma: safety and efficacy of re-treatment. *J Clin Oncol* 2000; **18**: 3135–3143
24 **Rastetter W**, Molina A, White CA. Rituximab: expanding role in therapy for lymphomas and autoimmune diseases. *Annu Rev Med* 2004; **55**: 477-503
25 **Wooldridge JE**, Link BK. Post-treatment surveillance of patients with lymphoma treated with curative intent. *Semin Oncol* 2003; **30**: 375-381
26 **Montravers F**, McNamara D, Landman-Parker J, Grahek D, Kerrou K, Younsi N, Wioland M, Leverger G, Talbot JN. [(18)F]FDG in childhood lymphoma: clinical utility and impact on management. *Eur J Nucl Med Mol Imaging* 2002; **29**: 1155-1165
27 **Blum RH**, Seymour JF, Wirth A, MacManus M, Hicks RJ. Frequent impact of [18F]fluorodeoxyglucose positron emission tomography on the staging and management of patients with indolent non-Hodgkin's lymphoma. *Clin Lymphoma* 2003; **4**: 43-49
28 **Schot B**, van Imhoff G, Pruim J, Sluiter W, Vaalburg W, Vellenga E. Predictive value of early 18F-fluoro-deoxyglucose positron emission tomography in chemosensitive relapsed lymphoma. *Br J Haematol* 2003; **123**: 282-287

Science Editor Guo SY **Language Editor** Elsevier HK

PO Box 2345, Beijing 100023, China
www.wjgnet.com
wjg@wjgnet.com

ELSEVIER

World J Gastroenterol 2005;11(20):3156-3158
World Journal of Gastroenterology ISSN 1007-9327

• *CASE REPORT* •

Small cell carcinoma of rectum: A case report

Enver Ihtiyar, Cem Algin, Serap Isiksoy, Ersin Ates

Enver Ihtiyar, Cem Algin, Serap Isiksoy, Ersin Ates, Department of General Surgery, Osmangazi University Faculty of Medicine, 26480 Eskisehir, Turkey
Correspondence to: Cem Algin, Assistant Professor, Health School, Dumlupinar University, 43270 Kutahya, Turkey. cemalgin@ttnet.net.tr
Telephone: +90-274-2652031-2086 Fax: +90-274-2652191
Received: 2004-06-22 Accepted: 2004-07-08

Abstract

We present a case of a 40-year-old woman with small-cell carcinoma (SCC) of the rectum. She had profuse bleeding in rectum for 5 d. By colonoscopy, polyps were determined in the rectum and biopsies were carried out. Histopathologically, the polyps were adenomatous. Because of the profuse bleeding in rectum, she underwent low anterior resection. After the diagnosis of SCC, she received intravenous chemotherapy with standard doses of siklofosfamid, adriamycin, and vepesid. Nevertheless, intracranial metastases were revealed and she died 6 mo after the operation.

Key words: Small cell carcinoma; Rectum

Ihtiyar E, Algin C, Isiksoy S, Ates E. Small cell carcinoma of rectum: A case report. *World J Gastroenterol* 2005; 11 (20): 3156-3158
http://www.wjgnet.com/1007-9327/11/3156.asp

INTRODUCTION

Small-cell carcinomas (SCC) are malignancies derived from cells of the neuroendocrine system. Colorectal SCC is a rare tumor[1-5] and its incidence is less than 0.2% among all kinds of colorectal cancers[6] such as small-cell undifferentiated carcinoma, neuroendocrine carcinoma and stem cell carcinoma[7]. In some cases these tumors are in close association with adenomatous polyps[2,3,5,8]. Some of these tumors show glandular and squamous differentiation. The morphological heterogeneity of these tumors support that these tumors develop on divergent differentiation from pluripotential stem cells derived from the endoderm[9,10].

Small-cell neuroendocrine carcinoma is an aggressive neoplasm, which was reported to occur frequently with distant metastasis and carries a poor prognosis, even if diagnosed in the early stage[2]. Primary SCC showing neuroendocrine differentiation has been observed in many sites, including the upper airway and lung, skin, thymus, kidney, breast, ovary, uterus, urinary bladder, hepatobiliary tree, pancreas, salivary glands and alimentary tract[11,12]. Through the amine precursor uptake and decarboxylation system, neuroendocrine cells are capable of synthesizing, storing and secreting a variety of neuroamines, neuropeptides and related substances[12]. The gastrointestinal tract has the largest component of neuroendocrine cells, and neoplastic proliferation of these cells occurs primarily in the appendix, ileum and rectum[13].

The choice of treatment for these kinds of tumors is chemotherapy, which is used for SCC of the lung. Surgery plus chemotherapy is another alternative for small localized tumors[1,3].

CASE REPORT

A 40-year-old woman was admitted to Osmangazi University Hospital with the complaint of anorexia, 9 kg of weight loss over 2 mo and profuse bleeding in rectum for 5 d.

Blood-stained bowel motions were found in digital rectum. Her hemoglobin was 7.2 mg/dL and other laboratory data were within normal range. Her chest and abdominal X-ray examinations indicated no specific abnormalities. Colonoscopy revealed a polypoid lesion and a large size rectal mass in the rectal wall about 8-12 cm from the anal verge. Biopsies were performed and the diagnosis of adenomatous polyps was made.

Abdominal tomography and ultrasonography revealed a large rectal mass consistent with neoplasm, multiple lesions probably due to metastasis in both right and left lobes of the liver and massive peri-aortic and peri-iliac enlarged lymph nodes. She was transfused 3 units of red blood cells. After preoperative bowel preparation for 3 d, laparotomy was performed. There were widespread liver metastases and lymphadenopathy in the abdomen and iliac region. Frozen rectal mass and liver lesions on the seventh segment were studied, the diagnosis of SCC was made and she underwent low anterior resection. Macroscopically, there was a sessile papillary lesion in the rectum indicating ulceration in the mid-portion. Cut section of the lesion revealed a solid tumor beneath the area of ulceration (Figure 1). Microscopically, surface epithelium was adenomatous and had villoglandular configuration, the solid tumor tissue extended through the entire bowel wall below the ulcer area and villous adenoma (Figure 2). Tumor infiltration was found in the surrounding fatty tissues as well. Tumor tissue was composed of solid sheets and partly trabecular structures of small round or oval undifferentiated cells with hyperchromatic nuclei and scanty cytoplasm. Nucleoli were not prominent. There was a focal peritheliomatous pattern produced by necrosis. Vascular invasion was determined. No transitional zone was observed between the adenoma and SCC. No histological

features were suggestive of glandular or squamous elements. Immunohistochemical staining tumor demonstrated positive immunoreactivity with chromogranin A and synaptophysin. Neuron-specific enolase was negative in tumor cells. Tumor cells were negative for Grimelius' argyrophilic reaction. Argyrophilic cells of mucosal crypts served as internal controls for the Grimelius stain. There were endocrine cells showing immunoreaction with chromogranin in adenomatous epithelium. Immunoreactivity with synaptophysin was not seen. In liver biopsy, SCC metastases were observed.

Computerized tomography scan and ultrasonography were performed 3 mo after operation and found an increasing metastatic focus in the liver. Thus, she was given intravenous chemotherapy with 800 mg/m^2 of siklofosfamid, 50 mg/m^2 of adriamycin and 120 mg/m^2 vepesid on d 1-3. However, 6 mo after the surgery, her condition deteriorated rapidly with vomiting, headache and hemiparesis due to intracranial metastases and died.

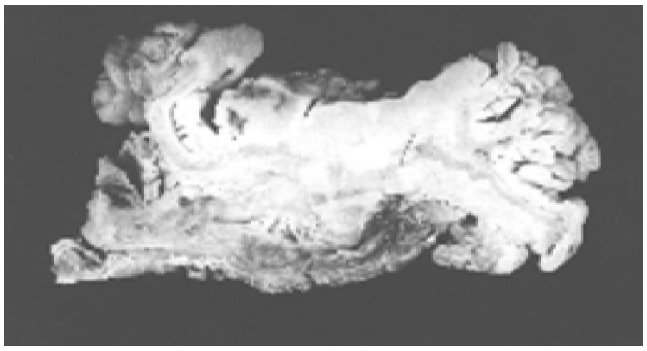

Figure 1 Solid tumor beneath the area of ulceration.

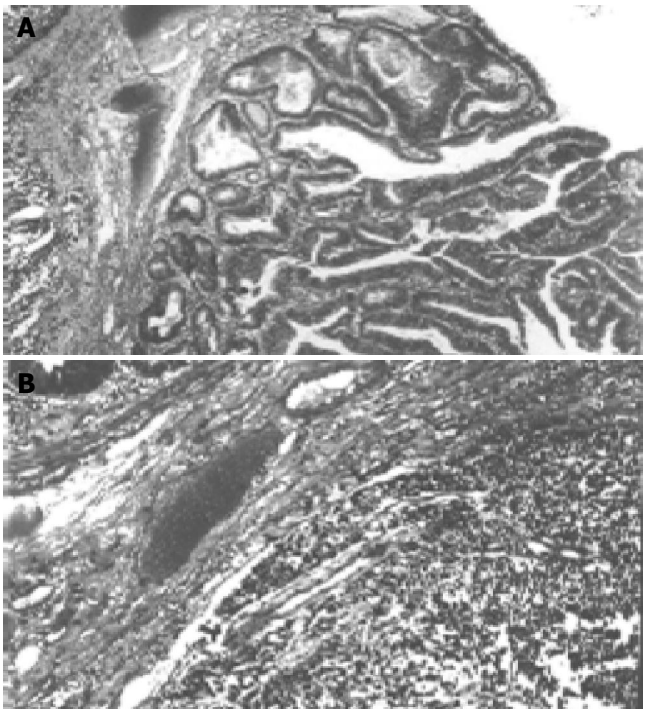

Figure 2 Solid tumor tissue below the ulcer area (**A**) and villous adenoma (**B**).

DISCUSSION

The incidence of neuroendocrine cancers is about 3.9% among all types of colorectal cancers[1,4] and 23-33% of colorectal neuroendocrine tumors arise in rectum[4,5]. Neuroendocrine tumors include well-differentiated carcinoid tumors and aggressive neuroendocrine carcinomas also called as SCC[14]. The frequency of SCC of colorectal region is less than 1%[1] and 1.5%[4] among all colorectal cancer types.

SCC involving rectum is large and ulcerative[6] and tumors of the colorectum are frequently associated with adenomatous polyps[2,5,8,10]. In our case, tubulovillous adenoma overlay the solid tumor. Their association with adenomas suggests that SCC derives from stem cells or cells in a preexisting adenoma[5,7,9,15]. However, as in many cases[5,8], we did not observe the transition between two lesions. In pathogenesis, the likely mechanism of divergent differentiation of stem cells seems more acceptable.

Through amine precursor uptake and decarboxylation system, neuroendocrine cells are capable of synthesizing, storing and secreting a variety of neuroamines, neuropeptides and related substances[12]. Neuroendocrine cells of the gut are originally thought to be of neuroectodermal origin[16], but recently it was suggested that these cells are endodermally originated[17,18]. Neuroendocrine nature of such cells and tumors arising from them can be demonstrated immunohistochemically. Electron microscopic studies have confirmed that the neuroendocrine differentiation is by demonstrating neurosecretory granules. As a neuroendocrine carcinoma, positive immunoreactivity to at least two neuroendocrine markers is required[4,19]. In these tumors immunoreactivity is shown with antibodies against neuron-specific enolase, chromogranin, synaptophysin and hormones[3-5,8,10]. In SCC, synaptophysin immunoreactivity is strongly positive, which is the most reliable finding in detecting this tumor[14]. In our case chromogranin immunoreactivity was determined in focal areas and synaptophysin showed widespread positivity.

These tumors have a high aggressive behavior[16,20], their 6-mo survival rate is 58% and 5-year survival rate is 6%[1,4,21]. Liver and lymph-node involvements are found in 70-80% of patients in their early evolution[21]. In our case, the patient had multiple metastases in both right and left lobes of the liver and massive periaortic and peri-iliac probably metastatic nodes.

Prognosis is favorable for some patients after radical surgery for these tumors. It is suggested that local control of SCC of the rectum can be achieved with multidrug chemotherapy and radiation therapy without radical surgery[22]. This tumor is as responsive to chemotherapy as is SCC of the lung[10]. Different results of therapy may be due to unusual examples of poorly differentiated small-cell malignancies. Electron microscopy may be helpful to confirm the diagnosis of poorly differentiated small-cell malignancies[22].

It has poor prognosis, even when the primary resection is radical[8]. Surgery should be performed only when the tumor is small and various non-surgical treatments should be given to patients with advanced disease[23].

REFERENCES

1 **Yaziji H**, Broghamer WL. Primary small cell undifferentiated

carcinoma of the rectum associated with ulcerative colitis. *South Med J* 1996; **89**: 921-924
2 **Okuyama T**, Korenaga D, Tamura S, Yao T, Maekawa S, Watanabe A, Ikeda T, Sugimachi K. The effectiveness of chemotherapy with cisplatin and 5-fluorouracil for recurrent small cell neuroendocrine carcinoma of the rectum: report of a case. *Surg Today* 1999; **29**: 165-169
3 **Sarsfield P**, Anthony PP. Small cell undifferentiated ("neuroendocrine") carcinoma of the colon. *Histopathology* 1990; **16**: 357-363
4 **Saclarides TJ**, Szeluga D, Staren ED. Neuroendocrine cancers of the colon and rectum. Results of a ten-year experience. *Dis Colon Rectum* 1994; **37**: 635-642
5 **Gaffey MJ**, Mills SE, Lack EE. Neuroendocrine carcinoma of the colon and rectum. A clinicopathologic, ultrastructural, and immunohistochemical study of 24 cases. *Am J Surg Pathol* 1990; **14**: 1010-1023
6 **Clery AP**, Dockerty MB, Waugh JM. Small-cell carcinoma of the colon and rectum. A clinicopathologic study. *Arch Surg* 1961; **83**: 164-172
7 **Vilor M**, Tsutsumi Y, Osamura RY, Tokunaga N, Soeda J, Ohta M, Nakazaki H, Shibayama Y, Ueno F. Small cell neuroendocrine carcinoma of the rectum. *Pathol Int* 1995; **45**: 605-609
8 **Palvio DH**, Sorensen FB, Klove-Mogensen M. Stem cell carcinoma of the colon and rectum: Report of two cases and review of the literature. *Dis Colon Rectum* 1985; **28**: 440-445
9 **Mills SE**, Allen MS, Cohen AR. Small-cell undifferentiated carcinoma of the colon. A clinicopathological study of five cases and their association with colonic adenomas. *Am J Surg Pathol* 1983; **7**: 643-651
10 **Wick MR**, Weatherby RP, Weiland LH. Small cell neuroendocrine carcinoma of the colon and rectum: clinical, histologic, and ultrastructural study and immunohistochemical comparison with cloacogenic carcinoma. *Hum Pathol* 1987; **18**: 9-21
11 **Ibrahim NB**, Briggs JC, Corbishley CM. Extrapulmonary oat cell carcinoma. *Cancer* 1984; **54**: 1645-1661
12 **Pearse AG**. The diffuse neuroendocrine system and the apud concept: related "endocrine" peptides in brain, intestine, pituitary, placenta, and anuran cutaneous glands. *Med Biol* 1977; **55**: 115-125
13 **Chejfec G**, Falkmer S, Askensten U, Grimelius L, Gould VE. Neuroendocrine tumors of the gastrointestinal tract. *Pathol Res Pract* 1988; **183**: 143-154
14 **Fenoglio-Preiser CM**, Noffsinger AE, Lantz PE, Stemmermann GN, Rilke FO. Gastrointestinal Pathology an Atlas and Text. 2nded. *Lippincott-Raven Pres: Philadelphia* 1999: 1043-1044
15 **Damjanov I**, Amenta PS, Bosman FT. Undifferentiated carcinoma of the colon containing exocrine, neuroendocrine and squamous cells. *Virchows Arch A Pathol Anat Histopathol* 1983; **401**: 57-66
16 **Ledermann JA**. Extrapulmonary small cell carcinoma. *Postgrad Med J* 1992; **68**: 79-81
17 **Sidhu GS**. The endodermal origin of digestive and respiratory tract APUD cells. Histopathologic evidence and a review of the literature. *Am J Pathol* 1979; **96**: 5-20
18 **Cox WF**, Pierce GB. The endodermal origin of the endocrine cells of an adenocarcinoma of the colon of the rat. *Cancer* 1982; **50**: 1530-1538
19 **Cebrian J**, Larach SW, Ferrara A, Williamson PR, Trevisani MF, Lujan HJ, Kassir A. Small-cell carcinoma of the rectum: report of two cases. *Dis Colon Rectum* 1999; **42**: 274-277
20 **Khansur TK**, Routh A, Mihas TA, Underwood JA, Smith GF, Mihas AA. Syndrome of inappropriate ADH secretion and diplopia: oat cell (small cell) rectal carcinoma metastatic to the central nervous system. *Am J Gastroenterol* 1995; **90**: 1173-1174
21 **Sterling RK**. Ectopic ACTH syndrome associated with anorectal carcinoma. Report of a case and review of the literature. *Dig Dis Sci* 1993; **38**: 955-959
22 **Robidoux A**, Monte M, Heppell J, Schurch W. Small-cell carcinoma of the rectum. *Dis Colon Rectum* 1985; **28**: 594-596
23 **Shirouzu K**, Morodomi T, Isomoto H, Yamauchi Y, Kakegawa T, Morimatsu M. Small cell carcinoma of the rectum. Clinicopathologic study. *Dis Colon Rectum* 1985; **28**: 434-439

Science Editor Wang XL **Language Editor** Elsevier HK

PO Box 2345, Beijing 100023, China
www.wjgnet.com
wjg@wjgnet.com

ELSEVIER

World J Gastroenterol 2005;11(20):3159-3160
World Journal of Gastroenterology ISSN 1007-9327

• *CASE REPORT* •

Atorvastatin-induced severe gastric ulceration: A case report

Ihab I El-Hajj, Fadi H Mourad, Nina S Shabb, Kassem A Barada

Ihab I El-Hajj, Fadi H Mourad, Kassem A Barada, Department of Internal Medicine, American University of Beirut Medical Center (AUBMC), Beirut, Lebanon
Nina S Shabb, Department of Pathology, AUBMC, Beirut, Lebanon
Correspondence to: Dr. Kassem Barada, Associate Professor, Department of Internal Medicine, Division of Gastroenterology, American University of Beirut Medical Center, PO Box, 113-6044, Hamra street, Beirut 110 32090, Lebanon. kb02@aub.edu.lb
Telephone: +961-1-350000 Fax: +961-1-370814
Received: 2004-06-24 Accepted: 2004-09-19

Abstract

A 41-year-old man presented with severe gastric ulceration 3 mo after beginning treatment with atorvastatin 20 mg once daily for hypercholesterolemia. The patient was not taking any ulcerogenic drugs and had no evidence of *Helicobacter pylori* infection. Proton pump inhibitor therapy was initiated and atorvastatin was replaced by simvastatin with complete resolution of gastrointestinal symptoms. To our knowledge, this is the first report of atorvastatin-induced gastric ulceration, which should be looked for in patients who develop abdominal pain while on this drug.

Key words: Atorvastatin; Drug toxicity; Gastric ulceration

El-Hajj II, Mourad FH, Shabb NS, Barada KA. Atorvastatin-induced severe gastric ulceration: A case report. *World J Gastroenterol* 2005; 11(20): 3159-3160
http://www.wjgnet.com/1007-9327/11/3159.asp

INTRODUCTION

Atorvastatin is generally well tolerated, with most adverse effects related to the gastrointestinal system[1]. Although drug-induced gastric ulcerations are listed as potential adverse effects on package inserts, published reports documenting these adverse effects are scarce[2]. We present a case of reversible drug-induced gastric ulceration, attributed to atorvastatin.

CASE REPORT

A 41-year-old man with a history of familial hypercholesterolemia was started on atorvastatin (Lipitor) 20 mg daily. Three months later, he started complaining of severe epigastric pain that frequently woke him up at night. He had no other gastrointestinal symptoms. On physical examination, epigastric and right upper quadrant tenderness was noted. Complete blood count, liver biochemistry, amylase and lipase were normal. Ultrasound of upper abdomen revealed a normal gall bladder and a thickened gastric wall suggestive of gastritis. Upper gastrointestinal endoscopy showed a small hiatal hernia, along with multiple superficial and irregular ulcers in the cardia, the body of stomach and the antrum (Figure 1). Multiple antral biopsies were taken. CLO-test for *Helicobacter pylori* turned out to be negative. Histologic examination of gastric biopsies revealed superficial ulcers associated with hemorrhage and acute inflammation in the lamina propria. There was no evidence of malignancy and *H pylori*-like organisms were not seen (Figure 2).

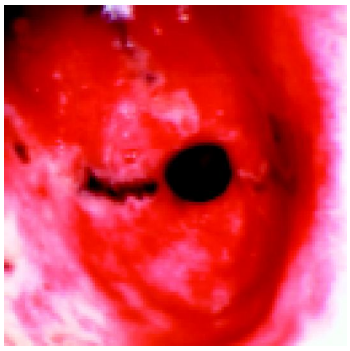

Figure 1 Gastroscopic morphological change of multiple superficial and irregular ulcers in the antrum.

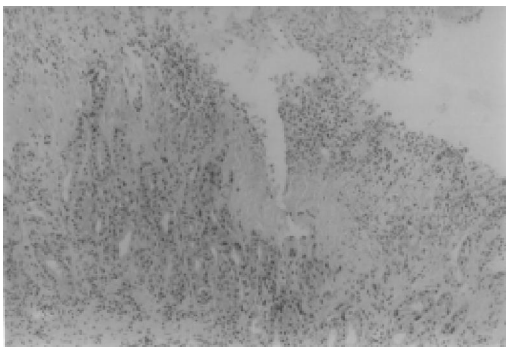

Figure 2 Histologic morphology of needle-biopsied specimens of primary gastric ulcerations.

The patient had no previous personal or family history of ulcer disease and was not on aspirin, nonsteroidal anti-inflammatory drugs, or other medications. Atorvastatin-induced gastric ulceration seemed to be the most probable diagnosis. Atorvastatin was discontinued and the patient was

put on rabeprazole 20 mg daily for a total of 6 wk and he had a quick relief from symptoms. Simvastatin was started at a dose of 20 mg once daily with no adverse effects during a 3-year follow-up.

DISCUSSION

Atorvastatin has a favorable risk-benefit profile[3]. Common side-effects of this drug (>2%) include constipation, flatulence, dyspepsia, abdominal pain and headache[2]. Infrequent adverse events (<2%) are reported, including diaphragmatic muscle impairment[4], myositis migrans[5], tendinopathy[6], peripheral neuropathy[7], external ophthalmoplegia and ataxia[8], skin and appendages changes/ alopecia[9], dermatomyositis[10], dermographism[11], toxic epidermal necrolysis[12], chronic urticaria[13], and severe thrombocytopenia[14]. The serious digestive system side-effects include acute hepatitis[15], cholestatic hepatitis[16], and acute pancreatitis[17].

Our patient developed severe symptoms that were compatible with gastric ulceration. Both endoscopy and histopathology confirmed the presence of significant mucosal injury. Other causes of gastric ulcerations were ruled out. There was no personal or family history of ulcer disease. The patient did not take any other medication. He had been taking atorvastatin for 3 mo before the onset of gastric ulceration.

To our knowledge, this is the first report about gastric ulcerations caused by atorvastatin and it further reinforces the fact that statins may cause gastric ulcers. The mechanism of this side effect is not known. As the use of statins increases, physicians should consider the diagnosis of gastric ulcerations in patients taking these medications who then develop abdominal pain which cannot be explained by any other process. If gastric ulcer is suspected, the drug should be stopped and replaced by another lipid lowering drug to reduce the possibility of further damage to the gastric mucosa.

REFERENCES

1 **Malinowski JM**. Atorvastatin: a hydroxymethylglutaryl-coenzyme A reductase inhibitor. *Am J Health Syst Pharm* 1998; **55**: 2253-2267; quiz 2302-2303
2 **Lacy C,** Armstrong L, Goldman M, Lance L. Atorvastatin. In: Drug information Handbook. 9th ed. Ohio: *Lexi-Comp, Inc,* 2001-2002: 109-110
3 **Andrejak M,** Gras V, Massy ZA, Caron J. Adverse effects of statins. *Therapie* 2003; **58**: 77-83
4 **Sulem P,** Bagheri H, Faixo Y, Montastruc JL. Atorvastatin-induced diaphragmatic muscle impairment. *Ann Pharmacother* 2001; **35**: 1292-1293
5 **Sinzinger H.** Statin-induced myositis migrans. *Wien Klin Wochenschr* 2002; **114**: 943-944
6 **Chazerain P,** Hayem G, Hamza S, Best C, Ziza JM. Four cases of tendinopathy in patients on statin therapy. *Joint Bone Spine* 2001; **68**: 430-433
7 **Ziajka PE,** Wehmeier T. Peripheral neuropathy and lipid-lowering therapy. *South Med J* 1998; **91**: 667-668
8 **Negevesky GJ,** Kolsky MP, Laureno R, Yau TH. Reversible atorvastatin-associated external ophthalmoplegia, anti-acetylcholine receptor antibodies, and ataxia. *Arch Ophthalmol* 2000; **118**: 427-428
9 **Segal AS.** Alopecia associated with atorvastatin. *Am J Med* 2002; **113**: 171
10 **Noêl B,** Cerottini JP, Panizzon RG. Atorvastatin-induced dermatomyositis. *Am J Med* 2001; **110**: 670-671
11 **Adcock BB,** Hornsby LB, Jenkins K. Dermographism: an adverse effect of atorvastatin. *J Am Board Fam Pract* 2001; **14**: 148-151
12 **Pfeiffer CM,** Kazenoff S, Rothberg HD. Toxic epidermal necrolysis from atorvastatin. *JAMA* 1998; **279**: 1613-1614
13 **Anliker MD,** Wuthrich B. Chronic urticaria to atorvastatin. *Allergy* 2002; **57**: 366
14 **Gonzalez-Ponte ML,** Gonzalez-Ruiz M, Duvos E, Gutierrez-Iniguez MA, Olalla JI, Conde E. Atorvastatin-induced severe thrombocytopenia. *Lancet* 1998; **352**: 1284
15 **Nakad A,** Bataille L, Hamoir V, Sempoux C, Horsmans Y. Atorvastatin-induced acute hepatitis with absence of cross-toxicity with simvastatin. *Lancet* 1999; **353**: 1763-1764
16 **Jimenez-Alonso J,** Osorio JM, Gutierrez-Cabello F, Lopez de la Osa A, Leon L, Mediavilla Garcia JD. Atorvastatin-induced cholestatic hepatitis in a young woman with systemic lupus erythematosus. Grupo Lupus Virgen de las Nieves. *Arch Intern Med* 1999; **159**: 1811-1812
17 **Belaiche G,** Ley G, Slama JL. Acute pancreatitis associated with atorvastatine therapy. *Gastroenterol Clin Biol* 2000; **24**: 471-472

Science Editor Wang XL **Language Editor** Elsevier HK

PO Box 2345, Beijing 100023, China
www.wjgnet.com
wjg@wjgnet.com

ELSEVIER

World J Gastroenterol 2005;11(20):3161-3164
World Journal of Gastroenterology ISSN 1007-9327

• *CASE REPORT* •

Long-term survival after intraluminal brachytherapy for inoperable hilar cholangiocarcinoma: A case report

Siu-Yin Chan, Ronnie T. Poon, Kelvin K. Ng, Chi-Leung Liu, Raymond T. Chan, Sheung-Tat Fan

Siu-Yin Chan, Ronnie T. Poon, Kelvin K. Ng, Chi-Leung Liu, Sheung-Tat Fan, Centre for the Study of Liver Disease and Department of Surgery, The University of Hong Kong, Pokfulam, Hong Kong, China
Raymond T. Chan, Department of Clinical Oncology, The University of Hong Kong, Pokfulam, Hong Kong, China
Correspondence to: Dr. Ronnie T. Poon, Department of Surgery, The University of Hong Kong, Queen Mary Hospital, 102 Pokfulam Road, Hong Kong, China. poontp@hkucc.hku.hk
Telephone: +852-285-53641 Fax: +852-281-75475
Received: 2004-07-12 Accepted: 2004-09-19

Abstract

Surgical resection with a tumor-free margin is the only curative treatment for hilar cholangiocarcinoma (Klatskin tumor). However, over half of the patients present late with unresectable tumors. Radiotherapy using external beam irradiation or intraluminal brachytherapy (ILBT) has been used to treat unresectable hilar cholangiocarcinoma with satisfactory outcome. We reported a patient with unresectable hilar cholangiocarcinoma surviving more than 6 years after combined external beam irradiation and ILBT.

Key words: Brachytherapy; Hilar cholangiocarcinoma

Chan SY, Poon RT, Ng KK, Liu CL, Chan RT, Fan ST. Long-term survival after intraluminal brachytherapy for inoperable hilar cholangiocarcinoma: A case report. *World J Gastroenterol* 2005; 11(20): 3161-3164
http://www.wjgnet.com/1007-9327/11/3161.asp

INTRODUCTION

Cholangiocarcinoma is a malignant tumor arising from either the extra-or intra-hepatic bile duct. The histological types include adenocarcinoma, carcinoma *in situ*, papillary adenocarcinoma, mucinous adenocarcinoma, and squamous cell carcinoma[1]. Hilar cholangiocarcinoma (Klatskin tumor) is a specific disease entity involving malignant tumors that locate in the biliary confluence at the liver hilum. Surgical resection with an adequate tumor-free margin is the only curative treatment[2]. The reported medium survival after surgical resection ranges from 16 to 46 mo[3-5]. A 5-year survival rate ranging from 21% to 25% after curative hepatectomy for hilar cholangiocarcinoma has been reported[6,7]. However, the prognosis of most patients with hilar cholangiocarcinoma is usually poor because of the low resectability rate, ranging from 28% to 37%[3,4,6,8]. This can be related to their locally advanced disease with extensive biliary and/or vascular involvement, presence of distant metastases, and poor pre-morbid conditions precluding a major operation. The median survival for patients with unresectable hilar cholangiocarcinoma has been reported to be 6-12 mo[3,4,6,9].

Among the palliative therapies for unresectable hilar cholangiocarcinoma, radiotherapy can achieve satisfactory local tumor control and possible survival benefit. It can be given in the form of external beam radiotherapy (EBRT), intraluminal brachytherapy (ILBT), or a combination of both. With the advancement in computerized 3D treatment planning system, the accuracy of the delivery of EBRT to the targeted tumor has been much improved. This technique leads to tumor shrinkage and improves bile drainage, thus reducing the incidence of septic complications. Likewise, ILBT imposes a high radiation dose to the tumor volume, bypasses the radiosensitive skin and superficial structures, and therefore spares the surrounding normal structures from radiation toxicity. The reported medium survival for unresectable hilar cholangiocarcinoma is 11 mo with ILBT alone[10] and 14.5 mo with combined EBRT and ILBT[11]. Both techniques offer satisfactory symptom palliation with minimal toxicity and are technically feasible for most patients. However, long-term survival beyond 5 years is very rare after radiotherapy for unresectable cholangiocarcinoma. We reported a patient with unresectable hilar cholangiocarcinoma surviving more than 6 years after combined treatment by EBRT and ILBT, and briefly reviewed the literatures of this treatment modality.

CASE REPORT

A 49-year-old gentleman presented with painless obstructive jaundice and significant weight loss in May 1998. Liver biochemistry showed elevated bilirubin (185 μmol/L) and alkaline phosphatase (285 IU/L) concentration. His carcino-embryonic antigen concentration was normal. Endoscopic retrograde cholangiopancreatography (Figure 1) showed a Bismuth type IV stricture[12]. Contrast computed tomography (CT) scan of the abdomen revealed enlarged lymph nodes along the hepatoduodenal ligament (Figure 2). Subsequent hepatic and superior mesenteric angiogram showed encasement of the common hepatic artery and main portal vein by the tumor. The tumor was considered unresectable and ultrasound-guided fine needle aspiration cytology of the hilar mass confirmed the diagnosis of hilar cholangiocarcinoma.

Bile duct decompression was performed by percutaneous transhepatic biliary drainage (PTBD), and the patient received combined EBRT and ILBT. A total of 40 Gy EBRT was

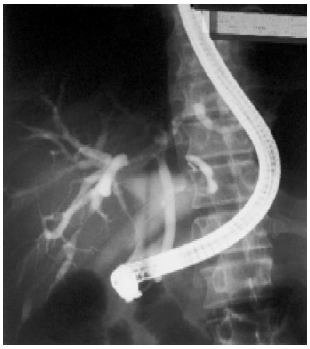

Figure 1 Endoscopic retrograde cholangiopancreatography showing bile duct stricture at liver hilum suggesting hilar cholangiocarcinoma.

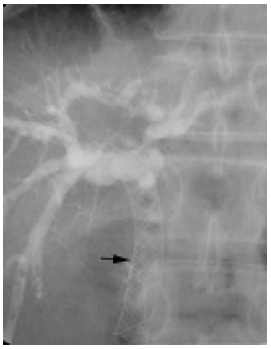

Figure 3 Metallic stent (black arrow) inside common duct on endoscopic retrograde cholangiopancreatography.

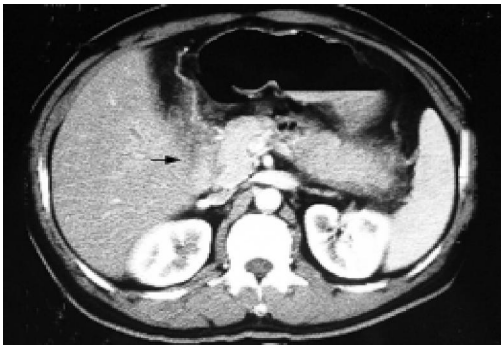

Figure 2 Contrast CT scan showing lymph node enlargement at hepatoduodenal ligament (black arrow).

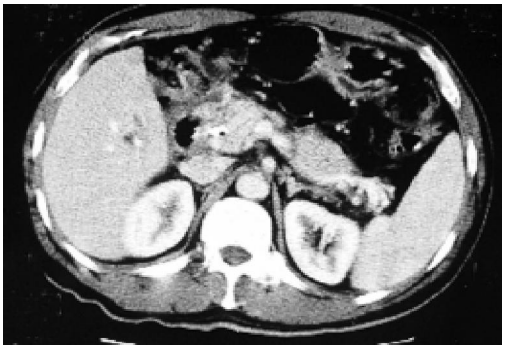

Figure 4 Contrast CT scan showing tumor regression after combined ILBT and external beam irradiation.

given to the tumor bed in 20 divided fractions, which was followed by 10 Gy ILBT using iridium 192 (Ir^{192}) wire. These radio-therapeutic procedures were not associated with any complication. A self-expandable metallic stent (Wallstent, Boston Scientific Ltd, USA) (Figure 3) was then inserted via the PTBD tract to bypass the stricture site, and the patency of the metallic stent lasted for 14 mo. Subsequently he required PTBD again when the metallic stent was blocked.

There was evidence of tumor regression on reassessment by CT scan in the first 2 years following the treatment (Figure 4). Subsequently there was slow disease progression with bile duct segregation and tumor infiltration to the second part of the duodenum. The patient relied on long-term PTBD for symptomatic control. Nevertheless, he has survived for more than 6 years since the initial diagnosis was made, and enjoyed a reasonable quality of life. He was able to work after the radiotherapy until the most recent 2 years of his disease course. At the time of writing the manuscript, the patient was still alive with satisfactory general condition.

DISCUSSION

In spite of its low incidence, hilar cholangiocarcinoma is a deadly tumor because the diagnosis is commonly not made until the disease progresses to its advanced stage which is not amenable to curative resection. The median survival is less than 1 year if the tumor is unresectable[3,4,6,9]. The treatment options for unresectable advanced hilar cholangiocarcinoma are limited. Orthotopic liver transplantation has been proposed to be a curative treatment modality for locally advanced hilar tumors with no evidence of extrahepatic tumors. However, it could be offered only to patients with locally advanced unresectable tumors without widespread metastases. The reported medial survival is 25 mo[13] and 5-year survival ranges from 30% to 87%[6,14,15]. Hassoun *et al*[14], achieved a high 5-year survival of 87% by very careful patient selection including staging laparotomy. Nonetheless, the practice of this treatment option is largely limited by the lack of organ donors and the potential risk of tumor recurrence following immunosuppressive therapy. For most patients with unresectable hilar cholangiocarcinoma, therapeutic efforts are mainly confined to palliation, which primarily involves relief and treatment of cholestasis. However, no palliative treatment is of proven value in prolonging survival.

Mortality of patients with hilar cholangiocarcinoma is usually caused by locoregional phenomena, as a result of liver failure secondary to bile duct obstruction, cholangitis, and sepsis. Bile duct decompression by endoscopic or radiological techniques is of paramount importance. This not only relieves patients' symptoms such as itching and cholangitis, but also facilitates biliary access and recovery of hepatic parenchymal function. In addition, it makes further oncological treatments of the tumor possible[9]. In fact, ILBT is regarded to be beneficial as it improves bile drainage in patients with hilar cholangiocarcinoma[10]. In case of significant biliary obstruction, prior establishment of patency of the common duct is important for a successful delivery of ILBT. This can be achieved by self-expandable metallic stent insertion, either percutaneously

Table 1 Survival after radiotherapy for extrahepatic cholangiocarcinoma

Study	No. of patients	Pathology	Mode of radiotherapy	Medium survival (mo)
Fletcher *et al*[10] (1983)	18	Hilar cholangiocarcinoma	ILBT	11
Kuvshinoff *et al*[11] (1995)	12	Hilar cholangiocarcinoma	ILBT+EBRT	14.5
Levitt *et al*[19] (1988)	20	Cholangiocarcinoma	ILBT	10
Ede *et al*[20] (1989)	14	Cholangiocarcinoma	ILBT	10.5
Veeze-Kuijpers *et al*[21] (1990)	31	Cholangiocarcinoma	ILBT+EBRT	8
Morganti *et al*[22] (2000)	20	Cholangiocarcinoma	ILBT+EBRT	13
Gonzalez *et al*[23] (2002)	38	Cholangiocarcinoma	ILBT+EBRT	10.4

ILBT, intraluminal brachytherapy; EBRT, external beam radiotherapy.

or endoscopically via the duodenum[16,17]. ILBT prolongs the patency of the metallic stent, which has been reported to range from 6 to 8 mo[9,17]. This minimizes the chance of stent occlusion, and delays the use of external biliary drain, which is associated with significant psychological problems and physiological disturbances such as dehydration and electrolyte imbalance[17]. Our patient received ILBT before metallic stent insertion, and the patency of the stent lasted for 14 mo after brachytherapy.

With regard to ILBT, there is no randomized controlled study to prove its effectiveness in patients with hilar cholangiocarcinoma[18]. The number of patients studied was small in most of the series in the literature[10,11,19-23]. The medium survival after ILBT for extrahepatic cholangiocarcinoma has been reported to range from 4 to 13 mo[19-23]. With respect to hilar cholangiocarcinoma *per se*, the reported medium survival ranges from 11 to 14.5 mo[10,11] (Table 1). ILBT was initially planned as a boost, as part of a treatment regimen for patients with inoperable tumors. This treatment modality was first reported in 1979 by Zimmon *et al*[24]. In that study, the iridium wire source was placed through PTBD in four patients. The treatment duration lasted for 24-72 h. It provides symptomatic palliation and significant tumor control without exacerbation of cholestasis or infective complication. It is suggested that early ILBT after PTBD might extend palliation of jaundice due to its effect on the limitation of tumor extension. Ir^{192}, with a half-life of 7 d, is the usual irradiation source for ILBT. The wire source can be put through PTBD or a nasobiliary catheter to reach the site of neoplastic stricture under fluoroscopic guidance. The wire can be placed across, parallel to or inside a stent. Au^{198} grains, with a shorter half-life of 2.7 d, have also been used for ILBT. It was found that the medical staff is better protected from radioactivity when the Au^{198} sources are withdrawn after brachytherapy[25].

The optimal irradiation dose and duration of brachytherapy are unknown. Our patient received a combination of 50-Gy external irradiation. The relationship between irradiation dosage and survival has been studied by Alden and Mohiuddin[26]. The patients with cholangiocarcinoma receiving high-dose combined brachytherapy and external beam radiation of more than 55 Gy showed significantly better survival than those who received smaller doses in unresectable cases. Among patients who received high-dose radiation, 48% of them experienced an extended 2-year survival. In another study, brachytherapy was given to five patients with Klatskin tumor for up to 5 d[27]. Two ribbons containing Ir^{192} seeds were threaded into the right and left percutaneous biliary drainage catheters in a "Y-shaped" configuration that corresponded well to the "Y-shaped" volume of the Klatskin tumor. Despite all these survival results, long-term survivors after radiation therapy for hilar cholangiocarcinoma, as in our case, have rarely been reported.

The procedure itself is not without risk. In the absence of any standardized protocol for brachytherapy, it is meaningless to compare the overall morbidity in different studies. The reported complication rate for cholangitis, which can be fatal, ranges from 6% to 30%[11,28,29]. Complications can be classified as those related to catheter introduction and those resulting from irradiation. There is an increased risk of bactobilia and bile duct perforation with either endoscopic or percutaneous biliary tract instrumentation. The wire source is introduced to the stricture site commonly via PTBD catheters, thus the potential risks are hemobilia, catheter dislodgement, superficial wound infection, liver abscess, and bile leakage. The complications related to ILBT itself are cholangitis and pancreatitis, as a result of blocked stent with biliary obstruction, as well as gastrointestinal tract upset with peptic ulcer or diarrhea[11,28].

There has been no report on the benefits of offering EBRT in advance to ILBT or vice versa. However, EBRT is given first in the majority of centers. This may be attributed to its effect on tumor shrinkage that prevents cholangitis during brachytherapy treatment. It is also questionable whether the addition of chemotherapy is beneficial to patients with inoperable Klatskin tumors. Basically, the use of chemotherapy is mainly limited to clinical trials. Nomura *et al*[30], reported a survival benefit in patients with unresectable extrahepatic bile duct cancer receiving brachytherapy combined with EBRT and repeated hepatic arterial infusion chemotherapy when compared with those receiving brachytherapy alone.

ILBT was intensely investigated 10 years ago, but it is still not commonly practiced nowadays. This case report showed that palliative combined EBRT and ILBT could be associated with long-term survival. Hence, it is worthwhile to reconsider its potential effect on local tumor control and possible survival benefits by proper randomized controlled trials. Hilar cholangiocarcinoma, once labeled as a dismal disease with poor outcome, can be associated with long-term survival as shown in our patient. In addition to improvement of life expectancy, the prolonging of symptom-free survival is an important target of the treatment as well.

REFERENCES

1 **Tumours of the biliary tract**. In Robert L.Souhami, Ian Tannock (eds). Oxford Textbook of Oncology. OXFORD University Press 2002: 1641-1652

2 **Reed DN,** Vitale GC, Martin R, Bas H, Wieman TJ, Larson GM, Edwards M, McMasters K. Bile duct carcinoma: trends in treatment in the nineties. *Am Surg* 2000; **66**: 711-714; discussion 714-715

3 **Jarnagin WR,** Fong Y, DeMatteo RP, Gonen M, Burke EC, Bodniewicz BS J, Youssef BA M, Klimstra D, Blumgart LH. Staging, resectability, and outcome in 225 patients with hilar cholangiocarcinoma. *Ann Surg* 2001; **234**: 507-517; discussion 517-519

4 **Burke EC,** Jarnagin WR, Hochwald SN, Pisters PW, Fong Y, Blumgart LH. Hilar Cholangiocarcinoma: patterns of spread, the importance of hepatic resection for curative operation, and a presurgical clinical staging system. *Ann Surg* 1998; **228**: 385-394

5 **Havlik R,** Sbisa E, Tullo A, Kelly MD, Mitry RR, Jiao LR, Mansour MR, Honda K, Habib NA. Results of resection for hilar cholangiocarcinoma with analysis of prognostic factors. *Hepatogastroenterology* 2000; **47**: 927-931

6 **Figueras J,** Llado L, Valls C, Serrano T, Ramos E, Fabregat J, Rafecas A, Torras J, Jaurrieta E. Changing strategies in diagnosis and management of hilar cholangiocarcinoma. *Liver Transpl* 2000; **6**: 786-794

7 **Nimura Y,** Kamiya J, Kondo S, Nagino M, Uesaka K, Oda K, Sano T, Yamamoto H, Hayakawa N. Aggressive preoperative management and extended surgery for hilar cholangiocarcinoma: Nagoya experience. *J Hepatobiliary Pancreat Surg* 2000; **7**: 155-162

8 **Bathe OF,** Pacheco JT, Ossi PB, Hamilton KL, Franceschi D, Sleeman D, Levi JU, Livingstone AS. Management of hilar bile duct carcinoma. *Hepatogastroenterology* 2001; **48**: 1289-1294

9 **Chamberlain RS,** Blumgart LH. Hilar cholangiocarcinoma: a review and commentary. *Ann Surg Oncol* 2000; **7**: 55-66

10 **Fletcher MS,** Brinkley D, Dawson JL, Nunnerley H, Williams R. Treatment of hilar carcinoma by bile drainage combined with internal radiotherapy using 192iridium wire. *Br J Surg* 1983; **70**: 733-735

11 **Kuvshinoff BW,** Armstrong JG, Fong Y, Schupak K, Getradjman G, Heffernan N, Blumgart LH. Palliation of irresectable hilar cholangiocarcinoma with biliary drainage and radiotherapy. *Br J Surg* 1995; **82**: 1522-1525

12 **Bismuth H,** Corlette MB. Intrahepatic cholangioenteric anastomosis in carcinoma of the hilus of the liver. *Surg Gynecol Obstet* 1975; **140**: 170-178

13 **Sudan D,** DeRoover A, Chinnakotla S, Fox I, Shaw B, McCashland T, Sorrell M, Tempero M, Langnas A. Radiochemotherapy and transplantation allow long-term survival for nonresectable hilar cholangiocarcinoma. *Am J Transplant* 2002; **2**: 774-779

14 **Hassoun Z,** Gores GJ, Rosen CB. Preliminary experience with liver transplantation in selected patients with unresectable hilar cholangiocarcinoma. *Surg Oncol Clin N Am* 2002; **11**: 909-921

15 **Robles R,** Figueras J, Turrion VS, Margarit C, Moya A, Varo E, Calleja J, Valdivieso A, Garcia-Valdelcasas JC, Lopez P, Gomez M, de Vicente E, Loinaz C, Santoyo J, Casanova D, Bernardos A, Fernandez JA, Marin C, Ramirez P, Bueno FS, Jaurrieta E, Parrilla P. Liver transplantation for hilar cholangiocarcinoma: Spanish experience. *Transplant Proc* 2003; **35**: 1821-1822

16 **Freeman ML,** Sielaff TD. A modern approach to malignant hilar biliary obstruction. *Rev Gastroenterol Disord* 2003; **3**: 187-201

17 **Hii MW,** Gibson RN, Speer AG, Collier NA, Sherson N, Jardine C. Role of radiology in the treatment of malignant hilar biliary strictures 2: 10 years of single-institution experience with percutaneoustreatment. *Australas Radiol* 2003; **47**: 393-403

18 **Khan SA,** Davidson BR, Goldin R, Pereira SP, Rosenberg WM, Taylor-Robinson SD, Thillainayagam AV, Thomas HC, Thursz MR, Wasan H. Guidelines for the diagnosis and treatment of cholangiocarcinoma: consensus document. *Gut* 2002; **51** Suppl 6: VI1-VI9

19 **Levitt MD,** Laurence BH, Cameron F, Klemp PF. Transpapillary iridium-192 wire in the treatmentof malignant bile duct obstruction. *Gut* 1988; **29**: 149-152

20 **Ede RJ,** Williams SJ, Hatfield AR, McIntyre S, Mair G. Endoscopic management of inoperable cholangiocarcinoma using iridium-192. *Br J Surg* 1989; **76**: 867-869

21 **Veeze-Kuijpers B,** Meerwaldt JH, Lameris JS, van Blankenstein M, van Putten WL, Terpstra OT. The role of radiotherapy in the treatment of bile duct carcinoma. *Int J Radiat Oncol Biol Phys* 1990; **18**: 63-67

22 **Morganti AG,** Trodella L, Valentini V, Montemaggi P, Costamagna G, Smaniotto D, Luzi S, Ziccarelli P, Macchia G, Perri V, Mutignani M, Cellini N. Combined modality treatment in unresectable extrahepatic biliary carcinoma. *Int J Radiat Oncol Biol Phys* 2000; **46**: 913-919

23 **Gonzalez Gonzalez D,** Gouma DJ, Rauws EA, van Gulik TM, Bosma A, Koedooder C. Role of radiotherapy, in particular intraluminal brachytherapy, in the treatment of proximal bile duct carcinoma. *Ann Oncol* 1999; **10** Suppl 4: 215-220

24 **Zimmon DS,** Bursa J, Chang J, Clemett AR. The management of hepatic duct cancer with percutaneous transhepatic biliary stent and intraluminal irradiation. *Gastroenterology* 1979; **77**: 49

25 **Hiratsuka J,** Imajo Y, Numaguchi K, Ohumi T, Shirabe T. Radiotherapy of bile duct carcinoma using intracatheter 198Au grains. *Radiat Med* 1991; **9**: 77-81

26 **Alden ME,** Mohiuddin M. The impact of radiation dose in combined external beam and intraluminal Ir-192 brachytherapy for bile duct cancer. *Int J Radiat Oncol Biol Phys* 1994; **28**: 945-951

27 **Kumar PP,** Good RR, McCaul GF. Intraluminal endocurietherapy of inoperable Klatskin's tumor with high-activity 192iridium. *Radiat Med* 1986; **4**: 21-26

28 **Lu JJ,** Bains YS, Abdel-Wahab M, Brandon AH, Wolfson AH, Raub WA, Wilkinson CM, Markoe AM. High-dose-rate remote afterloading intracavitary brachytherapy for the treatment of extrahepatic biliary duct carcinoma. *Cancer J* 2002; **8**: 74-78

29 **Montemaggi P,** Costamagna G, Dobelbower RR, Cellini N, Morganti AG, Mutignani M, Perri V, Brizi G, Marano P. Intraluminal brachytherapy in the treatment of pancreas and bile duct carcinoma. *Int J Radiat Oncol Biol Phys* 1995; **32**: 437-443

30 **Nomura M,** Yamakado K, Nomoto Y, Nakatsuka A, Ii N, Shoji K, Takeda K. Clinical efficacy of brachytherapy combined with external-beam radiotherapy and repeated arterial infusion chemotherapy in patients with unresectable extrahepatic bile duct cancer. *Int J Oncol* 2002; **20**: 325-331

Science Editor Wang XL and Guo SY **Language Editor** Elsevier HK

PO Box 2345, Beijing 100023, China
www.wjgnet.com
wjg@wjgnet.com

ELSEVIER

World J Gastroenterol 2005;11(20):3165-3166
World Journal of Gastroenterology ISSN 1007-9327

• *CASE REPORT* •

Retrotracheal thymoma masquerading as esophageal submucosal tumor

Sheung-Fat Ko, Yuan-Hsiung Tsai, Hsuan-Ying Huang, Shu-Hang Ng, Fu-Ming Fang, Yeh Tang, Ming-Tse Sung, Ming-Jang Hsieh

Sheung-Fat Ko, Yuan-Hsiung Tsai, Shu-Hang Ng, Fu-Ming Fang, Departments of Radiology, Chang Gung University, Chang Gung Memorial Hospital at Kaohsiung, Kaohsiung Hsien, Taiwan, China
Hsuan-Ying Huang, Ming-Tse Sung, Departments of Pathology, Chang Gung University, Chang Gung Memorial Hospital at Kaohsiung, Kaohsiung Hsien, Taiwan, China
Yeh Tang, Departments of Oncology, Chang Gung University, Chang Gung Memorial Hospital at Kaohsiung, Kaohsiung Hsien, Taiwan, China
Ming-Jang Hsieh, Departments of Thoracic Surgery, Chang Gung Memorial Hospital at Kaohsiung, Kaohsiung Hsien, Taiwan, China
Correspondence to: Ming-Jang Hsieh MD, Department of Thoracic Surgery, Chang Gung Memorial Hospital at Kaohsiung, 123 Ta-Pei Road, Niao-Sung, Kaohsiung 833, Taiwan, China. sfatko@adm.cgmh.org.tw
Telephone: +886-7-7317123-2579 Fax: +886-7-7338762
Received: 2004-09-21 Accepted: 2004-09-30

Abstract

A 42-year-old man presented with a two-year history of progressive dysphagia and hoarseness. Esophagogram and endoscopy revealed submucosal mass effect on the upper esophagus. Computed tomography and magnetic resonance imaging revealed an elongated mass in the retrotracheal region of the lower neck with extension to the posterior mediastinum. Partial tumor resection and histopathological evaluation revealed a WHO type B2 thymoma. Adjuvant radiation and chemotherapy were subsequently administered resulting in complete tumor regression. To our knowledge, this is the first report of ectopic retrotracheal thymoma with clinical and imaging manifestations mimicking those for esophageal submucosal tumor.

Key words: Dysphagia; Hoarseness

Ko SF, Tsai YH, Huang HY, Ng SH, Fang FM, Tang Y, Sung MT, Hsieh MJ. Retrotracheal thymoma masquerading as esophageal submucosal tumor. *World J Gastroenterol* 2005; 11(20): 3165-3166

http://www.wjgnet.com/1007-9327/11/3165.asp

INTRODUCTION

Thymoma is an epithelial neoplasm of the thymus, which usually lies in the anterior mediastinum[1-4]. Uncommonly, thymomas can also be found in other locations including the neck, the middle or posterior mediastinum, and the lung[4-9]. These ectopic thymomas are considered to arise from aberrantly distributed thymic tissues due to failure of normal caudal migration into the anterosuperior mediastinum[4-11]. Herein, we described a rare case of retrotracheal thymoma presenting with progressive dysphagia due to compression of the esophagus. To our knowledge, a thymoma developing in such an unusual location and mimicking an esophageal submucosal tumor on endoscopy and imaging studies has not been previously described.

CASE REPORT

A 42-year-old male presented with a 2-year history of progressive dysphagia and hoarseness. A mass with elastic consistency was palpable in the left lower neck. Otherwise, physical examination was normal. Laboratory work-up was also unremarkable. Endoscopy revealed an intact esophageal mucosa and a submucosal mass compressing the anterior wall of the upper esophagus. Esophagogram confirmed extraluminal compression and right-side deviation of the upper esophagus in the lower neck and upper mediastinum (Figure 1A). Extrinsic compression of the upper posterior tracheal wall was demonstrated from bronchoscopy. Computed tomography (CT) of the neck and thorax demonstrated a well-defined, homogeneously enhanced mass measuring 6 cm×3 cm×2 cm posterior to the trachea in the lower neck and upper posterior mediastinum, while the esophageal lumen was markedly compressed (Figure 1B). Magnetic resonance imaging (MRI) revealed a slightly elongated inhomogeneous mass posterior to the upper tracheal wall, highly suggestive of the presence of an esophageal submucosal mass (Figure 1C). The patient underwent surgical treatment under the initial impression of esophageal submucosal tumor. During the operation, instead of the expected esophageal growth, an elongated mass in the lower neck with extension to the mediastinum lying between the posterior wall of the trachea and anterior wall of the esophagus was found. Only partial resection of the mass via the low-neck approach was possible. Histopathological examination revealed a tumor composed of neoplastic epithelial component cells appearing as scattered plump cells with vesicular nuclei and distinct nucleoli among a heavy population of lymphocytes, compatible with the type B2 WHO classification. The patient refused further thoracotomy for complete tumor resection. Adjuvant chemotherapy and radiotherapy (60 Gy) were performed postoperatively and recovery was unremarkable. Complete resolution of the tumor was noted on 1-year CT follow-up. At the time of writing, there had been no evidence of recurrence in the intervening 5 years.

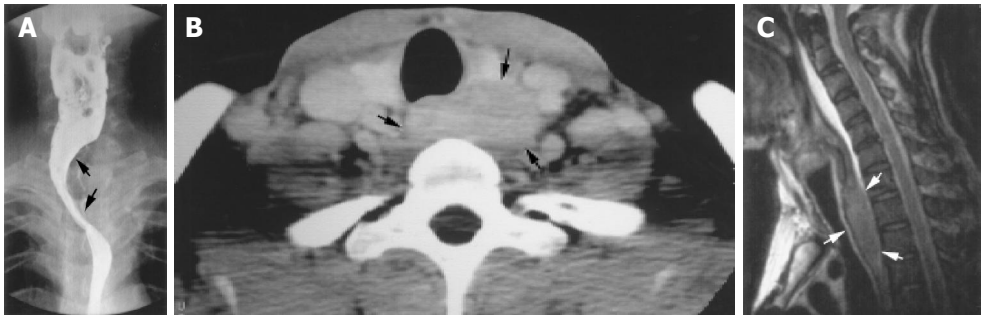

Figure 1 **A:** Barium esophagogram shows extraluminal compression and right side deviation of the upper esophagus (arrows); **B:** Enhanced CT scan at the level of the lower neck shows a mildly lobulated homogeneous mass (arrows) posterior to the trachea; **C:** T2 weighted sagittal MR image shows a slightly inhomogeneous, enlongated mass (arrows) with compression on the posterior wall of the trachea, mimicking an esophageal submucosal mass.

DISCUSSION

Embryologically, the thymic epithelium originates bilaterally from the ventral portions of the third pharyngeal pouches and descends caudally with the third parathyroid to a level lower than the thyroid tissue, eventually migrating to the anteriosuperior mediastinum by the fifth or sixth week of gestation[4,10]. Aberrant migration may occur anywhere along this pathway, especially adjacent to the thyroid glands or in the anterior neck[4-10]. Rarely, aberrant thymic tissues identified in the skull base, preaortic and retrocarinal fat during autopsies have also been reported.

Thymoma is the most common anterior mediastinal neoplasm, usually occurring at 30-40 and 60-70 years of age in patients with and without myasthenia gravis, respectively[1-4]. Corresponding to the frequencies for thymus location, 75% of thymomas are in the anterior mediastinum, 15% involve both the anterior and superior mediastinum, and 6% are within the superior mediastinum[4]. The remaining 4% of thymomas occur ectopically, affecting the neck, middle and posterior mediastinum, and the lung[4-9]. To our knowledge, however, isolated ectopic thymoma occurring in the retrotracheal region masquerading as an esophageal submucosal mass has not previously been documented.

Approximately one-third of patients with a thymic tumor are asymptomatic[1,2]. In symptomatic patients, 30% present with myasthenia gravis, and the remainder usually present with chest pain, cough, and dyspnea. Superior vena cava syndrome, weight loss, fever and night sweats can also be found in patients with more aggressive tumors [1,2]. On the other hand, although extremely unusual, our case illustrated that thymoma may be present with progressive dysphagia, which could be related to the unusual anatomic location, leading to initial endoscopic and esophagographic evaluations and a tentative diagnosis of esophageal submucosal tumor.

On CT, thymomas usually appear as homogeneous soft-tissue density oval or lobulated masses, which are usually sharply demarcated and project to one side of the anterior mediastinum[3,6-8]. On MRI, thymomas typically have a low signal intensity on T1-weighted images, which increases with T2-weighted images, and may be homogeneous or inhomogeneous in intensity[3,5]. In retrospect, we found that the tumor morphology on CT and MRI in this particular case was compatible with thymoma. However, owing to the rarity of its location, an accurate preoperative diagnosis was, indeed, difficult and the differential diagnosis included leiomyoma or leimyosarcoma, gastrointestinal stromal tumor, and lymphoma.

Surgical resection is the mainstay of treatment for thymoma[1,2]. Recently, multimodality therapy has been stressed for thymoma, especially for subtotally resected tumors[1,2]. Significant reduction of the rate of thymoma metastasis has also been reported in chemotherapy patients. Adjuvant radiotherapy and chemotherapy were successful in our patient. CT follow-up revealed total tumor regression 1 year after surgery, and the patient remained disease-free 5 years after treatment.

In summary, this report documents a rare occurrence of retrotracheal thymoma presenting with progressive dysphagia. In light of this case, retrotracheal thymoma may be included as one of the unusual differential considerations when submucosal mass effect on the esophagus is encountered.

REFERENCES

1 **Detterbeck FC,** Parsons AM. Thymic tumors. *Ann Thorac Surg* 2004; **77**: 1860-1869
2 **Moore KH,** McKenzie PR, Kennedy CW, McCaughan BC. Thymoma: trends over time. *Ann Thorac Surg* 2001; **72**: 203-207
3 **Naidich DP,** Webb WR, Muller NL, Krinsky GA, Zerhouni EA, Siegelman SS. Computed tomography and magnetic resonance of the thorax. 3rd ed. Philadelphia: *Lippincott Raven* 1999: 58-76
4 **Rosai J,** Levine GD. Tumors of the thymus. In: Firminger HI, ed. Atlas of tumor pathology. Fascicle 13, 2nd series. Washington: *Armed Forces Institute Pathol* 1976: 34-161
5 **Nagasawa K,** Takahashi K, Hayashi T, Aburano T. Ectopic cervical thymoma: MRI findings. *AJR Am J Roentgenol* 2004; **182**: 262-263
6 **Kanzaki M,** Oyama K, Ikeda T, Yoshida T, Murasugi M, Onuki T. Noninvasive thymoma in the middle mediastinum. *Ann Thorac Surg* 2004; **77**: 2209-2210
7 **Kojima K,** Yokoi K, Matsuguma H, Kondo T, Kamiyama Y, Mori K, Igarashi S. Middle mediastinal thymoma. *J Thorac Cardiovasc Surg* 2002; **124**: 639-640
8 **Tan A,** Holdener GP, Hecht A, Gelfand C, Baker B. Malignant thymoma in an ectopic thymus: CT appearance. *J Comput Assist Tomogr* 1991; **15**: 842-844
9 **Moran CA,** Suster S, Fishback NF, Koss MN. Primary intrapulmonary thymoma. A clinicopathologic and immunohistochemical study of eight cases. *Am J Surg Pathol* 1995; **10**: 304-312
10 **Richardson MA,** Sie KYC. The neck: embryology and anatomy. In: Bluestone CD, Stool SE, Kenna MA, eds. Pediatric Otolaryngology. 3rd ed. Philadelphia: *WB Saunders Company* 1996: 1464-1479

Science Editor Guo SY **Language Editor** Elsevier HK

PO Box 2345, Beijing 100023, China
www.wjgnet.com
wjg@wjgnet.com

ELSEVIER

World J Gastroenterol 2005;11(20):3167-3169
World Journal of Gastroenterology ISSN 1007-9327

• *CASE REPORT* •

Submucous colon lipoma: A case report and review of the literature

Hong Zhang, Jin-Chun Cong, Chun-Sheng Chen, Lei Qiao, En-Qing Liu

Hong Zhang, Jin-Chun Cong, Chun-Sheng Chen, Lei Qiao, En-Qing Liu, Department of General Surgery, The Second Hospital of China Medical University, Shenyang 110004, Liaoning Province, China
Correspondence to: Dr Hong Zhang, Department of General Surgery, The Second Hospital of China Medical University, Shenyang 110004, Liaoning Province, China. zhanghong1203@yahoo.com.cn
Telephone: +86-24-24139358 Fax: +86-24-23896876
Received: 2004-05-27 Accepted: 2004-06-17

Abstract

Colon lipoma is remarkably rare in clinical practice. We reported a case of ascending colon lipoma in an 83-year-old woman. She was asymptomatic with a lipoma of 35 mm×30 mm×24 mm in size which was found by routine colonoscopy. Right hemicolectomy was performed uneventfully. The diagnosis was made by histological examination. Reviewing the literature and combining with our experience, we discussed the clinical features, diagnosis and treatment of this uncommon disease.

Key words: Colon lipoma; Case report; Review literature

Zhang H, Cong JC, Chen CS, Qiao L, Liu EQ. Submucous colon lipoma: A case report and review of the literature. *World J Gastroenterol* 2005; 11(20): 3167-3169
http://www.wjgnet.com/1007-9327/11/3167.asp

INTRODUCTION

Colon lipoma is generally mildly symptomatic or asymptomatic. Even in the condition of presenting with dramatic characteristics in colonoscopy, barium enema and CT scan, colon lipoma is still underemphasized and misdiagnosed. We report a case of submucous ascending colon lipoma and review the literature to evaluate the clinical features, diagnosis and treatment of this disease.

CASE REPORT

An 83-year-old woman was admitted to the General Surgery Department of our hospital on January 2003 for intermittent mild anal pain. She denied any abdominal pain, constipation, diarrhea, hematochezia or melena. She had a past medical history of cerebral infarction for at least 10 years, and no cancer records were available. She received appendectomy for acute appendicitis 9 years ago. No meaningful findings were obtained in abdominal examination. Complete evaluations of the ano-rectum were carried out which included visual inspection, digital examination and anoscopy. The diagnosis of external hemorrhoid was established and conservative treatment was adopted. Detailed laboratorial studies showed all results within normal limits, including complete peripheral blood cell counts, blood biochemistry and carcinoembryonic antigen. Fecal occult blood test was negative thrice consecutively. Colonoscopy was performed afterward, and a yellowish hemispherical tumor of 45 mm in diameter was detected at the site of ascending colon. The overlying mucosa was smooth, and the lesion was soft and compressible (Figure 1A). According to these features, the diagnosis of submucous tumor (SMT) was made by colonoscopy. Biopsy showed non-specific colitis. Barium enema revealed an ovoid filling defect with smooth border at the proximal area of colon hepatic flexure (Figure 1B). Abdominal CT scan found a pedunculated neoplasm protruding into the lumen of ascending colon with sharp margin and soft tissue density (Figure 1C). Lipoma was considered to be the most probable cause, but malignancy could not be excluded. Finally, the patient underwent laparotomy, although she was asymptomatic and the tumor showed benign features. Right hemicolectomy was performed uneventfully. Surgery certified the diagnosis of colon lipoma. Macroscopic inspection of the resected colon segment showed a smooth round polypoid submucous tumor with elastic character and 35 mm×30 mm×24 mm in size (Figure 2A). Fault of the specimen demonstrated the tumor with pedunculated appearance. The base of the lesion was 8 mm in size. The tumor was covered by normal mucosa and had uniform parenchyma in bright yellow color (Figure 2B). Histological examination revealed characteristic lipoma of colon (Figure 3).

DISCUSSION

Colon lipoma was described initially by Bauer in 1757. The incidence was estimated to be about 0.26%[1] 10 years ago, however the available data was kept insufficient during the recent decade. Rogy *et al*[2], reported that colon lipoma constituted 0.3% of the cases treated for colorectal diseases and 1.8% of the cases of benign colorectal tumor during the same period. Elders are more likely to be involved, and neither male nor female was found to be predominant according to most of the current literatures, but this conception was disagreed by some authors who reported a higher incidence in women than in men[2,3]. Most of the lesions were located at the right side of large bowel, accounting for nearly 90% of cases. The majority of colon lipomas presented as single while only 10% of cases were multiple. The most frequent type was submucous lipoma with sessile or pedunculate appearance, the remainder as

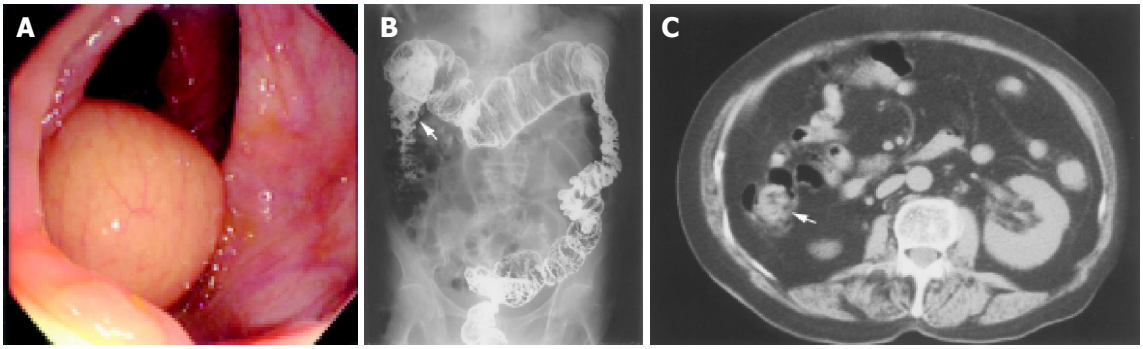

Figure 1 **A**: The preoperative examination: Colonoscopy showed a yellowish hemispherical tumor at the site of ascending colon. The overlying mucosa was smooth, and the lesion was soft and compressible; **B**: The preoperative examination: Barium enema revealed an ovoid filling defect with smooth border at the proximal area of colon hepatic flexture; **C**: The preoperative examination: CT scan found a pedunculated neoplasm protruding into the lumen at the site of ascending colon with sharp margin and soft tissue density.

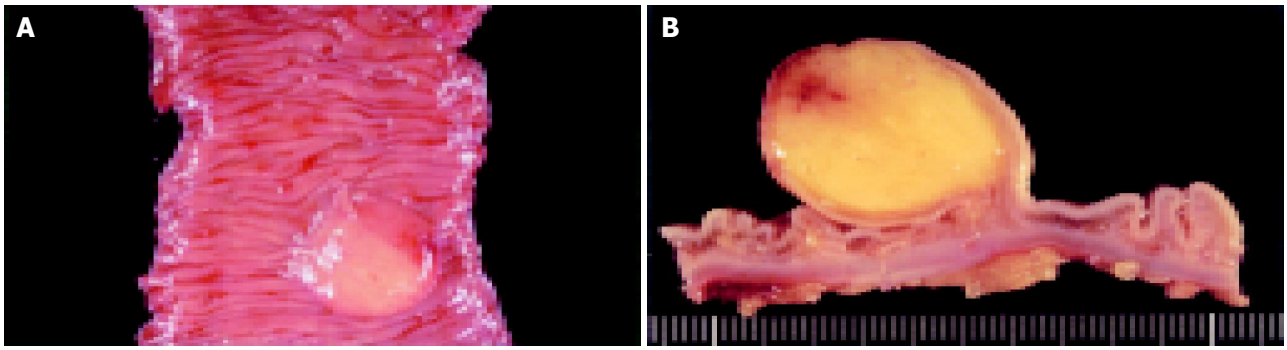

Figure 2 **A**: The macroscopic inspection: Macroscopic inspection of the resected colon segment showed a smooth round polypoid submucous tumor with elastic character and 35 mm×30 mm×24 mm in size; **B**: The macroscopic inspection: Fault of the specimen demonstrated the tumor with pedunculated appearance. The base of the lesion was 8 mm in size. The tumor was covered by normal mucosa and had uniform parenchyma in bright yellow color (one scale mark = 1 mm).

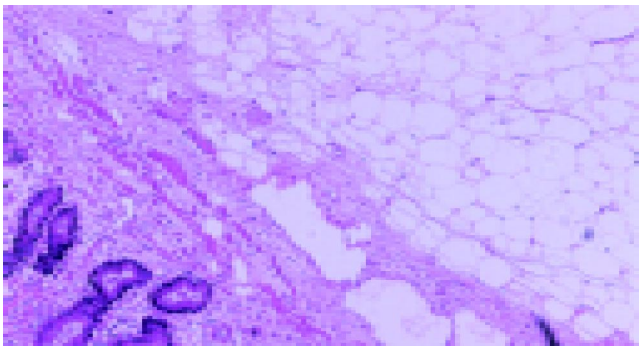

Figure 3 The histological examination: Histological examination showed characteristic lipoma of colon. No evidence of malignancy was detected (hematoxylin and eosin, original magnification ×40).

subserosal lipoma was less than 10%. Generally, colon lipoma is mildly symptomatic or asymptomatic. Sometimes it was detected accidentally in examinations for other purpose. Rogy *et al*[2], insisted that the clinical manifestations were associated with the size of tumor and not related to the involved segment of large bowel. As widely accepted, lipoma larger than 20 mm in diameter, is likely to be symptomatic, it is quite unusual that the lipoma with a maximum diameter of 35 mm is asymptomatic. The common symptoms of colon lipomas include abnormal bowel habits, abdominal pain, diarrhea, rectal bleeding, abdominal discomfort and melena. Occasionally, patients may complain that a lump of hemorrhagic tissues defecate from the rectum due to self-amputation of the lipoma[3]. The episode of intussusception or intestinal obstruction can also be seen in the patients with larger lipoma[4]. Even in some situations, abdominal emergency due to the complications of colon lipoma was the first manifestation of these patients. Sometimes colon lipoma can also be the source of massive lower gastrointestinal bleeding[5].

Since no specific symptoms and physical signs are available, accurate preoperative diagnosis is difficult to achieve. Regarding the age and symptoms of these patients, malignant colon tumors are often considered. With the development of colonoscopy, barium enema and CT scan, some characteristic findings of colon lipomas are useful in making diagnosis, even there is a case report that colon lipoma was correctly diagnosed by sonography[6]. For the submucous lipoma, colonoscopy may directly visualize the mass with tenting of the mucosa, which may be easily indented with a closed biopsy forceps. As the forceps are withdrawn, the tumor will soon spring back to resume its previous shape (pillow or cushion sign)[7]. The pressure exerted on the lesion may compress the superficial vessels and the distinctive yellow color of fat will disclose. Adipose tissue may protrude through the biopsy site (naked fat sign) which reveals fatty characteristic of the tumor[1]. But usually

biopsy is not recommended in the patients with suspected lipoma, because the lesion is beneath the normal mucosa and biopsy often cannot promote diagnosis just as the result of non-specific colitis in our case report, on the contrary, it increases the risks of bleeding and perforation. According to the radiolucency of fatty tissue, barium enema is helpful in making diagnosis by showing a relatively radiolucent mass. Generally, lipoma appears as an ovoid, well-demarcated filling defect. The characteristic of lipoma on barium enema is so-called "squeeze-sign" which means that the tumor can deform by external pressure or peristalsis. Computerized tomography is considered to be the definitive diagnostic measure in recognizing colon lipomas because the masses present characteristic fatty densitometric values[8]. On CT scan image, lipoma has uniform appearance with fat-equivalent density and smooth border. But for small lipoma, the diagnostic value of CT is low.

Patients with small asymptomatic colon lipomas need regular follow-up, and additional treatments are unnecessary. Larger lipoma may cause symptoms, so resection should be considered for those bigger than 20 mm in diameter[9]. Currently, the indication of endoscopic resection of colonic lipoma is still a controversial subject. In our opinion, lipoma is unreliable to endoscopic removal, partly because the fatty tissue is inefficient conductor for electronic current and may result in a significantly high rate of complication[10]. The risk of perforation or hemorrhage is notably increased when the lesion is sessile or broadly-based. Surgical resection seems to be the ideal choice of treatment, especially when the malignancy cannot be completely excluded. Colotomy excision or segmental colon resection is recommended for complete removal of the lipoma. If the preoperative diagnosis of colon lipoma can be made correctly, extent of surgery may be appropriately limited.

REFERENCES

1 **Notaro JR,** Masser PA. Annular colon lipoma: a case report and review of the literature. *Surgery* 1991; **110**: 570-572
2 **Rogy MA,** Mirza D, Berlakovich G, Winkelbauer F, Rauhs R. Submucous large-bowel lipomas-presentation and management. An 18-year study. *Eur J Surg* 1991; **157**: 51-55
3 **Radhi JM.** Lipoma of the colon: self amputation. *Am J Gastroenterol* 1993; **88**: 1981-1982
4 **Kabaalioglu A,** Gelen T, Aktan S, Kesici A, Bircan O, Luleci E. Acute colonic obstruction caused by intussusception and extrusion of a sigmoid lipoma through the anus after barium enema. *Abdom Imaging* 1997; **22**: 389-391
5 **Rodriguez DI,** Drehner DM, Beck DE, McCauley CE. Colonic lipoma as a source of massive hemorrhage. Report of a case. *Dis Colon Rectum* 1990; **33**: 977-979
6 **Alkim C,** Sasmaz N, Alkim H, Caglikulekci M, Turhan N. Sonographic findings in intussusception caused by a lipoma in the muscular layer of the colon. *J Clin Ultrasound* 2001; **29**: 298-301
7 **Ryan J,** Martin JE, Pollock DJ. Fatty tumours of the large intestine: a clinicopathological review of 13 cases. *Br J Surg* 1989; **76**: 793-796
8 **Liessi G,** Pavanello M, Cesari S, Dell'Antonio C, Avventi P. Large lipomas of the colon: CT and MR findings in three symptomatic cases. *Abdom Imaging* 1996; **21**: 150-152
9 **Tamura S,** Yokoyama Y, Morita T, Tadokoro T, Higashidani Y, Onishi S. "Giant" colon lipoma: what kind of findings are necessary for the indication of endoscopic resection? *Am J Gastroenterol* 2001; **96**: 1944-1946
10 **Chase MP,** Yarze JC. "Giant" colon lipoma-to attempt endoscopic resection or not? *Am J Gastroenterol* 2000; **95**: 2143-2144

Science Editor Ma JY and Guo SY **Language Editor** Elsevier HK

PO Box 2345, Beijing 100023, China
www.wjgnet.com
wjg@wjgnet.com

ELSEVIER

World J Gastroenterol 2005;11(20):3170
World Journal of Gastroenterology ISSN 1007-9327

Acknowledgements to Reviewers of *World Journal of Gastroenterology*

Many reviewers have contributed their expertise and time to the peer review, a critical process to ensure the quality of *World Journal of Gastroenterology*. The editors and authors of the articles submitted to the journal are grateful to the following reviewers for evaluating the articles (including those were published and those were rejected in this issue) during the last editing period of time.

Julio Horacio Carri, Professor
Internal Medicine – Gastroenterology, Universidad Nacional de Córdoba, Av. Estrada 160 - P 5 - Dpt. D, Córdoba 5000, Argentina

Er-Dan Dong, Professor
Department of Life Science, Division of Basic Research in Clinic Medicine, National Natural Science Foundation of China, 83 Shuanqing Road, Haidian District, Beijng 100085, China

Xue-Gong Fan, Professor
Xiangya Hospital, Changsha 410008, Hunan Povince, China

Jin Gu, Professor
Peking University School of Oncology, Beijing Cancer Hospital, Beijing 100036, China

De-Wu Han, Professor
Shanxi Medical University, 86 Xinjian South Road, Taiyuan 030001, Shanxi Povince, China

Shao-Heng He, Professor
Medical College of Shantou University, 22 Xinling Rd, Shantou, Guangdong, Shantou 515031, Guangdong Povince, China

Fu-Lian Hu, Professor
Department of Gastroenterology, Peking University First Hospital, 8 Xishiku St, Xicheng District, Beijing 100034, China

Keiji Hirata, M.D.
Surgery 1, University of Occupational and Environmental Health, 1-1 Iseigaoka, Yahatanishi-ku, Kitakyushu 807-8555, Japan

Joachim Labenz, Associate Professor
Jung-Stilling Hospital, Wichernstr. 40, Siegen 57074, Germany

Martin Lipkin, Professor
Weill Medical College of Cornell University, Strang Cancer Research Lab Rockefeller Univ., 1230 York Avenue, The Rockefeller University, New York 10021, United States

Ai-Ping Lu, Professor
China Academy of Traditional Chinese Medicine, Dongzhimen Nei, 18 Beixincang, Beijing 100700, China

You-Yong Lu, Professor
Beijing Molecular Oncology Laboratory, Peking University School of Oncology and Beijing Institute for Cancer Reaearch, #1, Da-Hong-Luo-Chang Street, Western District, Beijing 100034, China

Sasa Markovic, Professor
Head,Department of Gastroenterology, Univercity Clinical Center Ljubljana, 2 Japljeva 1525 Ljubljana, Slovenia

Jae-Gahb Park, Professor
Seoul National University College of Medicine, 28 Yongon-dong, Chongno-gu, Seoul 110-744, Korea

Lun-Xiu Qin, Professor
Liver Cancer Institute and Zhongshan Hospital, Fudan University, 180 Feng Lin Road, Shanghai 200032, China

Christian Rabe, M.D.
Resident, Department of Medicine 1, University of Bonn Sigumund-Freud-Strasse 25 D 53105 Bonn, Germany

Peng Shang, Professor
Department of Cell Biology, Faculty of Life Sciences, 127 Western Youyi Road, Northwestern Polytechnological University, Xi'an, 710072, Shaanxi Povince, China

Dino Vaira, Professor
Department of Internal Medicine and Gastroent, University of Bologna, S.Orsola-Malpighi Hospital - Nuove Patologie, Pad. 5 - via Massarenti 9, Bologna 40138, Italy

Chun-Yang Wen, M.D.
Department of Molecular Pathology, Atomic Bomb Disease Institute, Nagasaki University Graduate School of Biomedical Sciences. 1-12-4 Sakamoto, Nagasaki 852-8523, Japan

Harry H-X Xia, M.D.
Department of Medicine, The University of Hong Kong, Pokfulam Road, Hong Kong, China

Yuan Yuan, Professor
Cancer Institute of China Medical University, 155 North Nanjing Street, Heping District, Shenyang 110001, Liaoning Province, China

Mu-Jun Zhao, M.D.
Institute of Biochemistry and Cell Biology, Chinese Academy of Sciences, 320 Yueyang Road, Shanghai 200031, China

Xiao-Hang Zhao, Professor
State Key Laboratory of Molecular Oncology, Cancer Institute of Chinese Academy of Medical Sciences, 17 Panjiayuan, Chaoyangqu, Beijing 100021, China

PO Box 2345, Beijing 100023, China
www.wjgnet.com
wjg@wjgnet.com

ELSEVIER

World J Gastroenterol 2005;11(20):Appendix 1
World Journal of Gastroenterology ISSN 1007-9327

Meetings

Major meetings coming up

Digestive Disease Week
106th Annual Meeting of AGA, The American Gastroenterology Association
May 14-19, 2005
www.ddw.org/
Chicago, Illinois

13th World Congress of Gastroenterology
September 10-14, 2005
www.wcog2005.org/
Montreal, Canada

13th United European Gastroenterology Week, UEGW
October 15-20, 2005
www.uegf.org/
Copenhagen, Denmark

American College of Gastroenterology Annual Scientific Meeting
October 28-November 2, 2005
www.acg.gi.org/
Honolulu Convention Center, Honolulu, Hawaii

Events and Meetings in the upcoming 6 months

World Congress on Gastrointestinal Cancer
June 15–18, 2005
Barcelona

Events and meetings in 2005

Canadian Digestive Disease Week Conference
February 26-March 6, 2005
www.cag-acg.org
Banff, AB

2005 World Congress of Gastroenterology
September 12–14, 2005
Montreal, Canada

International Colorectal Disease Symposium 2005
February 3–5, 2005
Hong Kong

13th UEGW meeting *United European Gastroenterology Week*
October 15–20, 2005
www.webasistent.cz/guarant/uegw2005/
Copenhagen-Malmoe

7th International Workshop on Therapeutic Endoscopy
September 10–12, 2005
www.alfamedical.com
Theodor Bilharz Research Institute

EASL 2005 the 40th annual meeting
April 13–17, 2005
www.easl.ch/easl2005/
Paris, France

Pediatric Gastroenterology, Hepatology and Nutrition
March 13, 2005
Jakarta, Indonesia

21st annual international congress *of Pakistan society of Gastroenterology & GI Endoscopy*
March 25–27, 2005
www.psgc2005.com
Peshawar

8th Congress of the Asian Society of HepatoBiliary Pancreatic Surgery
February 10–13, 2005
Mandaluyong, Philippines

APDW 2005 - Asia Pacific Digestive Week 2005
September 25–28, 2005
www.apdw2005.org
Seoul, Korea

World Congress on Gastrointestinal Cancer
June 15–18, 2005
Barcelona

British Society of Gastroenterology Conference (BSG)
March 14–17, 2005
www.bsg.org.uk
Birmingham

Digestive Disease Week *DDW 106th Annual Meeting*
May 15–18, 2005
www.ddw.org
Chicago, Illinois

70th ACG Annual Scientific Meeting and Postgraduate Course
October 28-November 2, 2005
Honolulu Convention Center, Honolulu, Hawaii

Events and Meetings in 2006

EASL 2006 - THE 41ST ANNUAL MEETING
April 26–30, 2006
Vienna, Austria

Canadian Digestive Disease Week Conference
March 4–12, 2006
www.cag-acg.org
Quebec City

XXX pan-american congress of digestive diseases *XXX congreso panamericano de anfermedades digestivas*
November 25-December 1, 2006
www.gastro.org.mx
Cancun

World Congress on Gastrointestinal Cancer
June 14–17, 2006
Barcelona, Spain

7th World Congress of the International Hepato-Pancreato-Biliary Association
September 3–7, 2006
www.edinburgh.org/conference
Edinburgh

71st ACG Annual Scientific Meeting and Postgraduate Course
October 20–25, 2006
Venetian Hotel, Las Vegas, Neveda

PO Box 2345, Beijing 100023, China
www.wjgnet.com
wjg@wjgnet.com

ELSEVIER

World J Gastroenterol 2005;11(20):Appendix 2-3
World Journal of Gastroenterology ISSN 1007-9327

Instructions to authors

GENERAL INFORMATION

World Journal of Gastroenterology (*WJG,* ISSN 1007-9327 CN 14-1219/R) is a weekly journal of more than 48 000 circulation, published on the 7th, 14th, 21st and 28th of every month.

Original Research, Clinical Trials, Reviews, Comments, and Case Reports in esophageal cancer, gastric cancer, colon cancer, liver cancer, viral liver diseases, *etc*., from all over the world are welcome on the condition that they have not been published previously and have not been submitted simultaneously elsewhere.

Published jointly by
The WJG Press and Elsevier Inc.

SUBMISSION OF MANUSCRIPTS

Manuscripts should be typed double-spaced on A4 (297×210 mm) white paper with outer margins of 2.5 cm. Number all pages consecutively, and start each of the following sections on a new page: Title Page , Abstract, Introduction, Materials and Methods, Results, Discussion, Acknowledgements, References, Tables, Figures and Figure Legends. Neither the Editors nor the Publisher is responsible for the opinions expressed by contributors. Manuscripts formally accepted for publication become the permanent property of The WJG Press and Elsevier Inc., and may not be reproduced by any means, in whole or in part without the written permission of both the Authors and the Publisher. We reserve the right to put onto our website and copy-edit accepted manuscripts. Authors should also follow the guidelines for the care and use of laboratory animals of their institution or national animal welfare committee.

Authors should retain one copy of the text, tables, photographs and illustrations, as rejected manuscripts will not be returned to the author(s) and the editors will not be responsible for the loss or damage to photographs and illustrations.

Online submission
Online submission is strongly advised. Manuscripts should be submitted through the Online Submission System at: http://www.wjgnet.com/index.jsp. Authors are highly recommended to consult the ONLINE INSTRUCTIONS TO AUTHORS (http://www.wjgnet.com/wjg/help/instructions.jsp) before attempting to submit online. Authors encountering problems with the Online Submission System may send an email describing the problem to wjg@wjgnet.com for assistance. If you submit manuscript online, do not make a postal contribution. A repeated online submission for the same manuscript is strictly prohibited.

Postal submission
Send 3 duplicate hard copies of the full-text manuscript typed double-spaced on A4(297×210 mm) white paper together with any original photographs or illustrations and a 3.5 inch computer diskette or CD-ROM containing an electronic copy of the manuscript including all the figures, graphs and tables in native Microsoft Word format or *.rtf format to:

World Journal of Gastroenterology
Apartment 1066 Yishou Garden,
58 North Langxinzhuang Road,
PO Box 2345, Beijing 100023, China
E-mail: wjg@wjgnet.com
http: //www.wjgnet.com

MANUSCRIPT PREPARATION

All contributions should be written in English. All articles must be submitted using a word-processing software. All submissions must be typed in 1.5 line spacing and in word size 12 with ample margins. The letter font is Tahoma. For authors originating from China, one copy of the Chinese translation of the manuscript is also required (excluding references). Style should conform to our house format. Required information for each of the manuscript sections is as follows:

Title page
Full manuscript title, running title, all author(s) name(s), affiliations, institution(s) and/or department(s) where the work was accomplished, disclosure of any financial support for the research, and the name, full address, telephone and fax numbers and email address of the corresponding author should be involved. Titles should be concise and informative (removing all unnecessary words), emphasize what is NEW, and avoid abbreviations. A short running title of less than 40 letters should be provided. List the author(s)' name(s) as follows: initials and/or first name, middle name or initial(s) and full family name.

Abstract
An informative, structured abstract of no more than 250 words should accompany each manuscript. Abstracts for original contributions should be structured into the following sections: AIM: Only the purpose should be included. METHODS: The materials, techniques, instruments and equipments, and the experimental procedures should be included. RESULTS: The observatory and experimental results, including data, effects, outcome, *etc*. should be included. Authors should present *P* value where necessary, and the significant data should accompany. CONCLUSION: Accurate view and the value of the results should be included.

The format of structured abstracts is at: http://www.wjgnet.com/wjg/help/11.doc

Key words
Please list 3-10 key words that could reflect content of the study.

Text
For most article types, the main text should be structured into the following sections: INTRODUCTION, MATERIALS AND METHODS, RESULTS and DISCUSSION, and should include appropriate Figures and Tables. Data should be presented in the body text or Figures and Tables, not both.

Illustrations
Figures should be numbered as 1, 2, 3 and so on, and mentioned clearly in the main text. Provide a brief title for each figure on a separate page. No detailed legend should be involved under the figures. This part should add into the text where the figures are applicable. Digital images: black and white photographs should be scanned and saved in TIFF format at a resolution of 300 dpi; color images should be saved as CMYK (print files) and not RGB (screen-viewing files). Place each photograph in a separate file. Print images: supply images of size no smaller than 126×76 mm printed on smooth surface paper; label the image by writing the Figure number and orientation using an arrow. Photomicrographs: indicate the original magnification and stain in the legend. Digital Drawings: supply files in EPS if created by Freehand and Illustrator, or TIFF from Photoshop. EPS files must be accompanied by a version in native file format for editing purposes. Scans of existing line drawings should be scanned at a resolution of 1200 dpi and as close as possible to the size at which they will appear when printed, not smaller. Please use uniform legends for the same subjects. For example: Figure 1 Pathological changes of atrophic gastritis after treatment. A: ...; B: ...;C: ...; D: ...; E: ...; F: ...; G: ...

Tables
Three-line tables should be numbered as 1, 2, 3 and so on, and mentioned clearly in the main text. Provide a brief title for each table. No detailed legend should be involved under the tables. This part should add into the text where the tables are applicable. The information should complement but not duplicate that contained in the text. Use one horizontal line under the title, a second under the column heads, and a third below the Table, above any footnotes. Vertical and italic lines should be omitted.

Notes in tables and illustrations
Data which is not statistically significant should not be noted. $^{a}P<0.05$, $^{b}P<0.01$ ($P>0.05$ should not be noted). If there are other series of *P* values, $^{c}P<0.05$ and $^{d}P<0.01$ are used; Third series of *P* values can be expressed as $^{e}P<0.05$ and $^{f}P<0.01$. Other notes in tables or under

illustrations should be expressed as ^1F, ^2F, ^3F; or some other symbols with a superscript (Arabic numerals) in the upper left corner. In a multi-curve illustration, each curve should be labeled with ●, ○, ■, □, ▲, △, *etc*. in a certain sequence.

Acknowledgments

Brief acknowledgments of persons who have made genuine contributions to the manuscripts and who endorse the data and conclusions are included. Authors are responsible for obtaining written permission to use any copyrighted text and/or illustrations.

References

Cited references should mainly be drawn from journals covered in the Science Citation Index (http://www.isinet.com) and/or Index Medicus (http://www.ncbi.nlm.nih.gov/PubMed) databases. Mention all references in the text, tables and figure legends, and set off by consecutive, superscripted Arabic numerals. References should be numbered consecutively in the order in which they appear in the text. Abbreviate journal title names according to the Index Medicus style (http://www.ncbi.nlm.nih.gov/entrez/query.fcgi?db=journals). Unpublished observations and personal communications are not listed as references. The style and punctuation of the references conform to ISO standard and the Vancouver style (5th edition); see examples below. Reference lists not conforming to this style could lead to delayed or even rejected publication status. Examples:

Standard jounal article (list all authors and include the PubMed ID [PMID] where applicable)

1 **Das KM,** Farag SA. Current medical therapy of inflammatory bowel disease. *World J Gastroenterol* 2000; 6: 483-489 [PMID: 11819634]
2 **Pan BR**, Hodgson HJF, Kalsi J. Hyperglobulinemia in chronic liver disease: Relationships between *in vitro* immunoglobulin synthesis, short lived suppressor cell activity and serum immunoglobulin levels. *Clin Exp Immunol* 1984; 55: 546-551 [PMID: 6231144]
3 **Lin GZ,** Wang XZ, Wang P, Lin J, Yang FD. Immunologic effect of Jianpi Yishen decoction in treatment of Pixu-diarrhoea. *Shijie Huaren Xiaohua Zazhi* 1999; 7: 285-287 [CMFAID:1082371101835979]

Books and other monographs (list all authors)

4 **Sherlock S,** Dooley J. Diseases of the liver and billiary system. 9th ed. Oxford: Blackwell Sci Pub, 1993: 258-296

Chapter in a book (list all authors)

5 **Lam SK.** Academic investigator's perspectives of medical treatment for peptic ulcer. In: Swabb EA, Azabo S. Ulcer disease: investigation and basis for therapy. New York: Marcel Dekker, 1991: 431-450

Electronic journal (list all authors)

6 **Morse SS.** Factors in the emergence of infectious diseases. Emerg Infect Dis serial online, 1995-01-03, cited 1996-06-05; 1(1):24 screens. Available from: URL: http//www.cdc.gov/ncidod/EID/eid.htm

PMID requirement

From the full reference list, please submit a separate list of those references embodied in PubMed, keeping the same order as in the full reference list, with the following information only: (1) abbreviated journal name and citation (e.g. *World J Gastroenterol* 2003;9(11): 2400-2403; (2) article title (e.g. Epidemiology of gastroenterologic cancer in Henan Province, China; (3) full author list (e.g. Lu JB, Sun XB, Dai DX, Zhu SK, Chang QL, Liu SZ, Duan WJ; (4) PMID (e.g. 14606064). Provide the full abstracts of these references, as quoted from PubMed on a 3.5 inch disk or CD-ROM in Microsoft Word format and send by post to The *WJG* Press. For those references taken from journals not indexed by *Index Medicus*, a printed copy of the first page of the full reference should be submitted. Attach these references to the end of the manuscript in their order of appearance in the text.

Inappropriate references

Authors should always cite references that are relevant to their article, and avoid any inappropriate references. Inappropriate references include those that are linked with a hyphen and the difference between the two numbers at two sides of the hyphen is more than 5. For example, [1-6], [2-14] and [1,3,4-10,22] are all considered as inappropriate references. Authors should not cite their own unrelated published articles.

Statistical data

Present as mean±SD and mean±SE.

Statistical expression

Express *t* test as *t*(in italics), *F* test as *F*(in italics), chi square test as χ^2 (in Greek), related coefficient as *r*(in italics), degree of freedom as γ(in Greek), sample number as *n*(in italics), and probability as *P*(in italics).

Units

Use SI units. For example: body mass, m(B) = 78 kg; blood pressure, p (B)=16.2/12.3 kPa; incubation time, t(incubation)=96 h, blood glucose concentration, c(glucose) 6.4±2.1 mmol/L; blood CEA mass concentration, p(CEA) = 8.6 24.5 μg/L; CO_2 volume fraction, 50 mL/L CO_2 not 5% CO_2; likewise for 40 g/L formaldehyde, not 10% formalin; and mass fraction, 8 ng/g, *etc*. Arabic numerals such as 23,243,641 should be read 23 243 641.

The format about how to accurately write common units and quantum is at: http://www.wjgnet.com/wjg/help/15.doc

Abbreviations

Standard abbreviations should be defined in the abstract and on first mention in the text. In general, terms should not be abbreviated unless they are used repeatedly and the abbreviation is helpful to the reader. Permissible abbreviations are listed in Units, Symbols and Abbreviations: A Guide for Biological and Medical Editors and Authors (Ed. Baron DN, 1988) published by The Royal Society of Medicine, London. Certain commonly used abbreviations, such as DNA, RNA, HIV, LD50, PCR, HBV, ECG, WBC, RBC, CT, ESR, CSF, IgG, ELISA, PBS, ATP, EDTA, mAb, can be used directly without further mention.

Italicization

Quantities: *t* time or temperature, *c* concentration, *A* area, *l* length, *m* mass, *V* volume.
Genotypes: *gyr*A, *arg* 1, *c myc*, *c fos*, *etc*.
Restriction enzymes: *Eco*RI, *Hin*dI, *Bam*HI, *Kbo* I, *Kpn* I, *etc*.
Biology: *Helicobacter pylori, H pylori, E coli, etc*.

SUBMISSION OF THE REVISED MANUSCRIPTS AFTER ACCEPTED

Please revise your article according to the revision policies of *WJG*. The revised version including manuscript and high-resolution image figures (if any) should be copied on a floppy or compact disk. Author should send the revised manuscript, along with printed high-resolution color or black and white photos, copyright transfer letter, the final check list for authors, and responses to reviewers by a courier (such as EMS) (submission of revised manuscript by e-mail or on the WJG Editorial Office Online System is NOT available at present).

Language evaluation

The language of a manuscript will be graded before sending for revision. (1) Grade A: priority publishing; (2) Grade B: minor language polishing; (3) Grade C: a great deal of language polishing; (4) Grade D: rejected. The revised articles should be in grade B or grade A.

Copyright assignment form

It is the policy of WJG to acquire copyright in all contributions. Papers accepted for publication become the copyright of WJG and authors will be asked to sign a transfer of copyright form. All authors must read and agree to the conditions outlined in the Copyright Assignment Form (which can be downloaded from http://www.wjgnet.com/wjg/help/9.doc).

Final check list for authors

The format is at: http://www.wjgnet.com/wjg/help/13.doc

Responses to reviewers

Please revise your article according to the comments/suggestions of reviewers. The format for responses to the reviewers' comments is at: http://www.wjgnet.com/wjg/help/10.doc

Proof of financial support

For paper supported by a foundation, authors should provide a copy of the document and serial number of the foundation.

Publication fee

Authors of accepted articles must pay publication fee.

PO Box 2345, Beijing 100023, China
www.wjgnet.com
wjg@wjgnet.com

ELSEVIER

World J Gastroenterol 2005;11(20):Appendix 4
World Journal of Gastroenterology ISSN 1007-9327

World Journal of Gastroenterology standard of quantities and units

Number	Nonstandard	Standard	Notice
1	4 days	4 d	In figures, tables and numerical narration
2	4 days	four days	In text narration
3	day	d	After Arabic numerals
4	Four d	Four days	At the beginning of a sentence
5	2 hours	2 h	After Arabic numerals
6	2 hs	2 h	After Arabic numerals
7	hr, hrs,	h	After Arabic numerals
8	10 seconds	10 s	After Arabic numerals
9	10 year	10 years	In text narration
10	Ten yr	Ten years	At the beginning of a sentence
11	0,1,2 years	0,1,2 yr	In figures and tables
12	0,1,2 year	0,1,2 yr	In figures and tables
13	4 weeks	4 wk	
14	Four wk	Four weeks	At the beginning of a sentence
15	2 months	2 mo	In figures and tables
16	Two mo	Two months	At the beginning of a sentence
17	10 minutes	10 min	
18	Ten min	Ten minutes	At the beginning of a sentence
19	50% (*V/V*)	500 mL/L	
20	50% (m/*V*)	500 g/L	
21	1 M	1 mol/L	
22	10 μM	10 μmol/L	
23	1N HCl	1 mol/L HCl	
24	1N H_2SO_4	0.5 mol/L H_2SO_4	
25	4rd edition	4^{th} edition	
26	15 year experience	15- year experience	
27	18.5 kDa	18.5 ku,18 500u or M_r18 500	
28	25 $g.kg^{-1}/d^{-1}$	25 g/(kg·d) or 25 g/kg per day	
29	6900	6 900	
30	1000 rpm	1 000 r/min	
31	sec	s	After Arabic numerals
32	1 pg $\cdot L^{-1}$	1 pg/L	
33	10 kilograms	10 kg	
34	13 000 rpm	13 000 *g*	High speed; *g* should be in italic and suitable conversion.
35	1000 *g*	1 000 r/min	Low speed. *g* cannot be used.
36	Gene bank	GenBank	International classified genetic materials collection bank
37	Ten L	Ten liters	At the beginning of a sentence
38	Ten mL	Ten milliliters	At the beginning of a sentence
39	umol	μmol	
40	30 sec	30 s	
41	1 g/dl	10 g/L	10-fold conversion
42	OD_{260}	A_{260}	"OD" has been abandoned.
43	One g/L	One microgram per liter	At the beginning of a sentence
44	*A*260 nm	A_{260}nm	*A* should be in italic.
	$^bP<0.05$	$^aP<0.05$	In Table, no note is needed if there is no significance in statistics: $^aP<0.05$, $^bP<0.01$ (no note if $P>0.05$). If there is a second set of *P* value in the same table, $^cP<0.05$ and $^dP<0.01$ are used for a third set: $^eP<0.05$, $^fP<0.01$.
45	**F*=9.87, §*F*=25.9, #*F*=67.4	^1F=9.87,^2F=25.9, ^3F=67.4	Notices in or under a table
46	KM	km	kilometer
47	CM	cm	centimeter
48	MM	mm	millimeter
49	Kg, KG	kg	kilogram
50	Gm, gr	g	gram
51	nt	N	newton
52	l	L	liter
53	db	dB	decibel
54	rpm	r/min	rotation per minute
55	bq	Bq	becquerel, a unit symbol
56	amp	A	ampere
57	coul	C	coulomb
58	HZ	Hz	
59	w	W	watt
60	KPa	kPa	kilo-pascal
61	p	Pa	pascal
62	ev	EV	volt (electronic unit)
63	Jonle	J	joule
64	J/mmol	kJ/mol	kilojoule per mole
65	10×10×10cm^3	10 cm×10 cm×10 cm	
66	N·km	KN·m	moment
67	$\bar{x}\pm s$	mean±SD	In figures, tables or text narration
68	Mean±SEM	mean±SE	In figures, tables or text narration
69	*im*	im	intramuscular injection
70	*iv*	iv	intravenous injection
71	Wang et al	Wang *et al.*	
72	EcoRI	*Eco*RI	*Eco* in italic and RI in positive. Restriction endonuclease has its prescript form of writing.
73	Ecoli	*E.coli*	Bacteria and other biologic terms have their specific expression.
74	Hp	*H pylori*	
75	Iga	*Iga*	writing form of genes
76	*igA*	IgA	writing form of proteins
77	-70 kDa	~70 ku	